Role of redox signaling by ascorbate in the performance of tomato fruit

Guillaume Decros

THESE

Présentée pour l'obtention du grade de
DOCTEUR DE L'UNIVERSITÉ DE BORDEAUX
École Doctorale des Sciences de la Vie et de la Santé

Spécialité : Biologie Végétale

Par

Guillaume DECROS

ROLE OF ASCORBATE REDOX SIGNALLING IN THE PERFORMANCE OF TOMATO FRUIT

-

RÔLE DE LA SIGNALISATION REDOX PAR L'ASCORBATE DANS LA PERFORMANCE DU FRUIT DE TOMATE

Sous la direction de Pierre Pétriacq
Présentée et soutenue publiquement le 08 Avril 2022

Director	M. Pierre PÉTRIACQ – Associate Professor, *University of Bordeaux*
President	M. Éric Gomes - Professor, *University of Bordeaux*
Rapporteurs	Mme. Christine Helen FOYER – Professor, *University of Birmingham* Mme. Emmanuelle ISSAKIDIS-BOURGUET – Researcher, *IPS2 Orsay*
Examinators	M. Christophe SALON – Research Director, *INRAE Dijon*
Guest	Mme. Rebecca STEVENS - Researcher, *INRAE Avignon*

AKNOWLEDGMENTS

Tout d’abord, je souhaiterais remercier les membres du jury, Christine H. Foyer, Emmanuelle Issakidis-Bourguet, Rebecca Stevens, Christophe Salon et Éric Gomès pour avoir accepté d’évaluer mes travaux.

J’adresse ensuite un grand merci à Yves Gibon, Directeur de l’équipe META, pour m’avoir accueilli dans son équipe durant ces trois années et demie et pour sa confiance dans mon projet de thèse. J’ai particulièrement apprécié les réunions thésards durant lesquelles tu as su m’aider à développer mon esprit scientifique mais aussi pour tous tes conseils avisés qui m’aideront, j’en suis sûr, à poursuivre une carrière dans la science.

Je remercie très chaleureusement mon encadrant Pierre Pétriacq qui m’a accordé une confiance sans égale durant ce projet. Pierre, je ne sais comment te remercier de tout ce que tu as fait pour moi, tu as su me guider tout en me laissant devenir autonome. Je te remercie très sincèrement pour toutes les opportunités que tu m’as offerte ces dernières années. Je pense particulièrement à tous les étudiants que j’ai pu encadrer durant ce projet, ce qui m’aura permis de confirmer mon gout pour l’enseignement. Grâce à toi, j’ai pu m’émanciper professionnellement et personnellement, travailler à tes côtés m’aura appris que bienveillance, rigueur et tolérance sont des valeurs essentielles pour le bon déroulement d’une carrière universitaire. Encore une fois, je suis très heureux d’avoir pu réaliser ce projet guidé par ta bienveillance, MERCI INFINIMENT !

Je voudrais aussi remercier très sincèrement Pierre Baldet et Kentaro Mori avec qui j’ai débuté dans les sciences végétales en stage de master 1, en tant que jeune padawan. Vous m’avez soutenu depuis le début dans mon projet d’aller à Tsukuba, ce que j’ai appris en 2 mois avec vous m’a permis de réussir mon année au Japon et je vous en suis infiniment reconnaissant, domo arigato gosaimasu ! D’un point de vue plus personnel, Pierrot je te remercie très sincèrement pour ton soutien continu depuis plus de 5 ans. Depuis ma première expérience en laboratoire jusqu’à la fin de cette thèse, ta bonne humeur contagieuse, ton soutien sans faille et ton immense bienveillance m’ont toujours accompagnées, même jusqu’à l’autre bout du monde dans les jardins de Tokyo. Je te remercie pour tous ces moments passés avec toi et pour tous les efforts que tu as fait pour moi, notamment à faire le bourdon en plein été dans la serre. Tu resteras pour moi un modèle, le maitre jedi que j’aspire à devenir plus tard.

Je remercie également toutes les personnes qui m'ont aidé, de prêt ou de loin, à réaliser ce projet : Cécile, Mickael, Michel, Joana, Sophie, Kentaro, ainsi que tous mes stagiaires, Biranty, Chloé, Camille, Thy, Lucie, Karen, Nahikari, Olivier, Vincent et Agathe.

Je remercie tout particulièrement Isabelle Atienza-Babin pour sa patience et le soin qu'elle a apporté à mes plantes et, Bertrand Beauvoit pour son aide concernant la modélisation mais aussi pour ses conseils tout au long de ce projet.

Mention particulière pour mes amis et compagnons de bureau qui m'ont accompagné durant ce projet : Amélie, Gabriel, Thomas, Sylvain, Cédric, Alice, JJ, Théo et Chloé. Je vous remercie sincèrement pour tous ces moments passés au labo ou en dehors, le bureau des thésards va énormément me manquer. J'en profite pour remercier également tous les participants des *jeudi plus plus*.

Enfin, je remercie plus que tous mes parents et ma sœur qui m'ont toujours soutenu et donné les moyens de réaliser mes projets même si le monde de la science leur est inconnu. Je remercie également mes amis de TARTEK qui sont toujours présent malgré mon attitude fantomatique ces dernières années.

Je remercie également le mystérieux T. pour m'avoir supporté tout au long de cette thèse, avec toutes les difficultés et les réussites qui se sont succédé, sans oublier mon chat Ronron pour son incroyable capacité antistress et ses ronrons apaisants !

ABSTRACT OF THE THESIS

The change of paradigm in redox biology, considering ROS as finely-tuned signals modulating plant metabolism, shed new light on redox networks, especially in plants where multiple sources of ROS are possible and associated with many “ROS processing systems” (Noctor et al., 2018), while major redox buffers (e.g. ASC, GSH and NAD) clearly appear at the forefront of oxidative regulations. ROS production and redox signals arising from are crucial to harmonious metabolism and participate in adaptive signalling pathways throughout development and in response to the environment. In parallel, the development of mathematical integrative modelling permitted by new approaches providing quantitative description through metabolic fluxes.

Progress in understanding the molecular signatures involved in the redox regulations controlling the trade-off between fruit development and stress pathways will help to define novel strategies for optimal fruit production and storage (Beauvoit et al., 2018). However, knowledge on redox biology in fruit is sparsely documented, although principles originating from leaves tissues are valuable while waiting for comprehensive studies that provide more extensive knowledge on fruits.

In this regard, my PhD project aims to provide the first quantitative description of core redox metabolism in a developmental context while developing and implementing protocols allowing the rapid quantification of major redox compounds. In addition, the use of an integrative modelling approach will allow deciphering the implication of redox flux in the control of redox balance during fruit development.

For this purpose:

1. A multiscale omics study focusing on NAD metabolism during tomato fruit development provides a better view of the implication of NAD metabolism in redox and central metabolism,

2. Major redox buffers and total antioxidant capacity are assessed using targeted biochemical analyses of the ascorbate-glutathione cycle, while untargeted LC-MS analysis provides a global comparison of developmental stages, in particular for secondary redox compounds. Furthermore, mutant plants enriched in ascorbate have been analysed to study the impact of an increase in ASC on tomato fruit,

3. The data sets obtained are finally used to develop a kinetic-based model of the ASC-GSH cycle, allowing the investigation of redox fluxes and their regulation during tomato fruit development.

Besides, I participate in developing a redox platform to implement at the Bordeaux Metabolome Facility, allowing me to participate in some other projects, such as the characterisation of new NAD kinase (Dell'Aglio et al., 2019) and the characterisation of ASC-enriched mutants (Deslous et al., 2021). I also had the opportunity to participate in the writing of reviews aiming to bring together the scattered knowledge available on redox metabolism in fruits and in response to extreme environments (Decros et al., 2019; Dussarrat et al., 2021). Furthermore, the preliminary data obtained allowed the designing of new projects more focused on the involvement of redox metabolism during the fruit setting phase. To this end, different ASC mutant fruits have been analysed at several flower and young fruit stages.

RÉSUMÉ DE LA THÈSE

Le changement de paradigme dans la biologie de l'oxydoréduction (redox), considérant les espèces réactives de l'oxygène (EROs) comme des signaux ajustés avec précision modulant le métabolisme des plantes, a mis en exergue les réseaux d'oxydoréduction, en particulier chez les plantes où de multiples sources d'EROs sont présentes et associées à de nombreux " systèmes de traitement des EROs " (Noctor et al., 2018). De plus, les principaux tampons redox (par exemple, l'acide ascorbique, le glutathion et les nucléotides à pyridine) apparaissent clairement au premier plan des régulations redox. La production d'EROs et les signaux redox qui en découlent sont cruciaux pour préserver l'harmonie du métabolisme du fait de leur participation aux voies de signalisation adaptatives tout au long du développement et en réponse à l'environnement. En parallèle, le développement de la modélisation mathématique intégrative a permis de nouvelles approches qui fournissent une description quantitative des flux métaboliques et de leurs régulations.

Les progrès dans la compréhension des signatures moléculaires impliquées dans les régulations redox, contrôlant le compromis entre le développement des fruits et les voies de stress, permettront de définir de nouvelles stratégies pour une production et un stockage optimal des fruits (Beauvoit et al., 2018). Cependant, les connaissances sur la biologie de l'oxydoréduction dans les fruits sont peu documentées. Bien que les principes provenant des tissus foliaires apportent une première compréhension du métabolisme redox, des études complètes fournissant des connaissances plus étendues sur les fruits restent manquantes.

A cet égard, mon projet de thèse vise à fournir la première description quantitative du métabolisme redox principal du fruit de tomate dans un contexte de développement, tout en développant et en mettant en œuvre des protocoles permettant la quantification rapide des principaux composés redox. En outre, l'utilisation d'une approche de modélisation cinétique permettra de déchiffrer l'implication des flux redox dans le contrôle de l'équilibre oxydoréducteur au cours du développement du fruit.

A cette fin :

1. Une étude omique multi-échelle axée sur le métabolisme du NAD au cours du développement du fruit de la tomate a permis de fournir une meilleure vue de l'implication du métabolisme du NAD dans les métabolismes redox et central,

2. Les principaux tampons redox et la capacité antioxydante totale ont été évalués à l'aide d'analyses biochimiques ciblées du cycle ascorbate-glutathion, tandis que l'analyse LC-MS non ciblée a permis une comparaison globale des stades de développement, en particulier vis à vis des composés redox secondaires. D'autre part, des plantes mutantes enrichies en ascorbate ont été analysées pour étudier l'impact d'une augmentation de l'ASC sur le métabolisme et le développement du fruit de tomate,

3. Les ensembles de données obtenus ont finalement été utilisées pour développer un modèle cinétique du cycle ASC-GSH, permettant l'étude des flux redox et de leur régulation au cours du développement du fruit de la tomate.

D'autre part, j'ai participé au développement d'un plateau d'analyses redox mis en place au sein de la plateforme Bordeaux Metabolome, ce qui m'a permis de participer à d'autres projets, tels que la caractérisation d'une nouvelle NAD kinase (Dell'Aglio et al., 2019) et la caractérisation de mutants enrichis en ASC (Deslous et al., 2021). J'ai également eu l'occasion de participer à la rédaction de revues visant à rassembler les connaissances éparses disponibles sur le métabolisme redox dans les fruits et en réponse aux environnements extrêmes (Decros et al., 2019; Dussarrat et al., 2021). Par ailleurs, les données préliminaires obtenues au cours de ce projet ont permis de concevoir de nouveaux projets plus ciblés sur l'implication du métabolisme redox pendant la phase de mise à fruit.

ABBREVIATION LIST

AA: amino acid
ABA: Abscisic acid
ADP: adenosine diphosphate
AGPase: ADP-Glucose pyrophosphorylase
AltDH: Alternative dehydrogenases
AO: Aspartate oxidase
AOX: Alternative oxidase
APX: Ascorbate peroxidase
ASC: Ascorbate
ASC OX: Ascorbate oxidase
Asp: Aspartate
ATP: adenosine triphosphate
BABA: β-aminobutyrate
cADPR(P): cyclic ADP-ribose (phosphate)
CAT: Catalase
cETC: chloroplastic electron transport chain
Chl: Chlorophyll
CI-V: Complex I-V
CP: Carboxypeptidase
Cys: Cysteine
cyt.c : Cytochrome c
DHA: Dehydroascorbate
DHAP: Dihydroxyacetone phosphate
DHAR: Dehydroascorbate reductase
DPA: Day post anthesis
ET: Ethylene
GA: Gibberellins
GABA: γ-aminobutyrate
GAP: 3-phosphoglyceric aldehyde
GAPDH: Glyceraldehyde-3-phosphate dehydrogenase
GGP: GDP-L-galactose phosphorylase
GGS: γ-glutamyl cycloytansferase
GGT: γ-glutamyl transpeptidase
Glu: Glutamic acid
Gly: Glycine
GME: GDP-D-mannose-3',5'-epimerase
GMP: GDP-D-mannose pyrophosphorylase
GOX: Glycolate oxidase
GP: Guaiacol peroxidase
GPP: L-galactose-1-P phosphatase
GPX: Glutathione peroxidase
GR: Glutathione reductase
GRX: Glutaredoxins
GS: Glutathione synthetase
GSH: Glutathione (reduced form)
GSSG: Disulfide glutathione (oxidized form)
GST: Glutathione S-transferase
IDH: Isocitrate dehydrogenase
JA: Jasmonic acid
LC-MS: Liquid chromatography - Mass spectrometry
L-GalDH: L-galactose dehydrogenase
L-GalLDH: L-galactono-1,4-lactone dehydrogenase
MDHA: Monodehydroascorbate
MDHAR: Monodehydroascorbate reductase
Met: Methionine
mtETC: Mitochondrial electron transfer chain
MSR: Met sulfoxide reductase
NaAD: Nicotinic acid adenine dinucleotide
NAD: Nicotinamide adenine dinucleotide
NADK: NAD kinase
NADP: Nicotinamide adenine dinucleotide phosphate
NADPPase: NADP phosphatase
NAD(P)HX: NAD(P)H hydrate

NADS: NAD synthetase

NaGT: Nicotinate N-glucosyltransferase

NaMN: Nicotinic acid mononucleotide

NaMNAT: NaMN adenylyltransferase

NaPT: Nicotinate phosphoribosyltransferase

NIC: Nicotinamidase

NMR: Nuclear magnetic resonance

NMT: Nicotinate N-methyltransferase

OAA: Oxaloacetate

OPP: Oxidative pentose phosphate pathway

PARP: Poly-ADP-ribose polymerase

PCS: Phytochelatin synthase

pETC: Photosynthetic electron transport chain

PGA: Phosphoglycerate

PMI: Phosphomannose isomerase

PMM: Phosphomannose mutase

PS: Photosystem

PRX: Peroxidase

PXN: peroxisomal NAD carrier

QPT: Quinolinate phosphoribosyltransferase

QS: Quinolinate synthase

RBOH: Respiratory Burst Oxidase Homolog

ROS: Reactive Oxygen Species

RuBP: Ribulose 1,5Bisphosphate

$^1O_2$: Singlet oxygen

H_2O_2: Hydrogen peroxide

$O_2^{\bullet-}$: Superoxide anion

OH•: Hydroxyl radical

SA: Salicylic acid

SOD: Superoxide dismutase

Sugar-P: sugar-phosphate

TCA: Tricarboxylic acid

THD: Transhydrogenases

TRXs: Thioredoxins

XDH: Xanthine dehydrogenases

γ-ECS: γ-glutamylcysteine synthetase

1,3BGPA: 1,3-bisphosphoglyceric acid

3PGA: 3-phosphoglyceric acid

5-OP: 5-oxoproline

5OPase: 5-oxoprolinase

TABLE OF CONTENT

CHAPTER I. GENERAL INTRODUCTION

CHAPTER II. MATERIALS AND METHODS

CHAPTER III. MULTIOMICS ANALYSES OF NAD(P) METABOLISM DURING TOMATO FRUIT DEVELOPMENT

CHAPTER IV. QUANTITATIVE DESCRIPTION OF THE ASC-GSH CYCLE DURING TOMATO FRUIT DEVELOPMENT

CHAPTER I

GENERAL INTRODUCTION

A. Tomato fruit (*Solanum lycopersicum*)

I. Origin

Tomato originated from the Andes, where it was cultivated by the peoples of South America. Its first description was documented in 1544 by Matthiolus, an Italian botanist (Figure I.1). At that time, the tomato already showed tremendous phenotypic diversity in terms of shape and colour (Figure I.2). Then, the Spanish conquistadors introduced it to Europe at the beginning of the 16th century, where it was first cultivated as an ornamental plant because of its similarity to *Mandragora* and *Belladona*, two plants also belonging to the nightshade family (Solanaceae). It was not until the 19th century that its usefulness in food was discovered (Rick, 1976).

II. Botanical description

In the 18th century, the founder of the modern binomial nomenclature system, Carl Von Linnaeus, renamed the tomato "*Solanum lycopersicum"* after the Greek words "*lycos"* and "*persicum"*, meaning "wolf" and "peach", respectively. The tomato, *Solanum lycopersicum*, is therefore a herbaceous plant that belongs to the large family of Solanaceae. This family of dicotyledons includes nearly 100 genus and 2700 species representing a great diversity of morphologies and habitats. The Solanaceae family includes species used in the food industry such as potatoes (*Solanum tuberosum*), peppers (*Solanum capsicum*) and aubergines (*Solanum melongena*), as well as various ornamental species such as datura (*Datura stramonium*) or belladonna (*Atropa belladonna*) (Figure I.2).

This family includes species known as toxic for humans because of their alkaloid content, such as atropine or scopolamine. The same applies to the tomato, whose vegetative parts are poisonous and only the fruit is edible.

The species *Solanum lycopersicum* comprises several thousand varieties, including the cultivated tomato (*Solanum lycopersicum* var. *esculentum*), from which almost all commercial cultivars are derived. The different tomato varieties are classified according to their growth habit (determinate or indeterminate) and the fruit phenotype (shape, size, colour). Genetic resources are preserved by cultivar collections maintained worldwide.

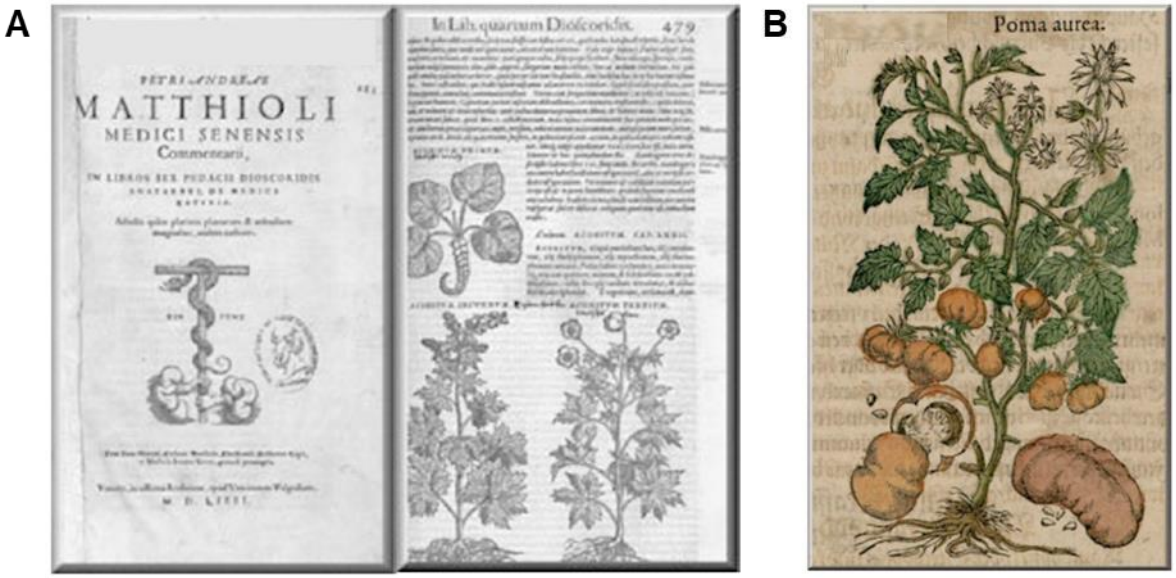

Figure I.1: First description of tomato. Book providing the first description of tomato (edited in 1554) **(A)** ; First illustration of a tomato plant by Piétro Andréa Matthioli (1550) **(B).**

Figure I.2: Example of Solanaceae fruits. Tomato (*Solanum lycopersicum*) **(A)**; Mandragore (*Mandragora officinarum*) **(B)**; Belladone (*Atropa belladonna*) **(C)**.

III. Economic, nutritional and scientific importance

According to the Food and Agriculture Organisation (FAO; https://www.fao.org/home/en/), tomatoes are grown across the entire globe (in 173 countries), although half of the world's production comes from Asia (Figure I.3). Tomato cultivation on a global scale is made possible by varietal selection and developments in cultivation methods (greenhouse or soilless) that allow tomatoes to be produced all year round. The fruit is intended for direct consumption but also numerous processing operations used by the food industry (sauces, juices, etc.). The demand for tomatoes has constantly been increasing since the 1990s, leading to a production of more than 100 million tonnes today, ranking tomatoes first in terms of fruit production (Figure I.4). In France, tomato is not the primary agricultural product, despite an annual production of about 700 thousand tonnes. Nonetheless, tomato is the most consumed fruit in France, with a yearly consumption of 13 kg per person per year for fresh tomatoes and 15.8 kg per person per year for processed tomatoes.

Besides, tomatoes are of great nutritional importance for humans. This fruit harbours a low sugar content (less than 20 kcal per 100 g of fresh material) but high amounts of antioxidants such as ascorbate (or vitamin C), lycopene, and numerous other carotenes and polyphenols that are beneficial to human health. Additionally, tomatoes are considered the primary source of vitamin C in the human diet because, even though they contain a lower level of vitamin C than citrus species, they are massively consumed in daily diet.

Apart from this nutritional and economic importance, tomato (*Solanum lycopersicum*) has a scientific interest as a model plant to study processes associated with the development of fleshy fruits. Indeed, tomato presents many biological advantages, such as its short generation cycle as well as its ease of crossing and control of fertilisation. Moreover, it is cultivable all year long and easily transformed by genome editing technics. Furthermore, the tomato genome has been fully sequenced and annotated since 2012 (The Tomato Genome Consortium, 2012). It has a total size of 900 Mb, spread over 12 chromosomes, and presents about 33 000 genes among which more than 5 000 are preferentially expressed in fruits (Fernandez-Pozo et al., 2017). Nowadays, many mutants have been generated and are available in several collections allowing the identification and characterisation of genes associated with interesting phenotypical traits (Okabe et al., 2011; Just et al., 2013).

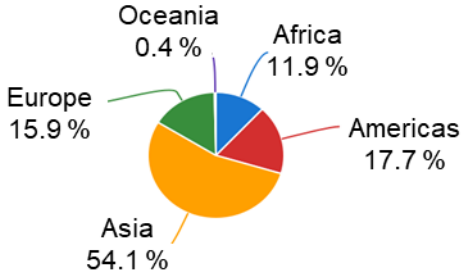

Figure I.3: Worldwide average (1994-2019) tomato production by region.

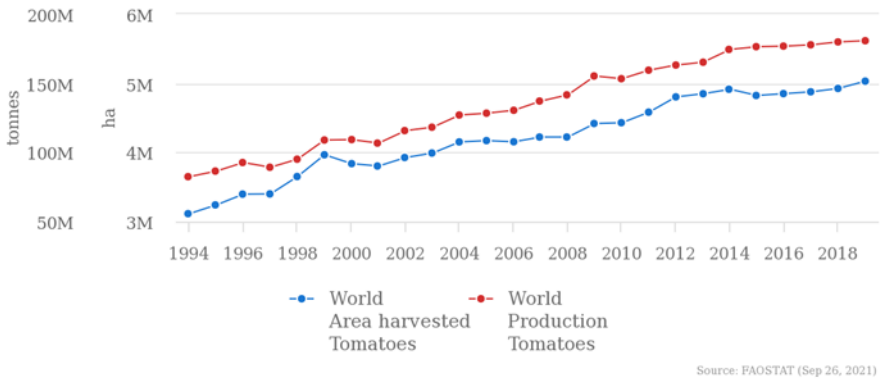

Figure I.4: Evolution of world tomato production during the last 30 years.

IV. Development of tomato reproductive tissues

Tomato is a perennial herbaceous plant in warm and temperate climates, and it is usually grown as an annual. The tomato is a neutral day plant, which means that its flowering depends on the photoperiod. Its development cycle from seed to seed is between 90 and 120 days, depending on the cultivar.

1. Flower development

Tomato flowers are hermaphroditic and self-fertile. They are actinomorphic flowers with pentameric symmetry (Figure I.5A), whose calyx consists of five green sepals that persist at the top of the fruit after fertilisation, the corolla carries five yellow petals fused at the base, and the androecium is composed of five stamens whose elongated anthers form a cone constricted around the pistil. The stamens have dehiscence, allowing the pollen to be released inwards, thus facilitating the self-fertilisation. Besides, the gynoecium consists of a pistil formed by two fused carpels, structuring an ovary generally bi- or trilocular with central placentation (Figure I.5B). When the flower reaches maturity, called the anthesis stage (Figure I.5C), the anther opens and allows the release of pollen that will be deposited on the stigma of the pistil, finally inducing the fertilisation of the ovule and the beginning of the development of the fruit. Sometimes, fruits can develop without necessary fertilisation and thus do not have seeds, referred to as parthenocarpy.

2. Fruit development

The tomato fruit is a fleshy berry-like fruit that consists of a pericarp (skin and fleshy part) and a pulp (placenta and seeds) (Figure I.6). From a histological point of view, after fertilization, the wall of the ovary is transformed into a pericarp, characterised by three cellular layers, namely the exocarp, the mesocarp and the endocarp. The exocarp is the outermost part of the fruit formed by a layer of epidermal cells associated with a collenchymatous tissue where starch and plastids can accumulate. Moreover, the exocarp is externally covered by a cuticle deposit which increases as the fruit grows. Next, the mesocarp is the intermediate layer of the pericarp, composed of a parenchyma formed by large cells carrying large vacuoles. The mesocarp cells are the site of endoreduplication, a process during which genetic material is replicated without cell division (Bourdon et al., 2010). Finally, the endocarp constitutes the innermost part of the pericarp formed by a cell bed lining the interior of the seed coat. On the other hand, inside the fruit, the fertilised ovules will evolve into seeds, and the placenta will be transformed into locular tissue, which will become gelatinous during ripening.

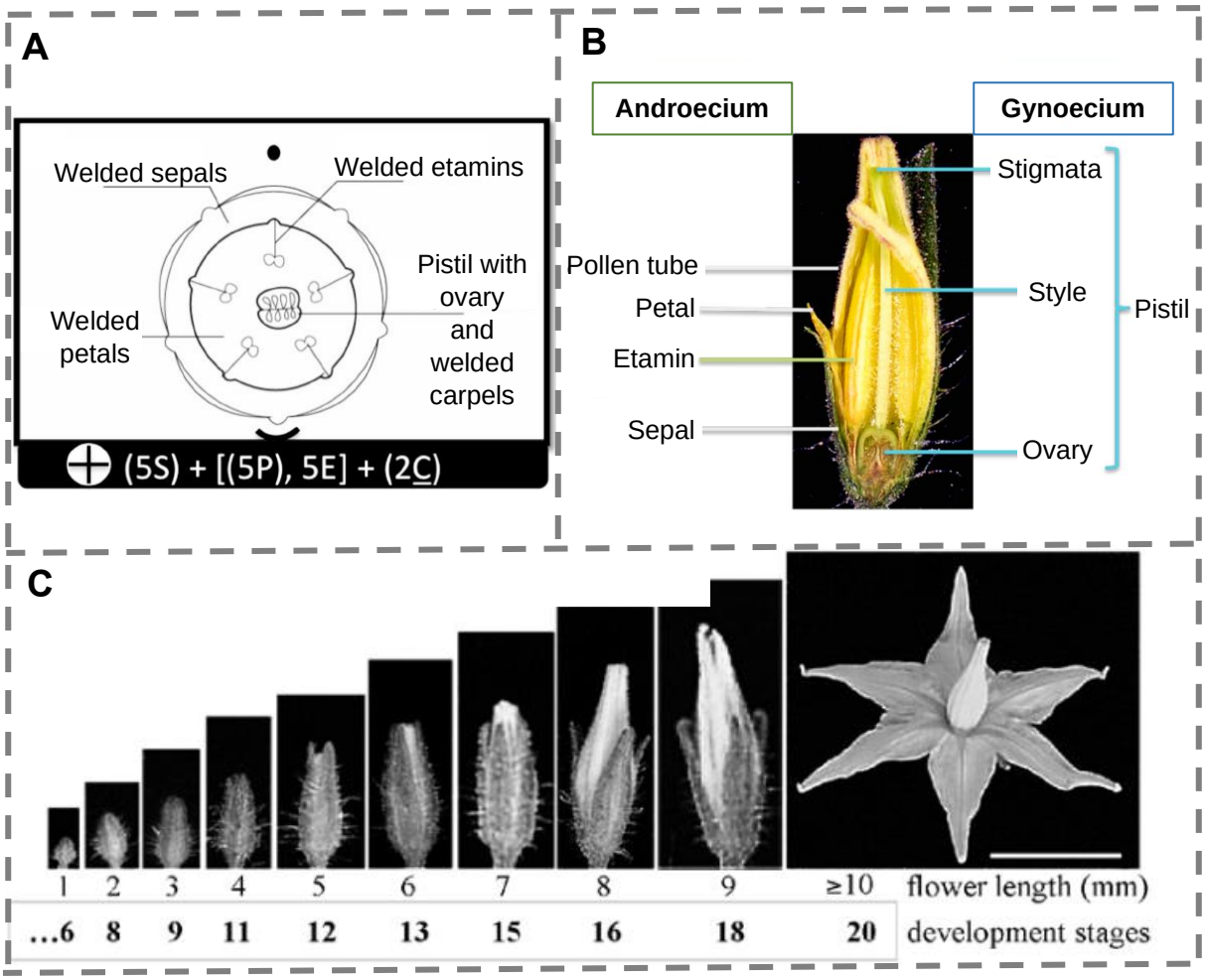

Figure I.5: Structure and development of *Solanum lycopersicum* flower. Floral diagram of tomato flower **(A)**; Longitudinal view of tomato flower **(B)**; Sequential development of tomato flower **(C)**, adapted from (Brukhin et al., 2003). S (sepal), P (petal), E (etamins), C (carpel).

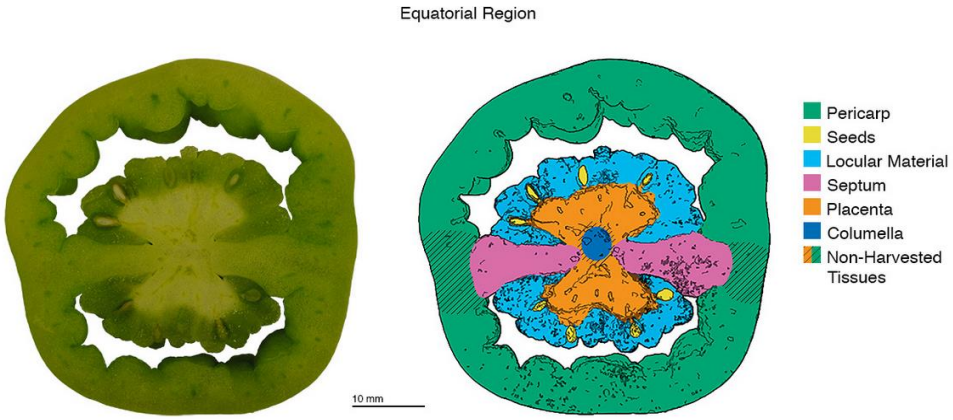

Figure I.6: Anatomical view of *Solanum lycopersicum* cv. M82 fruit at mature green stage (all tissues are fully developed), from Tomato Expression Atlas (Fernandez-Pozo et al., 2017).

From a physiological point of view, the development of the fruit is characterised by three distinct phases of development: the cell division phase, the cell expansion phase and the maturation phase (Figure I.7).

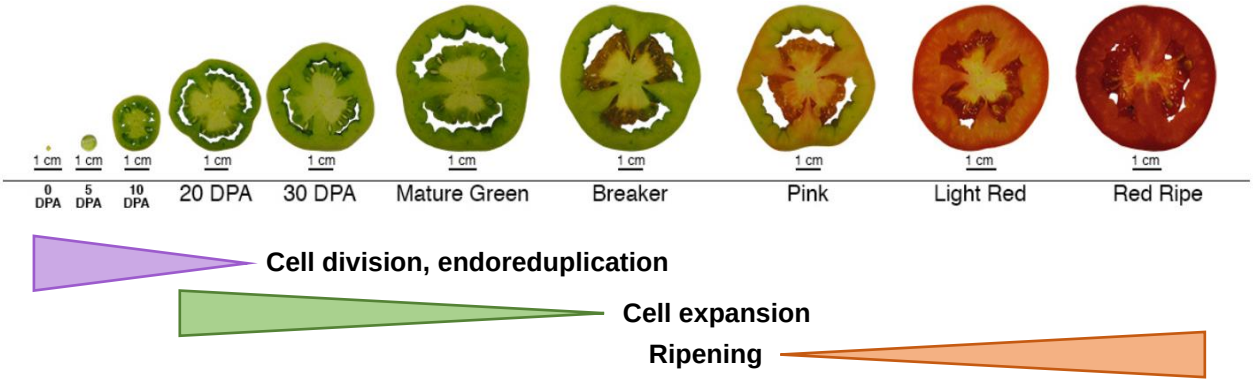

Figure I.7: Tomato fruit development, adapted from Tomato Expression Atlas (Fernandez-Pozo et al., 2017). DPA: day post anthesis

a. Cell division phase

The first phase of fruit development is characterised by an intense cell division activity resulting in an increase in the number of cell layers within the pericarp. This phase starts with fertilisation and lasts for about ten days, depending on the variety. We can distinguish two types of divisions: the anticlinal divisions, characterised by a division plane perpendicular to the surface of the fruit, and the periclinal divisions, in which the division plane is parallel to the surface of the fruit. During the cell division phase in tomato fruit, there is a considerable increase in anticlinal divisions (about 70%) in the epidermal layers leading to a rise in the number of cell bases and thus an increase in the fruit surface (Renaudin et al., 2017).

b. Cell expansion phase

Cell expansion starts when the division phase ends and mainly determines the final size of the fruit. Cell expansion in plants occurs primarily by turgor. In short, the accumulation of metabolites (mainly sugars, organic acids and ions) in the vacuole induces a difference in osmotic potential resulting in an influx of water into the vacuole leading to its enlargement and cell expansion eventually. Moreover, we can observe during this expansion phase augmented cell volumes up to 100 times their initial volumes, thus reinforcing the role of cellular expansion as a crucial process to influence fruit size.

c. Ripening

The last stage of fruit development, ripening, is associated with the maturation of the seeds. It is a complex and species-dependent process whose purpose is to make the fruits attractive to encourage their consumption and promote the dissemination of seeds.

The ripening process involves many biochemical, physiological and structural changes in all the tissues of the fruit. Tomato belongs to climacteric fruit, therefore tomato ripening depends on a specific phytohormone, ethylene (Lelievre et al., 1997). The beginning of the ripening phase is characterised by an increase in ethylene content concomitant with an increase in respiratory flow. Once this climacteric crisis is achieved, fruits can ripe either attached or detached from the plant. Moreover, during ripening, the starch stored in the fruit is remobilised to be transformed into soluble sugars, which is associated with an active respiratory metabolism. In addition, ripening involves the transition of chloroplasts into chromoplasts that will accumulate antioxidant metabolites such as polyphenols and carotenoids, inducing the colour change of the fruit.

To conclude, the development of the tomato fruit is thus characterised by three distinct developmental phases (Figure I.7), with dynamic physiological and metabolic activities suggesting an active antioxidative metabolism during all developmental steps. Meanwhile, tomato is composed of many antioxidant molecules that accumulate mainly during ripening concomitantly with the climacteric crisis. However, no detailed analysis of redox metabolism during development has been performed to date.

B. Basics of redox biology in plants

Reduction-oxidation (redox) processes are electron transfers from a reductive agent to an oxidising agent, thus including both an oxidation of the reductive agent and a reduction of the oxidising agent (Figure I.8). Oxygen ($^{16}_{8}O$) is the third-most abundant element in the universe after hydrogen and helium, and the major oxidative compound found on Earth (ground state oxygen, constituting c.a. 20.8% of the atmosphere). Oxygen was discovered by Scheele, Joseph Priestley and Antoine Lavoisier in the late 18th century. The French chemist Antoine Lavoisier named it after the Greek words *oxy* and *genes*, meaning respectively “acid” and “producer” because of its oxidant properties (Figure I.9). It was later demonstrated that O_2 can be produced by plants and is necessary for animals to survive by allowing them to propagate and release the energy they collect from their environment. In short, oxygen and the resulting redox processes are the basis of life on earth.

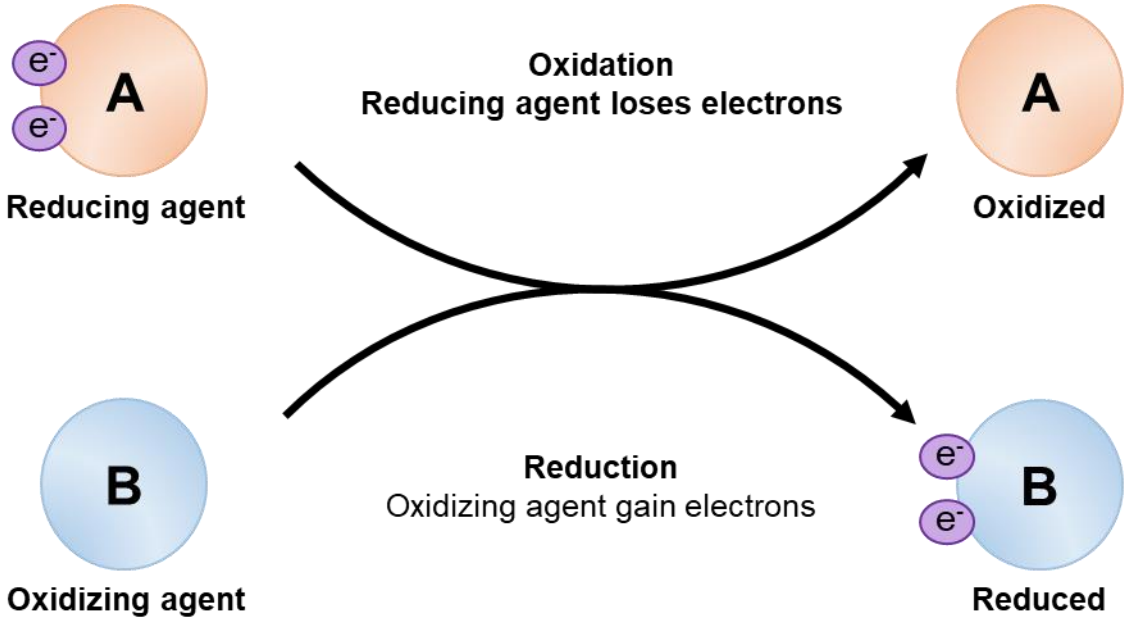

Figure I.8: Mechanism of reduction-oxidation (redox) reaction.

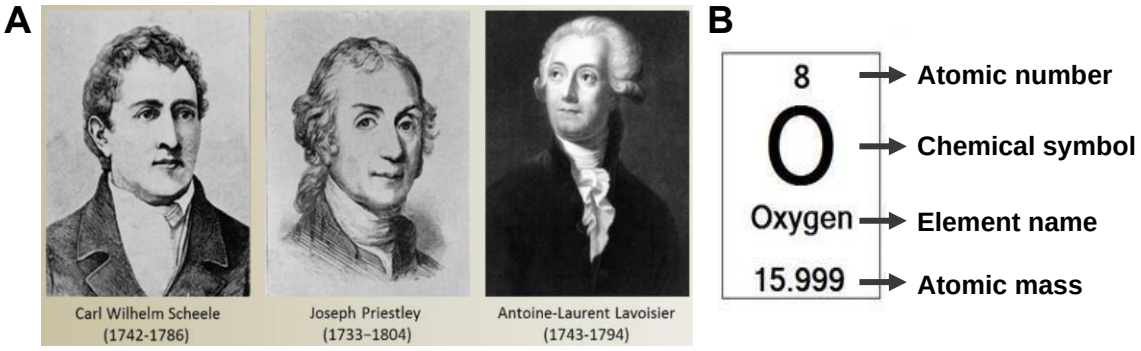

Figure I.9: Diatomic oxygen. Scientists that participate to the discovery of oxygen as an element **(A).** ID card of oxygen **(B)**.

I. Oxidative metabolism in plants

Plants and others photosynthetic organisms, such as green algae and cyanobacteria, drive electron flow from the light-driven splitting of water (H_2O) to produce O_2 during photosynthesis (Foyer, 2018). In tissues with low or no photosynthesis activity, such as fruits and roots, chemical redox couples can also drive the flow of electrons to generate the energy needed for growth during mitochondrial respiration (Schertl and Braun, 2014). In other words, central metabolism produces reducing power (*i.e.* NADH and NADPH) that will be used during oxidative respiration and allows plants to create the energy necessary for their growth. Consequently, this redox biochemistry generates the famous reactive oxygen species (ROS).

1. Natures and sources of ROS in plant cells

ROS encompass highly reactive molecules that are partially reduced or excited forms of O_2, including, *e.g.* singlet oxygen ($^1O_2$), the superoxide anion ($O_2^{\bullet-}$), hydrogen peroxide (H_2O_2), and the hydroxyl radical (OH•) (Apel and Hirt, 2004) (Figure I.10). Among these ROS, H_2O_2 shows a longer lifespan, diffusion distance and stability, making it the best candidate for oxidative signalling (Exposito-Rodriguez et al., 2017; Mittler, 2017). Plant ROS are mainly produced during three fundamental biological processes: chloroplastic photosynthesis, peroxisomal photorespiration, and mitochondrial respiration.

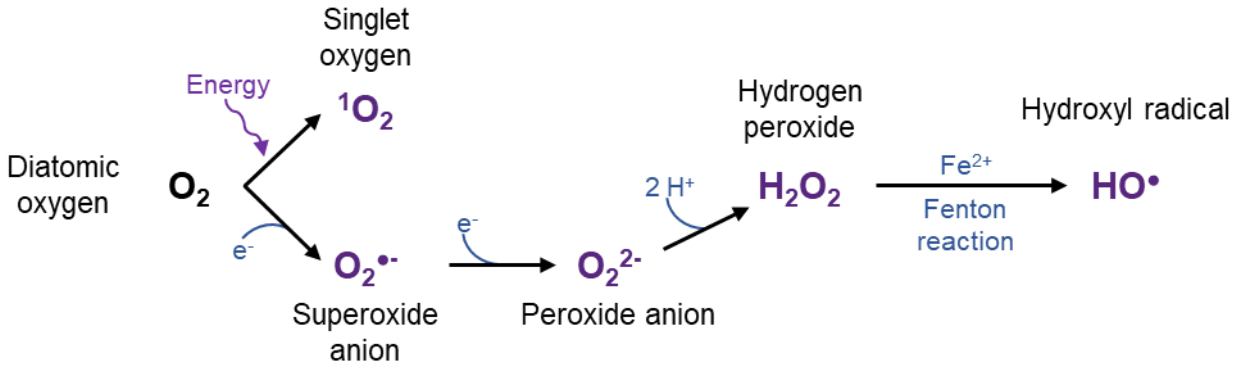

Figure I.10: Reactive oxygen species (ROS) produced from atmospheric diatomic oxygen gas.

From a quantitative perspective, chloroplastic photosynthesis is the primary ROS producer in photosynthetic tissues, especially in producing H_2O_2 and $O_2^{\bullet-}$. Firstly, superoxide anion and hydrogen peroxide can be produced by photosystem I (PSI) (Figure I.11) by reducing molecular oxygen through the Mehler reaction. This reaction is concurrent to the reduction of $NADP^+$, meaning that O_2 competes with $NADP^+$ to collect the electron from PSI. In this context, the photoreduction of O_2 can be considered an outlet to dissipate excess of reducing power (*i.e.* NADPH) or a non-expected leak of electrons leading to superoxide anion production. Secondly, superoxide anion inherently dismutates or could be enzymatically dismutated by superoxide dismutases (EC 1.15.1.1; SODs) to H_2O_2 that can subsequently be reduced to form $HO^{\bullet}$ via the Fenton reaction. Finally, singlet oxygen is synthetised by photodynamic oxidation of ground-state oxygen that can be driven by the energy transfer from excited chlorophylls triplet to O_2 in photosystem II (PSII) (Figure I.11) (Fischer et al., 2013).

In non-photosynthetic tissues, ROS mainly originate from the mitochondrial electron transport chain (mETC) that consists of four main enzymatic complexes, CI (EC 1.6.5.3; NADH:ubiquinone oxidoreductase), CII (EC 1.3.5.1; succinate dehydrogenase), CIII (EC 1.10.2.2; cytochrome *c* reductase) and CIV (EC 1.9.3.1; cytochrome *c* oxidase) linked to the ATP synthase (CV) (Figure I.11). Among these complexes, CI and CIII are known to be the major contributors to mitochondrial superoxide production (Markevich and Hoek, 2015). In complex I, NADH oxidation allows the reduction of flavine mononucleotide (FMN) to $FMNH^{\bullet}$ resulting in the production of $O_2^{\bullet-}$ by electron transfer to O_2, thereby generating H_2O_2 through the activity of specific SODs (Smirnoff and Arnaud, 2019).

Besides ROS-generating systems, plant mitochondria specifically harbour alternative NADP(H) dehydrogenases (AltDH) that face both the matrix and the intermembrane space, and the alternative oxidase (AOX) (Figure I.11). These enzymes are alternative respiratory routes, which do not produce energy, but allow viability when the enzymes of the main pathway are overworked by removing excess of reducing power in the mitochondria, which will balance the redox poise (Rasmusson et al., 2008, 2009; Schertl and Braun, 2014).

Photorespiration is a highly compartmentalised pathway occurring in plant cells due to the oxygenase activity of ribulose-1,5-bisphosphate carboxylase/oxygenase (RuBisCO; EC 4.1.1.30) that leads to the synthesis of a toxic compound, 2-phosphoglycolate (2PG) (Hodges et al., 2016). This pathway allows 2PG processing using chloroplastic, peroxisomal and mitochondrial enzymes. First, 2PG is converted into glycolate in the chloroplast that will be transported to the peroxisome to be oxidised in glyoxylate by the glycolate oxidase (EC 1.1.3.15, GOX), thereby generating H_2O_2. Next, glyoxylate is converted into glycine that will be exported to the mitochondria allowing reducing power regeneration during glyoxylate conversion to serine. Finally, serine is converted to glycerate then 3PG, thus re-joining the sugar-phosphate synthesis pathway (Figure I.11). Quantitatively, the contribution of peroxisomal volume to total cell volume is small: 1% for peroxisomes compared to 12% for chloroplasts

in leaves (Queval et al., 2011). Nonetheless, peroxisomes are predicted to be a major source of hydrogen peroxide in active photorespiratory cells.

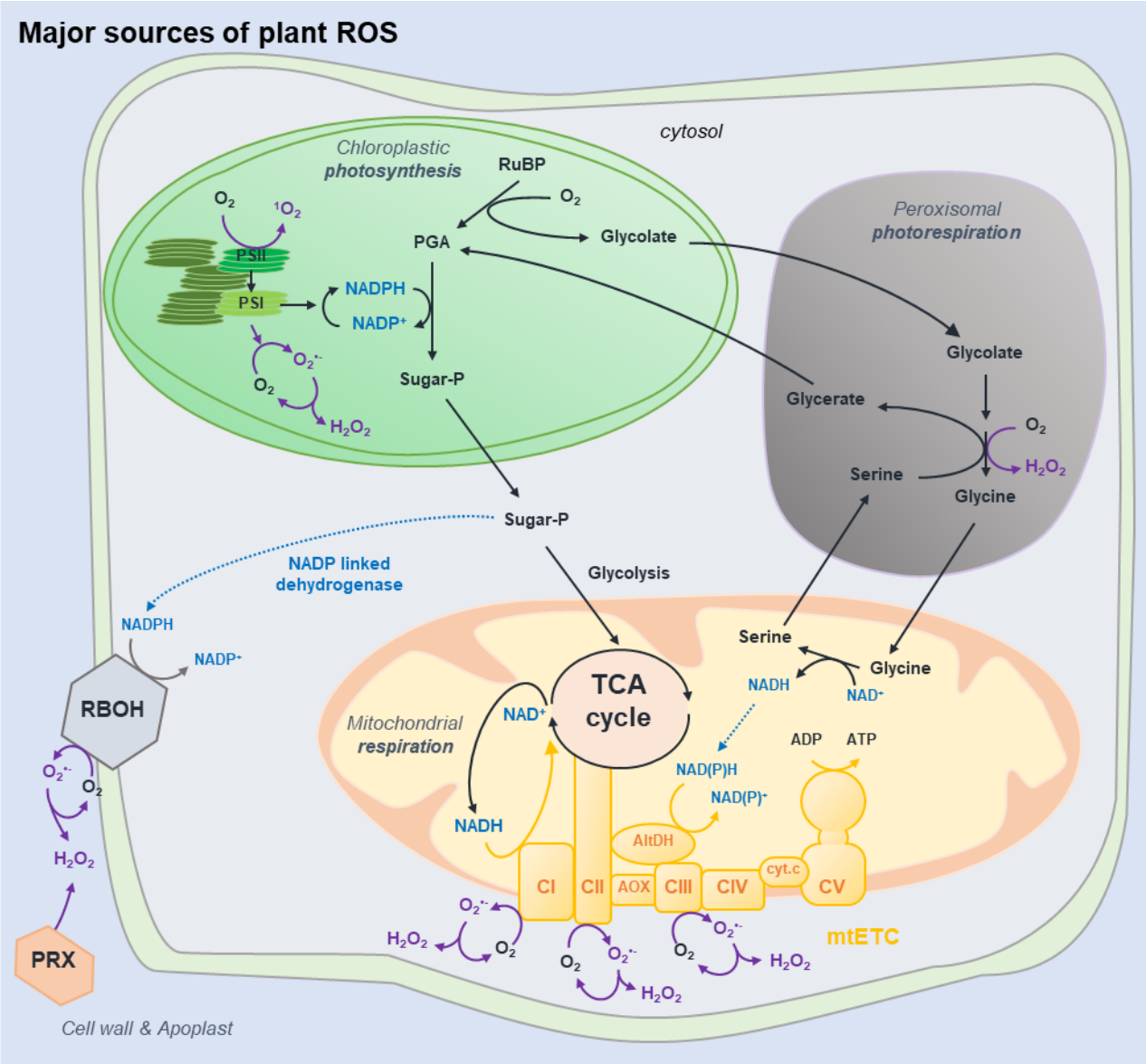

Figure I.11: Basics of ROS biology in plants.

mtETC, mitochondrial electron transfer chain; PRX, peroxidase; TCA, tricarboxylic acid; CI-V, complex I-V; AOX, alternative oxidase; AltDH, alternative dehydrogenase; cyt. c, cytochrome c; RuBP, ribulose 1,5Bisphosphate; PGA, phosphoglycerate; Sugar-P, sugar-phosphate; PS, photosystem. From (Decros et al., 2019a).

In addition, plants harbour several other ROS producing systems such as xanthine dehydrogenases (EC 1.17.1.4; XDH) or NADPH oxidases (EC; 1.6.3.1), which generate $O_2^{\bullet-}$ by single-electron reduction of oxygen. XDH are important enzymes involved in the hydroxylation of hypoxanthine to xanthine but can also form $O_2^{\bullet-}$ when molecular oxygen is used as the electron acceptor. While XDHs in mammals can be converted into xanthine oxidases (EC; 1.17.3.2) that produce both $O_2^{\bullet-}$ and H_2O_2, plant XDHs only form $O_2^{\bullet-}$, which will swiftly dismutate into H_2O_2 (Yesbergenova et al., 2005; Ma et al., 2016). The NADPH oxidases, also named Respiratory Burst Oxidase Homolog (RBOH), are well known key players in extracellular ROS production, especially in response to biotic and abiotic environmental challenges (Torres and Dangl, 2005; Suzuki et al., 2011). These plasma membrane-bound flavoproteins can oxidise NADPH to produce $O_2^{\bullet-}$ in the apoplast. Moreover, RBOHs appear active in several other organelles (*e.g.* mitochondria, vacuole, endoplasmic reticulum, nucleus) and may be regulated by calcium and several (de)phosphorylation reactions (Gilroy et al., 2014; Mittler, 2017; Chapman et al., 2019; Lee et al., 2020).

Furthermore, class III peroxidases (EC 1.11.1.7, PX) are heme-containing enzymes that produce $O_2^{\bullet-}$ and H_2O_2 at the apoplast (Bindschedler et al., 2006; Cosio and Dunand, 2009; O'Brien et al., 2012). Although H_2O_2 formation is enhanced at high pH in the presence of reductants (O'Brien et al., 2012), spontaneous dismutation might also occur. Remarkably, data from the literature highlight a substantial contribution of the apoplast in generating ROS in metabolically active leaves: > 90 nmoles.g^{-1} FW for the apoplast, *versus* 0.95, 0.04, 0.015 and 0.48 nmoles.g^{-1} FW for the chloroplast, mitochondrion, peroxisome and cytosol, respectively (Foyer and Noctor, 2016). This can also result from the redox status of each compartment since chloroplasts, mitochondria, peroxisomes and cytosol are more reduced, while the apoplast and the vacuole appear to be more oxidised (Foyer and Noctor, 2016).

Hence, by focusing on the metabolically active, highly reduced organelles, the proportion in ROS formation would be 1% for the peroxisomes, 3% for the mitochondria, 32% for the cytosol and 64% for the chloroplasts.

However, knowledge is still fragmentary on the contribution of each source of ROS for fruit tissues. Of course, due to low photosynthetic metabolism in fruit, one could predict different values, which further depends on the plant species that exhibit diverse biochemical pathways able to scavenge and process cellular ROS. Regardless, mitochondria, peroxisomes and the apoplast are assumed to be leaders in ROS production in flowers and fruits (Qin et al., 2009a, 2009b; Rogers and Munné-Bosch, 2016).

2. Dual effects of ROS: damages and signals

ROS were first identified as toxic by-products of aerobic metabolism, but decades of research on redox biology pointed to a dual role for ROS in plants where they both act as toxic by-products of aerobic metabolism, and powerful signals that modulate plant functions (Mittler et al., 2011; Mittler, 2017; Foyer, 2018).

The harmful effects of ROS are mainly the oxidation of DNA bases, proteins and the lipid peroxidation of polyunsaturated fatty acids (Figure I.12) (Apel and Hirt, 2004; Qin et al., 2009a; Nimse and Pal, 2015). In DNA, ROS can oxidise deoxyribose and nitrogenous bases leading to DNA breaks or changes of DNA bases, which in turn increases mutation rates, thus endangering cell viability. Moreover, ROS may inflict damages to protein structures inducing changes in the catalytic activity of enzymes and perturbations in the regulation of metabolic pathways. The effects of ROS on proteins can be several: cleavage of peptide bonds, oxidation of amino acids and aggregation between proteins. Briefly, cysteine (Cys) thiol radicals can be oxidised by H_2O_2 inducing a switch of thiols (-RSH) into disulfides (-RSSR-) or trisulfides and even into tetrasulfides (Noctor et al., 2011). These changes result in structural changes within target proteins and modifications of their function that can affect enzymatic properties, transcription, phosphorylation and other signalling processes. As the contrary of nucleotides, damaged proteins need to be processed by the proteasome to avoid undesired proteins interactions and perturbations of signalling network. Lastly, membrane phospholipids can be oxidised by ROS leading to lipid peroxidation and compromising membrane integrity, and thus, cell viability. Lipid peroxidation by ROS can be described in three sequential steps that are initiation, propagation and termination (Figure I.12). It starts with the initiation phase during which ROS oxidise the double carbon bond of polyunsaturated fatty acids forming a carbon-centred lipid radical that will be stabilised by molecular rearrangement of adjacent double carbon bonds.

Then, during the propagation phase, lipid radical will promptly react with oxygen to create a lipid peroxyl radical that detaches one hydrogen from another lipid and thus produces a new lipid radical and a lipid hydroperoxide. Finally, during the termination step, an antioxidant reduces the lipid peroxyl radical resulting in the production of nonradical products such as malondialdehyde (MDA), which is a powerful mutagenic product and a marker of oxidative stress. Nevertheless, all the damages caused by ROS can be grouped under the name “oxidative stress” which represents the perturbation of redox homeostasis in which the antioxidant capacity is no longer sufficient to prevent ROS from causing cellular damage.

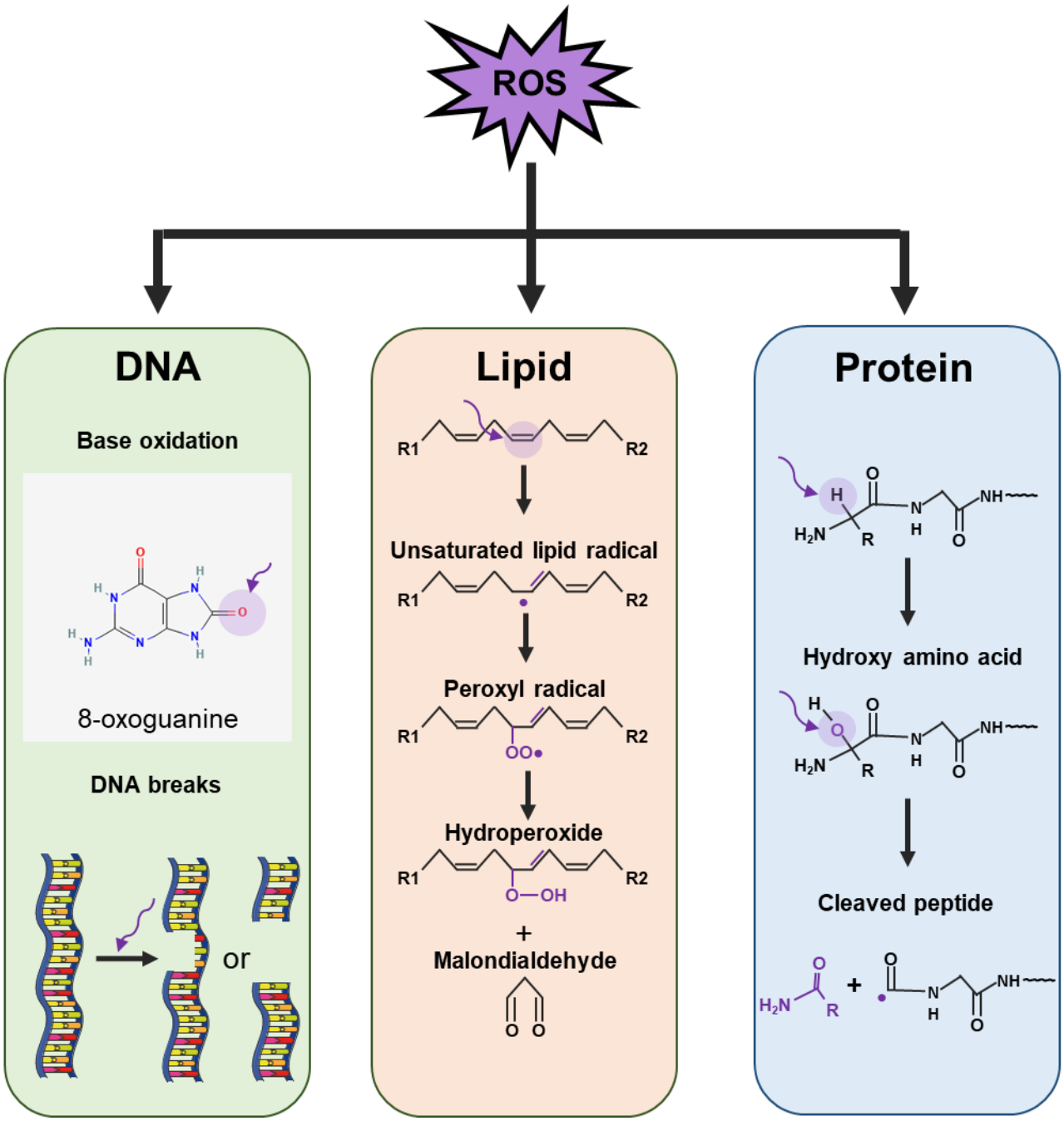

Figure I.12: Global view of ROS damages on DNA, lipids and proteins. Adapted from (Mittler et al., 2017)

On the other hand, ROS have been identified to participate in numerous biological processes by their signalling ability. For instance, cell death was first described as a result of the damaging effect of oxidative stress but is now considered as the result of a physiological pathway using ROS to trigger cell death signals (Berghe et al., 2014). Another example of ROS beneficial aspects is the induction of innate immune responses during biotic stress, where pathogen recognition by pathogen associated molecular patterns (PAMPs) triggers an oxidative burst producing ROS by phosphorylating NAPDH-dependent

RBOH allowing rapid and long-distance signalling (Lee et al., 2020). Furthermore, ROS-mediated redox signalling appears to be a crucial actor in stem cell research topic by regulating their differentiation, expansion and survival (Owusu-Ansah and Banerjee, 2009; Sart et al., 2015).

Hence, low levels of ROS in pluripotent stem cells (PSC), due to their low content in mitochondria, sustain the capacity of self-renewal and increase the retention of multipotency. Upon differentiation, mitochondrial synthesis is increased leading to a higher levels of ROS production, and thus changes in cellular redox state. The discrepancies in redox profiles of PSCs will define their differentiation pathways, in osteoblast or adipocyte lineage for example, by activating different transcriptional factors (Imhoff and Hansen, 2011). These are a few examples of the implication of ROS in plant physiology, which has been extensively reviewed over the past decades (Foyer and Noctor, 2016; Rogers and Munné-Bosch, 2016; Chaput et al., 2020; Lee et al., 2020).

It therefore appears that a physiological level of ROS is required for normal organism development and that ROS-mediated redox signalling (detailed below in part C) is involved in numerous crucial developmental steps and in response to the environment (Figure I.13).

II. Antioxidant metabolism and ROS scavenging systems

As scientists like to point out the sessile nature of plants life, they developed a myriad of antioxidant metabolites to handle the ROS processing during growth, which regulates the cellular redox balance. ROS produced in the plant cell can be scavenged, or more precisely *processed*, by highly efficient antioxidant systems. If not, ROS levels exceeding the requirement of metabolic processes would induce oxidative stress damaging cellular structures and functions (Muñoz and Munné-Bosch, 2018). Basically, antioxidants refer to all biomolecules, including metabolites, that can process ROS and/or reactive nitrogen species to delay or avoid cell damages and for signalling processes (Nimse and Pal, 2015). Antioxidants include metabolites with antioxidative properties that are found in every organelle, and which are profuse in diversity and quantity in plants, particularly in fruits (Muñoz and Munné-Bosch, 2018; Decros et al., 2019a). Besides metabolites, the antioxidant machinery is illustrated by a few major enzymes that are tightly linked to the pool of major redox buffers in order to process ROS rapidly (Figure I.13). These ROS-processing systems are key components of plant metabolism, and they could link to developmental processes or responses to environmental changes, as detailed further below.

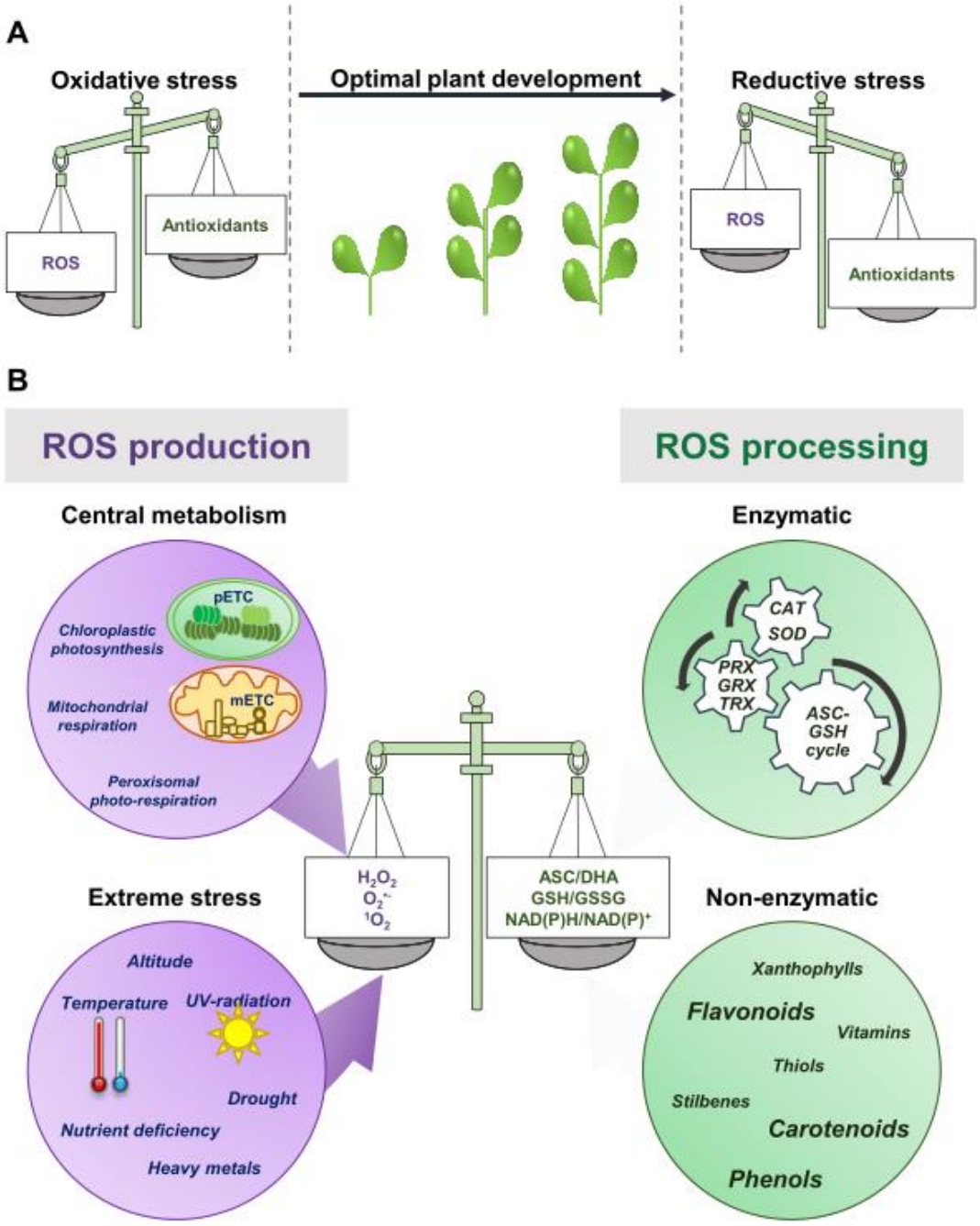

Figure I.13: Redox poise is pivotal to plant growth and acclimation. Harmonious plant growth requires a finely tuned redox homeostasis to avoid oxidative or reductive stress when the ROS/antioxidant balance is altered **(A)**. Plants produce ROS and other redox signals during growth and in response to environmental stimuli. Redox homeostasis relies on the balance between ROS production (left side) and processing (right side) **(B)**. ASC, ascorbate; CAT, catalase; DHA, dehydroascorbate; GRX, glutaredoxins; GSH, glutathione; GSSG, disulfide glutathione; mETC, mitochondrial electron transport chain; pETC, photosynthetic electron transport chain; PRX, peroxiredoxins; ROS, reactive oxygen species; SOD, superoxide dismutase; TRX, thioredoxins. From (Dussarat et al., 2021).

1. Diversity of plant antioxidant metabolites

Because of their complex oxidative metabolism (ROS production, described above), plants have developed a wide range of antioxidative metabolites as well as pathways to synthetise, catabolise and regenerate them. Plant antioxidant metabolites have been intensively studied because of their numerous benefits for human diets, particularly in fruit tissues, and even more in citrus and berry fruits, representing our main source of major antioxidants. Antioxidants can be distributed into several biochemical classes (Figure I.14), including phenolics, terpenoids, thiol-derivatives and vitamins, for which common metabolites and their antioxidative mechanisms are listed in Table I.1.

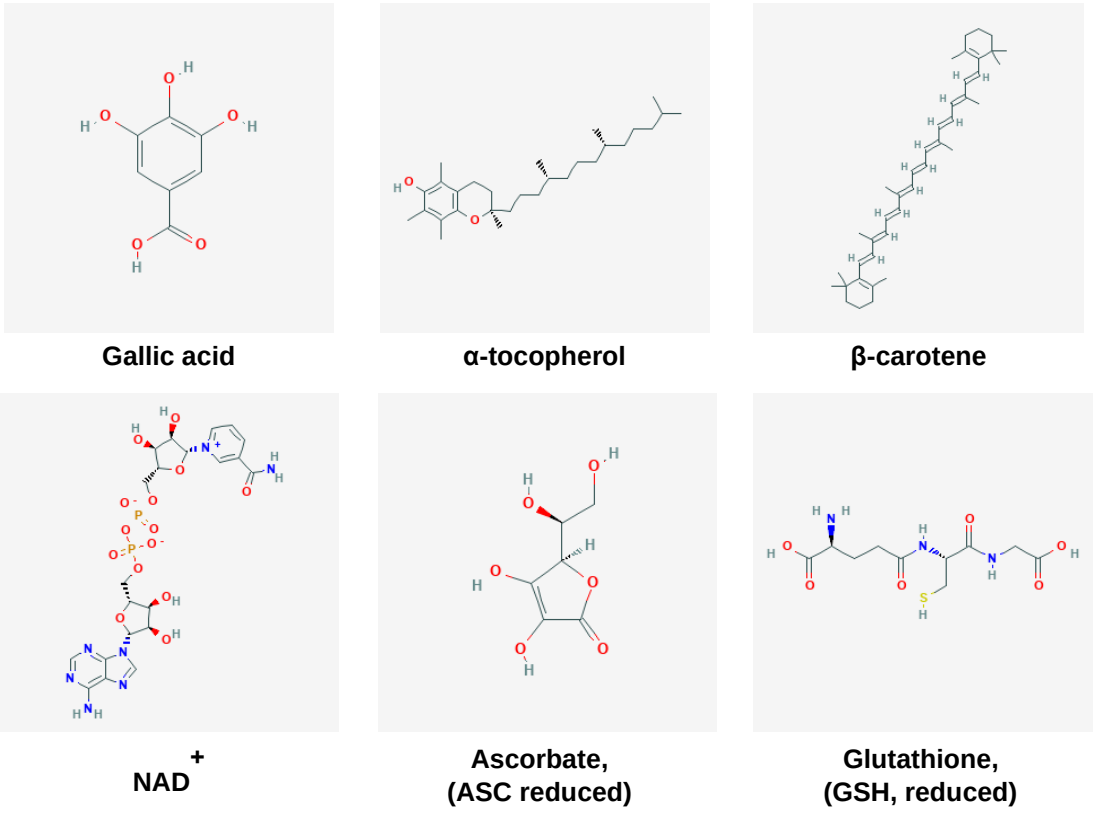

Figure I.14: Examples of fruit antioxidants. Chemical structures of several metabolites presenting antioxidative properties. The major redox buffer NAD, ASC and GSH are also presented. For further detail, please refer to Table I.1. (Images taken from PubChem)

Terpenoids, also known as isoprenoids for their core structure, can be divided into several classes based on their carbon skeleton (Graßmann, 2005). Carotenoids are the main group of terpenoids with more than 600 identified and characterised. They are pigments used for light harvesting, preventing photooxidation and increasing fruit attraction for seed dispersion (Young and Lowe, 2018). Here, I will focus on carotenoids among other terpenoids because they are widely studied concerning their antioxidant properties and biological effects in plants and mammals. While antioxidants are often shared by plant species, most plant families have developed their own range of specific antioxidant metabolites within their botanical taxa. Quite importantly, some major redox buffers shared between species, such

as ferredoxins, pyridine nucleotides, thioredoxins, glutathione (GSH) and ascorbate (ASC), can be distinguished as they play a fundamental role in the development of plants and their responses to the environment, thus in plant performance (Balmer et al., 2004; Geigenberger and Fernie, 2014; Geigenberger et al., 2017; Gakière et al., 2018a; Noctor et al., 2018).

Due to the wide diversity of fruit metabolites harbouring antioxidant activity, they can process ROS in many ways. Most antioxidants spontaneously react with ROS, although enzymes such as peroxidases and "redoxins" catalyse several reactions. Moreover, antioxidants remarkably participate in recycling pathways, such as the glutathione-ascorbate cycle, to maintain the redox state of the main redox buffers through the activity of specific enzymes. The importance of such systems for fruit biology is detailed further. However, a large number of studies have focused on plant antioxidants and demonstrated their numerous health benefits (Kelley et al., 2018; Pohl and Kong Thoo Lin, 2018). They are used as potential treatments for some chronic diseases, including diabetes, cardiovascular and neurodegenerative pathologies, as well as various types of cancer due to anti-inflammatory, anti-aging, anti-cancer effects on *in-vitro* cultivated cells and *in-vivo* studies (Cory et al., 2018; Kelley et al., 2018), and references therein). The main class of antioxidant metabolites found in plants and especially in fruits will be shortly described below.

a. Polyphenols

Among fruits antioxidants, phenolic compounds, or polyphenols, constitute a very diverse class of biochemicals (for updated details about their classification and fruit bioavailability see http://phenol-explorer.eu/compounds/classification). These specialised metabolites are composed of at least one aromatic cycle carrying hydroxyl groups such as gallic acid (Figure I.14). They exist as free forms or as conjugates with diverse acids, sugars and other molecules that are either hydrophilic or lipophilic. Phenolics can be subdivided into four main groups according to their core structure, namely, hydroxycinnamic acid derivatives, hydroxybenzoic acid derivatives, flavonoids and stilbenes, which mainly act through direct scavenging of ROS (Singh et al., 2017). For each category, common fruit polyphenols and their antioxidant activities are presented in Table I.1. Noteworthy, their total concentrations considerably vary between plant species. For instance, plum (sanhua), tomato and watermelon (red pulp) contain 495.12 ± 0.91, 30.74 ± 1.58 and 10.32 ± 1.43 mg of gallic acid equivalent for 100 g of fresh weight, respectively (Chen et al., 2014). Nowadays, phenolic compounds have been intensively studied for their various health benefits for human health, more particularly for their anti-inflammatory, anti-cancer and anti-diabetes properties (Gorzynik-Debicka et al., 2018; Olas, 2018).

b. Carotenoids

Carotenoids are a major family of hydrophilic and lipophilic plant antioxidants that are present in red/yellow-coloured fruits. These tetraterpenes are formed by the conjugation of two C20-units and harbour a polyene backbone composed of a series of C=C conjugated bonds, providing pigmenting and photoprotective properties through the scavenging of singlet oxygen and peroxyl radicals. Based on their functional group, they can be divided into carotenes composed of carbon and hydrogen atoms only (Figure I.14), and xanthophylls containing at least one oxygen atom (Graßmann, 2005; Young and Lowe, 2018). Based on the radical species, carotenoids employ different mechanisms of antioxidant action. Their distinguishing feature is the ability to process singlet oxygen both physically and chemically. In most cases, energy transfer physically processes singlet oxygen, and the excess of energy is dissipated as thermal energy to bring back carotenoids to their ground state. Subsequently, chemical quenching by carotenoids induce their breaking and the release of smaller molecules with various activities and signalling in cells (Graßmann, 2005; Edge and Truscott, 2018). Besides their interactions with radical species, carotenoids can also interact with other antioxidants, for instance, to regenerate α-tocopherol, or be regenerated by ascorbate. However, carotenoids can also exhibit pro-oxidant activity, for instance, by enhancing ascorbate oxidation depending on the oxygen concentration (Edge and Truscott, 2018). The major carotenoids present in fleshy coloured fruits are listed in Table I.1. For example, red and orange pigments such as lycopene and carotene are contained in tomato (7.8-18.1 and 0.1-1.2 mg.100 gFW^{-1}, respectively), in apricot (1.5-3.8 mg.100 gFW^{-1} of β-carotene) and in buffalo berry (1.82-3.6 g.100 gFW^{-1} of lycopene) (Sass-Kiss et al., 2005; Riedl et al., 2013; Martí et al., 2016). As a result of their capacity to process radical species and reduce other antioxidants, carotenoids are recognised as healthy compounds for their anti-inflammatory, anti-cancer and pro-vitamin A effects (Martí et al., 2016; Chaudhary et al., 2018).

c. Thiols

Thiols are organosulfur compounds characterised by the presence of a sulfhydryl group that is highly sensitive to oxidation leading to a perturbation of the cellular redox homeostasis. Two main groups of thiol components can be distinguished: the key thiol reduction enzymes, described below, and the crucial thiol metabolite, glutathione (GSH) (Figure I.14). GSH is a eukaryotic ubiquitous thiol, essential for the maintenance of cellular redox homeostasis. Several evidences indicate that GSH is part of the signalling cascade from ROS, controlling crucial metabolic steps for plant development (*i.e.*, cell cycle, stress tolerance and apoptosis), and in the control of blossom-end rot in tomato fruits for example (Mestre et al., 2012). The thiol group of GSH allows it to act as a free antioxidant, scavenging directly or enzymatically radical species or by regenerating other oxidised compounds such as ascorbate.

From a quantitative perspective, GSH is contained in mango at 1.3 mg.100 gFW^{-1} (≈ 4.2 µmol.100g.FW^{-1}) and in tomato from 19.5 to 46 mg.100 gFW^{-1} (≈ 60 to 150 µmol.100g.FW^{-1})

(Giovinazzo et al., 2004; Cervilla et al., 2007; Ding et al., 2007). Glutathione metabolism will be further detailed below in this chapiter.

d. Vitamins

The class of vitamins includes a large number of molecules, either lipophilic or hydrophilic, with antioxidant properties that are beneficial for human health. Among the liposoluble vitamins, tocochromanols represent the biggest category and refer to tocopherols and tocotrienols, also known as vitamin E in humans, which are lipophilic chain-breaking antioxidants in plants (Table I.1). The most studied form is α-tocopherol (Figure I.14), due to its high content in numerous fruits and well-studied effects on human health (Knecht et al., 2015). α-tocopherol is an essential macronutrient for human beings maintaining cell membrane integrity and limiting lipid peroxidation by scavenging free radicals with a higher affinity than β-carotene or polyunsaturated fatty acids. To process ROS, α-tocopherol loses a hydrogen atom and produces an α-tocopheroxyl radical that can be regenerated in tocopherol by ascorbate or go through additional reduction leading to the production of α-tocopherol quinones and hydroquinones, which are used as markers of oxidative stress *in-vivo*. Nevertheless, in conditions with low ascorbate concentrations, tocopherols switch to a pro-oxidant activity (Bowry et al., 1992). As an example, tomato and green olives contain 0.5-1.1 and 3.8 mg.100 gFW^{-1} of tocochromanols, respectively (Chun et al., 2006; Raiola et al., 2015). Several reports indicate the beneficial effects of tocochromanols for human health, such as for cancer, neurodegenerative diseases (*i.e.* Alzheimer), cardiovascular pathologies and other physiological disorders (Shahidi and de Camargo, 2016; Gugliandolo et al., 2017).

At the top of hydrosoluble vitamin sits ascorbic acid, or ascorbate (ASC), also known as vitamin C in humans, which is an essential water-soluble macronutrient for life because of its antioxidant properties (Nimse and Pal, 2015; Smirnoff, 2018). Briefly, ASC is a ubiquitous sugar-derivative organic acid with antioxidant properties that are essential in the human diet due to a loss of synthesis ability during evolution. The main sources of ASC in food come from plants and fruits, among which tomato constitutes the most important contribution in terms of consumption. For example, ASC is found in commercial cultivars of tomato from 10 to 15 mg.100 gFW^{-1}, in strawberries from 54 to 87 mg.100 gFW^{-1} and one of the highly concentrated fruit is the camu-camu, from 2.4 to 3 g.100 gFW^{-1} (Justi et al., 2000; Skupien and Oszmianski, 2004; Stevens et al., 2007). As for glutathione, ascorbate metabolism will be reviewed in the following section.

Table I.1: Examples of major antioxidant metabolites in fruits.

Biochemical class	Compound class	Antioxidative metabolite	Antioxidant activity	Effect on human health	Source example (per 100 g FW)	Key references
Polyphenols	Hydroxycinnamic aci	Caffeic acid	Scavenge ROS and peroxyl radicals Inhibit lipid peroxidation	Anti-inflammatory Preventive effects for diabete Cardiovascular protective effects	0.1 - 1.3 mg in tomato 0.4 - 35 µg in blueberries	L.Fu et al., 2011 Wolfe et al., 2008 Wang et al., 2017 Olas., 2018
		Ferulic acid			0.2 - 0.5 mg in tomato 26 - 185 µg in blueberries	Martí et al., 2016 Wang et al., 2017
		p-coumaric acid			0 - 0.6 mg in tomato 89 - 225 µg in blueberries 15 - 42 mg in strawberries	Skupien and Oszmianski., 2004 Martí et al., 2016
	Hydroxybenzoic acic	**Gallic acid**	Scavenge peroxyl radicals and ROS		2 - 9 mg in differents cultivars of blackberries	Wada and Ou., 2002 Wang et al., 2017
	Flavonoids	Anthocyanins	Scavenge free radicals Acylation of anthocyanins with phenolic acid increase the antioxidant activity Prevent lipid peroxidation	Neuroprotective effects Anti-cancer involved in treatment of cardiovascular diseases	154 - 1001 µg in blueberries of Cyanidin 25-40 mg in strawberries of total anthocyanins	Skupien and Oszmianski., 2004 Khoo et al., 2017 Wang et al., 2017
		Catechin	Prevent lipid peroxydation Scavenge NO and ROS	Regulate superoxide production Regulation of transcription factors involved in oxidative stress responses	180 - 338 µg in blueberies 6-19 mg in different cultivars of strawberries	Fraga et al., 2018 Wang et al., 2017 Skupien and Oszmianski., 2004
		Quercitin		Neuroprotective and cardioprotective effects Anti-cancer	0.7 - 4.4 mg in tomato 202 - 266 µg in blueberries	Chaudhary et al., 2018 Martí et al., 2016 Wang et al., 2017
	Stilbenes	Resveratrol	Scavenge ROS and peroxyl radicals Inhibit lipid peroxidation	Neuroprotective and cardioprotective effects	51 - 97 µg in blueberries	Wang et al., 2017 Cory et al., 2018
Carotenoids		Lycopene	Process singlet oxygen Trap peroxyl radicals Inhibit radical-induced lipid peroxidation Reduce ROS production by nonphotochemical quenching of chlorophyll fluorescence	Anti-inflammatory Pro-vitamin A activity, converted to retinoids after breaking (oculo protective effects) Enhance immune system Anti-proliferative and anti-carcinogenic	7.8 - 18.1 mg in tomato 1.82-3.6 g in different buffaloberry cultivars	Eldashan and Singab., 2018 Martí et al., 2016 Chaudhary et al., 2018 Murillo et al., 2010 Graßmann 2005 Riedl et al., 2013
		Zeaxanthin			200 µg in mandarins 7.92mg in South American sapote 6 mg in orange pepper 340 µg in tomato	Murillo et al., 2010
		β-carotene			0.1-1.2 mg in tomato 1.5-3.8 mg in apricot	Martí et al., 2016 Sass-Kiss et al., 2005
Thiols		**Glutathione**	Process ROS via enzymatic and non-enzymatic reactions ROS scavenging Maintain thiol equilibrium S-glutathionylation of Cys residues allowing regulation of central metabolism during oxidative stresses	Neuroprotective effects Involve in asthma prevention and treatment	1,3 mg in mango 210-298 µg in strawberries 16-19.5 mg in tomato	Ding et al., 2007 Fitzpatrick et al., 2012 Smeyne and Smeyne., 2014 Erkan et al., 2008 Martins et al., 2018 Noctor et al., 2018 Keutgen and Pawelzik 2007
Vitamins	Tocochromanols	**α-tocopherol (Vitamin E)**	Prevent lipid peroxidation by scavenging free radicals (donating hydrogens) using ascorbate to be regenerated Prevent the oxidation of carotenoids Essential macronutrient for human maintaining cell membrane integrity	Anti-anemia Neuroprotective effects	0.5 - 1,1 mg in tomato; 0.6-0.8 µg in MoneyMaker cultivar 1,6 - 3,2 mg in red sweet pepper 3.8 mg in green olives of total tocopherol + tocotrienols	A. Gugliandolo et al., 2017 Giovinazzo et al., 2004 Chaudhary et al., 2018 Amitava and Kimberley., 2014 Raiola et al., 2015 Chun et al., 2006
		Ascorbate (Vitamin C)	Process ROS via enzymatic and non-enzymatic reactions Allow the regeneration of tocopherols and carotenoids	Anti-scurvy Anti-inflammatory Anti-cancer	10-15 mg in commercial cultivars of tomato and until 70 mg in ancestral cultivars 54-87 mg in different cultivars of strawberries 2.4-3g in camu-camu	Chaudhary et al., 2018 Martí et al., 2018 Stevens et al., 2007 Skupien and Oszmianski., 2004 Justi et al., 2000

2. Major redox buffers

Ascorbate and glutathione are at the forefront of plant soluble antioxidants because they constitute the first ubiquitous layer of metabolic defence against oxidative damages in plant cells. Indeed, ROS react preferentially with ASC and GSH, in non-enzymatic and/or in enzymatic mechanisms that can induce redox signalling mechanisms thus participating in the monitoring of plant development. These major cellular redox buffers interact together in a *ménage-à-trois* to promptly process ROS, while maintaining their redox state in highly reduced condition, within the ascorbate-glutathione pathway (also known as Foyer-Asada-Halliwell) (Foyer and Halliwell, 1976; Asada, 1999; Foyer and Noctor, 2011) using reducing power from pyridine nucleotides (*i.e.* NADH and NADPH), which are other ubiquitous redox carriers (Pétriacq et al., 2016a; Gakière et al., 2018b). However, few limited data is available in fruit, some are listed in Table I.2. These three cellular redox buffers have been the most studied because of their ubiquity between kingdoms, the conservation of associated redox pathways during plant evolution and their implication in a plethora of fundamental developmental processes. The following sections will describe each of these main chemical redox couples and their role in plant performance.

Table I.2: Examples of ASC, GSH and NAD/P(H) sources in fruits. From (Decros et al., 2019a).

	Source example (per 100 g FW)	References
ASC	10 to 15 mg in tomato 54-87 mg in strawberries 2.4-3 g in camu-camu	Stevens et al., 2007 Skupien and Oszmianski., 2004 Justi et al., 2000
GSH	1.3 mg in mango 16-19.5 mg in tomato 210-298 µg in strawberries	Ding et al., 2007 Giovinazzo et al., 2005 Cervilla et al., 2007 Keutgen and Pawelzik 2007
NAD+	3.2 mg in red fruits and 2.2 mg at breaker stage in tomato 780 µg in orange 400 µg in grapefruit	Osorio et al., 2013a Centeno et al., 2011 Bruemmer., 1969
NADH	5.8 mg in red fruits and 4.9 mg at breaker stage in tomato 170 µg in orange 50 µg in grapefruit	Osorio et al., 2013a Centeno et al., 2011 Bruemmer., 1969
NADP+	0.5 mg in red fruits and 0.8 mg at breaker stage in tomato 89 µg in orange 69 µg in grapefruit	Osorio et al., 2013a Centeno et al., 2011 Bruemmer., 1969
NADPH	3.9 mg in red fruits and 3.2 mg at breaker stage in tomato 119 µg in orange 89 µg in grapefruit	Osorio et al., 2013a Centeno et al., 2011 Bruemmer., 1969

a. Ascorbate

i. History

In 1753, the first report of a molecule to treat scurvy, a disease from which many seafarers suffered at that time, was published. An English physician named James Lind published "A treatise of the scurvy". This work pioneered the link between the prevention of scurvy and the consumption of fruit, especially citrus fruits. It was not until the 20th century that this molecule was purified in 1928 by the Hungarian biochemist Albert Szent Györgyi (Nobel Prize for Medicine and Physiology in 1937) (Figure I.15) from the adrenal gland and then from lemon. The name ascorbic acid was not given until 1932, in reference to its anti-scurvy effects. Like most antioxidants, this molecule was first studied from a medical perspective in mammals but its precise role in plant development and the regulation of its metabolism (*i.e.* synthesis, degradation and transport) remain to be deciphered.

Figure I.15: Albert Sznet Györgyi (1893-1986). Nobel price of medicine and physiology for the discovery of ascorbate and flavonoids.

ii. Structure

As previously mentioned, ASC is a hydrosoluble organic acid derived from glucose. It is made up of 6 carbon, 6 oxygen and 8 hydrogen atoms ($C_6H_8O_6$) and has 3 different oxidation levels. It is found in reduced form (L-ascorbic acid), in semi-reduced or mono-oxidised form (MonoDeHydroAscorbate; MDHA) and in oxidised form (DeHydroAscorbate; DHA) (Figure I.16). The sum of these three forms constitutes the total pool of vitamin C, which can be more or less oxidised depending on the redox status of the cell. Nevertheless, only the reduced form possesses an antioxidant activity thanks to its capacity to release a proton from the hydroxyl group of carbon 3.

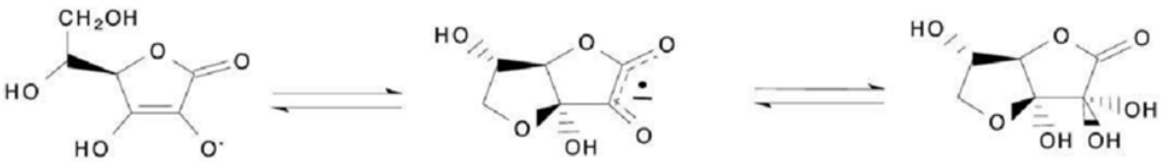

Figure I.16: Reduced and oxidized forms of ascorbate. From (Potters et al., 2002)

iii. Localisation

Ascorbate shows a great disparity in concentration between plants, for example, some exotic fruits like camu-camu or goji berry have extremely high ascorbate levels (2.4-3g and about 2.5g. 100 gFW^{-1}, respectively). Moreover, there is also great diversity between different species of the same genus. For instance, tomato has a high natural variability that has been reduced during domestication. Indeed, wild species (*Solanum pennelli*) have up to five times more ascorbate than agronomic species *(Solanum lycopersicum*) (Gest et al., 2013).

On another scale, ascorbate is heterogeneously distributed in the different organs of the plant but also between the different tissues in an organ and then in the subcellular compartments. Source organs (*i.e.* leaves) have a stronger capacity to synthetise ascorbate than sink organs (*i.e.* fruits, roots, meristem, etc.). Indeed, a substrate supply increases synthesis by 3 to 7 times in *Arabidopsis* leaves while it does not affect flowers and siliques (Franceschi and Tarlyn, 2002). Furthermore, the tomato fruit displays a gradient of ascorbate from the outside to the inside, in other words, the pericarp possesses a higher ascorbate content than the gel and seeds. Finally, it was shown that ascorbate is distributed evenly between the subcellular compartments. In a photosynthetically active *Arabidopsis* leaf cell, the peroxisome and cytosol show the highest concentrations (22.8 and 21.7 mM, respectively), the nucleus, chloroplasts and mitochondria also show ascorbate contents above 10 mM (16.3, 10.8 and 10.4, respectively) while the vacuole shows lower contents (2.3 mM) (Figure I.17) (Gest et al., 2013).

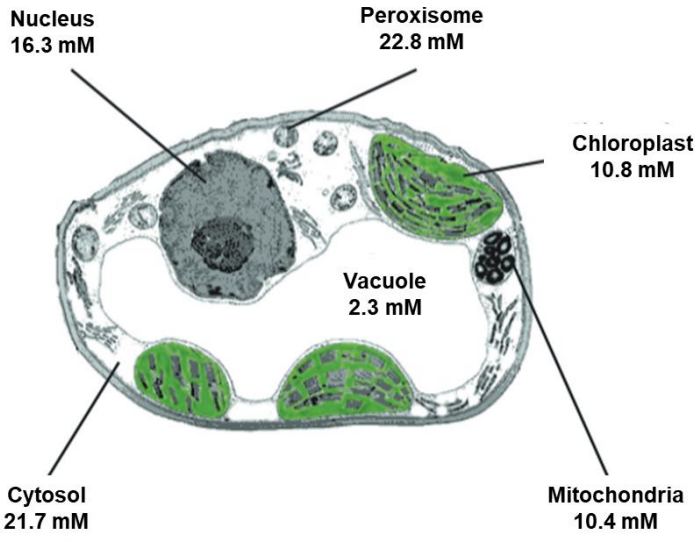

Figure I.17: Subcellular repartition of ascorbate in a photosynthetically active leaf cell of *Arabidopsis thaliana*. From (Gest et al. 2012)

iv. Synthesis

In 1954, the ascorbate biosynthetic pathway in plants was partially described for the first time, based on the pathway identified in animals. It was then in 1998 that the study of *Arabidopsis* mutants led to the identification of the main biosynthetic pathways of ascorbate in plants, namely the D-mannose/L-galactose pathway (Wheeler et al., 1998). Following, alternative ascorbate synthesis pathways have been identified in plants, all ending in the formation of L-gulono-1,4-lactone or L-galactono-1,4-lactone as the final substrate for ascorbate synthesis (Figure I.18) (Bulley et al., 2009).

Main ascorbate biosynthesis pathway: the D-mannose/L-galactose pathway

The main ascorbate biosynthetic pathway called the L-galactose or Smirnoff-Wheeler pathway was first fully identified in *Arabidopsis* in 2006 (Ishikawa et al., 2006). It is a mainly cytosolic pathway where only the last step, catalysed by the L-galactono-1,4-lactone (GLDH), is mitochondrial. This pathway involves 10 steps starting from D-glucose, coming from UDP-D-glucose, itself derived from starch as precursor. The six first steps are also common to cell wall precursors synthesis pathway (*i.e.* GDP-D-mannose and GDP-L-galactose) whereas the 4 following steps are specific to the ascorbate synthesis pathway (Figure I.18).

It starts from the hexose phosphate pool with D-glucose-6-phosphate (G6P). Then, G6P is sequentially converted into D-fructose-6-phosphate (F6P), D-mannose-6-phosphate (M6P), D-mannose-1-phosphate (M1P) by phosphoglucose isomerase (PGI), phosphomannose isomerase (PMI) and phosphomannomutase (PMM). Following, D-M1P is transformed into GDP-D-mannose by GDP-D-mannose pyrophosphorylase (GMP and then be epimerized by GDP-D-mannose epimerase (GME) into GDP-L-galactose. Thereafter, GDP-L-galactose will be transformed by GDP-L-galactose phosphorylase (GGP) leading to galactose-1-phosphate (Gal1P) synthesis. Next, Gal1P is dephosphorylated by L-galactose-1-phosphate phosphatase to produce L-galactose (Gal) which will be oxidised by the L-galactose dehydrogenase (LGalDH) into L-galactono-1,4-lactone. Finally, the l-galactono-1,4-lactone will be exported in the mitochondria to be oxidised by the GLDH to produce L-ascorbic acid at the external face of the internal mitochondrial membrane. Several evidences support that GGP, also known as VTC2 in *Arabidopsis*, can be considered as the most controlling enzyme of the ascorbate synthesis pathway (Laing et al., 2007, 2017; Fenech et al., 2021). However, depending on the species, GME and GPP enzymes can also have significant regulatory effects on ascorbate synthesis such as in tomato (Stevens et al., 2007; Decros et al., 2019a).

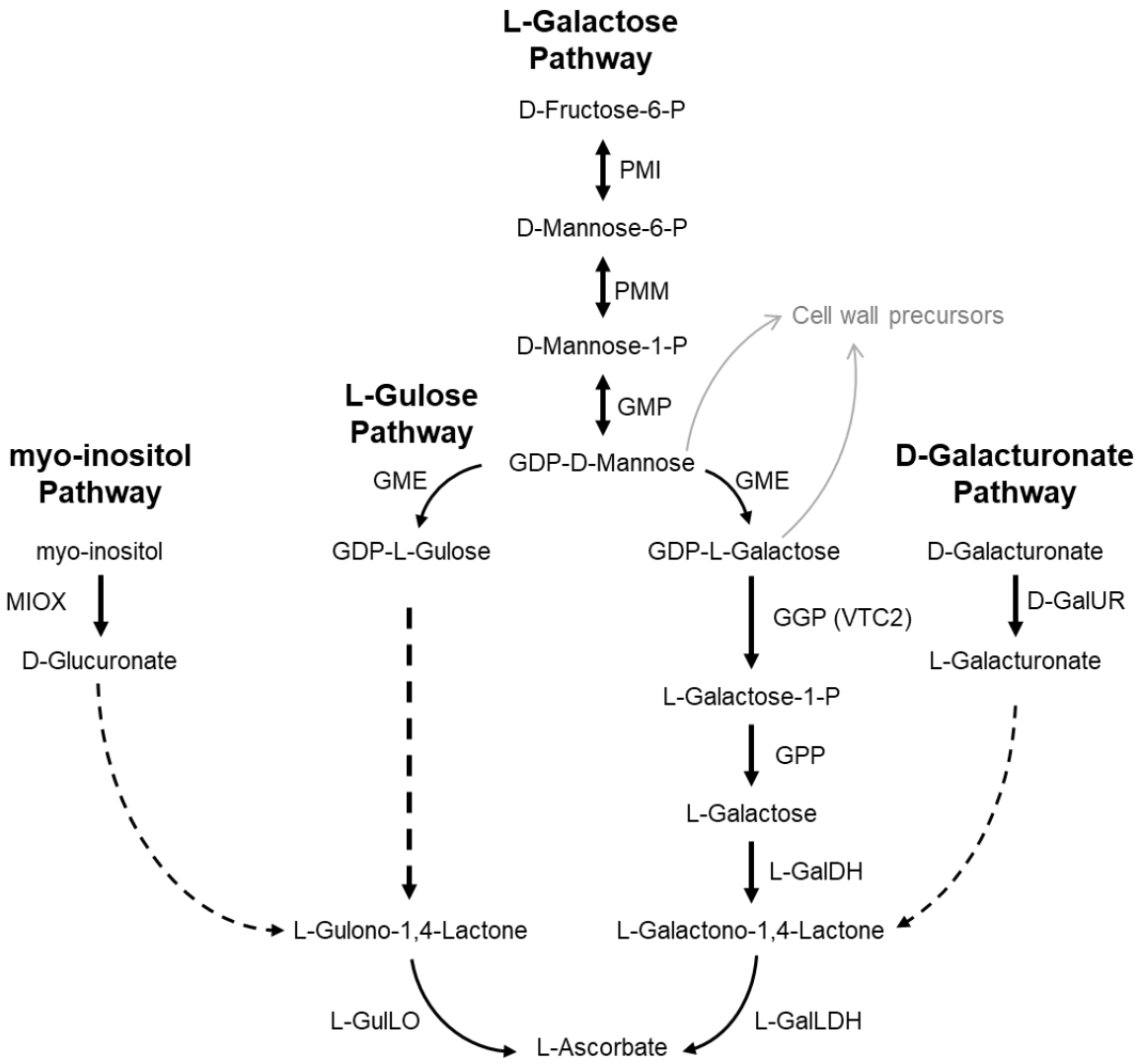

Figure I.18: The four proposed ascorbic acid biosynthetic pathways in plants. Dashed arrows indicate multiple and/or unknown biosynthetic steps. Name in brackets indicate the homolog genes in *Arabidopsis.* GGP: GDP-L-galactose phosphorylase, GME: GDP-D-mannose-3',5'-epimerase, GMP: GDP-D-mannose pyrophosphorylase, GPP: L-galactose-1-P phosphatase, L-GalDH: L-galactose dehydrogenase, L-GalLDH: L-galactono-1,4-lactone dehydrogenase, PMI: phosphomannose isomerase, PMM: phosphomannose mutase. Adapted from (Bulley et al., 2009)

Myo-inositol pathway

Myo-inositol pathway is the main biosynthetic pathway of ascorbate in animals, the possibility that an animal biosynthetic pathway is present in plants has never been ruled out. Overexpression in lettuce and tobacco of the gene coding for rat L-gulono-1,4-lactone oxidase induces an approximately sevenfold increase in ascorbate content (Jain and Nessler, 2000). In addition, ectopic expression of this gene in leaves of *Arabidopsis* mutants containing lower levels of ASC (*vtc1*), restores ascorbate levels (Radzio et al., 2003). In animals the substrate used for this enzyme is L-gulono-1,4-lactone, interestingly the *Arabidopsis vtc1* mutant produces very little quantity of this intermediate. In plants, the myo-inositol is an osmolyte accumulated under stress conditions, which is converted to D-glucuronic acid by myo-inositol oxygenase (Brown et al., 2006; Zhu et al., 2014). Thus, under certain conditions, these data suggest the presence of an alternative pathway that can compensate for the L-galactose pathway.

D-galacturonate pathway

D-galacturonate pathway is an analogous pathway to the biosynthetic pathway characterised in animals, which proposes the conversion of D-Gal by a carbon skeleton inversion mechanism (Isherwood et al., 1954). It was shown that galacturonic acid methyl ester could be directly converted to ascorbate by bypassing reactions involving the hexose phosphate pathway. Later, the gene coding for an NADPH-dependent D-galacturonate reductase able to catalyse this reaction was then identified in strawberry, thus demonstrating the existence of this pathway in plants (Agius et al., 2003; Badejo et al., 2012; Wheeler et al., 2015). The substrate of this pathway, the D-galacturonate is an abundant component of the cell wall and accumulates during the senescence and ripening processes of fruits.

Furthermore, the activity of two enzymes specifically associated with this pathway, D-galacturonate reductase and aldonolactonase, has been detected in insoluble fractions of red fruits (Carrari, 2006). Unfortunately, little is currently known about these enzymes and this pathway is not fully characterised in plants yet. Nevertheless, this pathway is assumed to act in ascorbate synthesis, especially during fruit development.

L-gulose pathway

During the L-galactose pathway, GDP-D-mannose is epimerised by GME producing GDP-L-galactose but also GDP-L-gulose. The following reactions have not been identified in plants but there are some reports about the characterisation of L-gulonic acid as an intermediate and L-gulono-1,4-lactone dehydrogenase activity (Wagner et al., 2003; Wolucka and Van Montagu, 2003). Besides, it has been shown that ascorbate levels display temporal variations during the circadian clock in leaves. Light regulation of main biosynthetic pathway enzymes such as GGP, GPP and GMP are upregulated during light exposure (Smirnoff and Wheeler, 2000; Massot et al., 2013). However, this effect is more pronounced in leaf tissue than in fruit (Massot et al., 2013).

It is worth remembering that the ascorbate biosynthesis pathway in plants is still a recent discovery (about 30 years), and that ASC displays numerous synthesis branches which show great variability between species and organs. Most of the existing data come from the study of model plants, mainly *Arabidopsis*, suggesting that many regulatory mechanisms and/or analogous synthetic pathways remain to be elucidated.

v. Recycling

One of the main roles of ascorbate refers to its antioxidant nature due to its ability to interact with ROS enzymatically and non-enzymatically. As described above, ascorbate has two different oxidation states, MDHA and DHA, both of which can be recycled into ascorbate. Firstly, MDHA can spontaneously react with another molecule of MDHA to produce DHA and reduced ascorbate. Secondly, MDHA can be recycled enzymatically by monodehydroascorbate reductase (MDHAR) through the reduction of NADH or NADPH. Finally, DHA can also be reduced to ascorbate by the action of dehydroascorbate reductase (DHAR) and the supply of glutathione. These two ascorbate recycling enzymes are involved within the ascorbate-glutathione cycle and in many stress responses by monitoring the redox state of ascorbate in the cell thus allowing signalling processes. In conclusion, the recycling of ascorbate requires a supply of reducing power, mainly via glutathione and pyridine nucleotides. It is a crucial activity to guarantee its antioxidant functions and thus allows the maintenance of the redox balance under optimal conditions.

vi. Degradation

Among the three mechanisms controlling the ascorbate pool in cells (*i.e.* synthesis, recycling and catabolism), *in-vivo* degradation is the one for which the least amount of research has been done. ascorbate catabolism in plants is species-dependent and starts from dehydroascorbate resulting mostly in the formation of oxalate and L-threonate (Green and Fry, 2005; Melino et al., 2009). These products can be further transformed such as threonate that turns into tartrate and participate in the quality of grape; however, it appears that ascorbate degradation has a little influence on the tartrate pool in grape (Melino et al., 2009). Ascorbate degradation takes place in the apoplast and involves enzymatic and non-enzymatic reactions (Green and Fry, 2005). The degradation of DHA can take place in different ways: (i) spontaneous oxidation in the presence of radicals leading to the formation of oxalyl-threonate, or (ii) spontaneous delactonation to 2,3-diketogulonate (DGK). After a series of reactions, these two different pathways come together to produce threonate (Truffault et al., 2017).

Furthermore, ascorbate degradation products can have some physiological roles in plants cells. Oxalate is a dicarboxylate found in vacuoles together with salts including potassium, sodium, magnesium or calcium. Calcium oxalate crystals are found in a wide diversity of animals and plants and are partially responsible for the regulation of the free calcium pool of cells (Franceschi and Nakata, 2005). Besides, calcium oxalate crystals may also serve as defence responses against herbivores. As for ascorbate synthesis, much remains to be elucidated about the mechanisms of ascorbate degradation and their regulations.

vii. Transport

Ascorbate is a small hydrophilic molecule, the last catalytic step is located in the intermembrane space of the mitochondria, and is present in all the different subcellular compartments as well as heterogeneously distributed between all the different plant organs. In addition, ascorbate is a negatively-charged metabolite at physiological pH, thus preventing its simple diffusion through lipidic membranes (Horemans et al., 2000; Foyer, 2015). However, DHA is neutral and thus easily passes through membranes. Hence, this suggests a controlled transport of this metabolite, with specific transporters for reduced ascorbate, at intracellular and at systemic levels.

Intracellular ascorbate transport

Whilst ascorbate intracellular transport received much attention in animals (Liang et al., 2001; Smirnoff, 2018), due to its health benefits, it remains mainly unknown in plants. Recently in *Arabidopsis*, a protein from the family of phosphate transporter has been identified in the chloroplastic membrane as a reduced ascorbate transporter (Miyaji et al., 2015). Concerning its oxidised form, a study on isolated mitochondria from tobacco shows a co-inhibition of glucose and DHA transports suggesting a potential role of glucose transporter in the import of DHA within cells, which is congruent with known mechanisms in animals (Szarka et al., 2004, 2013).

Systemic ascorbate transport

All plants organs can synthetise their own ascorbate, but source organs display a higher content than sink organs (*e.g.* 6 and 4 µmol.gFW^{-1} in leaves and fruits, respectively) (Mounet-Gilbert et al., 2016). Ascorbate has been localised in vascular cells suggesting that it can be transported through vascular organs to sink tissues to complement their synthesis capacity. However, it is still impossible to distinguish the proportion of ascorbate transport and synthesis involved in the total ascorbate pool of fruits.

viii. Role

Ascorbate is an essential metabolite for plant life due to its numerous functions in various developmental processes and in responses to environmental stimuli. Beyond these redox functions, the study of mutants affected in its synthesis has identified its role in the regulation of cell division and elongation. It also participates in seed germination, root development, flowering and embryogenesis (Ortiz-Espín et al., 2017). As such, ascorbate is a central metabolite for plant performance (Figure I.19).

During development

Apart from its antioxidant properties, ascorbate serves also as a cofactor of oxygenase enzymes by reacting with their copper or iron catalytic centre. Moreover, ascorbate participates in the regulation of plant development through its involvement in the biosynthetic pathways of several phytohormones, such as gibberellins (GA), auxins, ethylene (ET) and abscisic acid (ABA) (Davey et al., 2000). Meanwhile, the oxidation ratio or redox state (*i.e.* DHA/total ascorbate) is known as a significant marker of oxidative signalling. Indeed, the redox activity of ASC relies on both absolute and relative content of oxidised and reduced forms. It is assumed that under physiological conditions ASC redox state oscillates between 0.8 and 1 indicating that ascorbate is maintained mainly reduced, thus allowing normal photosynthesis activity (Baldet et al., 2013; Decros et al., 2019a). However, the ASC redox state can display discrepancies in response to numerous developmental events and in response to environmental stimuli as detailed below.

Cell division

The redox state of ascorbate, often expressed as the DHA/ total ASC ratio (*e.g.* typically 0.8 ± 0.1 in physiological conditions), plays an important role in cell cycle regulation by affecting the transition from the cell growth and replication preparation phase (G1 phase) to the DNA replication phase (S phase) (Potters et al., 2002). Indeed, several studies have shown that an increase in ascorbate induces an increase in cell division (Davey et al., 1999). Moreover, root cells show a high ascorbate oxidase (AO) activity concomitant with many cells blocked in the G1 phase, but the addition of exogenous ascorbate allows a reactivation of the cell cycle (Liso et al., 1988).

Although both ascorbate and other redox buffers such as GSH act in the cell cycle, they appear to perform their functions independently because changes in glutathione did not affect the ascorbate pool and did not inhibit the effects of DHA on cell division (Potters et al., 2010). This suggests that the recycling of DHA may occur independently from DHAR and that these two antioxidants have distinct functions in controlling the cell cycle.

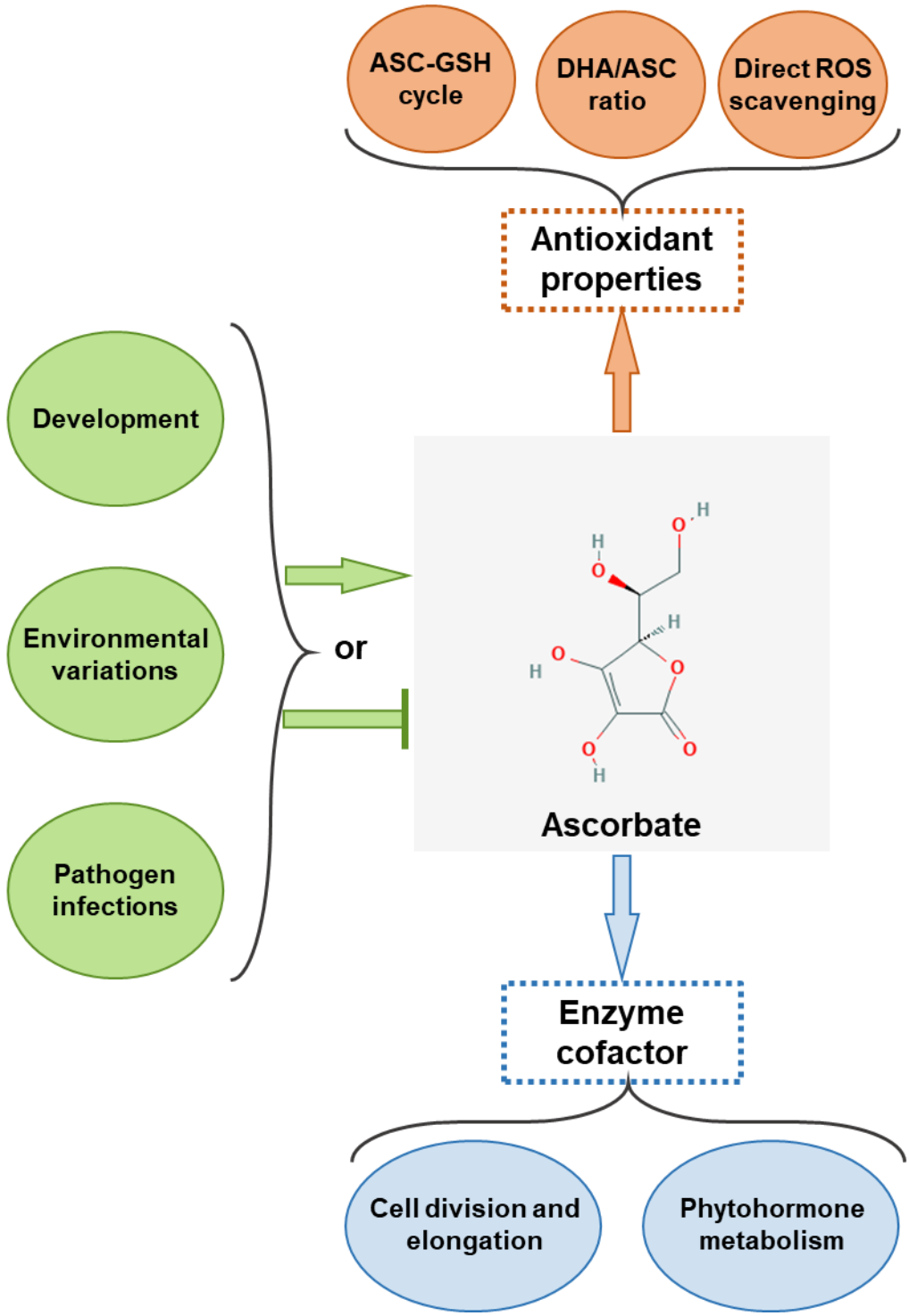

Figure I.19: Main roles of ascorbate in plants. Ascorbate is not only an antioxidant metabolite (orange) but also participates in fundamental biological processes acting as an enzyme cofactor (blue).

Cell expansion

Ascorbate synthesis is intimately linked with parietal sugar synthesis suggesting a strong link between wall synthesis and ascorbate metabolism. Furthermore, ascorbate also specifically influences cell expansion, notably through the stimulation of ascorbate oxidase activity which causes an increase in oxidised ascorbate thus stimulating cell elongation without affecting cell division (Pignocchi et al., 2003; de Pinto, 2004). Regulation of the redox state of ascorbate in the apoplast is one of the mechanisms proposed to explain how ascorbate promotes cell expansion and elongation. An increase in AO concomitant with higher levels of MDHA and DHA are detected in rapidly elongating tissues in cotton plants (Li et al., 2017a). MDHA serves as an electron acceptor in transmembrane electron transport, where cytochrome b transports electrons from NADH across the plasma membrane, inducing reduction of MDHA into ASC. The intensification of this process leads to hyperpolarisation of the plasma membrane, then followed by the activation of the plasma membrane H^+-ATPase. Thereby, this terminates by an acidification of the apoplast which favours the relaxation of the cell wall (Gonzalez-Reyes et al., 1995). Meanwhile, the NADH oxidation increases acidification in the cytoplasm, activating the vacuolar H^+-ATPase, thus triggering cell expansion (Horemans et al., 2000).

Seed germination and embryogenesis

The development cycle of a seed is composed of three phases: development, maturation and germination. Water imbibition of the seed reactivates the metabolism and growth of seminal tissues involving an increase in ROS and antioxidants including ASC, as well as redox proteins such as thioredoxin (Trx) or peroxiredoxin (Prx) (De Gara et al., 1997; Ortiz-Espín et al., 2017) necessary to balance the redox poise. An increase in ascorbate synthesis activity by GLDH together with a reduction in APX activity induces an increase in ASC content in the early germination stages (De Gara et al., 1997; Tommasi et al., 1999, 2001). Therefore, the higher levels of ASC seem to be due to *de novo* synthesis rather than recycling (Tommasi et al., 2001). Furthermore, seed germination is governed by an appropriate ABA/GA ratio and, during this process, ABA levels decrease in favour of GA which increases germination up to the seedling stage (Kucera et al., 2005; Finkelstein et al., 2008). The application of ABA to soaked seeds causes a decrease in ROS that leads to an inhibition of ASC production and repression of GA biosynthesis. In addition, GA biosynthesis was inhibited by lycorine, an inhibitor of ASC biosynthesis, and by the reduction of ROS levels.

Furthermore, the application of exogenous ASC can partially rescue seed germination after ABA treatment (Ye et al., 2012). These studies suggest that ASC participates in the regulation of the ABA/GA ratio during seed germination. In short, all these evidence support the role of ASC as an inducer of seed germination via a complex metabolic network integrated by ROS, hormones, and redox actors that regulate the development of the process.

Embryogenesis in higher plants leads to the formation of mature dry seeds and consists of three phases, i) morphogenesis, where the polar axis of the plant is defined (West and Harada, 1993), ii) embryo maturation, where storage reserves are accumulated and finally, iii) desiccation, during which the embryo dries out and seed formation ends. During morphogenesis, a reduced state of ASC promotes transverse cell division, while an increase in DHA causes longitudinal division (Chen and Gallie, 2012) suggesting a regulatory role for ASC in the establishment of polarity and formation of twins. A decline in reduced ASC continues until the end of seed maturation, resulting in near-total oxidation. These results agree with the general oxidative status observed in dry seeds. Under this condition, a steady metabolic state and long-term storage can easily be maintained (Tommasi et al., 2001). Moreover, during the embryogenesis of white spruce (*Picea glauca*), ASC metabolism displays an interesting dynamic (Stasolla and Yeung, 2007). Indeed, during the first days of germination, embryos accumulate high levels of ASC, mainly in their reduced state, and show a decrease in ASC degradation through APX activity. In addition, inhibition of ascorbate synthesis by lycorine resulted in a decrease in DNA synthesis, thus slowing down embryogenesis. Therefore, an increase in the ASC pool and a higher ASC/DHA ratio towards the reduced state are necessary for the progression of cell divisions in developing embryos (Becker et al., 2014).

On the other hand, the stimulatory role of ASC during meristem formation in apical shoots involves the inactivation of peroxidase-dependent cell wall stiffening. An increase in ASC content decreases the activities of ferulic acid and guaiacol peroxidases allowing cell division and growth, while their activities increase in lycorine-treated embryos, resulting in meristem abortion (Stasolla and Yeung, 2007; Becker et al., 2014). Another example is the lack of apical dominance and early formation of auxiliary buds in tomato where ASC synthesis is suppressed (Zhang, 2013). All these experiments demonstrate that the antioxidant pool and redox state of ASC is very important in the development of meristem.

Flowering and pollen fertility

Flowering time is crucial for plant reproduction, its initiation under unfavourable conditions can lead to aborted fruit development and thus to a reduction of the agronomic performance of plants. Therefore, plants finely control their flowering in response to different environmental cues. Indeed, light has a strong influence (photoperiod, light quality, light intensity) in the transition from vegetative to reproductive state (Imaizumi and Kay, 2006; Johansson and Staiger, 2015; Song et al., 2015). Other environmental factors such as temperature, water availability (Kenney et al., 2014), CO_2 concentration (Jagadish et al., 2016) and nutrient levels (Levy and Dean, 1998) are equally important. Depending on the conditions, ASC can act as a repressor or activator of flowering, for example, suppression of ASC oxidase gene expression induces delayed flowering (Yamamoto et al., 2005), while exogenous addition

of ASC or its precursor delays growth and flowering of wild-type *Arabidopsis* plants grown under long-day conditions (Attolico and De Tullio, 2006) but increases growth and induces early flowering under short-day conditions (Figure I.20) (Barth, 2006). In contrast, ASC-deficient *Arabidopsis vtc* mutants showed early flowering whereas the addition of exogenous ASC delayed flowering (Conklin and Barth, 2004; Kotchoni et al., 2009) independently of the photoperiod. Therefore, all these experiments show that ascorbate is controlling the timing of flowering, acting as a repressor or activator, depending on the environment. Moreover, the transition of a plant from the vegetative to the reproductive stage increases antioxidant and ROS levels, suggesting that plants must undergo perturbation of redox balance during the flowering process (Shen et al., 2009). Gene expression studies reinforce the link between ascorbate and flowering by showing that the expression of flowering-related genes such as LEAFY, a key transcription factor in flowering induction is affected by ASC (Attolico and De Tullio, 2006). In addition, transcriptomic analysis of *vtc* mutants showed up-regulation of genes related to flowering, the circadian clock and photoperiod (Kotchoni et al., 2009; Song et al., 2015).

On the other hand, flowering is an inherently hormone-driven process, including GA, SA and ABA (Barth, 2006). It has been shown that the application of GA or SA induces early flowering, while the application of ABA represses it (Figure I.20). As mentioned above, ascorbate is a key cofactor in hormone biosynthesis, so one would expect the influence of this antioxidant in flowering, which (i) is consistent with the analysis of *vtc* mutants, and (ii) show high levels of ABA (Pastori et al., 2003) and SA (Conklin and Barth, 2004) associated with low levels of GA (Foyer and Noctor, 2011), the whole resulting in delayed flowering. Furthermore, it has recently been shown that an increase in ascorbate synthesis induces a loss of pollen viability in tomato flowers (Deslous et al., 2021) leading to inhibition of fertilisation and thus to flower abortion and yield loss. Furthermore, this study shows that ascorbate content is related to flower morphogenesis consistent with the involvement of ASC in embryogenesis processes.

Overall, there is considerable evidence for the involvement of ASC in flowering: the early or delayed phenotype observed in ASC-overexpressed and ASC-deficient mutants, respectively, the regulation of ASC-dependent flowering-related genes and changes in phytohormone levels (Pastori et al., 2003; Foyer and Noctor, 2011; Foyer et al., 2012). Ascorbate seems to have more of a role here as a hormone synthesis factor than as an antioxidant, even though the overall redox balance is also involved in the flowering process.

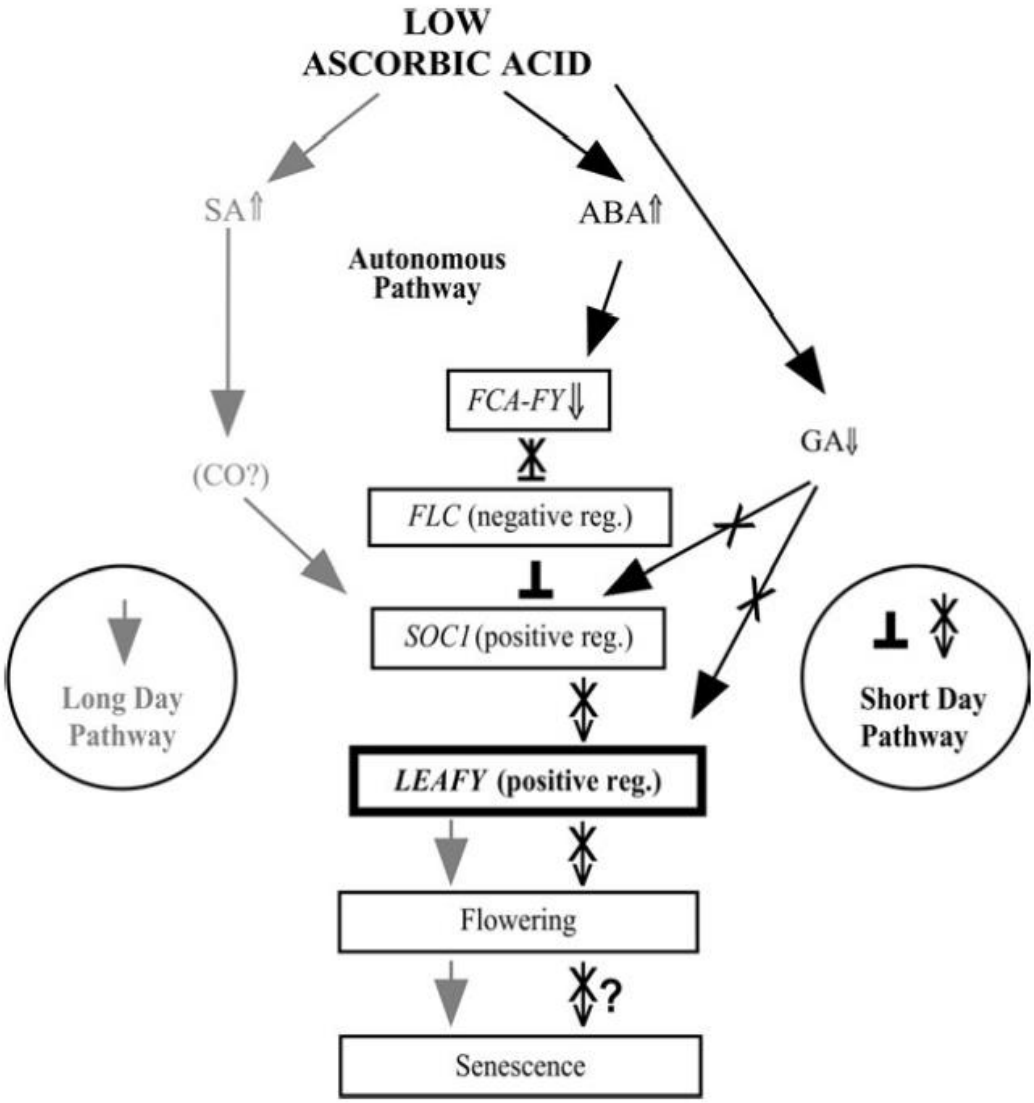

Figure I.20: Simplified scheme of hypothetical role of ascorbate during flowering in *Arabidopsis*. Ascorbate deficiency affects the long-day pathway through elevated levels of salicylic acid (SA), thus resulting in early flowering and senescence under long-day conditions. On the opposite, low levels of ascorbate inhibit the gibberellin (GA) pathway thus delay flowering and senescence under short days. Finally, ascorbate stimulate abscisic acid (ABA) accumulation under short days, that may delay flowering and senescence via an inhibition of the autonomous pathway. CO: CONSTANS; FCA-FY: negative regulator of flowering repressor FLC (Flowering Locus C); SOC1: Suppressor of overexpression of Constans 1. From (Barth et al., 2006)

In stress response

Alongside its role in the fundamental developmental processes of plants, ascorbate appears as a key actor in the regulation of redox homeostasis and signalling in response to biotic and/or abiotic stresses. As a matter of fact, it is assumed that every environmental constraint induces secondary oxidative stress. Indeed, overproduction of ROS and/or reduction of antioxidant capacity perturbates the antioxidative metabolism and thereby serves as a signal transductor that initiate plant response. As ascorbate is one of the main redox buffers of plant cells, it shows a role in abiotic and biotic responses, mainly by balancing the redox state but also by acting as a hormone synthesis cofactor.

Abiotic stress response

Numerous studies report variations in ascorbate content, its redox state as well as the activity of enzymes allowing its recycling, use and synthesis, in response to various abiotic stresses such as temperature, drought, nitrogen deficiency and exposure to strong light for example. Due to its main activity as a ROS processor during photosynthesis, many studies show a strong link between light and ascorbate metabolism. Therefore, among all the environmental factors, the one that seems to influence ascorbate metabolism the most is light (see above, Chapter I. part B.II.2.a.iv). Because ASC role during abiotic stress responses usually involves regulation of the ROS pool through the activity of the ASC-GSH cycle, the redox regulation of plant adaptation to environmental changes will be detailed below (see below, Chapter I. part B.II.2.d.II). However, it should be noted that ascorbate peroxidase has been extensively studied at the transcriptomic level in a large number of studies dealing with various abiotic stresses (Pandey et al., 2017 and reference therein).

Biotic stress response

The innate immune response of plants is characterised by an oxidative burst and production of ROS mainly *via* membrane NADPH oxidases following recognition of the pathogen by PAMPs (Daudi et al., 2012). This oxidative burst will disturb the redox balance as a signal that *in fine* will initiate plant responses. As in the vast majority of processes involving the redox balance, the ascorbate-glutathione cycle is a major player (see below, Chapter I. part B.II.2.d.II).

Nevertheless, a specific role of ascorbate can be distinguished here, mainly by interacting with the hormonal signalling pathways of the main defence hormones, namely JA, SA, ABA and ET (Pignocchi et al., 2006; Foyer et al., 2012; Denancé et al., 2013). In particular, the involvement of ASC in the defence response against pathogens is dependent on the pathogen lifestyle (Hossain et al., 2017). Indeed, *Arabidopsis* mutants with low levels of ASC show an increase in SA, pathogenesis-related proteins and camalexin, as well as better resistance to the hemibiotrophic bacteria *Pseudomonas syringae*, for

example (Pastori et al., 2003; Pavet et al., 2005; Barth, 2006; Mukherjee et al., 2010). On the contrary, the same mutants are more susceptible to the necrotrophic ascomycete *Alternaria brassicicola* (Botanga et al., 2012). In brief, defence against necrotrophic pathogens is mediated by JA and ET signalling (Paciolla et al., 2019), whereas SA-mediated signalling is involved in defence against biotrophic pathogens. Nevertheless, exogenous addition of ASC acts as an inducer of disease resistance in different plant-pathogen interactions in citrus crops (Egan et al., 2007; Fujiwara et al., 2013; Li et al., 2016).

b. Glutathione

i. History

In 1888, De Rey-Pailhade discovered a substance that he named "philothion" in yeast cells. This substance can form hydrogen sulphide after spontaneously reacting with elemental sulphur (Meister, 1988). Thereafter, he identified this molecule in various animal and plant tissues and concluded that the compound contained cysteine, which in the presence of oxygen, can undergo reversible oxidation to a disulphide form. It was then in 1921 that Hopkins identified an auto-oxidisable compound from muscle tissue containing cysteine and glutamate, for which he proposed the name glutathione. Finally, in 1929 the structure of glutathione, as a tripeptide of glutamic acid, cysteine and glycine, was achieved through its crystallisation (Figure I.21) (Hopkins, 1929). Hence, glutathione exists as reduced form namely GSH and oxidized form, namely GSSG. For this and other works on vitamins, Hopkins will receive a Nobel Prize that year. This discovery led to a great deal of research into the role of GSH in plants. Indeed, the discovery of ASC and that it is predominantly found in the reduced state in leaves, despite the presence of oxidases and oxidative catalysts, led to the conclusion that a reducing mechanism, *i.e.* glutathione, must be present, (Hopkins and Morgan, 1936). Having identified these two essential partners in redox balance, further research was carried out to place ascorbate-glutathione interactions in a physiological context leading to the discovery and characterisation of the ASC-GSH cycle. Today, there is unequivocal evidence that this small thiol compound is a multifunctional metabolite that acts as a cornerstone in redox homeostasis and signalling, as well as in environmental and plant defence responses. However, most of studies on GSH have been done in *Arabidopsis* leaves and GSH metabolism and regulation remain to be deciphered in other plants species and tissues.

ii. Structure

Glutathione (γ-L-glutamyl-L-cysteinylglycine; GSH), is a thiol tripeptide, present in most organisms. The binding of the γ-carboxyl group of glutamate to the amine group of cysteine distinguishes this bond from peptide bonds in proteins. It is suggested that this bond confers higher stability to the molecule as it allows it to be degraded by specific amino acid transferases. GSH is mainly found in the reduced free form (GSH) in cells but can be oxidised to disulphide glutathione (GSSG), thereby forming disulfide bonds between the two sulphur atoms in the cysteine residues (Figure I.21). Reduced GSH can be recycled from GSSG through the activity of glutathione reductase (EC 1.8.1.7; GR) using reducing power provided by NAPDH.

A **Reduced glutathione**

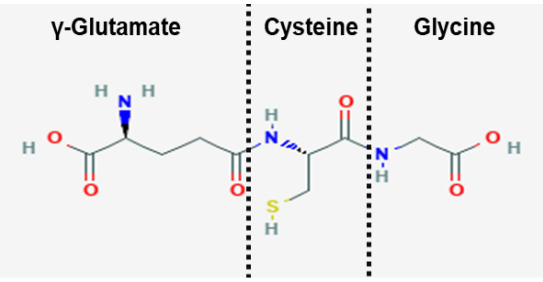

B **Oxidised glutathione**

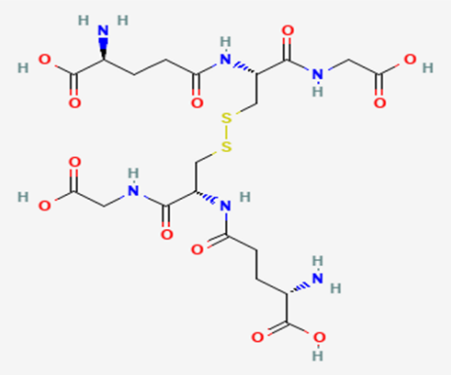

Figure I.21: Reduced (A) and oxidized (B) glutathione chemical structure. Images taken from PubChem.

However, homologous forms of glutathione are found, in some species, containing other C-terminal amino acids such as serine, β-alanine, or glutamate instead of glycine (Rennenberg, 1980; Klapheck et al., 1992; Meuwly et al., 1993). For example, homoglutathione (γ- Glu-Cys-β-Ala), in leguminous plants, is synthesised by distinct enzymes encoded by different genes (Frendo et al., 2005). The disulphide forms of homoglutathione and γ-Glu-Cys-Ser are still reducible by glutathione reductase (Klapheck et al., 1992; Oven et al., 2001). To our knowledge, such GSH homologues have not been reported in significant amounts in *Arabidopsis*, although analyses of purified GSH suggest that other new homologues may exist in some species (Skipsey et al., 2005; Noctor et al., 2011).

iii. Localisation

Glutathione concentration and redox state are highly variable between species, plant organs and even between different subcellular compartments. In plants, glutathione generally accumulates in cells at millimolar concentrations, with tissue levels exceeding 10 to 50 times the free cysteine (Noctor et al., 2011). Immunolocalisation studies report a high mitochondrial concentration although, due to their larger volume, it is estimated that the cytosol and chloroplasts account for about 50 and 30%, respectively, of the total glutathione in *Arabidopsis* leaf cells (Queval et al., 2011). The vacuole and apoplast have low GSH content, so it was considered negligible (Zechmann et al., 2008). However, the accumulation of GSSG in these compartments could have a physiological significance, important during oxidative stress responses (Queval et al., 2011). Furthermore, nuclear concentrations appear to be variable depending on the phase of the cell cycle. For example, during cell division, at the quiescent stage (G0), the nucleus seems to have similar glutathione concentrations to those found in the cytosol. However, it appears that the concentration of GSH increases in the nucleus at the beginning of the cell cycle in plant and animal cells (Markovic et al., 2007; Vivancos et al., 2010). Furthermore, the peroxisomal glutathione concentration is similar to the cytosolic concentration (Zechmann et al., 2008).

Nevertheless, not all these organelles possess enzymes of the glutathione biosynthetic pathway suggesting a controlled transport of this metabolite, whereas the transporters responsible for this activity remain to be characterised. Besides, we are witnessing the development of redox-sensitive fluorescent probes (Aller et al., 2013) that allow the microscopic detection of glutathione and its oxidation state within the different cellular compartments. However, these observations mainly allow qualitative comparisons between several conditions and will help to elucidate the distribution of GSH and GSSG and associate signalling pathways within plant cells (Meyer and Dick, 2010; Ming et al., 2017).

iv. Synthesis

The glutathione biosynthetic pathway in plants is a short pathway that has been well described (Noctor, 2002; Mullineaux and Rausch, 2005). It involves two enzymatic steps catalysed by ATP-dependent enzymes and requires glutamate, cysteine and glycine, three essential amino acids, as substrates. Firstly, γ-glutamylcysteine synthetase (EC 6.3.2.2; γ-ECS) combines cysteine with glutamate to form γ-glutamylcysteine (γ-EC), which is then used by glutathione synthetase (EC 6.3.2.3; GS) to add glycine that produces reduced glutathione. Studies on wheat and *Arabidopsis* leaves have shown that γ-ECS activity is confined to the chloroplast (Noctor, 2002), however, the study of the gene coding for GS in *Arabidopsis* shows alternative splicing phenomena leading to plastid and cytosolic localisation of the enzyme (Wachter et al., 2004). Thus, the first step of glutathione synthesis is confined to the

chloroplast while the second step can occur in both chloroplasts and cytosol (Figure I.22). This suggests an export of γ-EC from the chloroplast to the cytosol, in which, transporters competent for both γ-EC and GSH transport have recently been described (Maughan et al., 2010).

Furthermore, GSH synthesis appears to be highly regulated at multiple levels, and by multiple factors. Among them, γ-ECS activity and cysteine concentration seem to have a major impact on the GSH biosynthetic pathway as overexpression of these enzymes induces the highest accumulation (Noctor et al., 1998; Noji and Saito, 2002; Wirtz and Hell, 2007). However, other factors such as ATP and glycine availability seem to regulate this biosynthetic pathway (Ogawa et al., 2004). Otherwise, an increase in GSH is also observed in response to many environmental factors and responses to pathogens. Furthermore, the overall flux of glutathione biosynthesis is relatively low compared to the fluxes of primary metabolism suggesting that this pathway is extremely controlled and sensitive to the cellular redox state.

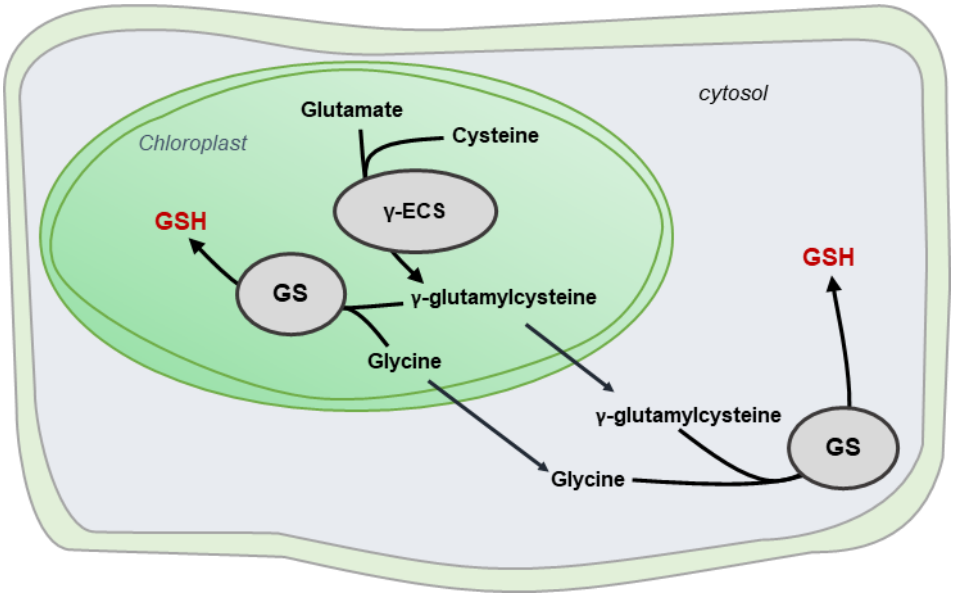

Figure I.22: Glutathione synthesis pathway.

GS: glutathione synthetase; γ-ECS: γ-glutamylcysteine synthetase; GSH: glutathione

v. Recycling

As previously, mentioned GSSG can be recycled into GSH by the glutathione reductase (GR), within the ASC-GSH cycle, using NADPH as a reductant cofactor. It is generally observed in plant cells that the GSH pool is maintained in a predominantly reduced state suggesting an active recycling activity. Specific glutathione reductase has been found in all subcellular compartments with a redox activity (*i.e.* cytosol, chloroplast, mitochondria and peroxisomes), which display high affinity for NADPH and GSSG (Halliwell and Foyer, 1978; Chew et al., 2003; Kataya and Reumann, 2010). Recently, a glutathione reductase (GR1) was found in the nucleus of *Arabidopsis*, suggesting that oxidised glutathione (GSSG) is actively reduced in the nucleus (Delorme-Hinoux et al., 2016). This suggests an active GSH recycling

in the organelles where oxidative metabolism occurs, thus reinforcing the role of glutathione as a major redox buffer but also as a transcription regulator.

vi. Transport

Glutathione is one of the main forms of organic sulphur, it is synthesised in the cytosol or chloroplast but present at different concentrations into the cell requiring an intracellular transport system. It can also be transported between cells apoplastically and/or symplastically (Bourgis et al., 1999; Mendoza-Cózatl et al., 2008). Observations on protoplasts have identified oligopeptide transporters (OPTs) as transporters of GSH, GSSG and other GS-derived products. In addition, transporters located on the inner chloroplast membrane, allowing the export of γ-EC across the chloroplast envelope and thus the cytosolic synthesis of GSH, have also been identified (Maughan et al., 2010). Furthermore, a restoration of the wild-type phenotype is observed in GR-deficient mutants by inducing cytosolic GR expression only (Pasternak et al., 2007) demonstrating that GSH can also be imported from the cytosol into the plastid. Moreover, tonoplastic transporters of the MRP (multidrug resistance-associated protein) family carrying an ATP-binding cassette have been identified and allow the storage of GSSG and GS-conjugates in the vacuole (Foyer et al., 2001). These transporters may play a role in maintaining the cytosolic redox state of predominantly reduced glutathione as they have a higher affinity for GSSG than GSH (Noctor et al., 2013). However, intracellular transporters for GSH and oxidised GSSG are still poorly characterised in plants.

vii. Degradation

Degradation of glutathione occurs enzymatically leading to dipeptides and amino acids production and is part of the γ-glutamyl cycle (Meister, 1988). This involves hydrolysis or transpeptidation of GSH by γ-glutamyl transpeptidase (EC 3.4.19.13; GGT), by γ-glutamyl cyclotransferases (EC 2.3.3.3; GGC) and 5-oxoprolinase (EC 3.5.2.9; 5-OPase) resulting *in fine* to the production of free glutamate (Figure I.23).

These enzyme activities were first characterized in tobacco (Steinkamp et al., 1987; Storozhenko et al., 2002). In addition, two GGTs purified from tomato were shown to have broad substrate specificity against GSH, GSSG and GS-conjugates and to localize to the cell wall or outer surface of the plasmalemma (Martin et al., 2007). Then, studies in maize (Masi et al., 2007) and barley also detected GGT activity in the apoplast (Ferretti et al., 2009), strikingly, the optimum pH of the enzyme detected in barley roots was reported to be basic, suggesting an increase of GSH degradation in response to alkalinisation of the apoplast. Another route for glutathione degradation from GS-conjugate could

involve cytosolic phytochelatin synthase (PCS) (Blum et al., 2007, 2010), although only a few reports are available concerning this pathway yet. Overall, rates of glutathione catabolism in *Arabidopsis* leaves have been estimated at about 30 $nmol.g^{-1}FW.h^{-1}$ (Ohkama-Ohtsu et al., 2007), suggesting that some pools of glutathione could turn over several times daily but the exact degradation mechanism remains unclear.

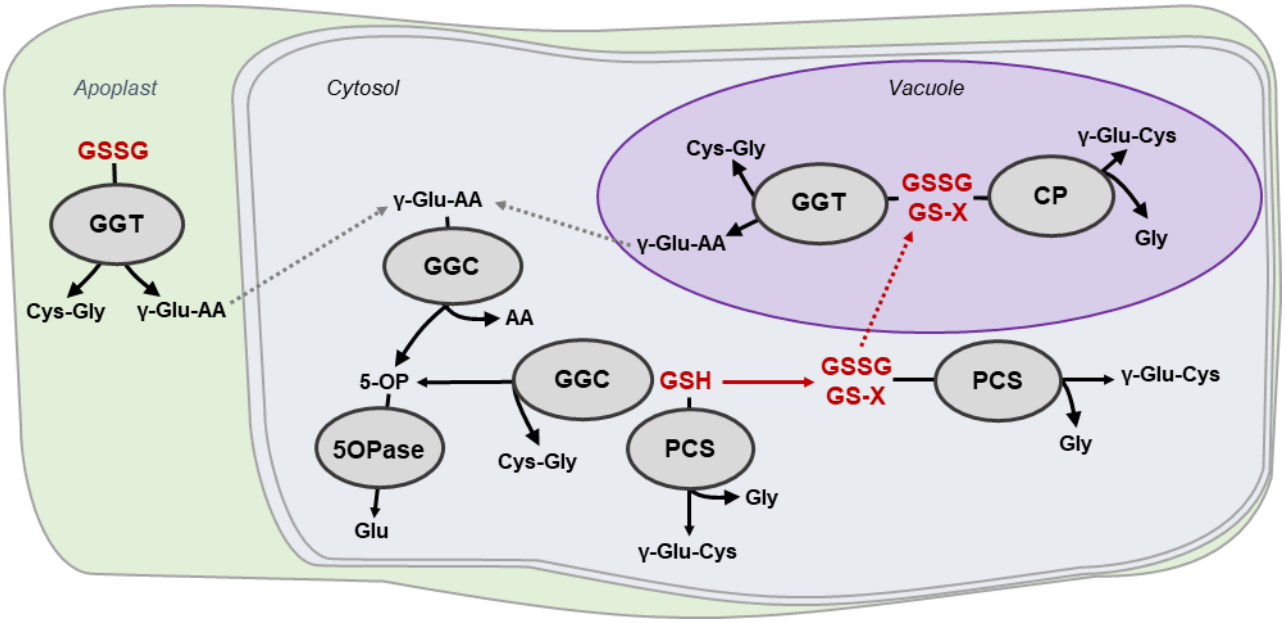

Figure I.23: Glutathione degradation pathways.

AA: amino acid; CP: carboxypeptidase; Cys: cysteine; GGS: γ-glutamyl cycloytansferase; GGT: γ-glutamyl transpeptidase; Glu: glutamic acid; Gly: glycine; GSH: glutathione; GSSG: glutathione disulfide; 5-OP: 5-oxoproline; 5OPase: 5-oxoprolinase; PCS: phytochelatin synthase; -X: S-conjugated compound.

viii. Role

The main role of GSH is as a reductant, intrinsically linked to the many possible reversible redox reactions of its cysteine sulphur group. Upon oxidation, either it forms GSSG by interacting with the cysteine residue of another GSH, or it can react with another thiol to form GS conjugates in which the thiol group is converted to sulfenic, sulfinic or sulphonic acids. However, the biochemistry of glutathione is not limited to these compounds; it can interact with nitric oxide (NO) to form S-nitrosoglutathione (GSNO). GSNO can then serve as either a signalling molecule or a reserve form of NO, suggesting an important physiological role for this GSH derivative (Lindermayr et al., 2005; Lindermayr, 2018). Similar to ascorbate, glutathione is a preferential target of ROS and serves as a major redox buffer by participating in their processing as well as in the recycling of ascorbate via the ascorbate-glutathione cycle. Moreover, the oxidation of glutathione does not only occur spontaneously but also enzymatically via the actions of thioredoxins and glutaredoxins, which are conserved enzymes during

evolution. However, thiol metabolism in plants is complex, with indispensable roles in many fundamental developmental mechanisms, but also in various responses to biotic and abiotic stresses. GSH is therefore an essential metabolite because of its action as a major redox buffer, participating in the regulation of the redox balance and as a signal molecule in many fundamental processes (Figure I.24).

Apart from its role as a redox buffer and its participation in the maintenance of the redox poise, GSH has a specific role in the synthesis of phytohormones as well as in the regulation of other physiological processes, such as apoptosis, notably via the glutathionylation and nitrosylation of proteins, and in the control of sulphur pool in plants.

Sulphur metabolism and accumulation

Glutathione is the perfect candidate for reduced sulphur management as cysteine is the main storage and transport form of reduced sulphur, and GSH is about 10 to 50 times higher than free cysteine levels (Kopriva, 2004; Maruyama-Nakashita and Ohkama-Ohtsu, 2017). Indeed, it has been shown that sulphur availability limits GSH accumulation in plants as *Arabidopsis* mutant deficient in the sulphate transporter shows decreased levels of glutathione (Maruyama-Nakashita et al., 2003; Nikiforova et al., 2003). In contrast, cysteine and glutathione levels were increased upon constitutive expression of a bacterial sulphate transporter, as well as upon overexpression of the cysteine synthesis pathway in *Arabidopsis* and tobacco (Noji and Saito, 2002; Tsakraklides et al., 2002; Wirtz and Hell, 2007). In addition, a retrocontrol phenomenon is observed in several species in which GSH suppresses the activity of sulphate transporters (Buchner et al., 2004) and sulphur uptake, particularly at the level of adenosine 5'-phosphosulphate reductase (APR) which is sensitive to GSH and its oxidation state (Leustek, 2002; Vauclare et al., 2002). Intracellular H_2O_2, cysteine, γ-EC and glutathione also induce genes encoding APRs in *Arabidopsis* roots (Queval et al., 2009), thus validating the role of GSH as an essential component in managing sulphur metabolism in plants.

Protein S-glutathionylation

S-glutathionylation of proteins involves the formation of a stable and reversible disulphide bond between glutathione and a cysteine residue of the targeted protein, resulting in a modification of its conformation, stability and/or activity. An inventory of potential target proteins has been carried out using several techniques, and most of the identified glutathionylation targets are relatively abundant proteins. Primary metabolic enzymes such as glyceraldehyde-3-phosphate dehydrogenase (GAPDH) and glycine decarboxylase (GDC) stand out (Michelet et al., 2005; Zaffagnini et al., 2007; Palmieri et al., 2010), however, the precise role of glutathionylation of these proteins has not been clearly established (Michelet et al., 2013). Overall, this suggests that the glutathione and thioredoxin systems

work closely together to fine-tune photosynthetic and respiratory metabolism through controlled modification of sensitive protein cysteine residues.

Protein S-nitrosylation

S-nitrosylation is another glutathione-related mechanism for regulating protein activity. Glutathione first forms GSNO by reacting with nitric oxide, which is then transferred to the cysteine residues, resulting, as for S-glutathionylation, in the modulation of the function of target proteins (Lindermayr et al., 2005; Romero-Puertas et al., 2008; Lindermayr, 2018). For instance, S-nitrosylation participates in the regulation of ethylene synthesis by specifically inhibiting a methionine adenosyltransferase (Lindermayr et al., 2006), thus influencing signalling processes mediated by ethylene.

Moreover, the same main targets are found for S-glutathionylation, (*i.e.* GADPH and GDC), for which these modifications lead to a decrease in their activity. It can be assumed that inhibition of GAPDH may contribute to the regulation of the trade-off between central metabolism and stress response pathways (Holtgrefe et al., 2008), while inhibition of GDC again highlights the importance of photorespiration-related redox regulation mechanisms (Foyer et al., 2009; Peterhansel et al., 2010).

Programmed cell death

Glutathione, and more specifically its oxidation ratio (GSSG/GSH), was first supposed to impact programmed cell death and dormancy (Kranner et al., 2006). According to this study, an increase in redox potential above the threshold value leads to cell death and/or growth arrest. Indeed, an increase in leaf glutathione content, caused by overexpression of γ-ECS in tobacco chloroplasts triggers the expression of pro-apoptotic gene expression and lesion formation (Creissen et al., 1999). However, GSSG accumulation is also observed in GSH synthesis deficient *Arabidopsis* mutants (*gsh1*), which are surprisingly aphenotypic (Marty et al., 2009; Mhamdi et al., 2010a). These studies show that high levels of glutathione (as GSH or GSSG) can be tolerated by plants and are not in themselves sufficient to trigger cell death pathways (Liedschulte et al., 2010). Subcellular compartmentalisation could be a key factor for a better understanding of GSH-triggered cell death. Currently, available data suggests that neither total glutathione nor GSSG accumulation necessarily induces cell death in leaves of several plant species. Further work is therefore needed to establish the importance of γ-EC accumulation in the mechanism of programmed cell death (Noctor et al., 2012).

Glutathione main functions have been briefly reviewed, but they participate in countless signalling pathways and regulatory networks involved in the responses of plants to abiotic and/or biotic stresses (for detailed reviews see (Noctor et al., 2011; Burritt et al., 2017; Hasanuzzaman et al., 2017 and reference therein).

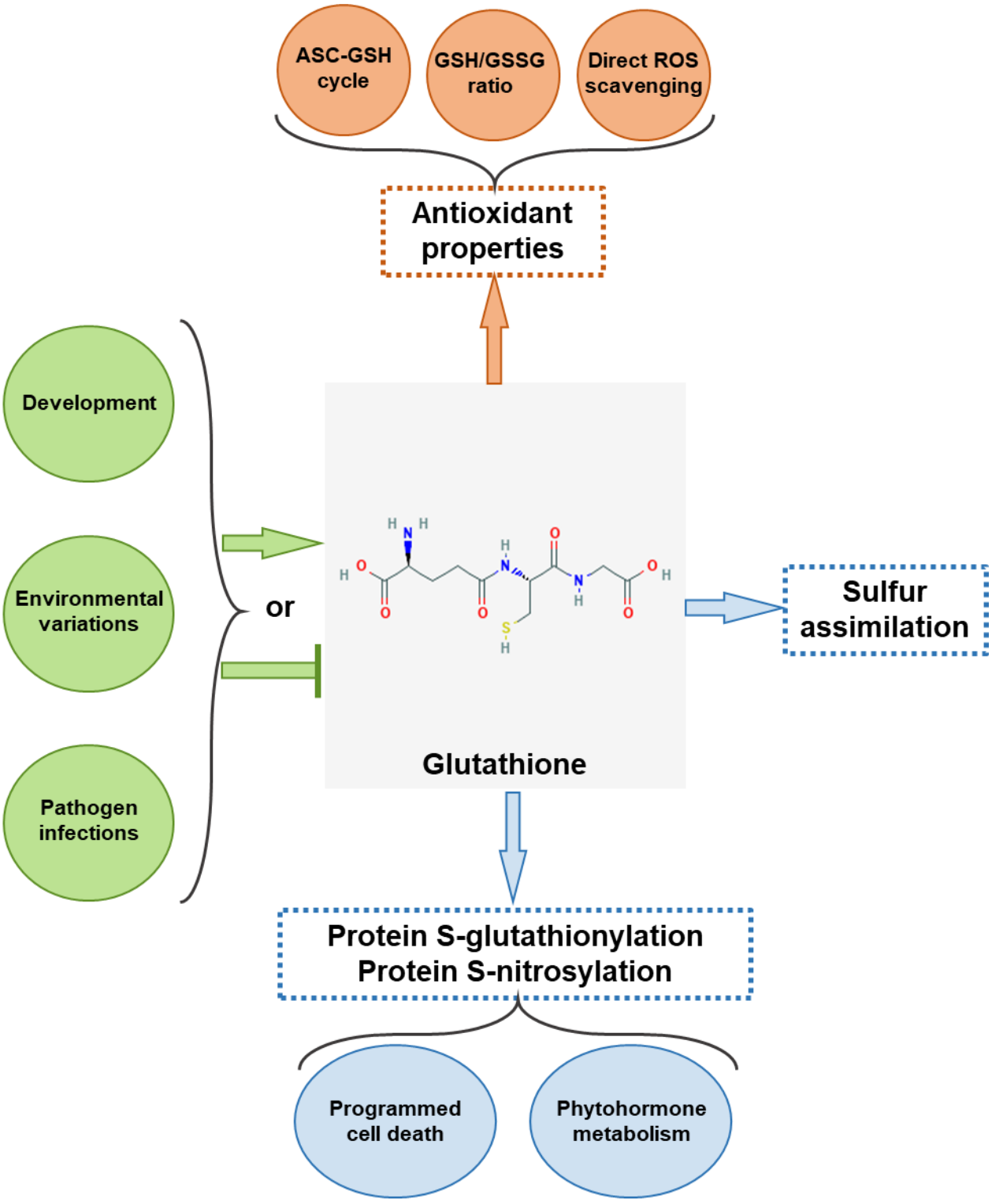

Figure I.24: Main roles of glutathione in plants. Glutathione is not only an antioxidant metabolite (orange) but also participates in fundamental biological processes by participating to sulfur assimilation and storage or by interacting with protein (glutathionylation or nitrosylation) (blue).

c. Pyridine nucleotides

i. History

At the beginning of the 20th century, in 1904, two English scientists, Arthur Harden and William Young, identified a molecule that accelerated the fermentation of glucose in yeast and named it "cozymase" (Harden and Young, 1906). It was not until about thirty years later that the structure of this molecule was identified as two nucleotides linked by a diphosphate bond (von Euler, 1930) and that its role in oxidation-reduction through its nicotinamide group was highlighted (Warburg and Christian, 1936). Nicotinamide adenine dinucleotide (NAD) was then characterised as an energy-transducing coenzyme that is ubiquitous in all living organisms. Furthermore, NAD is present in cells at millimolar concentrations and is involved in virtually all metabolic pathways in the cell (Noctor, 2006).

ii. Structure

Pyridine nucleotides are dinucleotides composed of an adenosine monophosphate (AMP) linked by a di-phosphate bridge to a nicotinamide mononucleotide (also known as niacin or vitamin B3) with a total mass of 664 daltons (Pollak et al., 2007) (Figure I.25). Moreover, NAD can also be phosphorylated by specific NAD kinases on the 2' hydroxyl residue of its ribose, linked to adenine, to form NAD phosphate (NADP) (Figure I.26). These two forms, NAD and NADP, are found in cells in oxidised (NAD^+ and $NADP^+$) or reduced (NADH and NADPH) state, thus participating in the maintenance of redox homeostasis and the activity of numerous enzymes (Gakière et al., 2018b). However, they are involved in different processes in plant cells. Indeed, NAD acts mainly as an oxidant and is most often used during catabolism, while NADP is primarily used as a reductant in biosynthetic pathways or photosynthesis during which it serves as a final electron acceptor of the photosynthetic electron transport chain (Figure I.26) (Gakière et al., 2018b).

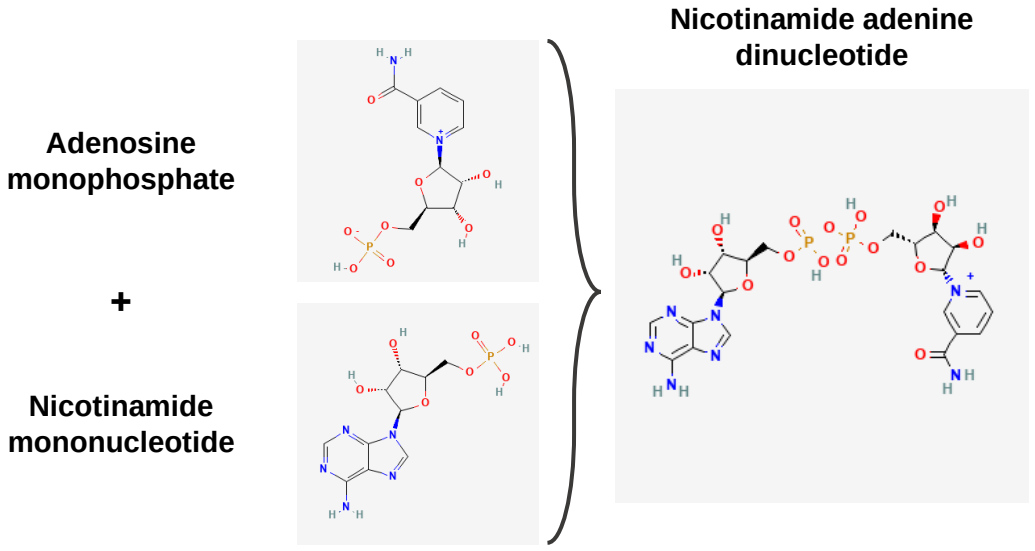

Figure I.25: Structure of nicotinamide adenine dinucleotide (NAD). Images taken from PubChem.

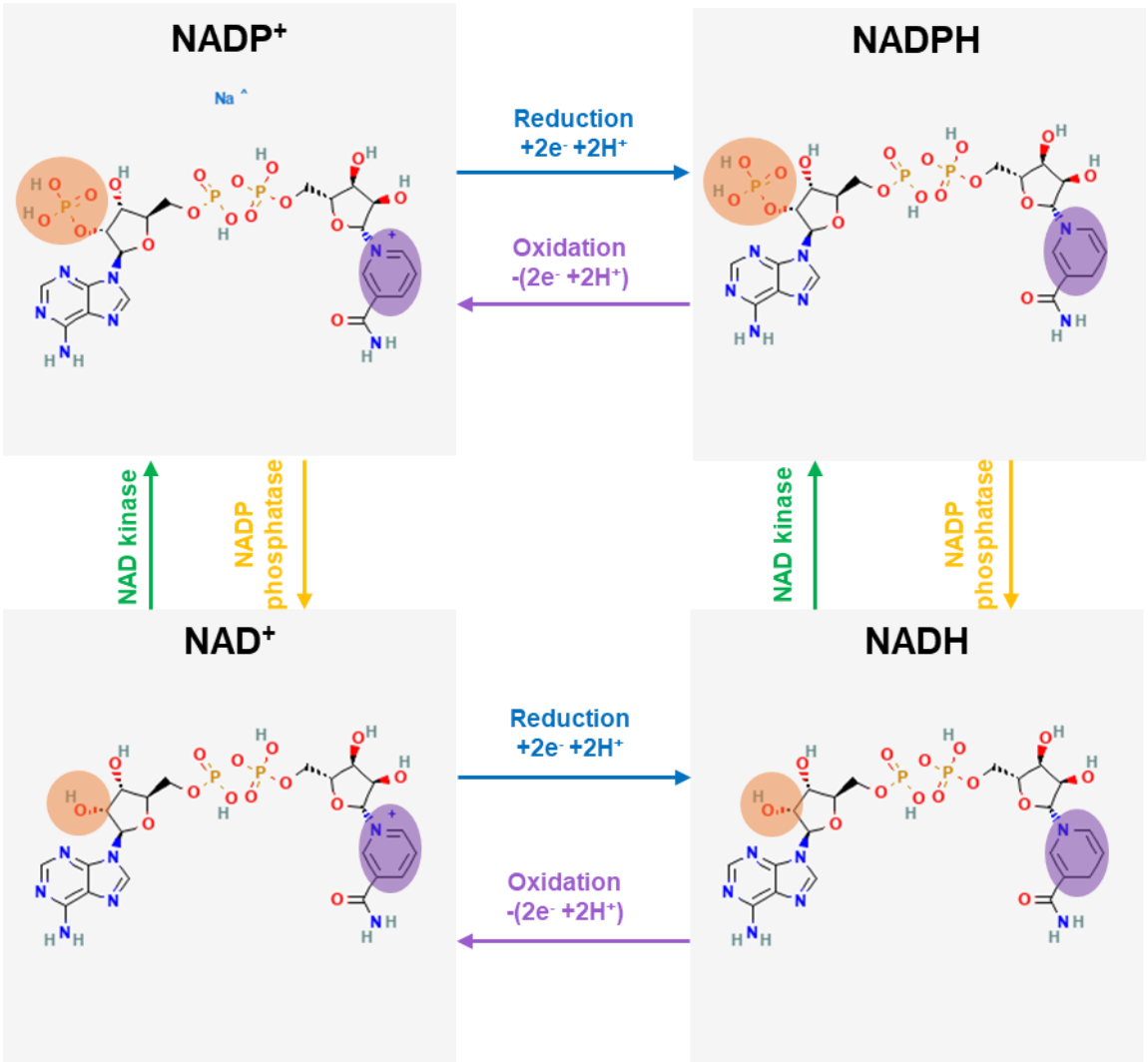

Figure I.26: Main forms of pyridine nucleotides. Images taken from PubChem.

iii. Localisation

As for the other major redox buffers, NAD in plant cells is heterogeneously distributed, both between species, organs, tissues and different subcellular compartments. The data currently available are mainly from non-aqueous cell fractionation studies of leaf tissue. It is observed that NAD(P) is primarily concentrated in the chloroplast, cytosol (from 0.1mM to 2mM; Figure I.27) (Igamberdiev and Gardeström, 2003; Szal et al., 2008; Gakière et al., 2018b). Interestingly, NAD(H) pools are highest in mitochondria, due to their involvement in mitochondrial metabolism. In contrast, the NADP(H) pool is most elevated in the chloroplast due to its participation in photosynthetic function. However, if the relative contribution of each compartment to the total cell volume is considered, the cytosolic NAD^+ pool contributes as a major part of the cellular NAD (Winter et al., 1994). Moreover, the redox state of NAD(P) also varies in response to light, with NAD and NADP pools being up to 10- and 6- fold more reduced, respectively, in mitochondria than in the chloroplast and cytosol (Igamberdiev and Gardeström, 2003; Szal et al., 2008).

On the other hand, very little data are available in the literature concerning NAD and NADP contents and their redox state in the different subcellular compartments (vacuole, peroxisome and nucleus) (Guérard et al., 2011; Pétriacq et al., 2012).

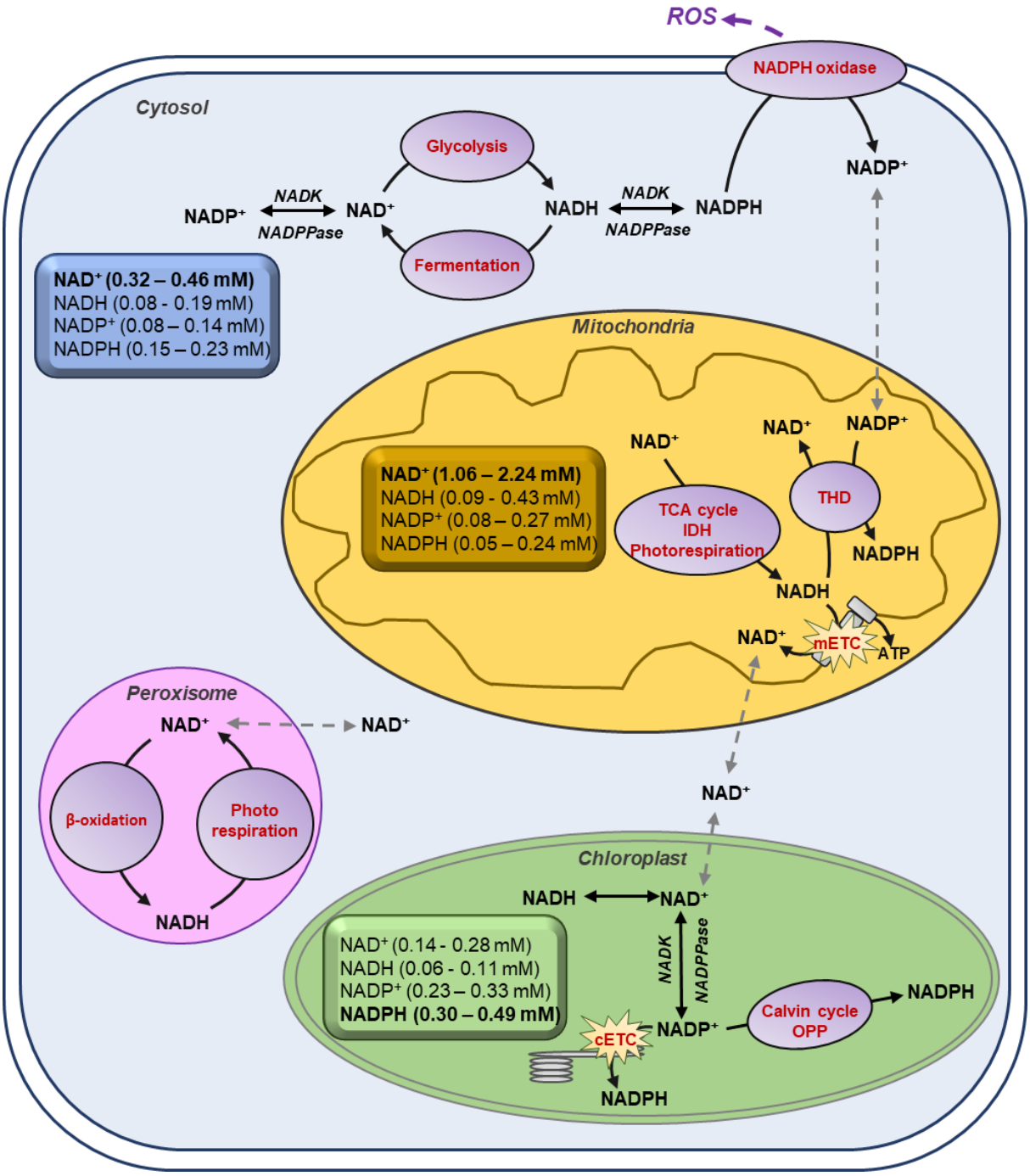

Figure I.27: Pyridine nucleotide turnover and concentrations in plant cells.

cETC: chloroplastic electron transport chain; mETC: mitochondrial electron transport chain; TCA: tricarboxylic acid; IDH: isocitrate dehydrogenase; OPP: oxidative pentose phosphate pathway; THD: transhydrogenases; NADK: NAD kinase; NADPPase: NADP phosphatase. Adapted from (Gakière et al., 2018b).

iv. Synthesis

In plant cells, NAD^+ *de novo* biosynthesis starts from the amino acid aspartate, which is oxidated by aspartate oxidase (AO; E.C. 1.4.3.16), producing iminoaspartate, then quinolinate by quinolinate synthase (QS; E.C. 2.5.1.72) in the chloroplast (Katoh et al., 2006). Quinolinate phosphoribosyltransferase (QPT; E.C. 2.4.2.19) catalyses the subsequent conversion of quinolinate to nicotinic acid (Na) mononucleotide (NaMN) that will be transported to the cytosol where the next biochemical reactions occur (Suda et al., 2003; Magni et al., 2004; Noctor et al., 2006; Hashida et al., 2007) (Figure I.28). However, the transporter responsible for the transfer of NaMN to the cytosol remains to be discovered. In the cytosol, NaMN is adenylated to nicotinic acid adenine dinucleotide (NaAD) by nicotinate mononucleotide adenylyl transferase (NaMNAT; E.C. 2.7.7.1), then NAD synthetase (NADS; E.C. 6.3.1.5) finally amidates NaAD to NAD^+ (Gakière et al., 2018b). Nevertheless, other synthesis pathways of NAD^+ using nicotinic acid conjugates as substrate, such as Na-glucosides, have been shown to play a role in seed germination in Brassicaceae (Li et al., 2017b).

Besides, NAD(H) can be phosphorylated into NADP(H) by NAD kinases (E.C. 2.7.1.23; NADK) and NADH kinases (E.C. 2.7.1.86), using ATP as substrate. NADK are present in several isoforms in the different subcellular compartments and can be regulated in a calcium/calmodulin-dependent manner (Gakière et al., 2018b). On the opposite, NADP phosphatases catalysed (EC 3.1.3.108; NADPPase) the conversion of NADP(H) to NAD(H), but little information is available yet. While the topology of NAD^+ synthesis is well documented in leaves (Noctor et al., 2006; Gakière et al., 2018b), the molecular and regulatory details of the corresponding biochemical pathways remain largely unknown, especially for fruit tissues.

v. Recycling

The salvage pathway consists of 2 specific enzymatic steps, NAD^+ can be recycled *via* the activity of nicotinamidases (NIC; E.C. 3.5.1.19), producing nicotinate from nicotinamide and by nicotinic acid phosphorybosyltransferase (NaPT; E.C. 2.4.2.11), which generates NaMN and thus reconnects with *de novo* synthesis pathway (Figure I.28). Due to its toxicity, nicotinate is stored in plant cells as Na-conjugates such as nicotinate glucosides and trigonelline (*i.e.* N-methylnicotinate) by glycosylation *via* Na glucosyltransferase (NaGT; E.C. 2.4.1.196) or methylation *via* Na-N-methyltransferase (NMT; E.C. 2.1.1.7) (Köster et al., 1989; Li et al., 2015, 2017b).

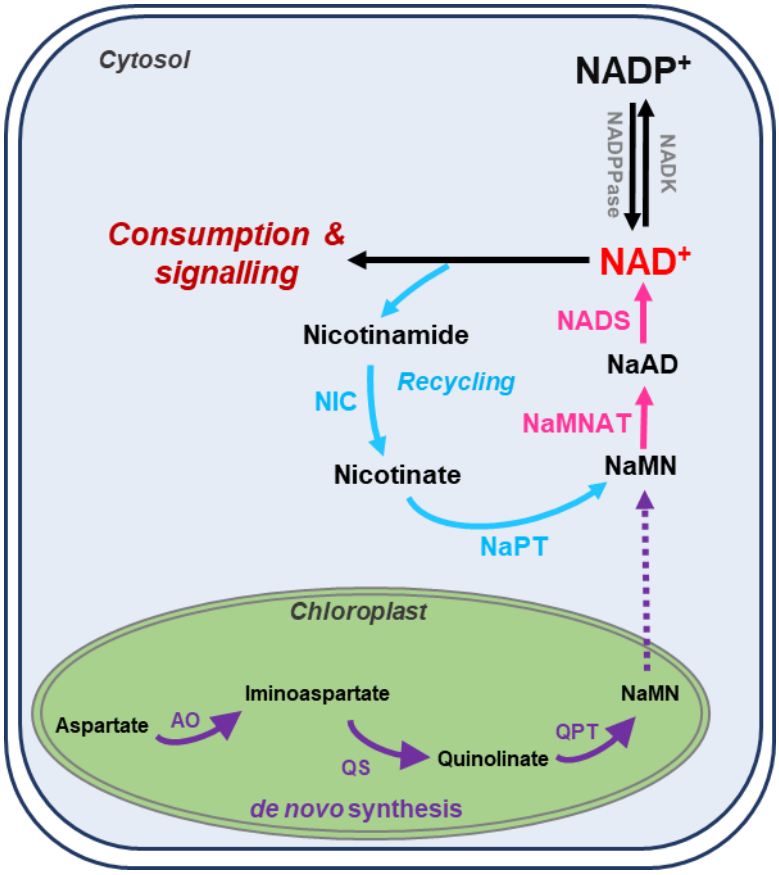

Figure I.28: NAD biosynthetic and recycling pathways. Dot arrows represent transport between the different cellular organelles. Purple and blue arrows indicate *de novo* synthesis pathway of NAD^+, and the recycling pathway, respectively. Pink arrows represent steps that are shared by these two synthesis pathways. AO: aspartate oxidase; NaAD: nicotinic acid adenine dinucleotide; NADK: NAD kinase; NADP: NAD phosphate; NADPPase: NADP phosphatase; NaMN: nicotinic acid mononucleotide; NaMNAT: NaMN adenylyltransferase; NADS: NAD synthetase; NaPT: nicotinate phosphoribosyltransferase; NIC: nicotinamidase; QPT: quinolinate phosphoribosyltransferase; QS: quinolinate synthase.

vi. Transport

Pyridine nucleotides can be transported intercellularly, intracellularly, and *via* shuttles of NAD(P) redox equivalents between compartments allowing the NAD(P) pools to be linked together and regulate the redox state of the different subcellular compartments (Stein and Imai, 2012; Hummel and Gröger, 2014; Kato and Lin, 2014). Several shuttles allow the transport of redox equivalents between compartments. Firstly, the triose phosphate/3-phosphoglycerate shuttle links chloroplast and cytosol (Heineke et al., 1991). Secondly, the malate/oxaloacetate shuttle, coupling both chloroplastic, cytosolic and mitochondrial NAD^+/NADH ratios (Day and Wiskich, 1981). In addition, the malate/aspartate shuttle allows the connection of mitochondria and cytosol (Mettler and Beevers, 1980) (Figure I.29).

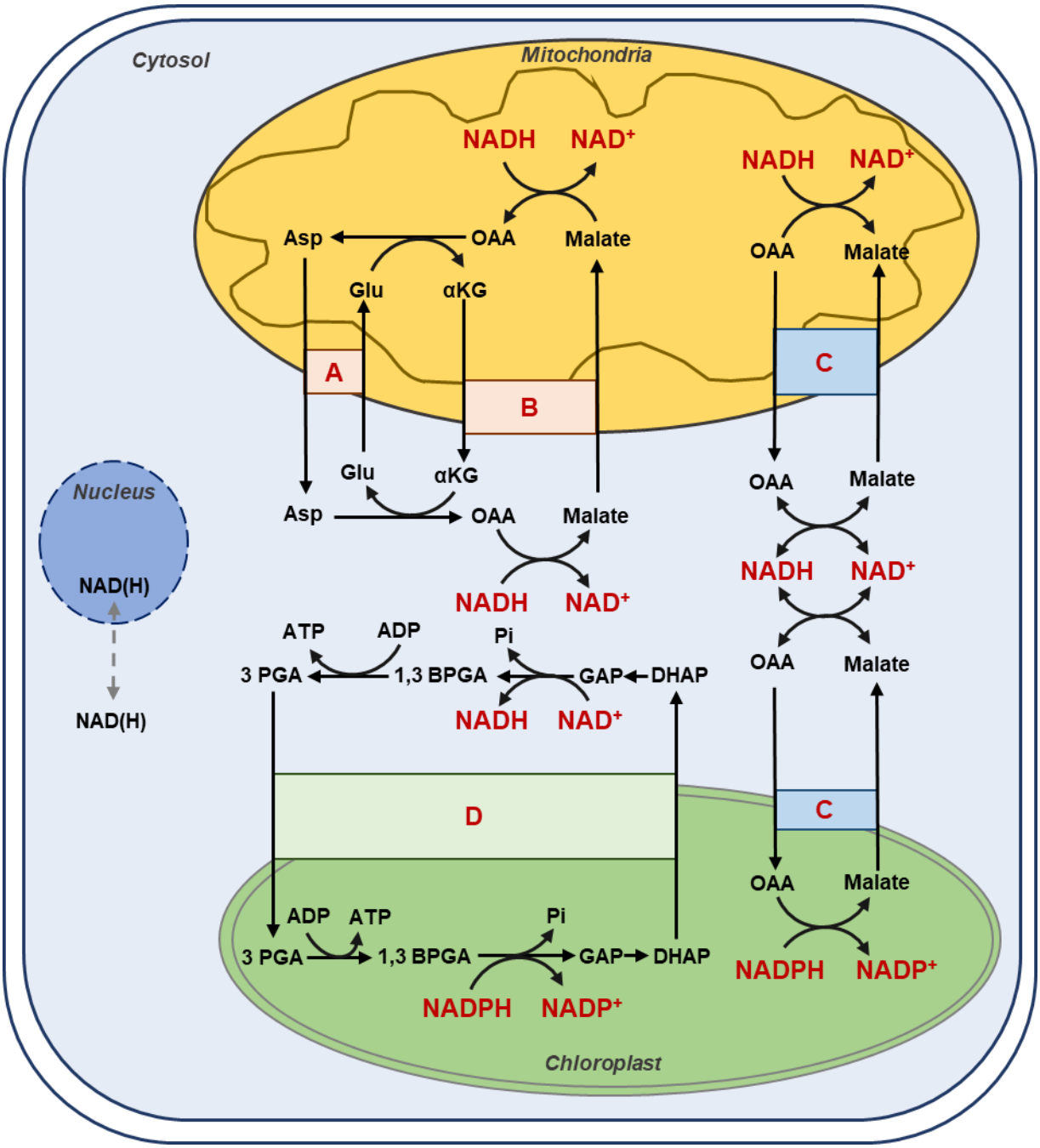

Figure I.29: Pyridine nucleotide shuttles. Glutamate-aspartate shuttle **(A)**; Malate-a-ketoglutarate shuttle **(B)**; Malate-oxaloacetate shuttle **(C)**; Triose phosphates shuttle **(D)**.
ADP: adenosine diphosphate; Asp: Aspartate; ATP: adenosine triphosphate; 1,3BGPA: 1,3-bisphosphoglyceric acid; DHAP: dihydroxyacetone phosphate; GAP: 3-phosphoglyceric aldehyde; Glu: Glutamate; OAA: oxaloacetate; 3PGA: 3-phosphoglyceric acid.

All these shuttles participate in the finely-tuned redox state of NAD(P) and are involved in many signalling processes (Gakière et al., 2018b). However, transporters capable of transporting nucleotides across mitochondrial and chloroplast membranes have also been identified in *Arabidopsis*, allowing the

movement of NAD^+ and other nucleotide mononucleotides (ADP or AMP) (Palmieri et al., 2009). It has also been shown that $NADP^+$ can be imported into isolated mitochondria, but the import mechanism remains to be elucidated (Bykova and Møller, 2001). Furthermore, NAD^+ and NADH can also be transported across the peroxisome membrane by a shuttle called PXN (Agrimi et al., 2012). Nonetheless, it is accepted that free NAD^+ passes through the nuclear pores to be used by different enzymes and thus modulates gene expression and/or chromatin organisation (Zhang et al., 2002; Fjeld et al., 2003). Hence, the cytosolic redox state of the NAD^+/NADH couple could link cellular metabolism with gene transcription (Fjeld et al., 2003).

Nevertheless, it is assumed that NAD^+ and $NADP^+$ cannot be directly imported into cells as infiltration of protoplasts with NAD^+ and $NADP^+$ did not result in an intracellular increase in their intracellular nucleotide content (Zhang and Mou, 2009). However, permease-type transporters of NAD^+ precursors have been reported for the transport of nicotinamide riboside and quinolinate (Belenky et al., 2011; Ohashi et al., 2013), inducing an increase in NAD^+ (Pétriacq et al., 2012). Finally, it has been shown that during infection, leakage of pyridine nucleotides increases their extracellular concentrations to trigger the expression of pathogenesis-related genes (PR) in a calcium-dependent manner (Zhang and Mou, 2009; Fu and Dong, 2013).

vii. Degradation

Catabolism of NAD occurs mainly during signalling processes involving the release of nicotinamide and a large amount of energy. Diverse enzymes can catabolise NAD^+ producing either cyclic ADP-ribose (cADPR), ADP-ribose conjugated with proteins or free ADP-ribose. cADPR is a secondary messenger produced by ADPR cyclases (EC 3.2.2.6) involved in plant defence response and linked with calcium signalling (Pétriacq et al., 2016a) (Figure I.30).

Besides, ADP-ribose polymerase (EC 2.4.2.30; PARP) are present in numerous isoforms and participate in fundamental processes, such as DNA repair and methylation, and regulatory processes by participating in the (de)compaction of chromatin (Briggs and Bent, 2011; Lamb et al., 2012; Swindall et al., 2013). Protein modification by PARP can be reversed by poly-ADP-ribose glycohydrolase (EC 3.2.1.143; PARG), releasing free ADP-ribose. Furthermore, silent information regulator type 2 histone deacetylases, also known as SIRTUINS in plants, consume NAD^+ to act in various signalling pathways, by modifying chromatin structure using acetylation/deacetylation of histones, or by post-translational acetylation of protein such as the large subunit of Rubisco (Finkemeier et al., 2011; Wu et al., 2011).

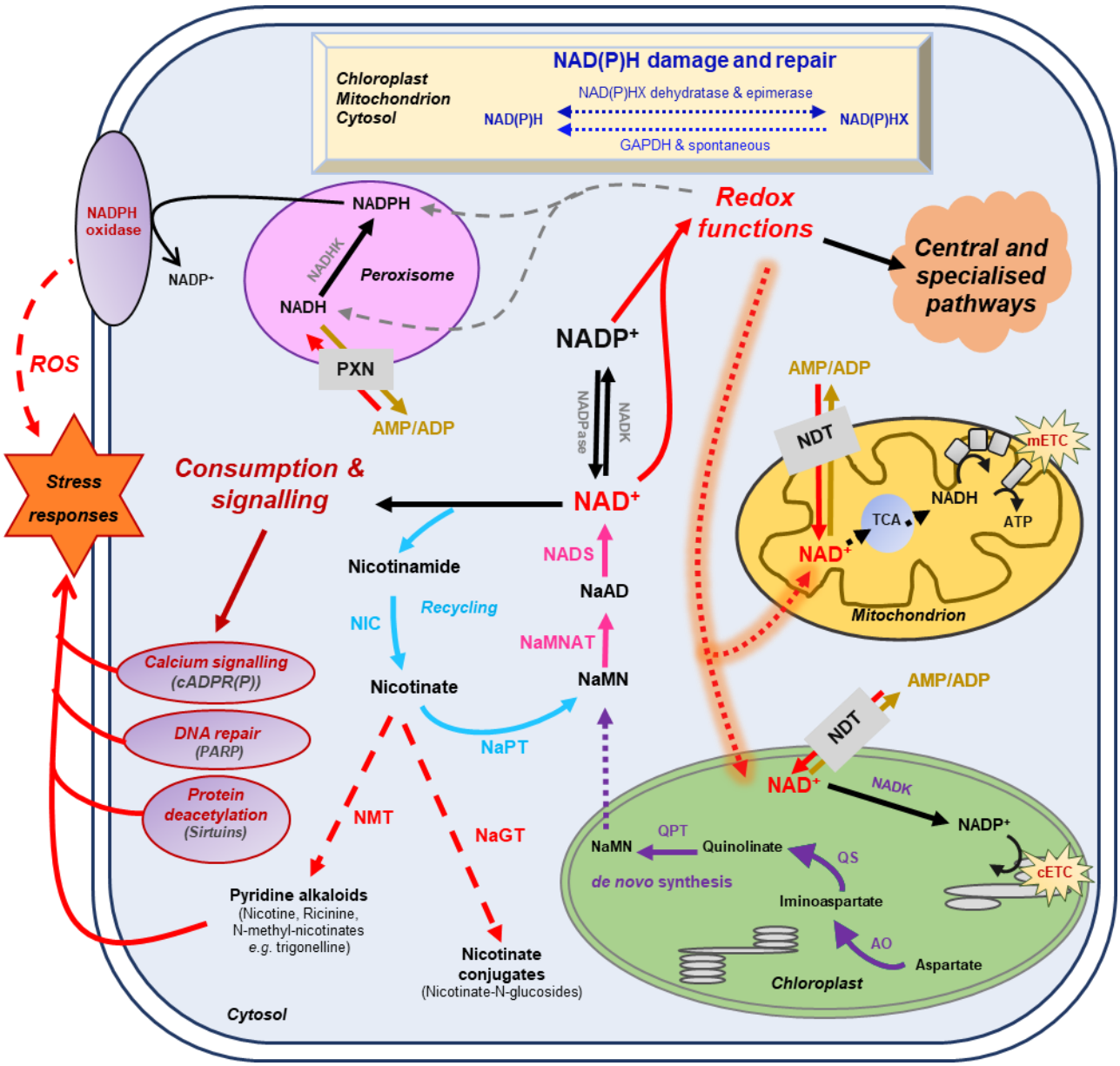

Figure I.30: Basics of nicotinamide adenine dinucleotide (NAD^+) metabolism in plant cells. Biosynthesis and utilisation of pyridine nucleotides. Purple and blue arrows indicate *de novo* synthesis pathway of NAD^+, and the recycling pathway, respectively. Pink arrows represent steps that are shared by these two synthesis pathways. AO: aspartate oxidase; ATP: adenosine triphosphate; cADPR(P): cyclic ADP-ribose (phosphate); cETC: chloroplastic electron transport chain; GAPDH: glyceraldehyde-3-phosphate dehydrogenase; mETC: mitochondrial electron transport chain; NaAD: nicotinic acid adenine dinucleotide; NADK: NAD kinase; NADP: NAD phosphate; NADPase: NADP phosphatase; NAD(P)HX: NAD(P)H hydrate; NaMN: nicotinic acid mononucleotide; NaMNAT: NaMN adenylyltransferase; NADS: NAD synthetase; NaGT: nicotinate N-glucosyltransferase; NaPT: nicotinate phosphoribosyltransferase; NDT: NAD^+ transporter; NIC: nicotinamidase; NMT: nicotinate N-methyltransferase; PARP: poly-ADP-ribose polymerase; PXN: peroxisomal NAD carrier; QPT: quinolinate phosphoribosyltransferase; QS: quinolinate synthase; ROS: reactive oxygen species; TCA: tricarboxylic acid cycle. From (Decros et al., 2019b).

Finally, NAD can be cleaved by NUDIX hydrolases (EC 3.6.1.13), leading to nicotinamide and free ADP-ribose production; NUDIX will also hydrolyse the later ones into free AMP and ribose-5-phosphate. Nudix hydrolase pathways are not well documented, but they have a role in numerous fundamental and signalling events like other NAD^+ catabolism pathways.

viii. Roles

Pyridine nucleotides, as energy transducers, are cornerstone metabolites involved in virtually all primary and secondary metabolic pathways. They participate actively in the regulation of redox balance in cells, especially by allowing the recycling of oxidised ASC and GSH within the ascorbate-glutathione cycle. Moreover, NAD is intrinsically linked to mitochondrial metabolism as NADH oxidation makes ATP synthesis possible (Dutilleul, 2005). From a redox perspective, a major role of NAD is during nitrogen assimilation from the soil. Indeed, NAD(P)H is required for nitrate reductase (EC 1.6.6.1; NR) activity, which is the starting step in nitrogen metabolism in plants (Pellny et al., 2008; Foyer et al., 2011). In addition, NAD homeostasis is pivotal for carbon assimilation during primary metabolism. Indeed, it permits C assimilation during photosynthesis as the final electron acceptor and is involved in numerous steps of sugar metabolism (*i.e.*glycolysis, etc.) (Figure I.30).

Besides, NAD also participates in fundamental developmental processes such as seed germination, development of pollen tube and root development, for instance (Hunt et al., 2007; Hashida et al., 2013, 2016) and signalling in response to various environmental stresses, either biotic or abiotic (Pétriacq et al., 2013, 2016b; Kollist et al., 2019). There is considerable evidence of the involvement of NAD metabolism in plant immunity (Pétriacq et al., 2012, 2016b; Mou, 2017; Kourelis et al., 2020) and in response to environmental changes, (*e.g.* drought, high light, temperature, etc.) (Torres and Dangl, 2005; Vanlerberghe, 2013; Gakière et al., 2018b). Briefly, NAD can regulate phytohormones such as ABA biosynthesis during dormancy break, for instance (Kucera et al., 2005; Hunt and Gray, 2009). In addition, in non-photosynthetic tissues such as seeds, anabolism requires reducing power supplied by NADPH produced by the oxidative pentose phosphate pathway (Hunt and Gray, 2009).

Nonetheless, NADPH oxidases appear crucial to control energy balance by producing extracellular ROS that subsequently induces cell wall remodelling and hormonal signalling, thus allowing pollen tube growth and root elongation (Müller et al., 2012; Hashida et al., 2013). Otherwise, pyridine nucleotides are pivotal for the trade-off between growth and response to stress in plants as they regulate carbon/nitrogen balance, mainly through the monitoring of respiration activity.

d. Enzymatic ROS processing

Alongside the metabolic ROS processing, plants harbour plentiful enzymes catalysing ROS processing using antioxidants as substrates. Two types can be distinguished, on the one hand, enzymes that are shared between all species and encoded by a large number of isoforms, in particular catalase, superoxide dismutase and redoxins (*e.g.* thioredoxins (TRXs), peroxiredoxins (PRX) and glutaredoxins (GRXs)), and on the other hand the enzymes that are part of the ASC-GSH cycle.

ix. Ubiquitous antioxidant enzymes

Catalase (EC 1.11.1.6; CAT) is the first ubiquitous antioxidant enzyme, encoded by a multigenic family, to be characterised and found in all aerobic and even some anaerobic organisms (Kirkman and Gaetani, 2007; Zamocky et al., 2008). Catalase can be distinguished from other ROS processing enzymes as it does not require any reductant cofactor supply. These heme-based enzymes catalyse the dismutation of two molecules of H_2O_2 to H_2O and O_2 (Figure I.31A) and comprise polypeptides of around 60 kDA organised into dimers or tetramers (Bernroitner et al., 2009). It starts with the concomitant generation of a water molecule, an oxy-ferryl intermediate and a porphyrin cation radical resulting from the splitting of O-O bond of H_2O_2. Then, the second molecule of H_2O_2 allows the production of O_2 and another water molecule by reducing the porphyrin cation radical (Alfonso-Prieto et al., 2009) (Figure I.31B). Thus, the first H_2O_2 substrate will be transformed into 2 H_2O molecules while the second is converted into O_2 (Kato et al., 2004).

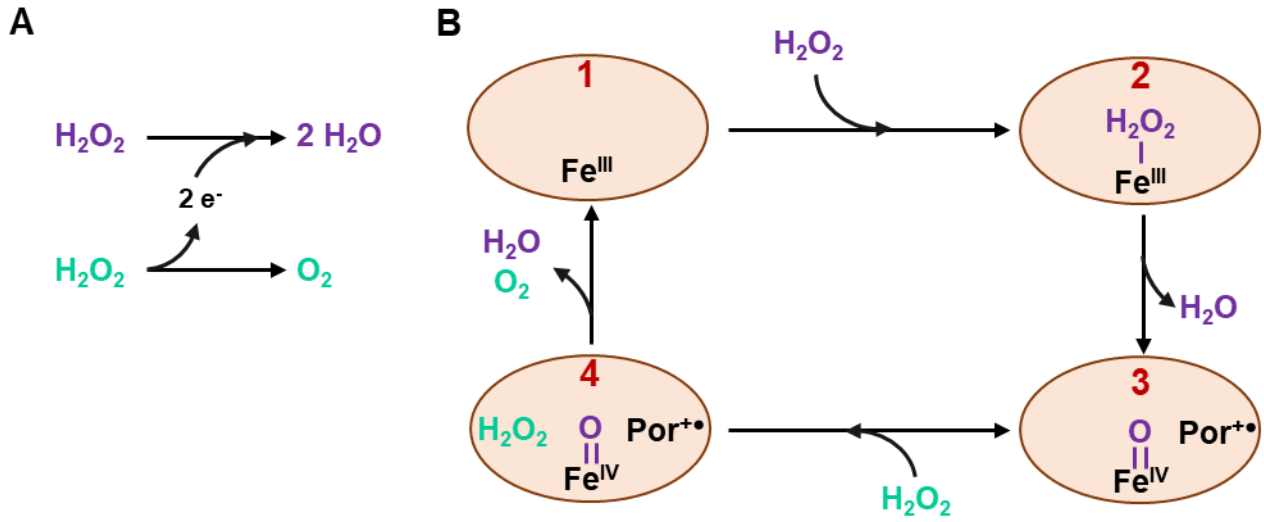

Figure I.31: Hydrogen peroxide dismutation by catalase. Classical dismutation reaction **(A)**. Simple scheme of catalase dismutation mechanism **(B)**.

Fe^{III} : ferric ion; Fe^{IV} : high valent iron; $Por^{+\bullet}$: porphirine cation radical. Coulors indicate the corresponding substract and product during the reaction.

Moreover, CAT displays a high specificity for H_2O_2 but low activity against other organic peroxides. Kinetic properties of catalase can be hard to determine precisely but reports indicate a Michaelis constant (K_M) for H_2O_2 comprised between 40 and 600 mM (Chelikani et al., 2004), suggesting that *in vivo* activity is much lower than its maximal capacity and that catalase activity can support transient high concentrations of H_2O_2. Genomic studies on plant species unveil the presence of at least three catalase genes, as identified in *Arabidopsis* and tobacco encoding for three catalase isoforms with high similarity (Willekens et al., 1995; Frugoli et al., 1996; Mhamdi et al., 2010b). Plant catalases can be classified into three classes; class I is expressed mainly on photosynthetic tissues, whereas class II is correlated with vascular tissues and class III with reproductive organs and seeds. Although these enzymes are characterised, they are all expressed in all tissues, and more analyses are required to decipher theirs *in vivo* significance in plant cells (Zimmermann et al., 2006). However, interrogations concerning the catalase subcellular localisation in plants remain to be unravelled. It is assumed that catalase is mostly found in peroxisomes enabled by an active import (Mullen et al., 1997).

In addition, catalase activity has been detected in cytosol, chloroplast and mitochondria (Kato et al., 1997; Petriv and Rachubinski, 2004). Nonetheless, catalase import into mitochondria has not been demonstrated yet, and it may be probable that contamination may account for reports of catalase activity in this organelle, hence highlighting the need for further studies to describe the precise involvement of this enzyme in the control of redox balance in plants.

Superoxide dismutases (EC 1.15.1.1; SOD) are ubiquitous antioxidant enzymes encoded by multiple homolog genes which allow the processing of $O_2^{\bullet-}$ to generate H_2O_2 and O_2 (Bowler et al., 1994). SODs are metalloenzymes classified into three groups: FeSOD using iron as a metal cofactor, MnSOD using manganese as a metal cofactor and Cu/ZnSOD containing zinc and copper ion, later one acting as redox cofactor. Interestingly, SODs are localised in different subcellular compartments depending on their catalytic centre. Indeed, FeSODs are specific to the chloroplast (Pilon et al., 2011), whereas MnSODs are found in mitochondria and peroxisomes (Kukavica et al., 2009), and Cu/ZnSODs are found in plastids, peroxisomes, cytosol and apoplast (Kröniger et al., 1992). Moreover, SODs exhibit differential expression and activity during developmental processes and especially in response to abiotic stimuli (Alscher, 2002; Szőllősi, 2014), even going so far as being considered as selection criteria for plant performance for some species (Saed-Moucheshi et al., 2021). Hence, superoxide dismutases are crucial in controlling the cell redox poise by rapidly scavenging superoxide radicals directly on their production site.

TRXs are small ubiquitous enzymes that display a dithiol in their active sites and operate as crucial redox regulators by catalysing a reversible disulphide-bond formation, using reduced ferredoxin or pyridine nucleotides as electron donors, hence monitoring protein structure and activity. Plants present plenty of TRX genes, with 20 identified in *Arabidopsis*, coding for mitochondrial, plastidial, nuclear and cytosolic proteins. TRXs have a myriad of roles in various primary and secondary metabolic pathways (*i.e.*, regulation of Calvin-Benson cycle, chlorophyll and ATP synthesis, transmitting redox signalling, defence against pathogens, etc.) (Geigenberger et al., 2017), and at the same time participate in fruit chilling tolerance (Wu et al., 2016).

PRXs are a large thiol peroxidases protein family, encoded by plenty of different genes, and distributed in all subcellular compartments (Rouhier and Jacquot, 2005). These abundant enzymes participating in multiple functions in redox signalling pathways can be classified into four groups based on their structural and biochemical properties. However, all contain a cysteinyl residue within their catalytic centre allowing the reduction of various peroxides. Next, thioredoxins and glutaredoxins act as electron donors during thiol-disulphide reactions, which regenerate PRX catalytic centre. PRXs are regulated by both transcriptional and post-translational modifications, such as phosphorylation, and play a role in redox metabolism and signalling, thus participating in the plant trade-off between growth and adaptation to the environment (Dietz, 2003; Liebthal et al., 2018, and reference therein).

GRXs, like TRXs, are small ubiquitous enzymes with oxidoreductase activity that catalyse binding of iron-sulfur (Fe-S) clusters and reduction of disulfide bonds using free glutathione as a reducing power supplier. In plants, glutaredoxins are distributed in all cellular compartments and classified into six different classes (Meyer et al., 2008). GRXs participate in the regeneration of antioxidant enzymes such as PRXs, and in the deglutathionylation of proteins, thereby, regulating post-transcriptionally their activity. Besides, GRXs participate in the regulation of iron pools of cells and transduction of redox signalling in response to developmental processes (Hofmann, 2009) in response to environmental stimuli (Rouhier, 2010). Overall, these redoxins are encoded by the multigenic family but display various functions and specie-dependent regulatory pathways. They participate actively in regulating the redox hub by acting at transcriptional, transcriptional and post-transcriptional levels. However, knowledge of the exact mechanism of these enzymes in plants, especially in fruits, is still lacking.

i. ASC-GSH cycle

After discovering ascorbate and glutathione and their role as crucial antioxidants for plant development. Firstly described in 1976 by Barry Halliwell and Christine H. Foyer (Foyer and Halliwell, 1976), the ascorbate-glutathione cycle (also known as the Foyer-Halliwell-Asada pathway) links the

three major redox buffers together in a *ménage-à-trois* allowing rapid ROS processing while maintaining a pool of antioxidants (Foyer and Noctor, 2011).

In brief, ROS react preferentially with GSH and ASC: the latter can reduce H_2O_2 *via* ascorbate peroxidase (EC 1.11.1.11; APX) to produce water and MDHA that will be reduced by MDHAR using NADPH, or be transformed spontaneously in DHA and thus be reduced by DHAR using GSH (Figure I.32). These repetitive redox cycles allow for the regeneration of the pools and the maintenance of the cellular redox buffers in a highly reduced state in most cellular compartments under unstressed conditions. Furthermore, these three major cellular redox buffers display distinct redox potential: -0.1, -0.23 and -0.32 mV for the ASC/DHA, GSH/GSSG and $NAD(P)^+$/NAD(P)H, couples respectively (Figure I.32). In this case, as pyridine nucleotides have a lower redox potential, they will be detrimental for electron transfer to GSH and ASC during redox mechanisms. Thus, pyridine nucleotides are crucial for the regeneration of GSH and ASC through GR and MDHAR enzymes as well as being involved in other metabolic pathways, thereby linking redox homeostasis to central metabolism (Gakière et al., 2018a). This clearly suggests a dynamic redox metabolism during growth as it influences the redox state of pyridine nucleotides and other redox buffers.

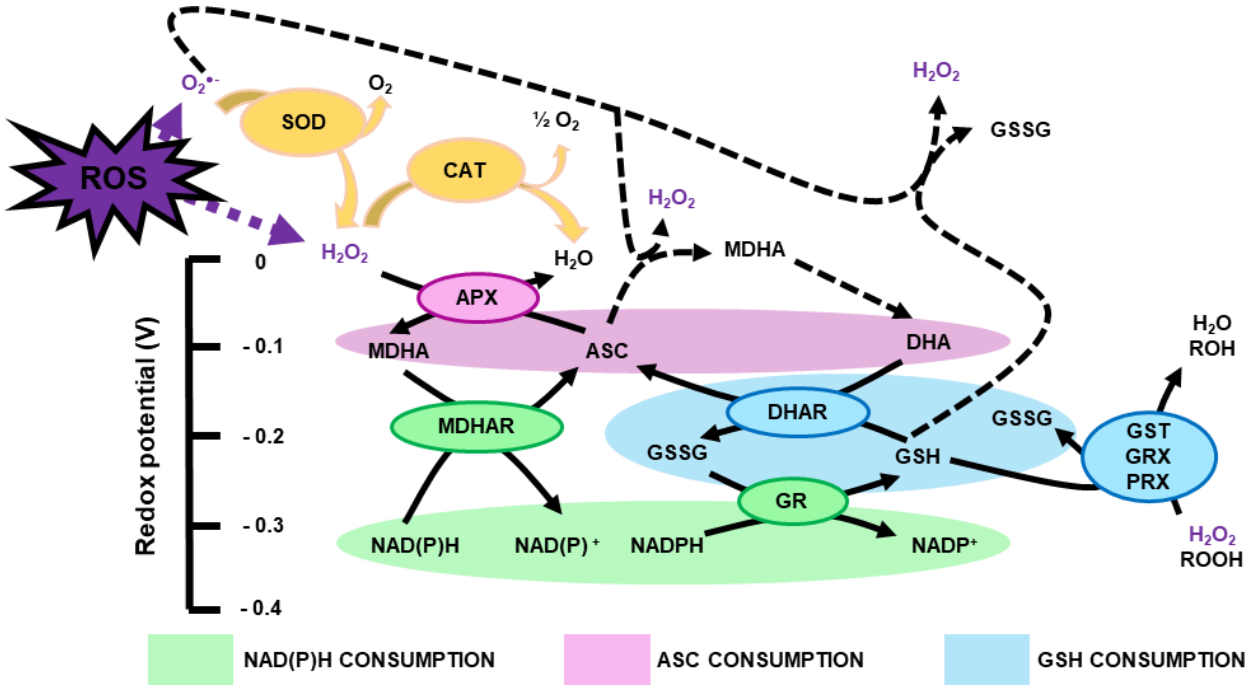

Figure I.32: Major cellular redox buffers: a *ménage-à-trois* to manage ROS. Plain and dashed arrows represent enzymatic and non-enzymatic reactions, respectively.

SOD: Superoxide dismutase; CAT: catalase; APX: ascorbate peroxidase; MDHA: monodehydroascorbate; ASC: reduced ascorbate; MDHAR: monodehydroascorbate reductase; DHA: dehydroascorbate; DHAR: dehydroascorbate reductase; GSH: reduced glutathione; GSSG: glutathione disulfide; GST: glutathione S-transferase; GRX: glutaredoxin; PRX: GRX-dependent peroxiredoxin; GR: glutathione reductase; ROH: organic compound with alcohol group; ROOH: organic compound with peroxide group. From (Decros et al., 2019a).

C. Redox hub and signalling in fruits

The redox hub consists of all the metabolites and enzymes able to generate, process or trigger oxidative signals, whilst the resulting redox signalling can modulate the physiology of fruits (Mittler, 2017; Noctor et al., 2018). Besides, redox status is also pivotal for the control of metabolic processes (Geigenberger and Fernie, 2014). It is assumed that oxidative stress typically comes as secondary stress, or signal, after primary stresses, being abiotic constraints (*e.g.* drought, flooding, wounding, high light, chill or heat stress), or biotic challenges (*e.g.* pest attacks, bacterial and fungal infections). Indeed, the generation of ROS is at the heart of the processes involved in the response of plants to various environmental challenges, and participates in the establishment of adaptive signalling pathways (Noctor et al., 2014). As previously mentioned, ascorbate, glutathione and pyridine nucleotides sit at the top of redox metabolites. In this section, recent advances in our understanding of key spatio-temporal redox signals occurring during developmental processes and in response to environmental stimuli, especially in fruits will be presented.

I. ROS signalling in response to developmental processes

Fruit development can be described in three main phases: cell division, cell expansion and ripening. Young fruits share similarities with leaves because of photosynthetically active chloroplasts driving central metabolism and thus developmental processes (Cocaliadis et al., 2014). Photosynthesis participates in the production of starch, which will be turned into soluble sugars during fruit ripening. It was shown in tomato that the mitochondrial malate valve is of significant importance in relaying redox status to the plastids, which will influence plastidial metabolism (Centeno et al., 2011; Osorio et al., 2013b). In fact, a reduction of malate content in the growing fruit led to enhanced starch and soluble sugar pools by triggering the activation state of AGPase (EC 2.7.7.27) in ripening tomatoes. Interestingly, such metabolic variations tend to provide tolerance of tomato to water loss, wrinkling, and pathogenic infections. This encourages the paradigm of a versatile role of redox signals in metabolic regulation during development and in response to stress (Tian et al., 2013). Another signature of ripening is the transition of chloroplasts to chromoplasts by decreasing green chlorophylls at the expense of coloured antioxidant metabolites such as carotenoids (Martí et al., 2009; Lado et al., 2015). Simultaneously, the expression of photosynthetic genes, both nuclear- and plastid-encoded, declines as the fruit ripens. Furthermore, the accumulation of carotenoids is stimulated by ROS synthesis (Pan et al., 2009), in particular β-carotene, tocopherol and plastoquinone, which build up mainly within lipophilic membranes (Miret and Munné-Bosch, 2015). Nevertheless, epigenetic processes displayed a crucial role in growing tomato fruit as the expression of genes involved in antioxidant biosynthesis (*e.g.* flavonoids, carotenoids) is influenced by DNA demethylation levels (Lang et al., 2017).

Therefore, fruits present considerable discrepancies in redox signalling, their source (*e.g.* chloroplastic, mitochondrial, peroxisomal, apoplastic), and the duration and extent of oxidative stress, during all their development in comparison to leaves (Muñoz and Munné-Bosch, 2018).

The final process of fruit development, ripening, is mediated by redox signalling, which is particularly involved during the chloroplast-chromoplast transition and in mitochondrial metabolism. Indeed, carbonylation of mitochondrial proteins induces an increase in respiration rates when sugar supply becomes limiting, thus affecting the cellular redox state (Qin et al., 2009a; Tian et al., 2013). Fruit ripening is characterised by a progressive increase in oxidative stress, inducing an accumulation of H_2O_2 concomitant with the change in colour of the skin of fruits (Jimenez et al., 2002; Martí et al., 2009; Qin et al., 2009a; Pilati et al., 2014; Kumar et al., 2016). Effectively, there are two peaks of ROS accumulation during fruit ripening: first at the beginning of ripening and then during overripening before or after harvest (Muñoz and Munné-Bosch, 2018). It can be assumed that increased oxidative stress weakens lipid membranes and hence promotes fruit softening, which is beneficial for seed release (Jimenez et al., 2002). Moreover, the observation that short-lived tomato cultivars are subjected to oxidative stress and display lower antioxidant activities (Cocaliadis et al., 2014) reinforces the idea that redox signalling impacts fruit development and storage properties.

ROS production during development induces oxidative signals that need to be processed by the antioxidant machinery to avoid potential cellular damage. For example, the accumulation of H_2O_2 during grape berry ripening is accompanied by an increase in CAT activity (Pilati et al., 2014). In addition, increases in the activities of other antioxidant enzymes such as APX, MDHAR and GR are observed in peach under oxidative stress conditions (Camejo et al., 2010). However, the biological diversity of fruits shows contrasting observations for peroxidase activity. In fact, fruits such as mango, apple and banana show an increase in PX activities while decreasing in fruits such as tomato, strawberry and pepper (Pandey et al., 2012), and references therein). On the other hand, ASC metabolism displays substantial discrepancies in its biosynthesis, recycling and catabolism during fruit development, especially in grapevine (Melino et al., 2009), where it is strongly linked to the accumulation of two derivatives of interest (tartaric and oxalic acids) for the wine industry. In fact, young berries show a rapid accumulation of ASC, mainly in reduced form (reflected by a low ASC/DHA redox ratio). In contrast, mature fruits also show an increased accumulation of ASC, but on the contrary, mainly oxidised (higher ASC/DHA ratio). Furthermore, differential regulation of the DHAR and MDHAR genes is observed during the ripening of acerola, an exotic fruit mainly cultivated for its ASC content (Eltelib et al., 2011). A comparison of ASC metabolism in two citrus species harbouring different ASC contents, mandarin and orange, revealed that the higher ASC content in ripening orange was associated with an increase in its

biosynthesis via stimulation of the expression of genes encoding GME, GGP, L-GalDH and L-GalLDH, as well as reduced ASC degradation activities by ASC oxidase and APX (Yang et al., 2011).

Another elegant work reported a global stimulation of the activity of the enzymes composing the ASC-GSH cycle in mitochondria isolated from ripening tomato fruits (López-Vidal et al., 2016). Recently, a systems biology approach in tomato, combining large-scale multi-omics and phenotypic data for maturing fruit from RNAi lines for three enzymes involved in ASC metabolism (AO, GLD and MDHAR) have been conducted (Stevens et al., 2018). The ASC/DHA ratio has been reported to impact the expression of genes involved in essential cellular functions such as protein synthesis, stability, and ribosomal function. In addition to its redox role, ASC synthesis is also crucial for tomato fruit growth (Garcia et al., 2009; Mounet-Gilbert et al., 2016), as illustrated by the strong growth inhibition of tomato fruits affected in mitochondrial ASC synthesis (Alhagdow et al., 2007). Finally, a recent study modelling protein turnover during tomato fruit development revealed a stage-specific response of redox protein profiles (Belouah et al., 2019). Differences in redox-related proteins occur in the young fruit (*e.g.* SOD, APX) and at ripening (*e.g.* MDHAR, GR), strengthening the role of ASC metabolism that appears crucial for regulating the redox poise and associate signalling during fruit development.

During ageing processes (*i.e.* senescence), oxidative stress occurs and can damage proteins, by targeting mainly methionine (Met) and cysteine, which contain thiols, resulting in conformational changes and thus impairing catalytic functions (Davies, 2005). Met sulfoxide reductase (MSR, EC 1.8.4.11/12) catalyses the reduction of oxidised Met (Emes, 2009; Rey and Tarrago, 2018), which has been reported to decrease the expression of *MSR* genes and thus play a role in litchi fruit senescence (Jiang et al 2017). Along with the regulation of *MSR* genes, mitochondrial antioxidant systems are related to differential carbonylation of mitochondrial proteins in ripening tomato fruits, which may be involved in protein degradation and cellular signalling (López-Vidal et al., 2016). Besides protein targeting, fruit ageing includes other redox-related changes. For instance, postharvest senescence and rotting are characterised by an accumulation of oxidative markers (*e.g.* MDA, ROS) concomitant with a decline of several antioxidant pathways (*e.g.* ascorbate, flavonoids, total phenolics) in the Kyoho grape (Ni et al., 2016). Interestingly, exogenous treatment with hydrogen sulphide could mitigate those redox perturbations by stimulating CAT and APX activities, and by reducing those of lipoxygenase in the pulp and peel of Kyoho grape (Ni et al., 2016).

In addition to central metabolism, more specialised pathways involving phytohormones link to redox signalling and fruit developmental processes (Symons et al., 2012; Leng et al., 2013) as some major antioxidants are involved in phytohormone synthesis pathways. In some fruits such as red raspberry, the ripening stage at harvest conditions the antioxidant contents (*e.g.* anthocyanins, ellagitannins, vitamin C and E, carotenoids) (Beekwilder et al., 2005; Miret and Munné-Bosch, 2016).

Moreover, the application of ascorbic acid after fruit set influences the redox state of ASC in young berries, inducing a more than a two-fold increase of ASC pool in ripe fruit. It was explained by perturbation of ASC oxidation (AO and APX) and recycling enzyme activities (DHAR and MDHAR) (Miret and Munné-Bosch, 2016).

Furthermore, fruit decay is a major issue in post-harvest conditions, caused by perturbation of the redox balance, including ROS production (Pétriacq et al., 2018).

Thus, antioxidant systems (*e.g.* ASC total pool and redox state, ASC-GSH cycle) are key components of fruit growth, which is further supported by the idea that ROS are signalling molecules requiring finely-tuned homeostasis. From an agri-food perspective, further research is required to decipher the involvement of each redox event monitoring fruit development so that efficient strategies can be developed to improve fruit production and storage.

II. ROS signalling in response to environmental constraints

As previously mentioned, abiotic constraints (*e.g.* drought, flooding, wounding, high light, chill or heat stress) or biotic challenges (*e.g.* pest attacks, bacterial and fungal infections) induce oxidative stress. Indeed, ROS production is a central mechanism in response of plants to various environmental changes and is involved in the establishment of adaptive signalling pathways (Noctor et al., 2014). ROS can be produced in the apoplast during biotic and abiotic environmental challenges by NADPH oxidases acting as signalling starting point (Torres and Dangl, 2005; Suzuki et al., 2011; Mittler, 2017). For example, upon cold stress, NADPH oxidases are regulated *via* ethylene and ROS signalling pathways in apple (Zermiani et al., 2015) and strawberry fruits (Zhang et al., 2018). To this day, it is well assumed that major redox couples (NAD, ASC, GSH) are integral regulators of stress responses in plants, including both abiotic and biotic stresses (Pétriacq et al., 2013; Noctor and Mhamdi, 2014; Gakière et al., 2018a; Smirnoff, 2018). For instance, resistance to citrus canker disease in citrus fruit can be induced by exogenous application of NAD^+ (Alferez et al., 2018). Additionally, redox metabolism overcomes hormonal signalling during stress responses, especially by regulating the stress hormones SA, JA and ABA, which are key actors of metabolic adjustments (Leng et al., 2013; Geigenberger and Fernie, 2014; Gakière et al., 2018a). Therefore, a complex signalling network linked with redox metabolism is devoted to designing the fruit stress responses. However, the relation and regulatory pathways between these multiple signalling partners are poorly understood.

As for developmental processes, a hallmark of plant responses to stress is the activation of the ASC-GSH cycle (Figure I.33). A detailed proteomic analysis of tomato fruit reported the implication of proteins, involved in ASC and/or GSH metabolism, in response to various abiotic stress (Marmiroli et

al., 2017). Moreover, upon toxic ion (arsenic and silicon) exposure, tomato fruits cultivars display differential redox discrepancies in ROS and antioxidant metabolite contents (*e.g.* lycopene, carotenoids, phenolics), ASC and GSH redox states, and lipid peroxidation depending on their cultivars (Marmiroli et al., 2017). This results in the proposition of some of these redox alterations (H_2O_2, ASC and GSH redox states, total carotenoids and phenolics) as reliable biomarkers in response to arsenic exposition (Marmiroli et al., 2017).

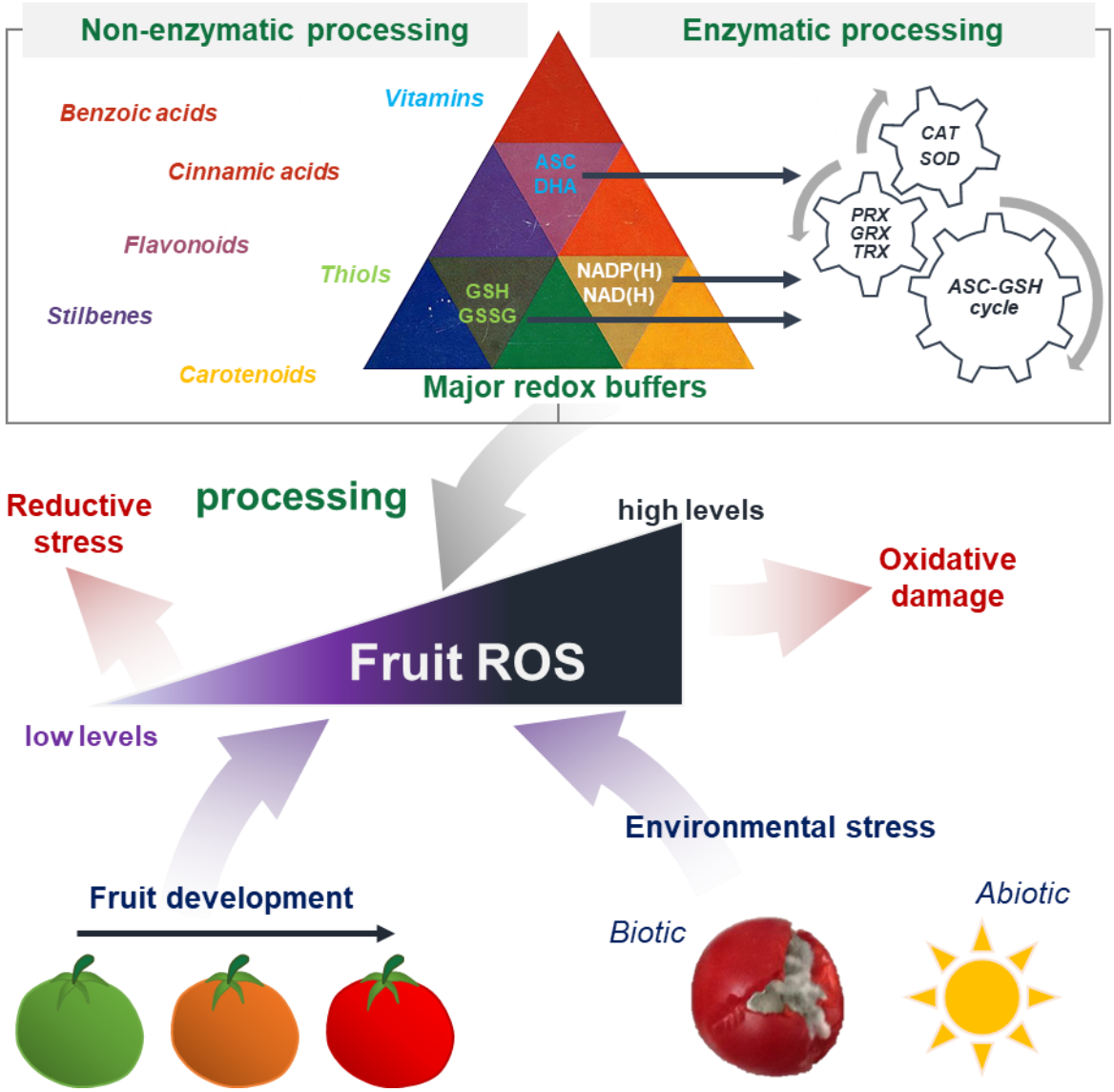

Figure I.33: Redox signalling is pivotal to fruit growth and stress responses. Fruits produce ROS and other redox signals during development and in response to environmental stress. ROS homeostasis is finely tuned between ROS production and processing. This involves several enzymatic and non-enzymatic mechanisms, including antioxidant metabolites and major redox buffers (NAD/P(H), ASC and GSH) that allow antioxidant cycles to process excess of ROS. When ROS levels are too high, the resulting oxidative stress would damage cellular structures. From (Decros et al., 2019a).

Besides arsenic, temperatures, and particularly hot air treatment, directly triggered the induction of ROS-processing enzymes (CAT, APX and SOD) in strawberry fruits, which induce a diminution of lesions caused by the fungal pathogen *Botrytis cinerea* (Jin et al., 2016). Furthermore, a study of cold and light stress in tomato fruit unveils regulation mechanisms of synthesis, recycling and oxidation of ASC by temperature and light in fruit (Massot et al., 2013). In fact, light has been shown to promote ASC and GSH accumulation in tomato fruit, thus supporting the previously reported hypothesis towards a light stimulation of ASC synthesis (Gautier et al., 2009; Massot et al., 2012; Baldet et al., 2013; Smirnoff, 2018). From a post-harvest perspective, fruit redox signalling is associated with physiological impairments under multiple storage conditions, such as for pome fruit, where redox-related metabolites (*e.g.* γ-aminobutyrate: GABA) are prone to accumulate or promptly decrease (*e.g.* ASC, GSH) after exposure to changing air conditions (*e.g.* low O_2 and/or elevated CO_2 environments) (Lum et al., 2016). As a consequence of these redox perturbations, disturbances of the energetic and oxidative balance occur, highlighting the crucial role of pyridine nucleotide redox states as they regulate both GABA and antioxidant metabolism, and which confirms the close relationship between major redox buffers and oxidative metabolism monitoring (Trobacher et al., 2013; Lum et al., 2016). In the context of the transport of agronomical products, interactions between redox metabolism and chilling stress are specifically critical since low temperatures are used to delay the senescence of many fruits, which has been recently reviewed (Valenzuela et al., 2017). In addition, thioredoxin genes have been shown to participate in the regulation of redox poise and improve tolerance to chilling stress in harvested banana fruits (Wu et al., 2016), which is of particular interest for post-harvest issues. New generation sequencing technics allowed the identification of 163 circular RNAs displaying differential expression during chilling stress in tomato fruit. Among them, several ones were predicted to be linked with redox reactions and diverse stress signalling pathways (*e.g.* heat/cold shock protein, energy metabolism, hormonal responses, salt stress, cold-responsive transcription factors) (Zuo et al., 2016).

Pathogens infection of fruits is a burning issue because of the dramatic post-harvest diseases that lead to the loss of 50% of the total production worldwide (Romanazzi et al., 2016; Pétriacq et al., 2018). The fungal elicitor chitosan and the benzothiadiazole (salicylate-mimicking compound) can modulate chloroplastic signals to trigger at transcriptional level various defence responses through redox alterations (*e.g. PX*, *GST*, *GRX*) in strawberry fruits (Landi et al., 2017). Accordingly, chitosan or SA also influences the redox status of the cell (*e.g.* TRX, SOD, PX), as illustrated by transcriptomic analysis of sweet orange (Coqueiro et al., 2015). Another instance validating the use of resistance inducers as promising strategies to elicit fruit biotic responses (Pétriacq et al., 2018), comes from *Peronophythora litchii*-infected litchi fruit, where a chitosan treatment allows a reduction of infection symptoms (Jiang et al., 2018).

Disease tolerance was supported in litchi pericarp by an increase of activities of defensive (chitinase, phenylalanine lyase, glucanase) and ROS-processing enzymes (SOD, CAT and APX), resulting in a lower O_2- generating rate and malondialdehyde pools, as well as a higher content of major redox buffers (ASC and GSH) and reducing power. Besides, a novel phytohormone (β-aminobutyrate; BABA) was shown to regulate antioxidant metabolites (*e.g.* flavonoids, polyphenols) and ABA contents (Wilkinson et al., 2018) and induce resistance against *Botrytis cinerea* in tomato fruit (Thevenet et al., 2017). This resistance was also related to a delay in fruit ripening, suggesting a metabolic trade-off between defence metabolisms and fruit growth.

Altogether, phytopathological studies confirm the implication of redox metabolism in response to pathogen infection by triggering an oxidative burst in infected fruit tissues. The oxidative signal provided by the excess of ROS is monitored by both stimulations of enzymatic antioxidative (ASC-GSH cycle) and non-enzymatic protective, scavenging molecules (Tian et al., 2013). Therefore, induction of antioxidant functions and especially function related to major redox buffers has proven to be successful in controlling post-harvest diseases in fruits (Romanazzi et al., 2016; Pétriacq et al., 2018).

D. Limits in redox studies

As stated in the introduction part, ROS are highly sensitive molecules, and redox reactions can be summarised as an electron transfer between an oxidant and a reductant. Since their discovery, there has been an increasing development of new methods to quantify and/or visualise the distribution of ROS and redox metabolites. However, there are still limitations to the study of redox metabolism and the interpretation of these results. Some parameters such as the subcellular distribution and transport mechanisms of the main antioxidants remain unclear, especially in fruit tissues.

I. Highly reactives molecules

Studying oxidative stress necessarily requires measuring ROS content. Three main categories of methods to estimate ROS can be identified among the numerous protocols available: by monitoring the ROS released in the cell medium (often applied to cell culture studies), by staining tissues allowing the visualisation of ROS distribution *in situ*, and by *in vitro* biochemical assays after extraction. Nevertheless, all these methods display limitations and artefact interferences and must be used with caution for data interpretation.

Moreover, for *in vitro* assays, it is necessary to take great precautions during sampling to avoid as much as possible any oxidative stress due to the handling of the plants, which could impact the ROS concentration and/or the cellular redox state.

Then, limits related to ROS stability, metabolic interference, and specificity remain during sample extraction and assays. Briefly, nitroblue tetrazolium (NBT) and 3,3'-diaminobenzidine (DAB) staining are the most common methods used to study *in situ* localisation and accumulation of $O_2^{\bullet-}$ and H_2O_2, respectively. However, it has been shown that these methods are not specific to ROS as NBT can be reduced by many dehydrogenases (Fridovich, 1997), but other oxidative stress markers can be analysed to validate the interpretation of the results as these methods still reflect oxidative stress *in situ*. *In vitro* assays are mainly restricted to the determination of H_2O_2 because the other ROS are very unstable and cannot be retained during the extraction step. In fact, hydrogen peroxide cannot be extracted using water or neutral buffer because it allows antioxidant machinery to process ROS during sample preparation. Specific acid extraction, inhibiting redox reactions, should be done to enable a proper *in vitro* H_2O_2 assay. In addition, the same precautions need to be taken for antioxidant metabolite assays to measure their redox state (Noctor et al., 2016). Besides, antioxidants encompass a plethora of metabolites either hydrophilic or lipophilic, making it virtually impossible to quantify antioxidants in a tissue fully. However, there are methods to translate this antioxidant capacity into equivalents of known molecules, including the TEAC assay, which allows an estimation of the proportion of hydrophilic and lipophilic antioxidants separately.

II. Subcellular localisation

Another major limitation of the study of redox metabolism is the limited knowledge available about the subcellular distribution and physiological concentrations of ROS and redox buffers within the different subcellular compartments. Indeed, the ROS concentrations observed using *in vitro* assay methods do not consider the distribution of ROS within the cell. It is assumed that under certain stress conditions, ROS can accumulate to very high concentrations, but are confined to a specific space in the cell (*e.g.* apoplast, vacuole, mitochondria, plastids), thus not inducing oxidative stress and redox signalling networks. The same applies to the major redox buffers, which are known to be heterogeneously distributed in the cell, but it is difficult to quantify them within a specific subcellular compartment. Indeed, the fractionation methods do not allow preservation of these metabolites and their redox state even if new emerging methods can bring solutions like non-aqueous fractionation and specific fluorescent probes. There are some examples of redox sensitive GMO lines for GSH and NAD(P) allowing us to investigate *in planta* their subcellular concentrations and redox states (Rosenwasser et al., 2010; Ming et al., 2017; Smith et al., 2021).

However, plants present a great variability between species, organs and tissues requiring specific methods of optimisation and further works on method development.

III. Transport of antioxidants

As stated in part II for the major redox buffers, the transport of antioxidants in plants is poorly documented. Nevertheless, some transporters have been identified but much remains undiscovered in this area. Antioxidant transport is often overlooked in studies of oxidative stress, although apoplastic and symplastic transports of ASC and GSH are partially known in plants. We can also suppose that specific transporters of antioxidants are present in the membrane of organelles as their heterogenic subcellular distribution supposes. However, some isotopic labelling experiments have been carried out, but they are more dedicated to the study of synthesis and catabolism pathways than transport systems (Truffault et al., 2017; Müller-Schüssele et al., 2020). Likewise, redox sensitive fluorescent biosensors are emerging that enable to monitor *in vivo* concentrations and/or redox of major redox buffers such as GSH and NAD(P) (Rosenwasser et al., 2010; Smith et al., 2021). These new technics have provided insight into the involvement of antioxidant transport in development and plant immunity (Elsässer et al., 2020; Feitosa-Araujo et al., 2020). Moreover, modelling appears as a good alternative to validate the hypothesis for transport of antioxidants even if the specific regulations remain to be discovered. Although fluorescent probes cannot quantify the underlying redox fluxes, they provide useful data that can be used to constraint computational models and thus quantify the redox fluxes associated with plant metabolism. Nonetheless, accurate calibration of fluorescent probes is critical for providing reliable quantitative data which remains an issue for redox sensor development (Smith et al., 2021).

Overall, although the current evidence has limitations, it has identified many links and interactions between redox metabolism and plant developmental processes, and during plant response to various stresses. Considering that ROS are now seen as signalling molecules and no longer toxic metabolic by-products, the research interest in redox metabolism has raised during the last decades and suggests that new methods will emerge to overcome these limitations and offer the potential to shed the light on a range of outstanding questions concerning redox metabolism in plants.

E. Integrative modelling of metabolism

The evolution of knowledge and *savoir-faire* in the topic of plant biology has led to the characterisation of plant metabolism as well as its regulation, at different omics levels. This resulted in the accumulation of a considerable amount of information on the physiological processes involved in development. All these data can be used to develop mechanistic models of metabolism able to make meaningful biological predictions (Bordbar et al., 2014; Beauvoit et al., 2018). Several types of models have been used in fruit research: reaction-based (stoichiometric), process-based (biophysical) and enzymatic-based (kinetic). These different models are complementary and can be integrated with each other allowing a better deciphering of fruit biology.

I. Stoichiometric modelling (constraint-based modelling)

Stoichiometric modelling is based on the assumption of a pseudo-steady state and a description of metabolism by stoichiometric reaction equations. A metabolic network is described by reactions, mainly catalysed by enzymes, in which substrates are metabolised into products, keeping the balance of the number of atoms (C, H, O, N and S) and the charge on each side of the equation. By maintaining these equilibrium principles, it is possible to reconstruct genome-wide metabolic networks that allow the distribution of metabolic fluxes in a cell to be estimated. These metabolic networks can be associated with constraints (input and/or output fluxes, minimum and/or maximum reaction rates) to predict the variations of metabolic fluxes and are also called constraint-based models. These models have been used to optimise the production of high-value molecules such as vanillin (Brochado et al., 2010) and lycopene (Alper et al., 2005) in single-cell systems. However, stoichiometric models are poorly developed in more complex systems such as plants that face many challenges, including sub-cellular compartmentalisation and tissue metabolic specificities. Nevertheless, they can predict fluxes, thus offering an interesting alternative to isotopic labelling, especially for fruits, which are very difficult to label (Sweetlove and Ratcliffe, 2011). Over the last decades, a large number of stoichiometric models have been published (Bordbar et al., 2014), including an increasing number of models describing plant metabolism. Stoichiometric models are attracting interest because they can be genome-wide, require few computational resources and overcome some experimental difficulties by using alternative modelling approaches (Shi and Schwender, 2016). For example, in tomato fruit, a stoichiometric model describing central metabolic fluxes throughout development, including a detailed description of respiratory metabolism, has been used to highlight the role of alternative oxidase and uncoupling proteins in fruit ripening (Colombié et al., 2015, 2017). This constraint-based modelling approach is a promising tool for estimating fruit respiration, which is difficult to measure directly on plants. Moreover, the flow analysis and modelling of a series of plant systems have shown that the supply of metabolic

inputs and the request for final products are major regulators of metabolic flows (Sweetlove et al., 2013). Thus, the use of constraint-based models could be very beneficial in developing our knowledge of the links between metabolism and fruit performance traits such as nutritional quality, taste and growth rate. This could allow, for example, the identification of genetic loci associated with fluxes, thus leading to the characterisation of genes involved in their control and ultimately to new selection strategies.

II. Kinetic modelling (enzymatic modelling)

Enzymatic kinetic model allows the reactions constituting a metabolic network to be described as a set of ordinary differential equations (ODEs). With the help of experimental data, this leads to the calculation of fluxes and the prediction of metabolite concentrations in the metabolic network. In addition, kinetic models allow the importance of each enzymatic step in regulating fluxes to be estimated. Thus, candidate enzymes can be identified that could be targeted to influence metabolism in the desired way (Rohwer, 2012). Robust experimental data on enzymes and metabolites are essential for building kinetic models, which explain why few validated kinetic models, especially in plants, are available (Rohwer, 2012; http://jjj.mib.ac.uk/ and http://www.ebi.ac.uk/biomodels-main/), despite their great potential. The development of an enzyme-based kinetic model requires several types of knowledge: (i) the topology of the reactions within the metabolic network and the enzymatic parameters of the enzymes involved; (ii) the cellular composition of accumulated metabolite cofactors; and (iii) the subcellular compartmentalisation (Schallau and Junker, 2010; Rohwer, 2012). Thus, it allows expressing fluxes using enzyme kinetic rate laws such as Michaelis-Menten and other ad hoc laws (Cornish-Bowden, 2004; Liebermeister and Klipp, 2006) based on the concentrations of reagents and kinetic properties of enzymes. Since enzyme capacities may vary during fruit development due to metabolic reprogramming (Biais et al., 2014), they must be determined experimentally. On the other hand, kinetic constants can be taken from the literature as well as from experimental measurements. Finally, the validation of these models requires independent data sets obtained, for example, with transgenic lines (Figure I.34) (Beauvoit et al., 2014). For example, during tomato fruit growth, an enzymatic model of sucrose metabolism highlighted the role of invertase and tonoplastic sugar transporters in controlling the osmotic pressure of the vacuole and thus in the regulation of the growth of the developing tomato fruit (Beauvoit et al., 2014). This model also allowed to test the physiological relevance of previous hypotheses. For example, the feedback inhibition of acid invertase and glucokinase, on the one hand, and the proton coupling mechanism of tonoplast transporters, on the other hand, were found to be essential to accommodate the experimentally measured sugar content throughout tomato fruit development (Beauvoit et al., 2014). Nevertheless, one of the challenges in building realistic kinetic models is the relatively small size of the networks, the rarity of data on enzymes, their post-translational modifications, and robust validation data sets (Beauvoit et al., 2018).

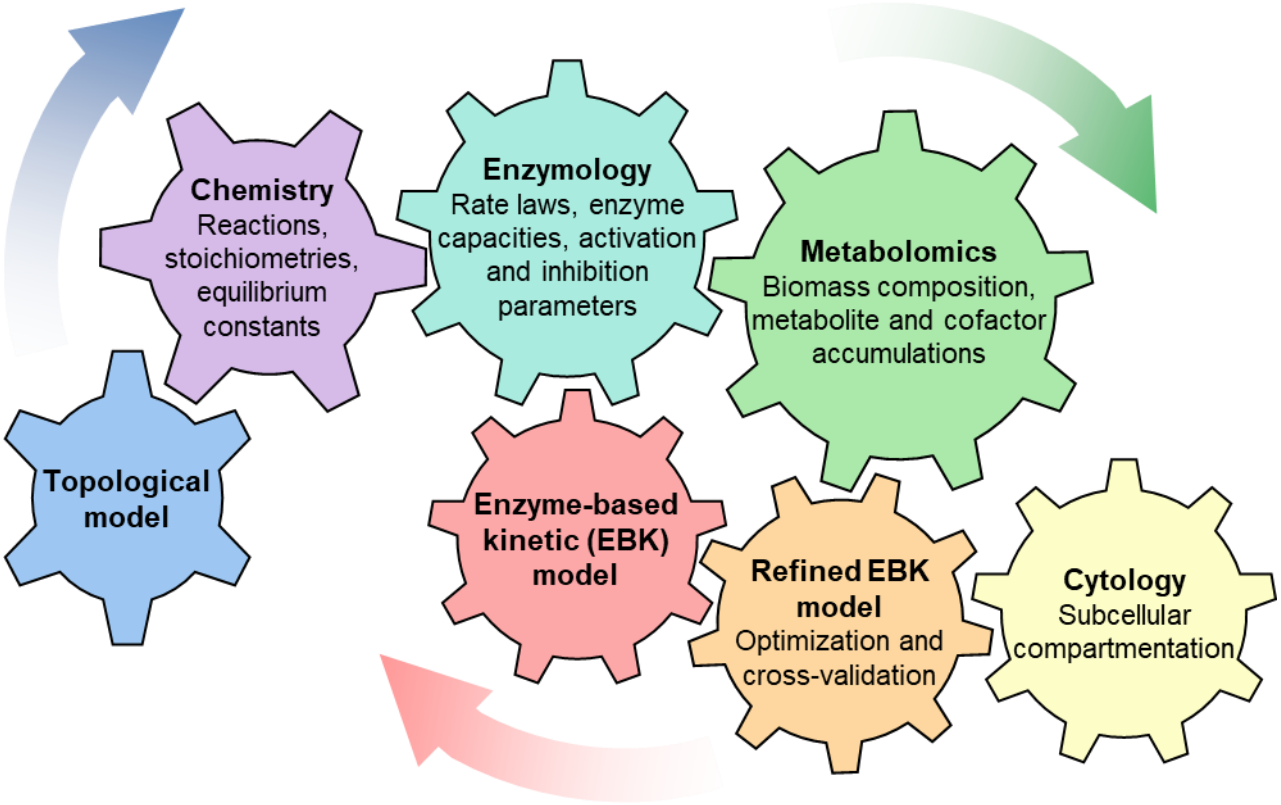

Figure I.34: Schematic representation of a data integration pipeline during construction and refinement of an enzyme-based kinetic (EBK) model.

Chemical information gives a structural framework describing the model topology. It is composed of chemical compounds connected through reactions and thermodynamic constants. The structural model is further enriched by enzyme data, which constrain the kinetic model. Enzyme rate laws are connected through a set of ordinary differential equations parameterized by numerous kinetic constants, e.g. enzyme capacity (Vmax), Michaelis–Menten constants (K_M), as well as activation and inhibition constants. The enzyme-based model is further realistically constrained by metabolomics, first by giving access to co-factor concentrations and output fluxes, and secondly by enabling model parameterization via least-square fit of experimentally determined metabolites. Ultimately, independent data sets, when available, can be used to cross-validate the refined model. An additional layer of information is provided by cytological data. Thus, knowing the volume fraction of subcellular compartments and implementing the model with carriers and enzyme isoforms located in different compartments allows the model to calculate local concentrations and fluxes. From (Beauvoit et al., 2018)

III. Process-based modelling

Process-based models describe the interactions between the different components of a system causally. These models allow the quantification of plant responses to different factors (genetic and/or environmental), thus allowing the dynamic simulation of physiological processes, which is very useful for agronomic applications (van Ittersum and Donatelli, 2003). However, not all processes involved in fruit performance can be integrated into this type of model. Nevertheless, there are models to study fruit yield and composition in response to various environmental conditions (de Jong et al., 2011) and agricultural practices (Louarn et al., 2007; Da Silva et al., 2011), thanks to a detailed description of the processes involved in the control of plant architecture. Another functional/structural model, developed in tomato, showed that fruits show compositional variations according to plant age and fruit position in the plant and also within the truss, by simulating carbohydrate concentration and water potential within the plant through modelling photosynthesis and leaf transpiration during plant development (Baldazzi et al., 2013). In addition, a virtual fruit model, integrating the major processes involved in fruit performance into a single system (Lescourret and Genard, 2005; Martre et al., 2011), has been applied to various species and provide the simulation of many conditions and the formulation of new hypotheses. For example, this model predicts that increased import of sugars into the fruit leads to an increase in the amount of water accumulated in the fruit, which in turn causes an increase in fruit size. However, this increase in fruit size through water supply leads to a dilutional decrease in the concentration of sugars in the fruit. Finally, these different models are complementary. The integration of process-based models with more mechanistic models represents an exciting alternative to identify the variables with the greatest impact on a trait of interest and thus improve fruit performance.

IV. Integrative modelling

Fruit performance depends on an integrative system that combines metabolic networks and biophysical processes at different levels of the plant. Only process-based modelling considers environmental variables, unlike mechanistic models of metabolism. Integrative models have several interests (Baldazzi et al., 2012). Firstly, it would allow linking environmental variables, agricultural practices or the developmental stage of the plants with omics data. Secondly, these models will make it possible to highlight the interactions between different plant organs and/or tissues during plant development (Chew et al., 2014). In short, integrative model development between process-based models and the genetic basis of metabolism could lead to powerful tools for deciphering key regulators of processes involved in fruit quality (Struik et al., 2005) (Figure I.35).

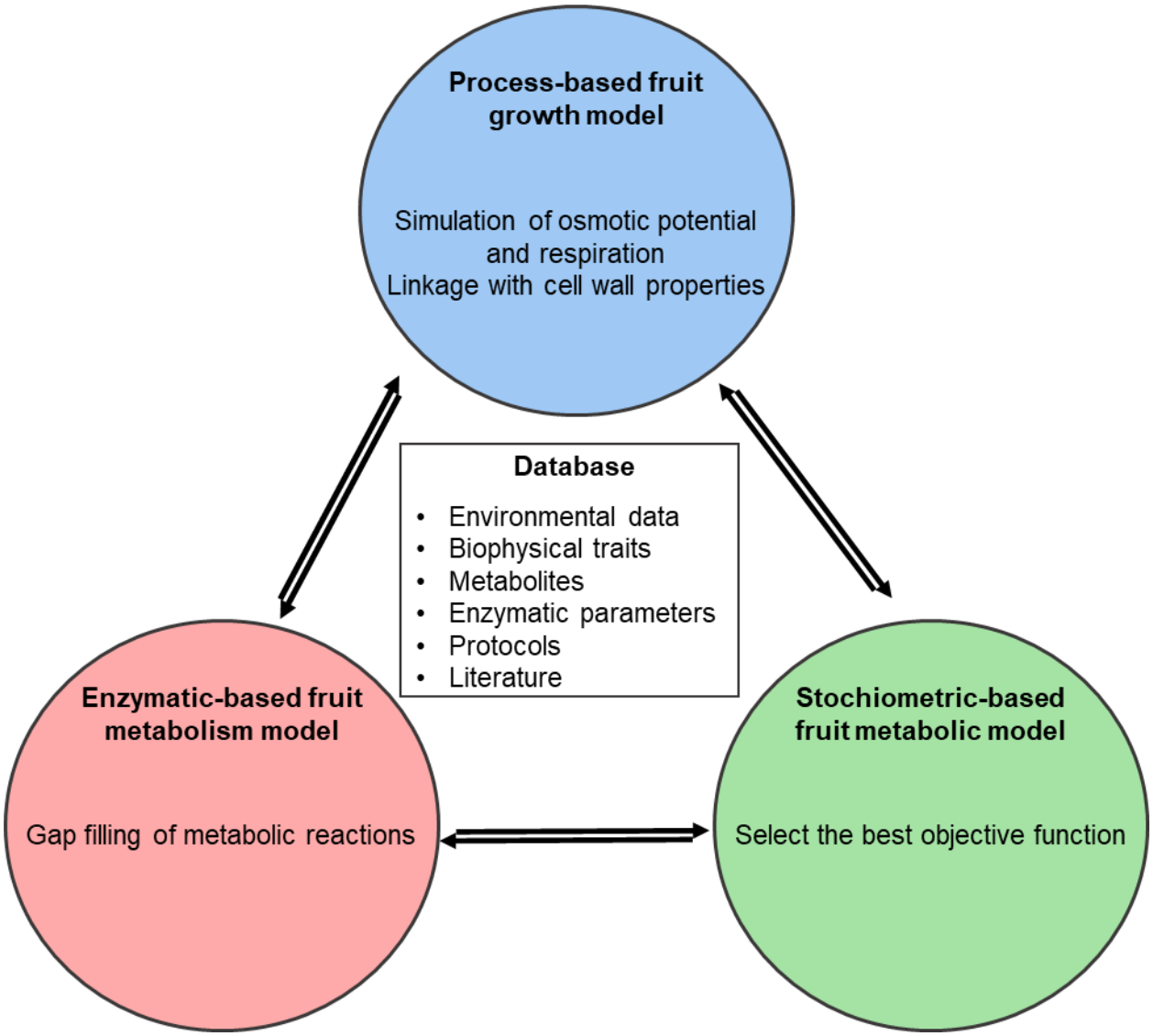

Figure I.35: Fruit model comparison and integration.

The comparison of common variables enables cross- validation. The arrows indicate examples of potential benefits that will be obtained by comparing or coupling kinetic, stoichiometric and/or process-based models describing fruit growth and metabolism. Model integration necessitates the archiving of data in common or translatable formats. Common variables are summarized in the box between the models. Adapted from (Beauvoit et al., 2018).

For instance, the integration of a kinetic model concerning sugar dynamics into a process-based model of central metabolism would highlight the steps (enzymatic and/or transport) that most influence a trait of interest (Fishman and Génard, 1998; Beauvoit et al., 2014). Finally, it can be assumed that the integrated models will enable *in silico* analyses of the interactions between the biophysical properties of the fruit and the distribution of metabolic fluxes, which will provide valuable clues for metabolic engineering. For instance, enzyme-based kinetic models can be used to obtain data for osmolyte concentrations (*i.e.* sugars and organic acids), which can then be used to improve simulations of the osmotic potential and its link with cell wall properties in process-based models.

Thereafter, both kinetic and stoichiometric models can be used to improve flux simulations for, for example, carbon influx or respiration within process-based models. In turn, process-based models can be used to constrain input and output variables (*e.g.* carbon influx and fluxes) towards biomass components (Figure I.35). Such constraining also makes it possible to study the effects of environmental variables such as temperature, light and watering on metabolic networks.

Overall, these integrative models could be a great asset for breeding by defining the most important parameters and could lead to the design of ideotypes (Constantinescu et al., 2016; Zhu et al., 2016; Chenu et al., 2017). However, these integrative models require a large amount of data using various omics technics. Nowadays, no integrated fruit model linking detailed fruit metabolism to biophysical fruit growth has been developed yet (Beauvoit et al., 2018).

Objectives of the PhD project

The change of paradigm in redox biology, considering ROS as finely-tuned signals modulating plant metabolism, shed new light on redox networks, especially in plants where multiple sources of ROS are possible and associated with many "ROS processing systems" (Noctor et al., 2018), while major redox buffers (*e.g.* ASC, GSH and NAD) clearly appear at the forefront of oxidative regulations. ROS production and redox signals arising from are crucial to harmonious metabolism and participate in adaptive signalling pathways throughout development and in response to the environment. In parallel, the development of mathematical integrative modelling permitted by new approaches providing quantitative description through metabolic fluxes.

Progress in understanding the molecular signatures involved in the redox regulations controlling the trade-off between fruit development and stress pathways will help to define novel strategies for optimal fruit production and storage (Beauvoit et al., 2018). However, knowledge on redox biology in fruit is sparsely documented, although principles originating from leaves tissues are valuable while waiting for comprehensive studies that provide more extensive knowledge on fruits.

In this regard, my PhD project aims to provide the first quantitative description of core redox metabolism in a developmental context while developing and implementing protocols allowing the rapid quantification of major redox compounds. In addition, the use of an integrative modelling approach will allow deciphering the implication of redox flux in the control of redox balance during fruit development.

For this purpose:

1. A multiscale omics study focusing on NAD metabolism during tomato fruit development provides a better view of the implication of NAD metabolism in redox and central metabolism,

2. Major redox buffers and total antioxidant capacity are assessed using targeted biochemical analyses of the ascorbate-glutathione cycle, while untargeted LC-MS analysis provides a global comparison of developmental stages. Furthermore, mutant plants enriched in ascorbate have been analysed to study the impact of an increase in ASC on tomato fruit,

3. The data sets obtained are finally used to develop a kinetic-based model of the ASC-GSH cycle, allowing the investigation of redox fluxes and their regulation during tomato fruit development.

Besides, I participate in developing a redox platform to implement at Bordeaux Metabolome Facility, allowing me to participate in some other projects, such as the characterisation of new NAD kinase (Dell'Aglio et al., 2019) and the characterisation of ASC-enriched mutants (Deslous et al., 2021). I also had the opportunity to participate in the writing of reviews aiming to bring together the scattered knowledge available on redox metabolism in fruits and in response to extreme environments (Dussarrat et al., 2021). Furthermore, the preliminary data obtained allowed the designing of new projects more focused on the involvement of redox metabolism during the fruit setting phase. To this end, different ASC mutant fruits have been analysed at several flower and young fruit stages.

CHAPTER II

MATERIALS AND METHODS

A. Plant material and growth conditions

I. Plant material and Growth Conditions for fruits used in chapter III

Tomato fruit pericarps were obtained from Solanum lycopersicum L. var. Moneymaker as previously described (Biais et al., 2014). Briefly, tomato plants were grown under usual production greenhouse conditions in southern western France (44°23′56″N, 0°35′25″E) from June to October, using a nutrient solution (detailed in (Biais et al., 2014)) to adjust plant growth and water supply to the climate via a drip irrigation system that maintained 20–30% drainage (pH adjusted to 5.9, electrical conductivity to 2.2 $mS.cm^{-1}$). Flower anthesis was monitored on trusses 5, 6 and 7, and fruits were harvested at nine developmental stages (thereafter referred to as GS1 to 9), at about 8, 15, 21, 28, 34, 42 (mature green), 49 (turning), 50 (orange) and 53 (red ripe) days post anthesis (dpa). Seeds, jelly and placenta were first removed for each fruit, and the resulting pericarp was cut into small pieces, which were immediately frozen in liquid nitrogen. Pericarp samples were ground to powder and stored at -80 °C until further analysis.

II. Plant material and Growth Conditions for fruits used in chapter IV and V

Tomato fruit pericarps were obtained from *Solanum lycopersicum L.* var. M82 under its determined form. Ascorbate-enriched plants from Micro-Tom were characterised in (Deslous et al., 2021). Briefly, ethyl methyl sulfonate (EMS) mutants were obtained using the *Solanum lycopersicum L.* var. MicroTom cultivar and characterised through two previous PhD works carried out in our laboratory (Thèses C. Bournonville, 2015 and P. Deslous 2018 (Deslous et al., 2021). ASC-enriched EMS mutant plants harbouring the causal mutation responsible for the phenotype were out-crossed with *Solanum lycopersicum L.* var. M82 during 6 generations (OC6) to obtain plants ASC^{+} phenotype in M82 genetic background with a negligible proportion of MicroTom genome (<2%). Besides CRISPR-Cas9 plants mimicking the causal mutation identified in the EMS line were also generated and out-crossed with *Solanum lycopersicum L.* var. M82 during 3 generations (OC3) allowing to obtain a M82-like phenotype enriched in ASC. After sowing, OC3F1 and OC6F1 seeds resulted in the culture WT-like plants (50%) and heterozygous plants (50%). Both out-crossed lines with original EMS- and CRISPR-lines were cultivated together with the WT M82 plants as well as the WT-like plants from the two out-cross progeny which we defined as control and the whole at the same period and same green house. For this experiment and the following analyses, each plant line (Mutants, WT M82, WT-like from both EMS and CRISPR crossed lines) and their corresponding fruits have been used individually. Remarkably, no difference was observed between the WT M82 and these WT-like in term of plant growth, fruit growth as well as metabolite content. Thus, to simplify the results presentation, data from

mutant lines have been pooled and compared to, what we consider as the more relevant reference that is the real WT M82 to build figures.

Tomato plants were grown under usual production greenhouse conditions from February to July, using long day photoperiod (16h day/ 8h night) and a temperature of 25°C during days and 20°C during nights. Plants were randomised on 2 tables of 24 plants allowing to distribute at least nine plants for each genetic condition.

III. Flower pollination and monitoring of fruit age

The pollination was carried out by gentle vibration of the fully opened flower at anthesis, corresponding to the self-pollination process for control and wild-type plants. For the ascorbate-enriched plants, which are impaired in pollen fertility and thus in self-pollination, flower emasculation was performed at the anthesis stage. Then, pollen from flowers of WT plants were used and thoroughly applied to the stigma by scraping the inner face of a fully opened anther cone or using a brush. To ensure the cross-pollination, this operation was repeated at least three times on the same emasculated flower. This operation allows the presence of pollen grains on stigma, then growth of pollen tubes in the style to reach the ovules inside the ovary leading to the set-up of fruit development process.

The age of fruit was recorded by tagging flowers on the day of their fertilization and the corresponding age was calculated for harvesting.

B. Harvesting conditions

Fruits were harvested according to their fertilisation tag, for anthesis and 4 DPA stages, fruits were entirely frozen while for other stages, a 1cm thick central strip in the fruit pericarp was harvested, cut into approximatively 2 mm sections and frozen immediately in liquid nitrogen in scintillation tubes (Polyvials V, Natural high-density polyethylene, 20 ml). Harvesting have been performed as quickly as possible to preserve redox metabolites. For each line and each stage, 3 vials containing at least three fruits from different plants within the line was collected. All further analyses have been conducted using the three biological replicates (n = 3).

C. PCR genotyping and sequencing

I. Genomic DNA extraction

Genomic DNA extraction is performed from young leaves or fruit pericarp (approx. 30 mg) frozen in liquid nitrogen and ground in 96-well plates with a tungsten ball using the Retsch MM300 grinder 2 times during 1 min at 25 Hz.sec^{-1}, inverting the plate between the two grinds. Once ground, the samples were centrifuged for 1 min at 5000 g (4 °C) and then 250 µL per tube of µPrep buffer (0.35 M sorbitol; 0.2 M Tris Base; 25 mM Na2EDTA; 2 M NaCl; 2% CTAB; Sarcosyl 5% (w/v); Bisulfilte 0.33%) was added. The tubes were homogenised in a grinder 2x30 sec at 25 Hz.sec^{-1} and then placed in a water bath at 65 °C for 1 hour, homogenising regularly by inversion.

After one hour, 225 µL of chloroform/isoamyl alcohol (24:1 v/v) were added and the whole was homogenised by manual inversion then centrifuged for 10 minutes at 5000 g at 20 °C. The aqueous phases are collected in new tubes and 250 µL of cold 100% ispropanol is added and homogenised by inversion until the DNA precipitates. Once precipitated, the tubes are centrifuged for 10 minutes at 5500 rpm at 4 °C, the ispropanol is removed and the pellets are rinsed with 250 µL of 70% ethanol. Finally, the tubes are centrifuged for 10 minutes at 5000 g at 4 °C, the ethanol is removed by inverting the tubes and the pellets are speedvac dried for 15 minutes at 65 °C. The pellet is finally recovered in 50 µL of mQ water and stored at -20 °C.

II. PCR reactions and sequencing

Routine PCR reactions were performed with GoTaq® DNA Polymerase (Promega) according to the conditions recommended by the supplier using purified gDNA or cDNA. For pre-sequencing amplification and cloning, PCRs were performed with the Q5® High-Fidelity DNA Polymerase kit (BioLabs) or the PrimeStarMax kit (Takara) to minimise the risk of sequence errors. The targeted DNA sequence responsible for the ASC-enriched phenotype (Upstream Open Reading Frame; uORF) was amplified using a specific forward primer, containing the SNP of the causal mutation: P17C5_WT_F1 (TTCTGAAGGTGGTAGTCCTG**C**) and P17C5_Mut_F1 (TTCTGAAGGTGGTAGTCCTG**T**) for WT and mutant, respectively. The same reverse primer for both WT and mutant was used: P17C5_WT_R1 (GAGATTCCTTTGTTTCATCGG).

Then, PCR results were further validated by sequencing using primers amplifying GGP DNA region (VTC2): VTC2seq_F1 (TAAACCGCCGACCACTTTTU) and VTC2seq_R1 (GGAACCCTCTTAATTTTGAGCA) *via* Eurofins company.

D. RNAseq and LC-MS/MS proteomics of developing tomato fruit

RNA and proteins were extracted and analysed as described previously (Belouah et al., 2019) by RNAseq (GeT-PlaGe core facility, INRA Toulouse, France, http://get.genotoul.fr) and LCMS/MS-based proteomics (PAPPSO, INRA Moulon, France, http://pappso.inra.fr/index.php), respectively.

I. RNA extraction and RNAseq analyses

Briefly, total RNA was isolated from frozen tissue powder of tomato pericarp using plant RNA Reagent (PureLink kit, Invitrogent) followed by DNase treatment (DNA-free kit, Invitrogen) and purification over RNeasy Mini spin columns (RNeasy Plant Mini kit, QIAGEN), according to the manufacturer's instruction. RNA integrity was assessed using the RNA 600 Nano kit with a Bioanalyzer 2100 system (Agilent Technologies). RNAseq was performed at the GeT-PlaGe core facility, INRA Toulouse (France). RNAseq libraries were prepared according to Illumina's protocols using the TruSeq Stranded mRNA sample prep kit to analyse mRNA. Library quality was assessed using an Agilent Bioanalyzer and libraries were quantified by quantitative PCR (qPCR) using the Kapa Library Quantification Kit. RNAseq experiments were performed on an Illumina HiSeq2000 or HiSeq2500 (2x100 bp).

II. Protein extraction and quantification

Total proteins from tomato pericarp were extracted as in (Faurobert et al., 2007). LC-MS/MS analyses were performed with a NanoLC-Ultra System (nano2DUltra, Eksigent, Les Ulis, France) coupled with a Q-Exactive mass spectrometer (Thermo Electron, Waltham, MA, USA) as in (Havé et al., 2018). For each sample, 800 ng (4 µl from a 0.200 ng.µl^{-1} solution) of protein digest were loaded onto a Biosphere C18 pre-column (0.1 × 20 mm, 100 Å, 5 µm; Nanoseparation) at 7.5 µl.min^{-1} and desalted with 0.1% (v/v) formic acid and 2% ACN. After 3 min, the pre-column was connected to a Biosphere C18 nanocolumn (0.075 × 300 mm, 100 Å, 3 µm; Nanoseparation). The raw MS output files and identification data were deposited online using the PROTICdb database (http://moulon.inra.fr/protic/tomato_fruit_development).

Protein identification was performed using the protein sequence database of *S. lycopersicum* Heinz assembly v 2.40 (ITAG2.4) downloaded from https://solgenomics.net/ (34,725 entries). A contaminant database, which contains the sequences of standard contaminants, was also interrogated. Criteria used for protein identification were (1) at least two different peptides identified with an E-value smaller than 0.01, and (2) a protein E-value (product of unique peptide E-values) smaller than 10^{-5}.

Using reversed sequences as a decoy database, the false discovery rate for peptide and protein identification were respectively 0.05% and 0%.

E. Data analysis of mRNA and protein profiles

Datasets consisted of 22,877 transcript and 2,375 protein profiles and were made publicly available via GEO repository (Barrett et al., 2013) with the accession number GSE12873 (https://www.ncbi.nlm.nih.gov/geo/query/acc.cgi?acc=GSE128739) for the transcripts. The proteomics data have been deposited to the ProteomeXchange Consortium via the PRIDE (Perez-Riverol et al., 2019) partner repository with the dataset identifier PXD012877.

Prior to uni- and multivariate statistical analyses, mRNA and protein data were pre-processed to normally distributed data by performing median normalisation, cube-root transformation and Pareto scaling of the data intensities as described previously (Belouah et al., 2019). Normalised datasets were then used to construct score plots of Principal Component Analysis (PCA) for transcriptomic and proteomic overview using MetaboAnalyst v 4.0 (http://www.metaboanalyst.ca/), or dendrograms of clustering analysis by Pearson's correlation with complete clustering linkage using MeV v 4.9.0 (http://mev.tm4.org/). Significant markers of both transcripts and proteins were determined by ANOVA after discarding false positives ($p < 0.01$ corrected for multiple testing by Bonferroni method). Transcript and protein features of NAD-dependent functions were selected by identifying domains (InterPro and GO) that were annotated to bind or process pyridine nucleotides using Assembly v 2.40 (ITAG v 2.4) from SolGenomics (https://solgenomics.net/) and UniProt (https://www.uniprot.org/). Datamining of publicly available gene expression data was conducted using Tomato Expression Atlas (http://tea.solgenomics.net/) (Fernandez-Pozo et al., 2017). Functional annotation of mRNA and protein markers was performed based on gene ontology using Mercator4 v1.0 (https://plabipd.de/portal/mercator4/) (Schwacke et al., 2019).

F. Sample preparation for targeted and untargeted biochemical assays

I. Grinding and storage

The samples were stored in scintillation tubes (20ml HDPE Polyvials® V, Zinsser Analytics) and ground under cryogenic conditions (liquid N_2) using the Genogrinder 2010 Mixer Mill at 30 Hz for 30 sec. The operation was repeated 2 to 3 times, separated with cooling sessions, depending on the samples. The grinding was done using three 8 mm diameter steel balls (BI08263 AISI 440C, CIMAP). The powders were then stored at -80 °C.

II. Lyophilisation of samples for untargeted metabolomic

The powders are vacuum freeze-dried using the PILOTE COMPACT freeze-dryer (Cryotec) in successive temperature steps over 5 days according to the following schedule:

Temperature (°C)	-20	--20	-10	-10	0	0	10	10	20	20
Duration	20 min	14 hours	20 min	14 hours	20 min	16 hours	20 min	15 hours	20 min	18 hours

The freeze-dried powders are then stored at -20°C in sealed bags containing Silica gel.

III. Extraction for targeted metabolite assays

For the absolute quantification of glucose, fructose, sucrose, citrate, malate, starch and soluble protein, 20 (± 3) mg of fresh ground material was weighed under cryogenic conditions, randomised onto roboracks (MP32033L, Micronic) and robotically extracted (Star 96 ML 6649, Hamilton).

In the first step, 250 µL of 80% ethanol, containing 10 mM HEPES/KOH buffer pH 6 is added to the frozen powders. The tubes were then agitated and heated for 20 min at 80 °C and centrifuged for 5 min at 2916 g (Centrifuges 5810R, Eppendorf). The first supernatant (S1) was transferred to a new Micronic tube and stored at 4 °C protected from light. The second extraction was performed on the pellet by adding 150 µl of the same solution and incubated at 80 °C for 20 min. After centrifugation, the second supernatant (S2) was added to S1 and stored at 4 °C protected from light. A third and final extraction is performed on the pellet by adding 250 µl of 50% EtOH, containing a 10 mM HEPES/KOH buffer solution pH 6 and the extract is incubated at 80°C for 20 min. After centrifugation, the third supernatant (S3) was added to the other two (S1 + S2). The supernatants (S1+S2+S3), as well as the pellets, were stored at -20 °C pending analysis of metabolites, starch and soluble proteins.

IV. Extraction for redox metabolite assays

Extraction of major redox buffer in their both oxidised and reduced form requires performing two different types of extraction adapted from (Queval and Noctor, 2007; Noctor et al., 2016).

1. Acidic extraction

Extraction of total ASC, total GSH, NAD^+ and $NADP^+$ was performed using 0.1 M HCl and with a ratio of 10 mg of ground fresh weight for 100 µL. The tubes are then shaken vigorously and centrifuged for 10 min at 12,000 g at 4°C. Then the supernatant will be split into three: (i) directly used for ASC assay, (ii) heat at 95 °C during 5 min and used for $NAD(P)^+$ assays and (iii) a further neutralisation step is required for GSH. Indeed, 200 µL of supernatant was neutralised using 50 µL of sodium phosphate buffer pH 5.6 and 15 µL of 1 M NaOH solution, to obtain a final pH of the supernatant about 4,5-5 (Figure II.1)

2. Basic extraction

Extraction of NADH and NADPH was performed using 0.1 M NaOH and with a ratio of 10 mg of ground fresh weight for 100 µL. The tubes are then shaken vigorously and centrifuged for 10 min at 12,000 g at 4°C. The supernatant was then incubated at 95 °C for 5 min to allow the degradation of the remaining oxidised forms.

V. Extraction for enzymatic assays

Extraction of soluble enzymes was performed using 20 to 50 mg of ground fresh material, depending on the growth stage, to which approximately 20 mg of insoluble PVPP was added to neutralise polyphenols. 500 µL of extraction buffer containing 20% glycerol (v/v), 0. 25% BSA (v/v), 1% triton (v/v), 50 mM HEPES/KOH buffer pH 7.5, 10 mM MgCl2, 1 mM ethylenediaminetetraacetic acid (EDTA), 1 mM egtazic acid (EGTA), 10 mM leupeptin are added to each tube. The tubes are then shaken vigorously and centrifuged for 10 min at 2916 g (5810R centrifuge, Eppendorf) at 4 °C. The supernatants are then collected, a portion of undiluted extract is retained and a portion of the supernatants is diluted 2, 4 or 8 times with extraction buffer to assay enzyme activities. Chemical standards are also included to check recoveries. Adapted extraction buffer for ascorbate peroxidase (APX) adding 10 mM sodium L-ascorbate.

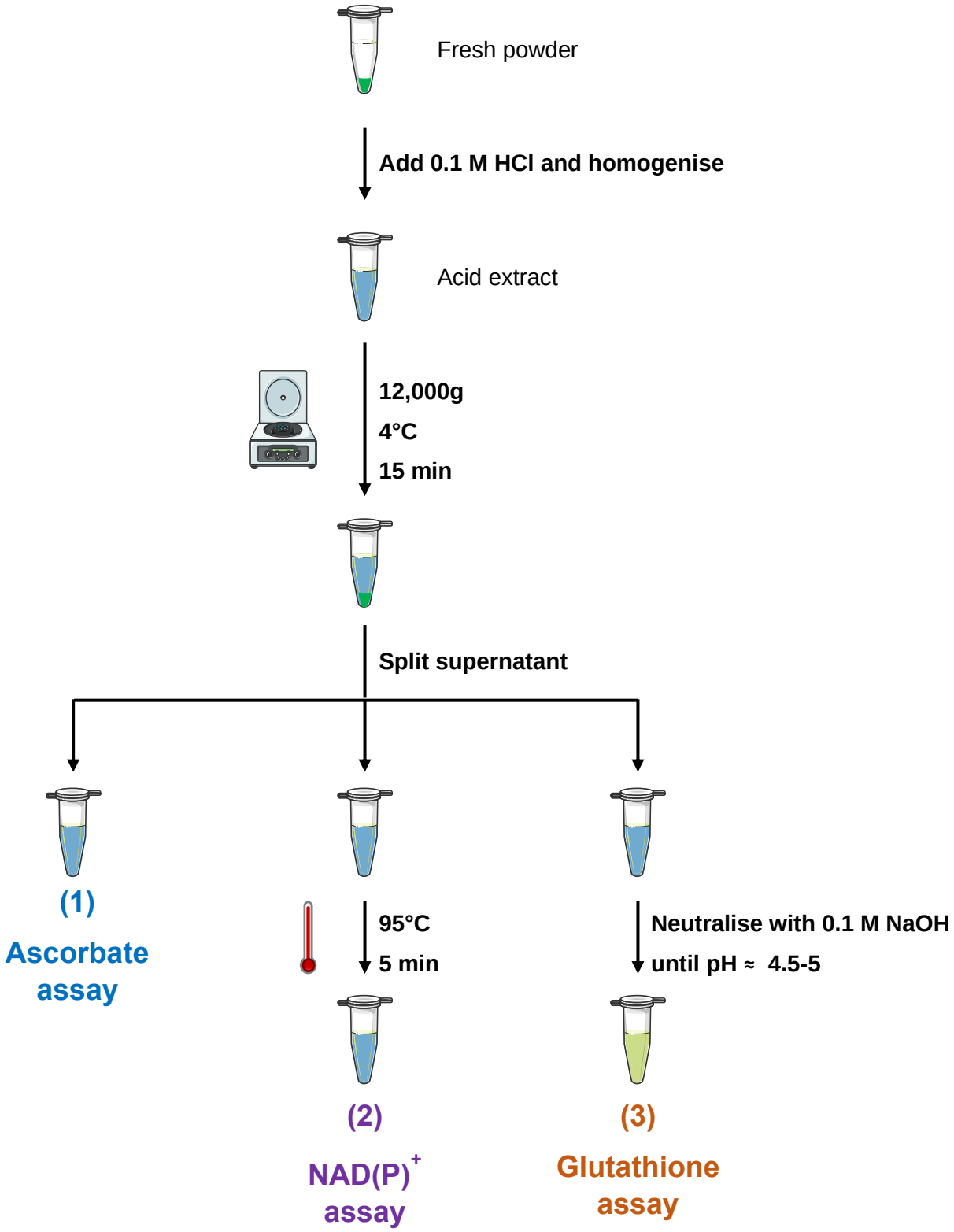

Figure II.1: Schematic view of acidic extraction for biochemical redox profiling.

VI. Extraction for untargeted LC-MS analysis

Twenty milligrams of each dried sample were weighed into 1.1 mL-micronic tubes (MP32033L, Micronic, Lelystad, Netherlands) and randomised onto a 96-micronic rack (MPW51001BC6, Micronic, Lelystad, Netherlands). Each rack also contained at least six empty tubes corresponding to the extraction blank. Extraction of metabolites was conducted on three biologically replicated pericarp samples (n = 3) using a robotised extraction method developed at Bordeaux Metabolome Facility (https://metabolome.cgfb.u-bordeaux.fr/en). The robot allowed for pipetting solvents, mixing, cooling and centrifuging racks of micronics. After decapping the micronics, the extraction started by adding 300 µL of 80% ethanol, 0.1% formic acid (v/v), and including 250 µg/mL methyl vanillate as the internal standard. Racks were agitated on the robot (30 sec, 500 rpm) then placed for 15 min into a sonicator containing ice-cold water (Elmasonic S300, Elma, Singen, Germany). Racks were then centrifuged (5 min, 1350 g). The first round of extraction stopped by pipetting 300 µL of the resulting supernatant into new 1.1 mL-micronic tubes. A second round of extraction was performed with 300 µl the same solvent, and the resulting pellet was finally washed with another solvent (50% ethanol (v/v)). The micronics-containing supernatants were kept for filtration and the micronics with the pellets were kept at -20 °C for further starch and total protein analysis. Filtration was also robotised (Microlab STARlet, Hamilton, Bienne, Switzerland) and allowed for the transfer of the supernatants onto a filtration 96-well sterile clear plate (MSGVS2210, 0.22 µM, Hydrophil. Low Protein Binding Durapore, Millipore, Molsheim, France) according to the supplier's instruction. Filtrates were subsequently collected into a new micronic tube. Finally, quality control (QC) samples were prepared by robotically pipetting 15 µL of each sample into a single tube (Microlab STARlet, Hamilton, Bienne, Switzerland). Each rack was supplemented with at least six micronic tubes containing the QC mix. The QC sample was replicated twenty-two times along the project run.

G. Central metabolites targeted biochemical assays

I. Soluble sugar quantification assay

Soluble sugars are measured in a microplate by coupling enzymatic reactions involving hexokinase (HK), phosphoglucose isomerase (PGI), invertase, and glucose-6-phosphate dehydrogenase (G6PDH) (Figure II.2). NADPH production is then measured at 340 nm. 20 µl of the ethanolic extract is added to 160 µL of the reaction mix.

Reaction mix:

- 150 µL HEPES/KOH 0.1 M, 3 mM MgCl2, pH 7

- 4.6 µL ATP 100 mM

- 4.6 µL $NADP^+$ 45 mM

- 0.8 µL G6PDH grade II 700 $U.mL^{-1}$

The plates are then incubated at 37 °C and the appearance of NADPH is measured at 340nm until a plateau is reached (OD1), then the following enzymes are added in succession:

- 1 µL of HK 900 $U.mL^{-1}$. Then when an OD plateau is reached (OD2),

- 1 µL of PGI 1000 $U.mL^{-1}$. Then when an OD plateau is reached (OD3),

- 1µL of invertase 30 000 $U.mL^{-1}$

The reaction is stopped when the last plateau is reached (OD4). The difference in OD between two consecutive plateaus (ΔDO) is calculated. ΔDO1 = OD2 - OD1 is used to quantify glucose, ΔDO2 = OD2 - OD3 is used to quantify fructose and ΔDO3 = OD3 - OD4 is used to quantify sucrose.

The amount of the measured metabolite is stoichiometrically proportional to the amount of NADPH produced in each reaction. Calculations were done following the formula:

$$NADPH\ (\mu mol) = \Delta DO_{340\ nm}/(l * \varepsilon)$$

Where ε is the extinction coefficient of NADPH at 340 nm (ε = 6.22 $L.mol^{-1}.cm^{-1}$) and l the optical path length (l = 2850 $cm.L^{-1}$). The amount of soluble sugar is finally expressed as µmol of glucose equivalent per gram of fresh material.

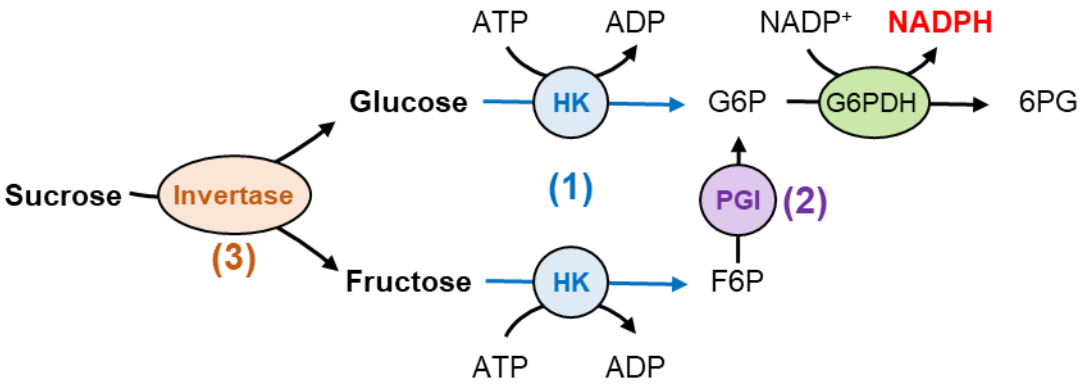

Figure II.2: Principle of soluble sugars assay.

HK: hexokinase; PGI: phosphoglucoisomerase; G6P: glucose-6-phosphate; G6PDH: G6P dehydrogenase; F6P: fructose-6-phosphate; 6PG: 6-phosphogluconate.

II. Total protein quantification assay

The protein assay is performed using the pellets from the ethanolic extraction to which 400 µL of 0.1 M NaOH has been added. The extracts were then heated for 30 minutes at 95 °C and centrifuged for 5 minutes at 2500 g. Protein determination was performed on the supernatants. For this purpose, between 5 µL of extracts are added to 180 µL of ready-to-use Bradford (B6916, Sigma Aldrich). After a 5-minute incubation at room temperature, the OD is measured at 595 nm. The amount of protein is calculated from a calibration curve performed with BSA (Bovine Serum Albumin - 0/80/160/230/640 $\mu g.mL^{-1}$ in NaOH 0.1 M).

III. Malic acid quantification assay

In the presence of NAD^+, malate is oxidised by MDH to oxaloacetate releasing one molecule of NADH per malate consumed. The oxaloacetate produced and the glutamate in the reaction mix are then used by glutamate-oxoglutarate aminotransferase (GOT) to give aspartate and 2-oxoglutarate to shift the equilibrium of the first reaction (Figure II.3). Shortly, 30 µL of the ethanolic extract is added to 90 µL of the following reaction mix:

Reaction mix:

- 69 µL Tricine/KOH 0.1 M pH 9
- 10 µL NAD^+ 30 mM
- 10 µL Glutamate 20 mM
- 1 µL GOT 200 $U.mL^{-1}$ diluted in 100 mM Tricine/KOH pH9

A first measurement of the reaction blank is performed at 340 nm, then 1 µl of MDH at 6000 $U.mL^{-1}$ is added to the mixture for the malate measurement. The ΔDO between the two plates is then calculated. The same formula as for NADPH is used to calculate the amount of NADH in the well.

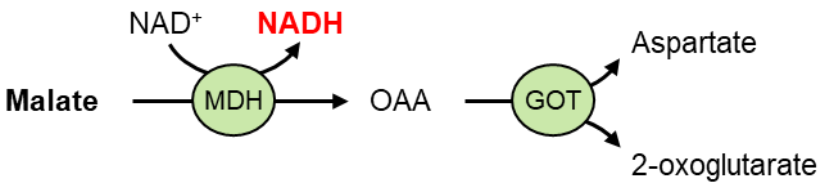

Figure II.3: Principle of malic acid assay.
MDH: malate dehydrogenase; OAA: oxaloacetate; GOT: glutamate-oxaloacetate transaminase.

IV. Citric acid quantification assay

Citrate was measured using the Citric Acid Assay Kit (K-CITR, Megazyme) following the recommendations of the supplier.

V. Starch quantification assay

The starch determination was done on the pellets from the ethanolic extraction and after the protein determination. The pH of the extracts is neutralised by adding 80 µL of 0.5 M HCl/0.1 M sodium acetate, pH 4.9.

The starch is then digested by the addition of 100 µL of digestion mix (Amyloglucosidase 140 $U.mL^{-1}$ with α-amylase 100 $U.mL^{-1}$ in 50 mM acetate buffer pH 4.9). The extracts were then incubated for 16 hours at 37 °C. After centrifugation, the starch determination is performed on the supernatant by determining the glucose in the same way as described above.

H. Redox metabolites targeted biochemical assays

All the targeted redox assays either metabolic or enzymatic were optimised following (Noctor et al., 2016). Recovery and dilutions assays have been performed and data for WT samples were assayed on two independent cultures during 2020 et 2021 years. Resulting metabolite levels were expressed in µ- or n- $mol.g^{-1}$ of fresh weight (FW) for independent bioreplicates ($n = 3$) and checked for statistical significance by ANOVA for global variation and by binary comparison of Student's *t* test or Tuckey test ($p < 0.05$) (see Chapter II, part II.K.I).

I. Ascorbate quantification assay

Ascorbate assay is based on the capacity of ASC to chemically reduce Methylthiazolyldiphenyl-tetrazolium bromide (MTT) to formazan that absorbs at 570 nm adapted from (White and Kennedy, 1985) (Figure II.4). Briefly, 20 µL of acid extract was added in buffer containing 95 µL 0.2 M Hepes/KOH pH 7.5, likewise, control samples are treated with 10 µL of ascorbate oxidase 100 $U.mL^{-1}$. After 10 min of room temperature incubation, 15 µL of determination mix containing 5 µL of 10 mM PES and 10 µL of 10 mM MTT (diluted in 0.2 M Na2HPO4, 0.2 M Citric acid, 2 mM EDTA and 3% (v/v) Triton X-100, pH 3.5). Then the optical density at 570 nm was recorded until it stabilises.

Concomitantly, a standard curve using a chemical standard of sodium L-ascorbate was performed ranging from 0 to 400 µM.

Besides, the same assay with a supplemental step, 20 µL of 5 mM dithiothreitol (DTT) treatment followed by 10 min incubation at room temperature and then 10 µl of 0.5% NEM was performed to reduce all the ASC present in the extract and thus allow the determination of total ASC content (Figure II.4). The difference between total and reduced ascorbate assays allows determining of the ASC redox state.

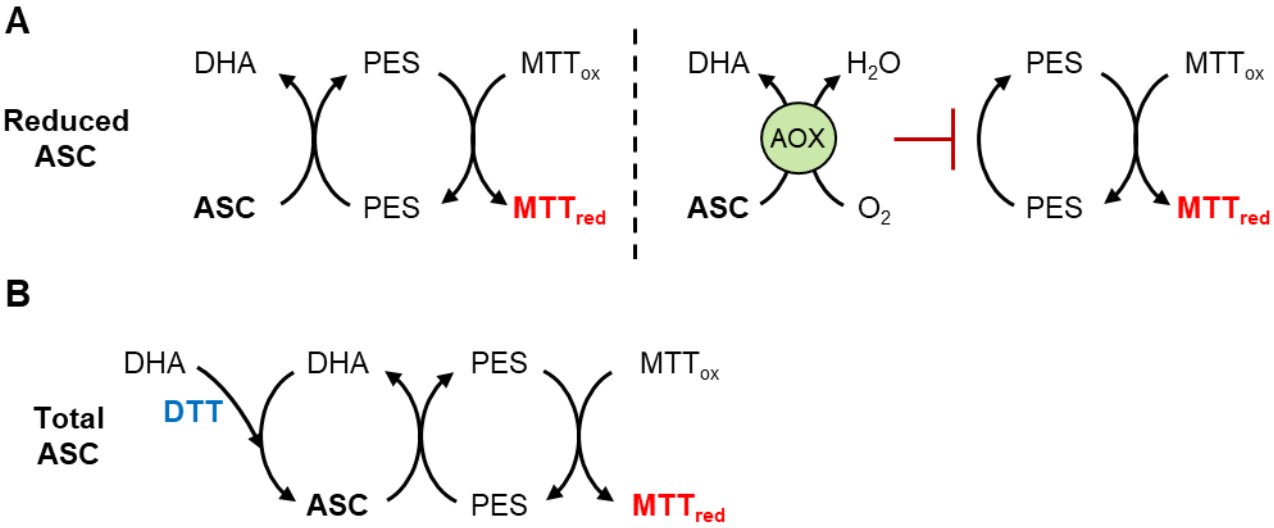

Figure II..4: Principle of ASC assay. Ascorbate oxidase (AOX) is used to consume reduced ASC and allow to measure the background signal. ASC: ascorbate; DHA: dehydroascorbate; DTT: dithiothreitol.

II. Glutathione quantification assay

Glutathione assay relies on the GR-dependent reduction of 5,5-dithiobis(2-nitro-benzoic acid) (DTNB, Ellman's reagent), monitored at 412 nm adapted from (Queval and Noctor, 2007) (Figure II.5). Without pre-treatment of extracts, the method measures total glutathione. The specific measurement of GSSG was achieved by pre-treatment of 200 µL of neutralised extract with 4 µL of 2-vinylpyridine (VPD) resulting in free GSH sequestration (Figure II.5). Then, treated extract was incubated for 30 min at room temperature and sequentially centrifuged 2 times at 12,000 g for 15 min at 4 °C to precipitate VPD. Finally, the treated supernatant was assayed as for total glutathione but using a standard curve based on GSSG, ranging from 0 to 50 µM.

To measure total glutathione, 10 µL of neutralized extract was added to 0.1 ml of 0.2 M $NaH2PO_4$, pH 7.5, 10 mM EDTA; 10 µl of 10 mM NADPH; 10 µl of 12 mM DTNB; and 60 µl of water. The reaction was started by the addition of 10 µl GR at 20 $U.mL^{-1}$ diluted in 0.2 M $NaH2PO_4$, pH 7.5, 10 mM EDTA. After shaking, the increase in optical density at 412 nm was monitored for 5 min. Standards of reduced GSH, ranging from 0 to 100 µM, were run concurrently in the same plates as triplicate assays to allow calibration of the assay.

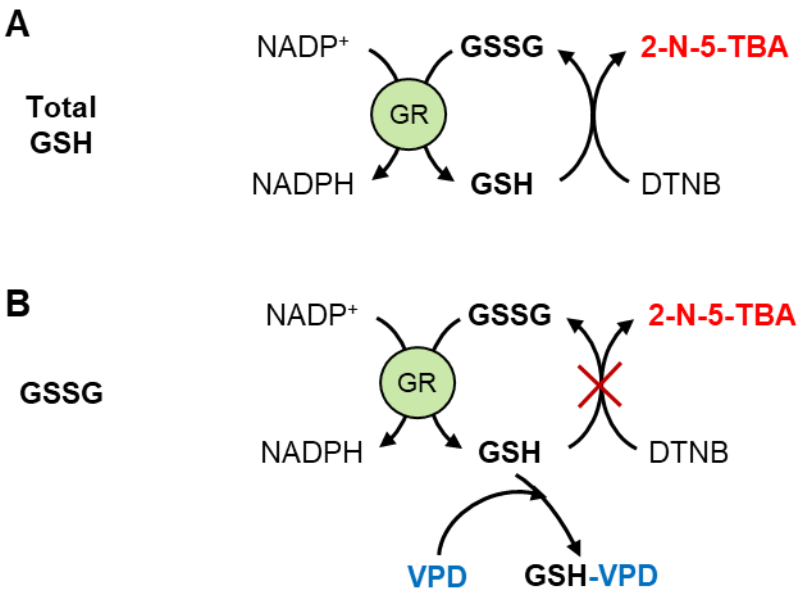

Figure II.5: Principle of GSH assay. Vinylpyridine (VPD) is used to sequestrate free GSH prior the assay inducing a specific signal from GSSG. GR: glutathione reductase

III. Pyridine nucleotides quantification assay

Total cellular soluble pools of NAD^+, NADH, $NADP^+$ and NADPH were measured from fruit pericarps of nine developmental stages of tomato fruit according to a coupled enzyme assay adapted from (Pétriacq et al., 2012) using either alcohol dehydrogenase (ADH) (Figure II..6) or glucose-6-phosphate dehydrogenase (G6PDH) (Figure II.6). Briefly, 5 to 10 µL of extract is added to the same volume of neutralisation solution (0.1 M NaOH or 0.1 M HCl for acid or basic extract, respectively), then 20 µL of 0.2 M Tricine/KOH buffer pH 9, 10 mM $MgCl_2$, 4 µL of 200 mM EDTA, 10 µL of 10 mM MTT, 5 µL of 4 mM PES and (2 µL 50% EtOH + 1 µL ADH at 2000 $U.mL^{-1}$) or (2 µL 250 mM G6P + 1 µL 500 $U.mL^{-1}$ G6PDH) for NAD(H) or NADP(H), respectively. Optical density was recorded at 570 nm before and after the addition of enzymes for a few minutes. Meanwhile, standard solutions of targeted nucleotide, ranging from 0 to 5 µM, were added to the plate as a calibration curve.

In chapter I, microplate measurements of oxidised NAD^+ and $NADP^+$ were confirmed from ethanolic extracts using ion pair liquid chromatography coupled to mass spectrometry (LCMS) technique described previously (Arrivault et al., 2009). Volumes of cytosol and all organelles, except

vacuole, were used to expressed metabolite pools as cellular concentrations by dividing pyridine nucleotide pools by the volume corresponding to each growth stage, as previously described (Beauvoit et al., 2014).

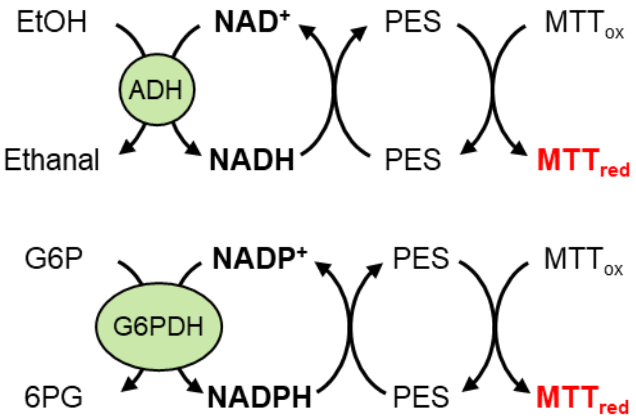

Figure II.6: Principle of NAD(H) and NADP(H) assays. ADH: alcool dehydrogenase; EtOH: ethanol. G6P: glucose-6-phosphate; G6PDH: G6P dehydrogenase; 6PG: 6-phosphogluconate.

IV. H_2O_2 quantification assay

H_2O_2 assay was adapted from a previously described assay in tomato fruits and has been selected for this study due to its non-interference by ASC in tomato as shown by (Junglee et al., 2014). This colorimetric assay is based on a one-step buffer (combining extraction and reaction) to overcome interferences from soluble antioxidants, especially ascorbate, and color background. This assay is based on the potassium iodide (KI) oxidation by hydrogen peroxide, thereby, inducing the formation of triiodide (I_3^-) from iodide ions (I^-) resulting in an increase of absorbance at 350 nm (Figure II.7).

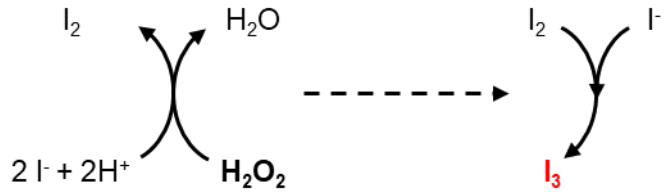

Figure II.7: Principle of H_2O_2 assay.

Shortly, 10 to 100 mg, depending on the growth stage, of ground fresh material was directly homogenised with 700 µL of a solution containing 175 µL of TCA (0.1%; w/v), 350 µL of 1 M KI and 175 µL of 10 mM phosphate buffer pH 8 at 4 °C for 10 min and protected from light. Meanwhile, a second sample aliquot was treated in the same way by replacing KI with H_2O as a control sample. Next, the homogenate was centrifuged at 12.000 g for 15 min at 4 °C. Next, 150 µL of supernatant was placed in microplate wells and optical density was recorded until it stabilises (about 20 min). Concomitantly, a

standard curve of H_2O_2 solution was prepared in 0.1% TCA, ranging from 0 to 100 µM, for calibration of the assay.

V. Trolox antioxidant capacity assay (TEAC)

Trolox equivalent antioxidant capacity (TEAC) method, allow the determination of the total antioxidant activity of an extract by quantifying its capacity to inhibit the $ABTS^{\bullet+}$ radical compared to a reference antioxidant: Trolox® (6-hydroxy-2,5,7,8-tetramethylchroman-2-carboxylic acid), whose cyclic molecular structure is similar to that of vitamin E (α-tocopherol). The cation radical is obtained by contacting ABTS with a peroxidation enzyme in the presence of H_2O_2, or an oxidant.

The $ABTS^{\bullet+}$ radical, in contact with an $H^{\bullet}$ donor, leads to $ABTSH^{\bullet+}$ and to the decolourisation at 734 nm of the solution. This method was adapted from (Fellegrini et al., 1999; Marc et al., 2004; Scalzo et al., 2005) and was applied to ethanolic extract thus allowing the detection of the total soluble antioxidant capacity only (Figure II.8).

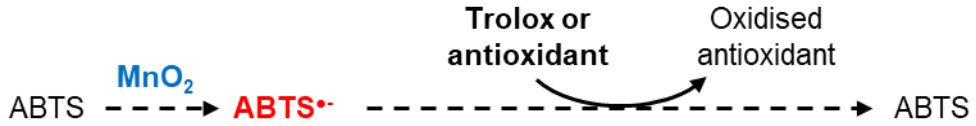

Figure II.8: Principle of TEAC assay.

Briefly, 10 µL of the ethanolic extract is added to 150 µL of $ABTS^{\bullet+}$ solution and the optical density at 740 nm is recorded until it became stable. The $ABTS^{\bullet+}$ solution was previously prepared by mixing 1 g of ABTS, 6 g of manganese oxide and 250 mL of H_2O which was protected from light and agitated overnight. Then, the solution is filtered through a 22 µM filter and kept at 4 °C up to 6 months. Finally, a standard curve of TROLOX ® was prepared in absolute ethanol ranging from 0 to 1 mM.

I. Targeted enzymatic capacity assays

As for metabolic assays, assays have been optimised by checking recoveries and dilutions and data for WT samples were assayed on two independent cultures during 2020 et 2021 years. Enzyme activities were assayed using a robotised platform at HiT-Me Facility (MetaboHUB-Bordeaux) http://metabolome.cgfb.u-bordeaux.fr/en). Resulting enzymatic capacities were expressed in µ- or n-mol.g^{-1} of fresh weight (FW) per minute, for independent bioreplicates ($n = 3$) and checked for statistical significance by ANOVA for global variation and by binary comparison of Student's t test or Tuckey test ($p < 0.05$), as described below (see Chapter II, part II.N.1).

I. Enzymatic activity of MDHAR

Monodehydroascorbate reductase activity is measured by direct colorimetric assay by determining the rate of oxidation of NADH to NAD^+. The assay is coupled to ascorbate using ascorbate oxidase to provide the substrate monodehydroascorbate (Figure II.9), and was adapted from (Dalton et al., 1986; Pritchard et al., 2000).

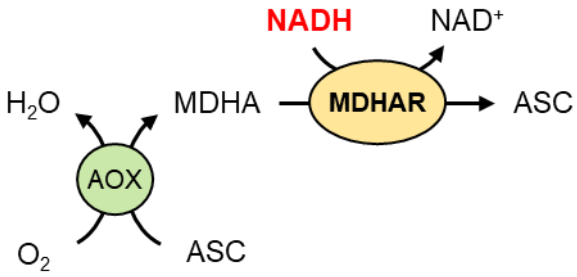

Figure II.9: Principle of MDHAR assay.

In brief, 15 µL of extract is added to 85 µL of 50 mM Hepes/KOH pH 7.5, 0.5 $U.mL^{-1}$ ascorbate oxidase, 0.5 mM NADH and 1.5 mM ASC. Control reaction was concomitantly performed in the same conditions but in absence of ASC. NADH consumption was monitored at 340 nm and its content was calculated using the same formula used for soluble sugar assays.

II. Enzymatic activity of DHAR

Dehydroascorbate oxidase activity is measured by direct monitoring of the rate of NADPH oxidation by Glutathione reductase (GR) at 340 nm. DHAR will transform GSH into GSSG that will allow NADPH oxidation by GR (Figure II.10).

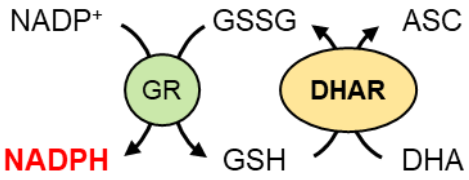

Figure II.10: Principle of DHAR assay.

Concisely, 20 µL of extract was added into 90 µL of 50 mM Hepes/KOH pH 7.5, 5 mM EDTA, 0.5 mM NAPDH and 1 $U.mL^{-1}$ of GR. The reaction was initiated by adding 10 µL of either 1 mM DHA or H_2O in the sample and blank well, respectively. Then, the optical density was recorded at 340 nm for 10 min. NADPH consumption was calculated with the same formula used for soluble sugar assays.

III. Enzymatic activity of GR

Glutathione reductase activity is measured by direct monitoring of the rate of reduction of oxidized glutathione by NADPH oxidation adapted from (Polle et al., 1990; Pritchard et al., 2000).

In short, 10 µL of extract is added to 90 µL of reaction mix containing 50 mM Hepes/KOH pH 7.5, 0.5mM EDTA, 0.5 mM NADPH and 0.25 mM of GSSG. Control reaction was concomitantly performed in the same conditions but in absence of GSSG. Then, the measure of change in optical density at 340 nm was recorded during 5min and NADH consumption was calculated with the same formula used for soluble sugar assays.

IV. Enzymatic activity of APX

Ascorbate peroxidase activity was measured by direct measurement of the rate of oxidation of ASC to DHA by H_2O_2. The change in absorbance was monitored at 290 nm using UV-spectrometer (SAFAS XENIUS XML) according to (Asada, 1984).

Succinctly, 10 to 30 µL of the enzymatic extract was added in 90 µL of 80 mM Hepes/KOH pH 7.5, 0.5 mM ASC. Besides, blank wells and ascorbate standards were also added within the plate. The reaction was started by the addition of 5 µL of 100 mM H_2O_2 and absorbance was recorded at 290 nm for 5 min. ASC content was calculated using the same formula as for NADH within sugar assay using an extinction coefficient of ASC at 290 nm (ε = 2.8 $L.mol^{-1}.cm^{-1}$)

V. Enzymatic activity of SOD

Superoxide dismutase activity was measured by monitoring the inhibition of MTT oxidation compared to a purified commercial enzyme. This assay used the xanthine oxidase as $O_2^{\bullet-}$ generator and was adapted from (Peskin and Winterbourn, 2017). In addition, catalase was added in the reaction mix to process produced H_2O_2 and thus allow a specific reaction between $O_2^{\bullet-}$ and MTT.

Briefly, 10 µL of extract was added to 130 µl of reaction mix containing 50 mM Tricine/KOH pH 8, 10 mM $MgCl_2$, 20 µg/mL catalase, 0.5 mM MTT and 0.1 mM xanthine. Next, 10 µL of 0.2 $U.mL^{-1}$ xanthine oxidase and 5 µL of PES 4 mM were added to each well to start the reaction. Control reaction was concomitantly performed in the same conditions but in absence of xanthine. Finally, absorbance was recorded at 570 nm and calibrated using a standard curve of purified SOD ranging from 0 to 8 units per well.

VI. Enzymatic activity of CAT

Catalase activity is measured by determining the amount of H_2O_2 remaining after a known incubation period adapted from (Summermatter et al., 1995). The remaining H_2O_2 is measured by the oxidation of potassium iodide that results in a yellowish colorimetric signal (340 nm) as described above in H_2O_2 assay.

Shortly, 10 µL of the enzymatic extract was added to 90 µL of 50 mM Hepes/KOH pH 7.5, 0.25 M NaCl. Control well was performed by pre-treating the extract with 0.5 M HCl for 10 min and then neutralised using 0.5 M NaOH to obtain the non-enzymatic H_2O_2 processing capacity of the extract. Simultaneously 0.5 M NaCl was added to other wells to maintain the ion concentrations. Then 30 µL of 100 mM H_2O_2 was added to each well and the reaction was stopped after 1 and 3 min by adding 50 µL of 0.5 M HCl. Finally, 10 µL of the reaction well was transferred to a new plate containing 100 µL of determination mix composed of 50 µL 1M KI, 25 µL TCA 0.1% and 25 µL 50 mM Hepes/KOH pH 7.5. The optical density was monitored at 340 nm until it become stable simultaneously with a H_2O_2 standard curve as described above.

J. Untargeted metabolic assay

I. Data collection

Untargeted metabolic profiling by UHPLC-LTQ-Orbitrap mass spectrometry (LCMS) was performed using an Ultimate 3000 ultra-high-pressure liquid chromatography (UHPLC) system coupled to an LTQ-Orbitrap Elite mass spectrometer interfaced with an electrospray (ESI) ionisation source (ThermoScientific, Bremen, Germany). The system was controlled by Thermo XCalibur v.3.0.63 software. Chromatographic separation was achieved at a flow rate of 350 µL.min^{-1} using a GEMINI UHPLC C18 column (150 × 2 mm, 3 µm, Le Pecq, Phenomenex, France) coupled to a C18 SecurityGuard GEMINI pre-column (4 × 2 mm, 3 µm, Le Pecq, Phenomenex, France). The column was maintained at 35 °C and the injection volume was 5 µL. The mobile phase consisted of solvent **(1)** (0.05% (v/v) formic acid in water) and solvent **(2)** (acetonitrile) with the following gradient: 0–0.5 min 3% **(2)**, 0.5–1 min 3% **(2)**, 1–9 min 50% **(2)**, 9–13 min 100% **(2)**, 13–14 min 100% **(2)**, 14–14.5 min 3% **(2)**, 14.5–18 min 3% **(2)**. Ionisation of samples was performed in negative mode with the following parameters: ESI- (Heater temp: 300 ◦C, Sheath Gas Flow Rate: 45 (arb), Aux Gas Flow Rate: 15 (arb), Sweep Gas Flow Rate: 10 (arb), I Spray Voltage: 2.5 kV, Capillary Temp: 300 ◦C, S-Lens RF Level: 60%). MS full scan detection of ions was operated by FTMS (50–1500 Da) at a resolution of 240 000. Prior to analyses, the LTQ-Orbitrap was calibrated by infusing a solution of the calibration dependent of the ionisation mode (Pierce© ESI Negative Ion Calibration Solution (ref: 88324). MS1 full scan

detection of ions was performed by FTMS (50 - 1500 Da) at a resolution of 240k at 200 *m/z*. Twenty-two QC samples and forty blank extracts were injected to correct for mass spectrometer signal drift, and to filter out variables detected in blanks, respectively. MS2 Data Dependent Analysis (DDA) was also performed on QC sample to generate fragmentation information for further annotation with the following parameters: FTMS (50 - 1500 Da) at a resolution of 60k at 200 *m/z*; activation type, CID; isolation width, 1 Da; normalised collision energy, 35 eV; activation Q, 0.250; activation time, 10 ms).

II. Data processing

Raw LCMS data were processed using MS-DIAL v 4.70 (Tsugawa et al., 2015), yielding 15 251 RT-*m/z* features. The precise parameter report is available as Annex 1. MS-DIAL parameters were as follows: MS1, tolerance, 0.01 Da; MS2 tolerance, 0.025 Da; retention time begin, 0 min; retention time end, 18 min; minimum peak height, 10000; mass slice width, 0.1 Da; smoothing filter, Savitzky-Golay; smoothing level, 4 scans; minimum peak width, 5 scans; sigma window value, 0.5. After data-cleaning (blank check, SN > 10, CV QC < 30%), 3742 variables were retained for further chemometrics. MS-DIAL annotation of metabolic features was performed using the online library MSMS-Public-Neg-VS15.msp (36,848 records) with the following parameters: retention time tolerance, 100 min; accurate mass tolerance (MS1), 0.01 Da; accurate mass tolerance (MS2), 0.05 Da; identification score cut off, 80%. Putative annotation of differentially expressed metabolites resulted from MS-DIAL screening of the MS1 detected exact HR *m/z* and MS2 fragmentation patterns against multiple online databases (http://prime.psc.riken.jp/compms/msdial/main.html#MSP) (Tsugawa et al., 2015).

Then, metabolic features were filtered based on their putative ontology (*i.e.* MS levels 2 and 3 and all the class associated with antioxidant activity (*i.e.* phenolics, flavonoids, terpenoids, thiols, vitamins and their derivatives) represented 733 annotated antioxidant metabolic features.

K. Enzyme based kinetic modelling

I. Computer modelling

The model was built from the mass balance equations of the ASC-GSH cycle. The general form of the differential equations used is:

$$\frac{dC_i}{dt} = \sum_{j=1}^{n} n_{i,j} \,.\, v_j \,.\, \frac{Vol_j}{\rho}$$

where C_i is the concentration of the ith species (in µmol.gFW^{-1}), $n_{i,j}$, the stoichiometry of the ith species in the reaction j, Vol_j, the volume fraction of the compartment (in mL$_{compartment}$.mL$_{tissue}^{-1}$) where the jth reaction occurs, ρ, the tissue density (in gFW.mL$_{tissue}^{-1}$), and v_j, the rate of the jth reaction (mM.min^{-1}) involved in the consumption and production of the ith species. The reaction rate equations, taking into account the measured maximal velocity (V_{max}) of the enzymes, the volume space where they are located, and their kinetic parameters are listed in Chapter V. The set of differential equations listed in Annex 2 was solved by the Copasy 4.34 software (Hoops et al., 2006) to satisfy the steady-state condition of metabolic intermediates, *i.e.*, dC/dt close to zero. Eight Copasi files corresponding to the eight developmental stages are available as Supplemental Data Sets 1 to 8.

The tissue contents of ASC, GSH and H_2O_2 at steady state were calculated by taking into account the local concentrations of the metabolites given by the model, the compartment volume, and the tissue density, according to the following equation:

$$X_{total} = \frac{[X]_{vac} \,.\, V_{vac} + [X]_{cyt} \,.\, V_{cyt} + [X]_{apo} \,.\, V_{apo}}{p}$$

where X_{total} is the tissue content of the metabolite X (in µmol.gFW^{-1}) and the subscripts *vac*, *cyt*, and *apo* represent the volume fraction (in mL.mL$_{tissue}^{-1}$) and the steady-state concentrations (in mM) for the cytosol, vacuole and apoplast respectively, and *p*, the tissue density (in gFW.mL^{-1}).

II. Model parameter optimization

Parameter optimization was performed using a random search algorithm and by minimizing an objective score, *i.e.*, the sum of the relative squared residuals weighted, according to the following equation:

$$Obj = \sum_{i=1}^{n} (\frac{X_{i\_cal} - X_{i\_exp}}{X_{i\_exp}})^2$$

where *Obj* is the objective score, n, the total number of variables, X_{i_cal}, the calculated value, and X_{i_exp}, the experimental value of a particular variable X_i (*i.e.* metabolite content, redox ratio). Sets of initial parameter values were randomly generated to avoid finding only local minima. At each developmental stage, the whole iterative process was repeated using the Curta cluster housed by Mésocentre de Calcul Intensif Aquitain (MCIA) and randomised initial conditions. The 100 best-scoring parameter sets were kept for statistical analysis, at the end of which the median values (Baker et al., 2010) were used to parameter the model to calculate steady state fluxes, concentrations and to perform sensitivity analysis.

III. Metabolic control analysis

According to the formalism of MCA (Kacser and Burns, 1973; Heinrich and Rapoport, 1974), flux ($C_{V_j}^{J_i}$) and concentration ($C_{V_j}^{X_i}$) control coefficients by a given enzyme are defined as the scaled partial derivative of the simulated values with respect to the enzyme activity:

$$C_{V_j}^{J_i} = \frac{\partial \ln J_i}{\partial \ln V_j}$$

and

$$C_{V_j}^{X_i} = \frac{\partial \ln X_i}{\partial \ln V_j}$$

Where V_j is the activity of the targeted enzyme j; J_i, a given flux; and X_i, a given metabolite concentration.

Coefficients were calculated using the implemented function in Copasy 4.34 and a delta factor of 0.001 for fixed parameters. Then, the control exerted by any enzyme j on the total ascorbate content was calculated as follows:

$$C_{V_j}^{ASC\_total} = \frac{C_{V_j}^{ASC}.\ [ASC] + C_{V_j}^{DHA}.\ [DHA] + C_{V_j}^{MDHA}.\ [MDHA]}{[ASC] + [DHA] + [MDHA]}$$

IV. Statistics and mathematical regressions

Data were cube root transformed and scaled using pareto scaling before hierarchical clustering analysis and heat map visualisation using Metaboanalyst (https://www.metaboanalyst.ca/) using Pearson correlation-based distance measure and the Ward linkage clustering method (Xia et al., 2009).

Linear and nonlinear regressions of the experimental data were performed using the R shiny interface EasyReg (http://sylvainprigent.fr:3838/easyReg/) using basic and nlstools R packages.

Right-tailed Chi square test for goodness of fit

A Chi square goodness of fit test was performed to evaluate the best model that accommodates the experimental measurements as described in … The Chi square is of the form:

$$\chi^2 = \sum_{i=1}^{n}\sum_{t=1}^{m} \frac{(X_{i,t}cal - X_{i,t}exp)^2}{X_{i,t}exp}$$

where $X_{i,t}cal$ refers to the tissue content of the metabolite i calculated by the model at the developmental stage t and $X_{i,t}exp$, the corresponding measurements. The Chi square value is then used to calculate a right tail p-value and knowing the degree of freedom df of the dataset. In our case, df is related to the number of measured variables n and to the number of developmental stages m, such as $df = (n-1) \times (m-1)$.

In the context of our modelling approach, a non-significant p-value ($p > 0.05$) means that there are no statistically significant differences between measured and simulated values throughout development.

L. Generalised multilinear modelling (GLM)

General multilinear models were used to (i) explore the correlation between metabolic variables and flux predictions and (ii) extract the best predictors of the ASC-GSH fluxes while preserving the developmental context. More specifically, we here deployed GLMs based on the normal distribution of the data using the glmnet package available in R (Friedman et al., 2010). Stratified sampling was used to define the training set (70%) and the testing set (20%) which were used to establish the model equation and the validation set (10%) to test the predictive capacity of the model. Variable selection was ensured via lasso, ridge and elastic net penalisation systems where a thousand penalty values were tested between 0 and 1 (the closer the penalty value is to 1, the smaller the number of variables used in the models). The final equation corresponded to the most parsimonious model ensuring the lowest mean square error (MSE) within one standard error of the minimal MSE.

In total, 500 models were developed to cover the multiple sampling possibilities arising from stratified partitioning. Whilst internal cross-validations were performed to establish the equation and limit the risks of overfitting, 500 permuted datasets were created to test the likelihood of spurious predictions. Besides, statistical validation was complemented with biological validation. In short, the equation of the model (as well as variable selection) was established using the first biological dataset and then applied to an independent dataset to validate the predictive capacity of the best metabolic markers.

M. Statistical analyses

I. Univariate analyses

Metabolic and enzymatic data were checked for normality and heteroscedasticity by Shapiro and Bartlett tests ($\alpha = 0.05$) using R software (https://www.r-project.org). Then, ANOVA and post-hoc (Tuckey's tests) ($p < 0.05$) were realised using the agricolae package (Mendiburu, 2021) on R software or directly on MetaboAnalyst v.5.0 (https://www.metaboanalyst.ca/) to identify differences between the metabolic compounds.

II. Multivariate analyses

Prior to multivariate statistical analyses, metabolic data were pre-processed to normally distributed data by performing median normalisation, cube-root transformation and Pareto scaling of the data intensities as described previously (Belouah et al., 2019). Normalised datasets were then used to construct score plots of Principal Component Analysis (PCA) overview using MetaboAnalyst v 5.0 (http://www.metaboanalyst.ca/), or *via* the factoextra and FactoMineR packages (Lê et al., 2008; Kassambara and Mundt, 2020).

Then, hierarchical clustering analysis (HCA) and visualisation through heatmaps were performed by Pearson's correlation with complete or Ward clustering linkage using Metaboanalyst or *via* the pheatmap and cluster packages in R (Kolde, 2019) using significant features previously determined by ANOVA ($p < 0.05$).

CHAPTER III

MULTIOMICS ANALYSES OF THE NAD(P) METABOLISM DURING TOMATO FRUIT DEVELOPMENT

ABSTRACT

Central metabolism is the engine of plant biomass, supplying fruit growth with building blocks, energy and biochemical cofactors. Among metabolic cornerstones, nicotinamide adenine dinucleotide (NAD) is particularly pivotal for electron transfer through reduction-oxidation (redox) reactions, thus participating in a myriad of biochemical processes. Besides redox functions, NAD is now assumed to act as an integral regulator of signalling cascades involved in growth and environmental responses. However, the regulation of NAD metabolism and signalling during fruit development remains poorly studied and understood.

Here, we benefit from RNAseq and proteomic data obtained from nine growth stages of tomato fruit (var. Moneymaker) to dissect mRNA and protein profiles that link to NAD metabolism, including *de novo* biosynthesis, recycling, utilisation and putative transport. As expected for a cofactor synthesis pathway, protein profiles failed to detect enzymes involved in NAD synthesis or utilisation, except for nicotinic acid phosphoribosyltransferase (NaPT) and nicotinamidase (NIC), which suggested that most NAD metabolic enzymes were poorly represented quantitatively. Further investigations on transcript data unveiled differential expression patterns during fruit development. Interestingly, among specific NAD metabolism-related genes, early *de novo* biosynthetic genes were transcriptionally induced in very young fruits, in association with NAD kinase, while later stages of fruit growth rather showed an accumulation of transcripts involved in later stages of *de novo* synthesis and in NAD recycling, which agreed with augmented NAD(P) levels. In addition, a more global overview of 119 mRNA and 78 protein significant markers for NAD(P)-dependent enzymes revealed differential patterns during tomato growth that evidenced clear regulations of primary metabolism, notably with respect to mitochondrial functions. Overall, we propose that NAD metabolism and signalling are very dynamic in the developing tomato fruit and that its differential regulation is certainly critical to fuel central metabolism linking to growth mechanisms.

Keywords: fruit, tomato, NAD, redox, development

Plant metabolism is maintained by universal metabolic cornerstones including pyridine nucleotides such as nicotinamide adenine dinucleotide (NAD) (Noctor, 2006; Gakière et al., 2018b). NAD and its phosphorylated form NADP are ubiquitous electron carriers modulating energy homeostasis through the transport of electrons within reduction-oxidation (redox) processes (Geigenberger and Fernie, 2014; Gakière et al., 2018a). As a result of its capacity to transfer electrons, NAD(P) is present in the cell as oxidised or reduced forms, $NAD(P)^+$ and NAD(P)H respectively, where NAD(P) refer to as the total pool of $NAD(P)^+$ and NAD(P)H. In plant cells, while NAD is mostly found as oxidised NAD^+, NADP mostly acts as a reductant (NADPH) (Noctor, 2006; Gakière et al., 2018b). For instance, the regeneration of reducing equivalents (NADPH) by the oxidative pentose phosphate pathway is necessary for the β-oxidation of fatty acids and for nitrogen assimilation in non-photosynthetic tissues (Neuhaus and Emes, 2000; Bowsher et al., 2007). Phosphorylation of NAD(H) to NADP(H) is catalysed via highly conserved NAD^+ kinases (E.C. 2.7.1.23) and NADH kinases (E.C. 2.7.1.86) playing essential roles in metabolic and redox reactions including photosynthesis performance and reactive oxygen species (ROS) homeostasis, which are both crucial for plant growth and responses to stress (Turner et al., 2004; Waller et al., 2010; Li et al., 2014, 2018a).

Plant cells produce NAD^+ from the amino acid aspartate via a de novo biosynthesis and a recycling pathway (Figure IIII.1) (Katoh et al., 2006; Gakière et al., 2018b). As for other nucleotides that are salvaged, NAD^+ can be recycled via the activity of nicotinamidases (NIC; E.C. 3.5.1.19) and nicotinic acid phosphorybosyltransferase (NaPT; E.C. 2.4.2.11) (Figure IIII.1).

While the topology of NAD^+ synthesis is well documented, the molecular and regulatory details of the corresponding biochemical pathways remain largely unknown, especially for fruit tissues. Deregulation of AO, QS and QPT levels in Arabidopsis thaliana leaves has shown that such enzymes are critical in the control of pyridine nucleotide levels and its derivatives (Schippers et al., 2008; Macho et al., 2012; Pétriacq et al., 2012, 2016b). Although the physiological role of trigonelline in plants remain unclear, trigonelline can also contribute, to a lesser extent, to the resynthesis of NAD^+ and undergoes long-distance transport in Arabidopsis (Upmeier et al., 1988; Wu et al., 2018).

For instance, research on pyridine nucleotide signalling mostly focuses on photosynthetic tissues, sometimes roots and seeds (Hunt et al., 2007; Hunt and Gray, 2009; Hashida et al., 2013). In Arabidopsis, changes in $NAD(P)^+$ contents drastically alter growth phenotype, as exemplified particularly for genotypes that are affected for the first three enzymes of de novo biosynthesis (for a review see (Gakière et al., 2018a)). Following NAD(H) and NADP(H) levels in Arabidopsis developing leaves further indicate a continuous accumulation of the cofactors during foliar growth until the pools drop with flowering (Queval and Noctor, 2007).

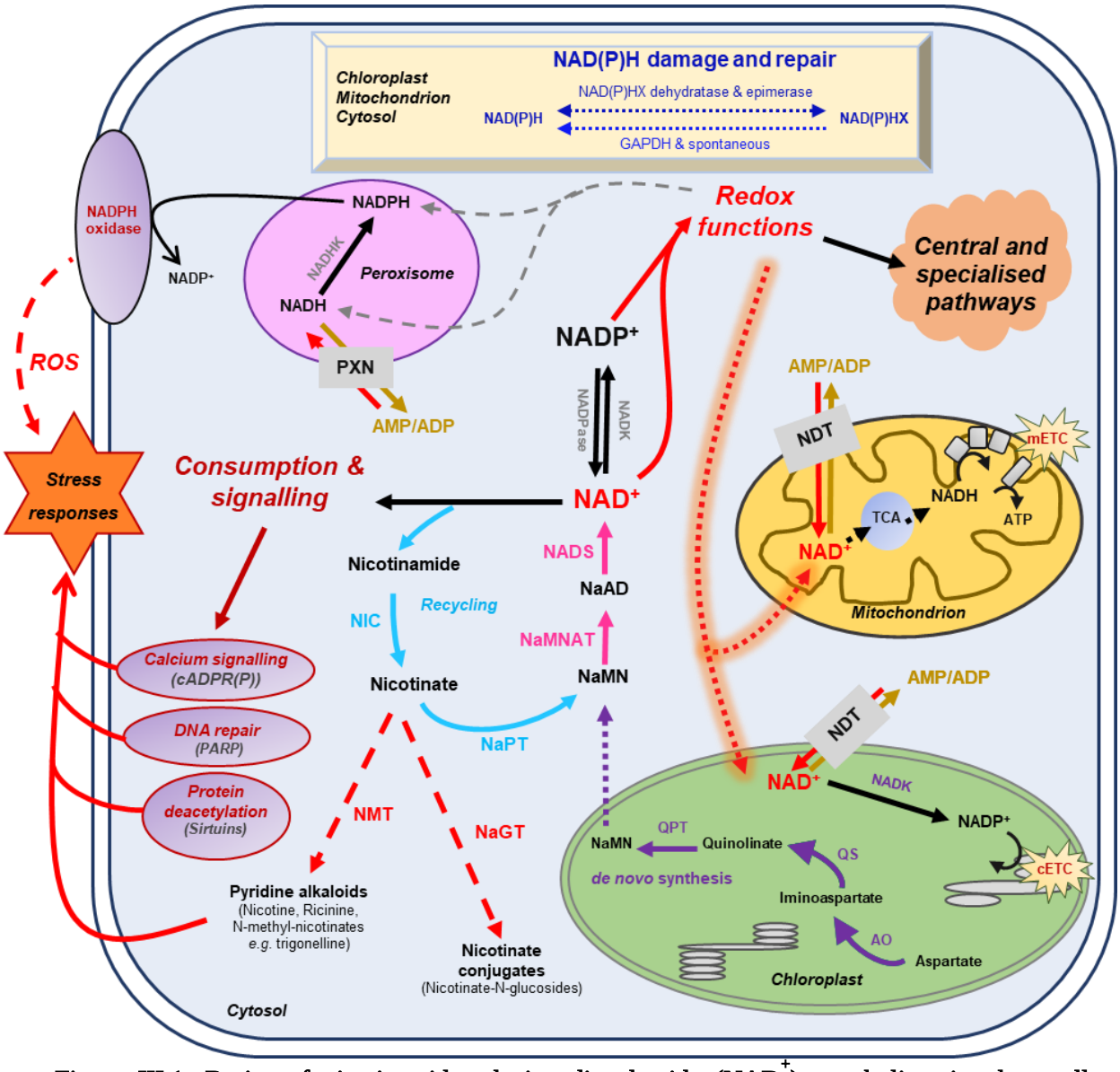

Figure III.1: Basics of nicotinamide adenine dinucleotide (NAD^+) metabolism in plant cells. Biosynthesis and utilisation of pyridine nucleotides. Dot arrows represent transport between the different cellular organelles. Purple and blue arrows indicate *de novo* synthesis pathway of NAD^+, and the recycling pathway, respectively. Pink arrows represent steps that are shared by these two synthesis pathways. Dashed red arrows indicate nicotinate metabolism. Indigo arrows show NAD(P)H damage and repair, which can be spontaneous or catalised by NAD(P)H-hydrate dehydratase and epimerase. AO: aspartate oxidase; ATP: adenosine triphosphate; cADPR(P): cyclic ADP-ribose (phosphate); cETC: chloroplastic electron transport chain; GAPDH: glyceraldehyde-3-phosphate dehydrogenase; mETC: mitochondrial electron transport chain; NaAD: nicotinic acid adenine dinucleotide; NADK: NAD kinase; NADP: NAD phosphate; NADPase: NADP phosphatase; NAD(P)HX: NAD(P)H hydrate; NaMN: nicotinic acid mononucleotide; NaMNAT: NaMN adenylyltransferase; NADS: NAD synthetase; NaGT: nicotinate N-glucosyltransferase; NaPT: nicotinate phosphoribosyltransferase; NDT: NAD^+ transporter; NIC: nicotinamidase; NMT: nicotinate N-methyltransferase; PARP: poly-ADP-ribose polymerase; PXN: peroxisomal NAD carrier; QPT: quinolinate phosphoribosyltransferase; QS: quinolinate synthase; ROS: reactive oxygen species; TCA: tricarboxylic acid cycle. From (Decros et al., 2019b).

Only a handful of studies provides fruit-specific concentrations of NAD(H) and NAD(P)H. Although previous changes in pyridine nucleotides have been observed between green and red tomato fruits of MicroTom and Moneymaker cultivars (Centeno et al., 2011; Osorio et al., 2013b), to our knowledge no developmental fruit series have been analysed so far. Tomato fruit is not only an important crop that is widely used for human diet but also pivotal for fruit research (Li et al., 2018b). During tomato fruit development, a medium-scale stoichiometric model suggested that biomass synthesis required NADPH and higher ATP hydrolysis at the end of cell expansion (Colombié et al., 2015). This was further associated with a peak of CO_2 at the end of tomato ripening coinciding with climacteric respiration of tomato fruit and involved energy dissipation by the mitochondrial alternative oxidase. This was further confirmed by a more detailed stoichiometric model of the respiratory pathway, including alternative oxidase and uncoupling proteins (Colombié et al., 2017). In grape berry, reducing power equivalents (NADH and NADPH) were also associated with major carbon fluxes, thus supporting a strong link between central metabolism and pyridine nucleotides (Soubeyrand et al., 2018).

In the present work, as a first attempt to clarify the importance of pyridine nucleotides in the developing fruit, we used a developmental fruit series of nine growth stages of tomato fruit (var. Moneymaker) and measured pyridine nucleotide pools. We further examined quantitative data for transcript and protein levels previously obtained by RNAseq and proteomics (Belouah et al., 2019) and revealed changes in NAD(P) metabolism during fruit development. Our studies show that NAD(P) metabolism and signalling are very dynamic and crucial to the developing tomato fruit, and link to central metabolism.

A. Tomato fruit development is associated with changes in NAD(P)pools

Fruit development can be divided into three partially overlapping phases, namely cell division, cell expansion and ripening (Figure IIII.2A), which all have their own metabolic specificity (Beauvoit et al., 2018). As a first attempt to clarify the importance of pyridine nucleotides for fruit growth, we measured total cellular NAD^+, $NADP^+$, NADH and NADPH pools from nine growth stages of tomato fruit (var. Moneymaker) (Figure IIII.2B). Oxidised pools were also confirmed by LCMS (Supplemental fig IIII.1). Global changes in the pools of these pyridine nucleotides were statistically significant (ANOVA followed by binary Student's t tests) and showed higher levels of both NAD(H) and NADP(H) in the very young fruit, with the highest pools observed at 8 days post anthesis (dpa) for growth stage 1 (GS1) and the lowest for mature green (GS6, 41 dpa) and for red ripe (GS9, 53 dpa) stages of tomato fruit, respectively. Reduced, oxidised and total content of NAD(H) decreased until the end of cell division (GS4), then firstly increased during cell expansion (GS5-7) and secondly during ripening (GS8-9), while maintaining the NAD(H) pool mainly oxidised during fruit development.

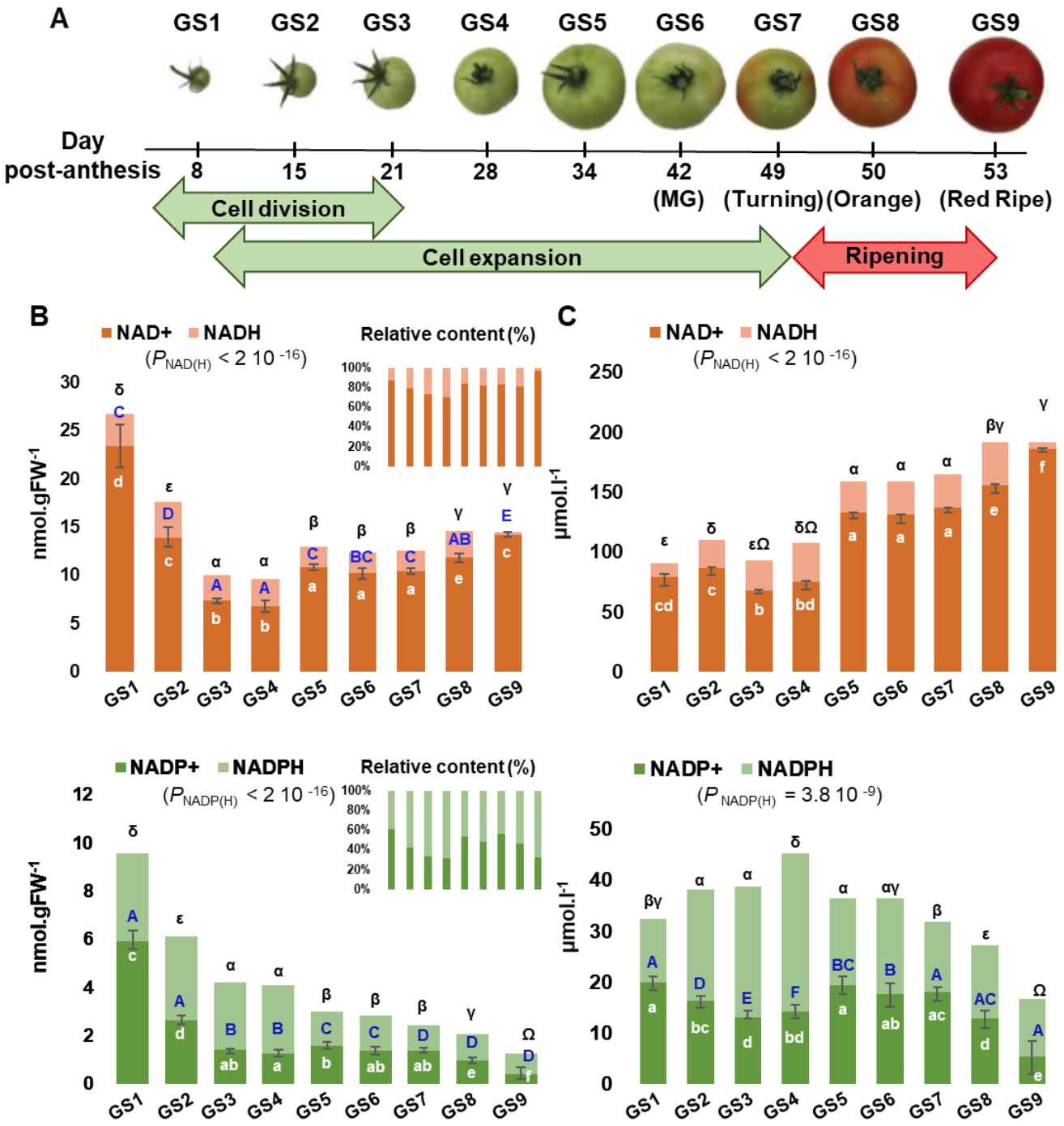

Figure III.2: Evolution of NAD(P) contents during tomato fruit development. NAD(P) pools were measured for nine sequential growth stages (GS) of tomato fruit development **(A)**. Shown are bar plots of NAD(P) contents (n = 3) **(B)** which have been normalised to the cytosol and organelles volumes **(C)**. Top and bottom error bars indicate SEM (Standard Error of the Mean) for the reduced and oxidised forms, respectively. Statistical significance for total NAD(P) content is indicated by ANOVA P value. Binary comparisons between conditions are indicated by letters (oxidised form, in white), capital letters (reduced form, in blue) and symbols (total content, in black), according to Student's t test ($p < 0.05$). Left panel indicates the concentrations of NAD(P) in nmol.gFW^{-1} whereas the right panel indicates the NAD(P) concentrations in µmol.l^{-1}. From (Decros et al., 2019b).

Since NAD(P) are mostly present in the chloroplasts, peroxisomes, mitochondria and cytosol, but not in the vacuole (Donaldson, 1982; Gakière et al., 2018b), we could rule out the dilution effect due to the cell expansion (Beauvoit et al., 2014) and express NAD(P) contents as concentrations (Figure III.2C). Differences in concentrations, except for NADH, were statistically significant during fruit growth (ANOVA followed by binary Student's t tests) and clearly indicated two distinct waves of accumulation for NAD(H) (*i.e.* GS5-7 and GS7-9). Simultaneously, NADP(H) only increased during the beginning of development (from GS1 to GS4) as a result of a higher NADPH concentration (Figure III.2C). Hence, this suggests a fine-tuned NAD(P) homeostasis during tomato fruit development.

B. Transcriptional changes of NAD biosynthesis and metabolism show distinct patterns during tomato fruit growth

Next, in order to substantiate the changes in NAD(P), we examined transcript and protein profiles during tomato fruit development that were obtained from RNAseq and proteomics techniques (Belouah et al., 2019). Raw data (22,877 transcript and 2,375 protein features) were normalised as described previously (median-centred, cube root-transformed and Pareto scaled) (Belouah et al., 2019). We first focused on genes that were associated with NAD^+ biosynthesis and NAD(P)H damage and repair (Figure III.1), which included 15 genes (Figure III.3A). Clustering analysis of mRNA profiles (Pearson's correlation and complete clustering, Figure III.3A) revealed two main statistically significant clusters (ANOVA with Bonferroni correction, $p < 0.01$ are listed in Supplemental table II.1): one associated with the young fruit (stages 1-4) and another with the ripening fruit (stages 5-9).

For the first cluster, early steps of de novo biosynthesis of NAD^+ and $NADP^+$ was transcriptionally up regulated in the young fruit, including AO, QS and QPT, and NADK1 and NADK2 (Figure III.3A). Interestingly, these enzymes are chloroplastic in Arabidopsis (Katoh et al., 2006), and assumed to be critical for NAD^+ and $NADP^+$ homeostasis, respectively (Pétriacq et al., 2012; Gakière et al., 2018a; Li et al., 2018a). For the second cluster, later stages of fruit growth coincided with the up regulation of the expression of genes involved in final steps of NAD^+ biosynthesis (NaMNAT and NADS), NAD^+ recycling (NIC and NaPT) and NADP(H) production (NADK3 and NADK4) (Figure III.3A). This suggests an accumulation of NAD^+ precursors during the beginning of development (GS1-4) followed by an active synthesis and recycling of $NAD(P)^+$ (GS5-9) concurrent with the increased NAD(H) content. Besides, NAD(P)XH epimerase and dehydratase genes are expressed all along fruit development suggesting a continuous NAD(P)H damage and repair (Figure III.3A). Remarkably, protein profiles failed to include enzymes involved in NAD^+ synthesis, except for NaPT and NIC that followed mRNA profiles with higher levels during ripening (Supplemental fig III.2).

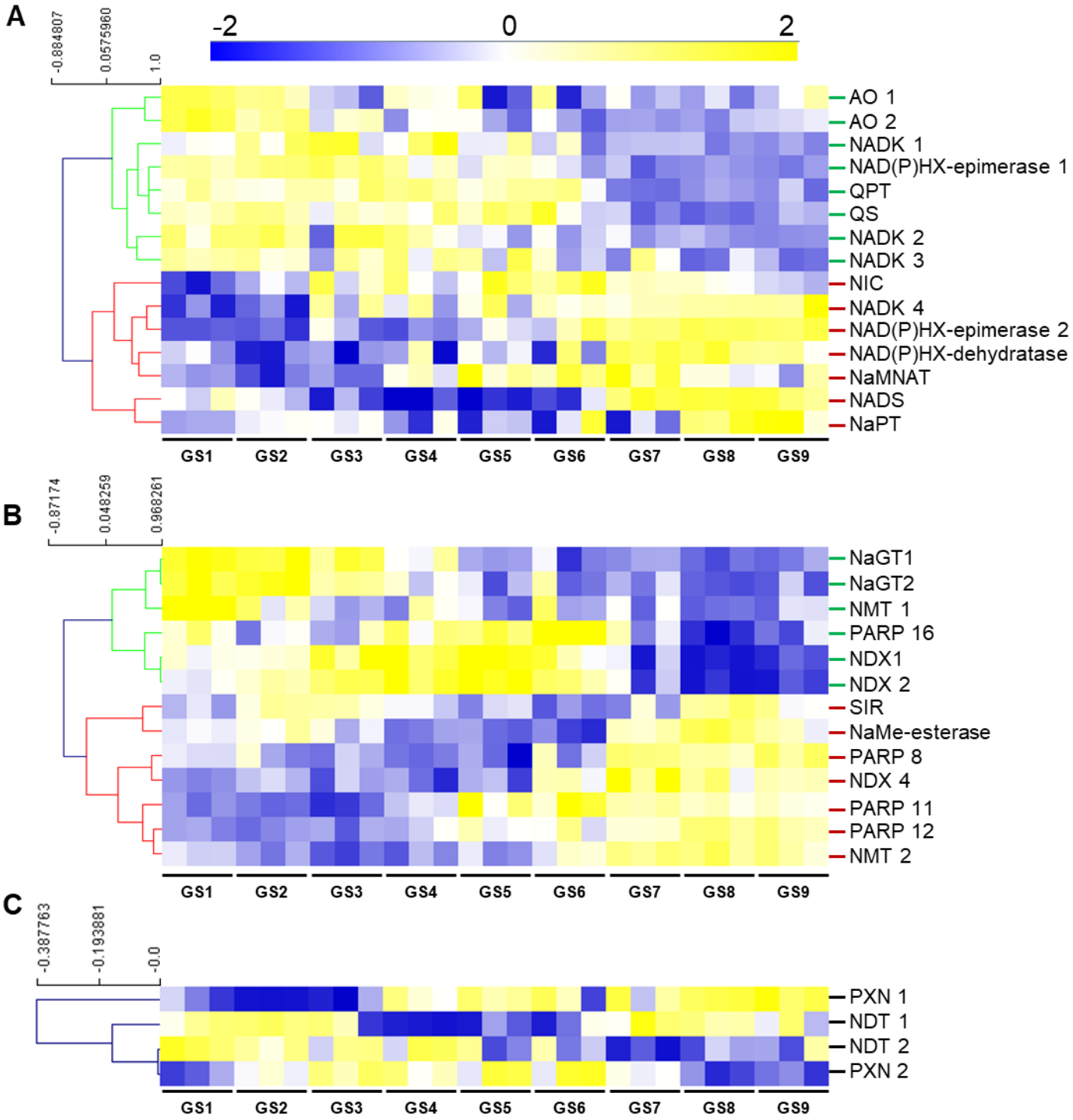

Figure III.3: NAD$^+$ synthesis (A), consumption (B) and transport (C) show transcriptional changes during tomato fruit development. Transcript data were normalised and filtered for statistically significant features (ANOVA with Bonferroni correction, $p < 0.01$) and subjected to clustering analysis. Shown are Pearson's correlations after complete clustering of mRNA profiles. Names on the right refer to as enzymes of NAD$^+$ synthesis **(A)**, consumption **(B)**, or putative transport **(C)**. AO: aspartate oxidase; GS: growth stage; NADK: NAD kinase; NAD(P)HX: NAD(P)H hydrate; NaMNAT: NaMN adenylyltransferase; NAD(P)HX: NAD(P)H hydrate NADS: NAD synthetase; NaGT: nicotinate N-glucosyltransferase; NaPT: nicotinate phosphoribosyltransferase; NaMe: nicotinate methyl; NMT: nicotinate methyltransferase; NDT: nicotinamide adenine transporter; NDX: nudix; NIC: nicotinamidase; PARP: poly-ADP-ribose polymerase; PXN: peroxisomal NAD carrier; QPT: quinolinate phosphoribosyltransferase; QS: quinolinate synthase; SIR: sirtuin. From (Decros et al., 2019b).

This might suggest that most NAD metabolism enzymes were poorly represented quantitatively (*i.e.* below threshold of protein detection). To test this hypothesis, we checked the absolute expression levels of genes involved in NAD^+ synthesis as compared to other genes of central cellular functions (Supplemental fig III.3). Raw data of mRNA profiles evidenced very low expression values for AO in tomato fruit, as compared to NIC and NaPT, and more remarkably, as compared to actin- and enolase-related genes (Supplemental fig III.3A). Complementarily, datamining of expression profiles from published datasets (http://tea.solgenomics.net/; (Fernandez-Pozo et al., 2017)) confirmed that the NAD^+ biosynthesis gene AO was expressed at low levels in fruit tissues as compared to other genes (Supplemental fig III.3B), which can explain the absence of proteomic hits in our dataset.

Furthermore, we analysed transcriptional changes of NAD^+ catabolism involved in signalling and synthesis of nicotinate derivatives including 13 genes of PARPs, SIRs, NDXs, NaGTs, and NMTs (Figure III.3B) (Gakière et al., 2018b). Clustering analysis (Pearson's correlation with complete clustering) unveiled three main significant clusters (ANOVA with Bonferroni correction, $p < 0.01$ are listed in Supplemental table II.1). The young fruit correlated with an up-regulation of genes associated with NaGT, SIR and NDX functions, while the ripening fruit was mostly associated with higher expression of genes associated with NMT, NaMe esterase and PARP (Figure III.3B).

Finally, we evaluated transcriptional changes of transporter genes that linked to putative pyridine nucleotide transport (Figure III.3C). Transcript levels observed during early fruit development (GS 1-4) correlated with the expression of NDT-like transporters suggesting an active transport of NAD(P) and its derivatives across the chloroplastic and mitochondrial membranes. Cell elongation (GS 4-6) and ripening (GS 7-9) phases were associated with higher expression of both PXN and NDT-like transporters, thus supporting the idea of an active NAD(P) transport during fruit development.

Altogether, RNAseq data demonstrate a profound reprogramming of NAD(P) metabolism during fruit growth, more specifically towards a stimulation of the synthesis of NAD^+ precursors (AO, QS and QPT) in chloroplast of young fruits, which was concurrent with the expression of NDT-like transporters. This was followed at later stages of fruit development by an active synthesis (NaMNAT and NADS) and recycling (NIC and NaPT) (Figure III.3), concomitantly with increased NAD(H) pools and concentrations (Figure III.2).

C. Transcriptional changes of genes associated with NAD(P)-dependent enzymes during tomato fruit growth

To get a more global overview of the metabolic functions relating to pyridine nucleotides during tomato fruit growth, we analysed the expression profiles of the genes that we could associate to NAD/P(H)-dependent functions. A selection of 442 NAD(P)-dependent features was subjected to Principal Component Analysis (PCA) to display the global impact of growth stages on transcriptional changes for those features (Figure III.4A). PCA explained 70% of the maximal variation in the mRNA profiles, where PC1 (59.6%) separated stages 1 to 6 from stages 7 to 9. This suggests a differential reprogramming at mRNA level of NAD(P)-dependent between cell division and expansion (GS1-6), and fruit ripening (GS7-9). Next, we filtered the same features for statistical significance (ANOVA with Bonferroni correction, $p < 0.01$ are listed in Supplemental table II.2), which provided 119 mRNA markers that were retained for subsequent clustering analysis (Pearson's correlation, complete clustering) (Figure III.4B).

Tomato fruit development was associated with four clusters distributed along the different growth stages, for which functional classification was performed based on gene ontology using Mercator4 v1.0 (https://plabipd.de/portal/mercator4; (Schwacke et al., 2019). This led to the identification of 13 different functional categories (Figure III.4C) in which mitochondrial activity (18% of the total significant features) is the largest category represented for all growth stages. Cluster 1 corresponded to the beginning of tomato fruit development (GS 1 to 5) and contained 19 genes mainly involved in energy supply for central metabolism, *i.e.* photosynthesis (21%) and mitochondrial activity (5%). Cluster 1 further harbours several genes linked to central metabolism such as lipid-, sugar-, lignin-, and cell wall-related metabolisms (11, 10, 16 and 5%, respectively). Cluster 2 covered cell division and cell expansion stages of fruit growth and contained 36 genes mostly related to central metabolism (*i.e.* cell wall, sugar, lipid, amino acid metabolism (28, 8, 8, 5%, respectively)) that are essential to cell proliferation by providing building blocks (Figure III.4C).

In addition, cluster 2 presented a substantial proportion (25%) of unknown functions or of genes involved in specialised metabolism (17 and 8%, respectively). Cluster 3 was represented only by 6 genes which were expressed from GS4 to GS6 (*i.e.* the end of fruit expansion) and that were annotated to pigment synthesis, lipid, amino acid and cell wall metabolisms (17% each) (Figure III.4C). Cluster 4 contained the larger number of significant mRNA markers (58) that coded for genes mostly involved in mitochondrial activity (34%), but also the maintenance of redox homeostasis, lipid, amino acid, secondary pathways (9% each) and protein degradation (2%).

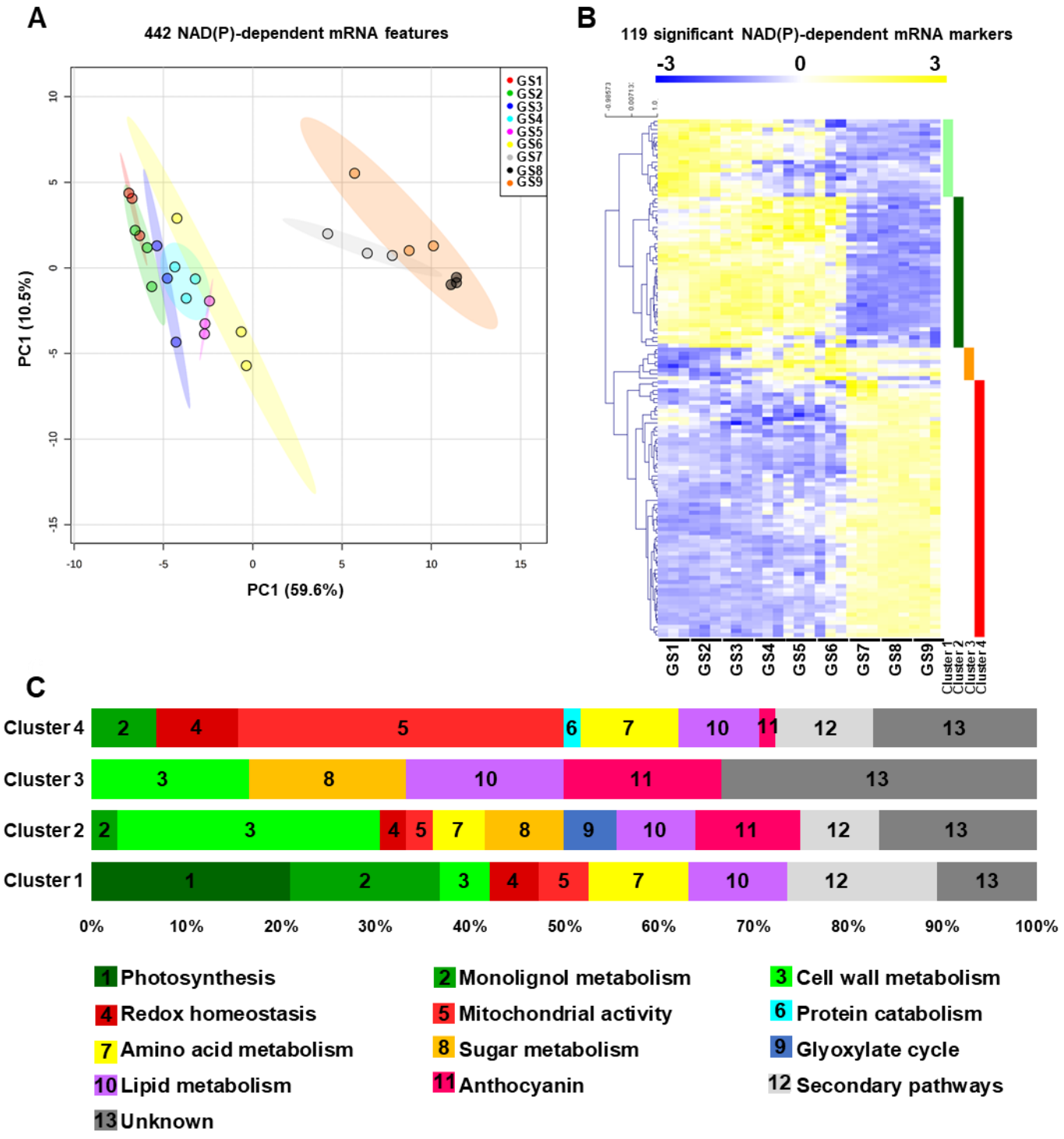

Figure III.4: **Expression of genes for NAD(P)-dependent enzymes reveals distinct clusters during tomato fruit growth.** Normalised transcript data of 442 transcript features of NAD(P)-dependent enzyme were visualised **(A)** for global impact of the growth stage of tomato fruit by PCA (with maximal variation given into brackets). Same features were then filtered (ANOVA with Bonferroni correction, $p < 0.01$) and subjected to clustering analysis **(B)**. Shown are Pearson's correlations after complete clustering of 119 significant mRNA profiles. Four clusters were identified and analysed for functional classification based on their gene ontology annotations **(C)**. GS: Growth Stage. From (Decros et al., 2019b).

Overall, gene expression for NAD(P)-dependent functions during fruit growth emphasises the importance of pyridine nucleotides as cornerstones of central metabolism, which provides building blocks and energy for development. Importantly, NAD(P)-related mitochondrial functions seem crucial for fruit growth, more specifically at the onset of ripening.

D. Protein profiles for NAD(P)-dependent enzymes during tomato fruit growth

In addition to mRNA profiles, we further examined protein profiles for NAD(P)-dependent enzymes through global analysis by PCA of 128 protein features from normalised data, and by clustering of 78 significant protein markers (ANOVA with Bonferroni correction, $p < 0.01$ are listed in Supplemental table II.3. In contrast to transcript signatures (Figure III.4A), PCA better segregated the protein patterns according to GS1, GS2 and GS3, then merged GS4 to GS6, separated GS7 and gathered GS8 and GS9 (Figure III.5A). This suggests that proteomics of NAD(P)-dependent enzymes is particularly sensitive to fruit growth. Complete clustering analysis by Pearson's correlation resulted in three main clusters (Figure III.5B) for which functional annotation of protein sequences was performed based on gene ontology using Mercator4 v1.0 leading to the identification of 12 different functional categories (Figure III.5C) in which mitochondrial activity (19% of the total significant markers) was the largest category represented across all growth stages. To confirm the proteomic output, we measured enzyme activities of isocitrate dehydrogenase ($NADP^+$-dependent) and malate dehydrogenase (NAD^+-dependent) (Supplemental fig III.4), which showed similar profile during fruit growth as compared to normalised protein concentration.

Firstly, cluster 1 is comprised of 27 NAD(P)-dependent proteins that accumulated mainly during the beginning of tomato fruit development (GS1-4) and during the ripening phases (GS7-9) for some of them (Figure 5C). This cluster could be divided into 3 segments, the first one contained enzymes involved in central metabolism (56%) such as cell wall-, sugar-, lipid-, nitrogen-related metabolism and pentose phosphate pathway (15, 15, 11, 11 and 4%, respectively). The second portion is devoted to the energy production via the mitochondrial activity, constituting 15% of this cluster. The remaining part is represented by enzymes involved in specialised metabolism or unknown functions (15 and 15%, respectively) (Figure III.5C).

Secondly, cluster 2 included 28 proteins, which coincided with the fruit enlargement (GS1-6) within half of them that are stimulated during cell expansion (GS4-GS6). The most represented enzymes in this cluster are those involved in secondary pathways (29%) and mitochondrial functions (18%) (Figure III.5C).

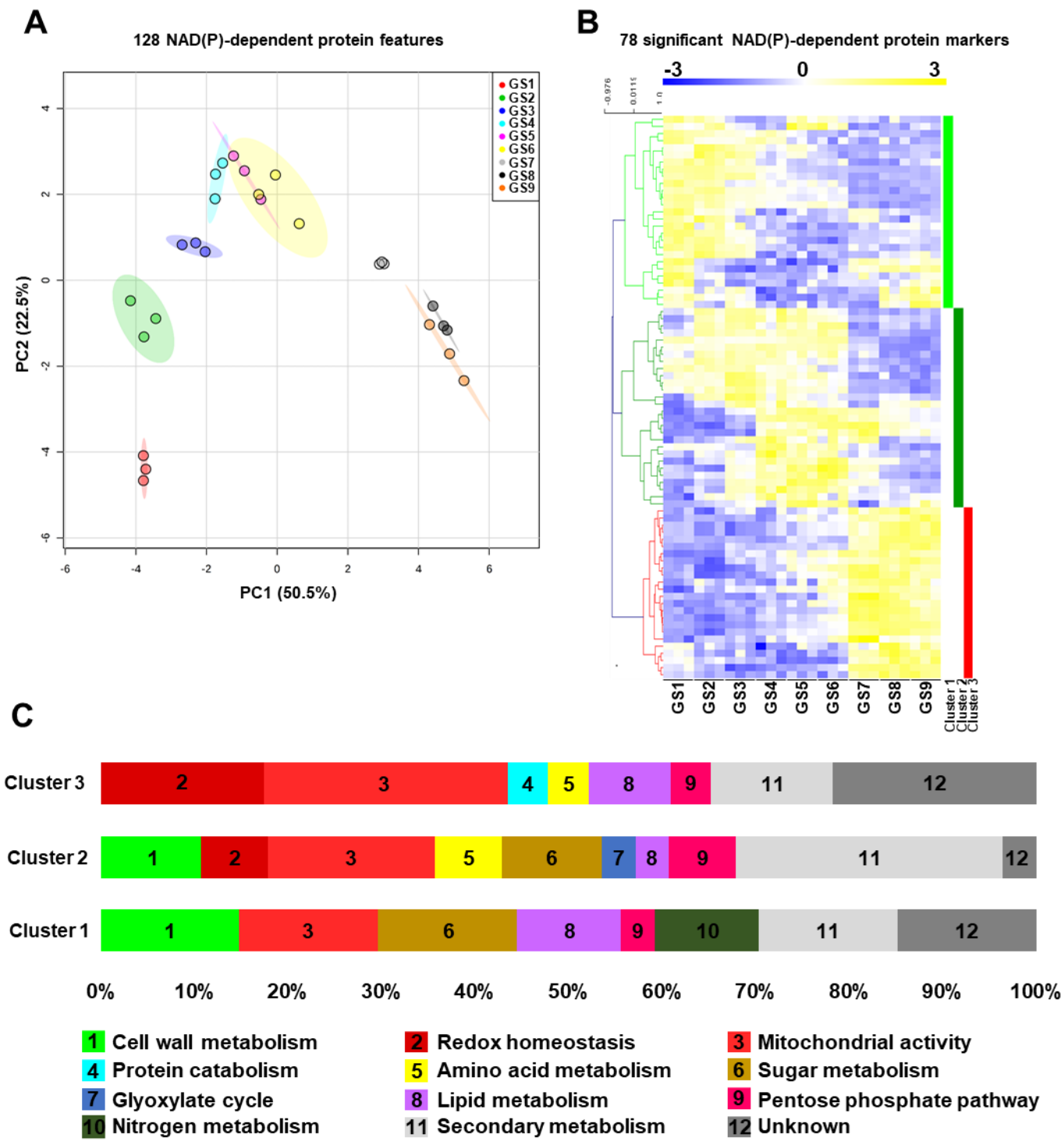

Figure III.5: Protein profiles for NAD(P)-dependent enzymes unveil distinct clusters during tomato fruit growth. Normalised protein data 127 NAD(P)-dependent enzymes were visualised **(A)** for global impact of the growth stage of tomato fruit by PCA (with maximal variation given into brackets). Same features were then filtered (ANOVA with Bonferroni correction, $p < 0.01$) and subjected to clustering analysis **(B)**. Shown are Pearson's correlations after complete clustering of 78 significant protein profiles. Four clusters were identified and analysed for functional classification based on their gene ontology annotations **(C)**. GS: Growth Stage. From (Decros et al., 2019b).

Strikingly, central metabolism accounted for 42%, mainly because of cell wall and sugar metabolism (11% each) but also because of amino acid and lipid metabolism, glyoxylate cycle and pentose phosphate pathway (7, 3, 3, and 7%, respectively) (Figure III.5C). Finally, cluster 3 was constituted by 23 NAD(P)-dependent enzymes that were found during fruit ripening (from GS7 to GS9). Quite importantly, enzymes involved in mitochondrial activity were mainly represented (26%) in this last cluster, followed by proteins participating in redox homeostasis (18%) and secondary pathways (13%). Central metabolism (21%) remained noticeable due to the presence of enzymes involved in lipid-, amino acid- metabolisms, pentose phosphate pathway and protein degradation (9, 4, 4 and 4%, respectively) (Figure III.5C). Hence, while protein and mRNA profiles of NAD(P)-dependent markers only showed partial overlap during tomato fruit growth, central metabolism and more particularly mitochondrial functions were critically linked to pyridine nucleotides.

E. Multiomics dynamic of NAD metabolism during fruit development.

Pyridine nucleotides have received considerable attention for their metabolic, redox and signalling functions in plant tissues (Hashida et al., 2009; Pétriacq et al., 2013; Gakière et al., 2018a, 2018b). However, very little is known about the importance of these metabolic cofactors for fruit growth. In this study, we examined the contribution of pyridine nucleotides to fruit growth by analysing NAD(P) metabolism at transcriptome and proteome scales as well as $NAD(P)^+$ and NAD(P)H contents and concentrations during nine sequential stages of tomato fruit development.

I. Growth dependent de novo synthesis and recycling of pyridine nucleotides

Although previous changes in pyridine nucleotides have been observed between green and red tomato fruits of MicroTom and Moneymaker cultivars (Centeno et al., 2011; Osorio et al., 2013b), our study presents for the first time the changes of NAD(P) contents and concentrations during nine sequential stages of tomato fruit development. As previously observed (Centeno et al., 2011), the highest contents ($nmol.gFW^{-1}$) were measured during early developmental phases (Figure III.2), concomitantly with the expression of genes involved in early reactions of NAD^+ de novo synthesis (AO, QS and QPT) (Figure III.3), also assumed to control critically NAD(P) levels and its derivatives (Pétriacq et al., 2012, 2016b). Firstly, NAD(H) contents and concentrations showed two distinct accumulations mainly caused by increased NAD^+ at the beginning of cell elongation and ripening (GS5 and GS8) (Figure III.2).

Concurrently, transcript analysis unveiled a stimulation of further steps of NAD^+ de novo synthesis and recycling pathway (Figure III.3A). Secondly, NADP(H) contents dropped during cell division (GS1-4) whereas concentrations were augmented as a result of increased NADPH concentrations. Furthermore,

cell expansion and ripening phases displayed a decrease in both NADP(H) contents and concentrations. Since NAD(P) are mostly present in organelles other than the vacuole (Donaldson, 1982; Gakière et al., 2018b), concentrations seem more relevant to understand the involvement of NADP(H) in fruit development (Figure III.2C). However, pyridine nucleotide concentrations that are reported here and in previous studies represent pooled contents of subcellular metabolites rather than the in vivo original compartmentalised concentrations, which are known to differ between organelles (Gakière et al., 2018b). Such differences in subcellular concentrations might affect the enzyme activities that depend on pyridine nucleotides as cofactor.

Meta-analysis of K_m values for plant dehydrogenases (Bar-Even et al., 2011) showed that total cellular concentrations of NAD(P) measured in our study were higher than the median K_m values of plant NAD(P)-dependent enzymes (Supplemental fig III.5). This indicates that concentrations of pyridine nucleotides in the developing fruit are sufficiently high that they would not limit NAD(P)-dependent enzyme activities, as previously suggested (Bennett et al., 2009). In growing tissues, such as Arabidopsis pollen tubes (Hashida et al., 2013), or here in young tomato fruit that is characterised by a turbo metabolism due to high enzyme activities (Biais et al., 2014), plant development requires higher NAD^+ and reducing power (NADPH) (Gakière et al., 2018b). High concentrations of NADP(H) in young fruits (Figure III.2C) might be associated with photosynthesis that remains active in green fruits, as detected in our transcript analysis (Figure III.4C) and previously reported (Lytovchenko et al., 2011). Furthermore, mRNA and protein analyses indicated a primary accumulation of NAD^+ precursors (GS1-4) before the activation of de novo and recycling (GS4-9) pathways during tomato fruit growth (Figure III.3), which correlated with both contents and concentrations of NAD(H). Interestingly, the stimulation of NaMNAT and NADS at transcript levels (Figure III.3A) occurred just before the increase in NAD(H) concentrations (Figure III.2C).

On the other hand, catabolism of NAD(P) via signalling functions appeared continuous during fruit development but resulted from different catabolic pathways (Figure III.3B) as well as transport of NAD(P) and their precursors (Figure III.3C). This indicates that NAD(P) contents are sustained as key metabolic regulators for fruit growth by different synthesis and degradation pathways. Precursors are synthesised by early enzymes of de novo synthesis of NAD^+ (AO, QS, QPT), then latter enzymes of synthesis and salvage routes (NaMNAT, NADS, NIC, NaPT, NaGT and NAD(P)H-hydrate epimerase and hydratase) (Figure III.1) allow for NAD(P) homeostasis.

This agrees with previous works which have demonstrated the importance of AO, QS and QPT in modulating NAD^+ levels that influence plant development (Katoh et al., 2006; Schippers et al., 2008; Pétriacq et al., 2012; Gakière et al., 2018a).

Likewise, Arabidopsis NICs were also reported to influence NAD^+ contents (Hunt et al., 2007; Wang and Pichersky, 2007). Metabolism of nicotinate has also received recent attention in various plant species (Matsui et al., 2007; Li et al., 2015; Wu et al., 2018). However, nicotinate conjugates are particularly difficult to measure via MS-based metabolomics due to unreliable ionisations of such compounds in the mass spectrometer, as it is the case for NAD^+ and nicotinamide (Guérard et al., 2011). Further research combining MS and NMR techniques is necessary to confirm the molecular and regulatory details of nicotinate metabolism in fruit.

II. Growth dependent mRNA and protein profiles of NAD(P)-dependent enzymes

In all biological systems, a plethora of cellular processes need NAD(P) as coenzymes, including both biosynthetic pathways and the catabolism of biomolecules which support energy production (Gakière et al., 2018a). Mitochondria are the powerhouse of the cell that ensure energy supply by regenerating NADH and providing ATP, and are considered to contain the highest proportion of cellular NAD(H). Several studies have shown that modifying mitochondrial functions result in changes of NAD(P) contents that not only greatly influence plant growth (Dutilleul et al., 2003a, 2003b, 2005; Pellny et al., 2008; Meyer et al., 2009; Centeno et al., 2011; Osorio et al., 2013b; Pétriacq et al., 2017) but also stress responses (Pétriacq et al., 2016b; Gakière et al., 2018b), thus placing pyridine nucleotides as critical regulators of plant performance. In line with this, we demonstrated that NAD(P)-dependent enzymes appeared mainly related to central metabolic pathways, including one-fifth of mitochondrial functions (Figure III.4C & II.5C). This agrees with a critical role of mitochondrial NAD(P) metabolism for tomato fruit growth, as elegantly demonstrated in mutant tomato fruit that are affected in TCA cycle (Araújo et al., 2012).

Additionally, we showed that mRNAs and proteins that related to NAD(P)-dependent enzymes exhibited distinguishable profiles during fruit development. We further identified a global separation between ripening and previous developmental stages (*i.e.* cell division and expansion) (Figure III.4A & II.5A), based on the profiles of both NAD(P)-dependent mRNAs and proteins. This suggests a growth stage-dependent reprogramming of NAD(P) metabolism. Concurrently, we observed a growth stage-dependent stimulation of the different central metabolism branches (amino acid-, lipid-, sugar- and cell wall-related metabolism) at both transcript and proteomic levels (Figure III.4C & II.5C), thus emphasising the link between NAD(P) and carbon and nitrogen metabolisms.

This raises the question about NAD(P) signalling during fruit development (Hashida et al., 2018), as further exemplified by a notable proportion of NAD(P)-dependent enzymes that related to redox homeostasis at mRNA and protein levels, especially those involved in ascorbate-glutathione cycle, and other specialised pathways (*e.g.* anthocyanins biosynthesis).

Here, we showed that cellular division phases displayed an increase in reducing power equivalent (NADPH) while cellular expansion and ripening phases harboured a higher oxidised state. Hence, pyridine nucleotides appear pivotal for fruit development in supplying energy and precursors for central metabolism while assuring redox homeostasis and secondary metabolites accumulation. For a better comprehension of NAD(P) involvement in cellular processes, future works should also include the study of protein turnover, especially protein synthesis rate that has been shown to control protein levels in developing tomato fruit (Belouah et al., 2019).

III. NAD metabolism is strongly linked with mitochondrial and redox processes during ripening

Climacteric species (*e.g.* tomato, banana, kiwi.) are characterised by a metabolic shift from normal development state, known as climacteric crisis, that is associated with the conversion of starch into soluble sugars and CO_2 (Moing et al., 2001; Colombié et al., 2017), and which is concomitant with higher ATP levels and respiratory fluxes. Interestingly, from a transcript perspective, 50% of the significant NAD(P)-dependent genes that were identified as up-regulated during ripening belonged to enzymes involved in the key respiratory burst during ripening of climacteric fruits (Figure III.4) in accordance with previous reports (Biais et al., 2014; Colombié et al., 2015, 2017).

Moreover, mitochondrial functions represented a notable proportion of both protein and transcript markers, and more specifically a greater proportion (>75%) within the NAD(P)-dependent ripening-related markers, thus supporting the idea that climacteric respiration is i) regulated by mitochondrial activity and ii) essential for fruit ripening (Figure III.4B & II.4C). In tomato fruit, the energy peak results from an excessive carbon supply coming from starch and cell wall degradation, and a decrease in carbon demand as a result of arrested cell expansion (Colombié et al., 2017). In agreement, several sugar- and cell wall-related NAD(P)-dependent markers are identified to be up-regulated shortly before and during ripening (Figure III.4 & II.5). Besides, NAD(P)-dependent markers involved in redox homeostasis were also up-regulated mainly during ripening (Figure III.4 & II.5). Despite the energy peak and the control of redox balance, ripening is also associated with a wide range of metabolic processes resulting in organoleptic changes reflected by an increased sweetness, and nutritional value. This further agrees with a concurrent accumulation of soluble sugars and others amino acids coming from starch and protein degradation, respectively (Beauvoit et al., 2018).

Here, functional clustering identified an increase of NAD(P)-dependent transcript and protein levels involved in protein catabolism only during ripening phases as well as amino acid-related metabolism markers (Figure III.4 & II.5). Finally, latter stages of NAD^+ synthesis and recycling were stimulated during ripening at both transcript and protein levels (Figure III.3) that resulted in an

augmented NAD(H) concentrations (Figure III.2), probably to sustain the high metabolic activity during fruit ripening process.

Collectively, these results indicate that NAD(P) is a core component of tomato fruit ripening, which not only participates in the climacteric respiration via a stimulation of mitochondrial activity, but also sustains energy supply for numerous biosynthetic pathways that relate pyridine nucleotides metabolism to fruit development and quality.

CONCLUSION

This study is one of the first steps towards a better comprehension of the implication of NAD(P) in fruit development. Our results demonstrate a crucial role of NAD(P) during the whole process of fruit growth with distinct functions between the cellular division, expansion and ripening stages. Further experiments are required to decipher which biochemical and molecular mechanisms are triggered by pyridine nucleotides and participate in the control of fruit development. Due to the high reactivity of such redox metabolites, metabolic modelling tools might provide a great alternative to predict fluxes of NAD(P) during fruit development and a better understanding of these mechanisms that will help to improve fruit performance, thus allowing better strategies for crop productions.

SUPPLEMENTAL DATA

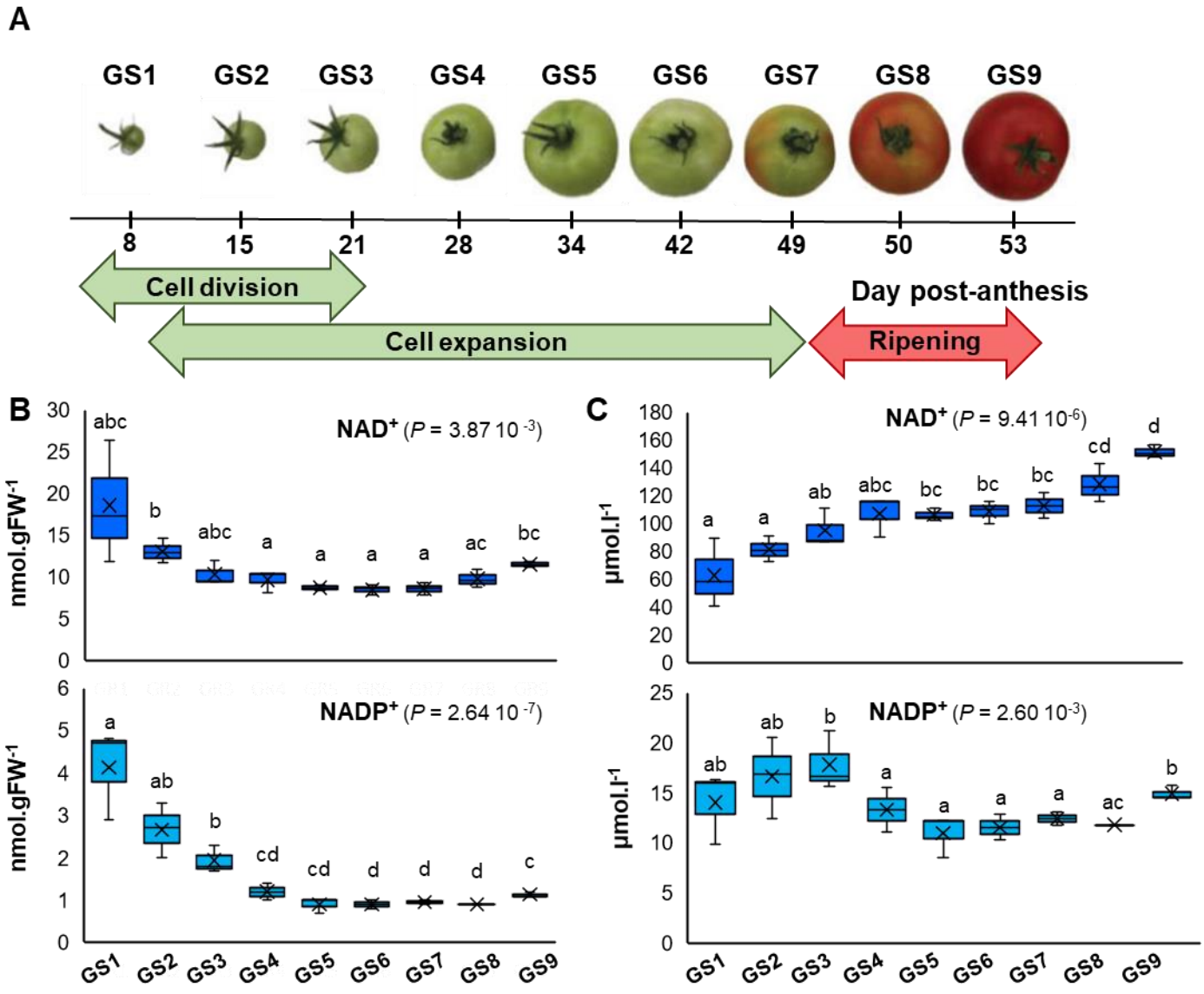

Supplemental fig III.1: **LCMS measurements of NAD(P)$^+$ contents during tomato fruit development. NAD$^+$ and NADP$^+$ pools were measured for nine sequential growth stages (GS) of tomato fruit development (A).** Shown are box plots of replicated metabolite quantifications (n = 3) **(B)** and of replicated metabolite quantifications (n = 3) normalised to the cytosol and organelles volumes **(C)**. where X indicates means and lines median, respectively. Statistical significance is indicated by ANOVA P value. Binary comparisons between conditions are indicated by letters above box plots, according to Student's t test ($p < 0.05$). Left panel indicates the concentrations of NAD(P)$^+$ in nmol.gFW^{-1} whereas the right panel indicates the NAD(P)$^+$ concentrations in µmol.l^{-1}.

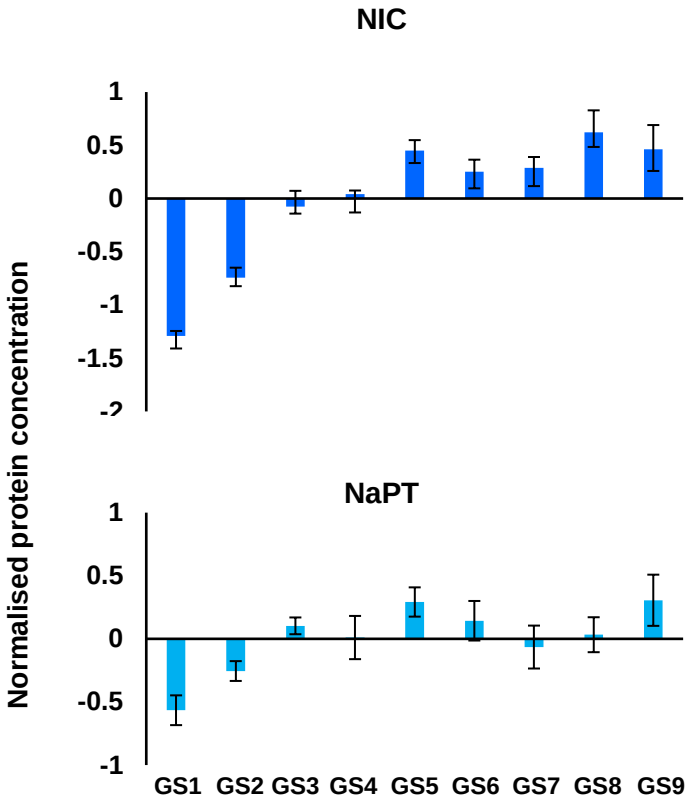

Supplemental fig III.2: Normalised protein profiles of NIC and NaPT during tomato fruit growth. Bar charts (n = 3, ± SEM) show normalised concentrations of NIC (Solyc01g007920) and NaPT (Solyc02g093290) enzymes involved in NAD^+ recycling. NaPT: Nicotinate phosphoribosyltransferase; NIC; Nicotinamidase.

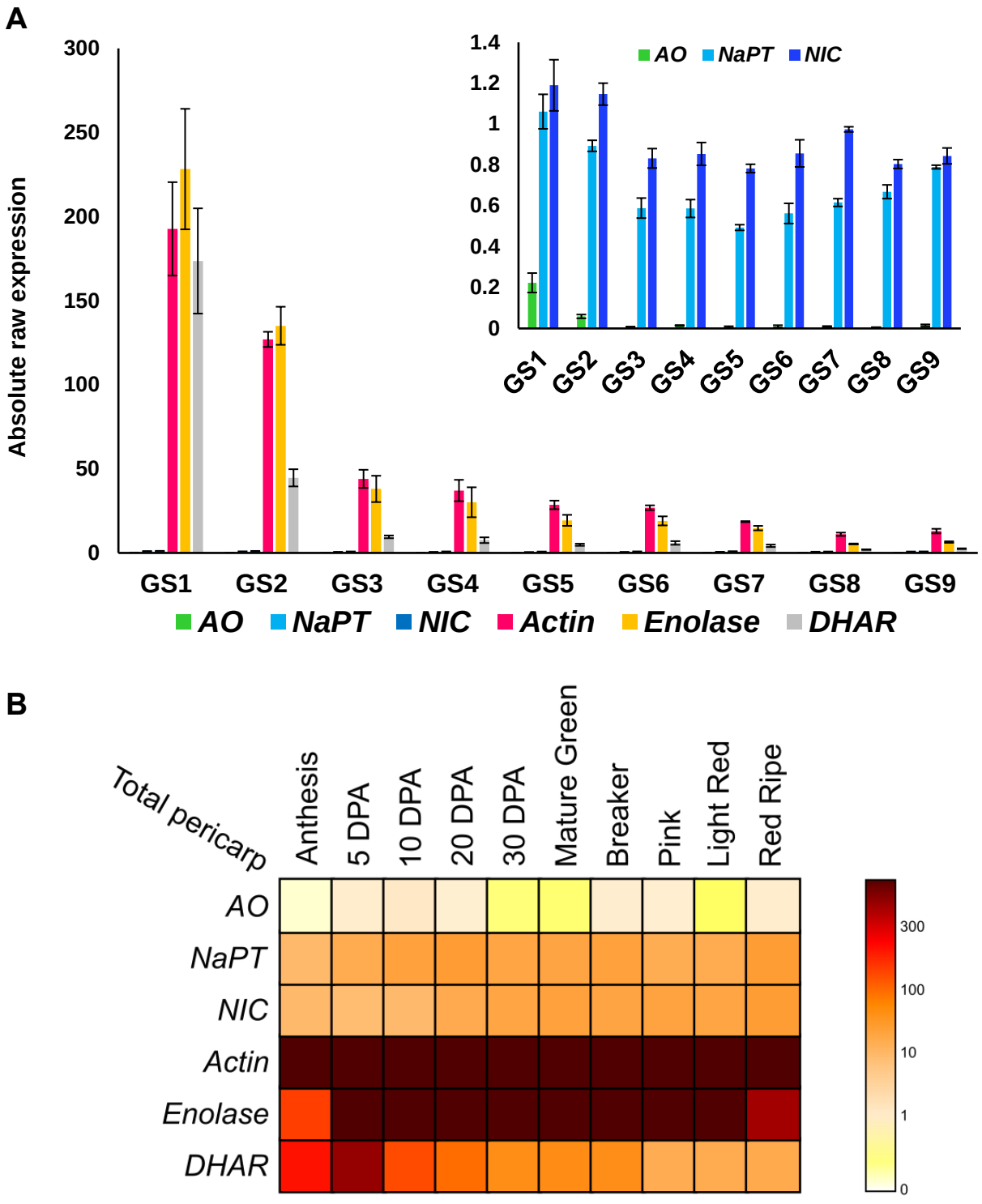

Supplemental fig III.3: Absolute expression of NAD$^+$ metabolism genes is low compared to central metabolism genes. Bar charts (n = 3, ± SEM) showing raw absolute expression of genes involved in NAD$^+$ synthesis, recycling, the house-keeping gene *Actin*, and two genes of central and redox metabolism. Insert shows absolute expression for only *AO*, *NIC* and *NaPT* genes **(A)**. Expression dataset from Tomato Expression Atlas (http://tea.solgenomics.net/) confirming the low expression levels of NAD$^+$ synthesis genes *AO* and compared to central metabolism and redox genes during tomato fruit development **(B)**. AO: Aspartate oxidase; NaPT: Nicotinate phosphoribosyltransferase; NIC; Nicotinamidase; DHAR: Dehydroascorbate reductase.

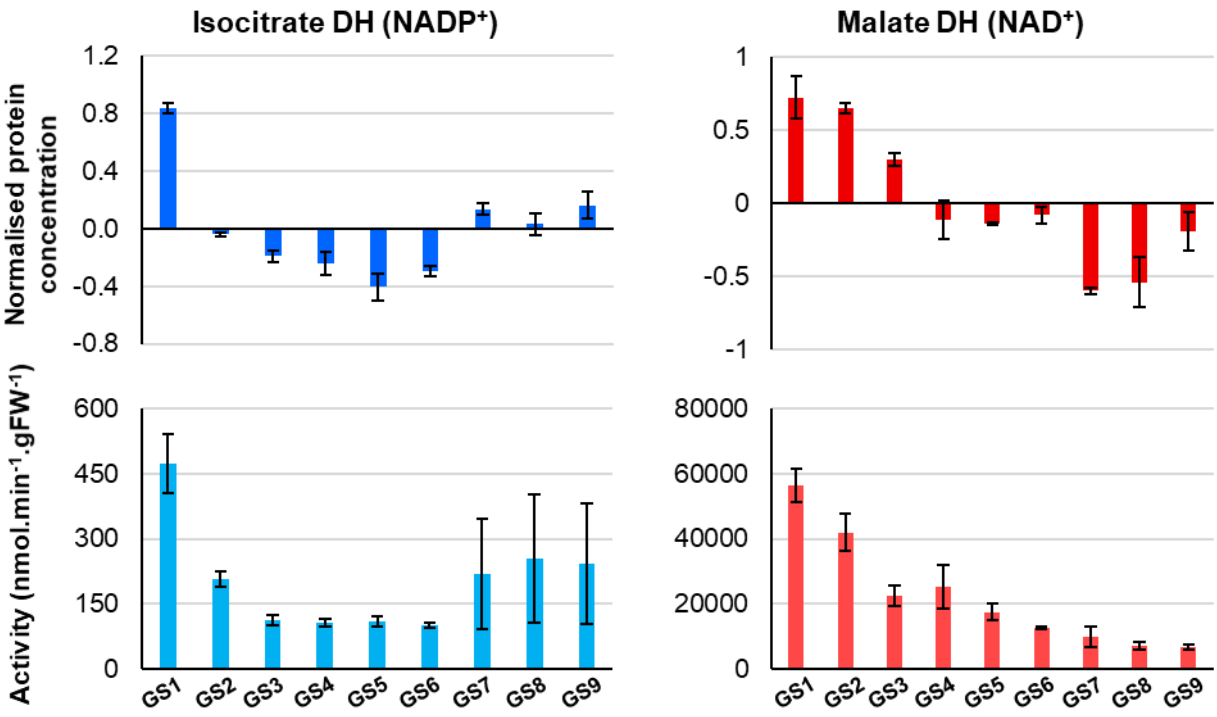

Supplemental fig III.4:. Example of NAD(P)-dependent enzyme activity. Activity of isocitrate dehydrogenase $NADP^+$-dependent (Solyc11g011930.1.1, in blue) and malate dehydrogenase NAD^+-dependent (Solyc01g106480.2, in red) during tomato fruit growth.

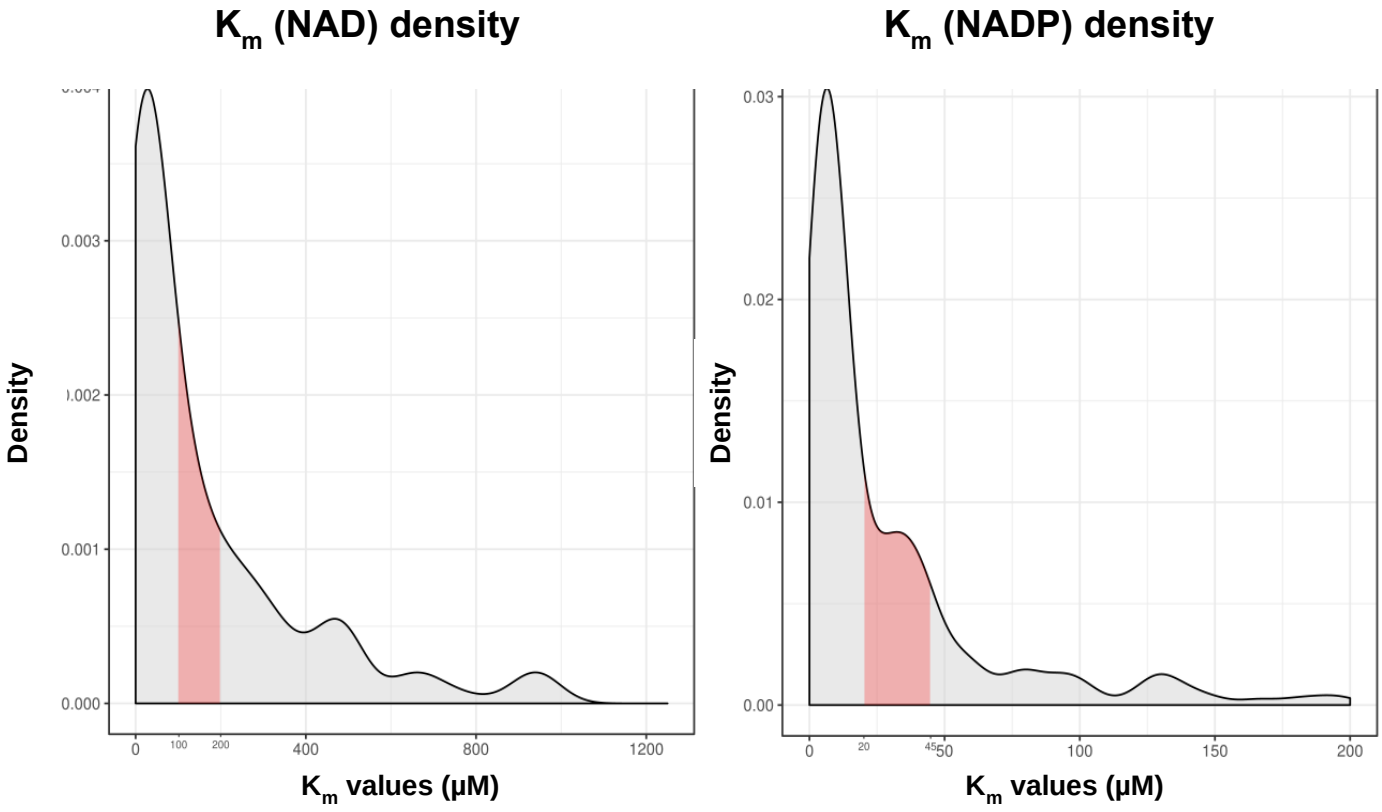

Supplemental fig III.5: Distribution of plant NAD(P)-dependent enzyme K_m. K_m values for plant species were filtered from (Bar-Even et al., 2011). Right panel shown the distribution of 171 K_m values of plant NAD-dependent dehydrogenases (K_m values < 1200) and left panel shown the distribution of 234 K_m values of plant NADP-dependent dehydrogenases (K_m values < 200). Red areas represent the NAD(P) concentrations observed in our study during tomato fruit development.

For supplemental tables, please follow this link:

https://www.frontiersin.org/articles/10.3389/fpls.2019.01201/full#supplementary-material

CHAPTER IV

QUANTITATIVE DESCRIPTION OF THE ASC-GSH CYCLE DURING TOMATO FRUIT DEVELOPMENT

ABSTRACT

Reactive oxygen species and redox metabolism are some of the key players in the control of plant development by participating in virtually all signalling processes. Among the myriad of antioxidant metabolites, ascorbate, glutathione and pyridine nucleotides have been identified as crucial metabolic cornerstones, orchestrating the regulations of the redox balance during development and in response to stresses (Foyer and Noctor, 2016; Decros et al., 2019a; Smirnoff and Arnaud, 2019). However, knowledge on the redox metabolism involvement during development remain scarce. Here, we provide the first quantitative description of the core redox metabolism, including ASC-GSH cycle metabolite contents and enzymatic capacities during the whole tomato fruit development. Moreover, mutant fruits displaying enhanced ASC synthesis have been analysed to investigate the role of ASC during fruit development.

This study unveiled a growth-dependent behaviour of the core redox metabolism during tomato fruit development, especially a complete shift in ASC oxidation ratio during cell division to expansion transition. Moreover, MDHAR and APX appeared as central actors in the control of ASC and GSH signalling during development, whereas DHAR and GR were probably more related to stress management.

Furthermore, analysis of these ASC-enriched mutant fruits showed a limited impact on fruit growth and metabolism but has enabled us to identify a co-regulation of GSH and ASC reduced form contents independently from the ASC-GSH cycle activity.

This unprecedented redox dataset represents valuable information for developing further a redox kinetic model (see Chapter V).

Reactive oxygen species and major redox buffers are key partners in orchestrating the redox poise in developing cells. However, the high reactivity of ROS leads to a scarcity of available quantitative data concerning them. The literature mainly contains semi-quantitative or qualitative data, but rarely obtained on developmental series, as well as for the other major redox buffers (Jozefczak et al., 2015; Foyer, 2018; Rosalie et al., 2018). Redox metabolism has often been specifically quantified during a definite event but not in a continuous way throughout the development, especially for fruits in which they have been assayed for post-harvest issues (Fu et al., 2011; Liu et al., 2016; Valenzuela et al., 2017).

The ascorbate-glutathione cycle is a major actor in the control of the redox balance by linking the three major redox buffers together in a *ménage-à-trois* allowing rapid ROS processing while controlling the redox state of major antioxidants (Foyer and Noctor, 2011; Decros et al., 2019a). High levels of oxidised ASC in young fruits of different species have been observed, however, no study including all three partners of the ASC-GSH cycle, as well as their redox state, and the associated ROS content has been reported yet (Roch et al., 2020).

Besides, antioxidant metabolites have been shown to benefit human health (Wargovich et al., 2012; Cory et al., 2018), and also participate in plant tolerance to various stresses (Foyer and Noctor, 2016; Pétriacq et al., 2016b; Choudhury et al., 2017). However, despite the ascorbate role in numerous fundamental processes, its content was gradually decreasing during tomato breeding in favour of the yield (Macknight et al., 2017; Mellidou et al., 2021). Additionally, studies aiming to increase fruit ascorbate content have shown limited success, which suggests a finely controlled ASC metabolism in fruits without totally identifying the underlying mechanism involved (Stevens et al., 2018). Lastly, a drastic increase of ASC content in the whole plant leads to developmental alterations in the flowers and pollen infertility, thus making fruit production impossible (Deslous et al., 2021). Although ASC synthesis and recycling pathways are well known in plants, ASC displays various roles within the different plant organs that remain to be deciphered (Bulley and Laing, 2016; Smirnoff, 2018). Concepts from foliar tissues, which are strongly linked to photosynthetic activity, can be transposed to fruits in a limited way leaving many questions about ASC role and metabolism unanswered.

The objective of this study is to describe, quantitatively, the core redox metabolism including ROS and major redox buffer contents throughout the development of the tomato fruit. Moreover, the impact of an internal perturbation of ASC metabolism for fruit development was analysed using ascorbate-enriched mutants affected in the ascorbate synthesis pathway.

A. Quantitative description of ROS and redox metabolite contents

I. ROS dynamic during fruit development

Remarkably, tomato fruit showed a very high content of H_2O_2 at the beginning of its development that dropped rapidly after 8 days post-anthesis (Figure IV.1). Then, ROS content continued to decline gradually during cell expansion. Furthermore, by optimising the scale of the data presented, a slight increase of the ROS content at the turning stage could be noticed. Although not significant, this increase was concurrent with the well-known climacteric crisis characterised by a respiratory burst (Colombié et al., 2017).

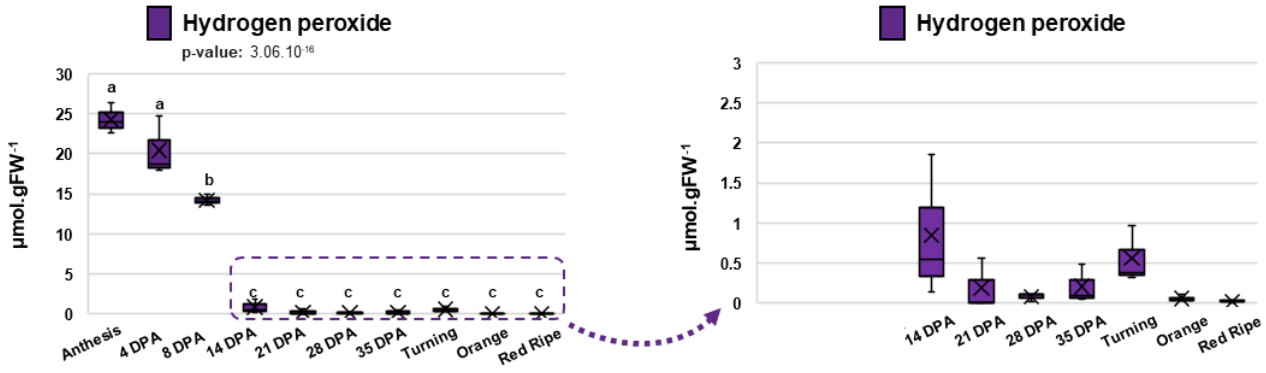

Figure IV.1: Hydrogen peroxide content during tomato fruit development. Statistical significance content is indicated by ANOVA p-value. Binary comparisons between growth stages are indicated by letters according to Tukey test ($p < 0.05$).

II. Major redox buffers dynamic during fruit development

It is interesting to note that the total ASC content showed a dynamic similar to that of H_2O_2 (Figure IV.2.A). Indeed, total ASC accumulated during young fruit development as compared to other stages, and slightly augmented during turning and orange stages before declining at the red stage. Furthermore, the reduced ASC content was lowest at anthesis and remained the minority form of ascorbate until 14 DPA, when a change in its redox state occurred, making it the majority form until late development (Figure IV.2A).

Besides, total GSH content remained relatively stable during green fruit development and increased after turning (Figure IV.2B). Moreover, GSSG content started high during anthesis but rapidly decreased, resulting in the maintenance of the total pool of GSH mainly reduced during all fruit development (Figure IV.2B). Discrepancies between ASC and GSH dynamics during development suggested a differential involvement of these redox buffers, where ASC was more likely involved in the early development, while GSH seemed to be more implicated during ripening.

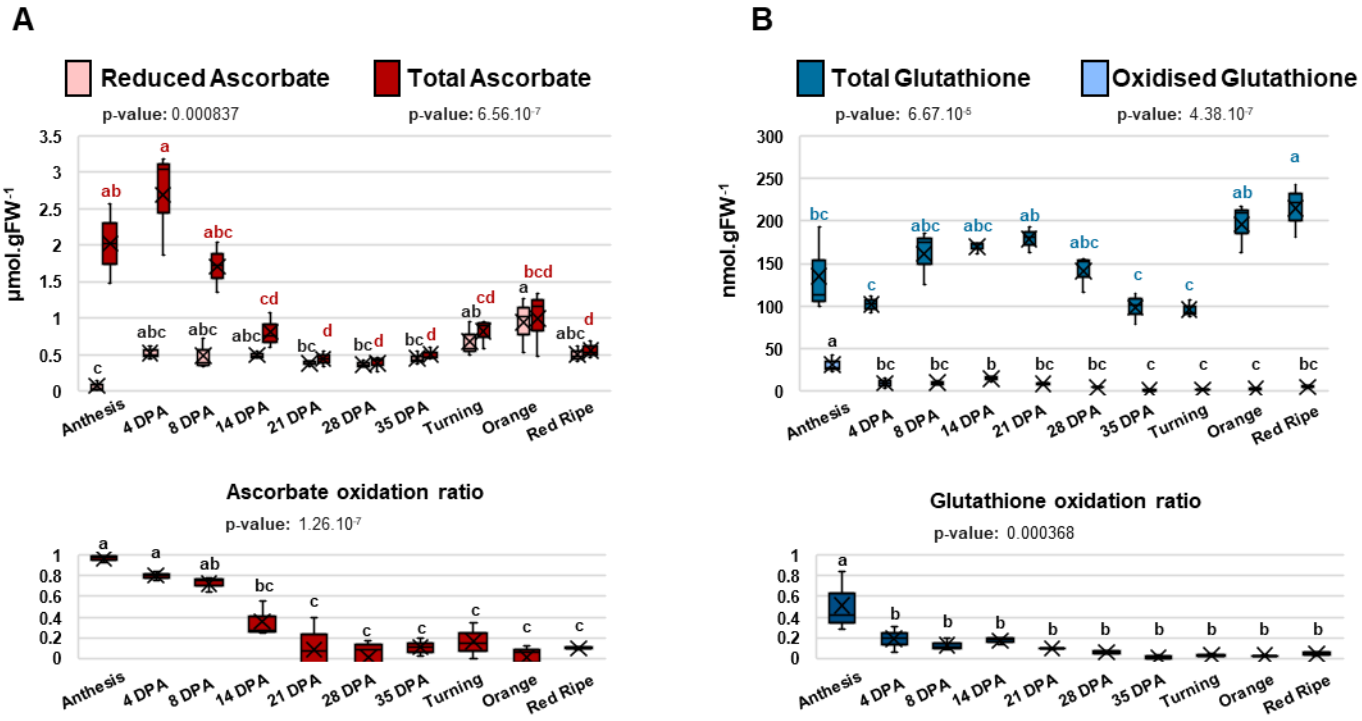

Figure IV.2: Ascorbate (A) and glutathione (B) content and their associated redox state during tomato fruit development. Statistical significance content is indicated by ANOVA p-value. Binary comparisons between growth stages are indicated by letters (total content in colors), according to Tukey test ($p < 0.05$).

On the other hand, pyridine nucleotide (*i.e.* NAD and NADP) contents harboured the same dynamic as observed for ASC and H_2O_2. In other words, their highest content was observed during the anthesis stage before decreasing and remaining stable until the end of development (Figure IV.3). Moreover, the NAD oxidation state remained largely oxidised during the fruit development, while the NADP oxidation state showed a slight decrease at the beginning before following the same trend as NAD.

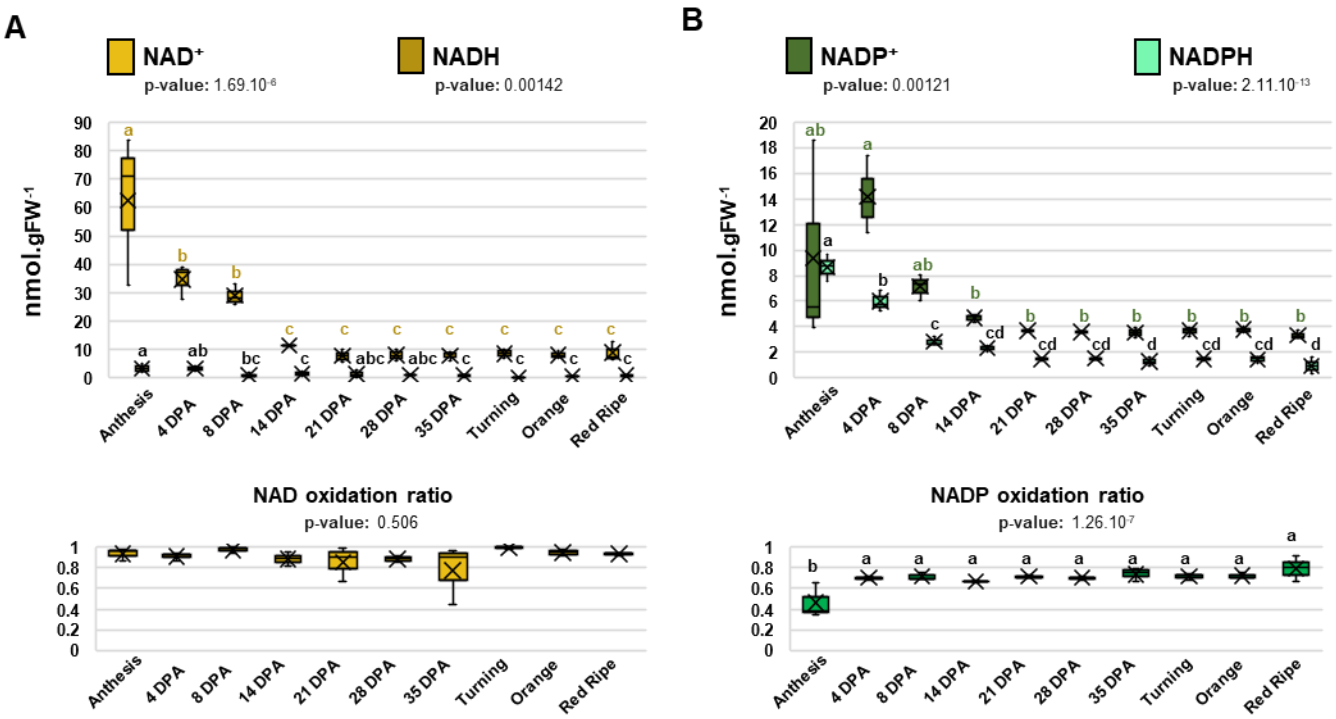

Figure IV.3: NAD(H) (A) and NADP(H) (B) content and their associated redox state during tomato fruit development. Statistical significance content is indicated by ANOVA p-value. Binary comparisons between growth stages are indicated by letters (oxdised form in colors, and reduced form in black), according to Tukey test ($p < 0.05$).

B. Redox enzymatic activities

I. Direct ROS scavenging enzymes

The two main enzymatic pathways for ROS processing in plants are catalase and ascorbate peroxidase. The former has a lower affinity for H_2O_2, but does not require an antioxidant as a substrate, while the latter allows rapid detoxification of ROS but is dependent on the available pool of reduced ascorbate (Bernroitner et al., 2009; Sarker and Oba, 2018). Unfortunately, due to experimental difficulties to obtain and assay anthesis samples, direct ROS scavenging data could not be obtained for this stage. Data presented for this section will start from 4 or 8 DPA stages.

Capacities (V_{max}) of these two enzymes exhibited distinct behaviour during tomato fruit development. APX displayed a dynamic close to the one of ROS and total ASC (Figure IV.4A), *i.e.*, a strong capacity during the early beginning of development that rapidly dropped and stayed stable until late development. On the other hand, CAT showed a steady activity during green fruit development followed by a peak at the turning stage that quickly returned to the basal level (Figure IV.4B).

Overall, ROS processing enzymes seems to modulate redox balance independently during development as they showed distinct patterns with a higher capacity at different developmental phases (*i.e.* APX during early stages and CAT at turning).

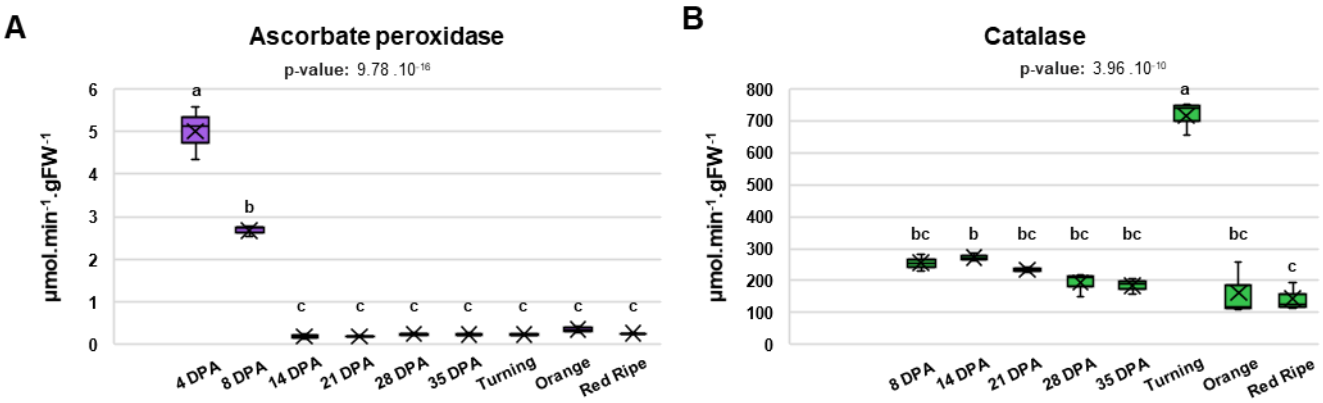

Figure IV.4: Ascorbate peroxidase (A) and catalase (B) capacities (V_{max}) during tomato fruit development. Statistical significance content is indicated by ANOVA p-value. Binary comparisons between growth stages are indicated by letters according to Tukey test ($p < 0.05$).

II. Antioxidant recycling enzyme

Ascorbate recycling enzymes displayed different patterns of evolution during fruit development. DHAR remained relatively steady but harboured a much lower activity (around 15 nmol.min^{-1}.gFW^{-1}) than MDHAR (lowest value < 150 nmol.min^{-1}.gFW^{-1}) (Figure IV.5A and B). Strikingly, MDHAR activity showed the lowest activity at anthesis, then raised until a peak at 14 DPA, concomitant with the switch of ascorbate oxidation ratio, followed by a stable decrease until the red ripe stage.

Besides, GR activity displayed a dynamic divided into two phases. Higher capacity was observed during fruit division phases before decreasing and remaining stable during further fruit development (Figure IV.5C). Interestingly, the highest GR capacity was concomitant with the lowest capacity of MDHAR and the highest ASC and GSH oxidation states. As both of these enzymes use the same substrate (*i.e.* NADPH) to reduce either GSSG or MDHA, this might suggest a potential co-regulation of these enzymes by the pyridine nucleotide supply.

Overall, as for ROS processing enzymes, main antioxidant recycling enzymes exhibited discrepancies in their behaviour during fruit development and seemed to control the redox poise in a development-dependent manner.

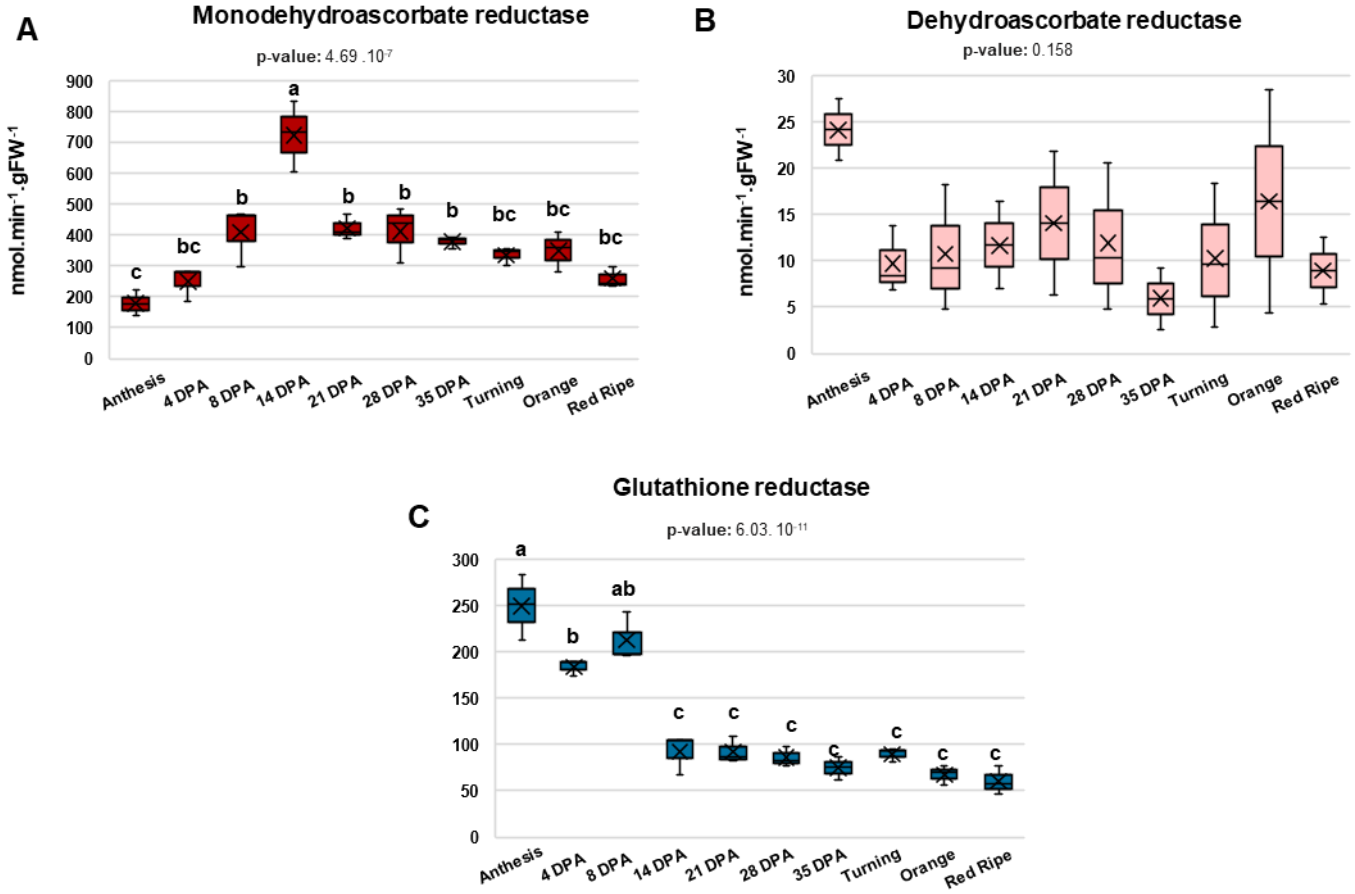

Figure IV.5: Monodehydroascorbate reductase (A), dehydroascorbate reductase (B) and glutathione reductase (C) capacities (V_{max}) during tomato fruit development. Statistical significance content is indicated by ANOVA p-value. Binary comparisons between growth stages are indicated by letters according to Tukey test ($p < 0.05$).

C. Dynamics of central and redox metabolism in developing tomato fruit

To obtain a better picture of the link between redox and central metabolism throughout tomato fruit development, targeted assays for soluble sugars, malic and citric acids, total protein content and total equivalent antioxidant capacity (TEAC, namely Trolox equivalent) were complemented. Principal component analysis of the biochemical phenotyping dataset revealed a distinct separation between tomato fruit developmental phases while explaining 66% of the variation in metabolite contents and enzyme capacities (Figure IV.6). PC1 (41.5%) separated each developmental stage gradually from anthesis to mature green stage (≈ 35 DPA), and PC2 (24.5%) segregated early and ripening stages from cell expansion stages.

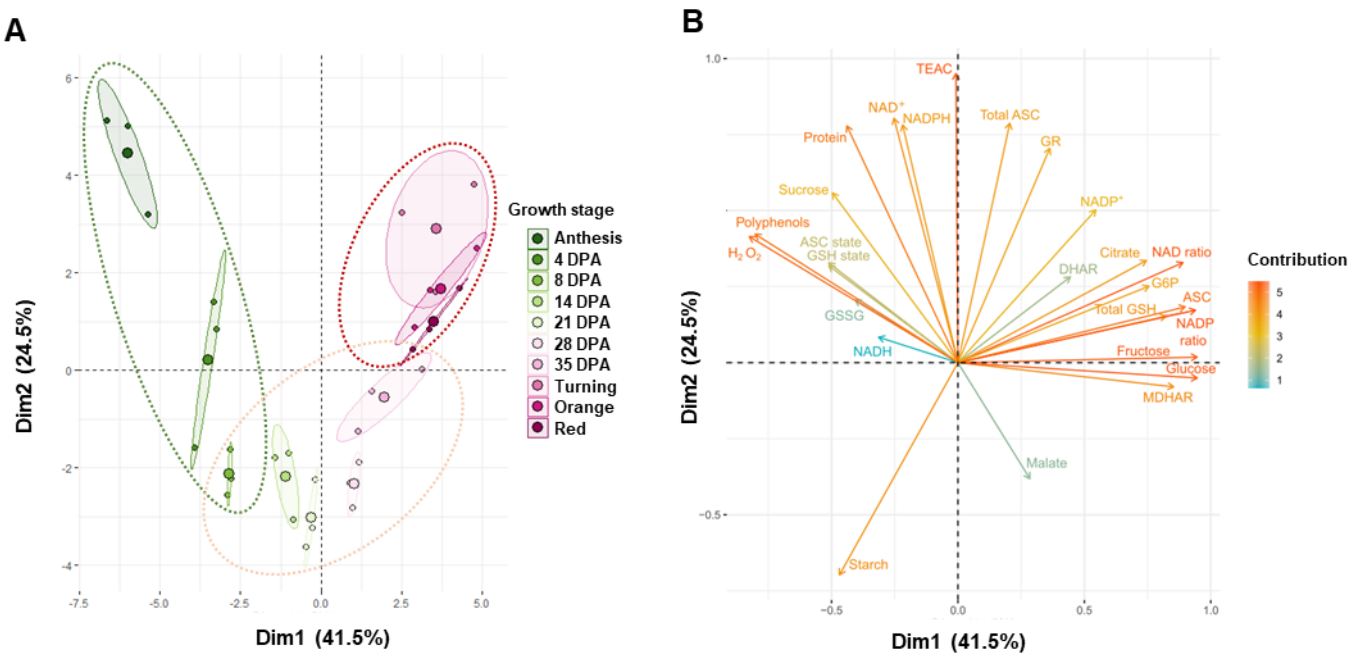

Figure IV.6: Central and core redox metabolism during tomato fruit growth. Normalised metabolites and protein contents, and enzymes capacities of 25 metabolic features of central and core redox metabolism were visualised **(A)** for global impact of the growth stage of tomato fruit and features contribution **(B)** by Principal Component Analysis (PCA with maximal variation given into brackets). Dotted circles indicates the different growth phase (cell division in green, cell expansion in orange, and ripening in purple).

Concomitantly, the contribution of variables through a loading plot demonstrated a predominant effect of TEAC, protein, NAD^+, NADPH, total ascorbate, GR and starch along PC2 (Figure IV.6). PC1 further represented ROS, polyphenols, reduced ascorbate, total glutathione, NAD(P) oxidation ratio, MDHAR and soluble sugars.

Besides, a hierarchical clustering analysis (HCA, Pearson's correlation, Ward clustering) of variables unveiled three main clusters (Figure IV.7). The first cluster (in blue) comprised variables depicting contrary evolution patterns, including starch and malate which showed the strongest values during cell expansion, while NADH, GSSG and GSH oxidation ratio were higher during early stages and ripening (Figure IV.7). This suggests a link between NADH and GSH redox state while highlighting the link between starch and malate with tomato fruit ripening, as already reported (Centeno et al., 2011). From a redox perspective, malate dehydrogenase serves NAD(P)H regeneration in fruit cells and participate in the control of NAD(H) distribution through the malate-aspartate shuttle (Mettler and Beevers, 1980; Gakière et al., 2018b). Hence, this emphasises MDH as a potential candidate in the crosstalk between central and redox metabolisms, especially during the ripening process.

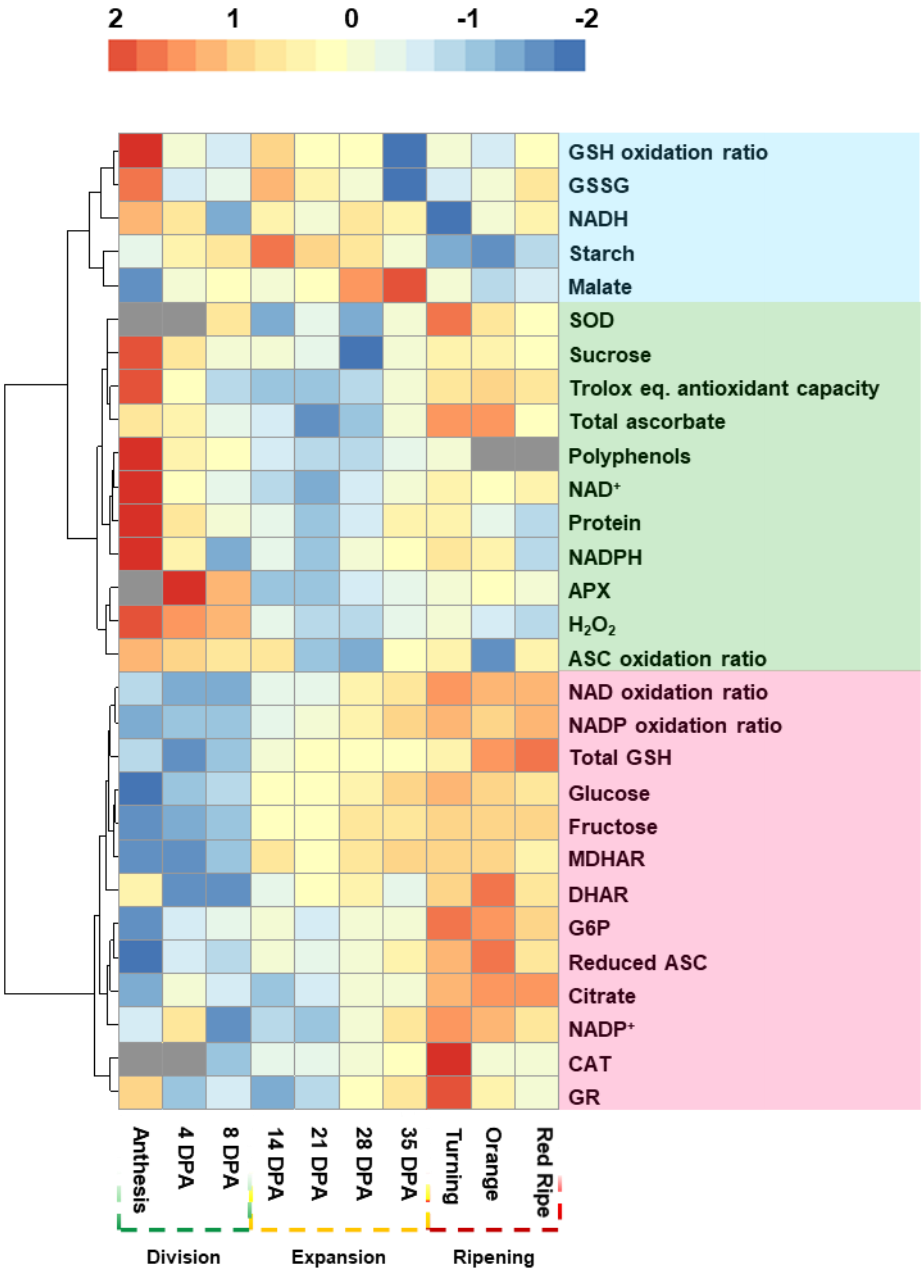

Figure IV.7: Central and core redox metabolism during tomato fruit growth. Same features as observed in Figure IV.6 were then filtered (ANOVA, $p < 0.05$) and subjected to unidimensional hierarchical clustering analysis. Shown are Pearson's correlations after complete clustering of 28 significant metabolic features.

The second cluster (in green) consisted of variables showing their maximum values at the early beginning of development that rapidly dropped until the ripening stages. Here, H_2O_2, APX, total ASC content and its oxidation ratio clustered together, associated with total antioxidant capacity and polyphenol content. Furthermore, NAD^+ and NADPH, which are the most commonly used forms of pyridine nucleotides, displayed a similar evolution profile. From a redox perspective, this cluster showed a correlation between APX, ASC content and its redox state, main forms of NAD(P) and H_2O_2 indicating

that ASC metabolism and oxidative signalling were more involved in ROS processing during development than GSH metabolism (Figure IV.7). Finally, the third cluster (in pink) encompassed metabolites and enzymes showing low levels or activities during cellular division stages (*i.e.* from anthesis to 8 DPA) that gradually increased during the cellular expansion phase (*i.e.* from 14 DPA to turning), and often displaying a peek at turning stages before remaining stable during ripening (*i.e.* from turning to red). Soluble hexoses, citrate and NAD(P) oxidation ratios followed the same pattern during fruit development. From a redox perspective, the most relevant variables included in this cluster were the antioxidant recycling enzymes (*i.e.* MDHAR, DHAR and GR) as well as total GSH, reduced ASC and CAT, suggesting maintenance of a potent antioxidant recycling capacity during cell expansion and ripening of fruit.

Altogether, PCA and HCA indicated an active and dynamic redox metabolism during tomato fruit development. Early development correlated with an important ROS content and a high ASC oxidation ratio, concomitant with a low MDHAR but strong APX capacities. In addition, glutathione also seemed to be involved during the cellular division phase as shown by its oxidation state and the high GR capacity. Thereafter, ascorbate and glutathione recycling activities together with reduced ascorbate and total glutathione correlated together until the end of tomato fruit development. Finally, ripening stood out by a peak for ROS producing enzymes, such as CAT and SOD, but maintained a highly reduced state and antioxidant recycling capacity. Overall, our results demonstrate that tomato fruit development is orchestrated by different events requiring a dynamic and flexible redox metabolism to handle the changing redox balance.

D. Effect of an increased ascorbate synthesis for fruit development

Ascorbate-enriched fruits have been obtained from previously characterised lines (Deslous et al., 2021). Briefly, the causal mutation is semi-dominant and localised in the regulatory upstream region of the open reading frame (uORF) of GDP-galactose phosphorylase (GGP), *i.e.* the main controlling enzyme of the ASC synthesis pathway (Bulley and Laing, 2016; Mellidou and Kanellis, 2017). Two independent mutant and control lines were analysed (see Chapter II.A.II). As we observed no differences between mutant or control lines, and between controls lines and M82 WT fruits, data from both mutant lines have been pooled and compared to M82 WT to facilitate the visualisation of the results.

I. *Effect of an increased ASC synthesis for fruit phenotype and growth*

The ASC-enriched (ASC^+) fruits harbour an enhanced ASC synthesis resulting in a higher ASC content in fruits, up to 5 times fold and 10 times the wild-type (WT) level at heterozygous and homozygous state, respectively (Deslous et al., 2021). Besides, ASC^+ plants displayed a similar phenotype to WT concerning their vegetative tissues. However, ASC^+ plants displayed an augmented number of flowers per truss (Figure IV.8) concomitant with pollen infertility problems and flower morphological disorders. Indeed, stills are no longer included within anthers which are inwardly twisted, thus hindering self-pollination (Figure IV.9).

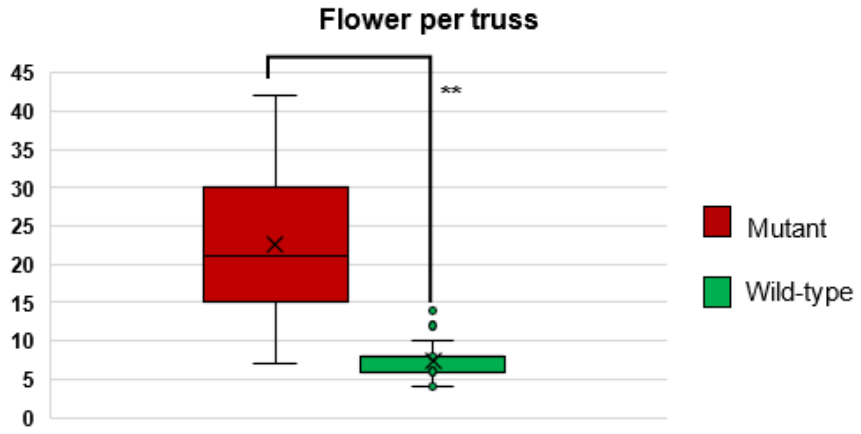

Figure IV.8: Number of flower per truss in mutant, control and wild-type plants. Statistical significance is indicated by stars (**) according to Student's test (p <0.01).

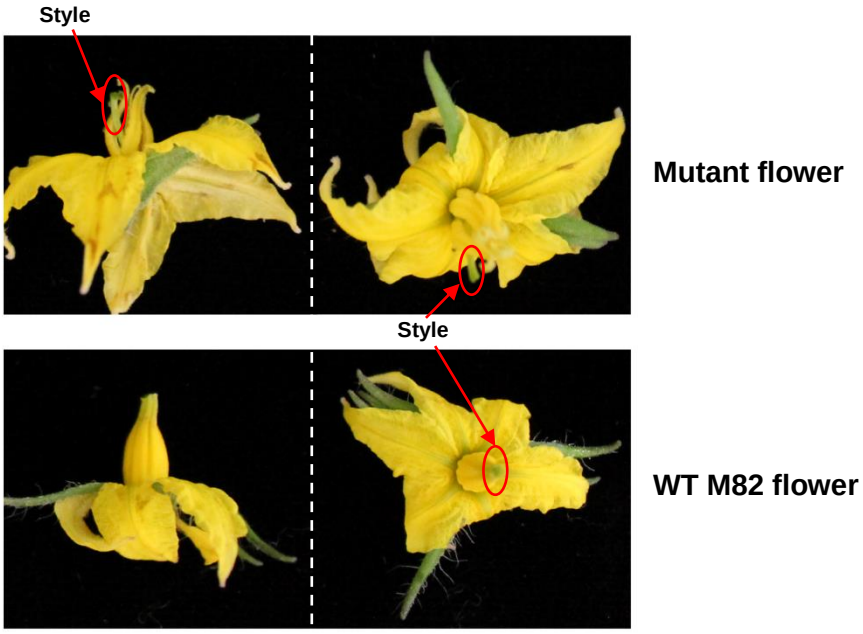

Figure IV.9: Longitudinal and top view of mutant and wild-type flowers. Still are circle in red to highlight their position in flower.

Thereby, auto-fecundation of ASC^+ mutants is almost impossible, and when it occurred, it led to several fruit disorders (*i.e.* gelless, seedless, smaller sized, development failures) or abortion. To encompass these issues, ASC^+ fruits were obtained through the crossing of heterozygous ASC^+ ovary and WT pollen, resulting in seeded fruits harbouring a WT phenotype (Figure IV.10).

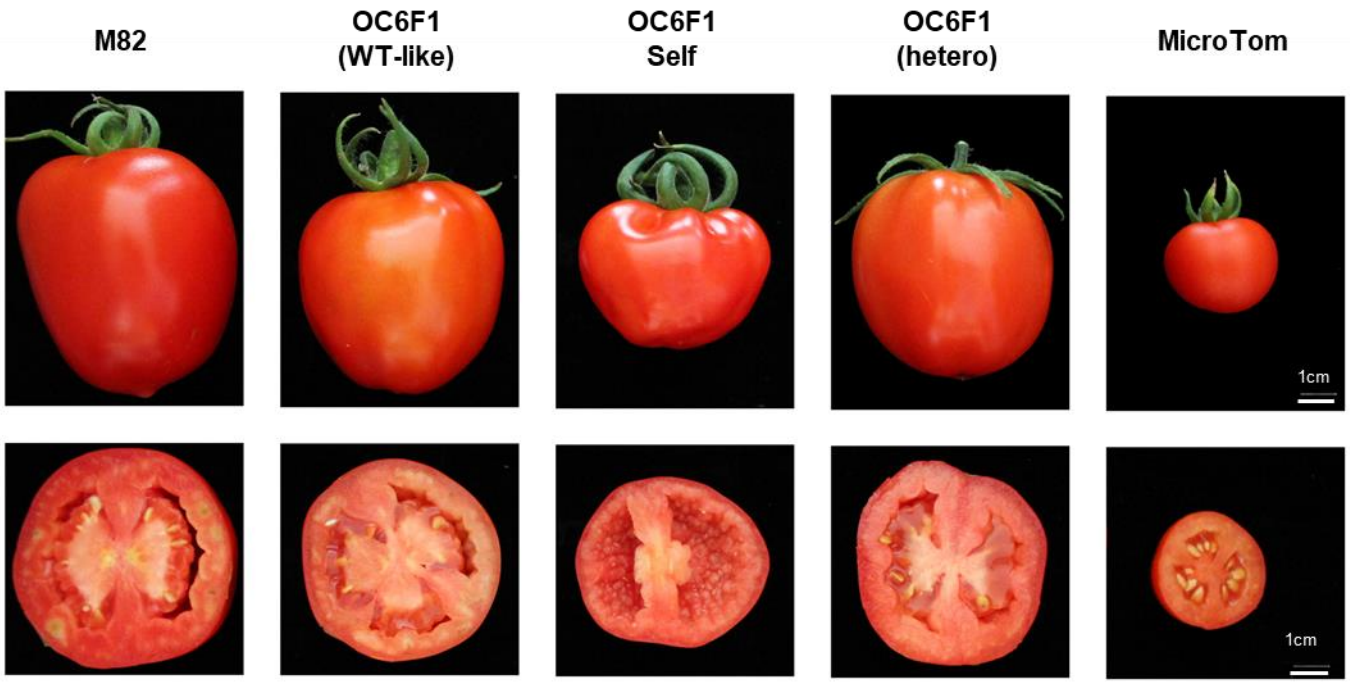

Figure IV.10: Pictures of fruits and associated transversal view. M82 and MicroTom represent commercial tomato cultivars. OC6F1 indicates the generation of the plant (Out-cross n°6, F1 generation) that can be wild-type-like (*i.e.* does not contain the causal mutation for ASC^+ phenotype) and is self-pollinated or heterozygous and in that case, flowers need to be crossed using WT M82 pollen.

These observations raise questions about the implication of ascorbate during flower and pollen development as well as its involvement during gel and seeds development. However, heterozygous fruits obtained through crossing displayed a wild-type phenotype suggesting that seeds and gel development were more associated with pollen metabolism and fertilisation than fruit development. Here, we investigated the effect of increased ASC synthesis in pericarp cells, which appears to be more dependent on maternal tissue. Thus, heterozygous fruits were analysed to specifically study the influence of an increased ASC synthesis on fruit metabolism. Overall, from a phenotypic perspective, mutant and control fruits showed a similar growth rate to WT during all fruit development (Figure IV.11). However, this indicates that an increase in ASC content of the pericarp does not affect tomato fruit growth (*i.e.* weight, shape and size), up to a certain limit, since homozygous fruits, when developed, were always smaller.

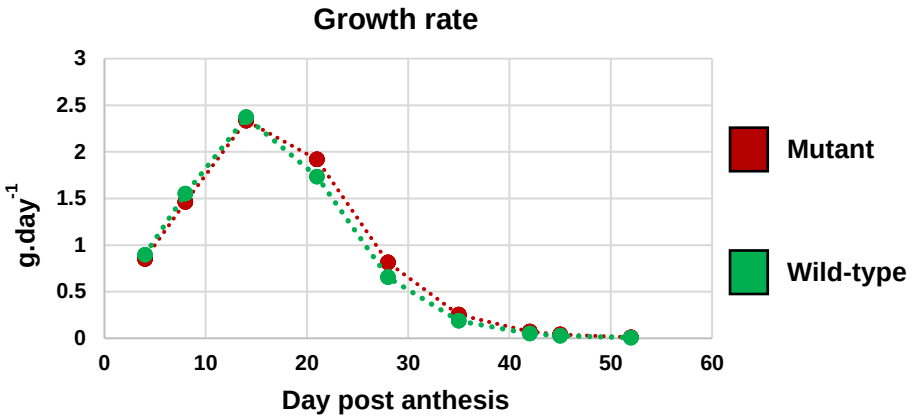

Figure IV.11: Growth rate of mutant, control and wild-type fruits during development.

II. Effect of an increased ASC synthesis on core carbon metabolism

Soluble sugar, major organic acids, starch and total protein content were assayed to determine the influence of an increased ASC synthesis on fruit central metabolism. For these variables, no difference was observed during development, and ASC$^+$ mutant fruits harboured a similar evolution pattern to WT fruits (Figure IV.12). Hence, this suggests that ASC synthesis did not influence core central metabolism even though the ASC synthesis pathway in this ASC-enriched mutant starts from glucose ((Davey et al., 1999; Bulley and Laing, 2016). Overall, this is consistent with the lack of differences observed for phenotypic variables, reinforcing the idea that ASC metabolism is not directly related to sugar metabolism, although there is a link to glucose through its synthetic pathway.

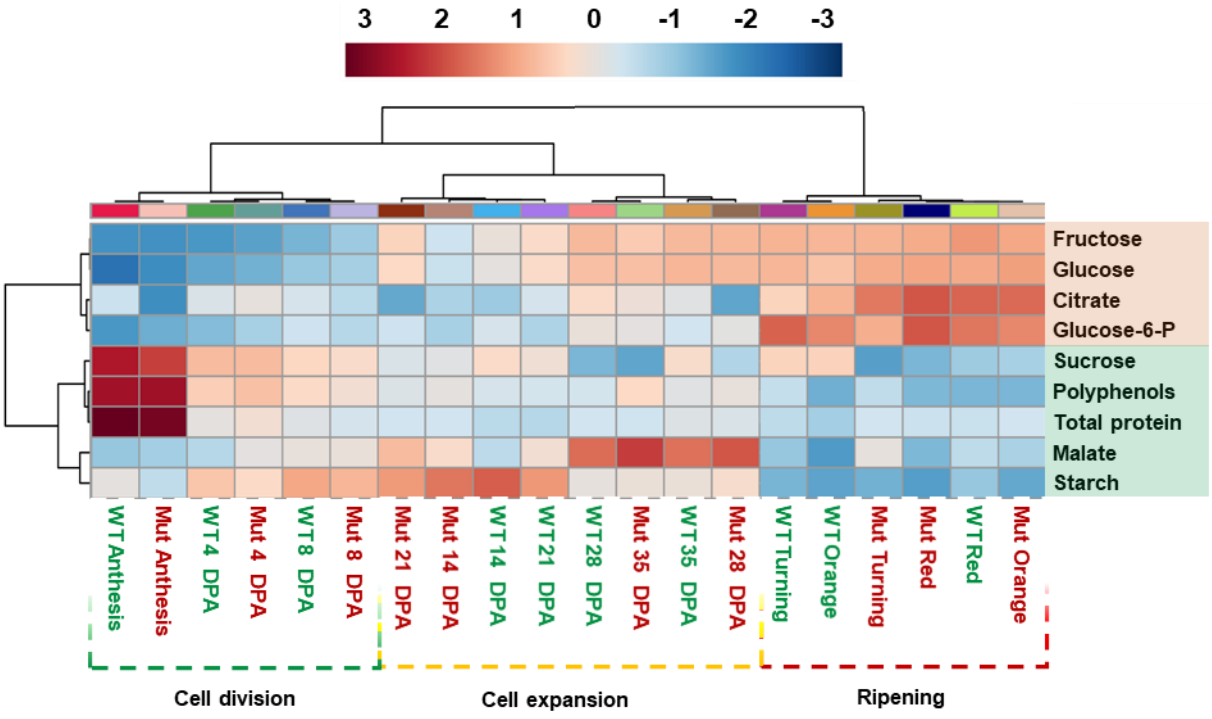

Figure IV.12: Central carbon metabolism in WT and ASC$^+$ mutant fruits during development. Nine features were filtered (ANOVA, $p < 0.05$) and subjected to bidimensional hierarchical clustering analysis. Shown are Pearson's correlations after Ward clustering that unveiled two metabolic clusters associated with three development cluster corresponding to developmental phases.

III. Effect of an increased ASC synthesis on core redox metabolism

1. ROS dynamic during fruit development

Strikingly, ROS content in ASC$^+$ fruits followed the same pattern as WT fruits. Moreover, H_2O_2 was significantly reduced only for the anthesis stage but remained clearly the highest concentrations of development (Figure IV.13). Thus, this indicates that an increase in ASC synthesis slightly affects the ROS content only during early development.

Besides, it is worth noting that the trend of ROS to augment at turning stage was not observed in ASC$^+$ mutant fruits despite a normal ripening phenotype (Figure IV.13). Therefore, this suggests that the increase in H_2O_2 observed at turning stage is a consequence of the climacteric crisis but does not act as a signal during ripening.

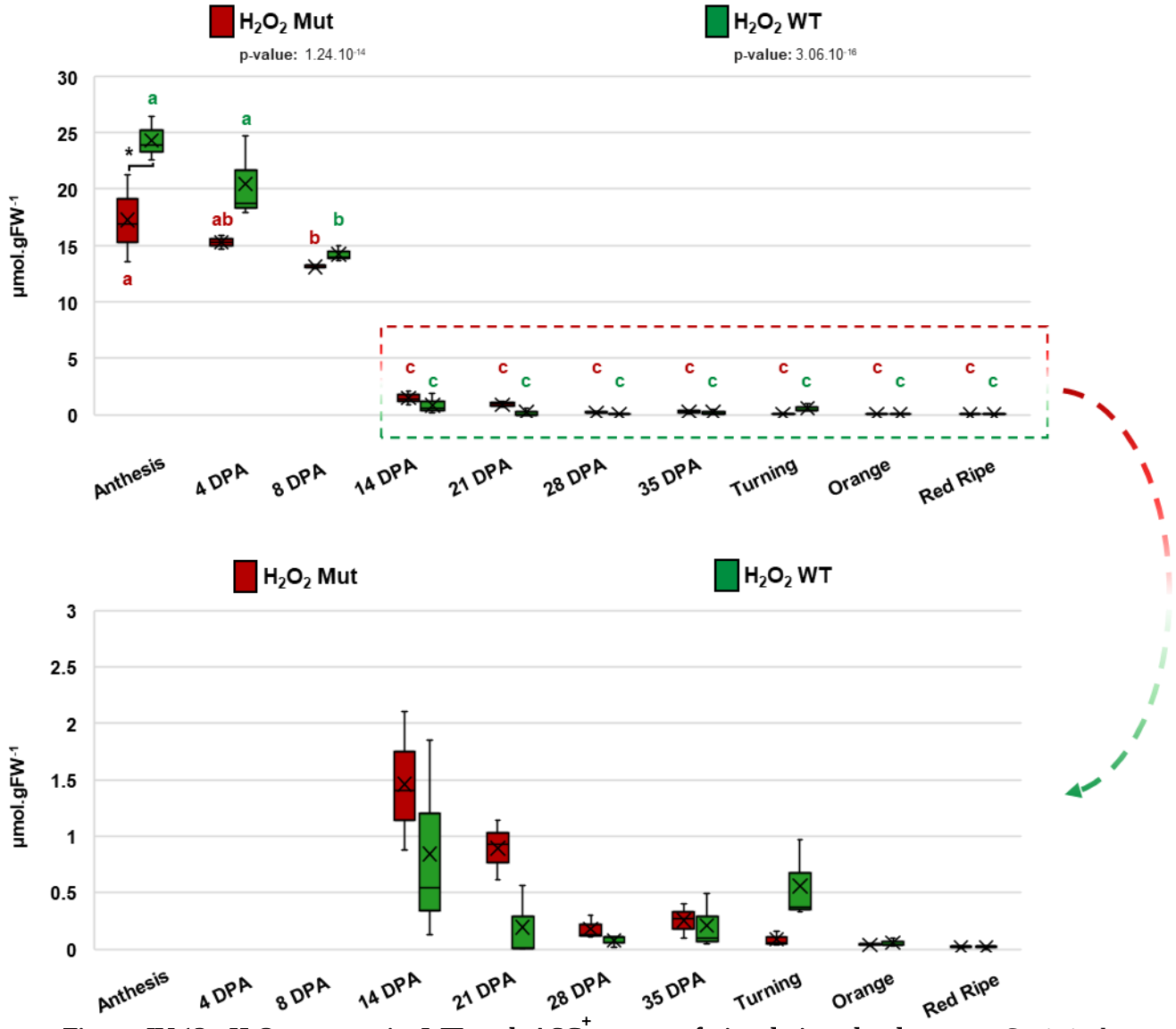

Figure IV.13: H_2O_2 content in WT and ASC$^+$ mutant fruits during development. Statistical significance content is indicated by ANOVA p-value. Binary comparisons between growth stages within the same genotype are indicated by letters (in colors according to legend) according to Tukey test ($p < 0.05$).

2. Major redox buffer dynamic during fruit development

From a redox perspective, both reduced and total ASC contents were significatively higher in ASC$^+$ mutant than in WT fruits, as expected (Figure IV.14). Interestingly, no difference was observed concerning the ASC redox state during the whole fruit development (Figure IV.14). Overall, ascorbate followed the same dynamic observed in WT fruits either in terms of its content or its redox status.

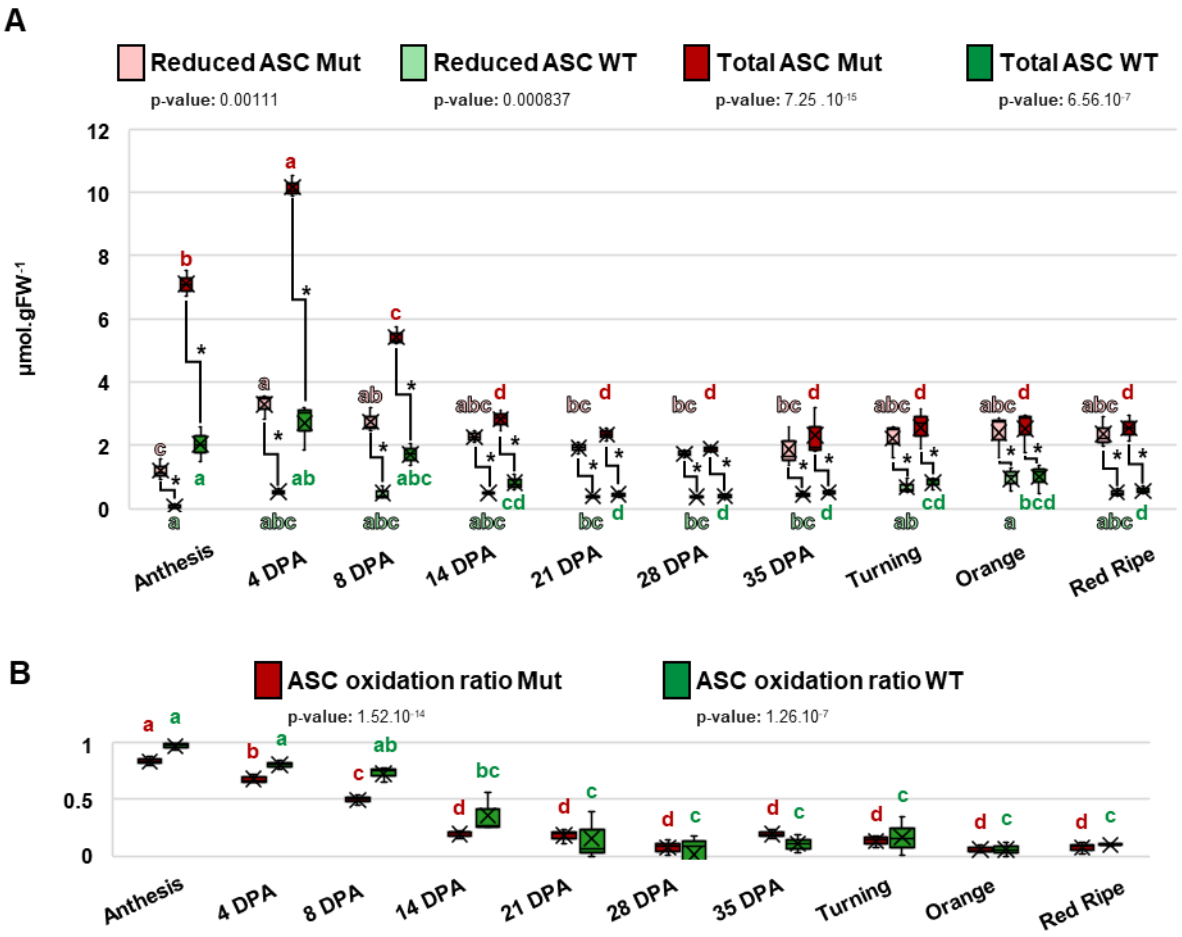

Figure IV.14: Ascorbate content (A) and its redox state (B) in WT and ASC$^+$ mutant fruits during development. Statistical significance content is indicated by ANOVA p-value. Binary comparisons between growth stages within the same genotype are indicated by letters (in colors according to legend) according to Tukey test ($p < 0.05$). Binary comparisons between WT and ASC$^+$ mutant for the same growth stage are indicated by stars according to Tukey test ($p < 0.05$).

In addition, GSH was increased at 4 and 8 DPA stages while it decreased at the red stage in ASC$^+$ fruits (Figure IV.15). However, no differences were observed in GSSG content as well as in GSH oxidation ratio, thus indicating that GSH discrepancies coul be attributed to variations in the content of reduced GSH (Figure IV.14).

Hence, this shows a complementary effect between GSH and ASC in terms of reduced antioxidant availability during cell division stages and at the end of ripening. Indeed, 4 and 8 DPA stages displayed an increase in both DHA and GSH content, whereas the increase in GSH content during maturation is inhibited by reduced ASC accumulation.

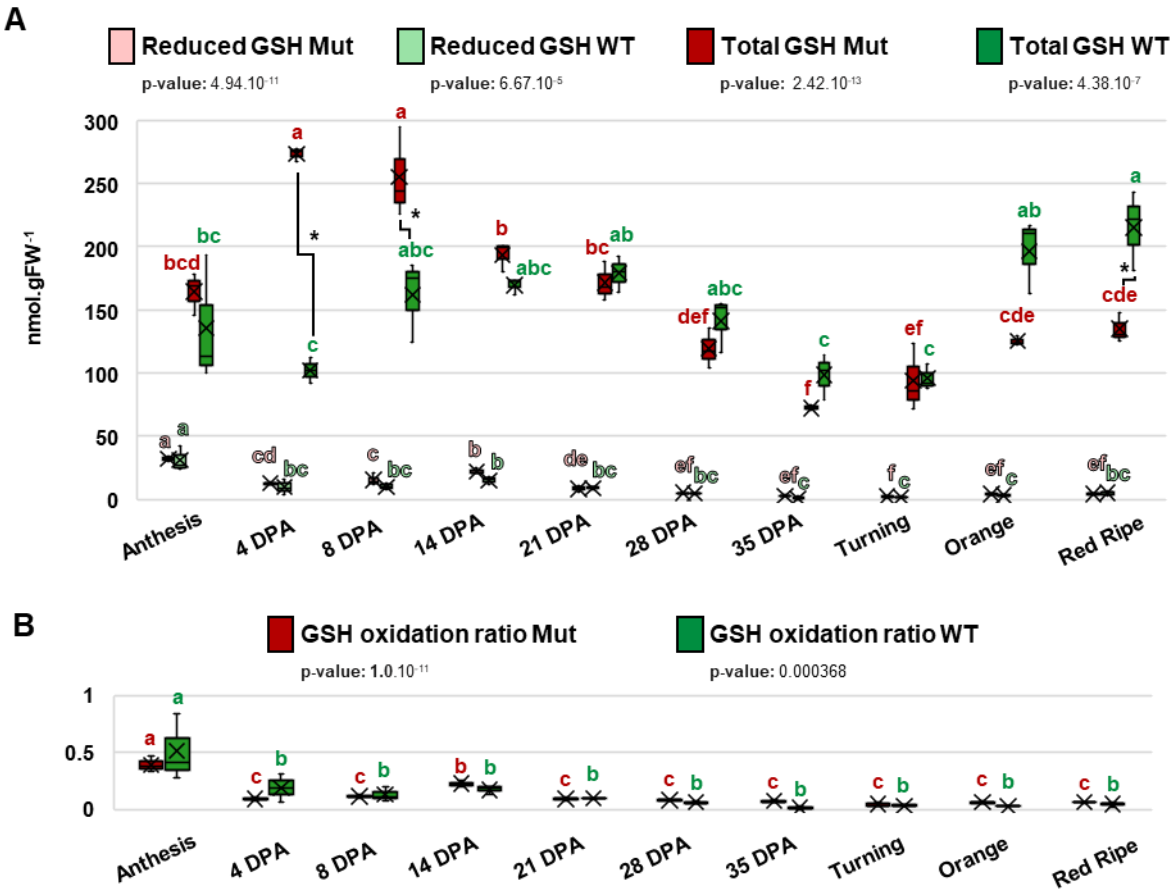

Figure IV.15: Glutathione content (A) and its redox state (B) in WT and ASC$^+$ mutant fruits during development. Statistical significance content is indicated by ANOVA p-value. Binary comparisons between growth stages within the same genotype are indicated by letters (in colors according to legend) according to Tukey test ($p < 0.05$). Binary comparisons between WT and ASC$^+$ mutant for the same growth stage are indicated by stars according to Tukey test ($p < 0.05$).

On the other hand, pyridine nucleotides were not affected by the increase in ASC synthesis either concerning their contents or redox states (Supplemental fig IV.1 and IV.2). As for ASC and H_2O_2, the dynamic of all the pyridine nucleotides content followed the same pattern in ASC$^+$ than in WT fruits.

3. Total soluble antioxidant capacity

Interestingly, despite a significant increase of total ASC, total soluble antioxidant capacity was significantly increased in ASC$^+$ mutants only from 35 DPA until the end of development. The increased ASC synthesis induced an accumulation of its oxidised form during cell division stages which is congruent with the stability of total soluble antioxidant capacity although the increase in GSH. However, the increase in total antioxidant capacity did not appear to be significantly increased during cell expansion stages despite an increased reduced ASC content (Figure IV.16). Nevertheless, it is worth noting during cell expansion ASC$^+$ seemed to display a higher antioxidant capacity, but this was not significant.

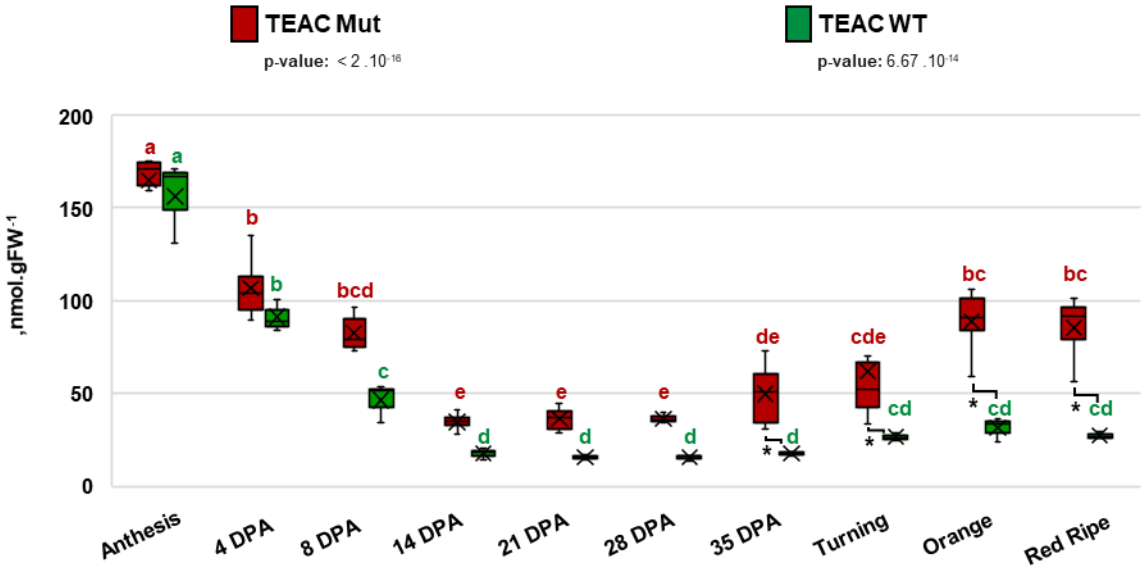

Figure IV.16: Total soluble antioxidant capacity in WT and ASC$^+$ mutant fruits during development. Statistical significance content is indicated by ANOVA p-value. Binary comparisons between growth stages within the same genotype are indicated by letters (in colors according to legend) according to Tukey test ($p < 0.05$). Binary comparisons between genotypes for the same growth stage are indicated by stars according to Tukey test ($p < 0.05$).

4. Enzymatic activities during fruit development

Interestingly, despite an increased ASC content during all fruit development and the variations of GSH for some stages, enzymes involved in antioxidant recycling (*i.e.* MDHAR, DHAR and GR) displayed no differences between WT and ASC$^+$ mutant fruits (Supplemental fig IV.3). Besides, ROS processing enzymes (*i.e.* APX and CAT) also showed the same evolution profiles as in WT fruits (Supplemental fig IV.4).

Overall, all enzymes involved in the ASC-GSH cycle showed a similar evolution pattern in both ASC$^+$ and WT fruits suggesting that ASC content is not involved in the regulation of their abundance.

5. Global metabolic changes in responses to an enhanced ASC synthesis

Altogether, the central and redox metabolic targeted metabolic features highlighted four main clusters associated with fruit developmental phases. HCA displayed a global pattern similar to the WT one (Figure IV.7), including two major clusters associated with either early development or cell division and ripening phases, as expected from the generally low difference levels observed between WT and mutant fruits (Figure IV.17).

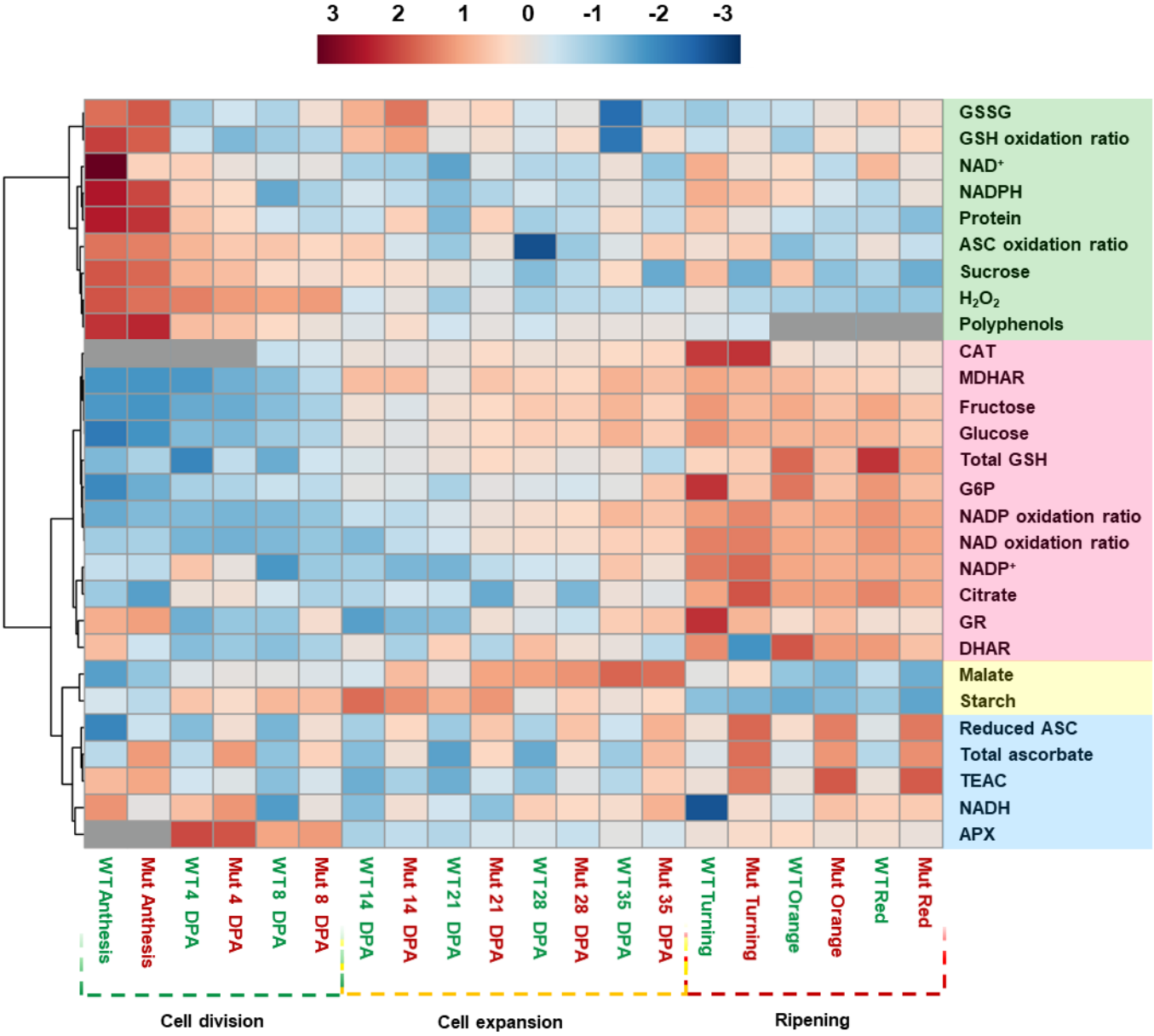

Figure IV.17: Central and core redox metabolism in WT and ASC$^+$ mutant fruits during development. 28 features were filtered (ANOVA, $p < 0.05$) and subjected to bidimensional hierarchical clustering analysis. Shown are Pearson's correlations after ward clustering that unveiled three metabolic clusters associated with three development cluster corresponding to developmental phases.

In the first cluster (in green), ROS content gathered with ASC and GSH redox state, NAD^+, NADPH as well as total protein and sucrose contents, which showed no relevant differences in ASC^+ mutants. This is in line with the 'turbo' metabolism observed during early development, which led to ROS accumulation and ASC oxidation due to the low recycling capacity, which was not influenced by ASC synthesis. (Figure IV.7 and IV.17).

In the second cluster (in pink), metabolic features associated with cell expansion and ripening included antioxidant recycling enzymes (*i.e.* MDHAR, DHAR and GR), total GSH content and both NAD(P) oxidation ratios as well as hexoses and CAT capacity (Figure IV.17). This agrees with the previous observation in WT fruits (Figure IV.7) This again highlighted the need to maintain reduced antioxidants available during these phases of fruit development and particularly at the turning stage. Strikingly, in the third cluster (in yellow), malate and starch stood out as they displayed a specific dynamic associated with cellular expansion only (Figure IV.17). In addition, NADH was still associated with malate and starch, but to a greater extent than previously observed (Figure IV.7). Finally, reduced and total ASC, as well as total antioxidant capacity, clustered together (in blue) and separated from the other variables, as expected. On the other hand, NADH and APX capacity were included in this cluster despite no differences observed (Figure IV.17). Nonetheless, their dynamic was close to ASC variations during development, thus enhancing the involvement of APX, especially during early development.

To conclude, from a redox perspective, an increase in ASC induces a slight decrease in H_2O_2 content at anthesis, followed by an increase in reduced GSH content during cell division. Subsequently, no differences were observed during cell expansion, suggesting a low contribution of ASC synthesis in redox regulations during this development phase. Finally, the resumption of H_2O_2 observed at turning stage in WT fruits was missing in ASC^+ fruits and followed by a decrease in reduced GSH content at red ripe. Hence, this indicates a complementation effect between GSH and ASC as a function of reduced ascorbate content. Overall, apart from this effect, ROS and major redox buffers in ASC^+ mutant fruits followed a similar pattern than in WT fruit. Thus, this suggests a limited involvement of ASC synthesis, and to a greater extent, of ASC in the control of core redox metabolism during tomato fruit development. Nonetheless, this reinforces the hypothesis of a growth-dependent involvement of the ASC-GSH cycle during fruit development, especially during cell division and ripening. On the other hand, central fruit metabolism and fruit growth were not affected by the increase in ASC synthesis despite auto-fecundation issues, which further highlights a tissue-dependent role of ASC signalling.

E. Untargeted metabolomic profiling

In the past decade, numerous metabolomics studies have been performed on fruits, especially tomato and strawberry, providing a global understanding of metabolic pathway dynamics and their interaction during fruit development and in response to various environmental stimuli (Hanhineva and Aharoni, 2010; Luna et al., 2020). Moreover, metabolomics studies allowed identifying discrepancies in the chemical compositions between diverse transgenic lines or physiological conditions, resulting in the identification of genomic regions associated with agronomical traits (Moing et al., 2020). In order to get a better idea of the fruit metabolome, an untargeted LC-MS analysis was performed on semi-polar compounds during fruit development. In a second step, metabolic features were filtered based on their putative annotations to select antioxidants metabolites (see Chapter II.K.II). Metabolomics is therefore a complementary approach to biochemical phenotyping that allows a broader coverage and description of redox metabolism during tomato fruit growth.

I. Global changes in metabolism during fruit development

A total number of 3742 metabolic features were identified in tomato pericarps, among which 3312 variated significatively during fruit development (ANOVA; $p < 0.05$ with Adjusted FDR), representing 88.7% of the total features retained for chemometrics. Principal component analysis enabled the separation of each early stage from the others along PC1 (41.9% of total variance) (Figure IV.18A), which corroborated the pronounced differences observed for central and redox metabolism for these stages (Figure IV.6A). Moreover, PC2 (28.2%) discriminated cell expansion stages, but did not contribute to the separation between cell division and ripening phases.

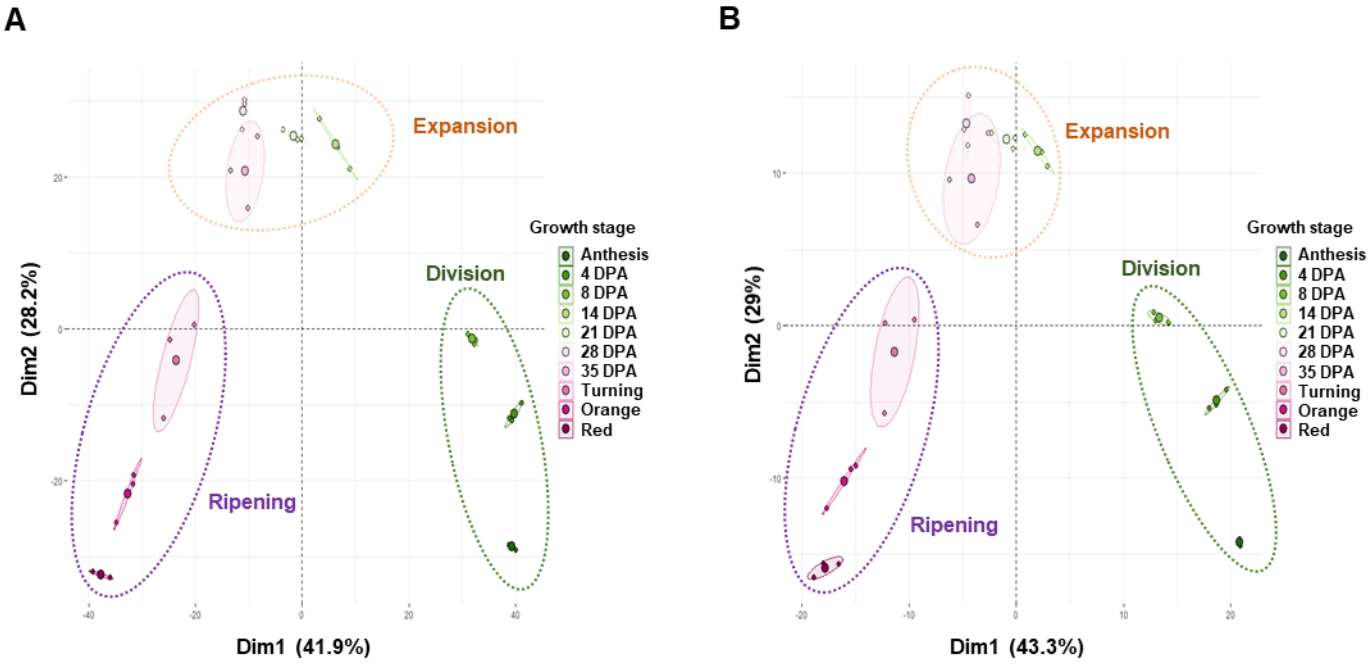

Figure IV.18: Principal component analysis of 3742 metabolic features (A) and of 733 putative antioxidant features (B) during tomato fruit development. Dotted circles indicate the different growth phase (cell division in green, cell expansion in orange, and ripening in purple).

Interestingly, hierarchical clustering analysis unveiled a clear association between metabolic profiles and the growth stage (Figure IV.19). Indeed, most metabolic markers identified (ANOVA; $p < 0.05$ with Adjusted FDR) showed a specific accumulation either for cell division, cell expansion or ripening phases. Altogether, this highlights a complete fruit metabolic reprogramming in terms of primary and secondary metabolites depending on the growth phase. Given the nature of the metabolomics approach (*i.e.* targeting semi-polar secondary compounds), our results thus demonstrate a specific involvement of several secondary metabolic pathways for harmonious fruit development.

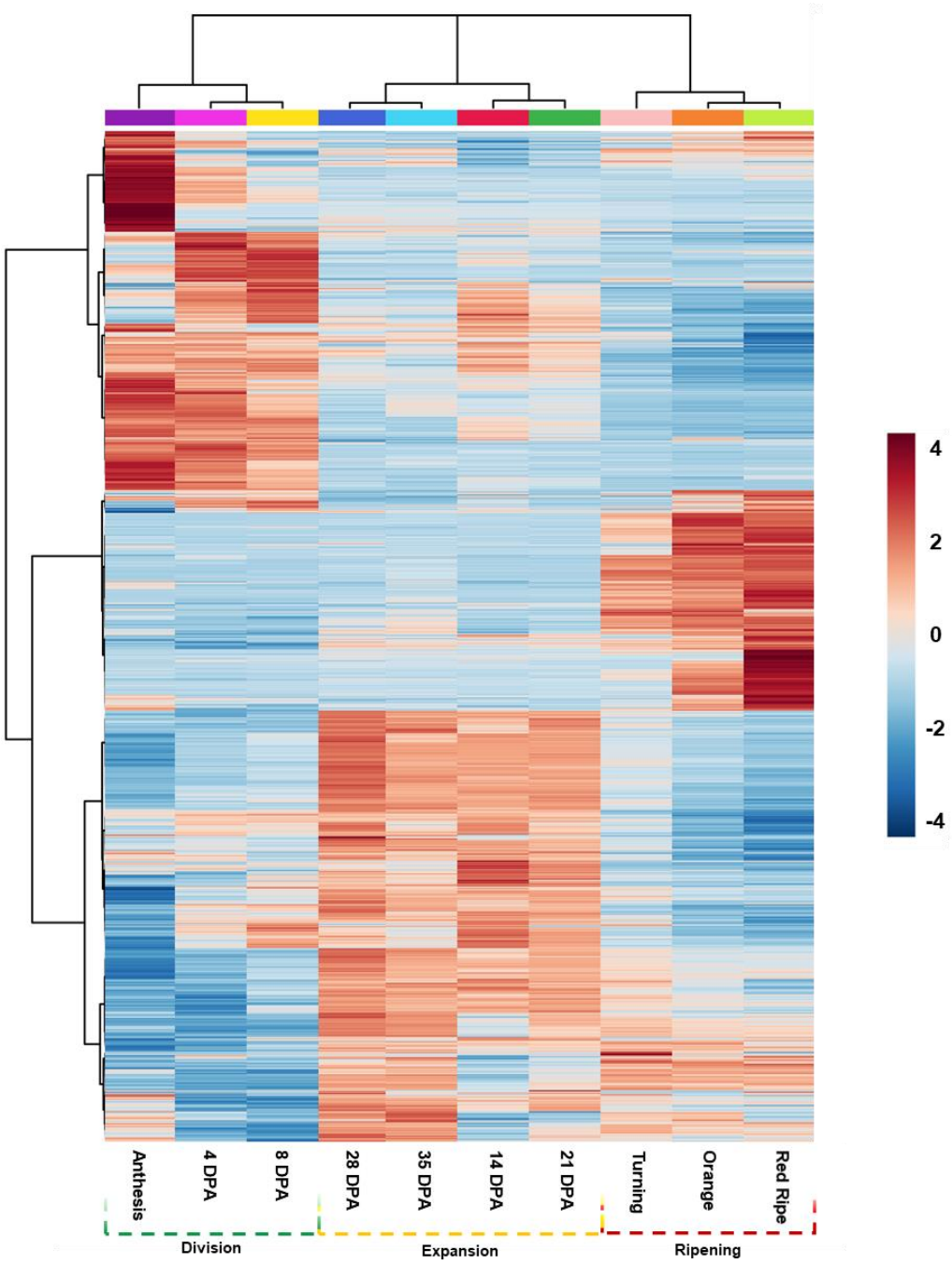

Figure IV.19: Hierarchical clustering analyses of 3312 significant (ANOVA, $p < 0.05$) metabolic features during tomato fruit development. Shown are Pearson's correlations after ward clustering that unveiled three metabolic clusters associated with three development cluster corresponding to developmental phases.

Besides, analysis of ASC^+ fruits only showed slight differences in the number of significant features identified, increasing from 3312 to 3482 within the global data set. However, PCA and HCA showed the same separation pattern between growth stages and displayed no differences between genotypes (Supplemental fig IV.6). Overall, global metabolic signals were not affected by increased ASC synthesis.

II. Dynamic of antioxidant secondary metabolites during fruit development

A total number of 733 metabolic features have been identified based on their putative antioxidant properties, among which 650 shifted significatively during fruit development (ANOVA; $p < 0.05$, Adjusted FDR), representing 88.6% of the total features identified. Similarly to the global analysis, PCA showed a marked separation between young stages and other developmental phases along PC1 (43.2%) (Supplemental figure IV.5B). Moreover, HCA displayed three feature clusters, each one associated with a development phase (Figure IV.20). On the other hand, analysis of the ASC^+ mutant fruits showed a similar pattern in which both genotypes clustered together for each growth stage (Supplemental figure IV.7). Overall, this indicates that secondary antioxidant metabolites are present in tomato fruit throughout development, but that their chemical abundance varies with growth which have been extensively documented (Hanhineva and Aharoni, 2010; Tohge et al., 2013; Tohge and Fernie, 2015; Decros et al., 2019a).

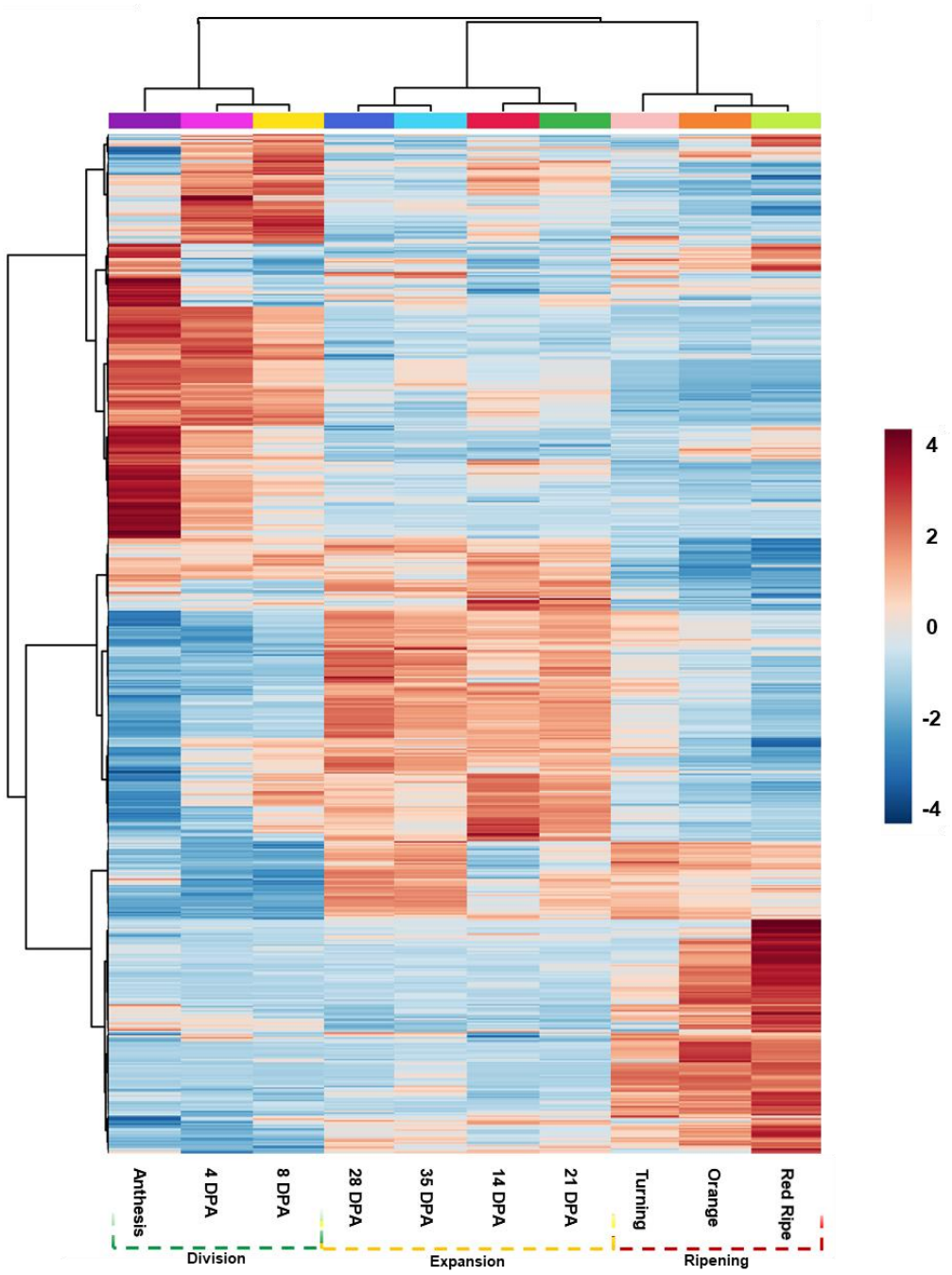

Figure IV.20: Hierarchical clustering analyses of 650 significant (ANOVA, $p < 0.05$) putative antioxidant features during tomato fruit development. Shown are Pearson's correlations after ward clustering that unveiled three metabolic clusters associated with three development cluster corresponding to developmental phases.

F. Discussion and conclusion

Core redox metabolism has received increasing attention for its involvement in fundamental cellular events and its role as a signalling contributor in response to virtually all stresses (Foyer and Noctor, 2016). Nonetheless, information is sparse about redox metabolism contribution to fruit development, leaving its role mainly unknown. Here is the first report on the quantitative description of ROS and major redox buffers during full development of the tomato fruit and in response to increased ASC synthesis.

I. *Fruit cell division is characterised by a strong ASC oxidation and ROS accumulation*

Fecundation event is associated with a peak of ROS production activity, which is considered as a signal for cellular reprogramming (Zafra et al., 2016). Here, we showed that the high ROS content was maintained throughout the cellular division developmental phase despite the strong APX activity (Figure IV.1 and IV.4). This suggests an intense cellular metabolism that agrees with a strong division activity occurring in tomato fruit pericarp cells from anthesis until 8-10 DPA (Fanwoua et al., 2013; Renaudin et al., 2017). Then, ROS content rapidly decreased from 14 DPA (about 10 times fold, Figure IV.1) and was maintained at a low level during the remaining development despite an upward trend at the turning stage. In addition, hierarchical clustering analysis (Figure IV.7) correlated ROS with total protein content, high sucrose content and both NAD^+ and NADPH, which are the most common forms required by central metabolism (Gakière et al., 2018b). As a sink tissue, the young fruit can be considered as a power plant brimming with building blocks and energy, resulting in an operational metabolism that induces a highly oxidised cell state, reflected in a high ROS content and a high oxidation rate of ASC and GSH. Hence, this reinforces the hypothesis of a "turbo metabolism" during the beginning of fruit development, as previously suggested by a global analysis of central enzymes and metabolites (Biais et al., 2014).

Besides, ASC^+ mutant fruits showed a slight decrease in H_2O_2 but maintained a high oxidation state of ASC despite the increased synthesis of reduced form. In addition, high APX activity and low MDHAR activity were observed simultaneously, indicating that ascorbate is oxidised by H_2O_2 and maintained in a highly oxidised state. Thus, this suggests that H_2O_2 is produced and/or accumulated in the same cellular compartments as ASC, resulting in its almost complete oxidation necessary for smooth cell division. Furthermore, high levels of ROS have been identified in mammals cells to participate in the maintenance of stem cells in an undifferentiated state (Sart et al., 2015).

Concomitantly, GSH harboured a moderately oxidised ratio and a stronger GR capacity without apparent correlation with H_2O_2 content and ASC metabolism (Figure IV.3). This suggests that reducing power is still available in cells but is not fully used. Thus, our study reinforces the hypothesis of a finely tuned production and/or a strictly controlled compartmentalisation of ROS. In addition, glutathione maintains its redox state mainly reduced, even in ASC^+ mutants where no difference in GSSG was apparent despite an increase in GSH and DHA contents (Figure IV.15).

Besides, untargeted metabolomic analysis revealed a specific accumulation of secondary antioxidant features (Figure IV.20) together with a high polyphenols content and TEAC (Figure IV.7 and IV.16). However, despite the occurrence of these antioxidant metabolic features and capacity, fruits showed a highly oxidised ASC content and ROS accumulation. Thus, this implies a strict regulation of the ROS distribution and oxidative signalling in cells during division phases. Besides, one might wonder whether the accumulation of these secondary compounds, known for their toxicity or anti-appetent role, does not accumulate to protect the young fruit against possible bio aggression.

To summarise, this emphasises that the fruit cell division phase is characterised by a "turbo metabolism" associated with a strong ASC oxidation activity but a low recycling activity resulting in ROS accumulation, in both WT and ASC^+ mutants (Biais et al., 2014). However, glutathione displayed a limited oxidation ratio suggesting that redox signalling during fruit cell division may rely more on ASC than thiols signalling pathways, as suggested by the high DHA content in diverse fruit species (Roch et al., 2019). Finally, the concomitance of high antioxidant capacity and high ROS accumulation pointed out a controlled redox metabolism, which is heterogeneously distributed among the subcellular compartments. Nonetheless, antioxidants transport remains mainly unknown and remain a central issue in redox studies.

II. Tomato fruit cell expansion is associated with a weak redox metabolism

The cellular expansion stage is characterised by an accumulation of specialised and central metabolites in the vacuole that triggers water influx and thus cell growth (Beauvoit et al., 2014). During this phase, sucrose is cleaved by neutral invertase and sucrose synthase and thus participate in the fruit sink strength (Beauvoit et al., 2014). Simultaneously, vacuole growth at the expense of the cytosol induces a dilution effect of cytosolic compounds. Considering that major redox buffers are present in the vacuole in small proportions, the decrease in their content observed from 14 DPA can be solely partially attributed to the increased vacuolar volume as shown by the pyridine nucleotides concentrations (see chapter III) (Decros et al., 2019b).

Besides, cell expansion is underpinned by the increase in growth rate and the decrease in central metabolism activity (Beauvoit et al., 2018; Roch et al., 2020), which is consistent with our observations in both WT and ASC$^+$ fruits (Figure IV.11). From a redox perspective, cell expansion is globally associated with a decreased content in both ROS and major redox buffers suggesting a weak redox metabolism (Figure IV.17). It is worth noting that the beginning of cell expansion (*i.*e the 14 DPA stage) displayed the highest ASC recycling capacity (*i.e.* MDHAR) associated with a low oxidation capacity resulting in a shift in ASC oxidation ratio, which could then be maintained in a reduced state throughout this development phase (Figure IV.2A and IV.5A). Concomitantly, the GSH oxidation state reached the almost completely reduced state despite a reduced GR capacity. Altogether, this indicates that MDHAR is highly implicated in the control of both ASC and GSH redox states using NAD(P)H and thus links central metabolism and redox signalling.

On the other hand, untargeted analysis unveiled a simultaneous shift of primary and secondary metabolic pathways from 14 DPA (Figure IV.17). This is in line with previously observed changes in hormonal contents, enzymatic activities and flavonoids accumulation, specifically associated with cell expansion phase (Tohge et al., 2013; Biais et al., 2014; Beauvoit et al., 2018). Overall, despite an apparent decline in central metabolism, the tomato fruit shows active metabolic reprogramming specific to the cell expansion phase.

At the same time, tomato fruits host endoreduplication, which starts at about 10 DPA depending on the variety and is considered one of the drivers of cell expansion (Chevalier et al., 2011; Fanwoua et al., 2013). Previous studies have already linked ASC and GSH with the control of the cell cycle, together or seperatelly (Potters et al., 2002; Hendrix et al., 2020). Here, we showed that cell expansion exhibits a distinct pattern than cell division, which is mainly characterised by a low ROS content and high antioxidant availability and recycling capacity (Figure IV.7). Besides, ASC$^+$ mutant fruits solely showed differences in reduced ASC content but not in phenotypic or other metabolic variables indicating that an increase in ASC did not influence the osmotic gradient driving the water influx (Figure IV.17). Hence, this suggests that ASC signalling during growth should be more dependent on the ASC redox state than its content.

Overall, cell expansion is characterised by a strong ASC recycling capacity and a weak oxidative metabolism resulting in a switch in ASC oxidation state from highly oxidised to reduced form at 14 DPA. Hence, this suggests that ascorbate signalling needs to be maintained in a reduced state for stable fruit cell expansion. From a more general perspective, this indicates that ASC might be involved in the underlying mechanisms controlling the trade-off between mitosis and endoreduplication through redox signalling. However, further research is needed to answer this specific question.

III. Tomato fruit ripening is defined by an increase in antioxidant capacity

Tomato is a climacteric species in which ripening is characterised by the arrest of growth (*i.e.* growth rate tending to 0) (Figure IV.11) associated with ethylene signalling and a greater starch accumulation compared to non-climacteric species (Roch et al., 2020). Moreover, tomato ripening is associated with a high respiratory burst resulting in an excess of energy, which is dissipated by non-phosphorylative oxidation implicating mitochondrial uncoupling proteins and alternative oxidases (Colombié et al., 2015, 2017). Interestingly, redox wise, the onset of ripening (*i.e.* the turning stage) displayed a specific behaviour. Indeed, ROS content tended to increase (Figure IV.1) and HCA highlighted an enhancement of antioxidant recycling capacities associated with a peak of CAT capacity. However, major redox buffer oxidation states remained mainly reduced together with a low APX activity (Figure IV.17). Hence, this suggests that the H_2O_2 produced during the climacteric respiratory burst is processed by CAT and not by APX using ASC in contrast to cell division. However, ASC^+ mutant fruits did not show this slight H_2O_2 increase suggesting that ROS production is more a consequence than a signal of maturation setup. Moreover, tomato fruit ripening is characterised by a strong accumulation in lycopenes and antioxidant volatile compounds which may participate in ROS processing during the onset of ripening (Tohge et al., 2013; Decros et al., 2019a).

Besides, GSH content increased during orange and red stages in WT fruits but remained steady in ASC^+ mutants, which suggests the need for increased antioxidant intake during maturation (Figure IV.15). The increase in reduced antioxidant supply is normally performed by GSH, and could be complemented by ASC, as showed by ASC^+ fruits. However, TEAC showed a similar capacity between both genotypes (Figure IV.16), thereby highlighting a co-regulation of ASC and GSH synthesis pathways linking these redox buffers based on their reduced form availability and/or capacity.

Finally, it is interesting to notice an increase in malic acid just before ripening, which can be associated with NAD(P)H regeneration, already been reported to be redox-regulated (Centeno et al., 2011; Yokochi et al., 2021). In addition, HCA showed a strong correlation between starch, malate and NADH, strengthening the link between redox and central metabolism before and during ripening (Figure IV.17). Thus, MDH appears as one of the main partners in the crosstalk between redox and central metabolism by acting on the reducing power availability, and to a further extent, on ASC-GSH cycle at the onset of fruit ripening.

Overall, in terms of redox, the onset of tomato fruit ripening is distinguished from other developmental stages by a restart of antioxidant capacities, in particular catalase, which allows the maintenance of a mainly reduced redox balance during the climacteric respiratory burst. Furthermore, malate dynamics suggest that MDH may participate in the crosstalk between central and redox metabolism. Nevertheless, an increase in ASC synthesis will not influence ripening from a phenotypic

point of view, although it induces differences in GSH content, suggesting that ripening fruit must maintain whatever reduced redox buffer is available.

CONCLUSION

To conclude, tomato fruit development is defined by a growth-phase dependent redox metabolism. Growth-dependent changes in hormonal content, central metabolism enzyme activities and secondary metabolic pathways have been previously reported in tomato (Tohge et al., 2013; Biais et al., 2014; Colombié et al., 2015; Beauvoit et al., 2018; Belouah et al., 2019). In this chapter, we provide additional quantitative data on central redox metabolism that has never been reported during fruit development. Moreover, we demonstrate that early development is characterised by active ascorbate oxidation resulting in a *quasi* total ASC oxidation, a ROS accumulation but a moderate GSH oxidation state indicating a finely spatially controlled redox metabolism within the cell during the cell division phase. Secondly, the central redox metabolism showed a strong recycling capacity associated with the transition to the cell expansion phase, highlighting the role of MDHAR as a guardian of the redox status of ASC and GSH during fruit development. Besides, DHAR showed a low and constant activity pointing to its negligible role from a developmental perspective as already reported in an *Arabidopsis* triple mutant, although a role during stress signalling by modulating glutathione redox state (Rahantaniaina et al., 2017). Furthermore, the turning stage is defined by a reboot of central metabolism activity whose redox repercussions will be managed by CAT, in contrast to the cell division phase. Finally, the increase in ASC synthesis within pericarp cells showed a limited impact, on fruit growth and metabolism but has enabled us to identify a co-regulation of GSH and ASC content independently from the ASC-GSH cycle activity. However, ascorbate is involved in a myriad of stress responses, and the effects of the increased synthesis remain to be assessed under various stress conditions.

Overall, core redox metabolism showed a growth-dependent behaviour during tomato fruit development, suggesting a dynamic reprogramming between developmental phases. Among the contributors of the ASC-GSH cycle, MDHAR appears as the major actor in the control of ASC and GSH redox state, whereas DHAR and GR seem less implicated in developmental processes. However, further studies are needed to decipher the regulations and mechanisms underlying this changing redox metabolism, in which antioxidant transport appears to be a bottleneck.

SUPPLEMENTAL FIGURES

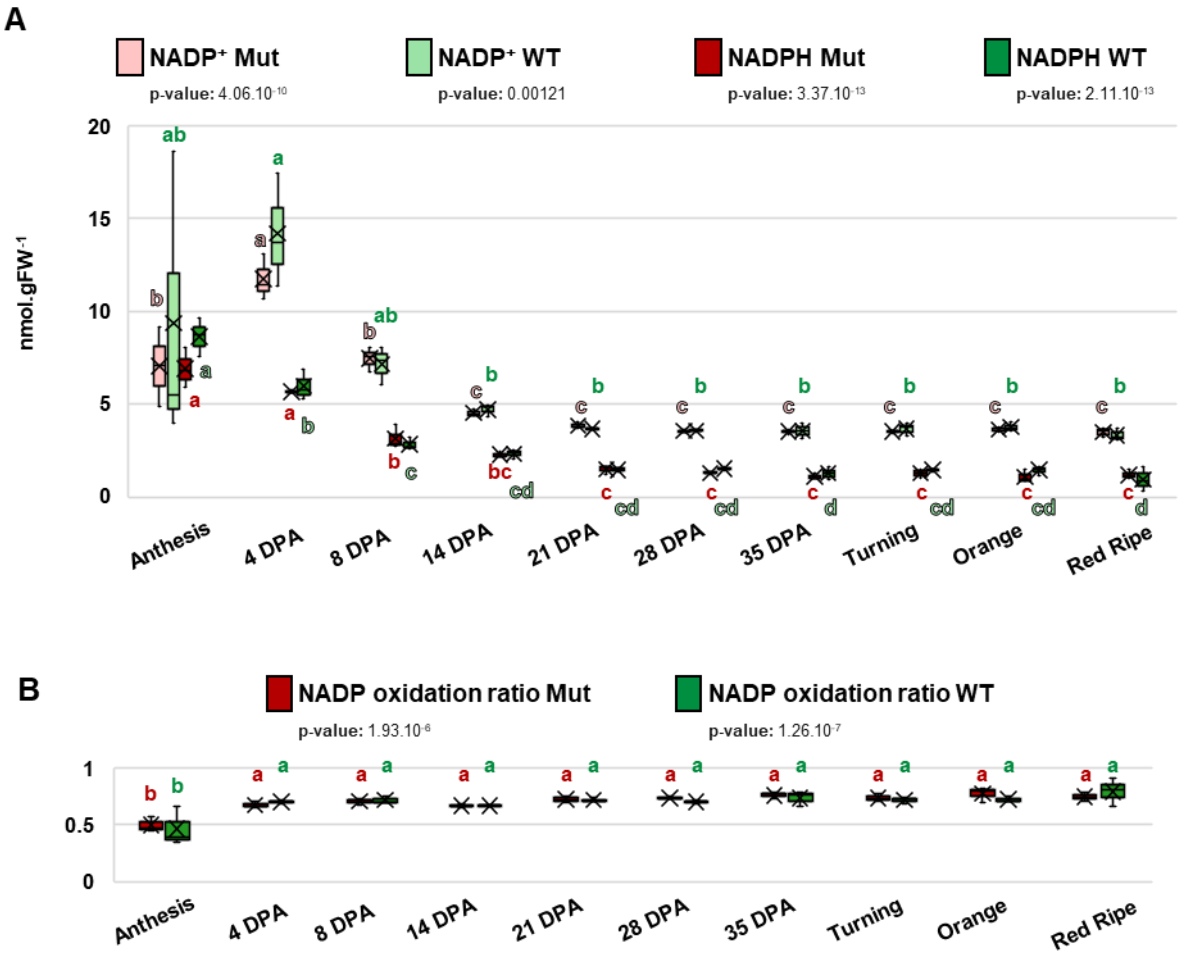

Supplemental fig IV.1: NADP(H) (A) and its redox state (B) in WT and ASC^{+} mutant fruits during development. Statistical significance content is indicated by ANOVA p-value. Binary comparisons between growth stages within the same genotype are indicated by letters (in colors according to legend) according to Tukey test ($p < 0.05$).

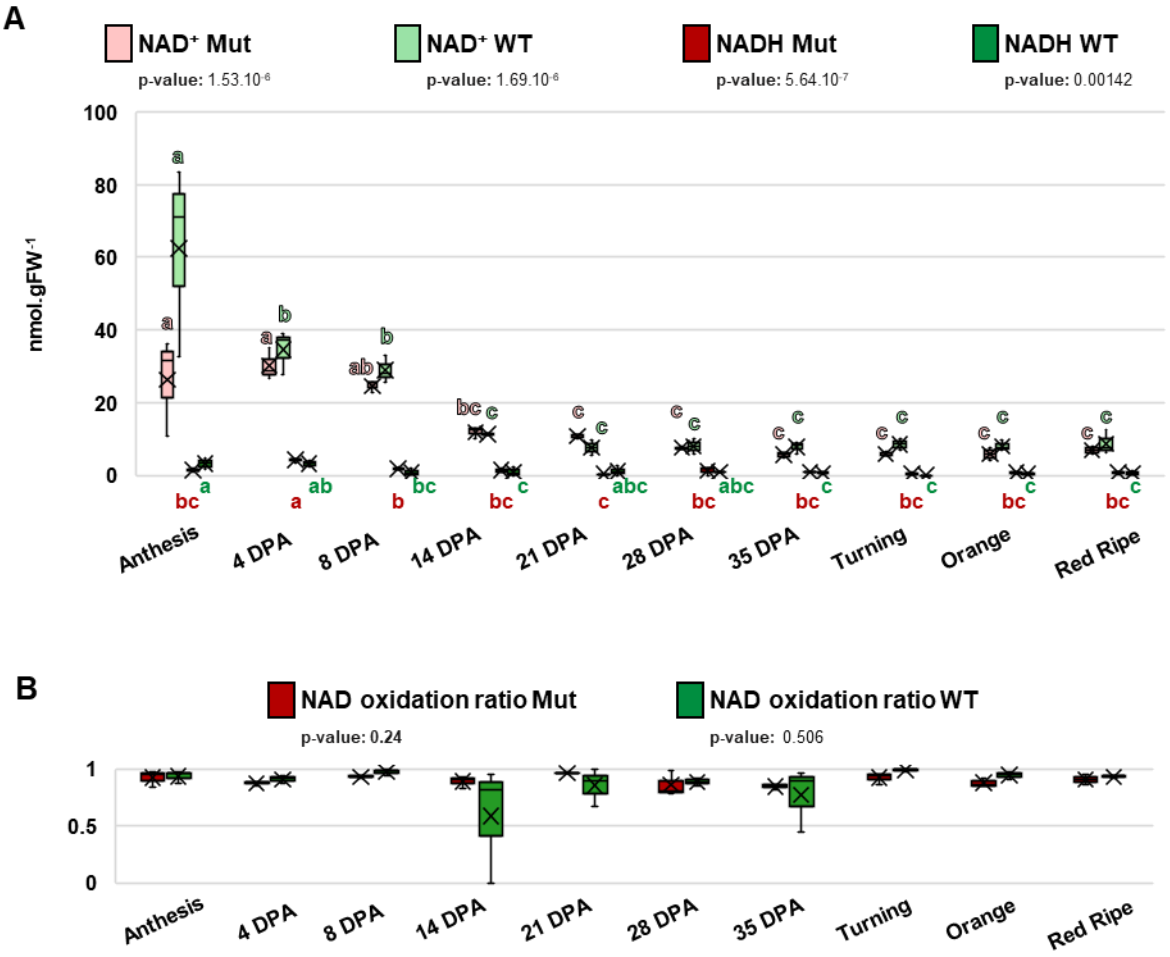

Supplemental fig IV.2: NAD(H) (A) and its redox state (B) in WT and ASC$^+$ mutant fruits during development. Statistical significance content is indicated by ANOVA p-value. Binary comparisons between growth stages within the same genotype are indicated by letters (in colors according to legend) according to Tukey test ($p < 0.05$).

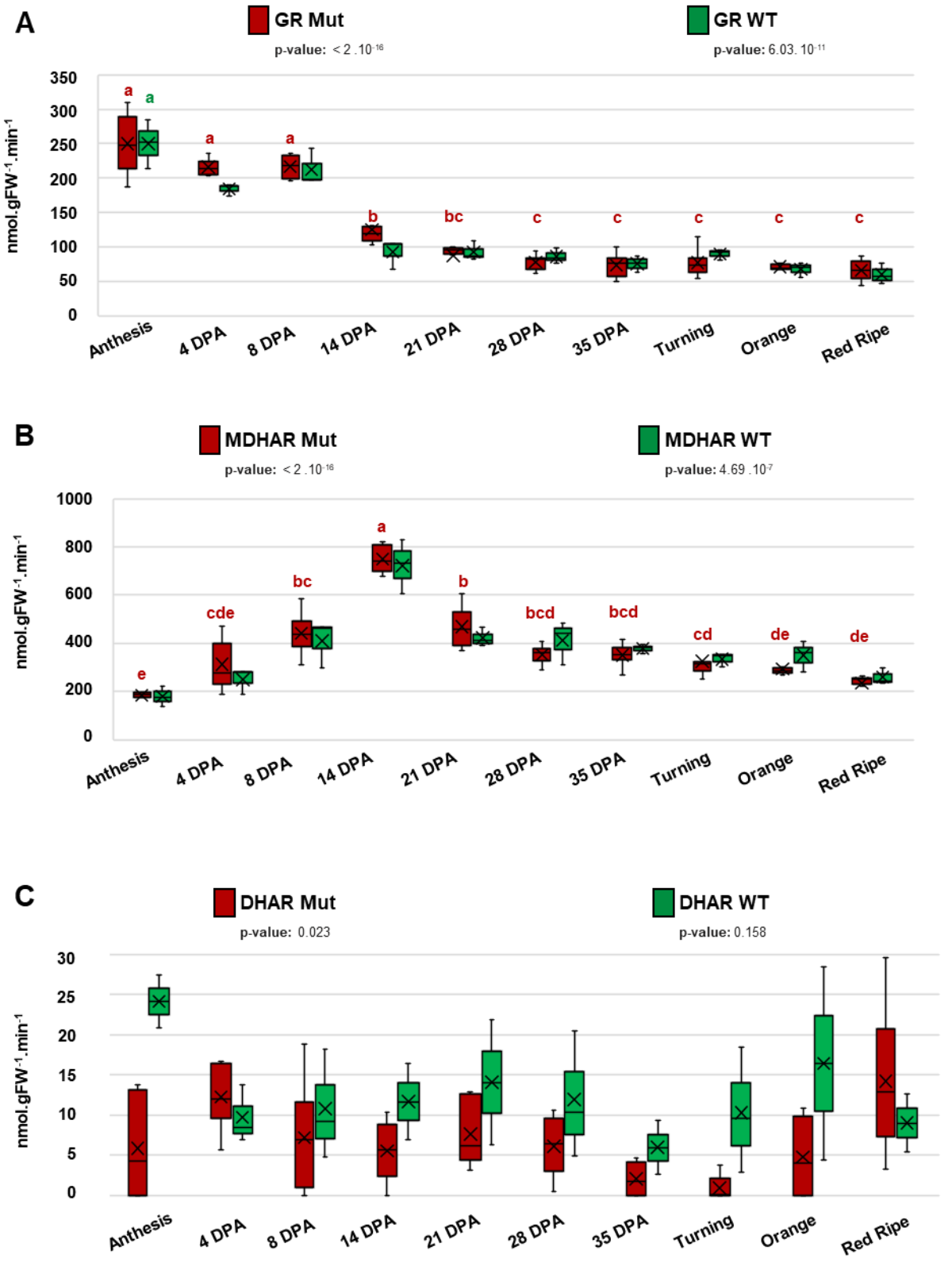

Supplemental fig IV.3: GR (A), MDHAR (B) and DHAR (C) in WT and ASC^{+} mutant fruits during development. Statistical significance content is indicated by ANOVA p-value. Binary comparisons between growth stages within the same genotype are indicated by letters (in colors according to legend) according to Tukey test ($p < 0.05$). Binary comparisons between genotypes for the same growth stage are indicated by stars according to Tukey test ($p < 0.05$).

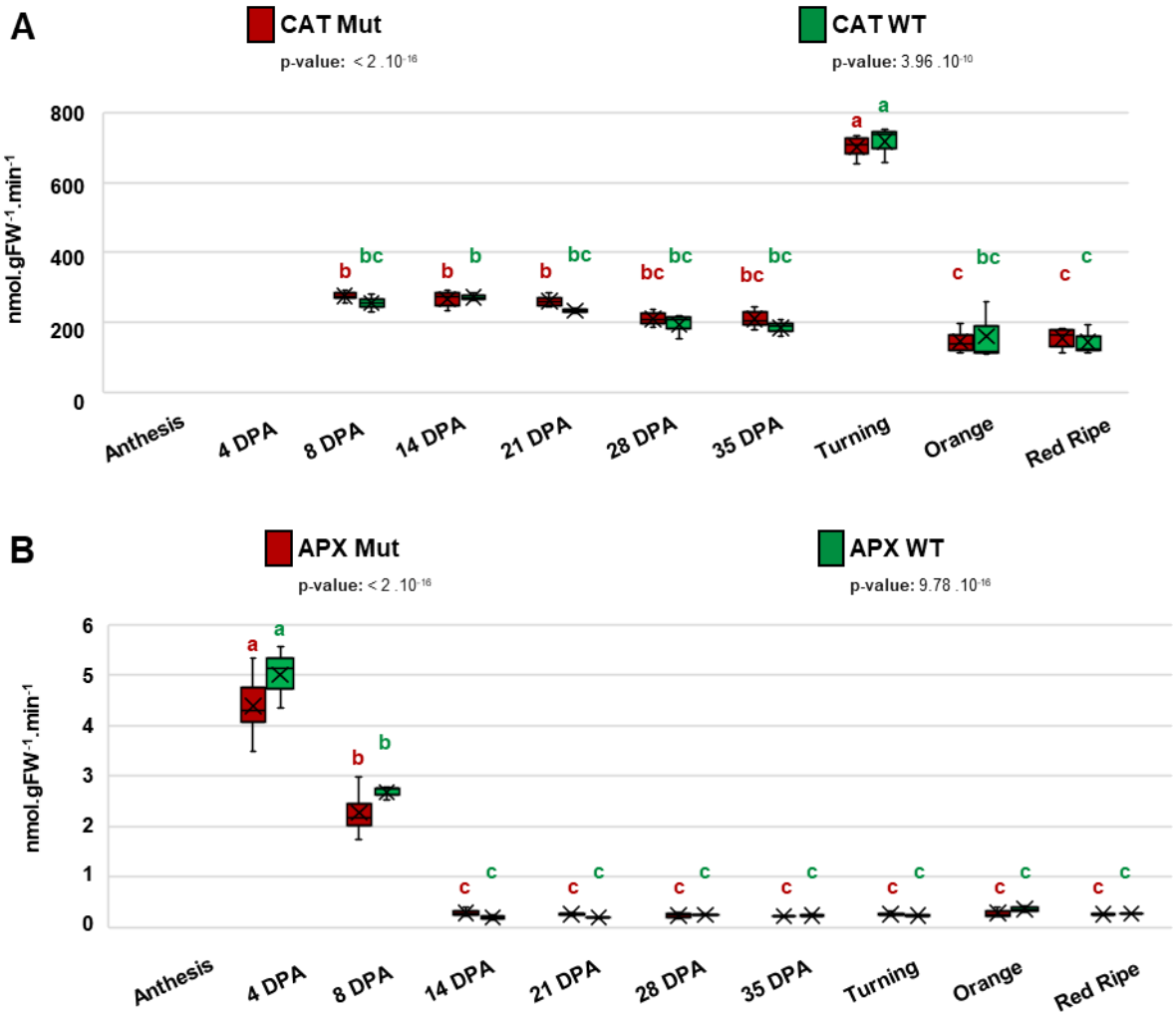

<u>Supplemental fig IV.4:</u> **APX (A) and CAT (B) in WT and ASC^{+} mutant fruits during development.** Statistical significance content is indicated by ANOVA p-value. Binary comparisons between growth stages within the same genotype are indicated by letters (in colors according to legend) according to Tukey test ($p < 0.05$). Binary comparisons between genotypes for the same growth stage are indicated by stars according to Tukey test ($p < 0.05$).

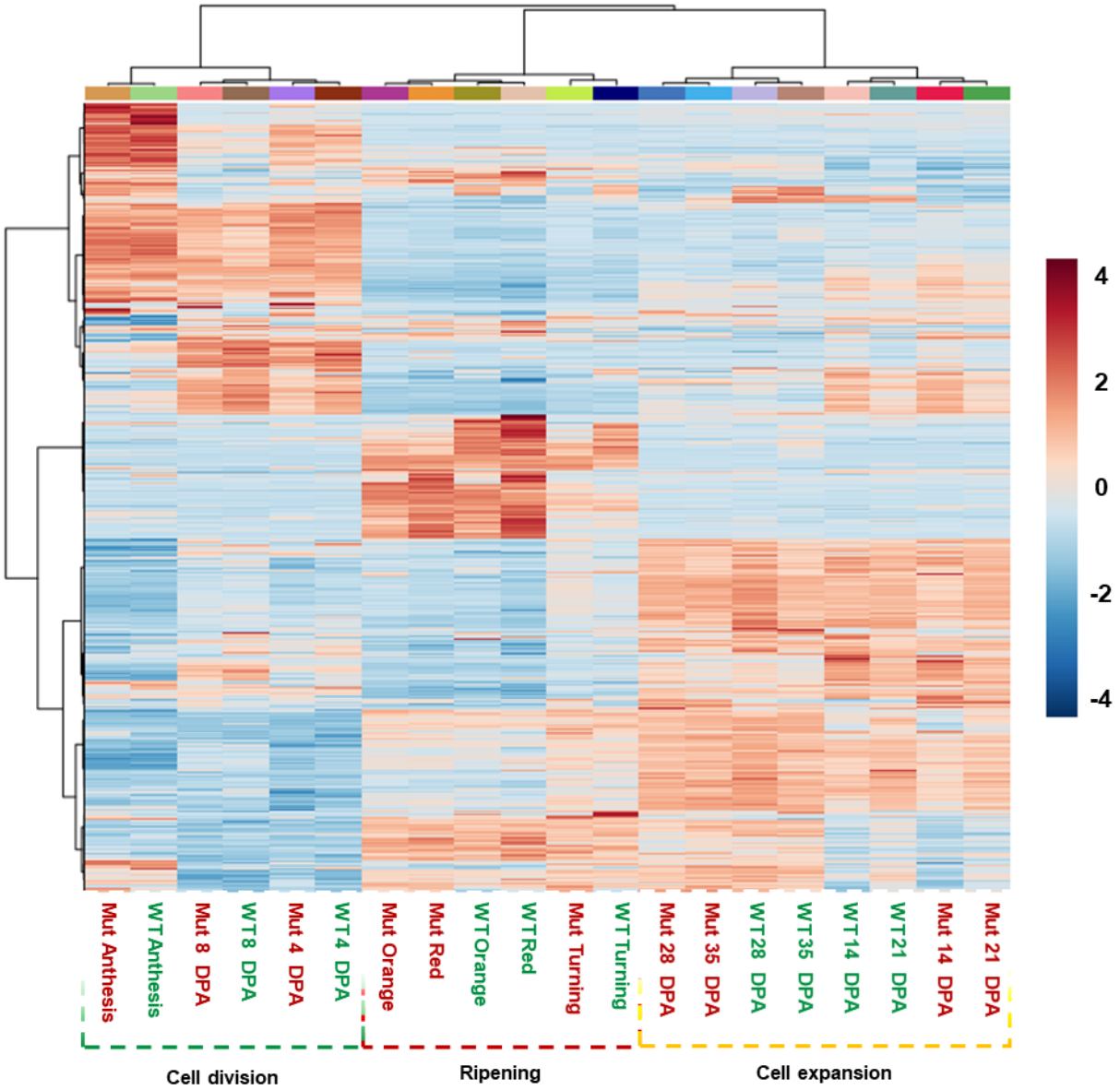

<u>Supplemental fig IV.6:</u> **Hierarchical clustering analyses of 3482 significant (ANOVA, $p < 0.05$) metabolic features during tomato fruit development.** Shown are Pearson's correlations after ward clustering that unveiled three metabolic clusters associated with three development cluster corresponding to developmental phases.

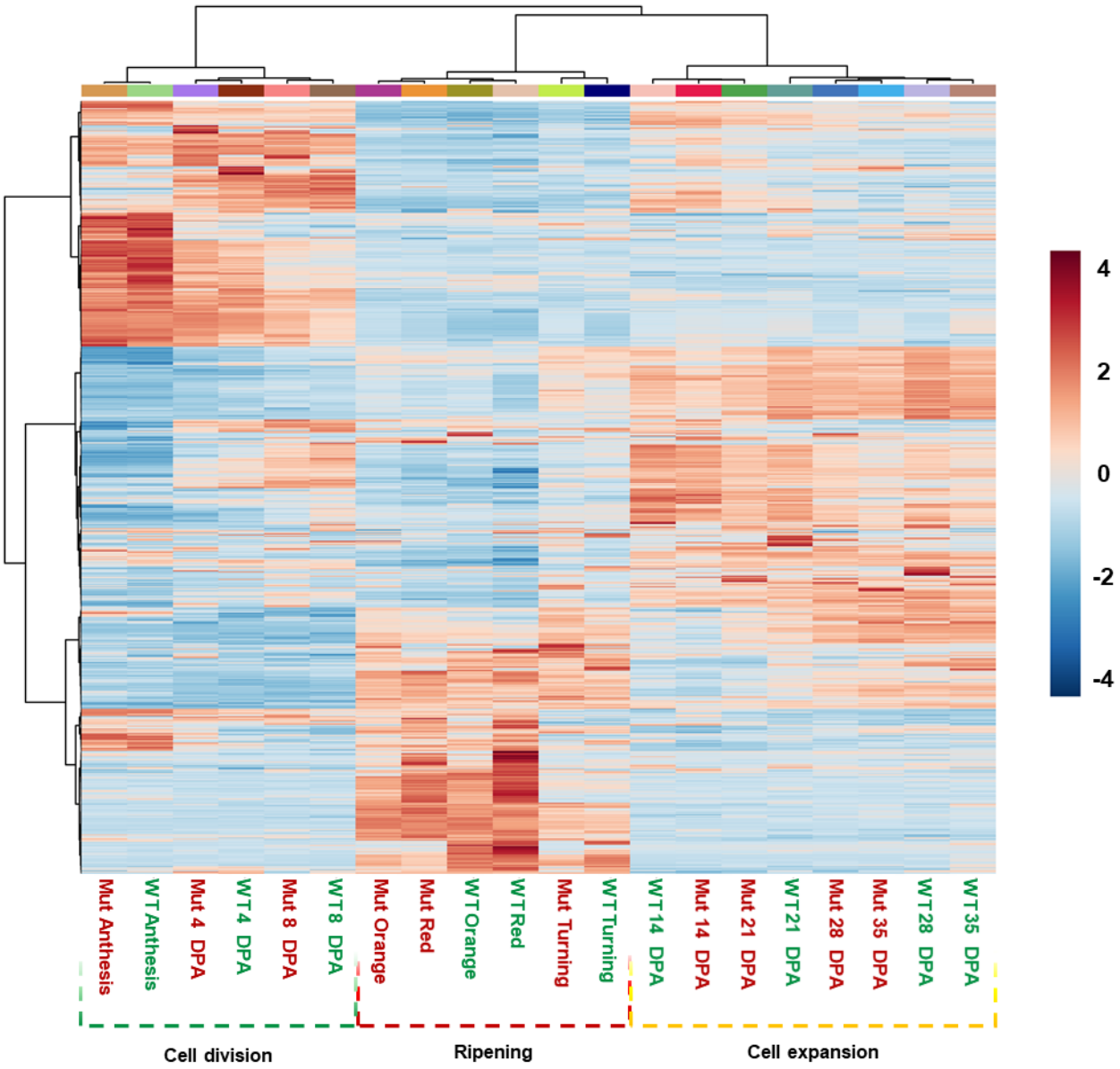

Supplemental fig IV.7: Hierarchical clustering analyses of 672 significant (ANOVA, $p < 0.05$) metabolic features during tomato fruit development. Shown are Pearson's correlations after Ward clustering that unveiled three metabolic clusters associated with three development cluster corresponding to developmental phases.

CHAPTER V

ENZYME-BASED KINETIC MODELLING OF THE ASC-GSH CYCLE DURING TOMATO FRUIT DEVELOPMENT

ABSTRACT

The ascorbate-glutathione cycle is at the heart of redox metabolism, linking the major redox buffer and their redox state with central metabolism through H_2O_2 processing and pyridine nucleotide metabolism. Previous changes in major redox buffer contents and their associated enzyme capacities have been observed during tomato fruit development but interactions between them remain unclear. Based on quantitative data obtained for the core redox metabolism (Chapter IV), we built an enzyme-based kinetic model able to predict core redox fluxes and metabolite content. This model was further validated using data from ASC-enriched mutants allowing us to investigate the control of ASC content within fruit tissues.

Dynamic and associated regulations of the ASC-GSH cycle throughout the whole fruit development were analysed and pointed to a sequential metabolic control of redox fluxes by ASC synthesis, NAD(P)H and H_2O_2 availability depending on the developmental phase. Moreover, MDHAR and reducing power availability were highlighted as the major regulators of ASC and GSH redox state during fruit growth in optimal conditions.

Finally, cross-validation using ASC-enriched fruits demonstrated that ASC content could be augmented in fruit solely by an increase of ASC synthesis up to a certain threshold, from which potential redox signalling was hindered.

The dynamic depiction of redox fluxes by deciphering redox signatures in plant biology is extremely tedious, if not impossible, probably due to the extreme reactivity of ROS and related redox signals, and to the intricacy of the redox hub. Moreover, the complexity of synthesis and degradation pathways of major redox buffers as well as their high level of reactivity complicate the analyses of redox fluxes. Multiple studies have evaluated the ASC-GSH cycle in photosynthetic cells (Foyer and Noctor, 2016; Foyer, 2018; Hashida et al., 2018; Terai et al., 2020). For decades, targeted studies based on reverse genetics and enzyme purification have focused on the functional and biochemical characterisation of the ROS processing enzymes of the ASC-GSH cycle (Mhamdi et al., 2010b; Sofo et al., 2015; Ortiz-Espín et al., 2017). However, metabolic control analysis in plant biology demonstrated that the influence of a specific enzyme could not be solely inferred from its over- or under- expression and that all enzymes and metabolites in the system needed further consideration (Thomas et al., 1997). Therefore, an exciting and promising alternative to measurements of redox pools and antioxidant systems is the use of mathematical modelling of metabolism (Rohwer, 2012; Salon et al., 2017), particularly for redox pathways. Enzyme-based kinetic modelling allows the description of metabolic and signalling networks by investigating fluxes and their regulations (Schallau and Junker, 2010). For instance, previous kinetic models of the ASC-GSH cycle have been developed, including studies on the mechanism of APX, which demonstrate a great sensitivity of the cycle in response to NADPH photoproduction or consumption by the Calvin cycle (Valero et al., 2009, 2015). In addition, the role of CAT in photosynthetically active leaves has also been investigated through kinetic modelling unveiling that low concentrations (below µM) of H_2O_2 rarely occur in cells and that ROS are processed by both APX and CAT under optimal conditions (Tuzet et al., 2019). Moreover, the authors demonstrate that the ASC turnover is largely independent of GSH metabolism until ASC peroxidation exceeds a certain value and that NAD(P)H availability indirectly influences the GSH redox ratio via the control of MDHAR activity (Tuzet et al., 2019). However, cross-validation of these models using independent datasets remains a critical issue.

Interestingly, kinetic models can be used to identify controlling steps of a specific pathway using *in silico* analysis, allowing new hypotheses to be generated (Morales et al., 2018). Furthermore, antioxidant metabolites are gaining interest because of their benefits for human health (Wargovich et al., 2012; Alseekh et al., 2021). Nevertheless, breeding strategies based on reverse genetic studies that aim to increase the ascorbate content in fruits encounter limited success (Gallie, 2013). However, emerging modelling approaches should be a useful complementary tool to investigate the regulations and the accumulation of a targeted metabolite. Indeed, kinetic models will provide a better understanding of the metabolic regulations in cells by identifying limiting steps or substrates, which are not highlighted by the classic genetic approach. Hence, the combination of metabolic modelling and reverse genetic will help to address breeding issues.

The present study aims to provide a kinetic model able to calculate steady-state concentrations of ROS and major redox buffers, including ASC, GSH and NAD(P)(H), as well as their oxidation state, and associated fluxes during tomato fruit development. In addition, this model allows analysing the effect of ascorbate synthesis on the ASC-GSH cycle during fruit development. This will help provide a deeper understanding of the reactive redox metabolism and, more specifically, ascorbate metabolism during fruit development. Even more so, our kinetic-based model represents a valuable tool that could benefit future studies of ASC-GSH cycle in a range of physiological contexts.

A. Ascorbate-glutathione model construction and parametrisation

A kinetic model of the ASC-GSH cycle was built according to Figure V.1. The model can be divided into 3 compartments: cytosol, vacuole, and apoplast where specific reactions occur. It is assumed that vacuole contains solely a few antioxidant metabolites, that no reactions occur, and its only role is to sequestrate oxidised glutathione, as already reported in a previous modelling study (Tuzet et al., 2019).

Apoplast has been included to account for the NADPH oxidase as an active ROS producing system and allow an extracellular ROS diffusion potentially involved in long-distance signalling pathways (Foyer and Noctor, 2016; Decros et al., 2019a).

The core network of the model is based on the *Arabidopsis* ascorbate-glutathione cycle described in chloroplasts by Polle (2001) and modified by Valero et al. (2015). However, these previous models have been dedicated to plastids and leave tissues and did not take into account either CAT (e.g. mostly peroxisomal) or MDHAR enzymes. The parameterisation of the model was based on the literature and novel experimental data. Since Michaelis constants (K_m) can display considerable discrepancies in the literature or database (https://www.brenda-enzymes.org/), we used K_m preferably from studies in tomato or other plants and assumed they remain constant during all the tomato fruit development (Table IV.1).

Enzyme capacities and metabolites concentrations were determined by fitting experimental data using linear or nonlinear regressions (Supplemental Table IV.1). Cytosolic and vacuolar volumes were obtained from a previous kinetic-based model focused on vacuolar sugar transport in growing tomato fruit (Beauvoit et al., 2014). The model consists of 8 differential equations as a function of the 19 reactions (see Annex 2), of which seven are enzymatic. Each enzymatic activity involved in the cycle has been implemented considering its specific catalytic mechanism. Biochemical reactions, rate equations, parameter setting and corresponding references are listed in Table IV.2 and IV.3. A model for each developmental stage has been generated to be solved at a quasi-stationary state, representing

the fruit development as a series of quasi-stationary state models. However, this model has limitations, such as the assumption that pyridine nucleotide concentrations remain constant at each stage but display discrepancies from one stage to another. Besides, relative measurements of ROS-processing secondary antioxidants using LCMS demonstrated that secondary redox metabolism was also highly plastic during tomato fruit growth (see chapter IV, Figure IV.20). However, the absence of quantitative data may hinder the global and comprehensive evaluation of the entire redox metabolism. These specific points will be discussed in light of the findings of our study.

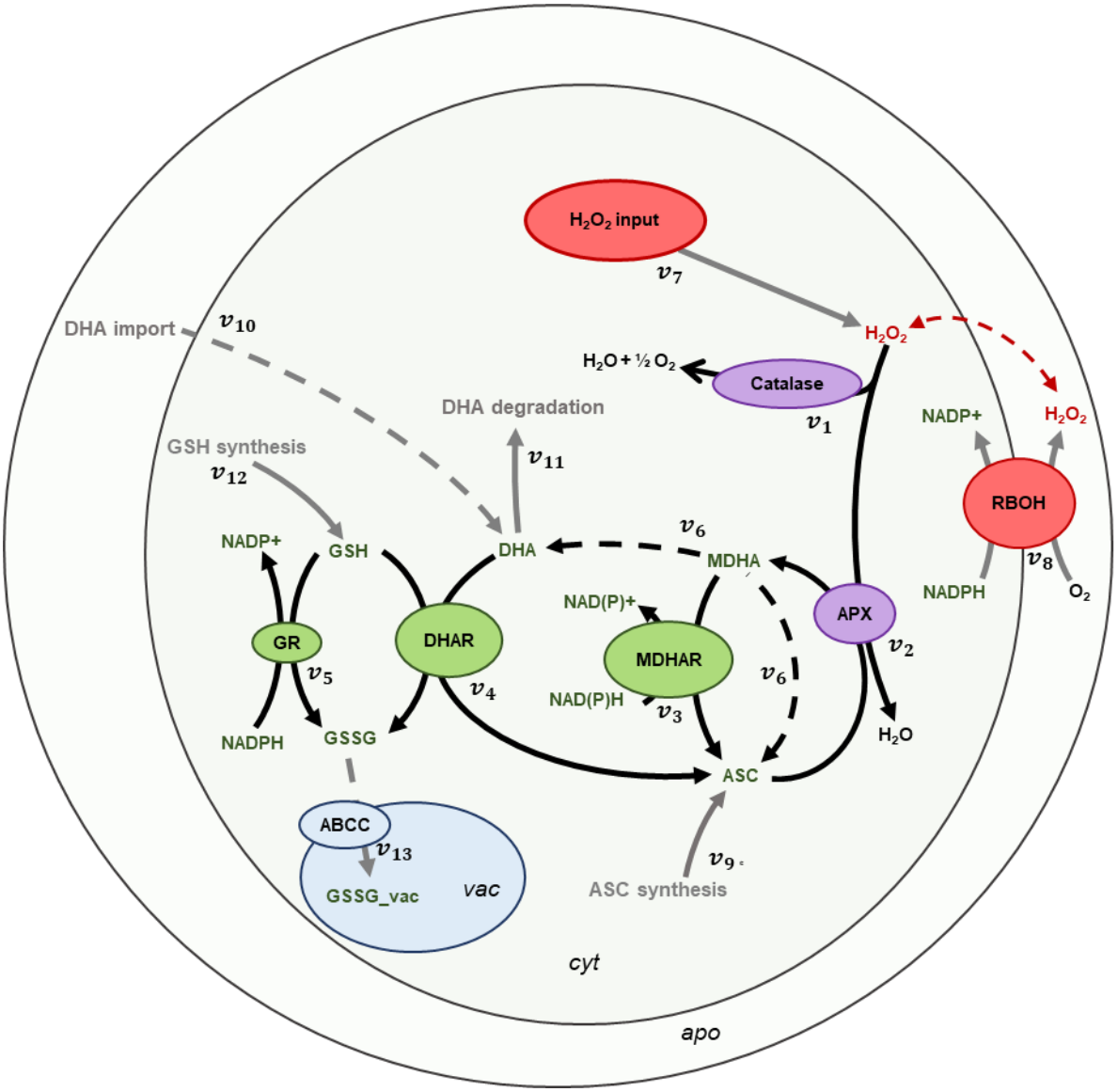

Figure V.1: Schematic network of ASC-GSH cycle in tomato fruit pericarp cell. Dashed arrow stands for non-enzymatic reactions (*i.e.* chemical reactions and transports) whereas full black arrows stand for enzymatic reaction included in the model (v_1 to v_5). vac: vacuole; cyt: cytosol; apo: apoplast; GSH: reduced glutathione; GSSG: oxidised glutathione; ASC: ascorbate; DHA: dehydroascorbate; MDHA: monodehydroascorbate; RBOH: respiratory burst NADPH oxidase; APX: ascorbate peroxidase; DHAR: dehydroascorbate reductase; MDHAR: monodehydroascorbate reductase; GR: glutathione reductase; H_2O_2: hydrogen peroxide.

Variable	Initial value	Unit	Reference
$K_{m_{ASC}^{APX}}$	0.325	mM	Polle, 2001; Tuzet et al., 2019
$K_{m_{H_2O_2}^{APX}}$	0.03	mM	Polle, 2001; Tuzet et al., 2019
$K_{m_{H_2O_2}^{CAT}}$	24	mM	Polle, 2001; Tuzet et al., 2019
$K_{m_{MDHA}^{MDHAR}}$	0.0014	mM	Hossain and Asada, 1985; Valero et al., 2009, 2015
$K_{m_{NAD(P)H}^{MDHAR}}$	0.023	mM	Hossain and Asada, 1985; Valero et al., 2009, 2015
$K_{m_{DHA}^{DHAR}}$	0.07	mM	Polle, 2001; Valero et al., 2009, 2015
$K_{i_{DHA}^{DHAR}} . K_{m_{GSH_1}^{DHAR}}$	0.5	mM^2	Polle, 2001; Valero et al., 2009, 2015
$K_{m_{GSH_1}^{DHAR}} + K_{m_{GSH_2}^{DHAR}}$	2.5	mM	Polle, 2001; Valero et al., 2009, 2015
$K_{m_{GSSG}^{GR}}$	0.2	mM	Polle, 2001; Valero et al., 2009, 2015
$K_{m_{NADPH}^{GR}}$	0.003	mM	Polle, 2001; Valero et al., 2009, 2015
$K_{m_{GSSG}^{ABCC}}$	0.4	mM	Tuzet et al., 2019
$k_{6_{MDHA\ dismutation}}$	0.03	$mM.min^{-1}$	Polle, 2001; Valero et al., 2009, 2015
$k_{5'_{DHA\ recycling}}$	1.6×10^{-7}	$mM.min^{-1}$	Polle, 2001; Valero et al., 2009, 2015
$k_{H_2O_{2diffusion}}$	0.1	min^{-1}	Valero et al., 2015

Table V.1: Km and catalytic constant values fixed during development in the model.

Flux	Reaction	Rate equation
CAT	$H_2O_2 \rightarrow H_2O + {}^1/_2\, O_2$	$\frac{V_{max_{CAT}}[H_2O_2]}{K_{m_{CAT}}}$
APX	$H_2O_2 + 2\ ASC \rightarrow 2\ H_2O + 2\ MDHA$	$\frac{V_{max_{APX}}[ASC][H_2O_2]}{K_{m_{ASC}}[H_2O_2] + K_{m_{H_2O_2}}[ASC] + [ASC][H_2O_2]}$
$MDHAR$	$MDHA + NAD(P)H \rightarrow ASC + NAD(P)^+$	$\frac{V_{max_{MDHAR}}[NAD(P)H][MDHA]}{K_{m_{NAD(P)H}}[MDHA] + K_{m_{MDHA}}[NAD(P)H] + [MDHA][NAD(P)H]}$
$DHAR$	$DHA + 2\ GSH \rightarrow ASC + GSSG$	$\frac{V_{max_{DHAR}}[GSH][DHA]}{K_{i_{DHA}} * K_{m_{GSH1}} + K_{m_{DHA}}[GSH] + \left(K_{m_{GSH1}} + K_{m_{GSH2}}\right)[DHA] + [DHA][GSH]}$
GR	$GSSG + NADPH \rightarrow GSH + NADP^+$	$\frac{V_{max_{GR}}[NADPH][GSSG]}{K_{m_{NADPH}}[GSSG] + K_{m_{GSSG}}[NADPH] + [NADPH][GSSG]}$
$ASC_{synthesis}$	$\rightarrow ASC$	*Optimised constant flux*
$DHA_{degradation}$	$DHA \rightarrow$	$k_{DHA_{degradation}} \times [DHA]$
$DHA_{chemical\ recycling}$	$DHA + GSH \rightarrow GSSG + ASC$	$k_{5'_{DHA\ recycling}} \times [GSH]_{cyt} \times [DHA]$
DHA_{import}	$\rightarrow DHA$	*Optimised constant flux*
$ASC_{dilution}$	$ASC \rightarrow$	$Vac_{expension_{factor}} \times [ASC]$
$DHA_{dilution}$	$DHA \rightarrow$	$Vac_{expension_{factor}} \times [DHA]$
$GSSG_{dilution}$	$GSSG_{vac} \rightarrow$	$Vac_{expension_{factor}} \times [GSSG]_{vac}$
$GSH_{synthesis}$	$\rightarrow GSH$	*Optimised constant flux*
$GSSG_{vacuolar_{accumulation}}$	$GSSG_{cyt} \rightarrow GSSG_{vac}$	$\frac{V_{max_{ABCC}} \times [GSSG]_{cyt}}{K_{m_{GSSG}^{ABCC}} + [GSSG]_{cyt}}$
$H_2O_{2_{diffusion}}$	$H_2O_{2_{cyt}} \leftrightarrow H_2O_{2_{apo}}$	$\left(k_{H_2O_{2_{diffusion}}} \times [H_2O_2]_{cyt}\right) - \left(k_{H_2O_{2_{diffusion}}} \times [H_2O_2]_{apo}\right)$
$H_2O_{2_{cytosolic\ production}}$	$\rightarrow H_2O_{2_{cyt}}$	*Optimised constant flux*
$MDHA_{chemical\ recycling}$	$2\ MDHA \rightarrow DHA + ASC$	$k_{6_{MDHA\ dismutation}} \times [MDHA]^2$
$NADPH\ oxidase$	$NADPH + O_2 \rightarrow NADP^+ + H_2O_{2_{apo}}$	$k_{NADPH\ oxidase} \times [NADPH] \times O_2$

Table V.2: Biochemical reactions and associated rate equations included in the model.

	8 DPA	14 DPA	21 DPA	28 DPA	35 DPA	Turning	Orange	Red
$V_{max_{GR}}$ (µmol.min^{-1}.gFW^{-1})	0.149373	0.113377	0.093566	0.084643	0.079827	0.074646	0.071467	0.060499
$V_{max_{APX}}$ (µmol.min^{-1}.gFW^{-1})	2.414462	0.186053	0.192455	0.184706	0.327797	0.291039	0.252357	0.280559
$V_{max_{MDHAR}}$ (µmol.min^{-1}.gFW^{-1})	0.384798	0.503311	0.533214	0.470354	0.380515	0.310963	0.293011	0.287270
$V_{max_{DHAR}}$ (µmol.min^{-1}.gFW^{-1})	0.011663	0.009793	0.008808	0.008547	0.008672	0.008919	0.008996	0.008938
$V_{max_{CAT}}$ (µmol.min^{-1}.gFW^{-1})	303.505	192.311	191.275	264.685	345.185	365.422	338.955	156.264
Vol_{cyt} (mL^{-1})	0.295007	0.160545	0.108439	0.090100	0.081962	0.076322	0.076215	0.075966
Vol_{apo} (mL^{-1})	0.07	0.07	0.07	0.07	0.07	0.07	0.07	0.07
RGR (min^{-1})	9.75 x10^{-5}	9.11 x10^{-5}	7.57 x10^{-5}	5.13 x10^{-5}	2.69 x10^{-5}	1.15 x10^{-5}	7.69 x10^{-6}	2.87 x10^{-6}
NAD^+ (µmol..gFW^{-1})	0.022299	0.012231	0.008346	0.007320	0.007495	0.008134	0.008374	0.008355
$NADH$ (µmol..gFW^{-1})	0.001467	0.000989	0.000607	0.000392	0.000289	0.000266	0.000280	0.000409
$NADP^+$ (µmol..gFW^{-1})	0.00714	0.00470	0.00367	0.00358	0.00356	0.00146	0.00377	0.00334
$NADPH$ (µmol..gFW^{-1})	0.00284	0.00233	0.00147	0.00152	0.00128	0.00367	0.00145	0.00095

Table V.3: Parameters setting during tomato fruit development.

I. ROS processing enzymes involved in the model

1. Catalase (CAT)

Catalase harbours a low affinity for H_2O_2 compared to other enzymes as it displays high K_m values in plants (from 10 to 140 mM), resulting in an almost linear CAT activity as H_2O_2 is increasing, even to values that are supra-physiological (Mhamdi et al., 2010b).

Thus, the catalytic mechanisms of catalase follow more pseudo-first-order kinetics than Michaelis-Menten kinetics within the range of physiological H_2O_2 range.

$$\boldsymbol{v_1} = \boldsymbol{V_{CAT}}(H_2O_2 \rightarrow H_2O + {}^1\!/_2\, O_2) = \frac{V_{max_{CAT}}[H_2O_2]}{K_{m_{CAT}}}$$

2. Ascorbate peroxidase (APX)

Ascorbate peroxidase possesses a higher affinity for H_2O_2 than catalase and leads to the oxidation of ascorbate to monodehydroascorbate. This enzyme is a class I heme peroxidase whose catalytic mechanism involves an oxidised intermediate (compound I), that will be subsequently reduced by two single-electron transfer steps. The APX flux can be expressed by the ping-pong bi-bi mechanism:

$$\boldsymbol{v_2} = \boldsymbol{V_{APX}}\,(H_2O_2 + 2\,ASC \rightarrow 2\,H_2O + 2\,MDHA) =$$

$$\frac{V_{max_{APX}}[ASC][H_2O_2]}{K_{m_{ASC}}[H_2O_2] + K_{m_{H_2O_2}}[ASC] + [ASC][H_2O_2]}$$

II. Antioxidant recycling enzymes involved in the model

1. Monodehydroascorbate reductase (MDHAR)

Monodehydroascorbate reductase catalyses the reduction of MDHA to ASC using NAD(P)H as an electron donor. This enzyme was previously described with a ping-pong mechanism and has been implemented in the model. To mimic the capacity of MDHAR to use either NADH or NADPH, MDHAR flux is expressed as two equations, each of one using a specifically reduced cofactor, whose K_m values were assumed to be the same.

$$\boldsymbol{v_3} = \boldsymbol{V_{MDHAR_{NADPH}}}(MDHA + NADPH \rightarrow ASC + NADP^+) =$$

$$\frac{V_{max_{MDHAR}}[NADPH][MDHA]}{K_{m_{NADPH}}[MDHA] + K_{m_{MDHA}}[NADPH] + [MDHA][NADPH]}$$

and

$$\boldsymbol{v_{3'}} = \boldsymbol{V_{MDHAR_{NADH}}}\ (MDHA + NADH \rightarrow ASC + NAD^+) =$$

$$\frac{V_{max_{MDHAR}}[NADH][MDHA]}{K_{m_{NADH}}[MDHA] + K_{m_{MDHA}}[NADH] + [MDHA][NADH]}$$

2. *Dehydroascorbate reductase (DHAR)*

Dehydroascorbate reductase catalyses the regeneration of ASC from DHA using GSH as an electron donor. Kinetic analysis revealed that this enzyme regenerates ASC by a bi uni uni uni ping-pong mechanism. The following equation has been used in the model:

$$\boldsymbol{v_4} = \boldsymbol{V_{DHAR}}\ (DHA + 2\ GSH \rightarrow ASC + GSSG) =$$

$$\frac{V_{max_{DHAR}}[GSH][DHA]}{K_{i_{DHA}} * K_{m_{GSH_1}} + K_{m_{DHA}}[GSH] + \left(K_{m_{GSH_1}} + K_{m_{GSH_2}}\right)[DHA] + [DHA][GSH]}$$

$K_{i_{DHA}}$ is the equilibrium constant between DHAR, DHA and the enzyme-substrate DHAR-DHA complex. $K_{m_{GSH_1}}$ and $K_{m_{GSH_2}}$ are K_m values for the first and second-binding molecules of GSH, respectively. The sum of these values has been used in the model since it is impossible to distinguish them separately in kinetic assays (Valero et al., 2015).

3. *Glutathione reductase (GR)*

Glutathione reductase achieves the recycling of GSH by reducing GSSG using NADPH as a reductant. Kinetic studies revealed that this enzyme operates according to a bi-ter ping-pong mechanism allowing the modelling of its rate as:

$$\boldsymbol{v_5} = \boldsymbol{V_{GR}}\ (GSSG + NADPH \rightarrow GSH + NADP^+) =$$

$$\frac{V_{max_{GR}}[\mathrm{NADPH}][\mathrm{GSSG}]}{K_{m_{NADPH}}[GSSG] + K_{m_{GSSG}}[NADPH] + [NADPH][GSSG]}$$

In addition, non-enzymatic reactions concerning superoxide anion dismutation, hydrogen peroxide processing have been excluded after showing negligible fluxes whereas non-enzymatic monodehydroascorbate reduction has been included (Figure V.1; v_6).

III. Parameters estimated by the model

The initial parameterisation of the model left seven parameters unknown, namely, H_2O_2 production (v_7), NADPH oxidase activity (v_8), ASC synthesis (v_9), DHA import (v_{10}), DHA degradation (v_{11}), GSH synthesis (v_{12}) and GSSG transport in the vacuole (v_{13}) (Figure V.1). Values of these parameters were optimised for each stage by fitting the experimentally measured contents for total and reduced ASC, total GSH and GSSG, H_2O_2 and both redox states of ASC and GSH. Briefly, parameter values were randomly searched by least square minimisation using a particle swarm algorithm. The whole iterative process was repeated using the Curta cluster housed by the Mésocentre de Calcul Intensif Aquitain (MCIA) using randomised initial conditions, at the end of which the 100 best values were retained for each stage. Median parameters obtained from optimisation results were used to calculate steady-state content in redox buffers, their redox state and total ROS concentration (Baker et al., 2010).

1. Antioxidant inputs

To obtain a realistic model of the ASC-GSH cycle in developing tomato fruits, inputs of reduced ASC and GSH (v_9 and v_{12} , respectively) have been added that stand for their synthesis pathways. An input of DHA (v_{10}) has also been inserted to mimic this potential transport of ascorbate from vegetative tissues as suggested by several lines of evidence (Horemans et al., 2000; Pignocchi and Foyer, 2003; Pignocchi et al., 2006). In addition, the occurrence of ascorbate oxidase activity in the apoplast has been reported to participate in numerous signalling pathways by maintaining the redox state of ascorbate mainly oxidised in the apoplast during various developmental and stresses events (de Pinto, 2004; Pignocchi et al., 2006; Li et al., 2017a).

2. Antioxidant outputs

As inputs were implemented in the model, some outputs were required to obtain an available steady-state. Outputs reflecting the dilution effect of growth during tomato development were added for ASC, DHA and GSSG according to the previous sugar metabolism kinetic models (Beauvoit et al., 2014; Génard et al., 2014). For each stage, a cytosolic and vacuolar expansion factor has been calculated by

multiplying the pool size by the relative growth rate and the respective compartment volume. Moreover, an ASC degradation pathway (v_{11}) has been included starting from DHA that leads to the accumulation of threonate and oxalate in tomato fruit (Truffault et al., 2017).

3. Hydrogen peroxide inputs

Considering that the stability of $O_2^{\bullet -}$ is extremely low, the most stable form of ROS is assumed to be H_2O_2 (Smirnoff and Arnaud, 2019). In addition, SODs are powerful enzymes that harbour pseudo-first-order kinetic rates as high as $2x10^9$ $.M^{-1}.s^{-1}$ (Ogawa et al., 1995), allowing an almost immediate dismutation of $O_2^{\bullet -}$ into H_2O_2 (Valero et al., 2015), thus ROS sources included in the model are considered to produce H_2O_2 directly.

Two ROS sources have been included in the model. The first one reflects the activity of mitochondrial and chloroplast metabolisms and glycolate oxidase activity within the photorespiratory cycle. Furthermore, the second H_2O_2 production flux aims at simulating the activity of the respiratory burst NADPH oxidase located in the apoplast. However, this model seeks to describe the redox metabolism at the cellular scale and will not be able to deepen the understanding of the contribution of the different ROS sources to the redox balance.

4. Transport processes

Although there are many lipophilic antioxidants, it is considered here that H_2O_2 can freely diffuse across the plasma membrane, thus linking the apoplastic and cytosolic ROS pools. Furthermore, the H_2O_2 diffusion across the plasma membrane combined with NADPH oxidase activity can be seen as a potential mechanism leading to the accumulation of ROS within the apoplast. A reversible mass action law was used to simulate H_2O_2 diffusion. Besides, a flux of vacuolar sequestration of GSSG has been included as previously modelled in *Arabidopsis* leaves (Tuzet et al., 2019), and corresponding to a Michaelis-Menten kinetic irreversible transport of GSSG using ABCC type transporter (Lu et al., 1998; Tommasini et al., 1998).

$$\boldsymbol{v_{13}} = \boldsymbol{V_{ABCC}}\left(GSSG_{cyt} \rightarrow GSSG_{vac}\right) =$$

$$\frac{V_{max_{ABCC}}[GSSG_{cyt}][GSSG_{vac}]}{K_{m_{ABCC}}[GSSG_{cyt}] + K_{m_{ABCC}}[GSSG_{vac}] + [GSSG_{cyt}][GSSG_{vac}]}$$

B. The necessity of a spatially controlled ROS production for model fitting

The model encompasses fruit growth from 8 DPA until 52 DPA, which corresponds to the red ripe stage of tomato fruit. The system of differential equations was solved for each of the 8 sequential development stages, thus making pericarp cell growth a succession of quasi-stationary states. It is worth noting that our model did not take into account the different ROS production sources (photosynthesis, photorespiration and respiration) within the cell because the lack of information concerning their dynamic during fruit growth makes it impossible to parameterise a such fine-tuned model. Moreover, superoxide synthesis was not implemented in the model, assuming this species to be entirely chemically and enzymatically dismutated to hydrogen peroxide owing to the high catalytic capacity of SOD (Bowler et al., 1994; Valero et al., 2015).

Unknown parameters (Figure V.1; v_7 to v_{13}) were optimised by least-square fitting using an unsupervised particule swarm algorithm, and the median value of the top 100 best scorings were used in the model (Baker et al., 2010). The median values for optimised parameters obtained through the optimisation procedure display discrepancies during fruit development (Supplemental fig V.1, 2). The dispersion of the optimisation results indicates to some extent the significance of these parameters for model fitting. For instance, ASC and GSH synthesis are more stringent than DHA import and V_{ABCC}, indicating that synthesis fluxes have a greater impact than transport fluxes on the model (Supplemental fig V.1). In general, optimised parameters show the same trend as metabolite data. For instance, ASC synthesis flux follows the dynamic of total ASC by harbouring its highest value during the beginning of the development, then rapidly drops during cell elongation before a small resumption, at the turning stage.

Furthermore, the median model for the 8 DPA stage obtained after optimisation showed a total absence of reduced ascorbate and a low H_2O_2 content (Supplemental fig V.2, 3) while displaying a very high ROS production flux (Supplemental fig V.3). Under these conditions, fitting the H_2O_2 content at an early stage was impossible because the ROS produced would be treated immediately either by APX, until it reached its maximum capacity and/or ASC had been totally consumed, or by catalase that could handle supra-physiological ROS production flux. In addition, we observed an increase in ascorbate oxidation ratio at turning followed by an increase in reduced and total glutathione at orange and red stages (Supplemental fig V.3, 5). Finally, this parameterisation was not able to produce a model that can reach a steady state at 35 DPA and thus failed to describe redox metabolism during the whole fruit development (Figure V.2A).

Overall, taking into consideration all measured variables (*i.e.* metabolites and redox ratio) and all stages, right-tailed Chi-square was performed to validate model prediction, which ended with a high value (Figure V.2.A; $Chi^2 = 57.68$, $p > 0.05$). Moreover, the log-log plot showed that this parameterisation of the model predicted values distant from the experimentally obtained for several variables (*i.e.* H_2O_2, GSH and ASC oxidation ratios and total GSH) (Figure V.2.A).

To address these limitations, we optimised our model by including two major redox functions: 1) apoplastic NADPH oxidase activity producing H_2O_2 that is not processed by cytosolic antioxidant machinery, and 2) a passive diffusion flux of ROS through the plasma membrane. Overall, the optimisation procedure provided suitable values for all unknown parameters and allowed matching between predicted values obtained using the model and the experimental values, throughout the whole fruit development (Figure V.1, 2B and Supplemental fig V.3, 4, 5). A good fit for total ASC content was observed, whereas model predictions for reduced and oxidised ASC, and thus its oxidation ratio, could be noticed at 8 DPA. Indeed, the model predicted an oxidation ratio close to 100% while the experimental data show a ratio of about 75% (Supplemental Fig V.3). However, the sum of weighted square errors showed a substantial decrease compared to the first model version (Figure V.3), and overall, the predictions obtained for all metabolic features ended with a lower Chi-square and higher goodness (Figure V.2B; $Chi^2 = 1.57$, $p >> 0.05$). Altogether, our results indicate that the optimised model allows predicting accurately ROS and major redox buffer contents during all tomato fruit development.

Meanwhile, apart from H_2O_2 production flux, the median values for optimised parameters did not show significant differences between the two versions of the model (Figure V.2). However, the dispersion of these parameters seemed reduced in the model including NADPH oxidase (Figure V.1). On the other hand, it was difficult to compare H_2O_2 cytosolic production flux and k1_NADPH oxidase, which represented a ratio of V_{max}/K_m (Figure V.2), Therefore, the model is intended to be used at the cell scale level, and the total H_2O_2 production flux should reflect the sum of the activities of ROS sources.

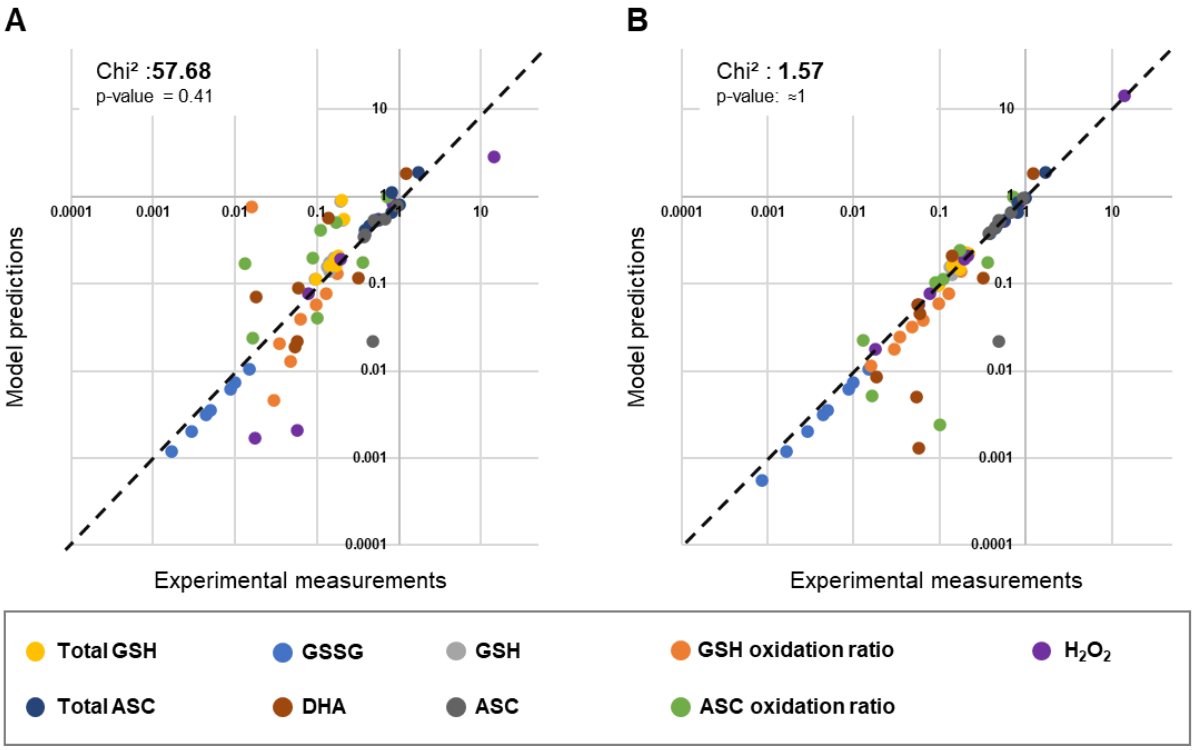

Figure V.2: Comparison between model predictions and experimental measurements during all fruit development using a model without **(A)** and with **(B)** apoplastic H_2O_2 production. Diagonals represent 100% match between experiments and predictions. p-values (alpha > 0.05).

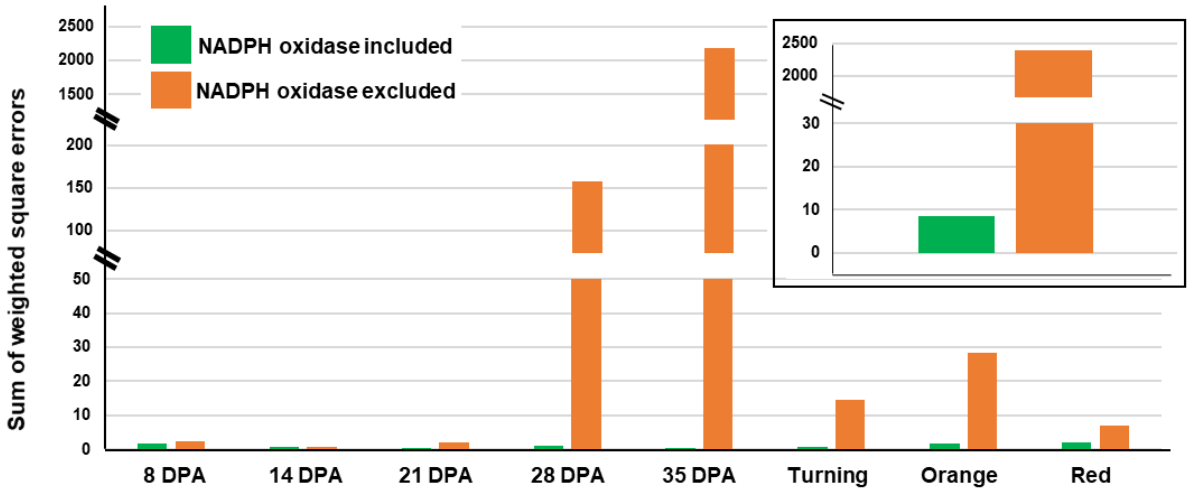

Figure V.3: Sum of weighted square errors calculated from original model (green) or using predicted values from model without NADPH oxidase (orange). Insert shows cumulative sum of squared residuals over all stages.

C. In silico approach to mimic ASC-enriched mutant behaviour for model validation

To ensure the robustness of the model predictions, cross-validation using independent experimental data set is required. Therefore, our model was validated using a heterozygous mutant line enriched in ASC due to higher ASC synthesis. This line was characterised in a previous study to which I contributed (Deslous et al., 2021). ASC-enriched mutant fruits displayed differences in ASC content without significant discrepancies neither in enzymatic capacities of enzymes involved in the ASC-GSH cycle nor in phenotypical variables (data shown in chapter II). Therefore, this allowed us to keep the same parameterisation from the original WT model to study the effects of an increase in ASC synthesis for fruit redox metabolism.

In the model, an increase in total ascorbate content was reproduced *in silico* for each developmental stage by enhancing only one parameter: either the input of ASC to mimic the rise in synthesis, or the input of DHA that simulated an import from sink tissues. Figure V.4 shows the results of a titration of the ASC synthesis flux up to 8 times the value of the WT, with all other parameters remaining at their WT values. Strikingly, an increase in ASC synthesis flux led to a sharp accumulation of reduced ASC and thus a swift rise in total ASC content. Discrepancies were observed between developmental stages but the maximum change in ASC synthesis compared to WT was up to 5-6 times at 8 DPA, suggesting that a too high increase in synthesis flux could result in unrealistic ASC content in pericarp cells.

Besides, an increase in DHA input up to 8 times the level of the original model was not able to induce a significant accumulation of ASC regardless of the developmental stage (Figure V.4). We then determined the response of the total ASC content to changes in its input values by using metabolic control analysis (MCA) to calculate response coefficients (Kacser and Burns, 1973; Heinrich and Rapoport, 1974). The total ASC content is positively sensitive to both DHA and ASC input but in different orders of magnitude, from 10^{-5} to 10^{-8} and from 0.5 to 6.5, respectively (Figure V.4). Moreover, discrepancies in the response coefficient were observed during fruit development, showing differential sensitivity to the increase in both inputs depending on the growth stage (Figure V.4). The sensitivity of total ASC content to augmented ASC synthesis was high as the vacuole expanded and low during ripening, thus following the trend of the relative growth rate.

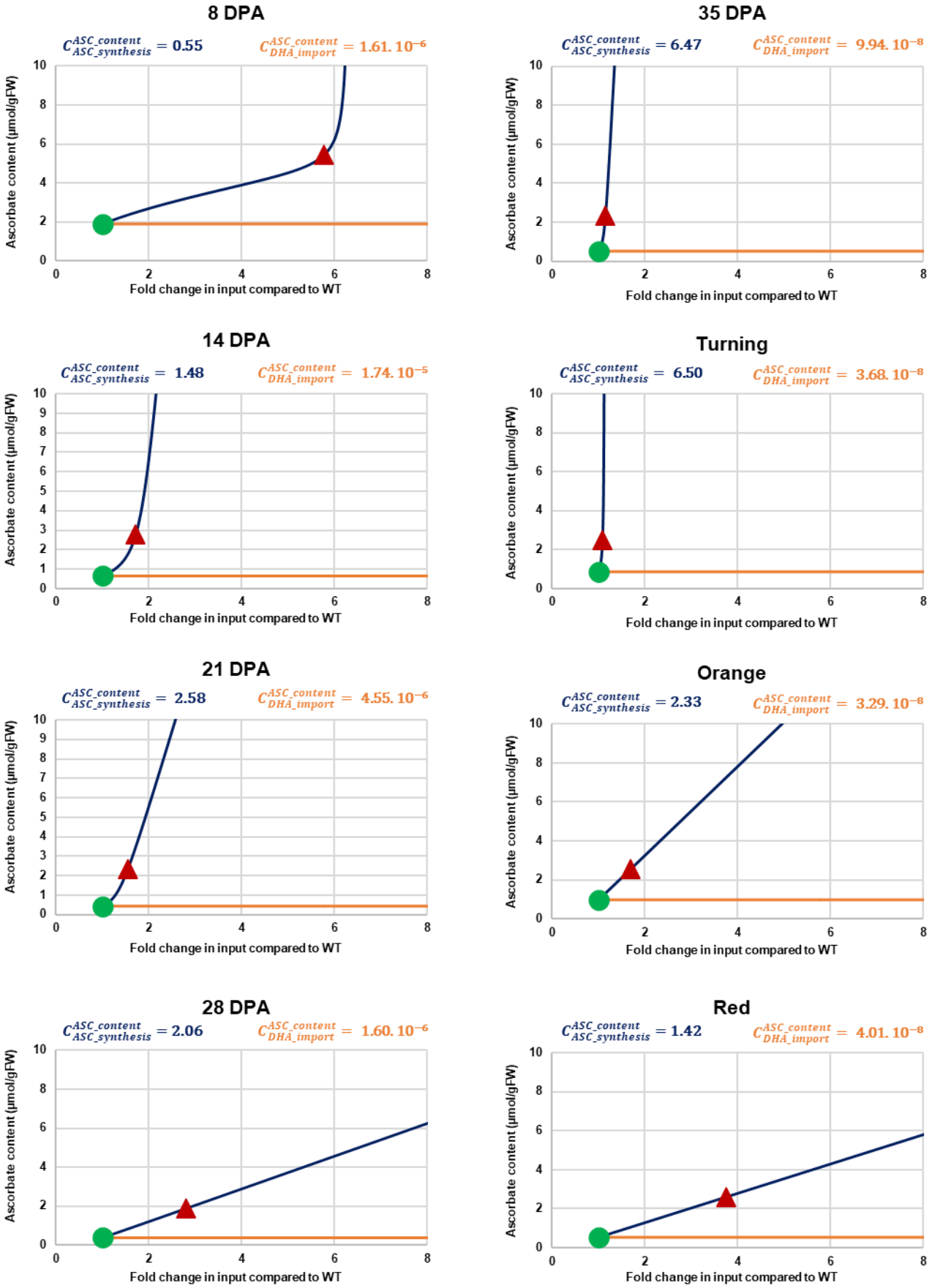

Figure V.4: Effect of an increase in ASC synthesis (blue) or DHA import (orange) on the pericarp ASC content. Green circles represent measured WT values and red triangles, the ascorbate-enriched mutant values. Inserted values represent the control coefficient of the ASC content to changes in ascorbate synthesis or import.

Overall, our *in silico* simulations emphasise that the ASC-enriched phenotype observed in mutant fruits can be reproduced by solely enhancing the ASC synthesis of fruit cells. According to the model, importing DHA from leaves could never achieve this level of ASC. This is congruent with the dispersion observed for these optimised parameters (Supplemental fig V.1) and a previous study reporting that the ASC level in fruit is not influenced by ASC synthesis in leaves (Gautier et al., 2009).

Simultaneously, the ASC oxidation ratio is strongly and negatively sensitive to an increase in ASC synthesis, resulting in an oxidation state of ASC sharply tending towards 0% and appearing buffered at this value which deviated from the experimental data (Supplemental Fig V.7). This could be explained by the oxidised forms of ASC (*e.g.* DHA and MDHA) that are unstable in the cytosol, which in turn could over-reduce the predicted ASC pool when the reduced form increased (Deutsch, 2000). Discrepancies between experimental and predicted values could be explained by the presence of several ASC oxidases present in the apoplast that maintain the apoplastic pool (Pignocchi and Foyer, 2003; Pignocchi et al., 2006; Li et al., 2017a). This pool is mainly oxidised and not considered in the model.

Interestingly, the 8 DPA stage showed a threshold value for ASC synthesis from which the total ASC content augmented exponentially together with a switch of oxidation state (Supplemental Fig V.6). Excessive increase in ASC synthesis led to higher total ascorbate while buffering its oxidation state near 0% and therefore inhibiting the associated signalling pathways required for normal plant development. Interestingly, this is congruent with the failure of this strategy during breeding history (Gest et al., 2013).

To analyse the goodness of fit of the mutant data, the WT model was run at each developmental stage by setting the respective ascorbate synthesis at a value that enabled ascorbate content to be close to that of the mutant (see Supplemental table IV.2 for values). Corresponding predictions regarding redox buffers and ROS were compared. Although differences in GSH content were to be noticed at the beginning and the end of development compared to ASC-enriched fruits (Supplemental Fig V.7). Overall, we noticed no significant differences with the experimental data ($Chi^2 = 9.36$; $p > 0.05$) at the scale of whole fruit development (Figure V.5). The sum of weighted square errors showed a reduced model fitness at the turning stage, mainly due to the slight peak of H_2O_2 observed in WT but missing in the mutant (Figure V.6 and Supplemental Fig V.8). Overall, predicted values obtained with an increased ascorbate synthesis were consistent with both the mutant experimental data and the original model optimised using the wild-type data.

Hence, our two-step modelling approach, *i.e.* a parameters optimisation using the wild-type data only and subsequent cross-validation of the model using independent mutant data, enabled us to investigate the control of major redox buffer content and ROS processing during the whole fruit development. This study thus provides a valuable tool to evaluate redox fluxes in various physiological contexts.

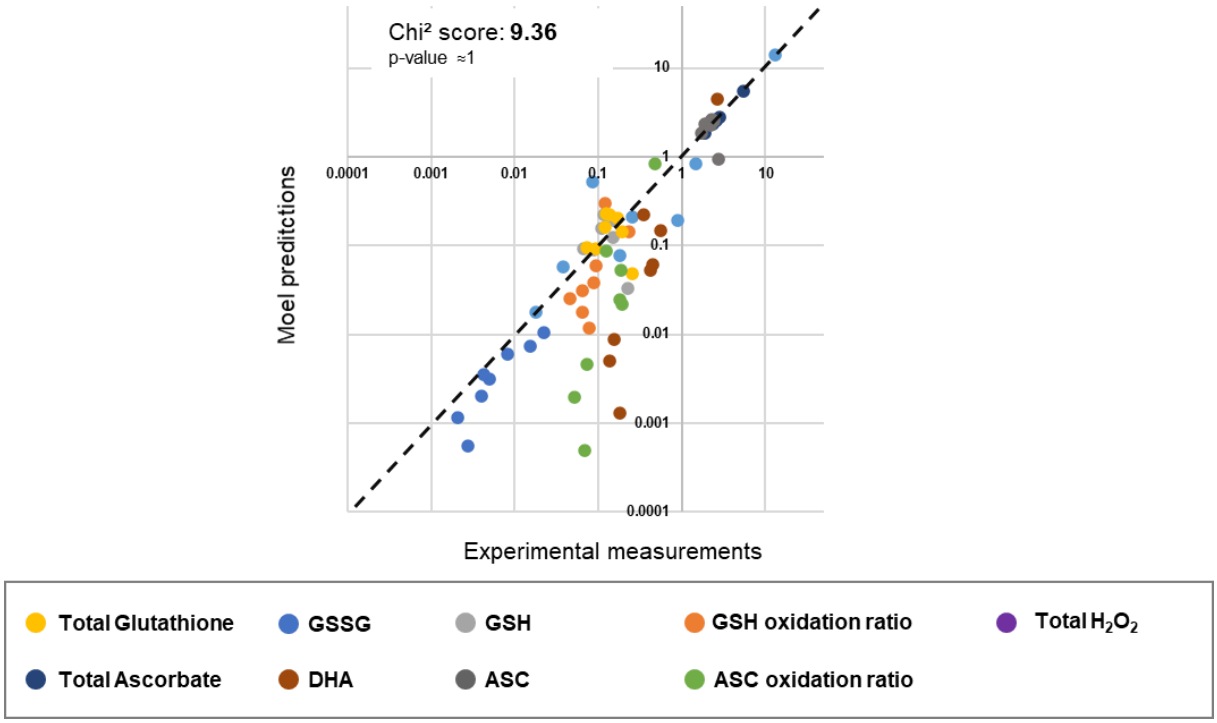

Figure V.5: Comparison between model predictions and experimental measurements performed on ASC enriched mutant. At each developmental stage, the model optimized using WT data was run using the ASC synthesis flux giving the ASC content measured for the mutant as shown in Figure V.4 Diagonal represents 100% match between experiments and predictions.

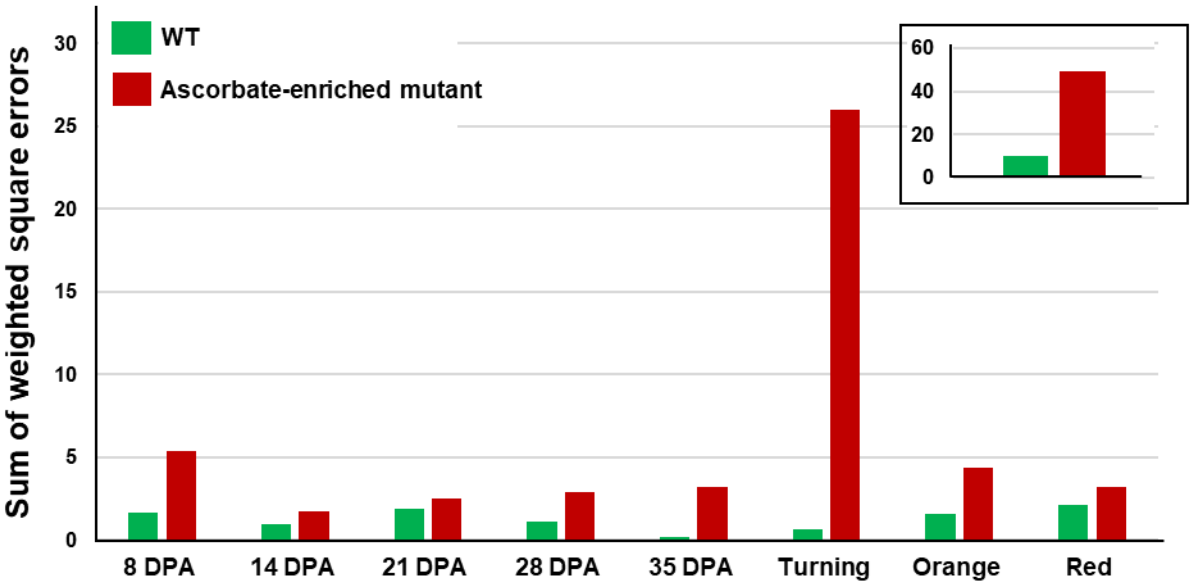

Figure V.6: Sum of weighted square errors calculated from original model (green) or using predicted values from *in silico* ascorbate-enriched mutant (red). Insert shows cumulative sum of squared residuals over all stages.

D. Dynamics of the ASC-GSH cycle during tomato fruit development

Using unidimensional hierarchical clustering analysis (HCA), the comparative analysis combining flux and enzymatic capacity evolution patterns revealed three distinct clusters (Figure V.7). The first cluster included variables involved in green fruit development before decreasing from 35 DPA until the end of development (*e.g.* DHAR, GR and GSH synthesis fluxes, MDHAR capacity and fruit relative growth rate). The second cluster encompassed maximal fluxes and capacities during cell division before rapidly decreasing during cell expansion, most of which rebounded specifically at the turning stage (*e.g.* APX, MDHAR, ASC synthesis, DHA import, DHA degradation and chemical recycling of MDHA fluxes). The last cluster separated clearly and contained only enzymes capacities that were high either during fruit growth (*e.g.* APX and DHAR) or maturation (*e.g.* CAT) (Figure V.7).

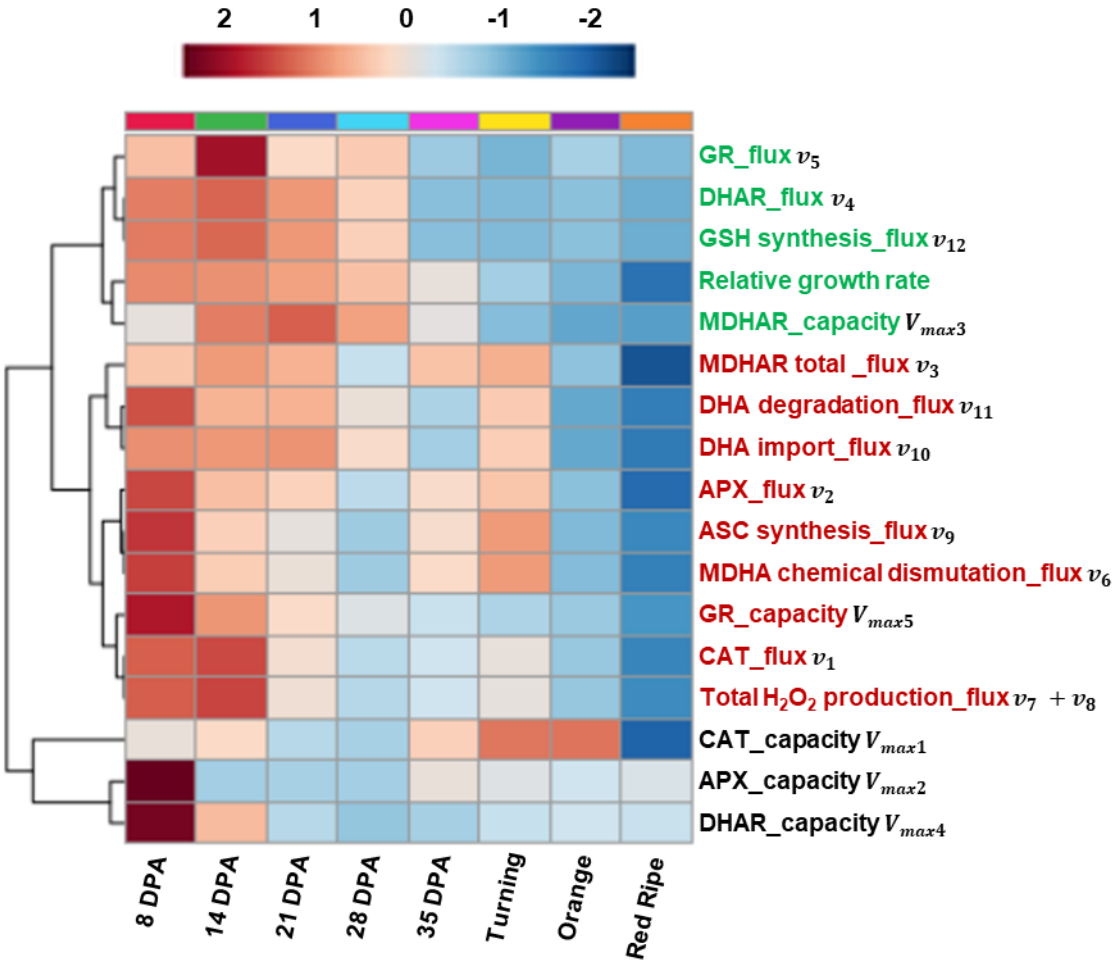

Figure V.7: Unidimensional hierarchical clustering analysis of fluxes and enzymes capacities involved in the ASC-GSH cycle and ROS processing.

It is worth noting that the modelled fluxes did not behave like the corresponding enzyme capacities (V_{max}). Indeed, none of the fluxes was found in the same cluster as their respective capacity. This thus suggests that variations in enzyme capacities, which was measured in optimal assay conditions,

do not reflect their actual *in vivo* activity (Beauvoit et al., 2014; Stitt and Gibon, 2014), at least for redox enzymes. Overall, this HCA suggests that redox metabolism, especially ROS processing and ASC recycling, is mostly represented during the cell division phase and the ripening of tomato fruit.

In the first cluster, the fact that DHAR, GR and GSH input fluxes were separated from total H_2O_2 production, CAT, APX and MDHAR fluxes suggests that ROS processing in tomato fruit is more dependent on ASC recycling through MDHAR activity and NADPH consumption than DHAR activity and GSH consumption. Moreover, MCA analysis of DHAR and GR fluxes (Supplemental Fig V.9) showed that they were mainly controlled by the GSH input and GR itself. This thus indicates that they act as pseudo first-order reactions limited by GSH availability. In addition, these fluxes were only weakly sensitive to the other parameters but were firmly controlled by a disturbance of GSH metabolism. Finally, the presence of the relative fruit growth rate in this cluster suggests that ROS processing and fruit growth exhibit different behaviours.

The second cluster showed a stronger association between ROS production and CAT flux than APX flux, since CAT processes the majority of ROS, especially at the beginning of development (Figure V.8). This agrees with previous statements indicating that fruit photosynthesis is negligible (Lytovchenko et al., 2011) and that majority of ROS would come from the photorespiratory pathway associated with CAT (Hagemann et al., 2016). However, the secondary antioxidant metabolites are not included in our model and their participation in ROS processing is attributed to CAT due to its high catalytic capacity. Nonetheless, APX and MDHAR fluxes displayed a strong increase at the turning stage together with a restart of ASC synthesis, suggesting an active ASC metabolism associated with a fine-tuning of its redox state at the onset of ripening. Remarkably, this further indicates that the ASC-GSH cycle is mainly driven by the APX-MDHAR duo than by the APX-DHAR-GR trio during tomato fruit development.

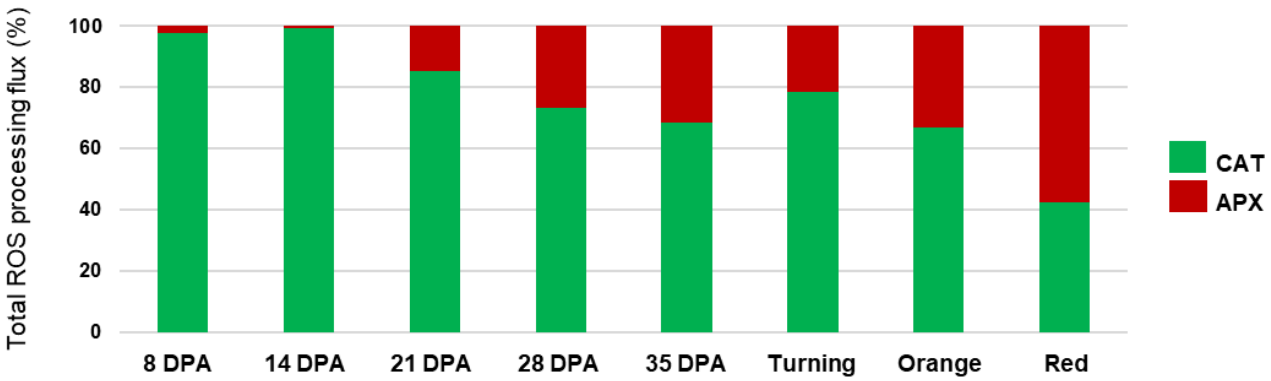

Figure V.8: Contribution of catalase (green) and ascorbate peroxidase (red) to the total ROS processing during tomato fruit development.

I. *ASC-GSH cycle fluxes are mainly limited by reduced ASC supply during fruit cell division*

Metabolic control analysis (MCA) was performed to analyse the regulation of the enzymes involved in cluster 2 (*i.e.* CAT, APX and MDHAR), thus identifying three distinct patterns during the development. Firstly, for the 8 DPA stage (*i.e.* during the cell division phase), APX flux was positively controlled mainly by the ASC synthesis and, to a lesser extent, by MDHAR (Figure V.9). This suggests a limitation of APX by the supply in reduced ASC (Supplemental fig V.10). At the same time, CAT flux was only influenced by ROS production, and MDHAR flux was positively controlled by itself but not by APX or ASC synthesis (Figure V.9), thus reflecting a limitation of the MDHAR activity by NADH and NADPH supply rather than MDHA availability (Supplemental fig V.11). Therefore, during fruit cell division, ROS production exceeds the capacity of APX flux, which is limited by the supply of reduced ASC, leading to H_2O_2 accumulation observed at this stage (Supplemental fig V.4).

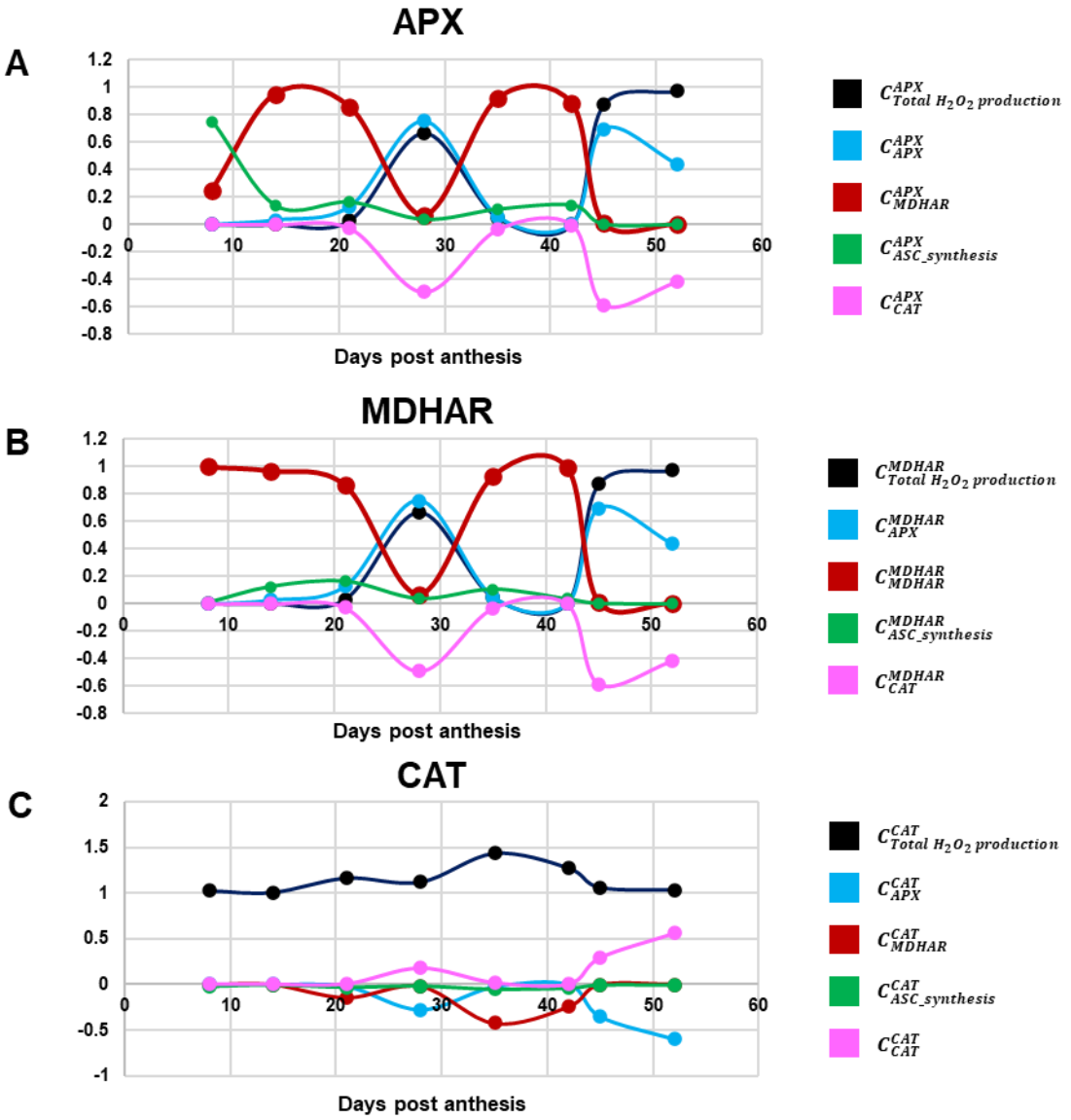

Figure V.9: Sensitivity coefficient of APX (A), MDHAR (B) and CAT (C) to various enzyme activities during fruit development. Solid lines refer to discontinuous data.

Furthermore, the reduced availability of reducing power (NAD(P)H) limited the flux of MDHAR, thus inducing a control of the ASC pool mainly by the ASC synthesis flux. In addition, the limitation of MDHAR flux by the NAD(P)H pool led to an accumulation of MDHA and thus to a higher ASC oxidation ratio, as observed for this stage (Supplemental fig V.3).

Overall, during the cell division stage, the activity of the ASC-GSH cycle mainly relies on central metabolism (ROS production and NAD(P)H supply) and ASC synthesis pathways.

II. *The availability of pyridine nucleotide modulates ASC and GSH redox states through MDHAR activity during fruit cell elongation and at the onset of ripening*

Then, for 14 DPA and 21 DPA (*i.e.* beginning of cell expansion), the APX flux was no longer controlled by ASC synthesis. However, it became strongly dependent on MDHAR activity, suggesting that APX still depended on reduced ASC supply. As for 8 DPA, APX is not under the control of ROS production, offering saturating ROS levels for this enzyme. Furthermore, MDHAR was still controlled by NAD(P)H supply (Supplemental fig V.11), further indicating that the ASC-GSH cycle was mainly regulated by NAD(P)H content when H_2O_2 provision was high enough to saturate APX. To a greater extent, NAD(P)H content strongly regulated the reduced ASC content and its oxidation ratio, as shown by the sensitivity coefficient (Figure V.10A).

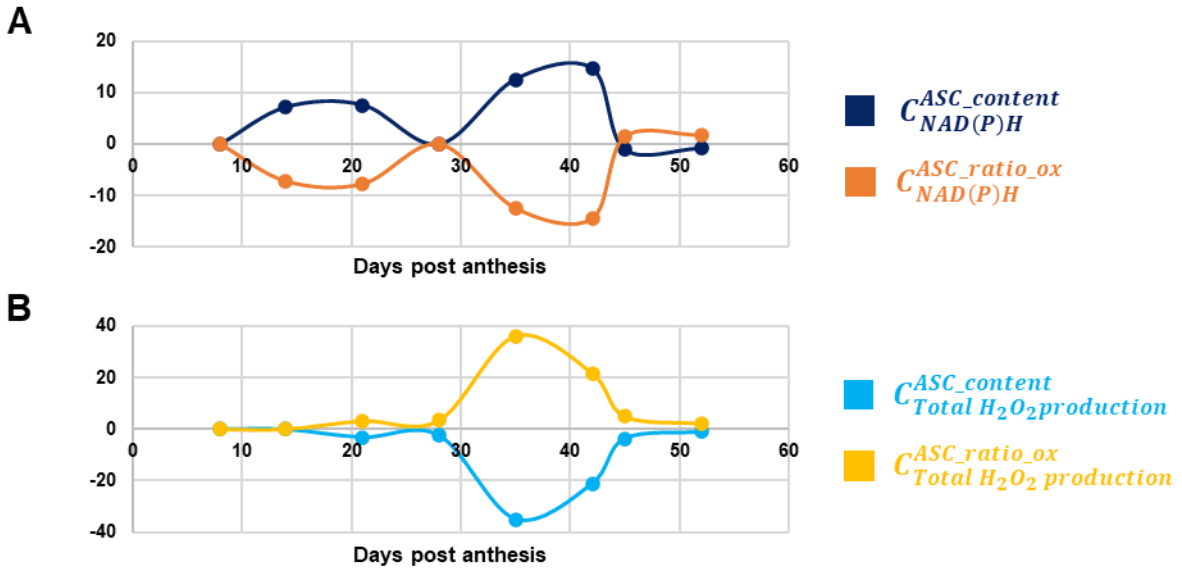

Figure V.10: Sensitivity coefficient of ASC total content (blue) and ASC oxidation ratio (orange) to the total reducing power (NAD(P)H) **(A)** and total ROS production flux **(B)** during fruit development. Solid lines refer to discontinuous data.

In other words, a perturbation of central metabolism and thus in NAD(P)H content could strongly impact the ASC oxidation ratio. Overall, during cell expansion, APX is saturated by H_2O_2 while its supply of reduced ASC was controlled by the MDHAR activity and NAD(P)H provision. The reducing power available will have the strongest impact on ASC oxidation ratio and thus on potential redox signalling. This suggests a role for the oxidative pentose phosphate pathway and thus in lipid metabolism for the regeneration of reducing power. Interestingly, this behaviour was also found for 35 DPA and Turning stages (*i.e.* onset of maturation) with the addition of a high influence of total H_2O_2 production flux on ASC content and oxidation ratio (Figure V.10B). During these stages, both NAD(P)H content and ROS production flux strongly modulated the ASC oxidation ratio. Thus, the ASC oxidation ratio is finely controlled by central metabolism during the transition from cell expansion to ripening.

III. Low metabolic activity during late cell elongation results in over-reduced ASC

Finally, the decrease in the total ROS production flux at 28 DPA, orange and red stages induced a switch in the control of APX and MDHAR. Indeed, the APX flux became positively regulated by the total ROS production while MDHAR and ASC synthesis fluxes no longer impacted it. Moreover, CAT negatively influenced the APX flux indicating a competition of these enzymes for H_2O_2, which is the limiting substrate at this stage. Here, reducing power (*i.e.* NAD(P)H) and reduced ASC supplies were in excess compared to ROS production, inducing a control of the ASC-GSH cycle through H_2O_2 supply and APX activity. Therefore, the strong decrease in H_2O_2 production at those stages compared to 21 DPA and Turning (Supplemental fig V.4) resulted in a shift in the behaviour of the ASC-GSH cycle in which the APX became the controlling step of the cycle itself restricted by the H_2O_2 production (Figure V.9A).

Simultaneously, ASC content and ASC oxidation ratio loss their sensitivity to both NAD(P)H content and total ROS production (Figure V.10), showing that the ASC-GSH cycle will ensure the maintenance of the ASC pool predominantly reduced for the stages with very low metabolic activity. This further highlights that the ASC oxidation ratio is a key component of redox signalling that needs to be maintained in a reduced state for normal fruit development.

E. Top-down modelling approach to identify a metabolic marker allowing accurate flux predictions

Top down modelling strategies, such as general multilinear modelling approach (GLMs), allows for investigating the predictive correlation between metabolic features while identifying the best predictive variables for a specific response (Luna et al., 2020; Roch et al., 2020). As mentioned before, enzyme capacities are not representative of their metabolic fluxes thus giving biased conclusions based only on their time course evolution (Figure V.7). Nevertheless, from one stage to another, the order of magnitude of some enzyme capacities may strongly control the whole network functioning (Figure V.9). Consequently, GLMs were used to identify potential metabolic features that represented relevant markers for flux predictions and that could be used for future, straight-forward biochemical redox phenotyping (Ma et al., 2013). To this end, we exploited a data set of 22 variables, enzyme capacities, total protein, ROS and major redox buffer contents as well as their redox state and total antioxidant capacity. Globally, apart from GR, all the fluxes of the enzymes involved in the ASC-GSH cycle showed a high Rsquare of the GLMs predictions (Figure V.11), thus indicating that dynamic redox fluxes could be predicted from steady-state metabolic data. Next, variables were filtered based on their occurrence in the models (>50%) resulting in similar flux predictions (Figure V.11), with reduced dispersion, particularly for the 8 DPA stage. (Supplemental fig V.12 to V.15). Additionally, permutated models were used to statistically cross-validate the predictions and, showed the relevance of the variables used for fluxes predictions, according to Tuckey's test ($p < 0.05$) (Figure V.11). Finally, for APX, CAT, MDHAR and DHAR, filtering by the variable's occurrence pointed out the total protein content, MDHAR capacity, GSSG content and both ASC and GSH oxidation ratio as best predictors (Supplemental fig V.12 to V.16). However, their contribution differed according to the targeted flux and no "universal" metabolic marker representative for ASC-GSH cycle fluxes could be identified. Nonetheless, this is consistent with previous reports which emphasise GSSG and GSH redox state as reliable markers of oxidative stress, and to a greater extent of redox metabolism (Kranner et al., 2006; Noctor et al., 2012). Altogether, this reinforces the role of these redox states as integral regulators of the ASC-GSH cycle and thus in the control of the redox balance.

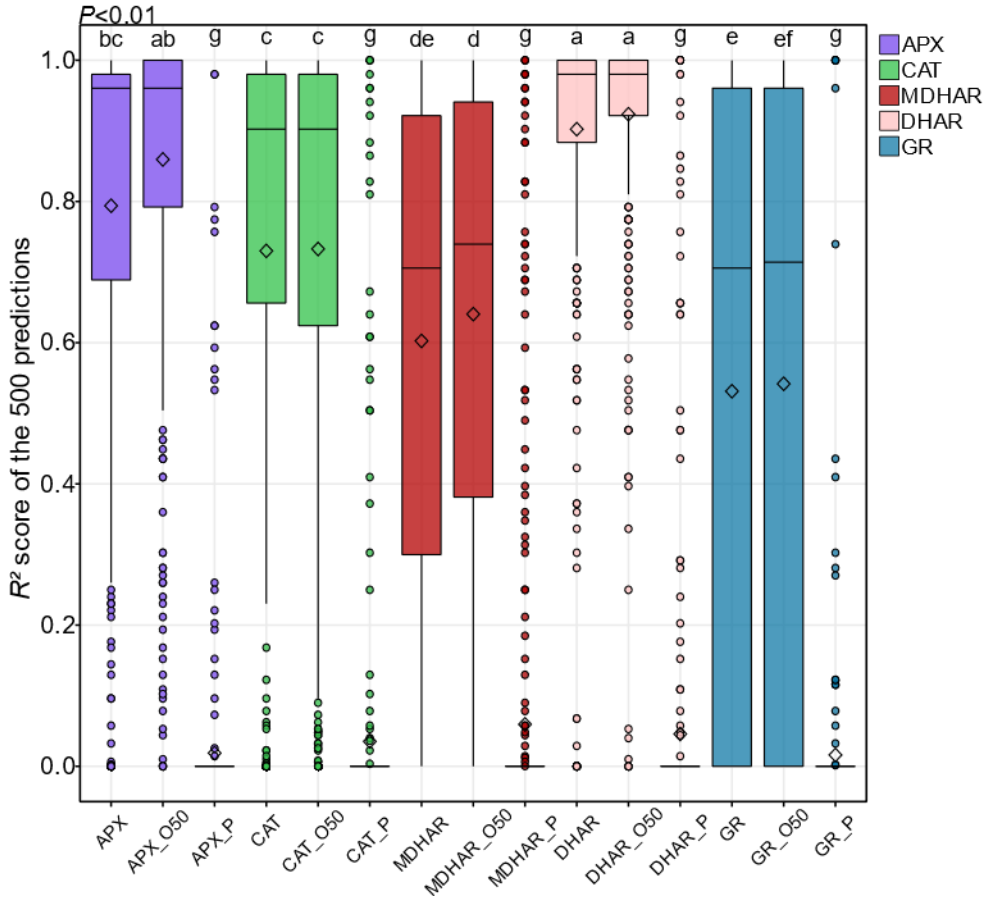

Figure V.11: Rsquare distribution of the GLMs predictions for fluxes involved in ASC-GSH cycle. O50 indicates that models have been performed by selecting the variables occurring in more than 50% of the models. P indicates the models run using random permutations.

CONCLUSION

In conclusion, the model demonstrates that (i) ROS production must be compartmentalised to allow H_2O_2 accumulation and (ii) ASC synthesis modulates the dynamics of the ASC-GSH cycle during cell division while allowing cross-validation by mimicking the ASC-enriched mutant phenotype. Besides, this study emphasises the role of MDHAR and APX as the two controlling enzymes of the ASC-GSH cycle fluxes during fruit development, which are sensitive to the availability of reduced ASC, H_2O_2 and NAD(P)H. Finally, ASC and more importantly GSH redox states appeared as the best reliable markers to estimate the activity of the ASC-GSH cycle.

SUPPLEMENTAL FIGURES

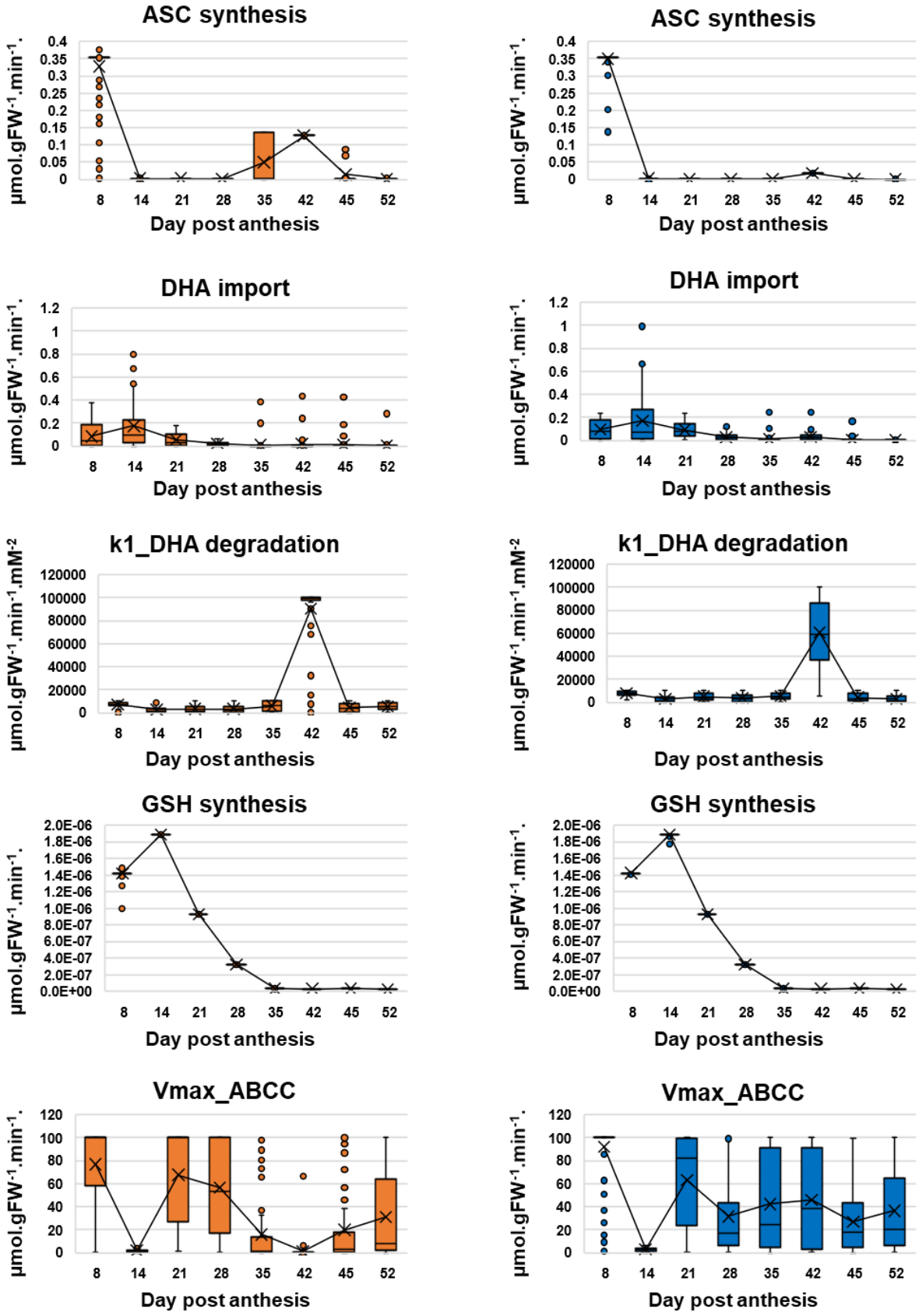

Supplemental fig V.1: Parameter estimated in the model without (left, orange) or with (right, blue) NADPH oxidase. k1_DHA degradation represent the ratio of V_{max}/K_m (µmol.gFW^{-1}.min^{-1}.**mM^{-2}**) and other parameter represent direct flux (µmol.gFW^{-1}.min^{-1}). Boxplot represent best 100 scoring values obtained through optimization procedure. Solid lines refer to discontinuous data.

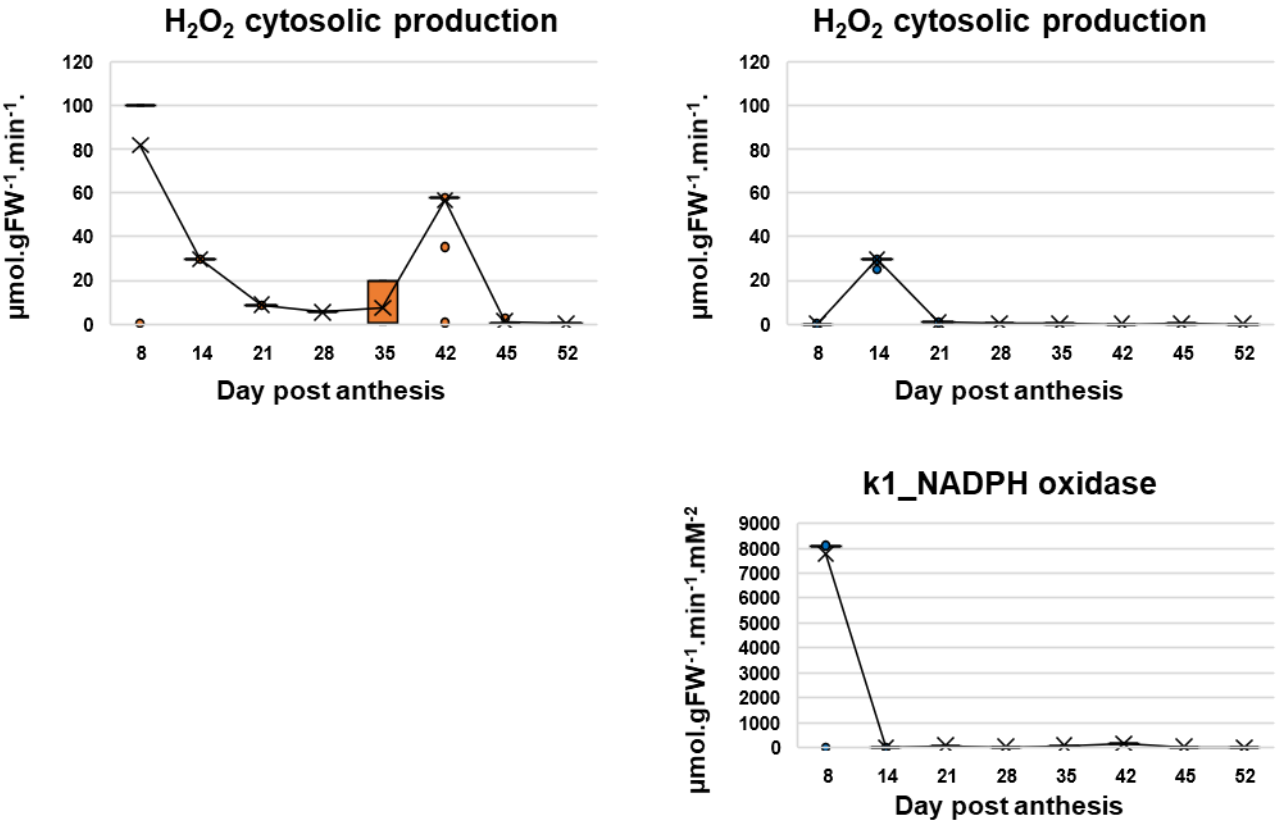

Supplemental fig V.2: Parameter estimated in the model without (left) or with (right) NADPH oxidase. k1_NADPH oxidase represent the ratio of V_{max}/K_m (µmol.gFW^{-1}.min^{-1}.**mM**$^{-2}$) and other parameter represent direct flux (µmol.gFW^{-1}.min^{-1}). Boxplot represent best 100 scoring values obtained through optimization procedure; median are represented by black crosses. Solid lines refer to discontinuous data.

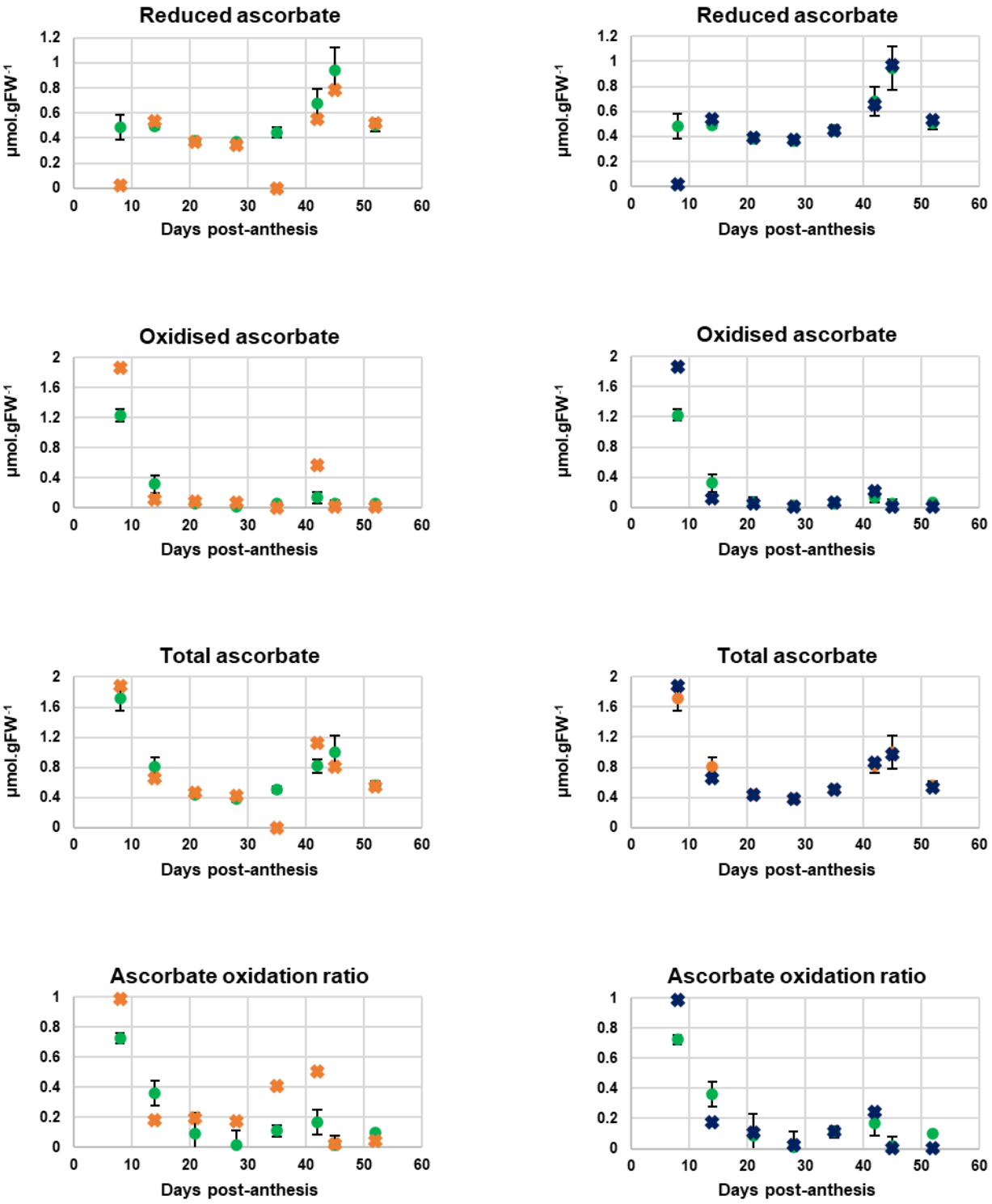

<u>Supplemental fig V.3:</u> **Experimental WT (green) and predicted values for ascorbate** using median parameters from optimization procedure without (orange, left) and with NADPH oxidase (blue, right).

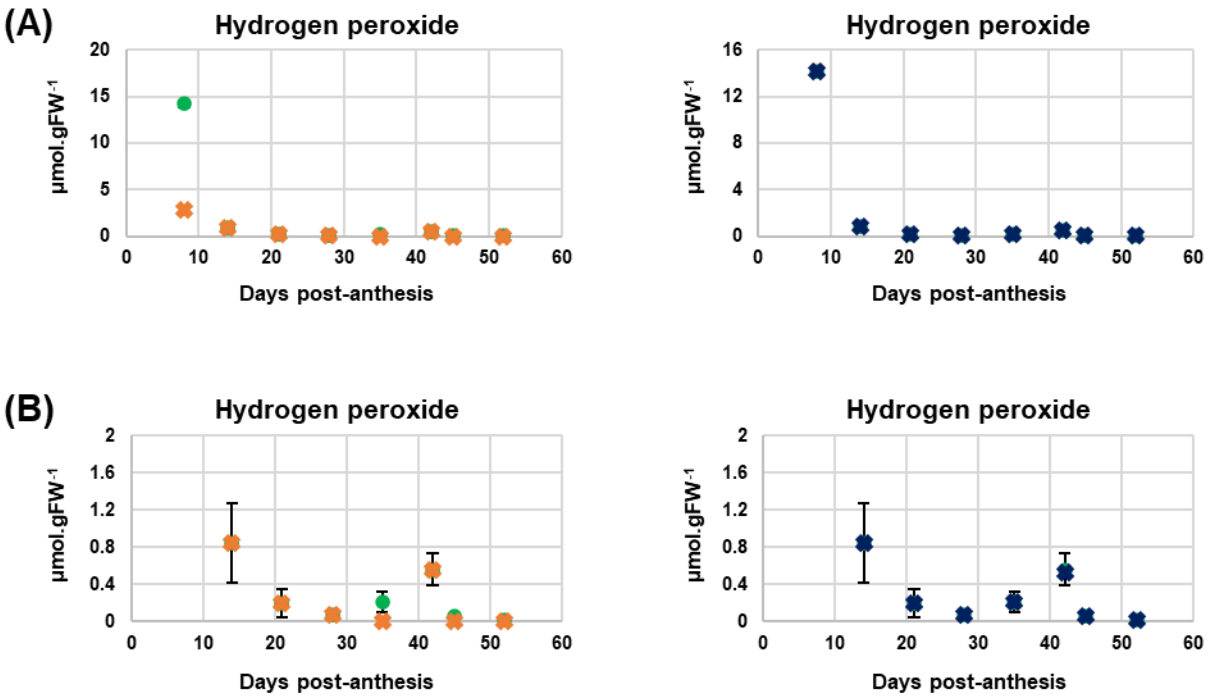

<u>Supplemental fig V.4:</u> **Experimental WT (green) and predicted values for H_2O_2** using median parameters from optimization procedure without (orange, left) and with NADPH oxidase (blue, right) **(A)**. Bottom panel have been scaled to allow visualization of differences during the end of development **(B)**.

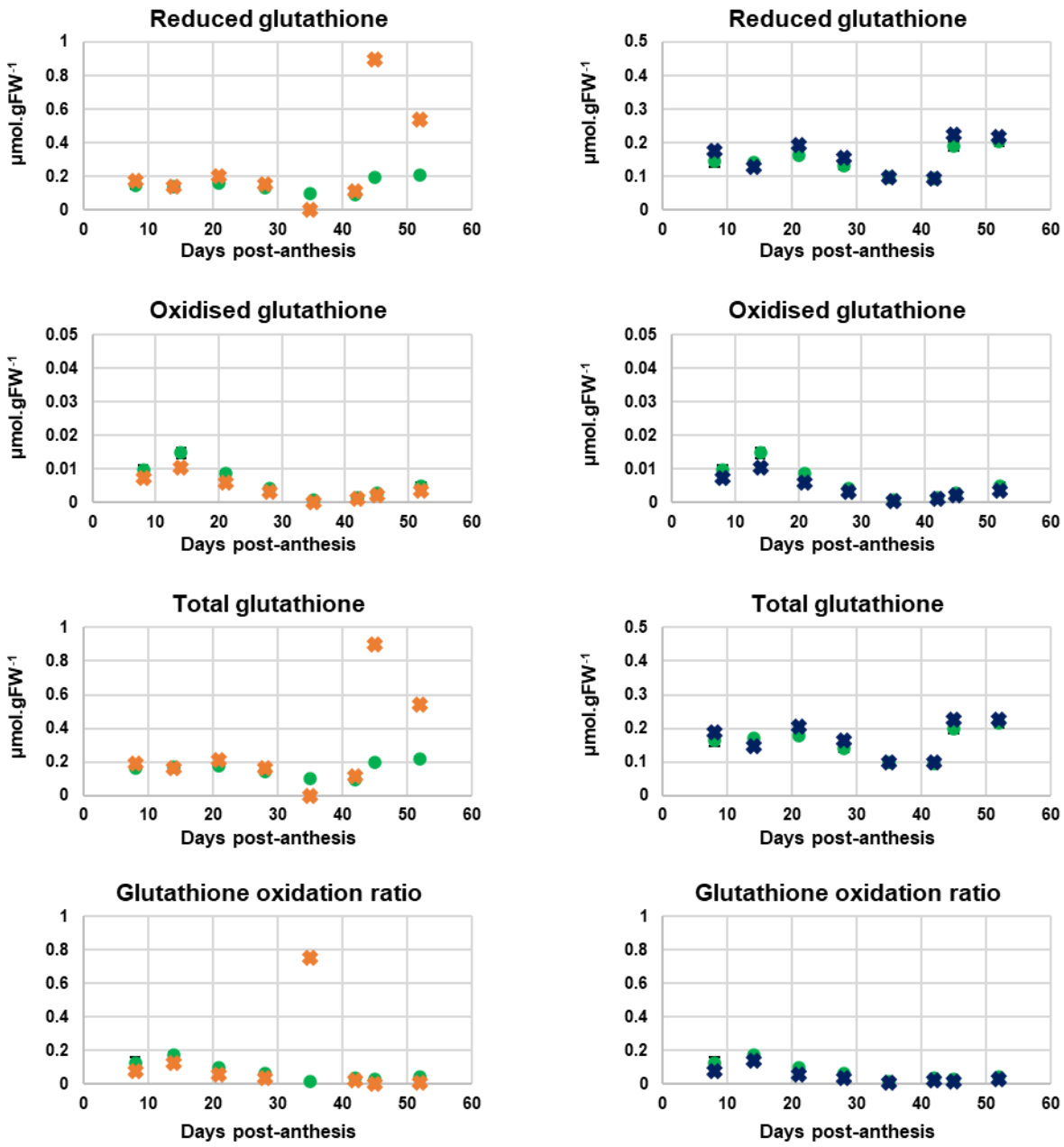

<u>Supplemental fig V.5:</u> **Experimental WT (green) and predicted values for glutathione** using median parameters from optimization procedure without (orange, left) and with NADPH oxidase (blue, right).

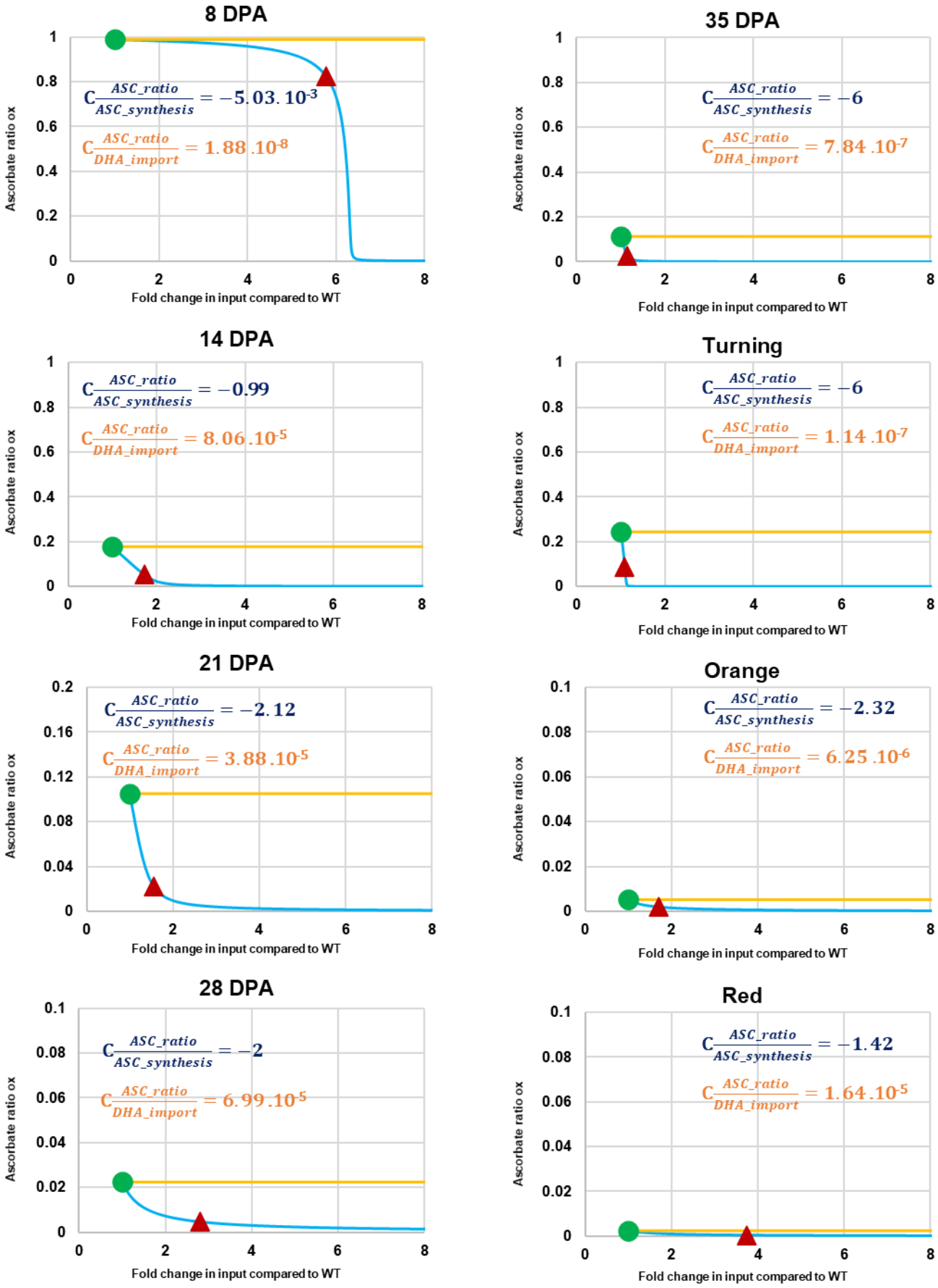

Supplemental fig V.6: *In silico* increase of ASC synthesis (blue) or DHA import (orange) and associated ASC oxidation ratio. Green dot represent predicted WT values and red triangle represent ascorbate-enriched mutant predicted values.

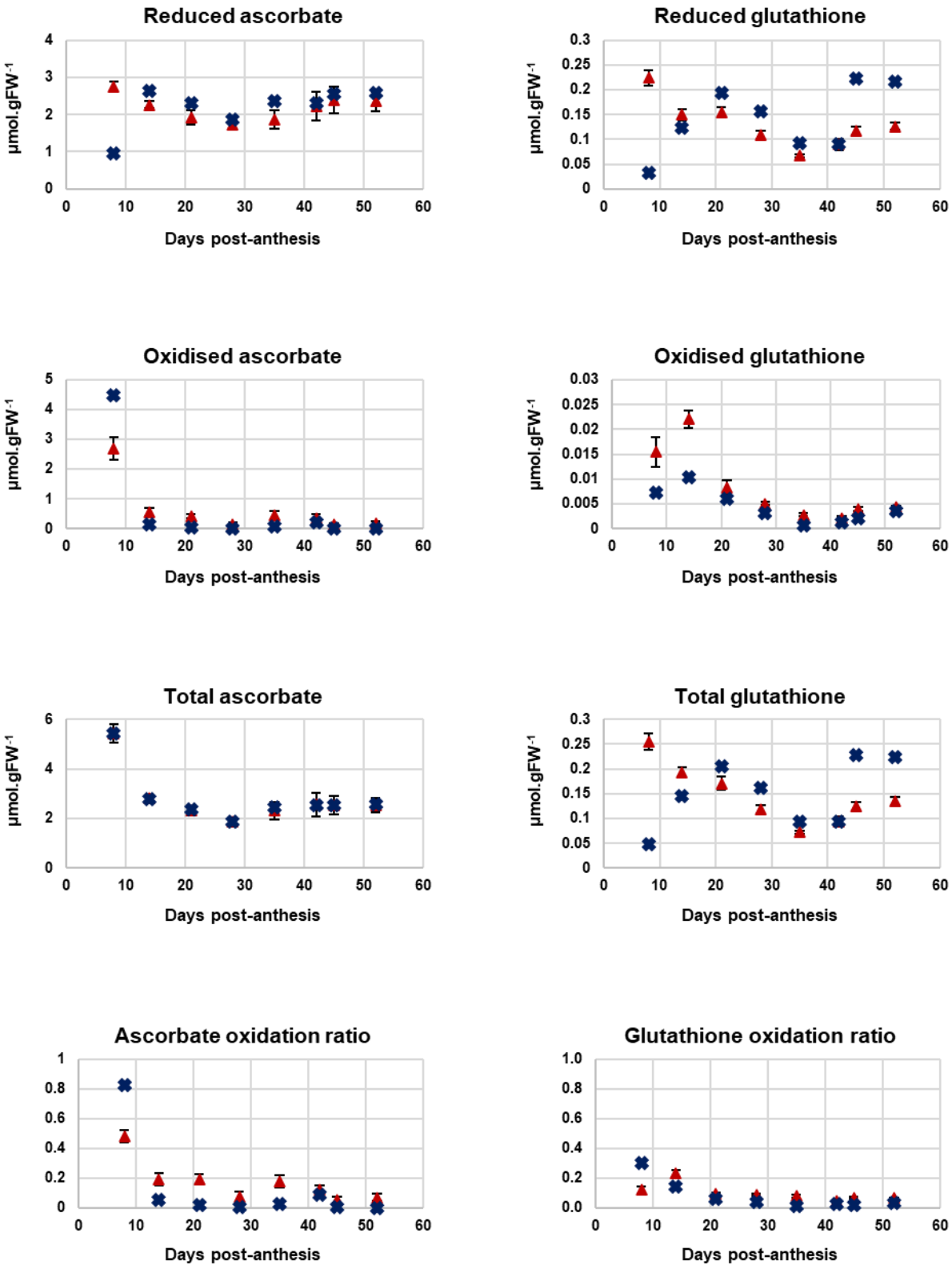

Supplemental fig V.7: **Experimental mutant (red) and predicted values (blue) for ascorbate (left) and glutathione (right)** using median parameter from optimization procedure and after increase ascorbate synthesis.

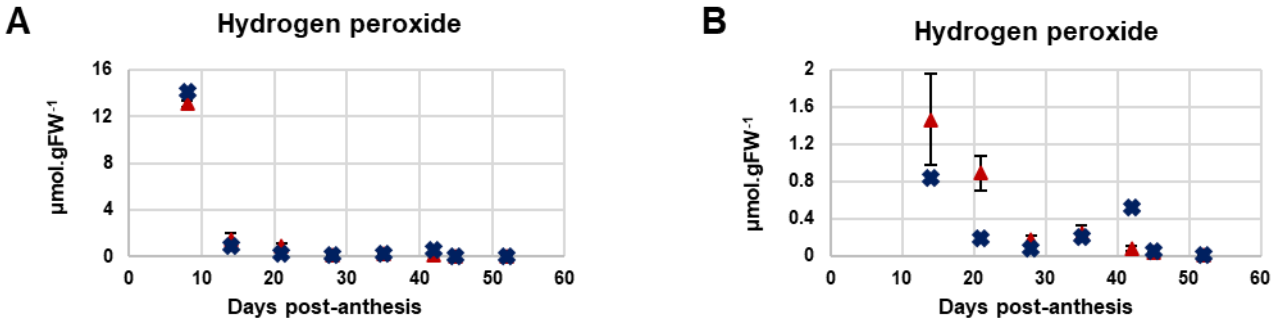

Supplemental fig V.8: **Experimental mutant (red) and predicted values (blue) for H_2O_2** using median parameter from optimization procedure and after increase ascorbate synthesis **(A)**. Same data but scaled-up **(B).**

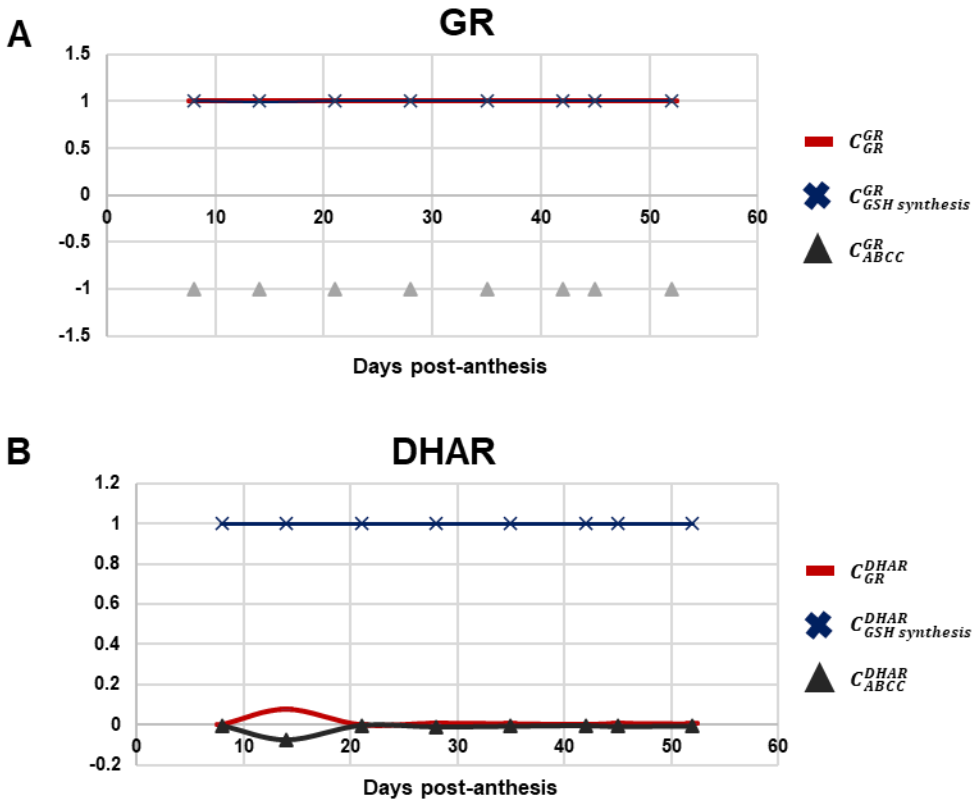

Supplemental fig V.9: Evolution of response coefficient for GR **(A)** and DHAR **(B)** to GSH-related fluxes during fruit development. Solid lines refer to discontinuous data.

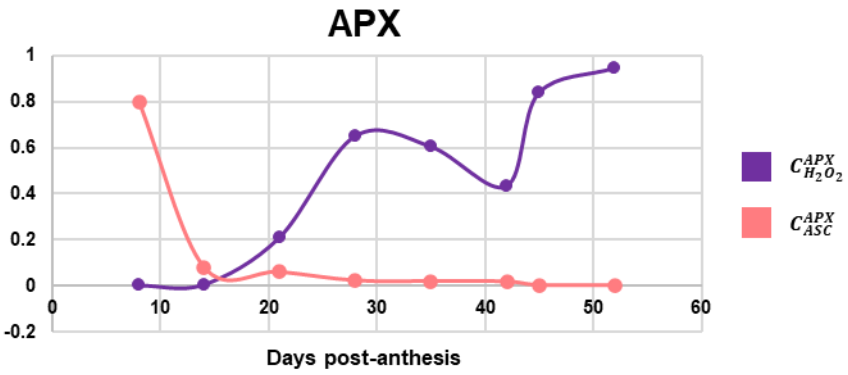

<u>Supplemental fig V.10:</u> **Sensitivity coefficient of APX flux to variations in substrate concentrations during fruit development.** Solid lines refer to discontinuous data.

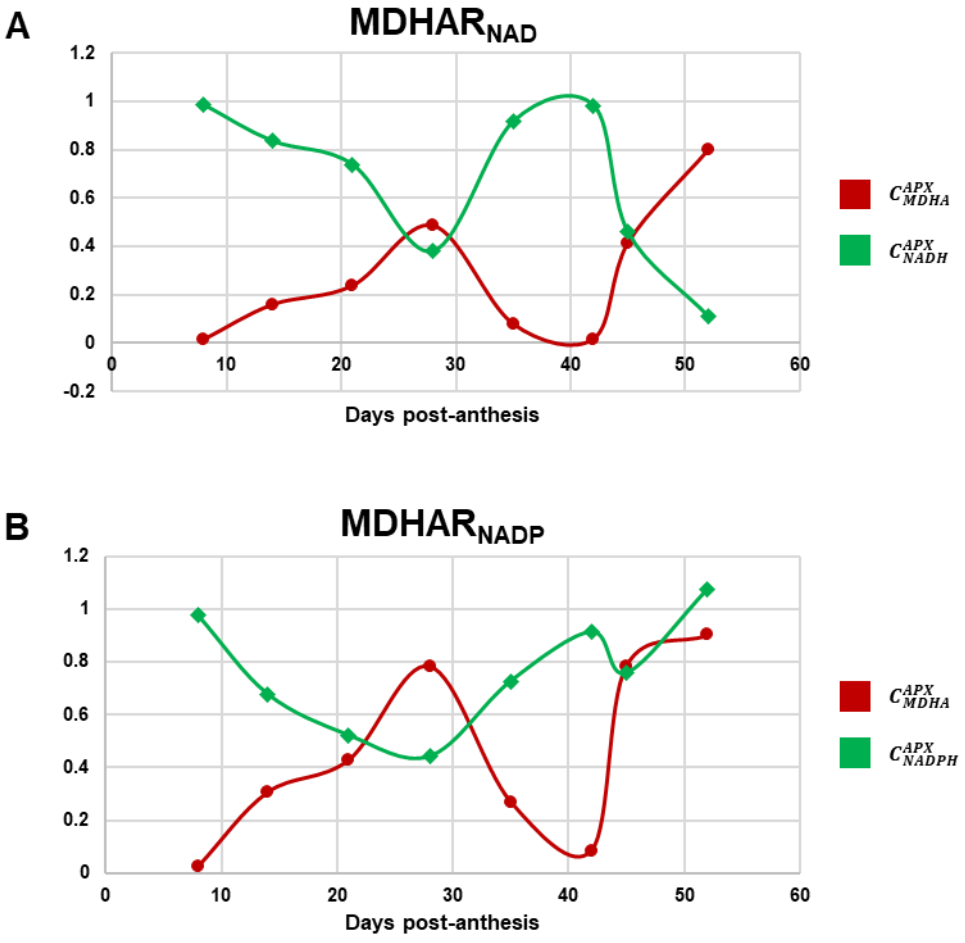

<u>Supplemental fig V.11:</u> **Sensitivity coefficient of MDHAR NAD (A) or NADP-dependent (B) to variations in substrate concentrations during fruit development.** Solid lines refer to discontinuous

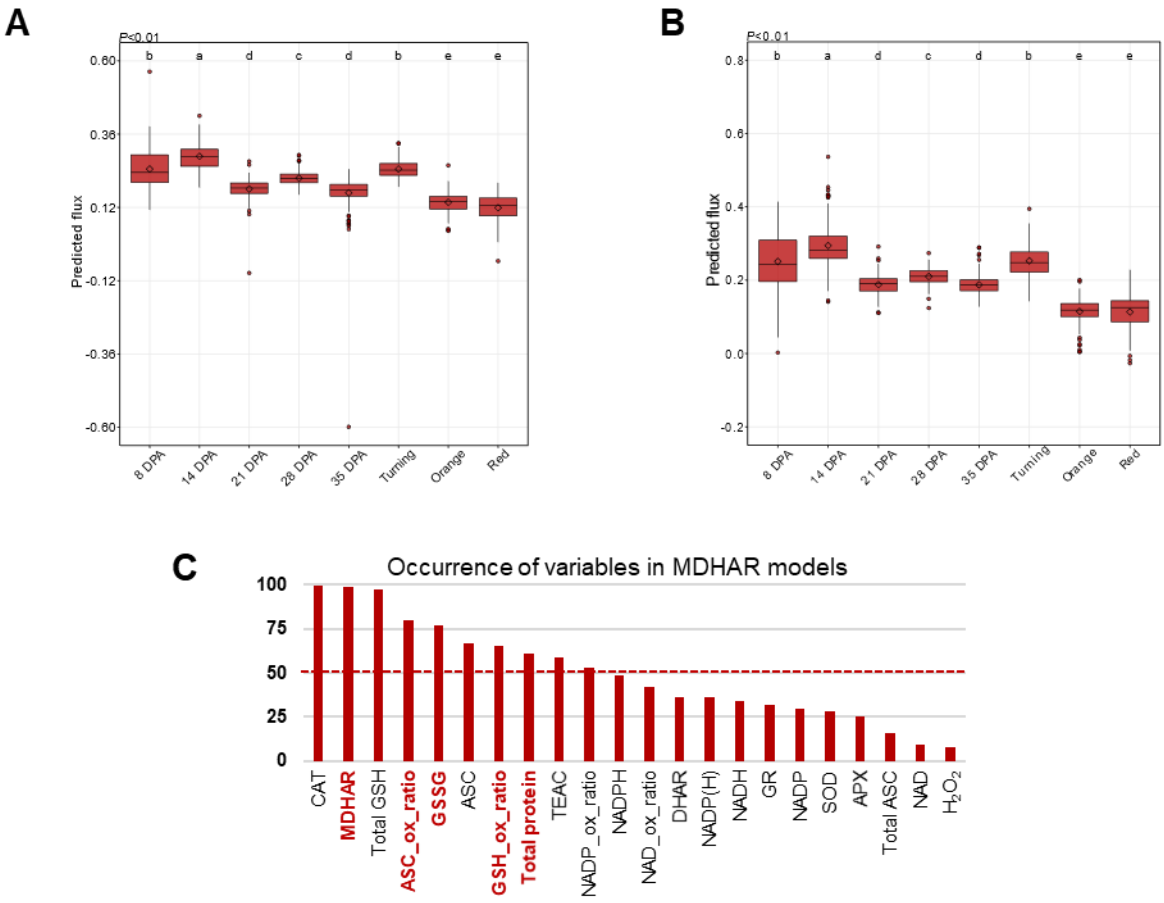

Supplemental fig V.12: GLMs predictions for MDHAR flux using all **(A)** or variables that occur in more than 50% of the model **(B)**. Occurrence of the metabolic features in GLMs **(C)**.

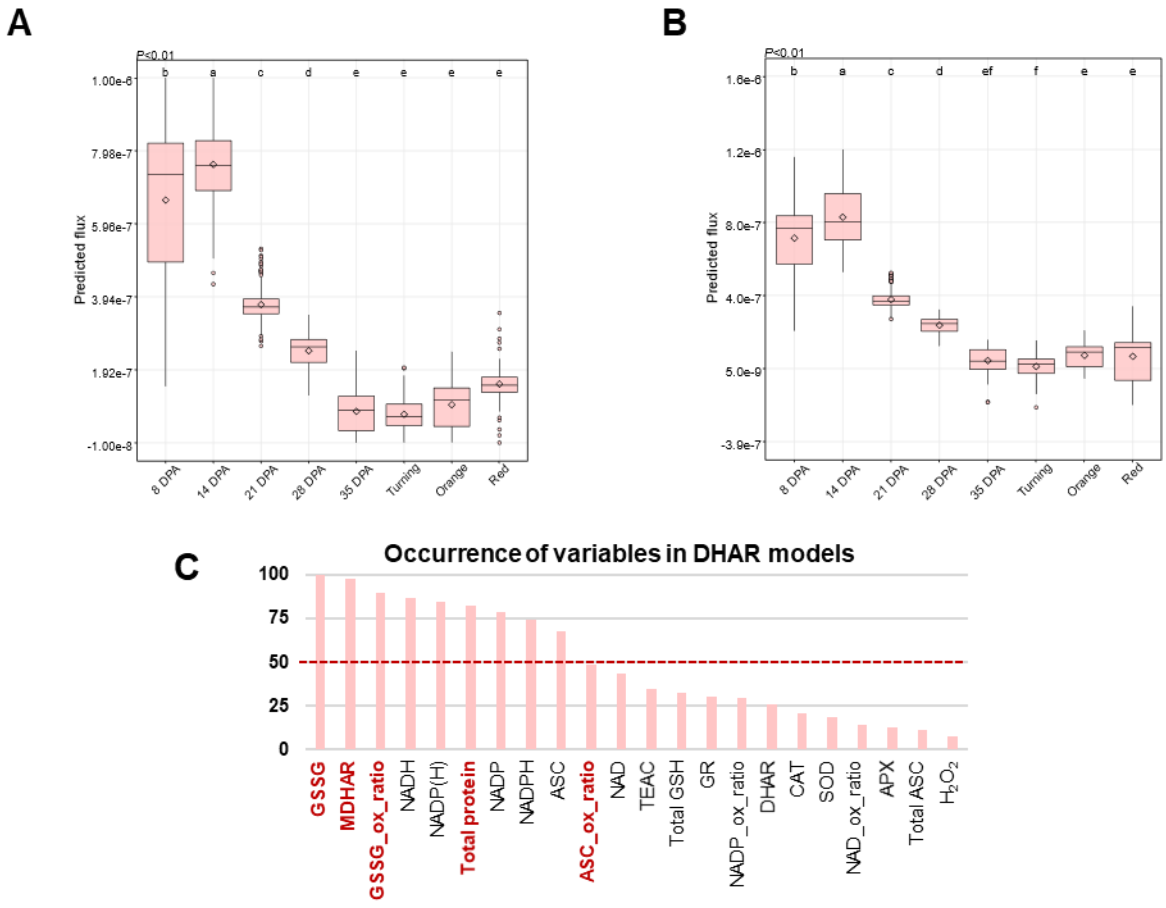

<u>Supplemental fig V.13:</u> **GLMs predictions for DHAR flux** using all **(A)** or variables that occur in more than 50% of the model **(B)**. Occurrence of the metabolic features in GLMs **(C)**.

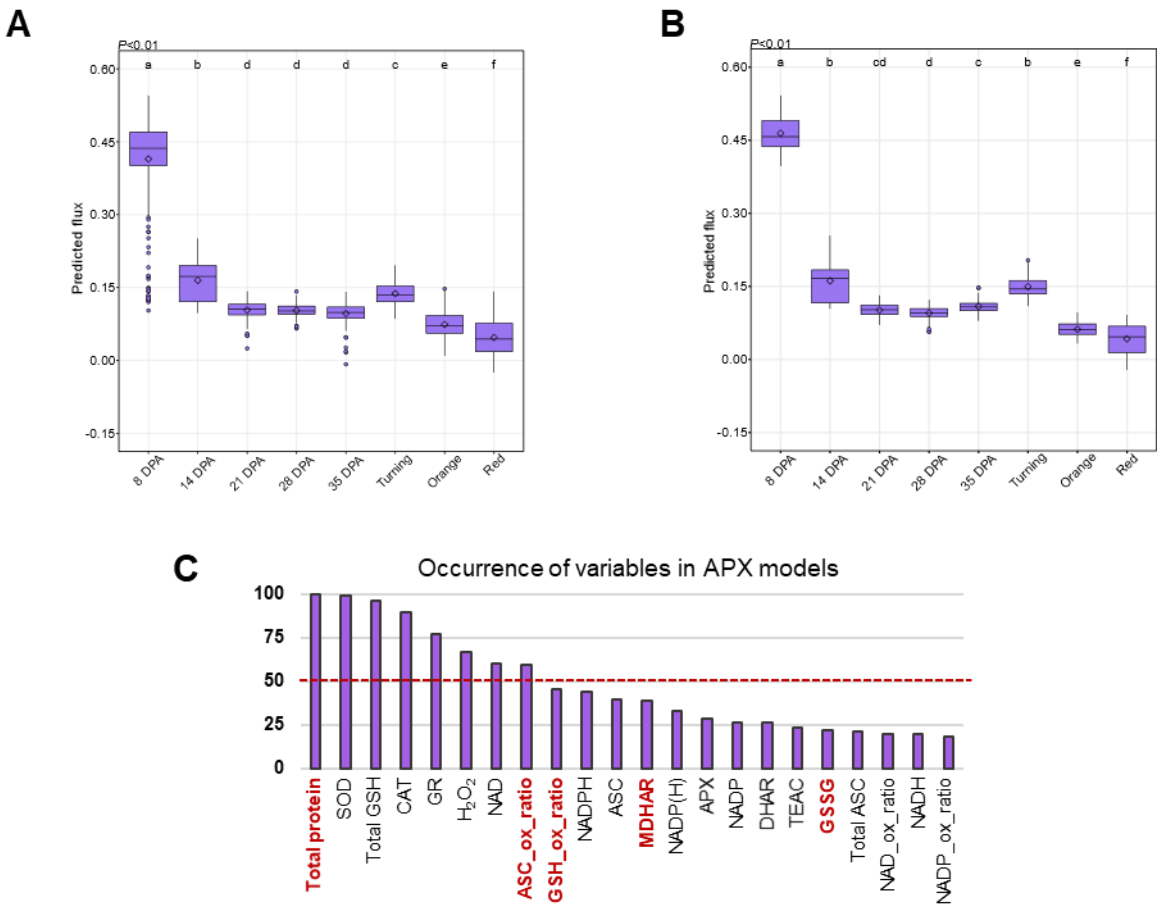

Supplemental fig V.14: GLMs predictions for APX flux using all **(A)** or variables that occur in more than 50% of the model **(B)**. Occurrence of the metabolic features in GLMs **(C)**.

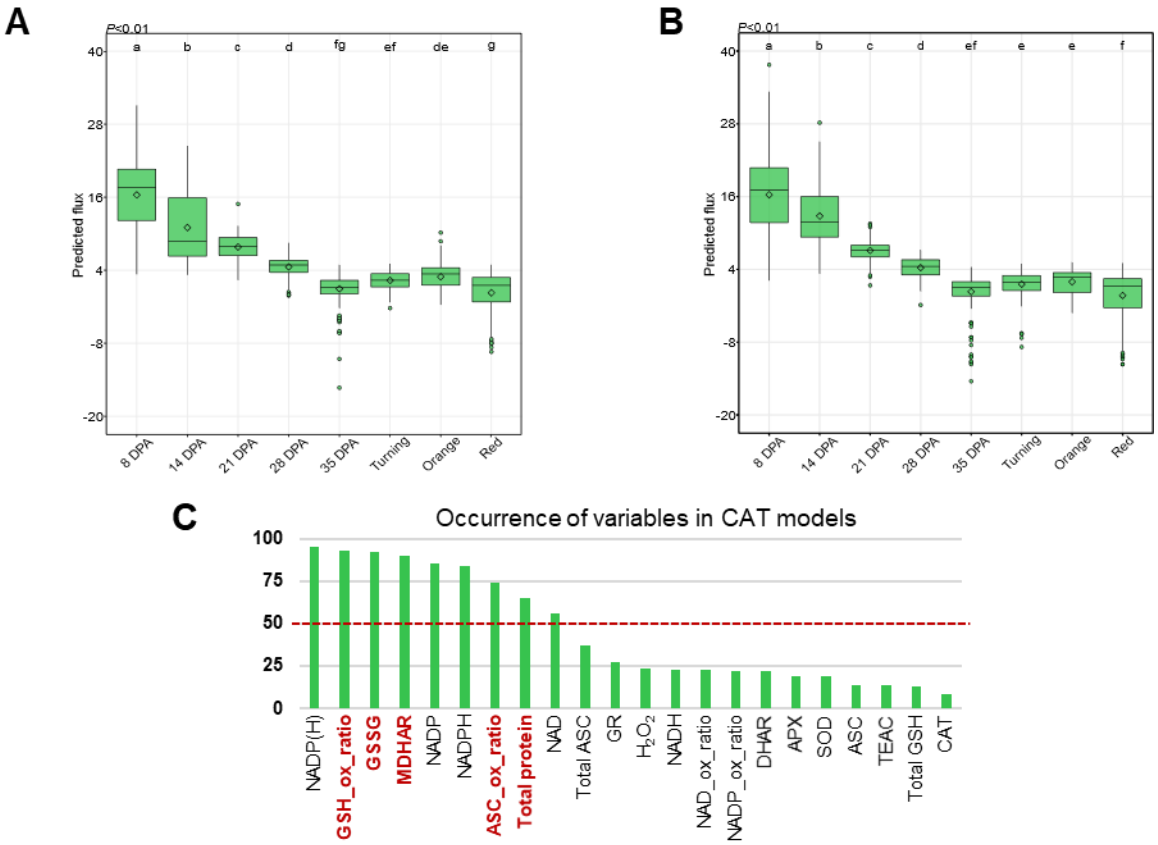

Supplemental fig V.15: GLMs predictions for CAT flux using all **(A)** or variables that occur in more than 50% of the model **(B)**. Occurrence of the metabolic features in GLMs **(C)**.

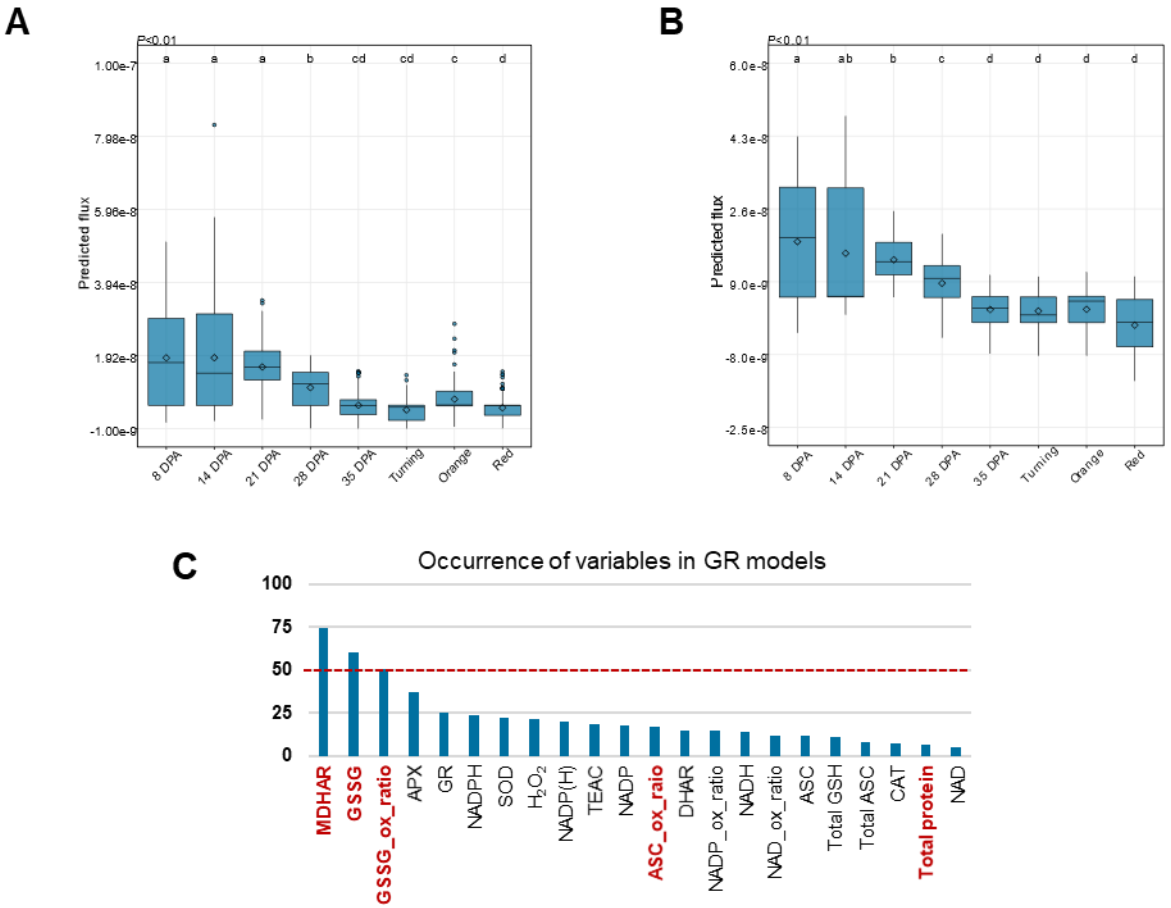

Supplemental fig V.16: GLMs predictions for GR flux using all **(A)** or variables that occur in more than 50% of the model **(B)**. Occurrence of the metabolic features in GLMs **(C)**.

For supplemental tables, please follow this link: https://drive.google.com/drive/folders/1N5ScrVfjt5W_XBUcp131hl5qAfE9k8iy?usp=sharing until the publication if these results.

CONCLUSION AND PERSPECTIVES

A. General discussion and conclusion

This PhD work aimed to provide a quantitative description of the core redox metabolism, especially the ascorbate-glutathione cycle, during tomato fruit development. Gathering such data, which are sparse in fruit science, is a first step in depicting the roles of redox metabolism in fruit development. In fruit tissues, redox metabolism has rarely been evaluated in a developmental context, although concepts from circadian clock studies in leaves remain valuable resources (Valero et al., 2015; Foyer, 2018; Noctor et al., 2018).

Here, we combined transcriptomic, proteomic, and metabolomic analyses using statistical and modelling approaches to investigate core redox metabolism through the ASC-GSH cycle during tomato fruit development. First, a study focused on pyridine nucleotides (*i.e.* NAD(P)) was carried out to link redox and central metabolisms at various omic scales. Secondly, growth, major central metabolites and ASC-GSH cycle were quantitatively described during fruit development. Finally, this enabled building an enzyme-based kinetic model of the ASC-GSH cycle to study the redox flux dynamics and regulations. Besides, ascorbate-enriched fruits affected in the main synthesis pathways were analysed to validate our kinetic models and further explore the implication of ASC during fruit development. Combining targeted analysis, computational kinetic-based modelling and global analyses allowed us to provide the first dynamic description of core redox metabolism during fruit development.

From a global perspective, redox metabolism exhibits several behaviours according to the fruit growth phase. Indeed, redox metabolism displayed a sequential activity in a “wave-shaped” pattern corresponding to the fruit development (*i.e.* cell division-elongation-ripening) with specific changes at phase transitions (*i.e.* 14 DPA and turning). Similarly, central fruit metabolism has also been defined by a “turbo” metabolism during cell division that rapidly drops at the beginning of cell elongation until growth arrest (Biais et al., 2014; Roch et al., 2020). Moreover, phytohormones have also been reported to fluctuate in a growth-dependent manner during fruit development (Zhang et al., 2009; McAtee et al., 2013).

The beginning of fruit development revealed a remarkably high ROS content despite a strong APX capacity. Simultaneously, ASC recycling enzymes (*i.e.* DHAR and MDHAR) showed low capacities, thus resulting in the nearly complete oxidation of ASC. Strikingly, such high levels of oxidised ascorbate during young fruit development have been previously reported in diverse fruit species, suggesting a common phenomenon between fruit species (Decros et al., 2019a; Roch et al., 2020). However, at the same time, tomato fruit also exhibited a moderate GSH oxidation ratio, while untargeted analysis showed a relative availability of secondary antioxidant metabolites. Besides, ASC-enriched fruits showed an increase in reduced GSH as a result of the increased DHA content. However,

no differences were observed regarding ASC and GSH redox states, thus indicating that reduced antioxidants were available in cells but not interacting with H_2O_2. Additionally, kinetic models emphasised the necessity of a ROS production source away from the antioxidant system and regulation of APX by the supply in reduced ASC. This is in line with previous reports of active fruit photosynthesis during early development and the role of ROS processing by ASC during this process (Pesaresi et al., 2014; Foyer, 2018; Decros et al., 2019b; Quinet et al., 2019). Moreover, GSH has been reported to be recruited in the nucleus during early cell proliferation and participate in thiol signalling pathways (Markovic et al., 2007; Vivancos et al., 2010). Overall, this demonstrates that during cell division phase, ROS accumulate in the same compartment as ASC and APX, resulting in a complete ASC oxidation, but separately from GSH, which remains moderately oxidised. In this regard, subcellular studies of the ROS production sources and/or the repartition of antioxidants emerge as key issues to go deeper in understanding redox metabolism involvement for fruit development. As such, subcellular fractionation experiments (Destailleur et al., 2021) or metabolic imaging (Gilmore et al., 2019) could lead to gaining further insights into the subcellular distribution of redox components at the metabolite levels.

Next, both ascorbate and glutathione presented noticeable variations in their redox state during the transition from cell division to elongation phase with, however, more pronounced differences in ASC, which displayed a drastic shift from totally oxidised to fully reduced. Furthermore, it is worth noting that the change in ASC redox state was concurrent with the increase of the fruit growth rate. This finding emphasises the global link between growth and redox metabolism.

Concomitantly, APX and MDHAR enzyme capacities showed a similar trend from ascorbate oxidation to full recycling. Complementarily, the kinetic model unveiled a simultaneous shift in the ASC-GSH flux sensitivity starting from a limitation by ASC supply during cell division to a restriction by NAD(P)H availability. Besides, GR and DHAR evolved independently from ROS, GSH and ASC in contrast to MDHAR and APX. In addition, the kinetic model highlighted GR and DHAR as minor fluxes compared to APX and MDHAR during fruit development. Altogether, this indicates that APX and MDHAR are the major regulators of ASC during tomato fruit development, and to a greater extent, GSH redox states. Besides, GR and DHAR presented a negligible role during fruit growth, which agrees with previous stress response studies (Rahantaniaina et al., 2017; Terai et al., 2020).

Furthermore, endoreduplication is also a hallmark of this growth phase transition in which redox metabolism involvement remains an incomplete puzzle (Chevalier et al., 2011; Fanwoua et al., 2013; Quinet et al., 2019). In addition, ASC has been reported to be present in the nucleus where it acts as a signalling molecule (Zechmann, 2011). Here, the shift in ASC redox state observed during this phase transition, concurrent with the increase in its recycling capacity through MDHAR, suggests that ASC metabolism participates in the control of the trade-off between division and endoreduplication.

Then, once the reduced state is established, it was maintained mainly reduced and showed a continuous decrease during the cell elongation phase. The concomitant reduction in redox and central metabolism activities suggested a decline of global metabolic activity at the expense of osmolytes influx (Beauvoit et al., 2014; Biais et al., 2014). However, untargeted metabolomic approach revealed an active metabolic reprogramming during this phase either from a global perspective or regarding secondary antioxidant metabolites. This agrees with a previous report of an increase in flavonoids content reported in mature green fruits (Tohge et al., 2013). Altogether, cell elongation can be characterised by dynamic maintenance of reduced redox buffers associated with a decrease in central metabolism. Nonetheless, this hides an active reprogramming of secondary metabolism during this phase, in which the fruit likely prepares the building blocks required for ripening.

Tomato fruit maturation starts at the turning stage when fruit changes colour. From a physiological perspective, ripening is defined by a reprogramming of metabolism driven by phytohormones, especially ethylene, during which starch is remobilised together with a respiratory burst ending in sugar accumulation and CO_2 release (Colombié et al., 2015; Roch et al., 2020). Interestingly, a stoichiometric model identified that an energy peak appeared just before ripening (Colombié et al., 2017). In addition, malic acid has been identified as a central actor and is also mobilised before the turning stage (Centeno et al., 2011; Osorio et al., 2013a, 2013b). This is consistent with our data, and the similar regulation pattern of the ASC-GSH cycle observed for 35 DPA and turning kinetic models. In addition, a prominent part of NAD(P)-dependent features was associated with redox and mitochondrial metabolisms during ripening, as well as active recycling and *de novo* synthesis of NAD(P). Hence, this suggests that carbon resource remobilisation impacts pyridine nucleotides metabolism, which in turn induces reprogramming of core redox metabolism. Moreover, the singular dynamic of malate suggests an involvement of malate dehydrogenase and aspartate-malate shuttle in the regulation of reducing power availably during the onset of ripening.

Furthermore, CAT capacity and MDHAR flux also showed a peak at turning, while APX capacity remained low. This indicates a change in ROS processing, which keeps the redox state of the ASC mainly reduced as opposed to early development. Besides, from a global redox perspective, tomato fruit ripening is associated with increased total antioxidant capacity and an accumulation of lycopene and volatile organic compounds (Riedl et al., 2013; Tohge et al., 2013). Lastly, ASC^+ fruits showed a reduction of GSH content in orange and red fruits compared to WT, suggesting the need for available reduced antioxidants, up to a certain threshold. Thus, this demonstrates that ROS processing and associated ASC signalling pathways are differentially involved between cell division and ripening. These results thus reinforce the importance of spatially tuned ROS production and processing.

On the other hand, the analysis of ASC enriched fruits validated the kinetic model and highlighted that ASC fruit content was mainly regulated by its own synthesis, and not by import from leaves such as for photo-assimilates (Lytovchenko et al., 2011). However, heterozygous ASC^+ fruits did not show a strong phenotype or considerable changes in core redox metabolism behaviour during fruit development. In addition, the untargeted metabolic analysis revealed a clear distinction between growth stages but not between genotypes. Nonetheless, the kinetic model showed a threshold effect for the ASC increase from which signalling through its redox state is hindered, congruent with the developmental disorders observed in homozygous fruits.

The main outcome from this study is the identification of a co-regulation between the reduced form of ASC and GSH depending on the sum of their contents. Indeed, early fruit development showed an accumulation in both DHA and GSH content, whereas the increase in GSH content during maturation was inhibited by reduced ASC accumulation. Furthermore, ASC-enriched plants displayed a slight decrease in H_2O_2 content at the anthesis stage associated with flower morphological disorders as well as pollen infertility (Deslous et al., 2021), suggesting that active ASC oxidation also occurs during fecundation process. In addition, ASC^+ plants harboured an increased number of flowers highlighting the crucial role of ASC in the control of flowering and the trade-off between the number and sustainability of flowers. In this regard, data obtained within this study allowed the development of a novel side project focusing on redox metabolism in flowers and fruits altered in ASC content during fruit set.

To summarise, core redox metabolism exhibited a growth stage-dependent dynamic. Here, we revealed that the fruit cell division phase is characterised by an active ROS production associated with a strong ASC oxidation by APX and a weak recycling activity resulting in ROS and oxidised ASC accumulation. In contrast, the GSH redox state remained moderately affected. Then, the transition to the elongation phase denoted a complete shift in ASC oxidative and recycling activities, concurrent with the decrease of ROS production ending in a full ASC reduction. This mechanism promoting ASC reduction and active recycling was maintained until the growth arrest at the beginning of fruit maturation. Next, ripening pointed out an increase in CAT capacity and MDHAR flux concomitant with an increased total antioxidant capacity, thus displaying another specific behaviour in which the ASC-GSH cycle was weakly involved in ROS processing. Furthermore, the kinetic modelling approach indicated that tomato fruit development displayed growth phase-dependent redox metabolism linked with central metabolism *via* pyridine nucleotides and H_2O_2 availability. Thereby, this emphasised the major role of ROS and reducing power (*i.e.* NAD(P)H) in controlling the ASC-GSH cycle during fruit development. Moreover, this highlighted that among the ASC-GSH cycle, MDHAR and APX stand out as major regulators of the redox balance in a developmental context. Overall, this demonstrates the

necessity of a strictly controlled subcellular distribution of ROS -production and -processing pathways. Hence, elucidating the mechanisms controlling antioxidant transport emerges as a critical issue in which fluorescent *in vivo* probes arise as promising tools (Ming et al., 2017; Smith et al., 2021).

In conclusion, this project provides the first comprehensive description of central redox metabolism and ASC-GSH cycle fluxes and their regulation during tomato fruit development. These complementary data allowed a deeper understanding of the intricate metabolic reprogramming occurring during fruit development. However, apart from growth processes, redox metabolism and oxidative signalling are involved in virtually all biotic and abiotic stress conditions in which the role of the ASC-GSH cycle for fruit has not been fully deciphered yet.

B. Perspectives

I. Perspectives from the ASC-GSH cycle kinetic model

The development of the ASC-GSH cycle kinetic model during this study provided a new tool for future investigations. For example, the model can be adapted to different fruit species to identify common and specific fruit redox alterations. The model will further allow *in silico* predictions of ASC-GSH cycle fluxes under various conditions that will benefit breeding issues while providing hypotheses about redox signalling. Besides, complementary pathways can be added to provide a bigger picture of redox metabolism. For instance, NAD(P) synthesis and recycling pathways as well as enzymes allowing their regeneration will help to go further in the crosstalk between central and redox metabolisms. Moreover, experiments aiming to measure photosynthesis and respiration of fruit *in planta* have been performed via gas exchanges in order to investigate the contribution of the different ROS sources in the total ROS production. Following their validation, these data will be implemented in the model in the future assuming that the percentage of electron leak within those systems to be known.

In addition, collecting data about the subcellular distribution and transport processes of ROS and antioxidant remains a bottleneck for deciphering redox signalling. In this regard, fluorescent probes as well as MS imaging techniques emerge as powerful tools to investigate the distribution of oxidative signals (Gilmore et al., 2019; Smith et al., 2021). Lastly, combining modelling approaches using previous models describing cell division, fruit growth and central metabolism will allow the development of integrative models that will deeper our understanding of fruit development (Fanwoua et al., 2013; Colombié et al., 2015). For example, implementing the redox flux predictions from the kinetic model into a process-based fruit growth model would highlight the steps most involved in a trait of interest (*i.e.* yield, fruit composition, stress resistance). These integrative models could be an asset for breeding issues and thus for the design of ideotypes (Chenu et al., 2017; Beauvoit et al., 2018). Finally,

top-down statistical modelling, *e.g.* using generalised linear modelling approach, will be performed on untargeted metabolomic data to unveil metabolic markers associated with fluxes predictions, and thus identify reliable proxies of the ASC-GSH cycle fluxes.

As a valuable tool for plant biologists interested in redox metabolism, the kinetic model could be implemented in future studies investigating the role of the ASC-GSH cycle in stress responses, including abiotic factors and bioagressor challenges. This would be particularly interesting and relevant in the context of trade-off studies examining the roles and regulations of redox metabolism between growth and stress pathways. For instance, this kinetic model could be exploited short terms in grapevine resilience to heat stress. The use of mutant lines affected at the level of regulators uncovered by the model would also expand our understanding of the roles of redox signalling in plant physiology.

II. Perspectives from the study of ascorbate mutant fruits

On the other hand, the study of ASC^+ mutant fruits highlighted a common regulation of glutathione and ascorbate contents based on the availability of their reduced form. Further analyses about their turnover in fruit are necessary to identify the scale and the associated signalling of this regulation (transcriptomic, proteomic or metabolic). Moreover, flowers and fruit set were noticeably affected by the increase in ASC synthesis, emphasising the role of ascorbate for fecundation and, to a greater extent, yield. ASC^+ plants also displayed an increased flower number per truss, which highlights the role of ASC in the control of flowering. In this regard, a study focusing on flowers and young fruits using both heterozygous and homozygous ASC^+ plants has been started and will provide new insights into the ASC control of flowering and fertilisation processes. Besides, despite the absence of the notorious effect of the increase in ASC synthesis for fruit development, studies on other traits are still needed. For example, challenging ASC mutants with various stress, either biotic or abiotic, should help to decipher the role of ASC in plant resistance and in the trade-off between growth and defence.

REFERENCES

Agius, F., González-Lamothe, R., Caballero, J. L., Muñoz-Blanco, J., Botella, M. A., and Valpuesta, V. (2003). Engineering increased vitamin C levels in plants by overexpression of a D-galacturonic acid reductase. *Nat Biotechnol* 21, 177–181. doi:10.1038/nbt777.

Alferez, F. M., Gerberich, K. M., Li, J.-L., Zhang, Y., Graham, J. H., and Mou, Z. (2018). Exogenous Nicotinamide Adenine Dinucleotide Induces Resistance to Citrus Canker in Citrus. *Frontiers in Plant Science* 9. doi:10.3389/fpls.2018.01472.

Alfonso-Prieto, M., Biarnés, X., Vidossich, P., and Rovira, C. (2009). The Molecular Mechanism of the Catalase Reaction. *J. Am. Chem. Soc.* 131, 11751–11761. doi:10.1021/ja9018572.

Alhagdow, M., Mounet, F., Gilbert, L., Nunes-Nesi, A., Garcia, V., Just, D., et al. (2007). Silencing of the mitochondrial ascorbate synthesizing enzyme L-galactono-1,4-lactone dehydrogenase affects plant and fruit development in tomato. *Plant Physiol.* 145, 1408–1422. doi:10.1104/pp.107.106500.

Aller, I., Rouhier, N., and Meyer, A. J. (2013). Development of roGFP2-derived redox probes for measurement of the glutathione redox potential in the cytosol of severely glutathione-deficient rml1 seedlings. *Front. Plant Sci.* 4. doi:10.3389/fpls.2013.00506.

Alper, H., Jin, Y.-S., Moxley, J. F., and Stephanopoulos, G. (2005). Identifying gene targets for the metabolic engineering of lycopene biosynthesis in Escherichia coli. *Metabolic Engineering* 7, 155–164. doi:10.1016/j.ymben.2004.12.003.

Alscher, R. G. (2002). Role of superoxide dismutases (SODs) in controlling oxidative stress in plants. *Journal of Experimental Botany* 53, 1331–1341. doi:10.1093/jexbot/53.372.1331.

Alseekh, S., Scossa, F., Wen, W., Luo, J., Yan, J., Beleggia, R., et al. (2021). Domestication of Crop Metabolomes: Desired and Unintended Consequences. *Trends in Plant Science*, S1360138521000340. doi:10.1016/j.tplants.2021.02.005.

Apel, K., and Hirt, H. (2004). REACTIVE OXYGEN SPECIES: Metabolism, Oxidative Stress, and Signal Transduction. *Annual Review of Plant Biology* 55, 373–399. doi:10.1146/annurev.arplant.55.031903.141701.

Araújo, W. L., Nunes-Nesi, A., Nikoloski, Z., Sweetlove, L. J., and Fernie, A. R. (2012). Metabolic control and regulation of the tricarboxylic acid cycle in photosynthetic and heterotrophic plant tissues: TCA control and regulation in plant tissues. *Plant, Cell & Environment* 35, 1–21. doi:10.1111/j.1365-3040.2011.02332.x.

Arrivault, S., Guenther, M., Ivakov, A., Feil, R., Vosloh, D., van Dongen, J. T., et al. (2009). Use of reverse-phase liquid chromatography, linked to tandem mass spectrometry, to profile the Calvin cycle and other metabolic intermediates in Arabidopsis rosettes at different carbon dioxide concentrations. *The Plant Journal* 59, 826–839. doi:10.1111/j.1365-313X.2009.03902.x.

Asada, K. (1984). "Chloroplasts: Formation of active oxygen and its scavenging," in *Methods in Enzymology* (Elsevier), 422–429. doi:10.1016/S0076-6879(84)05059-X.

Asada, K. (1999). THE WATER-WATER CYCLE IN CHLOROPLASTS: Scavenging of Active Oxygens and Dissipation of Excess Photons. *Annual Review of Plant Physiology and Plant Molecular Biology* 50, 601–639. doi:10.1146/annurev.arplant.50.1.601.

Attolico, A. D., and De Tullio, M. C. (2006). Increased ascorbate content delays flowering in long-day grown Arabidopsis thaliana (L.) Heynh. *Plant Physiology and Biochemistry* 44, 462–466. doi:10.1016/j.plaphy.2006.08.002.

Badejo, A. A., Wada, K., Gao, Y., Maruta, T., Sawa, Y., Shigeoka, S., et al. (2012). Translocation and the alternative D-galacturonate pathway contribute to increasing the ascorbate level in ripening tomato fruits together with the D-mannose/L-galactose pathway. *Journal of Experimental Botany* 63, 229–239. doi:10.1093/jxb/err275.

Baker, S. M., Schallau, K., and Junker, B. H. (2010). Comparison of different algorithms for simultaneous estimation of multiple parameters in kinetic metabolic models. doi:10.2390/BIECOLL-JIB-2010-133.

Baldazzi, V., Bertin, N., de Jong, H., and Génard, M. (2012). Towards multiscale plant models: integrating cellular networks. *Trends in Plant Science* 17, 728–736. doi:10.1016/j.tplants.2012.06.012.

Baldazzi, V., Pinet, A., Vercambre, G., Bénard, C., Biais, B., and Génard, M. (2013). In-silico analysis of water and carbon relations under stress conditions. A multi-scale perspective centered on fruit. *Front. Plant Sci.* 4. doi:10.3389/fpls.2013.00495.

Baldet, P., Bres, C., Okabe, Y., Mauxion, J.-P., Just, D., Bournonville, C., et al. (2013). Investigating the role of vitamin C in tomato through TILLING identification of ascorbate-deficient tomato mutants. *Plant Biotechnology* 30, 309–314. doi:10.5511/plantbiotechnology.13.0622b.

Balmer, Y., Vensel, W. H., Tanaka, C. K., Hurkman, W. J., Gelhaye, E., Rouhier, N., et al. (2004). Thioredoxin links redox to the regulation of fundamental processes of plant mitochondria. *Proceedings of the National Academy of Sciences* 101, 2642–2647. doi:10.1073/pnas.0308583101.

Bar-Even, A., Noor, E., Savir, Y., Liebermeister, W., Davidi, D., Tawfik, D. S., et al. (2011). The Moderately Efficient Enzyme: Evolutionary and Physicochemical Trends Shaping Enzyme Parameters. *Biochemistry* 50, 4402–4410. doi:10.1021/bi2002289.

Barrett, T., Wilhite, S. E., Ledoux, P., Evangelista, C., Kim, I. F., Tomashevsky, M., et al. (2013). NCBI GEO: archive for functional genomics data sets--update. *Nucleic Acids Res.* 41, D991-995. doi:10.1093/nar/gks1193.

Barth, C. (2006). The role of ascorbic acid in the control of flowering time and the onset of senescence. *Journal of Experimental Botany* 57, 1657–1665. doi:10.1093/jxb/erj198.

Beauvoit, B., Belouah, I., Bertin, N., Cakpo, C. B., Colombié, S., Dai, Z., et al. (2018). Putting primary metabolism into perspective to obtain better fruits. *Annals of Botany* 122, 1–21. doi:10.1093/aob/mcy057.

Beauvoit, B. P., Colombié, S., Monier, A., Andrieu, M.-H., Biais, B., Bénard, C., et al. (2014). Model-Assisted Analysis of Sugar Metabolism throughout Tomato Fruit Development Reveals Enzyme and Carrier Properties in Relation to Vacuole Expansion. *Plant Cell* 26, 3224–3242. doi:10.1105/tpc.114.127761.

Becker, M. G., Chan, A., Mao, X., Girard, I. J., Lee, S., Elhiti, M., et al. (2014). Vitamin C deficiency improves somatic embryo development through distinct gene regulatory networks in Arabidopsis. *Journal of Experimental Botany* 65, 5903–5918. doi:10.1093/jxb/eru330.

Beekwilder, J., Hall, R. D., and Ric Vos, C. H. D. (2005). Identification and dietary relevance of antioxidants from raspberry. *BioFactors* 23, 197–205. doi:10.1002/biof.5520230404.

Belenky, P., Stebbins, R., Bogan, K. L., Evans, C. R., and Brenner, C. (2011). Nrt1 and Tna1-Independent Export of NAD+ Precursor Vitamins Promotes NAD+ Homeostasis and Allows

Engineering of Vitamin Production. *PLoS ONE* 6, e19710. doi:10.1371/journal.pone.0019710.

Belouah, I., Nazaret, C., Pétriacq, P., Prigent, S., Bénard, C., Mengin, V., et al. (2019). Modeling Protein Destiny in Developing Fruit. *Plant Physiol.* 180, 1709–1724. doi:10.1104/pp.19.00086.

Bennett, B. D., Kimball, E. H., Gao, M., Osterhout, R., Van Dien, S. J., and Rabinowitz, J. D. (2009). Absolute metabolite concentrations and implied enzyme active site occupancy in Escherichia coli. *Nat Chem Biol* 5, 593–599. doi:10.1038/nchembio.186.

Berghe, T. V., Linkermann, A., Jouan-Lanhouet, S., Walczak, H., and Vandenabeele, P. (2014). Regulated necrosis: the expanding network of non-apoptotic cell death pathways. *Nat Rev Mol Cell Biol* 15, 135–147. doi:10.1038/nrm3737.

Bernroitner, M., Zamocky, M., Furtmüller, P. G., Peschek, G. A., and Obinger, C. (2009). Occurrence, phylogeny, structure, and function of catalases and peroxidases in cyanobacteria. *Journal of Experimental Botany* 60, 423–440. doi:10.1093/jxb/ern309.

Biais, B., Bénard, C., Beauvoit, B., Colombié, S., Prodhomme, D., Ménard, G., et al. (2014). Remarkable Reproducibility of Enzyme Activity Profiles in Tomato Fruits Grown under Contrasting Environments Provides a Roadmap for Studies of Fruit Metabolism. *Plant Physiol.* 164, 1204–1221. doi:10.1104/pp.113.231241.

Bindschedler, L. V., Dewdney, J., Blee, K. A., Stone, J. M., Asai, T., Plotnikov, J., et al. (2006). Peroxidase-dependent apoplastic oxidative burst in Arabidopsis required for pathogen resistance. *Plant J.* 47, 851–863. doi:10.1111/j.1365-313X.2006.02837.x.

Blum, R., Beck, A., Korte, A., Stengel, A., Letzel, T., Lendzian, K., et al. (2007). Function of phytochelatin synthase in catabolism of glutathione-conjugates: Catabolism of glutathione-conjugates. *The Plant Journal* 49, 740–749. doi:10.1111/j.1365-313X.2006.02993.x.

Blum, R., Meyer, K. C., Wünschmann, J., Lendzian, K. J., and Grill, E. (2010). Cytosolic Action of Phytochelatin Synthase. *Plant Physiology* 153, 159–169. doi:10.1104/pp.109.149922.

Bordbar, A., Monk, J. M., King, Z. A., and Palsson, B. O. (2014). Constraint-based models predict metabolic and associated cellular functions. *Nat Rev Genet* 15, 107–120. doi:10.1038/nrg3643.

Botanga, C. J., Bethke, G., Chen, Z., Gallie, D. R., Fiehn, O., and Glazebrook, J. (2012). Metabolite Profiling of *Arabidopsis* Inoculated with *Alternaria brassicicola* Reveals That Ascorbate Reduces Disease Severity. *MPMI* 25, 1628–1638. doi:10.1094/MPMI-07-12-0179-R.

Bourdon, M., Frangne, N., Mathieu-Rivet, E., Nafati, M., Cheniclet, C., Renaudin, J.-P., et al. (2010). "Endoreduplication and Growth of Fleshy Fruits," in *Progress in Botany, Vol. 71* Progress in Botany., eds. U. E. Lüttge, W. Beyschlag, B. Büdel, and D. Francis (Berlin, Heidelberg: Springer Berlin Heidelberg), 101–132. doi:10.1007/978-3-642-02167-1_4.

Bourgis, F., Roje, S., Nuccio, M. L., Fisher, D. B., Tarczynski, M. C., Li, C., et al. (1999). S-Methylmethionine Plays a Major Role in Phloem Sulfur Transport and Is Synthesized by a Novel Type of Methyltransferase. *Plant Cell* 11, 1485–1497. doi:10.1105/tpc.11.8.1485.

Bowler, C., Van Camp, W., Van Montagu, M., Inzé, D., and Asada, K. (1994). Superoxide Dismutase in Plants. *Critical Reviews in Plant Sciences* 13, 199–218. doi:10.1080/07352689409701914.

Bowry, V. W., Ingold, K. U., and Stocker, R. (1992). Vitamin E in human low-density lipoprotein. When and how this antioxidant becomes a pro-oxidant. *Biochem. J.* 288 (Pt 2), 341–344.

Bowsher, C. G., Lacey, A. E., Hanke, G. T., Clarkson, D. T., Saker, L. R., Stulen, I., et al. (2007). The effect of Glc6P uptake and its subsequent oxidation within pea root plastids on nitrite reduction and glutamate synthesis. *Journal of Experimental Botany* 58, 1109–1118. doi:10.1093/jxb/erl269.

Briggs, A. G., and Bent, A. F. (2011). Poly(ADP-ribosyl)ation in plants. *Trends in Plant Science* 16, 372–380. doi:10.1016/j.tplants.2011.03.008.

Brochado, A. R., Matos, C., Møller, B. L., Hansen, J., Mortensen, U. H., and Patil, K. R. (2010). Improved vanillin production in baker's yeast through in silico design. *Microb Cell Fact* 9, 84. doi:10.1186/1475-2859-9-84.

Brown, P. M., Caradoc-Davies, T. T., Dickson, J. M. J., Cooper, G. J. S., Loomes, K. M., and Baker, E. N. (2006). Crystal structure of a substrate complex of myo-inositol oxygenase, a di-iron oxygenase with a key role in inositol metabolism. *Proceedings of the National Academy of Sciences* 103, 15032–15037. doi:10.1073/pnas.0605143103.

Buchner, P., Stuiver, C. E. E., Westerman, S., Wirtz, M., Hell, R., Hawkesford, M. J., et al. (2004). Regulation of Sulfate Uptake and Expression of Sulfate Transporter Genes in *Brassica oleracea* as Affected by Atmospheric H2S and Pedospheric Sulfate Nutrition. *Plant Physiology* 136, 3396–3408. doi:10.1104/pp.104.046441.

Bulley, S., and Laing, W. (2016). The regulation of ascorbate biosynthesis. *Current Opinion in Plant Biology* 33, 15–22. doi:10.1016/j.pbi.2016.04.010.

Bulley, S. M., Rassam, M., Hoser, D., Otto, W., Schünemann, N., Wright, M., et al. (2009). Gene expression studies in kiwifruit and gene over-expression in Arabidopsis indicates that GDP-L-galactose guanyltransferase is a major control point of vitamin C biosynthesis. *Journal of Experimental Botany* 60, 765–778. doi:10.1093/jxb/ern327.

Burritt, D. J., Diaz-Vivancos, P., Fujita, M., Hossain, M. A., Mostofa, M. G., and Tran, L.-S. P. eds. (2017). *Glutathione in Plant Growth, Development, and Stress Tolerance*. 1st ed. 2017. Cham: Springer International Publishing : Imprint: Springer doi:10.1007/978-3-319-66682-2.

Bykova, N. V., and Møller, I. M. (2001). Involvement of matrix NADP turnover in the oxidation of NAD+ linked substrates by pea leaf mitochondria. *Physiologia Plantarum* 111, 448–456. doi:10.1034/j.1399-3054.2001.1110404.x.

Camejo, D., Martí, M. C., Román, P., Ortiz, A., and Jiménez, A. (2010). Antioxidant system and protein pattern in peach fruits at two maturation stages. *J. Agric. Food Chem.* 58, 11140–11147. doi:10.1021/jf102807t.

Carrari, F. (2006). Metabolic regulation underlying tomato fruit development. *Journal of Experimental Botany* 57, 1883–1897. doi:10.1093/jxb/erj020.

Centeno, D. C., Osorio, S., Nunes-Nesi, A., Bertolo, A. L. F., Carneiro, R. T., Araújo, W. L., et al. (2011). Malate Plays a Crucial Role in Starch Metabolism, Ripening, and Soluble Solid Content of Tomato Fruit and Affects Postharvest Softening. *Plant Cell* 23, 162–184. doi:10.1105/tpc.109.072231.

Cervilla, L. M., Blasco, B., Rios, J. J., Romero, L., and Ruiz, J. M. (2007). Oxidative Stress and Antioxidants in Tomato (Solanum lycopersicum) Plants Subjected to Boron Toxicity. *Annals of Botany* 100, 747–756. doi:10.1093/aob/mcm156.

Chapman, J. M., Muhlemann, J. K., Gayomba, S. R., and Muday, G. K. (2019). RBOH-Dependent ROS Synthesis and ROS Scavenging by Plant Specialized Metabolites To Modulate Plant Development and Stress Responses. *Chem. Res. Toxicol.* 32, 370–396. doi:10.1021/acs.chemrestox.9b00028.

Chaput, V., Martin, A., and Lejay, L. (2020). Redox metabolism: the hidden player in carbon and nitrogen signaling? *Journal of Experimental Botany* 71, 3816–3826. doi:10.1093/jxb/eraa078.

Chaudhary, P., Sharma, A., Singh, B., and Nagpal, A. K. (2018). Bioactivities of phytochemicals present in tomato. *Journal of Food Science and Technology* 55, 2833–2849. doi:10.1007/s13197-018-3221-z.

Chelikani, P., Fita, I., and Loewen, P. C. (2004). Diversity of structures and properties among catalases. *Cellular and Molecular Life Sciences (CMLS)* 61, 192–208. doi:10.1007/s00018-003-3206-5.

Chen, C., Letnik, I., Hacham, Y., Dobrev, P., Ben-Daniel, B.-H., Vanková, R., et al. (2014). ASCORBATE PEROXIDASE6 protects Arabidopsis desiccating and germinating seeds from stress and mediates cross talk between reactive oxygen species, abscisic acid, and auxin. *Plant Physiol.* 166, 370–383. doi:10.1104/pp.114.245324.

Chen, Z., and Gallie, D. R. (2012). Induction of Monozygotic Twinning by Ascorbic Acid in Tobacco. *PLoS ONE* 7, e39147. doi:10.1371/journal.pone.0039147.

Chenu, K., Porter, J. R., Martre, P., Basso, B., Chapman, S. C., Ewert, F., et al. (2017). Contribution of Crop Models to Adaptation in Wheat. *Trends in Plant Science* 22, 472–490. doi:10.1016/j.tplants.2017.02.003.

Chevalier, C., Nafati, M., Mathieu-Rivet, E., Bourdon, M., Frangne, N., Cheniclet, C., et al. (2011). Elucidating the functional role of endoreduplication in tomato fruit development. *Annals of Botany* 107, 1159–1169. doi:10.1093/aob/mcq257.

Chew, O., Whelan, J., and Millar, A. H. (2003). Molecular Definition of the Ascorbate-Glutathione Cycle in Arabidopsis Mitochondria Reveals Dual Targeting of Antioxidant Defenses in Plants. *Journal of Biological Chemistry* 278, 46869–46877. doi:10.1074/jbc.M307525200.

Chew, Y. H., Wenden, B., Flis, A., Mengin, V., Taylor, J., Davey, C. L., et al. (2014). Multiscale digital *Arabidopsis* predicts individual organ and whole-organism growth. *Proc Natl Acad Sci USA* 111, E4127–E4136. doi:10.1073/pnas.1410238111.

Choudhury, F. K., Rivero, R. M., Blumwald, E., and Mittler, R. (2017). Reactive oxygen species, abiotic stress and stress combination. *Plant J* 90, 856–867. doi:10.1111/tpj.13299.

Chun, J., Lee, J., Ye, L., Exler, J., and Eitenmiller, R. R. (2006). Tocopherol and tocotrienol contents of raw and processed fruits and vegetables in the United States diet. *Journal of Food Composition and Analysis* 19, 196–204. doi:10.1016/j.jfca.2005.08.001.

Cocaliadis, M. F., Fernández-Muñoz, R., Pons, C., Orzaez, D., and Granell, A. (2014). Increasing tomato fruit quality by enhancing fruit chloroplast function. A double-edged sword? *J. Exp. Bot.* 65, 4589–4598. doi:10.1093/jxb/eru165.

Colombié, S., Beauvoit, B., Nazaret, C., Bénard, C., Vercambre, G., Le Gall, S., et al. (2017). Respiration climacteric in tomato fruits elucidated by constraint-based modelling. *New Phytol* 213, 1726–1739. doi:10.1111/nph.14301.

Colombié, S., Nazaret, C., Bénard, C., Biais, B., Mengin, V., Solé, M., et al. (2015). Modelling central metabolic fluxes by constraint-based optimization reveals metabolic reprogramming of developing *Solanum lycopersicum* (tomato) fruit. *Plant J* 81, 24–39. doi:10.1111/tpj.12685.

Conklin, P. L., and Barth, C. (2004). Ascorbic acid, a familiar small molecule intertwined in the response of plants to ozone, pathogens, and the onset of senescence. *Plant Cell Environ* 27, 959–970. doi:10.1111/j.1365-3040.2004.01203.x.

Constantinescu, D., Memmah, M.-M., Vercambre, G., Génard, M., Baldazzi, V., Causse, M., et al. (2016). Model-Assisted Estimation of the Genetic Variability in Physiological Parameters Related to Tomato Fruit Growth under Contrasted Water Conditions. *Front. Plant Sci.* 7. doi:10.3389/fpls.2016.01841.

Coqueiro, D. S. O., de Souza, A. A., Takita, M. A., Rodrigues, C. M., Kishi, L. T., and Machado, M. A. (2015). Transcriptional profile of sweet orange in response to chitosan and salicylic acid. *BMC Genomics* 16. doi:10.1186/s12864-015-1440-5.

Cornish-Bowden, A. (2004). *Fundamentals of enzyme kinetics*. Third ed. London: Portland press.

Cory, H., Passarelli, S., Szeto, J., Tamez, M., and Mattei, J. (2018). The Role of Polyphenols in Human Health and Food Systems: A Mini-Review. *Frontiers in Nutrition* 5. doi:10.3389/fnut.2018.00087.

Cosio, C., and Dunand, C. (2009). Specific functions of individual class III peroxidase genes. *Journal of Experimental Botany* 60, 391–408. doi:10.1093/jxb/ern318.

Creissen, G., Firmin, J., Fryer, M., Kular, B., Leyland, N., Reynolds, H., et al. (1999). Elevated Glutathione Biosynthetic Capacity in the Chloroplasts of Transgenic Tobacco Plants Paradoxically Causes Increased Oxidative Stress. *Plant Cell* 11, 1277–1291. doi:10.1105/tpc.11.7.1277.

Da Silva, D., Favreau, R., Auzmendi, I., and DeJong, T. M. (2011). Linking water stress effects on carbon partitioning by introducing a xylem circuit into L-PEACH. *Annals of Botany* 108, 1135–1145. doi:10.1093/aob/mcr072.

Dalton, D. A., Russell, S. A., Hanus, F. J., Pascoe, G. A., and Evans, H. J. (1986). Enzymatic reactions of ascorbate and glutathione that prevent peroxide damage in soybean root nodules. *Proceedings of the National Academy of Sciences* 83, 3811–3815. doi:10.1073/pnas.83.11.3811.

Daudi, A., Cheng, Z., O'Brien, J. A., Mammarella, N., Khan, S., Ausubel, F. M., et al. (2012). The Apoplastic Oxidative Burst Peroxidase in Arabidopsis Is a Major Component of Pattern-Triggered Immunity. *The Plant Cell* 24, 275–287. doi:10.1105/tpc.111.093039.

Davey, M. W., Gilot, C., Persiau, G., Østergaard, J., Han, Y., Bauw, G. C., et al. (1999). Ascorbate Biosynthesis in Arabidopsis Cell Suspension Culture. *Plant Physiology* 121, 535–544. doi:10.1104/pp.121.2.535.

Davey, M. W., Montagu, M. V., Inzé, D., Sanmartin, M., Kanellis, A., Smirnoff, N., et al. (2000). Plant L-ascorbic acid: chemistry, function, metabolism, bioavailability and effects of processing. *Journal of the Science of Food and Agriculture* 80, 825–860. doi:10.1002/(SICI)1097-0010(20000515)80:7<825::AID-JSFA598>3.0.CO;2-6.

Davies, M. J. (2005). The oxidative environment and protein damage. *Biochim. Biophys. Acta* 1703, 93–109. doi:10.1016/j.bbapap.2004.08.007.

Day, D. A., and Wiskich, J. T. (1981). Glycine Metabolism and Oxalacetate Transport by Pea Leaf Mitochondria. *Plant Physiol.* 68, 425–429. doi:10.1104/pp.68.2.425.

De Gara, L., Pinto, M. C., and Arrigoni, O. (1997). Ascorbate synthesis and ascorbate peroxidase activity during the early stage of wheat germination. *Physiol Plant* 100, 894–900. doi:10.1111/j.1399-3054.1997.tb00015.x.

de Pinto, M. C. (2004). Changes in the ascorbate metabolism of apoplastic and symplastic spaces are associated with cell differentiation. *Journal of Experimental Botany* 55, 2559–2569. doi:10.1093/jxb/erh253.

Decros, G., Baldet, P., Beauvoit, B., Stevens, R., Flandin, A., Colombie, S., et al. (2019a). Get the balance right: ROS homeostasis and redox signalling in fruit. *Front. Plant Sci.* 10. doi:10.3389/fpls.2019.01091.

Decros, G., Beauvoit, B., Colombié, S., Cabasson, C., Bernillon, S., Arrivault, S., et al. (2019b). Regulation of Pyridine Nucleotide Metabolism During Tomato Fruit Development Through Transcript and Protein Profiling. *Front. Plant Sci.* 10, 1201. doi:10.3389/fpls.2019.01201.

Dell'Aglio, E., Giustini, C., Kraut, A., Couté, Y., Costa, A., Decros, G., et al. (2019). Identification of the Arabidopsis Calmodulin-Dependent NAD+ Kinase That Sustains the Elicitor-Induced Oxidative Burst. *Plant Physiology* 181, 1449–1458. doi:10.1104/pp.19.00912.

Delorme-Hinoux, V., Bangash, S. A. K., Meyer, A. J., and Reichheld, J.-P. (2016). Nuclear thiol redox systems in plants. *Plant Science* 243, 84–95. doi:10.1016/j.plantsci.2015.12.002.

Denancé, N., Sánchez-Vallet, A., Goffner, D., and Molina, A. (2013). Disease resistance or growth: the role of plant hormones in balancing immune responses and fitness costs. *Front. Plant Sci.* 4. doi:10.3389/fpls.2013.00155.

Deslous, P., Bournonville, C., Decros, G., Okabe, Y., Mauxion, J.-P., Jorly, J., et al. (2021). Overproduction of ascorbic acid impairs pollen fertility in tomato. *Journal of Experimental Botany* 72, 3091–3107. doi:10.1093/jxb/erab040.

Destailleur, A., Poucet, T., Cabasson, C., Alonso, A. P., Cocuron, J.-C., Larbat, R., et al. (2021). The Evolution of Leaf Function during Development Is Reflected in Profound Changes in the Metabolic Composition of the Vacuole. *Metabolites* 11, 848. doi:10.3390/metabo11120848.

Deutsch, J. C. (2000). Dehydroascorbic acid. *Journal of Chromatography A* 881, 299–307. doi:10.1016/S0021-9673(00)00166-7.

Dietz, K.-J. (2003). PLANT PEROXIREDOXINS. *Annu. Rev. Plant Biol.* 54, 93–107. doi:10.1146/annurev.arplant.54.031902.134934.

Ding, Z.-S., Tian, S.-P., Zheng, X.-L., Zhou, Z.-W., and Xu, Y. (2007). Responses of reactive oxygen metabolism and quality in mango fruit to exogenous oxalic acid or salicylic acid under chilling temperature stress. *Physiologia Plantarum* 130, 112–121. doi:10.1111/j.1399-3054.2007.00893.x.

Donaldson, R. P. (1982). Nicotinamide cofactors (NAD and NADP) in glyoxysomes, mitochondria, and plastids isolated from castor bean endosperm. *Archives of Biochemistry and Biophysics* 215, 274–279. doi:10.1016/0003-9861(82)90305-8.

Dussarrat, T., Decros, G., Díaz, F. P., Gibon, Y., Latorre, C., Rolin, D., et al. (2021). "Another Tale from the Harsh World: How Plants Adapt to Extreme Environments," in *Annual Plant Reviews online*, ed. J. A. Roberts (Wiley), 551–603. doi:10.1002/9781119312994.apr0758.

Dutilleul, C. (2005). Mitochondria-Driven Changes in Leaf NAD Status Exert a Crucial Influence on the Control of Nitrate Assimilation and the Integration of Carbon and Nitrogen Metabolism. *PLANT PHYSIOLOGY* 139, 64–78. doi:10.1104/pp.105.066399.

Dutilleul, C., Driscoll, S., Cornic, G., De Paepe, R., Foyer, C. H., and Noctor, G. (2003a). Functional Mitochondrial Complex I Is Required by Tobacco Leaves for Optimal Photosynthetic Performance in Photorespiratory Conditions and during Transients. *Plant Physiol.* 131, 264–275. doi:10.1104/pp.011155.

Dutilleul, C., Garmier, M., Noctor, G., Mathieu, C., Chétrit, P., Foyer, C. H., et al. (2003b). Leaf Mitochondria Modulate Whole Cell Redox Homeostasis, Set Antioxidant Capacity, and Determine Stress Resistance through Altered Signaling and Diurnal Regulation. *Plant Cell* 15, 1212–1226. doi:10.1105/tpc.009464.

Dutilleul, C., Lelarge, C., Prioul, J.-L., De Paepe, R., Foyer, C. H., and Noctor, G. (2005). Mitochondria-Driven Changes in Leaf NAD Status Exert a Crucial Influence on the Control of Nitrate Assimilation and the Integration of Carbon and Nitrogen Metabolism. *Plant Physiol.* 139, 64–78. doi:10.1104/pp.105.066399.

Edge, R., and Truscott, T. (2018). Singlet Oxygen and Free Radical Reactions of Retinoids and Carotenoids—A Review. *Antioxidants* 7, 5. doi:10.3390/antiox7010005.

Egan, M. J., Wang, Z.-Y., Jones, M. A., Smirnoff, N., and Talbot, N. J. (2007). Generation of reactive oxygen species by fungal NADPH oxidases is required for rice blast disease. *Proceedings of the National Academy of Sciences* 104, 11772–11777. doi:10.1073/pnas.0700574104.

Elsässer, M., Feitosa-Araujo, E., Lichtenauer, S., Wagner, S., Fuchs, P., Giese, J., et al. (2020). Photosynthetic activity triggers pH and NAD redox signatures across different plant cell compartments. Plant Biology doi:10.1101/2020.10.31.363051.

Eltelib, H. A., Badejo, A. A., Fujikawa, Y., and Esaka, M. (2011). Gene expression of monodehydroascorbate reductase and dehydroascorbate reductase during fruit ripening and in response to environmental stresses in acerola (Malpighia glabra). *Journal of Plant Physiology* 168, 619–627. doi:10.1016/j.jplph.2010.09.003.

Emes, M. J. (2009). Oxidation of methionine residues: the missing link between stress and signalling responses in plants. *Biochemical Journal* 422, e1–e2. doi:10.1042/BJ20091063.

Exposito-Rodriguez, M., Laissue, P. P., Yvon-Durocher, G., Smirnoff, N., and Mullineaux, P. M. (2017). Photosynthesis-dependent H2O2 transfer from chloroplasts to nuclei provides a high-light signalling mechanism. *Nat Commun* 8, 49. doi:10.1038/s41467-017-00074-w.

Fanwoua, J., de Visser, P. H. B., Heuvelink, E., Yin, X., Struik, P. C., and Marcelis, L. F. M. (2013). A dynamic model of tomato fruit growth integrating cell division, cell growth and endoreduplication. *Functional Plant Biol.* 40, 1098. doi:10.1071/FP13007.

Faurobert, M., Pelpoir, E., and Chaïb, J. (2007). Phenol extraction of proteins for proteomic studies of recalcitrant plant tissues. *Methods Mol. Biol.* 355, 9–14. doi:10.1385/1-59745-227-0:9.

Feitosa-Araujo, E., Fonseca-Pereira, P., Pena, M. M., Medeiros, D. B., Perez de Souza, L., Yoshida, T., et al. (2020). Changes in intracellular NAD status affect stomatal development in an abscisic acid-dependent manner. *Plant J* 104, 1149–1168. doi:10.1111/tpj.15000.

Fellegrini, N., Ke, R., Yang, M., and Rice-Evans, C. (1999). “Screening of dietary carotenoids and carotenoid-rich fruit extracts for antioxidant activities applying 2,2′-azinobis(3-

ethylenebenzothiazoline-6-sulfonic acid radical cation decolorization assay," in *Methods in Enzymology* (Elsevier), 379–389. doi:10.1016/S0076-6879(99)99037-7.

Fenech, M., Amorim-Silva, V., Esteban del Valle, A., Arnaud, D., Ruiz-Lopez, N., Castillo, A. G., et al. (2021). The role of GDP-l-galactose phosphorylase in the control of ascorbate biosynthesis. *Plant Physiology* 185, 1574–1594. doi:10.1093/plphys/kiab010.

Fernandez-Pozo, N., Zheng, Y., Snyder, S. I., Nicolas, P., Shinozaki, Y., Fei, Z., et al. (2017). The Tomato Expression Atlas. *Bioinformatics* 33, 2397–2398. doi:10.1093/bioinformatics/btx190.

Ferretti, M., Destro, T., Tosatto, S. C. E., La Rocca, N., Rascio, N., and Masi, A. (2009). Gamma-glutamyl transferase in the cell wall participates in extracellular glutathione salvage from the root apoplast. *New Phytologist* 181, 115–126. doi:10.1111/j.1469-8137.2008.02653.x.

Finkelstein, R., Reeves, W., Ariizumi, T., and Steber, C. (2008). Molecular Aspects of Seed Dormancy. *Annu. Rev. Plant Biol.* 59, 387–415. doi:10.1146/annurev.arplant.59.032607.092740.

Finkemeier, I., Laxa, M., Miguet, L., Howden, A. J. M., and Sweetlove, L. J. (2011). Proteins of Diverse Function and Subcellular Location Are Lysine Acetylated in Arabidopsis. *Plant Physiology* 155, 1779–1790. doi:10.1104/pp.110.171595.

Fischer, B. B., Hideg, É., and Krieger-Liszkay, A. (2013). Production, Detection, and Signaling of Singlet Oxygen in Photosynthetic Organisms. *Antioxidants & Redox Signaling* 18, 2145–2162. doi:10.1089/ars.2012.5124.

Fishman, S., and Génard, M. (1998). A biophysical model of fruit growth: simulation of seasonal and diurnal dynamics of mass. *Plant, Cell & Environment* 21, 739–752. doi:10.1046/j.1365-3040.1998.00322.x.

Foyer, C. H. (2015). Redox homeostasis: Opening up ascorbate transport. *Nature Plants* 1, 14012. doi:10.1038/nplants.2014.12.

Foyer, C. H. (2018). Reactive oxygen species, oxidative signaling and the regulation of photosynthesis. *Environmental and Experimental Botany* 154, 134–142. doi:10.1016/j.envexpbot.2018.05.003.

Foyer, C. H., Bloom, A. J., Queval, G., and Noctor, G. (2009). Photorespiratory Metabolism: Genes, Mutants, Energetics, and Redox Signaling. *Annu. Rev. Plant Biol.* 60, 455–484. doi:10.1146/annurev.arplant.043008.091948.

Foyer, C. H., and Halliwell, B. (1976). The presence of glutathione and glutathione reductase in chloroplasts: A proposed role in ascorbic acid metabolism. *Planta* 133, 21–25. doi:10.1007/BF00386001.

Foyer, C. H., Kerchev, P. I., and Hancock, R. D. (2012). The ABA-INSENSITIVE-4 (ABI4) transcription factor links redox, hormone and sugar signaling pathways. *Plant Signaling & Behavior* 7, 276–281. doi:10.4161/psb.18770.

Foyer, C. H., and Noctor, G. (2011). Ascorbate and Glutathione: The Heart of the Redox Hub. *Plant Physiol.* 155, 2–18. doi:10.1104/pp.110.167569.

Foyer, C. H., and Noctor, G. (2016). Stress-triggered redox signalling: what's in pROSpect?: What's in pROSpect? *Plant, Cell & Environment* 39, 951–964. doi:10.1111/pce.12621.

Foyer, C. H., Noctor, G., and Hodges, M. (2011). Respiration and nitrogen assimilation: targeting mitochondria-associated metabolism as a means to enhance nitrogen use efficiency. *Journal of Experimental Botany* 62, 1467–1482. doi:10.1093/jxb/erq453.

Foyer, C. H., Theodoulou, F. L., and Delrot, S. (2001). The functions of inter- and intracellular glutathione transport systems in plants. *Trends in Plant Science* 6, 486–492. doi:10.1016/S1360-1385(01)02086-6.

Franceschi, V. R., and Nakata, P. A. (2005). CALCIUM OXALATE IN PLANTS: Formation and Function. *Annu. Rev. Plant Biol.* 56, 41–71. doi:10.1146/annurev.arplant.56.032604.144106.

Franceschi, V. R., and Tarlyn, N. M. (2002). L-Ascorbic Acid Is Accumulated in Source Leaf Phloem and Transported to Sink Tissues in Plants. *Plant Physiology* 130, 649–656. doi:10.1104/pp.007062.

Frendo, P., Harrison, J., Norman, C., Jiménez, M. J. H., Van de Sype, G., Gilabert, A., et al. (2005). Glutathione and Homoglutathione Play a Critical Role in the Nodulation Process of *Medicago truncatula*. *MPMI* 18, 254–259. doi:10.1094/MPMI-18-0254.

Fridovich, I. (1997). Superoxide Anion Radical ($O^{\cdot}_2$), Superoxide Dismutases, and Related Matters. *Journal of Biological Chemistry* 272, 18515–18517. doi:10.1074/jbc.272.30.18515.

Friedman, J., Hastie, T., and Tibshirani, R. (2010). Regularization Paths for Generalized Linear Models via Coordinate Descent. *J Stat Softw* 33, 1–22.

Frugoli, J. A., Zhong, H. H., Nuccio, M. L., McCourt, P., McPeek, M. A., Thomas, T. L., et al. (1996). Catalase Is Encoded by a Multigene Family in Arabidopsis thaliana (L.). *Plant Physiology* 112, 327–336. doi:10.1104/pp.112.1.327.

Fu, L., Xu, B.-T., Xu, X.-R., Gan, R.-Y., Zhang, Y., Xia, E.-Q., et al. (2011). Antioxidant capacities and total phenolic contents of 62 fruits. *Food Chemistry* 129, 345–350. doi:10.1016/j.foodchem.2011.04.079.

Fu, Z. Q., and Dong, X. (2013). Systemic Acquired Resistance: Turning Local Infection into Global Defense. *Annu. Rev. Plant Biol.* 64, 839–863. doi:10.1146/annurev-arplant-042811-105606.

Fujiwara, A., Shimura, H., Masuta, C., Sano, S., and Inukai, T. (2013). Exogenous ascorbic acid derivatives and dehydroascorbic acid are effective antiviral agents against Turnip mosaic virus in Brassica rapa. *J Gen Plant Pathol* 79, 198–204. doi:10.1007/s10327-013-0439-5.

Gakière, B., Fernie, A. R., and Pétriacq, P. (2018a). More to NAD+ than meets the eye: A regulator of metabolic pools and gene expression in Arabidopsis. *Free Radical Biology and Medicine* 122, 86–95. doi:10.1016/j.freeradbiomed.2018.01.003.

Gakière, B., Hao, J., de Bont, L., Pétriacq, P., Nunes-Nesi, A., and Fernie, A. R. (2018b). NAD^+ Biosynthesis and Signaling in Plants. *Critical Reviews in Plant Sciences* 37, 259–307. doi:10.1080/07352689.2018.1505591.

Gallie, D. R. (2013). Increasing Vitamin C Content in Plant Foods to Improve Their Nutritional Value—Successes and Challenges. *Nutrients* 5, 3424–3446. doi:10.3390/nu5093424.

Garcia, V., Stevens, R., Gil, L., Gilbert, L., Gest, N., Petit, J., et al. (2009). An integrative genomics approach for deciphering the complex interactions between ascorbate metabolism and fruit growth and composition in tomato. *C. R. Biol.* 332, 1007–1021. doi:10.1016/j.crvi.2009.09.013.

Gautier, H., Massot, C., Stevens, R., Sérino, S., and Génard, M. (2009). Regulation of tomato fruit ascorbate content is more highly dependent on fruit irradiance than leaf irradiance. *Annals of Botany* 103, 495–504. doi:10.1093/aob/mcn233.

Geigenberger, P., and Fernie, A. R. (2014). Metabolic Control of Redox and Redox Control of Metabolism in Plants. *Antioxidants & Redox Signaling* 21, 1389–1421. doi:10.1089/ars.2014.6018.

Geigenberger, P., Thormählen, I., Daloso, D. M., and Fernie, A. R. (2017). The Unprecedented Versatility of the Plant Thioredoxin System. *Trends Plant Sci.* 22, 249–262. doi:10.1016/j.tplants.2016.12.008.

Génard, M., Baldazzi, V., and Gibon, Y. (2014). Metabolic studies in plant organs: don't forget dilution by growth. *Front. Plant Sci.* 5. doi:10.3389/fpls.2014.00085.

Gest, N., Gautier, H., and Stevens, R. (2013). Ascorbate as seen through plant evolution: the rise of a successful molecule? *EXBOTJ* 64, 33–53. doi:10.1093/jxb/ers297.

Gilmore, I. S., Heiles, S., and Pieterse, C. L. (2019). Metabolic Imaging at the Single-Cell Scale: Recent Advances in Mass Spectrometry Imaging. *Annual Rev. Anal. Chem.* 12, 201–224. doi:10.1146/annurev-anchem-061318-115516.

Gilroy, S., Suzuki, N., Miller, G., Choi, W.-G., Toyota, M., Devireddy, A. R., et al. (2014). A tidal wave of signals: calcium and ROS at the forefront of rapid systemic signaling. *Trends in Plant Science* 19, 623–630. doi:10.1016/j.tplants.2014.06.013.

Giovinazzo, G., D'Amico, L., Paradiso, A., Bollini, R., Sparvoli, F., and DeGara, L. (2004). Antioxidant metabolite profiles in tomato fruit constitutively expressing the grapevine stilbene synthase gene: Antioxidant levels in tomato synthesizing resveratrol. *Plant Biotechnology Journal* 3, 57–69. doi:10.1111/j.1467-7652.2004.00099.x.

Gonzalez-Reyes, J. A., Alcain, F. J., Caler, J. A., Serrano, A., Cordoba, F., and Navas, P. (1995). Stimulation of onion root elongation by ascorbate and ascorbate free radical inAllium cepa L. *Protoplasma* 184, 31–35. doi:10.1007/BF01276898.

Gorzynik-Debicka, M., Przychodzen, P., Cappello, F., Kuban-Jankowska, A., Marino Gammazza, A., Knap, N., et al. (2018). Potential Health Benefits of Olive Oil and Plant Polyphenols. *International Journal of Molecular Sciences* 19, 686. doi:10.3390/ijms19030686.

Graßmann, J. (2005). "Terpenoids as Plant Antioxidants," in *Vitamins & Hormones* (Elsevier), 505–535. doi:10.1016/S0083-6729(05)72015-X.

Green, M., and Fry, S. (2005). Apoplastic degradation of ascorbate: Novel enzymes and metabolites permeating the plant cell wall. *Plant Biosystems - An International Journal Dealing with all Aspects of Plant Biology* 139, 2–7. doi:10.1080/11263500500056849.

Guérard, F., Pétriacq, P., Gakière, B., and Tcherkez, G. (2011). Liquid chromatography/time-of-flight mass spectrometry for the analysis of plant samples: A method for simultaneous screening of common cofactors or nucleotides and application to an engineered plant line. *Plant Physiology and Biochemistry* 49, 1117–1125. doi:10.1016/j.plaphy.2011.06.003.

Gugliandolo, A., Bramanti, P., and Mazzon, E. (2017). Role of Vitamin E in the Treatment of Alzheimer's Disease: Evidence from Animal Models. *International Journal of Molecular Sciences* 18, 2504. doi:10.3390/ijms18122504.

Hagemann, M., Weber, A. P., and Eisenhut, M. (2016). Photorespiration: origins and metabolic integration in interacting compartments. *EXBOTJ* 67, 2915–2918. doi:10.1093/jxb/erw178.

Halliwell, B., and Foyer, C. H. (1978). Properties and physiological function of a glutathione reductase purified from spinach leaves by affinity chromatography. *Planta* 139, 9–17. doi:10.1007/BF00390803.

Hanhineva, K., and Aharoni, A. (2010). "Metabolomics in Fruit Development," in *Molecular Techniques in Crop Improvement*, eds. S. M. Jain and D. S. Brar (Dordrecht: Springer Netherlands), 675–693. doi:10.1007/978-90-481-2967-6_29.

Harden, A., and Young, W. (1906). The alcoholic ferment of yeast-juice. *Proc. R. Soc. Lond. B.* 78, 369–375. doi:10.1098/rspb.1906.0070.

Hasanuzzaman, M., Nahar, K., Anee, T. I., and Fujita, M. (2017). Glutathione in plants: biosynthesis and physiological role in environmental stress tolerance. *Physiol Mol Biol Plants* 23, 249–268. doi:10.1007/s12298-017-0422-2.

Hashida, S., Itami, T., Takahara, K., Hirabayashi, T., Uchimiya, H., and Kawai-Yamada, M. (2016). Increased Rate of NAD Metabolism Shortens Plant Longevity by Accelerating Developmental Senescence in *Arabidopsis*. *Plant Cell Physiol* 57, 2427–2439. doi:10.1093/pcp/pcw155.

Hashida, S., Miyagi, A., Nishiyama, M., Yoshida, K., Hisabori, T., and Kawai-Yamada, M. (2018). Ferredoxin/thioredoxin system plays an important role in the chloroplastic NADP status of Arabidopsis. *Plant J* 95, 947–960. doi:10.1111/tpj.14000.

Hashida, S., Takahashi, H., Kawai-Yamada, M., and Uchimiya, H. (2007). Arabidopsis thaliana nicotinate/nicotinamide mononucleotide adenyltransferase (AtNMNAT) is required for pollen tube growth: AtNMNATis required for pollen tube growth. *The Plant Journal* 49, 694–703. doi:10.1111/j.1365-313X.2006.02989.x.

Hashida, S., Takahashi, H., Takahara, K., Kawai-Yamada, M., Kitazaki, K., Shoji, K., et al. (2013). NAD+ Accumulation during Pollen Maturation in Arabidopsis Regulating Onset of Germination. *Molecular Plant* 6, 216–225. doi:10.1093/mp/sss071.

Hashida, S., Takahashi, H., and Uchimiya, H. (2009). The role of NAD biosynthesis in plant development and stress responses. *Annals of Botany* 103, 819–824. doi:10.1093/aob/mcp019.

Havé, M., Balliau, T., Cottyn-Boitte, B., Dérond, E., Cueff, G., Soulay, F., et al. (2018). Increases in activity of proteasome and papain-like cysteine protease in Arabidopsis autophagy mutants: back-up compensatory effect or cell-death promoting effect? *J. Exp. Bot.* 69, 1369–1385. doi:10.1093/jxb/erx482.

Heineke, D., Riens, B., Grosse, H., Hoferichter, P., Peter, U., Flügge, U.-I., et al. (1991). Redox Transfer across the Inner Chloroplast Envelope Membrane. *Plant Physiol.* 95, 1131–1137. doi:10.1104/pp.95.4.1131.

Heinrich, R., and Rapoport, T. A. (1974). A Linear Steady-State Treatment of Enzymatic Chains. General Properties, Control and Effector Strength. *Eur J Biochem* 42, 89–95. doi:10.1111/j.1432-1033.1974.tb03318.x.

Hendrix, S., Jozefczak, M., Wójcik, M., Deckers, J., Vangronsveld, J., and Cuypers, A. (2020). Glutathione: A key player in metal chelation, nutrient homeostasis, cell cycle regulation and the DNA damage response in cadmium-exposed Arabidopsis thaliana. *Plant Physiology and Biochemistry* 154, 498–507. doi:10.1016/j.plaphy.2020.06.006.

Hodges, M., Dellero, Y., Keech, O., Betti, M., Raghavendra, A. S., Sage, R., et al. (2016). Perspectives for a better understanding of the metabolic integration of photorespiration within a complex plant primary metabolism network. *J. Exp. Bot.* 67, 3015–3026. doi:10.1093/jxb/erw145.

Hofmann, N. R. (2009). Glutaredoxin Functions in Floral Development. *Plant Cell* 21, 363–363. doi:10.1105/tpc.109.210210.

Holtgrefe, S., Gohlke, J., Starmann, J., Druce, S., Klocke, S., Altmann, B., et al. (2008). Regulation of plant cytosolic glyceraldehyde 3-phosphate dehydrogenase isoforms by thiol modifications. *Physiol Plant* 133, 211–228. doi:10.1111/j.1399-3054.2008.01066.x.

Hoops, S., Sahle, S., Gauges, R., Lee, C., Pahle, J., Simus, N., et al. (2006). COPASI--a COmplex PAthway SImulator. *Bioinformatics* 22, 3067–3074. doi:10.1093/bioinformatics/btl485.

Hopkins, F. G., and Morgan, E. J. (1936). Some relations between ascorbic acid and glutathione. *Biochemical Journal* 30, 1446–1462. doi:10.1042/bj0301446.

Horemans, N., Foyer, C. H., and Asard, H. (2000). Transport and action of ascorbate at the plant plasma membrane. *Trends in Plant Science* 5, 263–267. doi:10.1016/S1360-1385(00)01649-6.

Hossain, M. A., Munné-Bosch, S., Burritt, D. J., Diaz-Vivancos, P., Fujita, M., and Lorence, A. eds. (2017). *Ascorbic Acid in Plant Growth, Development and Stress Tolerance*. Cham: Springer International Publishing doi:10.1007/978-3-319-74057-7.

Hummel, W., and Gröger, H. (2014). Strategies for regeneration of nicotinamide coenzymes emphasizing self-sufficient closed-loop recycling systems. *Journal of Biotechnology* 191, 22–31. doi:10.1016/j.jbiotec.2014.07.449.

Hunt, L., and Gray, J. E. (2009). The relationship between pyridine nucleotides and seed dormancy. *New Phytologist* 181, 62–70. doi:10.1111/j.1469-8137.2008.02641.x.

Hunt, L., Holdsworth, M. J., and Gray, J. E. (2007). Nicotinamidase activity is important for germination: Nicotinamidase activity and germination. *The Plant Journal* 51, 341–351. doi:10.1111/j.1365-313X.2007.03151.x.

Igamberdiev, A. U., and Gardeström, P. (2003). Regulation of NAD- and NADP-dependent isocitrate dehydrogenases by reduction levels of pyridine nucleotides in mitochondria and cytosol of pea leaves. *Biochimica et Biophysica Acta (BBA) - Bioenergetics* 1606, 117–125. doi:10.1016/S0005-2728(03)00106-3.

Imaizumi, T., and Kay, S. (2006). Photoperiodic control of flowering: not only by coincidence. *Trends in Plant Science* 11, 550–558. doi:10.1016/j.tplants.2006.09.004.

Imhoff, B., and Hansen, J. (2011). Differential redox potential profiles during adipogenesis and osteogenesis. *Cellular and Molecular Biology Letters* 16. doi:10.2478/s11658-010-0042-0.

Isherwood, F. A., Chen, Y. T., and Mapson, L. W. (1954). Synthesis of l-ascorbic acid in plants and animals. *Biochemical Journal* 56, 1–15. doi:10.1042/bj0560001.

Ishikawa, T., Dowdle, J., and Smirnoff, N. (2006). Progress in manipulating ascorbic acid biosynthesis and accumulation in plants. *Physiol Plant* 126, 343–355. doi:10.1111/j.1399-3054.2006.00640.x.

Jagadish, S. V. K., Bahuguna, R. N., Djanaguiraman, M., Gamuyao, R., Prasad, P. V. V., and Craufurd, P. Q. (2016). Implications of High Temperature and Elevated CO2 on Flowering Time in Plants. *Front. Plant Sci.* 7. doi:10.3389/fpls.2016.00913.

Jain, A. K., and Nessler, C. L. (2000). Metabolic engineering of an alternative pathway for ascorbic acid biosynthesis in plants. *Molecular Breeding* 6, 73–78. doi:10.1023/A:1009680818138.

Jiang, X., Lin, H., Lin, M., Chen, Y., Wang, H., Lin, Y., et al. (2018). A novel chitosan formulation treatment induces disease resistance of harvested litchi fruit to Peronophythora litchii in association with ROS metabolism. *Food Chem* 266, 299–308. doi:10.1016/j.foodchem.2018.06.010.

Jimenez, A., Creissen, G., Kular, B., Firmin, J., Robinson, S., Verhoeyen, M., et al. (2002). Changes in oxidative processes and components of the antioxidant system during tomato fruit ripening. *Planta* 214, 751–758. doi:10.1007/s004250100667.

Jin, P., Zheng, C., Huang, Y., Wang, X., Luo, Z., and Zheng, Y. (2016). Hot air treatment activates defense responses and induces resistance against Botrytis cinerea in strawberry fruit. *Journal of Integrative Agriculture* 15, 2658–2665. doi:10.1016/S2095-3119(16)61387-4.

Johansson, M., and Staiger, D. (2015). Time to flower: interplay between photoperiod and the circadian clock. *Journal of Experimental Botany* 66, 719–730. doi:10.1093/jxb/eru441.

Jozefczak, M., Bohler, S., Schat, H., Horemans, N., Guisez, Y., Remans, T., et al. (2015). Both the concentration and redox state of glutathione and ascorbate influence the sensitivity of arabidopsis to cadmium. *Annals of Botany* 116, 601–612. doi:10.1093/aob/mcv075.

Junglee, S., Urban, L., Sallanon, H., and Lopez-Lauri, F. (2014). Optimized Assay for Hydrogen Peroxide Determination in Plant Tissue Using Potassium Iodide. *AJAC* 05, 730–736. doi:10.4236/ajac.2014.511081.

Just, D., Garcia, V., Fernandez, L., Bres, C., Mauxion, J.-P., Petit, J., et al. (2013). Micro-Tom mutants for functional analysis of target genes and discovery of new alleles in tomato. *Plant Biotechnology* 30, 225–231. doi:10.5511/plantbiotechnology.13.0622a.

Justi, K. C., Visentainer, J. V., Evelázio de Souza, N., and Matsushita, M. (2000). Nutritional composition and vitamin C stability in stored camu-camu (Myrciaria dubia) pulp. *Arch Latinoam Nutr* 50, 405–408.

Kacser, H., and Burns, J. A. (1973). The control of flux. *Symp Soc Exp Biol* 27, 65–104.

Kassambara, A., and Mundt, F. (2020). *factoextra: Extract and Visualize the Results of Multivariate Data Analyses*. Available at: https://CRAN.R-project.org/package=factoextra.

Kataya, A. R. A., and Reumann, S. (2010). Arabidopsis glutathione reductase 1 is dually targeted to peroxisomes and the cytosol. *Plant Signaling & Behavior* 5, 171–175. doi:10.4161/psb.5.2.10527.

Kato, J., Yamahara, T., Tanaka, K., Takio, S., and Satoh, T. (1997). Characterization of catalase from green algae Chlamydomonas reinhardtii. *Journal of Plant Physiology* 151, 262–268. doi:10.1016/S0176-1617(97)80251-9.

Kato, M., and Lin, S.-J. (2014). Regulation of NAD+ metabolism, signaling and compartmentalization in the yeast Saccharomyces cerevisiae. *DNA Repair* 23, 49–58. doi:10.1016/j.dnarep.2014.07.009.

Kato, S., Ueno, T., Fukuzumi, S., and Watanabe, Y. (2004). Catalase Reaction by Myoglobin Mutants and Native Catalase. *Journal of Biological Chemistry* 279, 52376–52381. doi:10.1074/jbc.M403532200.

Katoh, A., Uenohara, K., Akita, M., and Hashimoto, T. (2006). Early Steps in the Biosynthesis of NAD in Arabidopsis Start with Aspartate and Occur in the Plastid. *Plant Physiol.* 141, 851–857. doi:10.1104/pp.106.081091.

Kelley, D., Adkins, Y., and Laugero, K. (2018). A Review of the Health Benefits of Cherries. *Nutrients* 10, 368. doi:10.3390/nu10030368.

Kenney, A. M., McKay, J. K., Richards, J. H., and Juenger, T. E. (2014). Direct and indirect selection on flowering time, water-use efficiency (WUE , δ^{13} C), and WUE plasticity to drought in *Arabidopsis thaliana*. *Ecol Evol* 4, 4505–4521. doi:10.1002/ece3.1270.

Kirkman, H. N., and Gaetani, G. F. (2007). Mammalian catalase: a venerable enzyme with new mysteries. *Trends in Biochemical Sciences* 32, 44–50. doi:10.1016/j.tibs.2006.11.003.

Klapheck, S., Chrost, B., Starke, J., and Zimmermann, H. (1992). γ-Glutamylcysteinylserine - A New Homologue of Glutathione in Plants of the Family Poaceae*. *Botanica Acta* 105, 174–179. doi:10.1111/j.1438-8677.1992.tb00284.x.

Knecht, K., Sandfuchs, K., Kulling, S. E., and Bunzel, D. (2015). Tocopherol and tocotrienol analysis in raw and cooked vegetables: A validated method with emphasis on sample preparation. *Food Chemistry* 169, 20–27. doi:10.1016/j.foodchem.2014.07.099.

Kolde, R. (2019). *pheatmap: Pretty Heatmaps*. Available at: https://CRAN.R-project.org/package=pheatmap.

Kollist, H., Zandalinas, S. I., Sengupta, S., Nuhkat, M., Kangasjärvi, J., and Mittler, R. (2019). Rapid Responses to Abiotic Stress: Priming the Landscape for the Signal Transduction Network. *Trends in Plant Science* 24, 25–37. doi:10.1016/j.tplants.2018.10.003.

Kopriva, S. (2004). Control of sulphate assimilation and glutathione synthesis: interaction with N and C metabolism. *Journal of Experimental Botany* 55, 1831–1842. doi:10.1093/jxb/erh203.

Köster, S., Upmeier, B., Komossa, D., and Barz, W. (1989). Nicotinic Acid Conjugation in Plants and Plant Cell Cultures of Potato (Solanum tuberosum). *Zeitschrift für Naturforschung C* 44, 623–628. doi:10.1515/znc-1989-7-813.

Kotchoni, S. O., Larrimore, K. E., Mukherjee, M., Kempinski, C. F., and Barth, C. (2009). Alterations in the Endogenous Ascorbic Acid Content Affect Flowering Time in Arabidopsis. *Plant Physiology* 149, 803–815. doi:10.1104/pp.108.132324.

Kourelis, J., Malik, S., Mattinson, O., Krauter, S., Kahlon, P. S., Paulus, J. K., et al. (2020). Evolution of a guarded decoy protease and its receptor in solanaceous plants. *Nat Commun* 11, 4393. doi:10.1038/s41467-020-18069-5.

Kranner, I., Birtić, S., Anderson, K. M., and Pritchard, H. W. (2006). Glutathione half-cell reduction potential: A universal stress marker and modulator of programmed cell death? *Free Radical Biology and Medicine* 40, 2155–2165. doi:10.1016/j.freeradbiomed.2006.02.013.

Kröniger, W., Rennenberg, H., and Polle, A. (1992). Purification of Two Superoxide Dismutase Isozymes and Their Subcellular Localization in Needles and Roots of Norway Spruce (*Picea abies* L.) Trees. *Plant Physiol.* 100, 334–340. doi:10.1104/pp.100.1.334.

Kucera, B., Cohn, M. A., and Leubner-Metzger, G. (2005). Plant hormone interactions during seed dormancy release and germination. *Seed Sci. Res.* 15, 281–307. doi:10.1079/SSR2005218.

Kukavica, B., Mojović, M., Vuččinić, Ž., Maksimović, V., Takahama, U., and Jovanović, S. V. (2009). Generation of Hydroxyl Radical in Isolated Pea Root Cell Wall, and the Role of Cell Wall-Bound Peroxidase, Mn-SOD and Phenolics in Their Production. *Plant and Cell Physiology* 50, 304–317. doi:10.1093/pcp/pcn199.

Kumar, V., Irfan, M., Ghosh, S., Chakraborty, N., Chakraborty, S., and Datta, A. (2016). Fruit ripening mutants reveal cell metabolism and redox state during ripening. *Protoplasma* 253, 581–594. doi:10.1007/s00709-015-0836-z.

Lado, J., Zacarías, L., Gurrea, A., Page, A., Stead, A., and Rodrigo, M. J. (2015). Exploring the diversity in Citrus fruit colouration to decipher the relationship between plastid ultrastructure and carotenoid composition. *Planta* 242, 645–661. doi:10.1007/s00425-015-2370-9.

Laing, W. A., Wright, M. A., Cooney, J., and Bulley, S. M. (2007). The missing step of the L-galactose pathway of ascorbate biosynthesis in plants, an L-galactose guanyltransferase, increases leaf ascorbate content. *Proceedings of the National Academy of Sciences* 104, 9534–9539. doi:10.1073/pnas.0701625104.

Laing, W., Norling, C., Brewster, D., Wright, M., and Bulley, S. (2017). Ascorbate concentration in *Arabidopsis thaliana* and expression of ascorbate related genes using RNAseq in response to light and the diurnal cycle. Plant Biology doi:10.1101/138008.

Lamb, R. S., Citarelli, M., and Teotia, S. (2012). Functions of the poly(ADP-ribose) polymerase superfamily in plants. *Cell. Mol. Life Sci.* 69, 175–189. doi:10.1007/s00018-011-0793-4.

Landi, L., De Miccolis Angelini, R. M., Pollastro, S., Feliziani, E., Faretra, F., and Romanazzi, G. (2017). Global Transcriptome Analysis and Identification of Differentially Expressed Genes in Strawberry after Preharvest Application of Benzothiadiazole and Chitosan. *Frontiers in Plant Science* 8. doi:10.3389/fpls.2017.00235.

Lang, Z., Wang, Y., Tang, K., Tang, D., Datsenka, T., Cheng, J., et al. (2017). Critical roles of DNA demethylation in the activation of ripening-induced genes and inhibition of ripening-repressed genes in tomato fruit. *Proc. Natl. Acad. Sci. U.S.A.* 114, E4511–E4519. doi:10.1073/pnas.1705233114.

Lê, S., Josse, J., and Husson, F. (2008). FactoMineR : An *R* Package for Multivariate Analysis. *J. Stat. Soft.* 25. doi:10.18637/jss.v025.i01.

Lee, D., Lal, N. K., Lin, Z.-J. D., Ma, S., Liu, J., Castro, B., et al. (2020). Regulation of reactive oxygen species during plant immunity through phosphorylation and ubiquitination of RBOHD. *Nat Commun* 11, 1838. doi:10.1038/s41467-020-15601-5.

Lelievre, J.-M., Latche, A., Jones, B., Bouzayen, M., and Pech, J.-C. (1997). Ethylene and fruit ripening. *Physiol Plant* 101, 727–739. doi:10.1111/j.1399-3054.1997.tb01057.x.

Leng, P., Yuan, B., and Guo, Y. (2013). The role of abscisic acid in fruit ripening and responses to abiotic stress. *Journal of Experimental Botany* 65, 4577–4588. doi:10.1093/jxb/eru204.

Lescourret, F., and Genard, M. (2005). A virtual peach fruit model simulating changes in fruit quality during the final stage of fruit growth. *Tree Physiology* 25, 1303–1315. doi:10.1093/treephys/25.10.1303.

Leustek, T. (2002). Sulfate Metabolism. *The Arabidopsis Book* 1, e0017. doi:10.1199/tab.0017.

Levy, Y. Y., and Dean, C. (1998). The Transition to Flowering. *Plant Cell* 10, 1973–1989. doi:10.1105/tpc.10.12.1973.

Li, B.-B., Wang, X., Tai, L., Ma, T.-T., Shalmani, A., Liu, W.-T., et al. (2018a). NAD Kinases: Metabolic Targets Controlling Redox Co-enzymes and Reducing Power Partitioning in Plant Stress and Development. *Front. Plant Sci.* 9, 379. doi:10.3389/fpls.2018.00379.

Li, J., Trivedi, P., and Wang, N. (2016). Field Evaluation of Plant Defense Inducers for the Control of Citrus Huanglongbing. *Phytopathology®* 106, 37–46. doi:10.1094/PHYTO-08-15-0196-R.

Li, R., Xin, S., Tao, C., Jin, X., and Li, H. (2017a). Cotton Ascorbate Oxidase Promotes Cell Growth in Cultured Tobacco Bright Yellow-2 Cells through Generation of Apoplast Oxidation. *IJMS* 18, 1346. doi:10.3390/ijms18071346.

Li, W., Zhang, F., Chang, Y., Zhao, T., Schranz, M. E., and Wang, G. (2015). Nicotinate O-Glucosylation Is an Evolutionarily Metabolic Trait Important for Seed Germination under Stress Conditions in Arabidopsis thaliana. *The Plant Cell* 27, 1907–1924. doi:10.1105/tpc.15.00223.

Li, W., Zhang, F., Wu, R., Jia, L., Li, G., Guo, Y., et al. (2017b). A Novel N-Methyltransferase in Arabidopsis Appears to Feed a Conserved Pathway for Nicotinate Detoxification among Land Plants and Is Associated with Lignin Biosynthesis. *Plant Physiol.* 174, 1492–1504. doi:10.1104/pp.17.00259.

Li, W.-Y., Wang, X., Li, R., Li, W.-Q., and Chen, K.-M. (2014). Genome-Wide Analysis of the NADK Gene Family in Plants. *PLoS ONE* 9, e101051. doi:10.1371/journal.pone.0101051.

Li, Y., Wang, H., Zhang, Y., and Martin, C. (2018b). Can the world's favorite fruit, tomato, provide an effective biosynthetic chassis for high-value metabolites? *Plant Cell Rep* 37, 1443–1450. doi:10.1007/s00299-018-2283-8.

Liang, W.-J., Johnson, D., and Jarvis, S. M. (2001). Vitamin C transport systems of mammalian cells. *Molecular Membrane Biology* 18, 87–95. doi:10.1080/09687680110033774.

Liebermeister, W., and Klipp, E. (2006). Bringing metabolic networks to life: convenience rate law and thermodynamic constraints. *Theor Biol Med Model* 3, 41. doi:10.1186/1742-4682-3-41.

Liebthal, M., Maynard, D., and Dietz, K.-J. (2018). Peroxiredoxins and Redox Signaling in Plants. *Antioxidants & Redox Signaling* 28, 609–624. doi:10.1089/ars.2017.7164.

Liedschulte, V., Wachter, A., Zhigang, A., and Rausch, T. (2010). Exploiting plants for glutathione (GSH) production: Uncoupling GSH synthesis from cellular controls results in unprecedented GSH accumulation: Exploiting plants for GSH production. *Plant Biotechnology Journal* 8, 807–820. doi:10.1111/j.1467-7652.2010.00510.x.

Lindermayr, C. (2018). Crosstalk between reactive oxygen species and nitric oxide in plants: Key role of S-nitrosoglutathione reductase. *Free Radical Biology and Medicine* 122, 110–115. doi:10.1016/j.freeradbiomed.2017.11.027.

Lindermayr, C., Saalbach, G., Bahnweg, G., and Durner, J. (2006). Differential Inhibition of Arabidopsis Methionine Adenosyltransferases by Protein S-Nitrosylation. *Journal of Biological Chemistry* 281, 4285–4291. doi:10.1074/jbc.M511635200.

Lindermayr, C., Saalbach, G., and Durner, J. (2005). Proteomic Identification of S-Nitrosylated Proteins in Arabidopsis. *Plant Physiology* 137, 921–930. doi:10.1104/pp.104.058719.

Liso, R., Innocenti, A. M., Bitonti, M. B., and Arrigoni, O. (1988). Ascorbic acid-induced progression of quiescent centre cells from G1 to S phase. *New Phytol* 110, 469–471. doi:10.1111/j.1469-8137.1988.tb00284.x.

Liu, Y., Yang, X., Zhu, S., and Wang, Y. (2016). Postharvest application of MeJA and NO reduced chilling injury in cucumber (Cucumis sativus) through inhibition of H2O2 accumulation. *Postharvest Biology and Technology* 119, 77–83. doi:10.1016/j.postharvbio.2016.04.003.

López-Vidal, O., Camejo, D., Rivera-Cabrera, F., Konigsberg, M., Villa-Hernández, J. M., Mendoza-Espinoza, J. A., et al. (2016). Mitochondrial ascorbate–glutathione cycle and proteomic analysis of carbonylated proteins during tomato (Solanum lycopersicum) fruit ripening. *Food Chemistry* 194, 1064–1072. doi:10.1016/j.foodchem.2015.08.055.

Louarn, G., Lecoeur, J., and Lebon, E. (2007). A Three-dimensional Statistical Reconstruction Model of Grapevine (Vitis vinifera) Simulating Canopy Structure Variability within and between Cultivar/Training System Pairs. *Annals of Botany* 101, 1167–1184. doi:10.1093/aob/mcm170.

Lu, Y.-P., Li, Z.-S., Drozdowicz, Y. M., Hörtensteiner, S., Martinoia, E., and Rea, P. A. (1998). AtMRP2, an Arabidopsis ATP Binding Cassette Transporter Able to Transport Glutathione *S*-Conjugates and Chlorophyll Catabolites: Functional Comparisons with AtMRP1. *Plant Cell* 10, 267–282. doi:10.1105/tpc.10.2.267.

Lum, G. B., Shelp, B. J., DeEll, J. R., and Bozzo, G. G. (2016). Oxidative metabolism is associated with physiological disorders in fruits stored under multiple environmental stresses. *Plant Science* 245, 143–152. doi:10.1016/j.plantsci.2016.02.005.

Luna, E., Flandin, A., Cassan, C., Prigent, S., Chevanne, C., Kadiri, C. F., et al. (2020). Metabolomics to Exploit the Primed Immune System of Tomato Fruit. *Metabolites* 10, 96. doi:10.3390/metabo10030096.

Lytovchenko, A., Eickmeier, I., Pons, C., Osorio, S., Szecowka, M., Lehmberg, K., et al. (2011). Tomato Fruit Photosynthesis Is Seemingly Unimportant in Primary Metabolism and Ripening But Plays a Considerable Role in Seed Development. *Plant Physiol.* 157, 1650–1663. doi:10.1104/pp.111.186874.

Ma, N. L., Rahmat, Z., and Lam, S. S. (2013). A Review of the “Omics” Approach to Biomarkers of Oxidative Stress in Oryza sativa. *Int J Mol Sci* 14, 7515–7541. doi:10.3390/ijms14047515.

Ma, X., Wang, W., Bittner, F., Schmidt, N., Berkey, R., Zhang, L., et al. (2016). Dual and Opposing Roles of Xanthine Dehydrogenase in Defense-Associated Reactive Oxygen Species Metabolism in Arabidopsis. *The Plant Cell* 28, 1108–1126. doi:10.1105/tpc.15.00880.

Macho, A. P., Boutrot, F., Rathjen, J. P., and Zipfel, C. (2012). Aspartate Oxidase Plays an Important Role in Arabidopsis Stomatal Immunity. *Plant Physiol.* 159, 1845–1856. doi:10.1104/pp.112.199810.

Macknight, R. C., Laing, W. A., Bulley, S. M., Broad, R. C., Johnson, A. A., and Hellens, R. P. (2017). Increasing ascorbate levels in crops to enhance human nutrition and plant abiotic stress tolerance. *Current Opinion in Biotechnology* 44, 153–160. doi:10.1016/j.copbio.2017.01.011.

Magni, G., Amici, A., Emanuelli, M., Orsomando, G., Raffaelli, N., and Ruggieri, S. (2004). Enzymology of NAD+ homeostasis in man. *Cellular and Molecular Life Sciences (CMLS)* 61, 19–34. doi:10.1007/s00018-003-3161-1.

Marc, F., Davin, A., Deglene-Benbrahim, L., Ferrand, C., Baccaunaud, M., and Fritsch, P. (2004). Méthodes d'évaluation du potentiel antioxydant dans les aliments. *Med Sci (Paris)* 20, 458–463. doi:10.1051/medsci/2004204458.

Markevich, N. I., and Hoek, J. B. (2015). Computational modeling analysis of mitochondrial superoxide production under varying substrate conditions and upon inhibition of different segments of the electron transport chain. *Biochimica et Biophysica Acta (BBA) - Bioenergetics* 1847, 656–679. doi:10.1016/j.bbabio.2015.04.005.

Markovic, J., Borrás, C., Ortega, Á., Sastre, J., Viña, J., and Pallardó, F. V. (2007). Glutathione Is Recruited into the Nucleus in Early Phases of Cell Proliferation. *Journal of Biological Chemistry* 282, 20416–20424. doi:10.1074/jbc.M609582200.

Marmiroli, M., Mussi, F., Imperiale, D., Lencioni, G., and Marmiroli, N. (2017). Abiotic Stress Response to As and As+Si, Composite Reprogramming of Fruit Metabolites in Tomato Cultivars. *Frontiers in Plant Science* 8. doi:10.3389/fpls.2017.02201.

Martí, M. C., Camejo, D., Olmos, E., Sandalio, L. M., Fernández-García, N., Jiménez, A., et al. (2009). Characterisation and changes in the antioxidant system of chloroplasts and chromoplasts isolated from green and mature pepper fruits. *Plant Biol (Stuttg)* 11, 613–624. doi:10.1111/j.1438-8677.2008.00149.x.

Martí, R., Roselló, S., and Cebolla-Cornejo, J. (2016). Tomato as a Source of Carotenoids and Polyphenols Targeted to Cancer Prevention. *Cancers* 8, 58. doi:10.3390/cancers8060058.

Martin, M. N., Saladores, P. H., Lambert, E., Hudson, A. O., and Leustek, T. (2007). Localization of Members of the γ -Glutamyl Transpeptidase Family Identifies Sites of Glutathione and Glutathione S-Conjugate Hydrolysis. *Plant Physiology* 144, 1715–1732. doi:10.1104/pp.106.094409.

Martre, P., Bertin, N., Salon, C., and Génard, M. (2011). Modelling the size and composition of fruit, grain and seed by process-based simulation models. *New Phytologist* 191, 601–618. doi:10.1111/j.1469-8137.2011.03747.x.

Marty, L., Siala, W., Schwarzlander, M., Fricker, M. D., Wirtz, M., Sweetlove, L. J., et al. (2009). The NADPH-dependent thioredoxin system constitutes a functional backup for cytosolic glutathione reductase in Arabidopsis. *Proceedings of the National Academy of Sciences* 106, 9109–9114. doi:10.1073/pnas.0900206106.

Maruyama-Nakashita, A., Inoue, E., Watanabe-Takahashi, A., Yamaya, T., and Takahashi, H. (2003). Transcriptome Profiling of Sulfur-Responsive Genes in Arabidopsis Reveals Global Effects of Sulfur Nutrition on Multiple Metabolic Pathways. *Plant Physiology* 132, 597–605. doi:10.1104/pp.102.019802.

Maruyama-Nakashita, A., and Ohkama-Ohtsu, N. (2017). "Sulfur Assimilation and Glutathione Metabolism in Plants," in *Glutathione in Plant Growth, Development, and Stress Tolerance*, eds. M. A. Hossain, M. G. Mostofa, P. Diaz-Vivancos, D. J. Burritt, M. Fujita, and L.-S. P. Tran (Cham: Springer International Publishing), 287–308. doi:10.1007/978-3-319-66682-2_13.

Masi, A., Destro, T., Turetta, L., Varotto, S., Caporale, G., and Ferretti, M. (2007). Localization of gamma-glutamyl transferase activity and protein in Zea mays organs and tissues. *Journal of Plant Physiology* 164, 1527–1535. doi:10.1016/j.jplph.2006.07.016.

Massot, C., Bancel, D., Lopez Lauri, F., Truffault, V., Baldet, P., Stevens, R., et al. (2013). High Temperature Inhibits Ascorbate Recycling and Light Stimulation of the Ascorbate Pool in Tomato despite Increased Expression of Biosynthesis Genes. *PLoS ONE* 8, e84474. doi:10.1371/journal.pone.0084474.

Massot, C., Stevens, R., Génard, M., Longuenesse, J.-J., and Gautier, H. (2012). Light affects ascorbate content and ascorbate-related gene expression in tomato leaves more than in fruits. *Planta* 235, 153–163. doi:10.1007/s00425-011-1493-x.

Matsui, A., Yin, Y., Yamanaka, K., Iwasaki, M., and Ashihara, H. (2007). Metabolic fate of nicotinamide in higher plants. *Physiol Plant* 0, 191–200. doi:10.1111/j.1399-3054.2007.00959.x.

Maughan, S. C., Pasternak, M., Cairns, N., Kiddle, G., Brach, T., Jarvis, R., et al. (2010). Plant homologs of the *Plasmodium falciparum* chloroquine-resistance transporter, *Pf* CRT, are required for glutathione homeostasis and stress responses. *Proc Natl Acad Sci USA* 107, 2331–2336. doi:10.1073/pnas.0913689107.

McAtee, P., Karim, S., Schaffer, R., and David, K. (2013). A dynamic interplay between phytohormones is required for fruit development, maturation, and ripening. *Front. Plant Sci.* 4. doi:10.3389/fpls.2013.00079.

Meister, A. (1988). On the discovery of glutathione. *Trends in Biochemical Sciences* 13, 185–188. doi:10.1016/0968-0004(88)90148-X.

Melino, V. J., Soole, K. L., and Ford, C. M. (2009). Ascorbate metabolism and the developmental demand for tartaric and oxalic acids in ripening grape berries. *BMC Plant Biol* 9, 145. doi:10.1186/1471-2229-9-145.

Mellidou, I., and Kanellis, A. K. (2017). Genetic Control of Ascorbic Acid Biosynthesis and Recycling in Horticultural Crops. *Front. Chem.* 5, 50. doi:10.3389/fchem.2017.00050.

Mellidou, I., Koukounaras, A., Kostas, S., Patelou, E., and Kanellis, A. K. (2021). Regulation of Vitamin C Accumulation for Improved Tomato Fruit Quality and Alleviation of Abiotic Stress. *Genes* 12, 694. doi:10.3390/genes12050694.

Mendiburu, F. de (2021). *agricolae: Statistical Procedures for Agricultural Research*. Available at: https://CRAN.R-project.org/package=agricolae.

Mendoza-Cózatl, D. G., Butko, E., Springer, F., Torpey, J. W., Komives, E. A., Kehr, J., et al. (2008). Identification of high levels of phytochelatins, glutathione and cadmium in the phloem sap of Brassica napus. A role for thiol-peptides in the long-distance transport of cadmium and the effect of cadmium on iron translocation. *Plant J* 54, 249–259. doi:10.1111/j.1365-313X.2008.03410.x.

Mestre, T. C., Garcia-Sanchez, F., Rubio, F., Martinez, V., and Rivero, R. M. (2012). Glutathione homeostasis as an important and novel factor controlling blossom-end rot development in calcium-deficient tomato fruits. *Journal of Plant Physiology* 169, 1719–1727. doi:10.1016/j.jplph.2012.07.013.

Mettler, I. J., and Beevers, H. (1980). Oxidation of NADH in Glyoxysomes by a Malate-Aspartate Shuttle. *Plant Physiol.* 66, 555–560. doi:10.1104/pp.66.4.555.

Meuwly, P., Thibault, P., and Rauser, W. E. (1993). γ-Glutamylcysteinylglutamic acid - a new homologue of glutathione in maize seedlings exposed to cadmium. *FEBS Letters* 336, 472–476. doi:10.1016/0014-5793(93)80858-R.

Meyer, A. J., and Dick, T. P. (2010). Fluorescent Protein-Based Redox Probes. *Antioxidants & Redox Signaling* 13, 621–650. doi:10.1089/ars.2009.2948.

Meyer, E. H., Tomaz, T., Carroll, A. J., Estavillo, G., Delannoy, E., Tanz, S. K., et al. (2009). Remodeled Respiration in ndufs4 with Low Phosphorylation Efficiency Suppresses Arabidopsis Germination and Growth and Alters Control of Metabolism at Night. *Plant Physiology* 151, 603–619. doi:10.1104/pp.109.141770.

Meyer, Y., Siala, W., Bashandy, T., Riondet, C., Vignols, F., and Reichheld, J. P. (2008). Glutaredoxins and thioredoxins in plants. *Biochimica et Biophysica Acta (BBA) - Molecular Cell Research* 1783, 589–600. doi:10.1016/j.bbamcr.2007.10.017.

Mhamdi, A., Hager, J., Chaouch, S., Queval, G., Han, Y., Taconnat, L., et al. (2010a). Arabidopsis GLUTATHIONE REDUCTASE1 Plays a Crucial Role in Leaf Responses to Intracellular Hydrogen Peroxide and in Ensuring Appropriate Gene Expression through Both Salicylic Acid and Jasmonic Acid Signaling Pathways. *Plant Physiology* 153, 1144–1160. doi:10.1104/pp.110.153767.

Mhamdi, A., Queval, G., Chaouch, S., Vanderauwera, S., Van Breusegem, F., and Noctor, G. (2010b). Catalase function in plants: a focus on Arabidopsis mutants as stress-mimic models. *Journal of Experimental Botany* 61, 4197–4220. doi:10.1093/jxb/erq282.

Michelet, L., Zaffagnini, M., Marchand, C., Collin, V., Decottignies, P., Tsan, P., et al. (2005). Glutathionylation of chloroplast thioredoxin f is a redox signaling mechanism in plants. *Proceedings of the National Academy of Sciences* 102, 16478–16483. doi:10.1073/pnas.0507498102.

Michelet, L., Zaffagnini, M., Morisse, S., Sparla, F., Pérez-Pérez, M. E., Francia, F., et al. (2013). Redox regulation of the Calvin–Benson cycle: something old, something new. *Frontiers in Plant Science* 4. doi:10.3389/fpls.2013.00470.

Ming, W., Feng, J., Chang, S., Xiang, K., Liu, Z., Tian, B., et al. (2017). Rhodamine-based fluorescent probes for selective detection of glutathione and cysteine. *Res Chem Intermed* 43, 7387–7398. doi:10.1007/s11164-017-3082-5.

Miret, J. A., and Munné-Bosch, S. (2015). Redox signaling and stress tolerance in plants: a focus on vitamin E. *Ann. N. Y. Acad. Sci.* 1340, 29–38. doi:10.1111/nyas.12639.

Miret, J. A., and Munné-Bosch, S. (2016). Abscisic acid and pyrabactin improve vitamin C contents in raspberries. *Food Chemistry* 203, 216–223. doi:10.1016/j.foodchem.2016.02.046.

Mittler, R. (2017). ROS Are Good. *Trends Plant Sci.* 22, 11–19. doi:10.1016/j.tplants.2016.08.002.

Mittler, R., Vanderauwera, S., Suzuki, N., Miller, G., Tognetti, V. B., Vandepoele, K., et al. (2011). ROS signaling: the new wave? *Trends in Plant Science* 16, 300–309. doi:10.1016/j.tplants.2011.03.007.

Miyaji, T., Kuromori, T., Takeuchi, Y., Yamaji, N., Yokosho, K., Shimazawa, A., et al. (2015). AtPHT4;4 is a chloroplast-localized ascorbate transporter in Arabidopsis. *Nat Commun* 6, 5928. doi:10.1038/ncomms6928.

Moing, A., Pétriacq, P., and Osorio, S. (2020). Special Issue on "Fruit Metabolism and Metabolomics." *Metabolites* 10, 230. doi:10.3390/metabo10060230.

Moing, A., Renaud, C., Gaudillère, M., Raymond, P., Roudeillac, P., and Denoyes-Rothan, B. (2001). Biochemical Changes during Fruit Development of Four Strawberry Cultivars. *Journal of the American Society for Horticultural Science* 126, 394–403. doi:10.21273/JASHS.126.4.394.

Morales, A., Yin, X., Harbinson, J., Driever, S. M., Molenaar, J., Kramer, D. M., et al. (2018). In Silico Analysis of the Regulation of the Photosynthetic Electron Transport Chain in C3 Plants. *Plant Physiol.* 176, 1247–1261. doi:10.1104/pp.17.00779.

Mou, Z. (2017). Extracellular pyridine nucleotides as immune elicitors in arabidopsis. *Plant Signaling & Behavior* 12. doi:10.1080/15592324.2017.1388977.

Mounet-Gilbert, L., Dumont, M., Ferrand, C., Bournonville, C., Monier, A., Jorly, J., et al. (2016). Two tomato GDP-D-mannose epimerase isoforms involved in ascorbate biosynthesis play specific roles in cell wall biosynthesis and development. *EXBOTJ* 67, 4767–4777. doi:10.1093/jxb/erw260.

Mukherjee, M., Larrimore, K. E., Ahmed, N. J., Bedick, T. S., Barghouthi, N. T., Traw, M. B., et al. (2010). Ascorbic Acid Deficiency in *Arabidopsis* Induces Constitutive Priming That is Dependent on Hydrogen Peroxide, Salicylic Acid, and the *NPR1* Gene. *MPMI* 23, 340–351. doi:10.1094/MPMI-23-3-0340.

Mullen, R. T., Lee, M. S., and Trelease, R. N. (1997). Identification of the peroxisomal targeting signal for cottonseed catalase. *Plant J* 12, 313–322. doi:10.1046/j.1365-313X.1997.12020313.x.

Müller, K., Linkies, A., Leubner-Metzger, G., and Kermode, A. R. (2012). Role of a respiratory burst oxidase of Lepidium sativum (cress) seedlings in root development and auxin signalling. *Journal of Experimental Botany* 63, 6325–6334. doi:10.1093/jxb/ers284.

Müller-Schüssele, S. J., Wang, R., Gütle, D. D., Romer, J., Rodriguez-Franco, M., Scholz, M., et al. (2020). Chloroplasts require glutathione reductase to balance reactive oxygen species and maintain efficient photosynthesis. *Plant J* 103, 1140–1154. doi:10.1111/tpj.14791.

Mullineaux, P. M., and Rausch, T. (2005). Glutathione, photosynthesis and the redox regulation of stress-responsive gene expression. *Photosynth Res* 86, 459–474. doi:10.1007/s11120-005-8811-8.

Muñoz, P., and Munné-Bosch, S. (2018). Photo-Oxidative Stress during Leaf, Flower and Fruit Development. *Plant Physiology* 176, 1004–1014. doi:10.1104/pp.17.01127.

Neuhaus, H. E., and Emes, M. J. (2000). Nonphotosynthetic Metabolism in Plastids. *Annu. Rev. Plant. Physiol. Plant. Mol. Biol.* 51, 111–140. doi:10.1146/annurev.arplant.51.1.111.

Ni, Z.-J., Hu, K.-D., Song, C.-B., Ma, R.-H., Li, Z.-R., Zheng, J.-L., et al. (2016). Hydrogen Sulfide Alleviates Postharvest Senescence of Grape by Modulating the Antioxidant Defenses. *Oxidative Medicine and Cellular Longevity* 2016, 1–14. doi:10.1155/2016/4715651.

Nikiforova, V., Freitag, J., Kempa, S., Adamik, M., Hesse, H., and Hoefgen, R. (2003). Transcriptome analysis of sulfur depletion in Arabidopsis thaliana : interlacing of biosynthetic pathways provides response specificity: Transcriptome analysis in Arabidopsis thaliana. *The Plant Journal* 33, 633–650. doi:10.1046/j.1365-313X.2003.01657.x.

Nimse, S. B., and Pal, D. (2015). Free radicals, natural antioxidants, and their reaction mechanisms. *RSC Advances* 5, 27986–28006. doi:10.1039/C4RA13315C.

Noctor, G. (2002). Interactions between biosynthesis, compartmentation and transport in the control of glutathione homeostasis and signalling. *Journal of Experimental Botany* 53, 1283–1304. doi:10.1093/jexbot/53.372.1283.

Noctor, G. (2006). NAD(P) synthesis and pyridine nucleotide cycling in plants and their potential importance in stress conditions. *Journal of Experimental Botany* 57, 1603–1620. doi:10.1093/jxb/erj202.

Noctor, G., Arisi, A.-C. M., Jouanin, L., and Foyer, C. H. (1998). Manipulation of Glutathione and Amino Acid Biosynthesis in the Chloroplast. *Plant Physiology* 118, 471–482. doi:10.1104/pp.118.2.471.

Noctor, G., and Mhamdi, A. (2014). Glutathione and NADPH in plant responses to H2O2. *Free Radic. Biol. Med.* 75 Suppl 1, S3-4. doi:10.1016/j.freeradbiomed.2014.10.830.

Noctor, G., Mhamdi, A., Chaouch, S., Han, Y., Neukermans, J., Marquez-Garcia, B., et al. (2012). Glutathione in plants: an integrated overview: Glutathione status and functions. *Plant, Cell & Environment* 35, 454–484. doi:10.1111/j.1365-3040.2011.02400.x.

Noctor, G., Mhamdi, A., and Foyer, C. H. (2014). The roles of reactive oxygen metabolism in drought: not so cut and dried. *Plant Physiol.* 164, 1636–1648. doi:10.1104/pp.113.233478.

Noctor, G., Mhamdi, A., and Foyer, C. H. (2016). Oxidative stress and antioxidative systems: recipes for successful data collection and interpretation: Methods in oxidative stress research. *Plant, Cell & Environment* 39, 1140–1160. doi:10.1111/pce.12726.

Noctor, G., Mhamdi, A., Queval, G., and Foyer, C. H. (2013). Regulating the Redox Gatekeeper: Vacuolar Sequestration Puts Glutathione Disulfide in Its Place. *PLANT PHYSIOLOGY* 163, 665–671. doi:10.1104/pp.113.223545.

Noctor, G., Queval, G., and Gakière, B. (2006). NAD(P) synthesis and pyridine nucleotide cycling in plants and their potential importance in stress conditions. *Journal of Experimental Botany* 57, 1603–1620. doi:10.1093/jxb/erj202.

Noctor, G., Queval, G., Mhamdi, A., Chaouch, S., and Foyer, C. H. (2011). Glutathione. *The Arabidopsis Book* 9, 1–32. doi:10.1199/tab.0142.

Noctor, G., Reichheld, J.-P., and Foyer, C. H. (2018). ROS-related redox regulation and signaling in plants. *Seminars in Cell & Developmental Biology* 80, 3–12. doi:10.1016/j.semcdb.2017.07.013.

Noji, M., and Saito, K. (2002). Molecular and biochemical analysis of serine acetyltransferase and cysteine synthase towards sulfur metabolic engineering in plants. *Amino Acids* 22, 231–243. doi:10.1007/s007260200011.

O'Brien, J. A., Daudi, A., Butt, V. S., and Paul Bolwell, G. (2012). Reactive oxygen species and their role in plant defence and cell wall metabolism. *Planta* 236, 765–779. doi:10.1007/s00425-012-1696-9.

Ogawa, K., Hatano-Iwasaki, A., Yanagida, M., and Iwabuchi, M. (2004). Level of Glutathione is Regulated by ATP-Dependent Ligation of Glutamate and Cysteine through Photosynthesis in Arabidopsis thaliana: Mechanism of Strong Interaction of Light Intensity with Flowering. *Plant and Cell Physiology* 45, 1–8. doi:10.1093/pcp/pch008.

Ogawa, K., Kanematsu, S., Takebe, K., and Asada, K. (1995). Attachment of CuZn-Superoxide Dismutase to Thylakoid Membranes at the Site of Superoxide Generation (PSI) in Spinach

Chloroplasts: Detection by Immuno-Gold Labeling After Rapid Freezing and Substitution Method. *Plant and Cell Physiology*. doi:10.1093/oxfordjournals.pcp.a078795.

Ohashi, K., Kawai, S., and Murata, K. (2013). Secretion of Quinolinic Acid, an Intermediate in the Kynurenine Pathway, for Utilization in NAD $^{+}$ Biosynthesis in the Yeast Saccharomyces cerevisiae. *Eukaryotic Cell* 12, 648–653. doi:10.1128/EC.00339-12.

Ohkama-Ohtsu, N., Radwan, S., Peterson, A., Zhao, P., Badr, A. F., Xiang, C., et al. (2007). Characterization of the extracellular γ-glutamyl transpeptidases, GGT1 and GGT2, in Arabidopsis: Apoplastic glutathione degradation in Arabidopsis. *The Plant Journal* 49, 865–877. doi:10.1111/j.1365-313X.2006.03004.x.

Okabe, Y., Asamizu, E., Saito, T., Matsukura, C., Ariizumi, T., Brès, C., et al. (2011). Tomato TILLING Technology: Development of a Reverse Genetics Tool for the Efficient Isolation of Mutants from Micro-Tom Mutant Libraries. *Plant and Cell Physiology* 52, 1994–2005. doi:10.1093/pcp/pcr134.

Olas, B. (2018). Berry Phenolic Antioxidants – Implications for Human Health? *Frontiers in Pharmacology* 9. doi:10.3389/fphar.2018.00078.

Ortiz-Espín, A., Sánchez-Guerrero, A., Sevilla, F., and Jiménez, A. (2017). "The Role of Ascorbate in Plant Growth and Development," in *Ascorbic Acid in Plant Growth, Development and Stress Tolerance*, eds. M. A. Hossain, S. Munné-Bosch, D. J. Burritt, P. Diaz-Vivancos, M. Fujita, and A. Lorence (Cham: Springer International Publishing), 25–45. doi:10.1007/978-3-319-74057-7_2.

Osorio, S., Scossa, F., and Fernie, A. R. (2013a). Molecular regulation of fruit ripening. *Front. Plant Sci.* 4, 198. doi:10.3389/fpls.2013.00198.

Osorio, S., Vallarino, J. G., Szecowka, M., Ufaz, S., Tzin, V., Angelovici, R., et al. (2013b). Alteration of the Interconversion of Pyruvate and Malate in the Plastid or Cytosol of Ripening Tomato Fruit Invokes Diverse Consequences on Sugar But Similar Effects on Cellular Organic Acid, Metabolism, and Transitory Starch Accumulation. *Plant Physiol.* 161, 628–643. doi:10.1104/pp.112.211094.

Oven, M., Raith, K., Neubert, R. H. H., Kutchan, T. M., and Zenk, M. H. (2001). Homo-Phytochelatins Are Synthesized in Response to Cadmium in Azuki Beans. *Plant Physiol.* 126, 1275–1280. doi:10.1104/pp.126.3.1275.

Owusu-Ansah, E., and Banerjee, U. (2009). Reactive oxygen species prime Drosophila haematopoietic progenitors for differentiation. *Nature* 461, 537–541. doi:10.1038/nature08313.

Paciolla, C., Fortunato, S., Dipierro, N., Paradiso, A., De Leonardis, S., Mastropasqua, L., et al. (2019). Vitamin C in Plants: From Functions to Biofortification. *Antioxidants* 8, 519. doi:10.3390/antiox8110519.

Palmieri, F., Rieder, B., Ventrella, A., Blanco, E., Do, P. T., Nunes-Nesi, A., et al. (2009). Molecular Identification and Functional Characterization of Arabidopsis thaliana Mitochondrial and Chloroplastic NAD+ Carrier Proteins. *Journal of Biological Chemistry* 284, 31249–31259. doi:10.1074/jbc.M109.041830.

Palmieri, M. C., Lindermayr, C., Bauwe, H., Steinhauser, C., and Durner, J. (2010). Regulation of Plant Glycine Decarboxylase by *S* -Nitrosylation and Glutathionylation. *Plant Physiology* 152, 1514–1528. doi:10.1104/pp.109.152579.

Pan, Z., Liu, Q., Yun, Z., Guan, R., Zeng, W., Xu, Q., et al. (2009). Comparative proteomics of a lycopene-accumulating mutant reveals the important role of oxidative stress on carotenogenesis in sweet orange (Citrus sinensis [L.] osbeck). *Proteomics* 9, 5455–5470. doi:10.1002/pmic.200900092.

Pandey, S., Fartyal, D., Agarwal, A., Shukla, T., James, D., Kaul, T., et al. (2017). Abiotic Stress Tolerance in Plants: Myriad Roles of Ascorbate Peroxidase. *Front. Plant Sci.* 8, 581. doi:10.3389/fpls.2017.00581.

Pandey, V. P., Singh, S., Singh, R., and Dwivedi, U. N. (2012). Purification and characterization of peroxidase from papaya (Carica papaya) fruit. *Appl. Biochem. Biotechnol.* 167, 367–376. doi:10.1007/s12010-012-9672-1.

Pasternak, M., Lim, B., Wirtz, M., Hell, R., Cobbett, C. S., and Meyer, A. J. (2007). Restricting glutathione biosynthesis to the cytosol is sufficient for normal plant development: Compartmentation of glutathione biosynthesis. *The Plant Journal* 53, 999–1012. doi:10.1111/j.1365-313X.2007.03389.x.

Pastori, G. M., Kiddle, G., Antoniw, J., Bernard, S., Veljovic-Jovanovic, S., Verrier, P. J., et al. (2003). Leaf Vitamin C Contents Modulate Plant Defense Transcripts and Regulate Genes That Control Development through Hormone Signaling. *Plant Cell* 15, 939–951. doi:10.1105/tpc.010538.

Pavet, V., Olmos, E., Kiddle, G., Mowla, S., Kumar, S., Antoniw, J., et al. (2005). Ascorbic Acid Deficiency Activates Cell Death and Disease Resistance Responses in Arabidopsis. *Plant Physiol.* 139, 1291–1303. doi:10.1104/pp.105.067686.

Pellny, T. K., Van Aken, O., Dutilleul, C., Wolff, T., Groten, K., Bor, M., et al. (2008). Mitochondrial respiratory pathways modulate nitrate sensing and nitrogen-dependent regulation of plant architecture in Nicotiana sylvestris. *Plant J* 54, 976–992. doi:10.1111/j.1365-313X.2008.03472.x.

Perez-Riverol, Y., Csordas, A., Bai, J., Bernal-Llinares, M., Hewapathirana, S., Kundu, D. J., et al. (2019). The PRIDE database and related tools and resources in 2019: improving support for quantification data. *Nucleic Acids Res.* 47, D442–D450. doi:10.1093/nar/gky1106.

Pesaresi, P., Mizzotti, C., Colombo, M., and Masiero, S. (2014). Genetic regulation and structural changes during tomato fruit development and ripening. *Front. Plant Sci.* 5. doi:10.3389/fpls.2014.00124.

Peskin, A. V., and Winterbourn, C. C. (2017). Assay of superoxide dismutase activity in a plate assay using WST-1. *Free Radical Biology and Medicine* 103, 188–191. doi:10.1016/j.freeradbiomed.2016.12.033.

Peterhansel, C., Horst, I., Niessen, M., Blume, C., Kebeish, R., Kürkcüoglu, S., et al. (2010). Photorespiration. *The Arabidopsis Book* 8, e0130. doi:10.1199/tab.0130.

Pétriacq, P., de Bont, L., Genestout, L., Hao, J., Laureau, C., Florez-Sarasa, I., et al. (2017). Photoperiod Affects the Phenotype of Mitochondrial Complex I Mutants. *Plant Physiol.* 173, 434–455. doi:10.1104/pp.16.01484.

Pétriacq, P., de Bont, L., Hager, J., Didierlaurent, L., Mauve, C., Guérard, F., et al. (2012). Inducible NAD overproduction in Arabidopsis alters metabolic pools and gene expression correlated with increased salicylate content and resistance to Pst-AvrRpm1: Inducible NAD overproduction. *The Plant Journal* 70, 650–665. doi:10.1111/j.1365-313X.2012.04920.x.

Pétriacq, P., de Bont, L., Tcherkez, G., and Gakière, B. (2013). NAD: Not just a pawn on the board of plant-pathogen interactions. *Plant Signaling & Behavior* 8, e22477. doi:10.4161/psb.22477.

Pétriacq, P., López, A., and Luna, E. (2018). Fruit Decay to Diseases: Can Induced Resistance and Priming Help? *Plants* 7, 77. doi:10.3390/plants7040077.

Pétriacq, P., Ton, J., Patrit, O., Tcherkez, G., and Gakière, B. (2016a). NAD Acts as an Integral Regulator of Multiple Defense Layers. *Plant Physiology* 172, 1465–1479. doi:10.1104/pp.16.00780.

Pétriacq, P., Ton, J., Patrit, O., Tcherkez, G., and Gakière, B. (2016b). NAD Acts as an Integral Regulator of Multiple Defense Layers. *Plant Physiol.* 172, 1465–1479. doi:10.1104/pp.16.00780.

Petriv, O. I., and Rachubinski, R. A. (2004). Lack of Peroxisomal Catalase Causes a Progeric Phenotype in Caenorhabditis elegans. *Journal of Biological Chemistry* 279, 19996–20001. doi:10.1074/jbc.M400207200.

Pignocchi, C., Fletcher, J. M., Wilkinson, J. E., Barnes, J. D., and Foyer, C. H. (2003). The Function of Ascorbate Oxidase in Tobacco. *Plant Physiology* 132, 1631–1641. doi:10.1104/pp.103.022798.

Pignocchi, C., and Foyer, C. H. (2003). Apoplastic ascorbate metabolism and its role in the regulation of cell signalling. *Current Opinion in Plant Biology* 6, 379–389. doi:10.1016/S1369-5266(03)00069-4.

Pignocchi, C., Kiddle, G., Hernández, I., Foster, S. J., Asensi, A., Taybi, T., et al. (2006). Ascorbate Oxidase-Dependent Changes in the Redox State of the Apoplast Modulate Gene Transcript Accumulation Leading to Modified Hormone Signaling and Orchestration of Defense Processes in Tobacco. *Plant Physiology* 141, 423–435. doi:10.1104/pp.106.078469.

Pilati, S., Brazzale, D., Guella, G., Milli, A., Ruberti, C., Biasioli, F., et al. (2014). The onset of grapevine berry ripening is characterized by ROS accumulation and lipoxygenase-mediated membrane peroxidation in the skin. *BMC Plant Biology* 14, 87. doi:10.1186/1471-2229-14-87.

Pilon, M., Ravet, K., and Tapken, W. (2011). The biogenesis and physiological function of chloroplast superoxide dismutases. *Biochimica et Biophysica Acta (BBA) - Bioenergetics* 1807, 989–998. doi:10.1016/j.bbabio.2010.11.002.

Pohl, F., and Kong Thoo Lin, P. (2018). The Potential Use of Plant Natural Products and Plant Extracts with Antioxidant Properties for the Prevention/Treatment of Neurodegenerative Diseases: In Vitro, In Vivo and Clinical Trials. *Molecules* 23. doi:10.3390/molecules23123283.

Pollak, N., Dölle, C., and Ziegler, M. (2007). The power to reduce: pyridine nucleotides – small molecules with a multitude of functions. *Biochemical Journal* 402, 205–218. doi:10.1042/BJ20061638.

Polle, A. (2001). Dissecting the Superoxide Dismutase-Ascorbate-Glutathione-Pathway in Chloroplasts by Metabolic Modeling. Computer Simulations as a Step towards Flux Analysis. *PLANT PHYSIOLOGY* 126, 445–462. doi:10.1104/pp.126.1.445.

Polle, A., Chakrabarti, K., Schürmann, W., and Renneberg, H. (1990). Composition and Properties of Hydrogen Peroxide Decomposing Systems in Extracellular and Total Extracts from Needles of Norway Spruce (*Picea abies* L., Karst.). *Plant Physiol.* 94, 312–319. doi:10.1104/pp.94.1.312.

Potters, G., De Gara, L., Asard, H., and Horemans, N. (2002). Ascorbate and glutathione: guardians of the cell cycle, partners in crime? *Plant Physiology and Biochemistry* 40, 537–548. doi:10.1016/S0981-9428(02)01414-6.

Potters, G., Jansen, M. A. K., Horemans, N., Guisez, Y., and Pasternak, T. (2010). Dehydroascorbate and glutathione regulate the cellular development of Nicotiana tabacum L. SR-1 protoplasts. *In Vitro Cell.Dev.Biol.-Plant* 46, 289–297. doi:10.1007/s11627-009-9266-y.

Pritchard, S. G., Ju, Z., van Santen, E., Qiu, J., Weaver, D. B., Prior, S. A., et al. (2000). The influence of elevated CO2 on the activities of antioxidative enzymes in two soybean genotypes. *Functional Plant Biol.* 27, 1061. doi:10.1071/PP99206.

Qin, G., Meng, X., Wang, Q., and Tian, S. (2009a). Oxidative damage of mitochondrial proteins contributes to fruit senescence: a redox proteomics analysis. *J. Proteome Res.* 8, 2449–2462. doi:10.1021/pr801046m.

Qin, G., Wang, Q., Liu, J., Li, B., and Tian, S. (2009b). Proteomic analysis of changes in mitochondrial protein expression during fruit senescence. *Proteomics* 9, 4241–4253. doi:10.1002/pmic.200900133.

Queval, G., Jaillard, D., Zechmann, B., and Noctor, G. (2011). Increased intracellular H2O2 availability preferentially drives glutathione accumulation in vacuoles and chloroplasts: Oxidative stress and glutathione compartmentation. *Plant, Cell & Environment* 34, 21–32. doi:10.1111/j.1365-3040.2010.02222.x.

Queval, G., and Noctor, G. (2007). A plate reader method for the measurement of NAD, NADP, glutathione, and ascorbate in tissue extracts: Application to redox profiling during Arabidopsis rosette development. *Analytical Biochemistry* 363, 58–69. doi:10.1016/j.ab.2007.01.005.

Queval, G., Thominet, D., Vanacker, H., Miginiac-Maslow, M., Gakière, B., and Noctor, G. (2009). H2O2-Activated Up-Regulation of Glutathione in Arabidopsis Involves Induction of Genes Encoding Enzymes Involved in Cysteine Synthesis in the Chloroplast. *Molecular Plant* 2, 344–356. doi:10.1093/mp/ssp002.

Quinet, M., Angosto, T., Yuste-Lisbona, F. J., Blanchard-Gros, R., Bigot, S., Martinez, J.-P., et al. (2019). Tomato Fruit Development and Metabolism. *Front. Plant Sci.* 10, 1554. doi:10.3389/fpls.2019.01554.

Radzio, J. A., Lorence, A., Chevone, B. I., and Nessler, C. L. (2003). L-Gulono-1,4-lactone oxidase expression rescues vitamin C-deficient Arabidopsis (vtc) mutants. *Plant Mol Biol* 53, 837–844. doi:10.1023/B:PLAN.0000023671.99451.1d.

Rahantaniaina, M.-S., Li, S., Chatel-Innocenti, G., Tuzet, A., Issakidis-Bourguet, E., Mhamdi, A., et al. (2017). Cytosolic and Chloroplastic DHARs Cooperate in Oxidative Stress-Driven Activation of the Salicylic Acid Pathway. *Plant Physiol.* 174, 956–971. doi:10.1104/pp.17.00317.

Raiola, A., Tenore, G., Barone, A., Frusciante, L., and Rigano, M. (2015). Vitamin E Content and Composition in Tomato Fruits: Beneficial Roles and Bio-Fortification. *International Journal of Molecular Sciences* 16, 29250–29264. doi:10.3390/ijms161226163.

Rasmusson, A. G., Fernie, A. R., and van Dongen, J. T. (2009). Alternative oxidase: a defence against metabolic fluctuations? *Physiologia Plantarum* 137, 371–382. doi:10.1111/j.1399-3054.2009.01252.x.

Rasmusson, A. G., Geisler, D. A., and Møller, I. M. (2008). The multiplicity of dehydrogenases in the electron transport chain of plant mitochondria. *Mitochondrion* 8, 47–60. doi:10.1016/j.mito.2007.10.004.

Renaudin, J.-P., Deluche, C., Cheniclet, C., Chevalier, C., and Frangne, N. (2017). Cell layer-specific patterns of cell division and cell expansion during fruit set and fruit growth in tomato pericarp. *Journal of Experimental Botany* 68, 1613–1623. doi:10.1093/jxb/erx058.

Rennenberg, H. (1980). Glutathione metabolism and possible biological roles in higher plants. *Phytochemistry* 21, 2771–2781. doi:10.1016/0031-9422(80)85045-X.

Rey, P., and Tarrago, L. (2018). Physiological Roles of Plant Methionine Sulfoxide Reductases in Redox Homeostasis and Signaling. *Antioxidants (Basel)* 7. doi:10.3390/antiox7090114.

Rick, C. M. (1976). Tomato, Lycopersicon esculentum (Solanaceae). *Simmonds, N.W. (Ed.), Evolution of Crop Plants. Longman Group, London, UK*, 268–273.

Riedl, K. M., Choksi, K., Wyzgoski, F. J., Scheerens, J. C., Schwartz, S. J., and Reese, R. N. (2013). Variation in Lycopene and Lycopenoates, Antioxidant Capacity, and Fruit Quality of Buffaloberry (*Shepherdia argentea* [Pursh]Nutt.): Buffaloberry carotenoids…. *Journal of Food Science* 78, C1673–C1679. doi:10.1111/1750-3841.12265.

Roch, L., Dai, Z., Gomès, E., Bernillon, S., Wang, J., Gibon, Y., et al. (2019). Fruit Salad in the Lab: Comparing Botanical Species to Help Deciphering Fruit Primary Metabolism. *Front. Plant Sci.* 10, 836. doi:10.3389/fpls.2019.00836.

Roch, L., Prigent, S., Klose, H., Cakpo, C.-B., Beauvoit, B., Deborde, C., et al. (2020). Biomass composition explains fruit relative growth rate and discriminates climacteric from non-climacteric species. *Journal of Experimental Botany* 71, 5823–5836. doi:10.1093/jxb/eraa302.

Rogers, H., and Munné-Bosch, S. (2016). Production and Scavenging of Reactive Oxygen Species and Redox Signaling during Leaf and Flower Senescence: Similar But Different. *Plant Physiol.* 171, 1560–1568. doi:10.1104/pp.16.00163.

Rohwer, J. M. (2012). Kinetic modelling of plant metabolic pathways. *Journal of Experimental Botany* 63, 2275–2292. doi:10.1093/jxb/ers080.

Romanazzi, G., Sanzani, S. M., Bi, Y., Tian, S., Gutiérrez Martínez, P., and Alkan, N. (2016). Induced resistance to control postharvest decay of fruit and vegetables. *Postharvest Biology and Technology* 122, 82–94. doi:10.1016/j.postharvbio.2016.08.003.

Romero-Puertas, M. C., Campostrini, N., Mattè, A., Righetti, P. G., Perazzolli, M., Zolla, L., et al. (2008). Proteomic analysis of S-nitrosylated proteins inArabidopsis thaliana undergoing hypersensitive response. *Proteomics* 8, 1459–1469. doi:10.1002/pmic.200700536.

Rosalie, R., Léchaudel, M., Dhuique-Mayer, C., Dufossé, L., and Joas, J. (2018). Antioxidant and enzymatic responses to oxidative stress induced by cold temperature storage and ripening in mango (Mangifera indica L. cv. 'Cogshall') in relation to carotenoid content. *J. Plant Physiol.* 224–225, 75–85. doi:10.1016/j.jplph.2018.03.011.

Rosenwasser, S., Rot, I., Meyer, A. J., Feldman, L., Jiang, K., and Friedman, H. (2010). A fluorometer-based method for monitoring oxidation of redox-sensitive GFP (roGFP) during development and extended dark stress. *Physiol Plant* 138, 493–502. doi:10.1111/j.1399-3054.2009.01334.x.

Rouhier, N. (2010). Plant glutaredoxins: pivotal players in redox biology and iron–sulphur centre assembly. *New Phytologist* 186, 365–372. doi:10.1111/j.1469-8137.2009.03146.x.

Rouhier, N., and Jacquot, J.-P. (2005). The plant multigenic family of thiol peroxidases. *Free Radic Biol Med* 38, 1413–1421. doi:10.1016/j.freeradbiomed.2004.07.037.

Saed-Moucheshi, A., Sohrabi, F., Fasihfar, E., Baniasadi, F., Riasat, M., and Mozafari, A. A. (2021). Superoxide dismutase (SOD) as a selection criterion for triticale grain yield under drought stress: a comprehensive study on genomics and expression profiling, bioinformatics, heritability, and phenotypic variability. *BMC Plant Biol* 21, 148. doi:10.1186/s12870-021-02919-5.

Salon, C., Avice, J.-C., Colombié, S., Dieuaide-Noubhani, M., Gallardo, K., Jeudy, C., et al. (2017). Fluxomics links cellular functional analyses to whole-plant phenotyping. *Journal of Experimental Botany* 68, 2083–2098. doi:10.1093/jxb/erx126.

Sarker, U., and Oba, S. (2018). Catalase, superoxide dismutase and ascorbate-glutathione cycle enzymes confer drought tolerance of Amaranthus tricolor. *Sci Rep* 8, 16496. doi:10.1038/s41598-018-34944-0.

Sart, S., Song, L., and Li, Y. (2015). Controlling Redox Status for Stem Cell Survival, Expansion, and Differentiation. *Oxidative Medicine and Cellular Longevity* 2015, 1–14. doi:10.1155/2015/105135.

Sass-Kiss, A., Kiss, J., Milotay, P., Kerek, M. M., and Toth-Markus, M. (2005). Differences in anthocyanin and carotenoid content of fruits and vegetables. *Food Research International* 38, 1023–1029. doi:10.1016/j.foodres.2005.03.014.

Scalzo, J., Politi, A., Pellegrini, N., Mezzetti, B., and Battino, M. (2005). Plant genotype affects total antioxidant capacity and phenolic contents in fruit. *Nutrition* 21, 207–213. doi:10.1016/j.nut.2004.03.025.

Schallau, K., and Junker, B. H. (2010). Simulating Plant Metabolic Pathways with Enzyme-Kinetic Models. *Plant Physiology* 152, 1763–1771. doi:10.1104/pp.109.149237.

Schertl, P., and Braun, H.-P. (2014). Respiratory electron transfer pathways in plant mitochondria. *Frontiers in Plant Science* 5. doi:10.3389/fpls.2014.00163.

Schippers, J. H. M., Nunes-Nesi, A., Apetrei, R., Hille, J., Fernie, A. R., and Dijkwel, P. P. (2008). The *Arabidopsis onset of leaf death5* Mutation of Quinolinate Synthase Affects Nicotinamide Adenine Dinucleotide Biosynthesis and Causes Early Ageing. *Plant Cell* 20, 2909–2925. doi:10.1105/tpc.107.056341.

Schwacke, R., Ponce-Soto, G. Y., Krause, K., Bolger, A. M., Arsova, B., Hallab, A., et al. (2019). MapMan4: A Refined Protein Classification and Annotation Framework Applicable to Multi-Omics Data Analysis. *Molecular Plant* 12, 879–892. doi:10.1016/j.molp.2019.01.003.

Shahidi, F., and de Camargo, A. (2016). Tocopherols and Tocotrienols in Common and Emerging Dietary Sources: Occurrence, Applications, and Health Benefits. *International Journal of Molecular Sciences* 17, 1745. doi:10.3390/ijms17101745.

Shen, C.-H., Krishnamurthy, R., and Yeh, K.-W. (2009). Decreased L-Ascorbate Content Mediating Bolting is Mainly Regulated by the Galacturonate Pathway in Oncidium. *Plant and Cell Physiology* 50, 935–946. doi:10.1093/pcp/pcp045.

Shi, H., and Schwender, J. (2016). Mathematical models of plant metabolism. *Current Opinion in Biotechnology* 37, 143–152. doi:10.1016/j.copbio.2015.10.008.

Singh, B., Singh, J. P., Kaur, A., and Singh, N. (2017). Phenolic composition and antioxidant potential of grain legume seeds: A review. *Food Research International* 101, 1–16. doi:10.1016/j.foodres.2017.09.026.

Skipsey, M., Davis, B. G., and Edwards, R. (2005). Diversification in substrate usage by glutathione synthetases from soya bean (Glycine max), wheat (Triticum aestivum) and maize (Zea mays). *Biochemical Journal* 391, 567–574. doi:10.1042/BJ20050718.

Skupien, K., and Oszmianski, J. (2004). Comparison of six cultivars of strawberries (Fragaria x ananassa Duch.) grown in northwest Poland. *European Food Research and Technology* 219, 66–70. doi:10.1007/s00217-004-0918-1.

Smirnoff, N. (2018). Ascorbic acid metabolism and functions: A comparison of plants and mammals. *Free Radical Biology and Medicine* 122, 116–129. doi:10.1016/j.freeradbiomed.2018.03.033.

Smirnoff, N., and Arnaud, D. (2019). Hydrogen peroxide metabolism and functions in plants. *New Phytol* 221, 1197–1214. doi:10.1111/nph.15488.

Smirnoff, N., and Wheeler, G. L. (2000). Ascorbic Acid in Plants: Biosynthesis and Function. *Critical Reviews in Biochemistry and Molecular Biology* 35, 291–314. doi:10.1080/10409230008984166.

Smith, E. N., Schwarzländer, M., Ratcliffe, R. G., and Kruger, N. J. (2021). Shining a light on NAD- and NADP-based metabolism in plants. *Trends in Plant Science* 26, 1072–1086. doi:10.1016/j.tplants.2021.06.010.

Sofo, A., Scopa, A., Nuzzaci, M., and Vitti, A. (2015). Ascorbate Peroxidase and Catalase Activities and Their Genetic Regulation in Plants Subjected to Drought and Salinity Stresses. *IJMS* 16, 13561–13578. doi:10.3390/ijms160613561.

Song, Y. H., Shim, J. S., Kinmonth-Schultz, H. A., and Imaizumi, T. (2015). Photoperiodic Flowering: Time Measurement Mechanisms in Leaves. *Annu. Rev. Plant Biol.* 66, 441–464. doi:10.1146/annurev-arplant-043014-115555.

Soubeyrand, E., Colombié, S., Beauvoit, B., Dai, Z., Cluzet, S., Hilbert, G., et al. (2018). Constraint-Based Modeling Highlights Cell Energy, Redox Status and α-Ketoglutarate Availability as Metabolic Drivers for Anthocyanin Accumulation in Grape Cells Under Nitrogen Limitation. *Front. Plant Sci.* 9, 421. doi:10.3389/fpls.2018.00421.

Stasolla, C., and Yeung, E. C. (2007). Cellular ascorbic acid regulates the activity of major peroxidases in the apical poles of germinating white spruce (Picea glauca) somatic embryos. *Plant Physiology and Biochemistry* 45, 188–198. doi:10.1016/j.plaphy.2007.02.007.

Stein, L. R., and Imai, S. (2012). The dynamic regulation of NAD metabolism in mitochondria. *Trends in Endocrinology & Metabolism* 23, 420–428. doi:10.1016/j.tem.2012.06.005.

Steinkamp, R., Schweihofen, B., and Rennenberg, H. (1987). γ-Glutamylcyclotransferase in tobacco suspension cultures: Catalytic properties and subcellular localization. *Physiol Plant* 69, 499–503. doi:10.1111/j.1399-3054.1987.tb09231.x.

Stevens, R., Buret, M., Duffé, P., Garchery, C., Baldet, P., Rothan, C., et al. (2007). Candidate Genes and Quantitative Trait Loci Affecting Fruit Ascorbic Acid Content in Three Tomato Populations. *Plant Physiol.* 143, 1943–1953. doi:10.1104/pp.106.091413.

Stevens, R. G., Baldet, P., Bouchet, J.-P., Causse, M., Deborde, C., Deschodt, C., et al. (2018). A Systems Biology Study in Tomato Fruit Reveals Correlations between the Ascorbate Pool and Genes Involved in Ribosome Biogenesis, Translation, and the Heat-Shock Response. *Front. Plant Sci.* 9, 137. doi:10.3389/fpls.2018.00137.

Stitt, M., and Gibon, Y. (2014). Why measure enzyme activities in the era of systems biology? *Trends in Plant Science* 19, 256–265. doi:10.1016/j.tplants.2013.11.003.

Storozhenko, S., Belles-Boix, E., Babiychuk, E., Hérouart, D., Davey, M. W., Slooten, L., et al. (2002). γ-Glutamyl Transpeptidase in Transgenic Tobacco Plants. Cellular Localization, Processing, and Biochemical Properties. *Plant Physiology* 128, 1109–1119. doi:10.1104/pp.010887.

Struik, P. C., Yin, X., and Visser, P. de (2005). Complex quality traits: now time to model. *Trends in Plant Science* 10, 513–516. doi:10.1016/j.tplants.2005.09.005.

Suda, Y., Tachikawa, H., Yokota, A., Nakanishi, H., Yamashita, N., Miura, Y., et al. (2003). Saccharomyces cerevisiae QNS1 codes for NAD+ synthetase that is functionally conserved in mammals. *Yeast* 20, 995–1005. doi:10.1002/yea.1008.

Summermatter, K., Sticher, L., and Metraux, J. P. (1995). Systemic Responses in Arabidopsis thaliana Infected and Challenged with Pseudomonas syringae pv syringae. *Plant Physiol.* 108, 1379–1385. doi:10.1104/pp.108.4.1379.

Suzuki, N., Miller, G., Morales, J., Shulaev, V., Torres, M. A., and Mittler, R. (2011). Respiratory burst oxidases: the engines of ROS signaling. *Curr. Opin. Plant Biol.* 14, 691–699. doi:10.1016/j.pbi.2011.07.014.

Sweetlove, L. J., and Ratcliffe, R. G. (2011). Flux-Balance Modeling of Plant Metabolism. *Front. Plant Sci.* 2. doi:10.3389/fpls.2011.00038.

Sweetlove, L. J., Williams, T. C. R., Cheung, C. Y. M., and Ratcliffe, R. G. (2013). Modelling metabolic CO2 evolution - a fresh perspective on respiration: Modelling metabolic CO2 evolution. *Plant Cell Environ* 36, 1631–1640. doi:10.1111/pce.12105.

Swindall, A., Stanley, J., and Yang, E. (2013). PARP-1: Friend or Foe of DNA Damage and Repair in Tumorigenesis? *Cancers* 5, 943–958. doi:10.3390/cancers5030943.

Symons, G. M., Chua, Y.-J., Ross, J. J., Quittenden, L. J., Davies, N. W., and Reid, J. B. (2012). Hormonal changes during non-climacteric ripening in strawberry. *Journal of Experimental Botany* 63, 4741–4750. doi:10.1093/jxb/ers147.

Szal, B., Dąbrowska, Z., Malmberg, G., Gardeström, P., and Rychter, A. M. (2008). Changes in energy status of leaf cells as a consequence of mitochondrial genome rearrangement. *Planta* 227, 697–706. doi:10.1007/s00425-007-0652-6.

Szarka, A., Bánhegyi, G., and Asard, H. (2013). The Inter-Relationship of Ascorbate Transport, Metabolism and Mitochondrial, Plastidic Respiration. *Antioxidants & Redox Signaling* 19, 1036–1044. doi:10.1089/ars.2012.5059.

Szarka, A., Horemans, N., Bánhegyi, G., and Asard, H. (2004). Facilitated glucose and dehydroascorbate transport in plant mitochondria. *Archives of Biochemistry and Biophysics* 428, 73–80. doi:10.1016/j.abb.2004.05.011.

Szőllősi, R. (2014). "Superoxide Dismutase (SOD) and Abiotic Stress Tolerance in Plants," in *Oxidative Damage to Plants* (Elsevier), 89–129. doi:10.1016/B978-0-12-799963-0.00003-4.

Terai, Y., Ueno, H., Ogawa, T., Sawa, Y., Miyagi, A., Kawai-Yamada, M., et al. (2020). Dehydroascorbate Reductases and Glutathione Set a Threshold for High-Light–Induced Ascorbate Accumulation. *Plant Physiol.* 183, 112–122. doi:10.1104/pp.19.01556.

The Tomato Genome Consortium (2012). The tomato genome sequence provides insights into fleshy fruit evolution. *Nature* 485, 635–641. doi:10.1038/nature11119.

Thevenet, D., Pastor, V., Baccelli, I., Balmer, A., Vallat, A., Neier, R., et al. (2017). The priming molecule β-aminobutyric acid is naturally present in plants and is induced by stress. *New Phytol.* 213, 552–559. doi:10.1111/nph.14298.

Thomas, S., Mooney, P. J. F., Burrell, M. M., and Fell, D. A. (1997). Metabolic Control Analysis of glycolysis in tuber tissue of potato (Solanum tuberosum): explanation for the low control coefficient of phosphofructokinase over respiratory flux. *Biochemical Journal* 322, 119–127. doi:10.1042/bj3220119.

Tian, S., Qin, G., and Li, B. (2013). Reactive oxygen species involved in regulating fruit senescence and fungal pathogenicity. *Plant Mol. Biol.* 82, 593–602. doi:10.1007/s11103-013-0035-2.

Tohge, T., Alseekh, S., and Fernie, A. R. (2013). On the regulation and function of secondary metabolism during fruit development and ripening. *Journal of Experimental Botany* 65, 4599–4611. doi:10.1093/jxb/ert443.

Tohge, T., and Fernie, A. R. (2015). Metabolomics-Inspired Insight into Developmental, Environmental and Genetic Aspects of Tomato Fruit Chemical Composition and Quality: Fig. 1. *Plant Cell Physiol* 56, 1681–1696. doi:10.1093/pcp/pcv093.

Tommasi, F., Paciolla, C., and Arrigoni, O. (1999). The ascorbate system in recalcitrant and orthodox seeds. *Physiologia Plantarum* 105, 193–198. doi:10.1034/j.1399-3054.1999.105202.x.

Tommasi, F., Paciolla, C., de Pinto, M. C., and De Gara, L. (2001). A comparative study of glutathione and ascorbate metabolism during germination of Pinus pinea L. seeds. *J Exp Bot* 52, 1647–1654.

Tommasini, R., Vogt, E., Fromenteau, M., Hörtensteiner, S., Matile, P., Amrhein, N., et al. (1998). An ABC-transporter of Arabidopsis thaliana has both glutathione-conjugate and chlorophyll catabolite transport activity. *The Plant Journal* 13, 773–780. doi:10.1046/j.1365-313X.1998.00076.x.

Torres, M. A., and Dangl, J. L. (2005). Functions of the respiratory burst oxidase in biotic interactions, abiotic stress and development. *Current Opinion in Plant Biology* 8, 397–403. doi:10.1016/j.pbi.2005.05.014.

Trobacher, C. P., Clark, S. M., Bozzo, G. G., Mullen, R. T., DeEll, J. R., and Shelp, B. J. (2013). Catabolism of GABA in apple fruit: Subcellular localization and biochemical characterization of two γ-aminobutyrate transaminases. *Postharvest Biology and Technology* 75, 106–113. doi:10.1016/j.postharvbio.2012.08.005.

Truffault, V., Fry, S. C., Stevens, R. G., and Gautier, H. (2017). Ascorbate degradation in tomato leads to accumulation of oxalate, threonate and oxalyl threonate. *The Plant Journal* 89, 996–1008. doi:10.1111/tpj.13439.

Tsakraklides, G., Martin, M., Chalam, R., Tarczynski, M. C., Schmidt, A., and Leustek, T. (2002). Sulfate reduction is increased in transgenic *Arabidopsis thaliana* expressing 5′-adenylylsulfate reductase from *Pseudomonas aeruginosa*: *Deregulation of Sulfate assimilation in Arabidopsis thaliana*. *The Plant Journal* 32, 879–889. doi:10.1046/j.1365-313X.2002.01477.x.

Tsugawa, H., Cajka, T., Kind, T., Ma, Y., Higgins, B., Ikeda, K., et al. (2015). MS-DIAL: Data independent MS/MS deconvolution for comprehensive metabolome analysis HHS public access. *Nat Methods* 12, 523–526. doi:10.1038/nmeth.3393.

Turner, W. L., Waller, J. C., Vanderbeld, B., and Snedden, W. A. (2004). Cloning and Characterization of Two NAD Kinases from Arabidopsis. Identification of a Calmodulin Binding Isoform. *Plant Physiol.* 135, 1243–1255. doi:10.1104/pp.104.040428.

Tuzet, A., Rahantaniaina, M.-S., and Noctor, G. (2019). Analyzing the Function of Catalase and the Ascorbate-Glutathione Pathway in H2O2 Processing: Insights from an Experimentally Constrained Kinetic Model. *Antioxid. Redox Signal.* 30, 1238–1268. doi:10.1089/ars.2018.7601.

Upmeier, B., Thomzik, J. E., and Barz, W. (1988). Nicotinic acid-N-glucoside in heterotrophic parsley cell suspension cultures. *Phytochemistry* 27, 3489–3493. doi:10.1016/0031-9422(88)80754-4.

Valenzuela, J., Manzano, S., Palma, F., Carvajal, F., Garrido, D., and Jamilena, M. (2017). Oxidative Stress Associated with Chilling Injury in Immature Fruit: Postharvest Technological and Biotechnological Solutions. *International Journal of Molecular Sciences* 18, 1467. doi:10.3390/ijms18071467.

Valero, E., Gonzalez-Sanchez, M. I., Macia, H., and Garcia-Carmona, F. (2009). Computer Simulation of the Dynamic Behavior of the Glutathione-Ascorbate Redox Cycle in Chloroplasts. *PLANT PHYSIOLOGY* 149, 1958–1969. doi:10.1104/pp.108.133223.

Valero, E., Macià, H., De la Fuente, I. M., Hernández, J.-A., González-Sánchez, M.-I., and García-Carmona, F. (2015). Modeling the ascorbate-glutathione cycle in chloroplasts under light/dark conditions. *BMC Systems Biology* 10. doi:10.1186/s12918-015-0239-y.

van Ittersum, M. K., and Donatelli, M. (2003). Modelling cropping systems—highlights of the symposium and preface to the special issues. *European Journal of Agronomy* 18, 187–197. doi:10.1016/S1161-0301(02)00095-3.

Vanlerberghe, G. C. (2013). Alternative Oxidase: A Mitochondrial Respiratory Pathway to Maintain Metabolic and Signaling Homeostasis during Abiotic and Biotic Stress in Plants. *Int J Mol Sci* 14, 6805–6847. doi:10.3390/ijms14046805.

Vauclare, P., Kopriva, S., Fell, D., Suter, M., Sticher, L., von Ballmoos, P., et al. (2002). Flux control of sulphate assimilation in *Arabidopsis thaliana* : adenosine 5′-phosphosulphate reductase is more susceptible than ATP sulphurylase to negative control by thiols. *The Plant Journal* 31, 729–740. doi:10.1046/j.1365-313X.2002.01391.x.

Vivancos, P. D., Dong, Y., Ziegler, K., Markovic, J., Pallardó, F. V., Pellny, T. K., et al. (2010). Recruitment of glutathione into the nucleus during cell proliferation adjusts whole-cell redox homeostasis in Arabidopsis thaliana and lowers the oxidative defence shield: Recruitment of GSH into the nucleus. *The Plant Journal* 64, 825–838. doi:10.1111/j.1365-313X.2010.04371.x.

Wachter, A., Wolf, S., Steininger, H., Bogs, J., and Rausch, T. (2004). Differential targeting of GSH1 and GSH2 is achieved by multiple transcription initiation: implications for the compartmentation of glutathione biosynthesis in the Brassicaceae: Differential targeting of GSH1 and GSH2. *The Plant Journal* 41, 15–30. doi:10.1111/j.1365-313X.2004.02269.x.

Wagner, C., Sefkow, M., and Kopka, J. (2003). Construction and application of a mass spectral and retention time index database generated from plant GC/EI-TOF-MS metabolite profiles. *Phytochemistry* 62, 887–900. doi:10.1016/S0031-9422(02)00703-3.

Waller, J. C., Dhanoa, P. K., Schumann, U., Mullen, R. T., and Snedden, W. A. (2010). Subcellular and tissue localization of NAD kinases from Arabidopsis: compartmentalization of de novo NADP biosynthesis. *Planta* 231, 305–317. doi:10.1007/s00425-009-1047-7.

Wang, G., and Pichersky, E. (2007). Nicotinamidase participates in the salvage pathway of NAD biosynthesis in Arabidopsis: Arabidopsis nicotinamidase. *The Plant Journal* 49, 1020–1029. doi:10.1111/j.1365-313X.2006.03013.x.

Wargovich, M. J., Morris, J., Moseley, V., Weber, R., and Byrne, D. H. (2012). "Developing Fruit Cultivars with Enhanced Health Properties," in *Fruit Breeding* Handbook of Plant Breeding., eds. M. L. Badenes and D. H. Byrne (Boston, MA: Springer US), 37–68. doi:10.1007/978-1-4419-0763-9_2.

West, Mal., and Harada, J. J. (1993). Embryogenesis in Higher Plants: An Overview. *Plant Cell*, 1361–1369. doi:10.1105/tpc.5.10.1361.

Wheeler, G., Ishikawa, T., Pornsaksit, V., and Smirnoff, N. (2015). Evolution of alternative biosynthetic pathways for vitamin C following plastid acquisition in photosynthetic eukaryotes. *eLife* 4, e06369. doi:10.7554/eLife.06369.

Wheeler, G. L., Jones, M. A., and Smirnoff, N. (1998). The biosynthetic pathway of vitamin C in higher plants. *Nature* 393, 365–369. doi:10.1038/30728.

White, C. A., and Kennedy, J. F. (1985). Methods of enzymatic analysis, 3rd edition, volume VI: Metabolites 1: Carbohydrates edited by H. U. Bergmeyer, J. Bergmeyer and M. GraRl, Verlag Chemie, Weinheim, 1984. ISBN 3-527-26046-3. *Brit. Poly. J.* 17. doi:10.1002/pi.4980170418.

Wilkinson, S. W., Pastor, V., Paplauskas, S., Pétriacq, P., and Luna, E. (2018). Long-lasting β-aminobutyric acid-induced resistance protects tomato fruit against *Botrytis cinerea*. *Plant Pathology* 67, 30–41. doi:10.1111/ppa.12725.

Willekens, H., Inzé, D., Van Montagu, M., and van Camp, W. (1995). Catalases in plants. *Mol Breeding* 1, 207–228. doi:10.1007/BF02277422.

Winter, H., Robinson, D. G., and Heldt, H. W. (1994). Subcellular volumes and metabolite concentrations in spinach leaves. *Planta* 193, 530–535. doi:10.1007/BF02411558.

Wirtz, M., and Hell, R. (2007). Dominant-Negative Modification Reveals the Regulatory Function of the Multimeric Cysteine Synthase Protein Complex in Transgenic Tobacco. *The Plant Cell* 19, 625–639. doi:10.1105/tpc.106.043125.

Wolucka, B. A., and Van Montagu, M. (2003). GDP-Mannose 3′,5′-Epimerase Forms GDP-L-gulose, a Putative Intermediate for the de Novo Biosynthesis of Vitamin C in Plants. *Journal of Biological Chemistry* 278, 47483–47490. doi:10.1074/jbc.M309135200.

Wu, F., Li, Q., Yan, H., Zhang, D., Jiang, G., Jiang, Y., et al. (2016). Characteristics of Three Thioredoxin Genes and Their Role in Chilling Tolerance of Harvested Banana Fruit. *International Journal of Molecular Sciences* 17, 1526. doi:10.3390/ijms17091526.

Wu, R., Zhang, F., Liu, L., Li, W., Pichersky, E., and Wang, G. (2018). MeNA, Controlled by Reversible Methylation of Nicotinate, Is an NAD Precursor that Undergoes Long-Distance Transport in Arabidopsis. *Molecular Plant* 11, 1264–1277. doi:10.1016/j.molp.2018.07.003.

Wu, X., Oh, M.-H., Schwarz, E. M., Larue, C. T., Sivaguru, M., Imai, B. S., et al. (2011). Lysine Acetylation Is a Widespread Protein Modification for Diverse Proteins in Arabidopsis. *Plant Physiology* 155, 1769–1778. doi:10.1104/pp.110.165852.

Xia, J., Psychogios, N., Young, N., and Wishart, D. S. (2009). MetaboAnalyst: a web server for metabolomic data analysis and interpretation. *Nucleic Acids Research* 37, W652–W660. doi:10.1093/nar/gkp356.

Yamamoto, A., Bhuiyan, Md. N. H., Waditee, R., Tanaka, Y., Esaka, M., Oba, K., et al. (2005). Suppressed expression of the apoplastic ascorbate oxidase gene increases salt tolerance in tobacco and Arabidopsis plants. *Journal of Experimental Botany* 56, 1785–1796. doi:10.1093/jxb/eri167.

Yang, X.-Y., Xie, J.-X., Wang, F.-F., Zhong, J., Liu, Y.-Z., Li, G.-H., et al. (2011). Comparison of ascorbate metabolism in fruits of two citrus species with obvious difference in ascorbate content in pulp. *J. Plant Physiol.* 168, 2196–2205. doi:10.1016/j.jplph.2011.07.015.

Ye, N., Zhu, G., Liu, Y., Zhang, A., Li, Y., Liu, R., et al. (2012). Ascorbic acid and reactive oxygen species are involved in the inhibition of seed germination by abscisic acid in rice seeds. *Journal of Experimental Botany* 63, 1809–1822. doi:10.1093/jxb/err336.

Yesbergenova, Z., Yang, G., Oron, E., Soffer, D., Fluhr, R., and Sagi, M. (2005). The plant Mo-hydroxylases aldehyde oxidase and xanthine dehydrogenase have distinct reactive oxygen species signatures and are induced by drought and abscisic acid. *Plant J.* 42, 862–876. doi:10.1111/j.1365-313X.2005.02422.x.

Yokochi, Y., Yoshida, K., Hahn, F., Miyagi, A., Wakabayashi, K., Kawai-Yamada, M., et al. (2021). Redox regulation of NADP-malate dehydrogenase is vital for land plants under fluctuating light environment. *Proc Natl Acad Sci USA* 118, e2016903118. doi:10.1073/pnas.2016903118.

Young, A., and Lowe, G. (2018). Carotenoids—Antioxidant Properties. *Antioxidants* 7, 28. doi:10.3390/antiox7020028.

Zaffagnini, M., Michelet, L., Marchand, C., Sparla, F., Decottignies, P., Le Maréchal, P., et al. (2007). The thioredoxin-independent isoform of chloroplastic glyceraldehyde-3-phosphate dehydrogenase is selectively regulated by glutathionylation: Glutathionylation of chloroplastic GAPDH. *FEBS Journal* 274, 212–226. doi:10.1111/j.1742-4658.2006.05577.x.

Zafra, A., Rejón, J. D., Hiscock, S. J., and Alché, J. de D. (2016). Patterns of ROS Accumulation in the Stigmas of Angiosperms and Visions into Their Multi-Functionality in Plant Reproduction. *Front. Plant Sci.* 7. doi:10.3389/fpls.2016.01112.

Zamocky, M., Furtmüller, P. G., and Obinger, C. (2008). Evolution of Catalases from Bacteria to Humans. *Antioxidants & Redox Signaling* 10, 1527–1548. doi:10.1089/ars.2008.2046.

Zechmann, B. (2011). Subcellular distribution of ascorbate in plants. *Plant Signaling & Behavior* 6, 360–363. doi:10.4161/psb.6.3.14342.

Zechmann, B., Mauch, F., Sticher, L., and Müller, M. (2008). Subcellular immunocytochemical analysis detects the highest concentrations of glutathione in mitochondria and not in plastids. *Journal of Experimental Botany* 59, 4017–4027. doi:10.1093/jxb/ern243.

Zermiani, M., Zonin, E., Nonis, A., Begheldo, M., Ceccato, L., Vezzaro, A., et al. (2015). Ethylene negatively regulates transcript abundance of ROP-GAP rheostat-encoding genes and affects

apoplastic reactive oxygen species homeostasis in epicarps of cold stored apple fruits. *J. Exp. Bot.* 66, 7255–7270. doi:10.1093/jxb/erv422.

Zhang, M., Yuan, B., and Leng, P. (2009). The role of ABA in triggering ethylene biosynthesis and ripening of tomato fruit. *Journal of Experimental Botany* 60, 1579–1588. doi:10.1093/jxb/erp026.

Zhang, X., and Mou, Z. (2009). Extracellular pyridine nucleotides induce *PR* gene expression and disease resistance in Arabidopsis. *The Plant Journal* 57, 302–312. doi:10.1111/j.1365-313X.2008.03687.x.

Zhang, Y. (2013). *Ascorbic Acid in Plants*. New York, NY: Springer New York doi:10.1007/978-1-4614-4127-4.

Zhang, Y., Li, Y., He, Y., Hu, W., Zhang, Y., Wang, X., et al. (2018). Identification of NADPH oxidase family members associated with cold stress in strawberry. *FEBS Open Bio* 8, 593–605. doi:10.1002/2211-5463.12393.

Zhu, L., Guo, J., Zhu, J., and Zhou, C. (2014). Enhanced expression of EsWAX1 improves drought tolerance with increased accumulation of cuticular wax and ascorbic acid in transgenic Arabidopsis. *Plant Physiology and Biochemistry* 75, 24–35. doi:10.1016/j.plaphy.2013.11.028.

Zhu, X.-G., Lynch, J. P., LeBauer, D. S., Millar, A. J., Stitt, M., and Long, S. P. (2016). Plants *in silico*: why, why now and what?-an integrative platform for plant systems biology research: Plants *in silico*. *Plant, Cell & Environment* 39, 1049–1057. doi:10.1111/pce.12673.

Zimmermann, P., Heinlein, C., Orendi, G., and Zentgraf, U. (2006). Senescence-specific regulation of catalases in Arabidopsis thaliana (L.) Heynh. *Plant Cell Environ* 29, 1049–1060. doi:10.1111/j.1365-3040.2005.01459.x.

Zuo, J., Wang, Q., Zhu, B., Luo, Y., and Gao, L. (2016). Deciphering the roles of circRNAs on chilling injury in tomato. *Biochemical and Biophysical Research Communications* 479, 132–138. doi:10.1016/j.bbrc.2016.07.032.

ANNEX

ANNEX 1.

MS-DIAL parameters for LS-MC raw data processing

MS-DIAL ver. 4.70

#Project

MS1 Data type Centroid

MS2 Data type Centroid

Ion mode Negative

Target Metablomics

Mode ddMSMS

#Data collection parameters

Retention time begin 0

Retention time end 18

Mass range begin 50

Mass range end 1500

MS2 mass range begin 50

MS2 mass range end 1500

#Centroid parameters

MS1 tolerance 0.01

MS2 tolerance 0.025

#Isotope recognition

Maximum charged number 2

#Data processing

Number of threads 10

#Peak detection parameters

Smoothing method SavitzkyGolayFilter

Smoothing level 4

Minimum peak width 5

Minimum peak height 10000

#Peak spotting parameters

Mass slice width 0.1

Exclusion mass list (mass & tolerance)

#Deconvolution parameters

Sigma window value 0.5
MS2Dec amplitude cut off 0
Exclude after precursor False
Keep isotope until 0.5
Keep original precursor isotopes False

#MSP file and MS/MS identification setting
MSP file C:\Users\ppetriacq\Desktop\MSDIAL\MSMS-Public-Neg-VS15.msp
Retention time tolerance 100
Accurate mass tolerance (MS1) 0.01
Accurate mass tolerance (MS2) 0.05
Identification score cut off 80
Using retention time for scoring False
Using retention time for filtering False

#Text file and post identification (retention time and accurate mass based) setting
Text file
Retention time tolerance 0.5
Accurate mass tolerance 0.01
Identification score cut off 85

#Advanced setting for identification
Relative abundance cut off 0
Top candidate report False

#Adduct ion setting
[M-H]-
[M-H2O-H]-
[M+Na-2H]-
[M+Cl]-
[M+K-2H]-
[M+FA-H]-
[M+Hac-H]-
[M+C2H3N+Na-2H]-
[M+Br]-
[M+TFA-H]-
[M-C6H10O4-H]-

[M-C6H10O5-H]-

[M-C6H8O6-H]-

[M+CH3COONa-H]-

[2M-H]-

[2M+FA-H]-

[2M+Hac-H]-

[3M-H]-

[M-2H]2-

[M-3H]3-

#Alignment parameters setting

Reference file D:\Metabolomics\GD\Neg\MET-2019-M03-PP_FSK240_Neg_116_QC013.abf

Retention time tolerance 0.1

MS1 tolerance 0.015

Retention time factor 0.5

MS1 factor 0.5

Peak count filter 0

N% detected in at least one group 0

Remove feature based on peak height fold-change True

Sample max / blank average 5

Sample average / blank average 5

Keep identified and annotated metabolites True

Keep removable features and assign the tag for checking True

Gap filling by compulsion True

#Tracking of isotope labels

Tracking of isotopic labels FALSE

#Ion mobility

Ion mobility data FALSE

ANNEX 2.

Differential equations used in the enzyme-based kinetic model.

(1) $$\frac{d[H_2O_2]_{cyt}}{dt} = -\left(\frac{V_{max_{CAT}} \times [H_2O_2]_{cyt}}{K_{m_{H_2O_2}^{CAT}}}\right) - \left(\frac{V_{max_{APX}} \times [H_2O_2]_{cyt} \times [ASC]}{K_{m_{ASC}^{APX}} \times [H_2O_2]_{cyt} + K_{m_{H_2O_2}^{APX}} \times [ASC] + [H_2O_2]_{cyt} \times [ASC]}\right)$$

$$+ H_2O_{2_{input}} - \left(\left(k_{H_2O_{2_{diffusion}}} \times [H_2O_2]_{cyt}\right) - \left(k_{H_2O_{2_{diffusion}}} \times [H_2O_2]_{apo}\right)\right)$$

(2) $$\frac{d[H_2O_2]_{apo}}{dt} = \left(\left(k_{H_2O_{2_{diffusion}}} \times [H_2O_2]_{cyt}\right) - \left(k_{H_2O_{2_{diffusion}}} \times [H_2O_2]_{apo}\right)\right)$$

$$+ (k_{NADPH\ oxidase} \times [NADPH] \times [O_2])$$

(3) $$\frac{d[GSH]_{cyt}}{dt} = GSH_{synthesis} - 2 \times \left(k_{5'_{DHA\ recycling}} \times [GSH]_{cyt} \times [DHA]\right)$$

$$-2 \times \left(\frac{V_{max_{DHAR}} \times [GSH]_{cyt} \times [DHA]}{K_{i_{DHA}^{DHAR}} \times K_{m_{GSH_1}^{DHAR}} + K_{m_{DHA}^{DHAR}} \times [GSH]_{cyt} + \left(K_{m_{GSH_1}^{DHAR}} + K_{m_{GSH_2}^{DHAR}}\right) \times [DHA] + [DHA] \times [GSH]_{cyt}}\right)$$

$$+2 \times \left(\frac{V_{max_{GR}} \times [GSSG]_{cyt} \times [NADPH]}{K_{m_{NADPH}^{GR}} \times [GSSG]_{cyt} + K_{m_{GSSG}^{GR}} \times [NADPH] + [GSSG]_{cyt} \times [NADPH]}\right)$$

(4) $$\frac{d[GSSG]_{cyt}}{dt} = -\left(\frac{V_{max_{ABCC}} \times [GSSG]_{cyt}}{K_{m_{GSSG}^{ABCC}} + [GSSG]_{cyt}}\right) + \left(k_{5'_{DHA\ recycling}} \times [GSH]_{cyt} \times [DHA]\right)$$

$$+\left(\frac{V_{max_{DHAR}} \times [GSH]_{cyt} \times [DHA]}{K_{i_{DHA}^{DHAR}} \times K_{m_{GSH_1}^{DHAR}} + K_{m_{DHA}^{DHAR}} \times [GSH]_{cyt} + \left(K_{m_{GSH_1}^{DHAR}} + K_{m_{GSH_2}^{DHAR}}\right) \times [DHA] + [DHA] \times}\right.$$

$$\left.-\left(\frac{V_{max_{GR}} \times [GSSG]_{cyt} \times [NADPH]}{K_{m_{NADPH}^{GR}} \times [GSSG]_{cyt} + K_{m_{GSSG}^{GR}} \times [NADPH] + [GSSG]_{cyt} \times [NADPH]}\right)\right.$$

(5) $$\frac{d[GSSG]_{vac}}{dt} = \left(\frac{V_{max_{ABCC}} \times [GSSG]_{cyt}}{K_{m_{GSSG}^{ABCC}} + [GSSG]_{cyt}}\right) - \left(Vac_{expension_{factor}} \times [GSSG]_{vac}\right)$$

(6)
$$\frac{d[ASC]}{dt} = -2 \times \left(\frac{V_{max_{APX}} \times [H_2O_2]_{cyt} \times [ASC]}{K_{m_{ASC}^{APX}} \times [H_2O_2]_{cyt} + K_{m_{H_2O_2}^{APX}} \times [ASC] + [H_2O_2]_{cyt} \times [ASC]} \right) + ASC_{synthesis}$$
$$+ \left(\frac{V_{max_{MDHAR}} \times [NADH] \times [MDHA]}{K_{m_{NADH}^{MDHAR}} \times [MDHA] + K_{m_{MDHA}^{MDHAR}} \times [NADH] + [NADH] \times [MDHA]} \right)$$
$$+ \left(\frac{V_{max_{MDHAR}} \times [NADPH] \times [MDHA]}{K_{m_{NADPH}^{MDHAR}} \times [MDHA] + K_{m_{MDHA}^{MDHAR}} \times [NADPH] + [NADPH] \times [MDHA]} \right)$$
$$+ \left(\frac{V_{max_{DHAR}} \times [GSH]_{cyt} \times [DHA]}{K_{i_{DHA}^{DHAR}} \times K_{m_{GSH_1}^{DHAR}} + K_{m_{DHA}^{DHAR}} \times [GSH]_{cyt} + \left(K_{m_{GSH_1}^{DHAR}} + K_{m_{GSH_2}^{DHAR}}\right) \times [DHA] + [DHA] \times [GSH]_{cyt}} \right)$$
$$+ \left(k_{5'_{DHA\,recycling}} \times [GSH]_{cyt} \times [DHA]\right) + \left(k_{6_{MDHA\,dismutation}} \times [MDHA]^2\right) - \left(Vac_{expension_{factor}} \times [ASC]\right)$$

(7)
$$\frac{d[MDHA]}{dt} = 2 \times \left(\frac{V_{max_{APX}} \times [H_2O_2]_{cyt} \times [ASC]}{K_{m_{ASC}^{APX}} \times [H_2O_2]_{cyt} + K_{m_{H_2O_2}^{APX}} \times [ASC] + [H_2O_2]_{cyt} \times [ASC]} \right)$$
$$- \left(\frac{V_{max_{MDHAR}} \times [NADH] \times [MDHA]}{K_{m_{NADH}^{MDHAR}} \times [MDHA] + K_{m_{MDHA}^{MDHAR}} \times [NADH] + [NADH] \times [MDHA]} \right)$$
$$- \left(\frac{V_{max_{MDHAR}} \times [NADPH] \times [MDHA]}{K_{m_{NADPH}^{MDHAR}} \times [MDHA] + K_{m_{MDHA}^{MDHAR}} \times [NADPH] + [NADPH] \times [MDHA]} \right)$$
$$-2 \times \left(k_{6_{MDHA\,dismutation}} \times [MDHA]^2\right)$$

(8)
$$\frac{d[DHA]}{dt} = DHA_{import} + \left(k_{6_{MDHA\,dismutation}} \times [MDHA]^2\right) - \left(k_{DHA_{degradation}} \times [DHA]\right)$$
$$- \left(\frac{V_{max_{DHAR}} \times [GSH]_{cyt} \times [DHA]}{K_{i_{DHA}^{DHAR}} \times K_{m_{GSH_1}^{DHAR}} + K_{m_{DHA}^{DHAR}} \times [GSH]_{cyt} + \left(K_{m_{GSH_1}^{DHAR}} + K_{m_{GSH_2}^{DHAR}}\right) \times [DHA] + [DHA] \times [GSH]_{cy} \right.$$
$$\left. - \left(Vac_{expension_{factor}} \times [DHA]\right) - \left(k_{5'_{DHA\,recycling}} \times [GSH]_{cyt} \times [DHA]\right) \right.$$

ANNEX 3.

Guillaume Decros, Pierre Baldet, Bertrand Beauvoit, Rebecca Stevens, Amélie Flandin, Sophie Colombié, Yves Gibon and Pierre Pétriacq (2019). Get the balance right: ROS Homeostasis and redox signalling in fruits.

frontiers in Plant Science

REVIEW
published: 18 September 2019
doi: 10.3389/fpls.2019.01091

Get the Balance Right: ROS Homeostasis and Redox Signalling in Fruit

Guillaume Decros[1], Pierre Baldet[1], Bertrand Beauvoit[1], Rebecca Stevens[2], Amélie Flandin[1,3], Sophie Colombié[1], Yves Gibon[1,3] and Pierre Pétriacq[1,3]**

[1] UMR 1332 BFP, INRA, Univ. Bordeaux, Villenave d'Ornon, France, [2] UR-1052 GAFL, INRA, CS60094, Montfavet, France, [3] MetaboHUB-Bordeaux, MetaboHUB, Phenome-Emphasis, Villenave d'Ornon, France

Plant central metabolism generates reactive oxygen species (ROS), which are key regulators that mediate signalling pathways involved in developmental processes and plant responses to environmental fluctuations. These highly reactive metabolites can lead to cellular damage when the reduction-oxidation (redox) homeostasis becomes unbalanced. Whilst decades of research have studied redox homeostasis in leaves, fundamental knowledge in fruit biology is still fragmentary. This is even more surprising when considering the natural profusion of fruit antioxidants that can process ROS and benefit human health. In this review, we explore redox biology in fruit and provide an overview of fruit antioxidants with recent examples. We further examine the central role of the redox hub in signalling during development and stress, with particular emphasis on ascorbate, also referred to as vitamin C. Progress in understanding the molecular mechanisms involved in the redox regulations that are linked to central metabolism and stress pathways will help to define novel strategies for optimising fruit nutritional quality, fruit production and storage.

Keywords: redox, fruit, ROS, metabolism, NAD, glutathione, tomato, ascorbate

OPEN ACCESS

Edited by:
Franco Famiani, University of Perugia, Italy

Reviewed by:
Robert D. Hancock, The James Hutton Institute, United Kingdom
Adriano Sofo, University of Basilicata, Italy

****Correspondence:***
Guillaume Decros
guillaume.decros@inra.fr
Pierre Pétriacq
pierre.petriacq@inra.fr

Specialty section:
This article was submitted to Plant Metabolism and Chemodiversity, a section of the journal Frontiers in Plant Science

Received: *13 February 2019*
Accepted: *09 August 2019*
Published: *18 September 2019*

Citation:
Decros G, Baldet P, Beauvoit B, Stevens R, Flandin A, Colombié S, Gibon Y and Pétriacq P (2019) Get the Balance Right: ROS Homeostasis and Redox Signalling in Fruit. Front. Plant Sci. 10:1091. doi: 10.3389/fpls.2019.01091

INTRODUCTION

Reduction-oxidation (redox) processes are a major consequence of the presence of ground-state oxygen gas (O_2, constituting c.a. 20.8% of the atmosphere) as a natural oxidant on Earth. Photosynthetic organisms (e.g. cyanobacteria, green algae, plants) produced O_2 by the light-driven splitting of water (H_2O) during oxygenic photosynthesis (Foyer, 2018). In other words, photosynthesis functionally houses redox reactions in plants that are underpinned by the transfer of electrons between a donor

Abbreviations: ABA, Abscisic acid; AGPase, ADP-glucose pyrophosphorylase; AltDH, Alternative dehydrogenases; AO, Ascorbate oxidase; AOX, Alternative oxidase; APX, Ascorbate peroxidase; ASC, Ascorbate; BABA, β-Aminobutyrate; CAT, Catalase; Chl, Chlorophyll; DHA, Dehydroascorbate; DHAR, Dehydroascorbate reductase; GABA, γ-Aminobutyrate; GP, Guaiacol peroxidase; GPX, Glutathione peroxidase; GR, Glutathione reductase; GRX, Glutaredoxins; GSH, Glutathione (reduced form); GSSG, Disulphide glutathione (oxidised form); GST, Glutathione S-transferase; JA, Jasmonic acid; LCMS, Liquid chromatography–mass spectrometry; MDHA, Monodehydroascorbate; MDHAR: Monodehydroascorbate reductase; Met, Methionine; MSR, Met sulphoxide reductase; NAD, Nicotinamide adenine dinucleotide; NADP, Nicotinamide adenine dinucleotide phosphate; NMR, Nuclear magnetic resonance; PS, Photosystem; PX, Peroxidase; RBOH, Respiratory burst oxidase homolog; ROS, Reactive oxygen species; $^1O_2$, Singlet oxygen; H_2O_2, Hydrogen peroxide; $O_2^{\bullet -}$, Superoxide anion; OH•, Hydroxyl radical; SA, Salicylic acid; SOD, Superoxide dismutase; TCA, Tricarboxylic acid; TRXs, Thioredoxins; XDH, Xanthine dehydrogenases.

and an acceptor. Consequently, this redox biochemistry generates the so-called reactive oxygen species (ROS). In tissues with low or no photosynthesis, such as roots and fruits, mitochondria can also drive the flow of electrons, thereby generating energy and ROS (Schertl and Braun, 2014).

Reactive oxygen species encompass highly reactive molecules that are partially reduced or excited forms of O_2 including singlet oxygen ($^1O_2$), hydrogen peroxide (H_2O_2), the superoxide anion ($O_2^{\bullet -}$) and the hydroxyl radical (OH•) (Apel and Hirt, 2004) (**Figure 1A**). Decades of research on redox biology pointed to a dual role for ROS both as toxic by-products of aerobic metabolism and as powerful signals that modulate plant functions (Mittler et al., 2011; Mittler, 2017; Foyer, 2018). With respect to this ambivalent concept, several ROS (e.g. H_2O_2) are produced during plant metabolism and development and in response to a fluctuating environment.

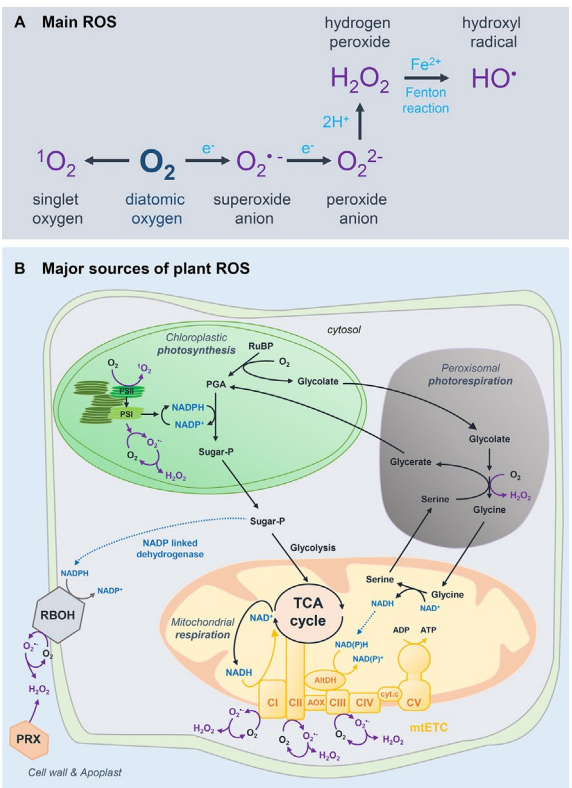

FIGURE 1 | Basics of ROS biology in plants. **(A)** Main reactive oxygen species (ROS) formed from atmospheric oxygen (O_2). **(B)** Major sources of ROS in plant cells. Excited triplet chlorophylls (Chl) can exacerbate the formation of singlet oxygen, mostly by the photosystem (PS) II reaction centre by photodynamic activation of ground-state oxygen (Fischer et al., 2013). In addition to singlet oxygen, superoxide and hydrogen peroxide can be formed in the chloroplast through the reduction of molecular oxygen, especially by the PSI. The four main complexes (CI–CIV) of the mitochondrial electron transport chain (mtETC) and the ATP synthase (CV) are represented in yellow. Among these complexes, CI (EC 1.6.5.3, NADH: ubiquinone oxidoreductase), CII (EC 1.3.5.1, succinate dehydrogenase) and CIII (EC 1.10.2.2, ubiquinol: cytochrome C oxidoreductase) are ROS-generating systems (Quinlan et al., 2012). mtETC, mitochondrial electron transfer chain; PRX, peroxidase; TCA, tricarboxylic acid; CI-V, complex I-V; AOX, alternative oxidase; AltDH, alternative dehydrogenase; cyt. c, cytochrome c; RuBP, ribulose 1,5-bisphosphate; PGA, phosphoglycerate; Sugar-P, sugar-phosphate; PS, photosystem.

Fruits, including fleshy fruits, are peculiar plant organs of great economic importance (e.g. 866 Mt worldwide in 2016, www.fao.org/faostat). They constitute a remarkable source of food worldwide and contain a plethora of natural compounds with various benefits for human health and nutrition, including vitamins, nutrients, fibres, proteins and minerals (Baldet et al., 2014; Rodriguez-Casado, 2016; Padayachee et al., 2017). Despite having high concentrations in carbohydrates, fruits usually exhibit reduced photosynthetic activity, but sometimes high respiration rates, in particular for climacteric fruits, such as tomato (Roch et al., 2019). As for other vegetative plant tissues, fruit biology involves redox reactions and generates ROS. Some fruits are major sources of antioxidants, such as ascorbate, which scavenge ROS (Gest et al., 2013b; Smirnoff, 2018).

To date, there is no global overview of the involvement of oxidative metabolism in fruit biology, despite some fairly recent reviews on ripening and photo-oxidative stress (Tian et al., 2013; Osorio et al., 2013a; Cocaliadis et al., 2014; Muñoz and Munné-Bosch, 2018). This present review aims at updating our current knowledge on redox biology of fleshy fruits. We provide an overview of the profusion of natural compounds having antioxidant properties and examine the importance of redox regulation in plant metabolism for development and stress responses. We also discuss the relevance of metabolic modelling for the study of redox fluxes in plants, which should help to improve knowledge on the link between metabolism and cell redox status and therefore to evaluate strategies for optimal fruit production and storage.

THE BASICS OF REDOX BIOLOGY IN PLANT CELLS

For decades, redox signalling has been perceived as a balance between low levels of ROS acting as signals to trigger signalling cascades that adjust plant functions and high levels of ROS causing oxidative cellular damage (Apel and Hirt, 2004). Currently, the paradigm of redox biology tends to display a bigger and clearer picture of the redox network, especially in plants where multiple sources of ROS are possible and associated with many 'ROS-processing systems' (Noctor et al., 2018). Spatial, temporal, metabolic and antioxidant specificities are multiple factors that can influence redox signalling. Whilst redox biology in fruit is clearly fragmentary, the concepts that originate from foliar tissues are useful whilst waiting for comprehensive studies that bring more substantial levels of knowledge. This section briefly describes the major sources of ROS that are found in plant cells and the systems that process them.

ROS Formation in Plants

The three main sources of plant ROS are the chloroplastic photosynthesis, the mitochondrial respiration and the peroxisomal photorespiration cycle (**Figure 1B**). The photosynthetic transport chain is assumed to be the major

source of plant ROS in photosynthetic tissues. Superoxide can directly exert its signalling function or be chemically reduced or dismutated to H_2O_2. Dismutation of H_2O_2 can be accelerated by superoxide dismutases (SODs; EC 1.15.1.1), which are pivotal in regulating the redox status of the plant cell (Smirnoff and Arnaud, 2019). Importantly, H_2O_2 is more likely to trigger transduction signals over longer cellular distances (e.g. into the nucleus) as it has a longer lifespan, a greater diffusion distance and stability as compared to $^1O_2$ (Exposito-Rodriguez et al., 2017; Mittler, 2017).

The photorespiratory cycle makes photosynthesis possible by scavenging 2-phosphoglycolate, which is toxic for the cell (Hodges et al., 2016). This highly compartmentalised pathway involving the chloroplast, peroxisome and mitochondrion is critical in generating H_2O_2 through the activity of peroxisomal glycolate oxidase (EC 1.1.3.15). Of course, the contribution of peroxisomal volume to total cell volume is small: 1% for peroxisomes compared to 12% for chloroplasts in leaves (Queval et al., 2011). Nonetheless, peroxisomes are predicted to be a major source of hydrogen peroxide in active photorespiratory cells. Furthermore, photorespiration-driven H_2O_2 is solely dismutated by peroxisomal catalase, which is commonly used as a redox marker of the peroxisome (Smirnoff and Arnaud, 2019, 202). In fruit, a high activity of the ascorbate recycling enzyme monodehydroascorbate reductase was observed in tomato fruit peroxisomes (Gest et al., 2013a), which supports the idea of an important role for peroxisomes in fruit redox homeostasis.

In nonphotosynthetic tissues, energy mostly originates from mitochondrial activity, which also contributes to generate ROS (Quinlan et al., 2012) (**Figure 1B**). The tricarboxylic acid cycle reduces NAD^+ into NADH in the mitochondrion, which is fundamental to ensure that cellular respiration produces ATP *via* oxidative phosphorylation (Millar et al., 2011) (**Figure 1B**). Thus, mitochondria are tightly linked to NAD(H) turnover (Gakière et al., 2018a). As for the chloroplast, specific SODs dismutate rapidly $O_2^{\bullet-}$ into H_2O_2 (Smirnoff and Arnaud, 2019). Besides ROS-generating systems, plant mitochondria specifically harbour alternative NADP(H) dehydrogenases that face both the matrix and the intermembrane space, as well as alternative oxidase (AOX) (**Figure 1B**). These enzymes are alternative respiratory routes, which do not produce energy, but allow viability when the enzymes of the main pathway are affected (Rasmusson et al., 2008, Rasmusson et al., 2009; Schertl and Braun, 2014). Alternative NADP(H) dehydrogenases can remove excess of reducing power in the mitochondria, which will balance the redox poise.

In addition, plant ROS can originate from other ROS-generating systems, including NADPH and xanthine oxidases. The NADPH oxidases (EC 1.6.3.1) are well-studied key players in ROS production (**Figure 1B**), most particularly with respect to biotic and abiotic environmental stresses (Torres and Dangl, 2005; Suzuki et al., 2011; Mittler, 2017). Xanthine dehydrogenases (EC 1.17.1.4, XDH) are important enzymes involved in the hydroxylation of hypoxanthine to xanthine, but can also form $O_2^{\bullet-}$ when molecular oxygen is used as the electron acceptor. Whilst XDHs in mammals can be converted into xanthine oxidases that produce both $O_2^{\bullet-}$ and H_2O_2, plant XDHs only form $O_2^{\bullet-}$, which can be swiftly dismutated into H_2O_2 (Yesbergenova et al., 2005; Ma et al., 2016). In complement, class III peroxidases (PXs; EC 1.11.1.7) are heme-containing enzymes that produce $O_2^{\bullet-}$ and H_2O_2 at the apoplast (Bindschedler et al., 2006; Cosio and Dunand, 2009; Daudi et al., 2012), although H_2O_2 formation is favoured at high pH in the presence of reductants (O'Brien et al., 2012). Peroxidases are also able to oxidise a donor and thereby process H_2O_2 (Lüthje and Martinez-Cortes, 2018).

For fruit tissues, however, knowledge is still lacking on the exact contribution of each source of ROS. Of course, due to low photosynthetic metabolism in fruit, one could predict different contributions than for leaves, which further depends on the plant species that exhibit diverse biochemical pathways able to scavenge and process cellular ROS. Even though mitochondria, peroxisomes and the apoplast are assumed to be leaders in ROS production in flowers and fruits (Qin et al., 2009a, Qin et al., 2009b; Rogers and Munné-Bosch, 2016), further research on fruit ROS is necessary to unveil the actual ROS-generating compartments and processes that mostly contribute to ROS production in fruit tissues.

Systems for ROS Scavenging and Processing in Plants

Reactive oxygen species produced in the plant cell can be scavenged, or processed, by highly efficient antioxidant systems. If this were not the case, ROS levels exceeding the requirement of metabolic processes would damage cellular structures and functions involving nucleic acids, proteins and lipids (Apel and Hirt, 2004; Muñoz and Munné-Bosch, 2018). Antioxidants include metabolites with antioxidant properties, which in fruit are profuse in their diversity and quantity and are found in all organelles. Besides metabolites, the antioxidant machinery is composed of a few major enzymes that rapidly process ROS, i.e. catalase (CAT; EC 1.11.1.21), SOD (EC 1.15.1.1), ascorbate peroxidase (APX; EC 1.11.1.11), monodehydroascorbate reductase (MDHAR; EC 1.6.5.4), dehydroascorbate reductase (DHAR; EC 1.8.5.1), glutathione S-transferase (GST; EC 2.5.1.18), glutathione peroxidase (**GPX**; EC 1.11.1.9), glutathione reductase (GR; EC 1.8.1.7) and guaiacol peroxidase (**GX**; EC 1.11.1.7). Hence, redox biology presents another level of ambiguity as enzymes such as peroxidase or dismutase can be considered as both ROS-generating and ROS-processing components (**Figure 2**). These enzymes tightly link to the pool of the redox buffers ascorbate, glutathione and pyridine nucleotides, which serve as reductants to recycle repeatedly glutathione and ascorbate *via* the so-called Foyer-Halliwell (or ascorbate-glutathione) cycle (Foyer and Noctor, 2011) (**Figure 2**). In addition, thioredoxins (TRXs) are widely distributed small proteins, which modulate the redox state of target proteins *via* transfer reactions of thiol-disulphide using NADP(H) as a cofactor (Geigenberger et al., 2017). These ROS-processing systems are also important for fruit metabolism, and they could link to developmental processes or responses to environmental changes, as we detail further below.

Fruit Antioxidants

Fruits, especially citrus and berry fruits, are well-known sources of antioxidants conferring plenty of beneficial effects for human

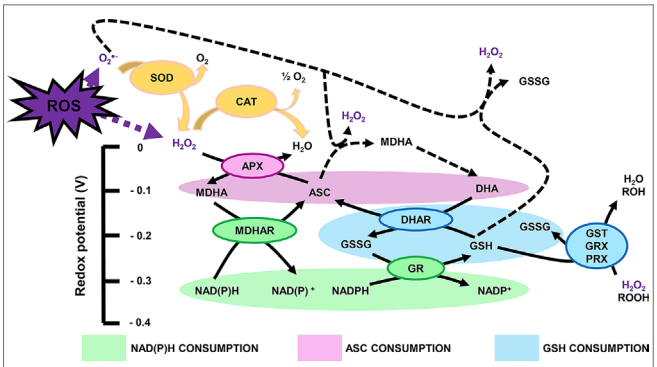

FIGURE 2 | Major cellular redox buffers: a *ménage-à-trois* to process ROS. Plain and dashed arrows represent enzymatic and nonenzymatic reactions, respectively. ASC, reduced ascorbate; APX, ascorbate peroxidase; CAT, catalase; DHA, dehydroascorbate; DHAR, dehydroascorbate reductase; GSH, reduced glutathione; GSSG, glutathione disulphide; GR, glutathione reductase; GRX, glutaredoxin; GST, glutathione S-transferase; MDHA, monodehydroascorbate; MDHAR, monodehydroascorbate reductase; PRX, GRX-dependent peroxiredoxin; ROH, organic compound with alcohol group; ROOH, organic compound with peroxide group; SOD, superoxide dismutase.

health (Gomes-Rochette et al., 2016). Because of their intricate oxidative metabolism (ROS production, described above), plants have developed a wide range of antioxidant metabolites as well as pathways to synthetize, catabolise and regenerate them. Basically, antioxidants refer to all biomolecules, including metabolites, which can process ROS and/or reactive nitrogen species to delay or avoid cell damage and for signalling processes (Nimse and Pal, 2015). Antioxidants can be distributed into several biochemical classes (**Figure 3**), including phenolics, terpenoids, thiol derivatives and vitamins, for which common metabolites and their antioxidant mechanisms are listed in

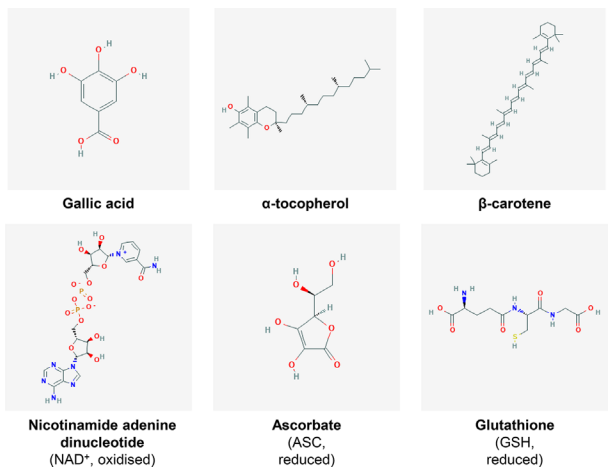

FIGURE 3 | Examples of fruit antioxidants. Chemical structures of several metabolites presenting antioxidant properties. The major redox buffers NAD^+, ASC and GSH are also presented. For further detail, refer to **Table 1**. Individual structures were obtained from PubChem (pubchem.ncbi.nlm.nih.gov/).

Table 1. Terpenoids, also known as isoprenoids for their core structure, can be divided into several classes based on their carbon skeleton, and among them, carotenoids are the main group with more than 600 having been identified and characterised (Graßmann, 2005). They are pigments used for light harvesting, preventing photo-oxidation and increasing fruit attractiveness for seed dispersion (Young and Lowe, 2018). Carotenoids among other terpenoids are widely studied with respect to their antioxidant properties and biological effects in plants and mammals. Whilst antioxidants are often shared by plant species, most plant families have developed their own range of specific antioxidant metabolites within their botanical taxa. Quite importantly, some major redox buffers shared between species, such as ferredoxins, pyridine nucleotides, TRXs, glutathione and ascorbate, can be distinguished as they play a fundamental role in the development of plants and their responses to the environment and thus in plant performance (Balmer et al., 2004; Geigenberger and Fernie, 2014; Geigenberger et al., 2017; Noctor et al., 2018; Gakière et al., 2018a).

Due to the wide diversity of fruit metabolites harbouring antioxidant activity, fruit antioxidants can process ROS in many ways. Most antioxidants spontaneously react with ROS, although enzymes such as APXs and glutaredoxins (GRX) catalyse several reactions. As previously mentioned, antioxidants remarkably participate in recycling pathways, such as the glutathione-ascorbate cycle, to maintain the redox state of the main redox buffers through the activity of GR, DHAR and MDHAR (**Figure 2**). The importance of such systems for fruit biology is detailed in Section 4.

Three Major Cellular Redox Buffers: A Ménage-À-Trois to Manage ROS

Ascorbate (ASC) and glutathione (GSH) sit at the top of plant soluble antioxidants because they process ROS rapidly using specific enzymes such as peroxidases belonging to the ascorbate-glutathione pathway (Foyer and Noctor, 2011) (**Figure 2**). In brief, ROS react preferentially with GSH and ASC: the latter can reduce H_2O_2 *via* APX to produce water and MDHA that will be reduced by MDHAR using NAD(P)H, or be transformed spontaneously in DHA that will be reduced by DHAR using GSH (**Figure 2**). These repetitive redox cycles allow for the regeneration of the pools and the maintenance of the cellular redox buffers in a highly reduced state in most cellular compartments under unstressed conditions. In addition, pyridine nucleotides (i.e. NAD(P)H and $NAD(P)^+$; **Figure 3**) are crucial for the regeneration of GSH and ASC through GR and MDHAR enzymes as well as being involved in other metabolic pathways, thereby linking redox homeostasis to central metabolism (Gakière et al., 2018a). Strikingly, fruit-specific concentrations and redox states of the pools are difficult to find in the literature (**Table 2**). In unstressed conditions, ASC and GSH are in a highly reduced state (> 90%), NAD(H) is 60% to 65% reduced, and NADP(H) is at 90% reduced in red ripe tomato fruits (Araújo et al., 2012; Centeno et al., 2011; Jimenez et al., 2002). However, NAD(H) is 12% to 20% reduced, and NADP(H) is 50% to 55% reduced in orange, apple, pear and

TABLE 1 | Examples of major antioxidant metabolites present in fruits.

Biochemical class	Compound class	Antioxidative metabolite	Antioxidant activity	Effect on human health	Source example (per 100 g FW)	Key references
Polyphenols	Hydroxycinnamic acids	Caffeic acid	Scavenge ROS and peroxyl radicals Inhibit lipid peroxidation	Anti-inflammatory Preventive effects for diabetes Cardiovascular protective effects	0.1–1.3 mg in tomato 0.4–35 µg in blueberries	Fu et al., 2011 Wolfe et al., 2008 Wang et al., 2017 Olas, 2018
		Ferulic acid			0.2–0.5 mg in tomato 26–185 µg in blueberries	Martí et al., 2016 Wang et al., 2017
		p-coumaric acid			0–0.6 mg in tomato 89–225 µg in blueberries 15–42 mg in strawberries	Skupien and Oszmianski, 2004 Martí et al., 2016 Wang et al., 2017
	Hydroxybenzoic acid	**Gallic acid**	Scavenge peroxyl radicals and ROS		2–9 mg in different cultivars of blackberries	Wada and Ou, 2002 Wang et al., 2017
	Flavonoids	Anthocyanins	Scavenge free radicals Acylation of anthocyanins with phenolic acid increase the antioxidant activity Prevent lipid peroxidation	Neuroprotective effects Anti-cancer involved in treatment of cardiovascular diseases	154–1001 µg in blueberries of Cyanidin 25–40 mg in strawberries of total anthocyanins	Skupien and Oszmianski, 2004 Khoo et al., 2017 Wang et al., 2017 Olas, 2018
		Catechin	Prevent lipid peroxydation Scavenge NO and ROS	Regulate superoxide production Regulation of transcription factors involved in oxidative stress responses	180–338 µg in blueberies 6–19 mg in different cultivars of strawberries	Fraga et al., 2018 Wang et al., 2017 Skupien and Oszmianski, 2004
		Quercitin		Neuroprotective and cardioprotective effects Anti-cancer	0.7–4.4 mg in tomato 202–266 µg in blueberries	Chaudhary et al., 2018 Martí et al., 2016 Wang et al., 2017
	Stilbenes	Resveratrol	Scavenge ROS and peroxyl radicals Inhibit lipid peroxidation	Neuroprotective and cardioprotective effects	51–97 µg in blueberries	Wang et al., 2017 Cory et al., 2018
Carotenoids		Lycopene	Process singlet oxygen Trap peroxyl radicals Inhibit radical-induced lipid peroxidation Reduce ROS production by nonphotochemical quenching of chlorophyll fluorescence	Anti-inflammatory Pro-vitamin A activity, converted to retinoids after breaking (oculo protective effects) Enhance immune system Anti-proliferative and anti-carcinogenic	7.8–18.1 mg in tomato 1.82–3.6 g in different buffaloberry cultivars	Eldahshan and Singab, 2013 Martí et al., 2016 Chaudhary et al., 2018 Murillo et al., 2010 Graßmann, 2005 Riedl et al., 2013
		Zeaxanthin			200 µg in mandarins 7.92 mg in South American sapote 6 mg in orange pepper 340 µg in tomato	Murillo et al., 2010
		β-Carotene			0.1–1.2 mg in tomato 1.5–3.8 mg in apricot	Martí et al., 2016 Sass-Kiss et al., 2005
Thiols		**Glutathione**	Process ROS *via* enzymatic and non-enzymatic reactions ROS scavenging Maintain thiol equilibrium S-glutathionylation of Cys residues allowing regulation of central metabolism during oxidative stresses	Neuroprotective effects Involve in asthma prevention and treatment	1,3 mg in mango 210–298 µg in strawberries 16–19.5 mg in tomato	Ding et al., 2007 Fitzpatrick et al., 2012 Smeyne and Smeyne, 2013 Erkan et al., 2008 Martins et al., 2018 Noctor et al., 2018 Keutgen and Pawelzik, 2007

(*Continued*)

TABLE 1 | Continued

Biochemical class	Compound class	Antioxidative metabolite	Antioxidant activity	Effect on human health	Source example (per 100 g FW)	Key references
Vitamins	Tocochromanols	**α-Tocopherol (VE)**	Prevent lipid peroxidation by scavenging free radicals (donating hydrogens) using ascorbate to be regenerated Prevent the oxidation of carotenoids Essential macronutrient for human maintaining cell membrane integrity	Anti-anemia Neuroprotective effects	0.5–1,1 mg in tomato; 0.6–0.8 µg in MoneyMaker cultivar 1,6–3,2 mg in red sweet pepper 3.8 mg in green olives of total tocopherol + tocotrienols	Gugliandolo et al., 2017 Giovinazzo et al., 2004 Chaudhary et al., 2018 Dasgupta and Klein, 2014 Raiola et al., 2015 Chun et al., 2006 Knecht et al., 2015
		Ascorbate (VC)	Process ROS *via* enzymatic and non-enzymatic reactions Allow the regeneration of tocopherols and carotenoids	Anti-scurvy Anti-inflammatory Anti-cancer	10–15 mg in commercial cultivars of tomato and until 70 mg in ancestral cultivars 54–87 mg in different cultivars of strawberries 2.4–3g in camu-camu	Chaudhary et al., 2018 Martins et al., 2018 Stevens et al., 2007 Skupien and Oszmianski, 2004 Justi et al., 2000

TABLE 2 | Examples of ASC, GSH and NAD/P(H) sources in fruits.

	Source example (per 100 g FW)	References
ASC	10 to 15 mg in tomato 54–87 mg in strawberries 2.4-3 g in camu-camu	Stevens et al., 2007 Skupien and Oszmianski, 2004 Justi et al., 2000
GSH	1.3 mg in mango 16–19.5 mg in tomato 210–298 µg in strawberries	Ding et al., 2007 Giovinazzo et al., 2004 Cervilla et al., 2007 Keutgen and Pawelzik, 2007
NAD^+	3.21 mg in red fruits and 2.22 mg at breaker stage in tomato 780 µg in orange 400 µg in grapefruit	Osorio et al., 2013b Centeno et al., 2011 Bruemmer, 1969
NADH	5.82 mg in red fruits and 4.94 mg at breaker stage in tomato 170 µg in orange 50 µg in grapefruit	Osorio et al., 2013b Centeno et al., 2011 Bruemmer, 1969
$NADP^+$	0.46 mg in red fruits and 0.77 mg at breaker stage in tomato 89 µg in orange 69 µg in grapefruit	Osorio et al., 2013b Centeno et al., 2011 Bruemmer, 1969
NADPH	3.88 mg in red fruits and 3.23 mg at breaker stage in tomato 119 µg in orange 89 µg in grapefruit	Osorio et al., 2013b Centeno et al., 2011 Bruemmer, 1969

grapefruits (Bruemmer, 1969), which is congruent with the redox status of photosynthetic tissues (Gakière et al., 2018b). This clearly suggests a diversity in fruit redox homeostasis as fruit growth influences the redox state of pyridine nucleotides. Furthermore, these three major cellular redox buffers display distinct redox potential: −0.1, −0.23 and −0.32 mV for the ASC/DHA, GSH/GSSG and $NAD(P)^+$/NAD(P)H couples, respectively (**Figure 2**). In this case, as pyridine nucleotides have a lower redox potential, they will be detrimental for electron transfer to GSH and ASC during redox mechanisms.

THE IMPORTANCE OF THE REDOX HUB FOR FRUIT SIGNALLING

The redox hub consists of all the molecular partners able to generate, process or trigger oxidative signals, whilst the resulting redox signalling can modulate the physiology of plant organs including fruits (Mittler, 2017; Noctor et al., 2018). Fruits are a major source of central metabolites (Osorio et al., 2013a; Roch et al., 2019), such as carbohydrates, lipids, amino and organic acids, but also vitamins and other antioxidant metabolites that play important roles in fruit biology (**Figure 3**). Besides, redox status is also at the heart of the control of metabolic processes (Geigenberger and Fernie, 2014). One among many reasons is the prominence of pyridine nucleotides (NAD/P(H)) as master regulators of hundreds of biochemical reactions (Gakière et al., 2018a), together with ascorbate/dehydroascorbate (ASC/DHA) and glutathione (GSH/GSSG) couples (Noctor et al., 2018). In this context, we will present recent advances in our understanding of key spatiotemporal redox signals that occur during developmental processes and in response to environmental changes, including redox buffers that balance the redox poise (**Figure 4**).

Redox and Central Metabolism During Fruit Development

Fruit development comprises three main phases: cell division, cell expansion and ripening. As green organs, young fruits and leaves share some similarities due to the presence of photosynthetically active chloroplasts driving central metabolism, hence developmental processes (Cocaliadis et al., 2014). Fruit photosynthesis can contribute to the production of starch, which can then be turned into soluble carbohydrates during ripening. In tomato, a number of studies points towards the importance of the mitochondrial malate valve in transmitting redox status to the plastids, which will influence plastidial metabolism (Centeno et al., 2011; Osorio et al., 2013b). In fact,

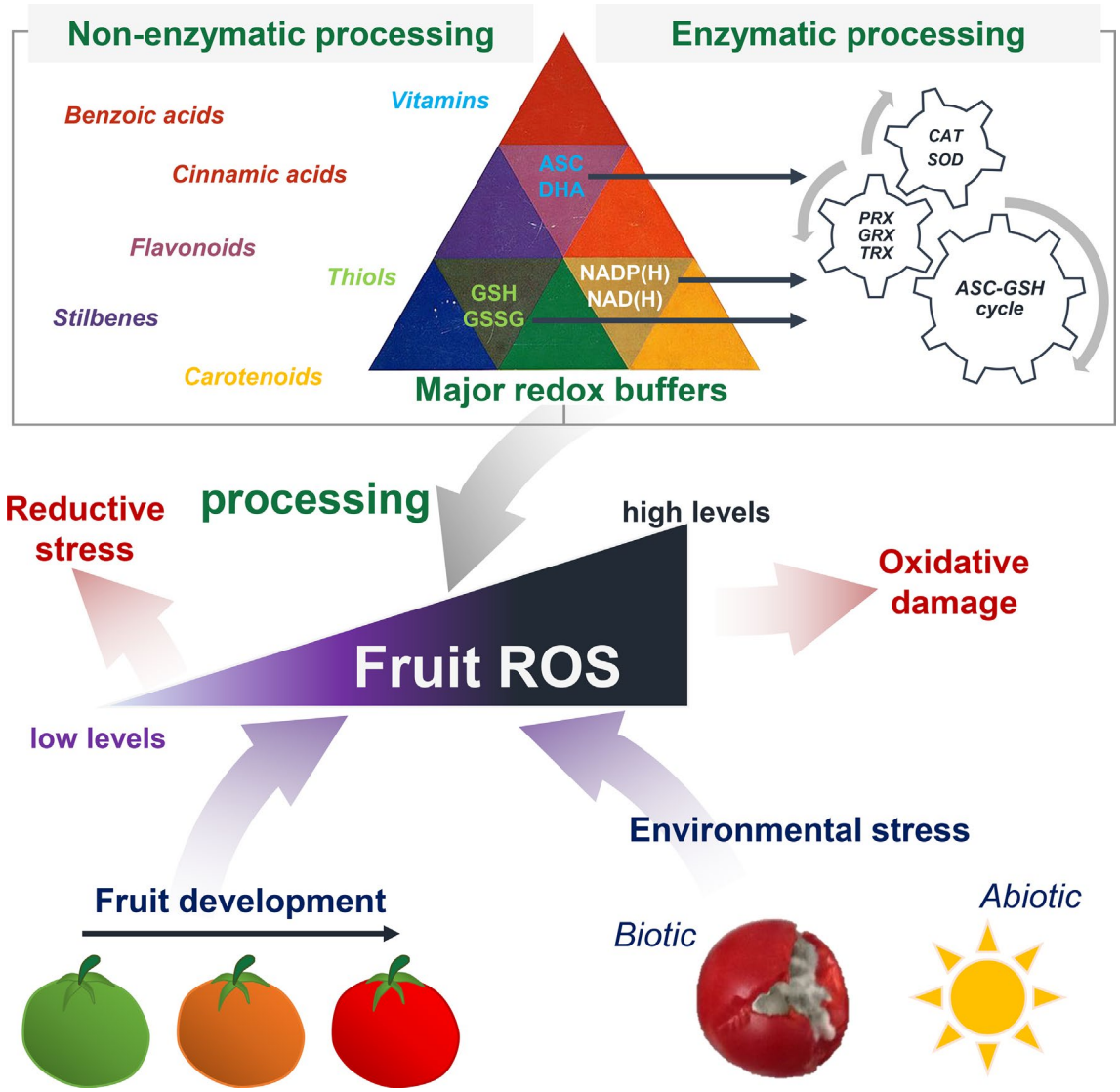

FIGURE 4 | Pivotal role of redox signalling for fruit growth and stress responses. Fruits produce ROS and other redox signals during development and in response to environmental stress. Reactive oxygen species homeostasis is finely tuned between ROS production and processing. This involves several enzymatic and non-enzymatic mechanisms, including antioxidant metabolites and major redox buffers (NAD/P(H), ASC and GSH) that allow antioxidant cycles to process excess of ROS. When ROS levels are too high, the resulting oxidative stress would damage cellular structures.

decreasing malate content in the growing fruit could stimulate the activation state of AGPase (EC 2.7.7.27), leading to increased starch and soluble sugar pools in ripening tomato. Intriguingly, such metabolic repercussions tend to provide tolerance of tomato to water loss, wrinkling and pathogenic infections. This supports the paradigm of a versatile role of redox signals in metabolic regulation throughout development and in response to stress (Tian et al., 2013). Another hallmark of this growth phase is when chloroplasts become chromoplasts by losing green chlorophylls at the expense of coloured antioxidants like carotenoids (Lado et al., 2015; Martí et al., 2009). Concomitantly, the expression of nuclear- and plastid-encoded photosynthetic genes drops as the fruit ripens. It is noteworthy that ROS synthesis influences the accumulation of carotenoids (Pan et al., 2009), which are major scavengers of singlet oxygen, specifically β-carotene, tocopherol and plastoquinone (Miret and Munné-Bosch, 2015). Besides carotenoids, anthocyanins can accumulate in the growing fruits and contribute to both red/purple/blue colours and antioxidant properties [**Table 1**; (Muñoz and Munné-Bosch, 2018)]. Whilst carotenoids accumulate primarily within lipophilic membranes, anthocyanins are stored in the vacuole where their colour depends on their chemical structure, which is influenced by vacuolar pH (Jaakola, 2013). In this context, recent studies have reported a critical role for epigenetic processes in growing tomato fruit by linking DNA demethylation levels with transcriptomic changes of genes involved in fruit antioxidant biosynthesis (e.g. flavonoids, carotenoids) (Lang et al., 2017). Conversely, however, development and ripening of orange,

a nonclimacteric fruit, were correlated with an increase in DNA methylation levels, together with repression of photosynthetic genes (Huang et al., 2019). Thus, fruit development is likely to present remarkable discrepancies in terms of redox signals, their source (e.g. chloroplastic, mitochondrial, peroxisomal, apoplastic) and the duration and extent of oxidative stress, even at early stages of fruit growth in comparison to leaves (Muñoz and Munné-Bosch, 2018).

Ripening is an important end process of fruit development that involves multiple molecular regulations (Osorio et al., 2013a). It is mediated by redox signalling, more specifically during the chloroplast-to-chromoplast transition and in the mitochondrial compartment, where protein carbonylation occurs and respiration rates increase, thus affecting the redox state when sugar supply becomes limiting (Qin et al., 2009a; Tian et al., 2013). As the fruit ripens, oxidative stress progressively augments, like in peach, tomato, pepper and grape berries (*Vitis vinifera*), where H_2O_2 pools accumulate upon changes in skin colour (Jimenez et al., 2002; Martí et al., 2009; Qin et al., 2009a; Pilati et al., 2014; Kumar et al., 2016). In fact, it is assumed that ROS accumulation produces two distinct peaks during fruit growth: first at the onset of ripening and second at overripening either preharvest or postharvest (Muñoz and Munné-Bosch, 2018). It is possible that increased oxidative stress might favour fruit softening, which is beneficial for seed release (Jimenez et al., 2002). This would explain why short life tomato cultivars are redox-stressed and present lower antioxidant activities (Cocaliadis et al., 2014).

Because of ROS imbalance, oxidative signals need processing *via* cellular redox buffering and the antioxidant machinery to avoid cellular damage (**Figure 4**). In ripening grape berries, accumulated levels of H_2O_2 are accompanied with a concomitant stimulation of CAT activity (Pilati et al., 2014). Moreover, under oxidative stress, increases in activities of APX, MDHAR and GR are seen in peach (Camejo et al., 2010). Contrasting observations are reported for peroxidases: ripening phase is associated with increased PX activities in mango, apples and banana fruit, whilst tomato, strawberry and capsicum show a decline in these activities (Pandey et al., 2012, and references therein). The importance of antioxidant systems for ripening is also exemplified in grapevines where there is a strong developmental modulation of ASC metabolism at the biosynthetic, recycling and catabolic levels (Melino et al., 2009). Fruit growth of wine grapes can witness a gradual induction of ASC biosynthesis and subsequent changes in the accumulation of ASC and two derivatives: tartaric and oxalic acids. Whilst immature berries showed a swift accumulation of ASC together with a low ASC/DHA redox ratio, ripe fruits instead showed an increased accumulation of ASC and higher ASC/DHA ratio. Additionally, acerola, an exotic fruit cultivated mostly for its ascorbic acid content, shows differential regulation of MDHAR and DHAR genes during fruit ripening (Eltelib et al., 2011). A comparison of ASC metabolism in mandarin and orange, two citrus species harbouring different ASC contents in pulp, deepens our understanding of the differences in ASC concentrations in fruit (Yang et al., 2011b). This study revealed that higher ASC in ripening orange was associated with an augmented expression of four genes involved in ASC biosynthesis, encoding GDP-D-mannose-3′,5′-epimerase (EC 5.1.3.18), GDP-L-galactose-phosphorylase (EC 2.7.7.69), L-galactose dehydrogenase (EC 1.1.1.316) and L-galactono-1,4-lactone dehydrogenase (EC 1.3.2.3), together with attenuated activities of ASC oxidase and ASC peroxidase, which are involved in ASC degradation. Another elegant work on isolated mitochondria from ripening tomato fruits has reported a global stimulation of the ASC-GSH cycle at the enzyme level (López-Vidal et al., 2016). Recently, a system biology approach in tomato has been conducted based on large-scale transcriptomic, proteomic, metabolic and phenotypic data for orange fruit of RNAi lines for three enzymes involved in ASC metabolism (AO, GLD and MDHAR) (Stevens et al., 2018). The ASC redox state has been reported to influence the expression of genes involved in cellular protein synthesis and stability and ribosomal function. Besides redox functions, synthesis of ASC is also crucial for tomato fruit growth (Garcia et al., 2009; Mounet-Gilbert et al., 2016), as exemplified by profound growth stunting of tomato fruits silenced in mitochondrial ASC synthesis (Alhagdow et al., 2007). Another recent study of protein turnover at global scale in the developing tomato fruit revealed a stage-specific response of protein profiles that were associated to various redox functions (Belouah et al., 2019). Changes in redox-related proteins were represented in the young fruit (e.g. SOD, APX) and at ripening (e.g. MDHAR, GR). Hence, ASC metabolism appears to be central to redox homeostasis during fruit development.

Upon stress and senescence (i.e. ageing), oxidative alterations can drastically target proteins, resulting in conformational changes and thus impairing their catalytic functions. Methionine (Met) and cysteine, which contain sulphur, are probably the most susceptible to ROS oxidation (Davies, 2005). In the case of Met, oxidation can be reversed by Met sulphoxide reductase (MSR, EC 1.8.4.11/12) (Emes, 2009; Rey and Tarrago, 2018), which has been reported to play a role in senescing litchi fruit through down-regulation of *MSR* genes (Jiang et al., 2018). In leaves, previous works have suggested a link between MSR and the homeostasis and redox balance of NAD/P(H) (Pétriacq et al., 2012, Pétriacq et al., 2013). Besides MSR, a stimulation of the antioxidant systems in tomato fruit mitochondria has been reported to be associated with a differential carbonylation of mitochondrial proteins in breaker and light red tomato fruits, which might participate in protein degradation and cellular signalling (López-Vidal et al., 2016). Besides targeting proteins, aging of fruit encompasses other redox-related changes. In the pulp of Kyoho grape, postharvest senescence and rotting are accompanied by an accumulation of oxidative signals (e.g. malondialdehyde, hydrogen peroxide, superoxide anion) and a concomitant depletion of several antioxidant systems (e.g. ascorbate, flavonoids, total phenolics, reducing sugars) (Ni et al., 2016). Interestingly, exogenous treatment with hydrogen sulphide could alleviate those redox perturbations by enhancing the activity of antioxidant enzymes, such as CAT and APX, and by attenuating those of lipoxygenase in the pulp and peel of Kyoho grape.

Additionally, not only central metabolism links to redox signalling in fruit but also more specialised pathways involving

phytohormones (Symons et al., 2012; Leng et al., 2013). In red raspberry, a nonclimacteric crop fruit, the stage of ripeness at the time of harvest determines the antioxidant contents (e.g. anthocyanins, ellagitannins, vitamins C and E, carotenoids) (Beekwilder et al., 2005; Miret and Munné-Bosch, 2016). Application of the carotenoid-derivative hormone ABA after fruit set modulates the ASC/DHA ratio in young berries and more than doubles ASC pools in ripe fruit. Such an effect was partially explained by alterations of ASC oxidation and recycling through the activities of AO, APX, DHAR and MDHAR (Miret and Munné-Bosch, 2016). In postharvest conditions, fruit decay is a major issue caused by perturbation of the redox balance, including ROS production (Pétriacq et al., 2018). Thus, antioxidant mechanisms (e.g. ASC total pool and redox state, ASC-GSH cycle) are important actors throughout fruit growth, which is further evidence for the idea that ROS act as metabolic by-products requiring a finely tuned homeostasis (**Figure 4**). In an agri-food context, further research is required to disentangle the implication of each redox event occurring during fruit development, so that efficient strategies can be adopted to improve fruit production and storage.

Nevertheless, the active depiction of redox fluxes by deciphering redox signatures in plant biology is extremely tedious, if not impossible, probably due to the extreme reactivity of ROS and related redox signals and to the intricacy of the redox hub. However, a very interesting and promising alternative to measurements of redox pools and antioxidant systems is the use of mathematical modelling of metabolism, in particular for redox branches. In the context of central metabolism, previous studies elegantly shed a different light on climacteric respiration in tomato fruit using stoichiometric models (Colombié et al., 2015, Colombié et al., 2017). Using a medium-scale stoichiometric model, energy and the redox cofactors NAD(H) and NADP(H) were defined as internal metabolites and balanced so that constraining of the metabolic network was possible not only through C and N homeostasis, but also through the redox and energy status (Colombié et al., 2015). This model suggested a consistent requirement of NADPH for biomass synthesis and demonstrated that higher ATP hydrolysis was required for growth starting at the end of cell expansion and that a peak of CO_2 was released at the end of tomato ripening. This coincided with climacteric respiration of tomato fruit and involved energy dissipation by the AOX (**Figure 1B**), a redox marker of the mitochondrial compartment (Polidoros et al., 2009; Pétriacq et al., 2016). This was further confirmed by a more detailed stoichiometric model of the respiratory pathway, including AOX and uncoupling proteins (Colombié et al., 2017). Moreover, the recent flux analysis performed with grape cells under nitrogen limitation showed differently regulated fluxes were involved in the flavonoid (phenylpropanoid) pathway and in major carbon fluxes supporting a strong link between central metabolism and cell redox status by energy (ATP) and reducing power equivalents (NADPH and NADH) (Soubeyrand et al., 2018). Thus, mitochondrial function plays a notable role along fruit development in mitigating the redox poise upon an imbalance between energy supply and demand. In complement, when omics strategies failed to measure oxidative fluxes accurately, kinetic modelling of metabolism has proven to be a complementary and promising approach as it offers, with enzymatic and metabolic parameters, the possibility to describe quantitatively fluxes of cycling pathways such as redox metabolism. For instance, this was achieved previously for sucrose metabolism in the developing tomato fruit *via* a model of 13 differential equations describing the variations of hexoses, hexoses-phosphates and sucrose as a function of 24 enzyme reactions (Beauvoit et al., 2014). Similar approaches to redox cycles are necessary to obtain novel insights into the active redox dynamics involved in fruit biology.

The Key Role of ROS and Cognate Redox Signals in Fruit Responses to Environmental Constraints

The generation of ROS is a crucial process in response of plants to a changing environment and contributes to establish adaptive signalling pathways (Noctor et al., 2014). Oxidative stress typically comes as a secondary stress after primary stresses, whether they are abiotic constraints (**Figure 4**), such as drought or flooding, wounding, high light, cold or heat stress or biotic stresses including pest attacks or bacterial and fungal infections. Fruits are no exception to this rule: ROS can originate from NADPH oxidases (**Figure 1B**), specifically with respect to biotic and abiotic environmental challenges (Torres and Dangl, 2005; Suzuki et al., 2011; Mittler, 2017). Upon cold stress in apple fruits, NADPH oxidases might function *via* a regulatory node that integrates ethylene and ROS signalling pathways (Zermiani et al., 2015). In strawberry fruits, recent identification of NAPDH oxidase genes indicated that *FvRbohA* and *FvRbohD* might be involved in cold stress and defence responses (Zhang et al., 2018).

At present, it is assumed that major redox couples (NAD/P(H), ASC, GSH) are integral regulators of stress responses in plants (**Figure 4**), including both abiotic and biotic stresses (Pétriacq et al., 2013; Noctor and Mhamdi, 2014; Smirnoff, 2018; Gakière et al., 2018a). For instance, exogenous application of NAD^+ confers resistance to citrus canker disease in citrus (Alferez et al., 2018). In coherence with a modulation of these redox buffers, the antioxidant system further contributes in processing excess of ROS within stressed tissues (Foyer and Noctor, 2011; Smirnoff and Arnaud, 2019) (**Figure 4**). Additionally, redox processes dominate hormonal signalling *via* the stress hormones salicylic (SA), jasmonic (JA) and abscisic acids, which play a critical role in metabolic adjustments under stress conditions (Leng et al., 2013; Geigenberger and Fernie, 2014; Gakière et al., 2018a). Thus, a complex signalling network is devoted to shaping the fruit responses to stress. However, the interrelation between these multiple signalling partners is poorly understood, and its study will necessitate further research.

As for developmental processes (**Figure 4**), a hallmark of plant responses to stress is the activation of the ASC-GSH cycle (**Figure 2**). Upon arsenic and silicon exposure, fruits of two tomato cultivars exhibited different but profound redox

perturbations of H_2O_2 and antioxidant contents (e.g. lycopene, carotenoids and phenolics), ASC and GSH redox states and lipid peroxidation (Marmiroli et al., 2017a). Alternatively, a detailed proteomic study on tomato fruit confirmed the implication of ASC- and GSH-related proteins in response to this abiotic stress (Marmiroli et al., 2017b). Some of these redox alterations (H_2O_2, ASC and GSH redox states, total carotenoids and phenolics) were proposed as reliable arsenic exposition biomarkers for further studies that could broaden our knowledge on arsenic-induced abiotic stress in fruit (Marmiroli et al., 2017a). Besides arsenic, hot air treatment of strawberry fruits directly triggered the induction of antioxidant enzymes (e.g. CAT, APX and SOD), which further leads to a reduction of necrotrophic lesions caused by the fungal pathogen *Botrytis cinerea* (Jin et al., 2016). Additionally, a study of cold and light stress in tomato fruit unveils an interaction between temperature and light to modulate synthesis, recycling and oxidation of ASC in fruit (Massot et al., 2013). Light promoted the accumulation of ASC and GSH in tomato fruit, thus supporting the hypothesis of a stimulation in ASC synthesis by light (Gautier et al., 2009; Massot et al., 2012; Baldet et al., 2013; Smirnoff, 2018).

Redox signalling is associated with physiological disorders in fruits stored under multiple environmental stresses, such as for pome fruit, where redox-related metabolites are likely to accumulate (e.g. γ-aminobutyrate [GABA]) or rapidly decline (e.g. ASC, GSH) after exposure to low O_2 and/or elevated CO_2 environments (Lum et al., 2016). This in turn results in disturbances of the energetic and oxidative balance. In this context, both GABA and antioxidant metabolism are regulated by NAD/P(H) ratios, which confirms the tight link between cellular redox buffers and the regulation of oxidative metabolism (Trobacher et al., 2013; Lum et al., 2016) (**Figure 4**). A characterisation of TRX genes in harvested banana fruit suggests that the protein MaTrx12 regulates redox homeostasis, which impacts chilling tolerance (Wu et al., 2016). In tomato fruit, a combination of deep sequencing and bioinformatics revealed 163 circular RNAs that exhibited chilling responsive expression, among them several ones predicted to be involved in redox reactions and various stress signalling pathways (e.g. heat/cold shock protein, energy metabolism, hormonal responses, salt stress, cold-responsive transcription factors) (Zuo et al., 2016).

Infection of fruits with pathogenic microbes is a pressing issue due to dramatic postharvest diseases that can claim up to 50% of the total production worldwide (Romanazzi et al., 2016; Pétriacq et al., 2018). Resistance inducers have been used as promising strategies to elicit fruit defences against phytopathogens (Pétriacq et al., 2018). A global transcriptional analysis of strawberry fruit has demonstrated that the fungal elicitor chitosan and the salicylate-mimicking compound benzothiadiazole modulate chloroplastic signals to trigger various defence responses through redox alterations (e.g. *PX*, *GST*, *GRX*) (Landi et al., 2017). Accordingly, induction of sweet orange with chitosan or salicylic acid also alters the redox status of the cell (e.g. TRX, SOD, PX), as exemplified through RNAseq data (Coqueiro et al., 2015). Another example comes from *Peronophythora litchii*–infected litchi fruits that exhibit lower infection symptoms after treatment with a novel chitosan formulation (Jiang et al., 2018). Disease tolerance was correlated in litchi pericarp with higher activities of defensive (e.g. chitinase, phenylalanine lyase, glucanase) and antioxidant enzymes (e.g. SOD, CAT, APX), a lower O_2^- generation rate and lower malondialdehyde levels and higher contents of redox buffers including ascorbic acid and glutathione and reducing power. Moreover, priming of tomato seedlings with β-aminobutyrate (BABA), a novel phytohormone (Thevenet et al., 2017), confers resistance of tomato fruits to the fungal pathogen *B. cinerea* through metabolic rearrangements including antioxidant (e.g. flavonoids, polyphenols) and ABA contents (Wilkinson et al., 2018). This resistance was also associated with a delay in fruit ripening, which suggests a metabolic trade-off for defence metabolism versus fruit growth. Together, phytopathologic studies confirm the trigger of an oxidative burst in infected fruit tissues, for which excess ROS are mitigated both by a stimulation of enzymatic antioxidant systems and nonenzymatic protective, scavenging molecules (Tian et al., 2013). Hence, unsurprisingly, induction of antioxidant functions has proven to be effective in controlling postharvest diseases in fruits (Romanazzi et al., 2016; Pétriacq et al., 2018).

Practical Applications Towards Modifying Redox Metabolism in Fruits

Although the precise functions of redox regulators remain to be evidenced, a few practical applications are currently explored towards modifying redox biology in fruits. From a human health perspective, fruit redox metabolism received much attention since fruits and vegetables are major sources of essential antioxidative metabolites and thus recommended in human diet (e.g. five a day, http://www.fao.org/). Due to the intensively studied health effects of antioxidants for their numerous benefits for aging, cancer and chronic disorders, research focused on strategies to increase the antioxidant contents in consumable product. Moderate success has been obtained in engineering plants to increase antioxidants content such as ASC, GSH and vitamin E (Wargovich et al., 2012; Gallie, 2013). However, the *Golden Rice*, enriched in β-carotene (provitamin A), remains a successful story for redox application in crops combining plant biotechnologies, antioxidant synthesis pathway and human health (Botella-Pavía and Rodríguez-Concepción, 2006). Nevertheless, due to the importance of ROS signalling in developmental processes, the modulation of oxidative mechanisms can alter fruit growth. For instance, engineering tomato fruits to increase levels of antioxidants by enhancing chloroplast functions results in longer-lasting and firmer fruits (Mehta et al., 2002; Zhang et al., 2013). Thus, future applications need to consider the spatial and temporal regulations of redox homeostasis during plant development to improve significantly plant productivity.

Fruit physiological disorders during storage under multiple environmental stresses are also associated with redox perturbations (Lum et al., 2016). Fruit decay is a major issue caused by changes of the redox balance, including ROS production, in postharvest conditions (Pétriacq et al., 2018). From an agri-food perspective, chilling stress is oxidative but also particularly critical as low temperatures are often used

to delay senescence of many fruits (Lallu, 1997; Bustamante et al., 2016; Valenzuela et al., 2017; Alhassan et al., 2019). Reactive oxygen species accumulate during fruit overripening, which thus puts the improvement of fruit storage conditions in the forefront of redox signalling applications (Muñoz and Munné-Bosch, 2018). Furthermore, diverse chemical treatments have been identified to limit ROS accumulation by affecting either their production or processing. For instance, nitric oxide postharvest treatment in cucumber was associated with a decrease in ROS content and an increase of APX, CAT and SOD activities (Yang et al., 2011a; Liu et al., 2016). Other examples come from the use of chlorine dioxide fumigation in longan fruit that displays a reduction in enzymatic fruit browning (Saengnil et al., 2014) and ozone applications in citrus industry that allow to improve fruit shelf-life (Karaca, 2010). In addition, the plant defence hormones methyl-jasmonate (MeJA) and methyl-salicylate (MeSA) promote AOX gene expression in green pepper (Purvis, 1997). More recently, it was reported that MeJA also improved chilling tolerance of cucumber by increasing both CAT gene expression and enzyme activity (Liu et al., 2016). Biotechnological approaches have been further used to reduce oxidative stress in fruits mostly by overexpressing main ROS-processing enzymes (**Figure 2**) but also by increasing the total antioxidant content. In this context, anthocyanin- and flavonoids-enriched mango fruits have shown a better tolerance to cold during storage (Sudheeran et al., 2018).

Importantly, practical applications to modulate redox metabolism trigger plant resistance to biotic stresses. Fruits can suffer substantial yield losses from diseases as fruit decay at a postharvest level can claim up to 50% of the total production worldwide (Pétriacq et al., 2018). Given that ROS signalling is central to plant-pathogen interactions (Mittler, 2017), and main redox buffers are linked to defence hormonal signalling (Pétriacq et al., 2013; Pétriacq et al., 2016; Pétriacq et al., 2018), diverse treatment building on hormonal and redox signalling has shown a lower disease incidence and symptoms. For instance, nitric oxide treatment inhibits anthracnose (*Colletotrichum gloeosporioides*) in ripening mango (Hu et al., 2014) and further improves chilling tolerance in banana fruit *via* an induction of the antioxidative defence system (Wu et al., 2014). Additionally, MeSA and MeJA treatments can be used to stimulate pathogen resistance and increase the antioxidant content without affecting fruit quality in kiwi, tomato and peach (Tzortzakis and Economakis, 2007; Zhang et al., 2008; Fatemi et al., 2013).

CONCLUDING REMARKS AND FUTURE OUTLOOKS

Not before time, the simple Manichean belief of 'good' reductants and 'bad' oxidants, such as ROS, has become erroneous. There is so much to learn from future molecular studies of redox metabolism, particularly in fruit, for which an obvious lack of fundamental knowledge needs to be addressed. Reactive oxygen species production and cognate redox signals are key to harmonious metabolism and contribute to establishing adaptive signalling pathways throughout development and in response of fruits to environmental events. Whilst redox buffers, specifically ascorbate, clearly appear at the forefront of oxidative regulation, these redox mechanisms also seem to depend on the fruit species. Recent years have witnessed a growing interest in developing both analytical technologies (e.g. LCMS, NMR, ROS detection, redox proteomics) and mathematical modelling to provide quantitative description of the central metabolism and specialised pathways including antioxidant processes (Qin et al., 2009a; Beauvoit et al., 2014; Colombié et al., 2015; Colombié et al., 2017; Deborde et al., 2017). In tomato fruit, for instance, spatially resolved distribution of metabolites including antioxidants will help to decipher the involvement of such redox compounds in physiological responses (Nakamura et al., 2017).

Studying key spatiotemporal redox processes involved in fruit is of paramount importance. Numerous fruits, such as the ones from the Solanaceae family (e.g. tomato, pepper, eggplant), not only contain a cocktail of antioxidants (vitamins A and C, flavonoids), but also domestication of these plants has reduced the content in prohealth molecules such as vitamin C. Indeed, ascorbate was higher in ancestral cultivars of tomato (Gest et al., 2013b; Palma et al., 2015). These are among the many reasons for ascorbate to be at the heart of research on the plant redox hub, where plant scientists endeavour to increase fruit ASC content, which should improve human nutrition and plant tolerance to stress (Macknight et al., 2017). Progress in understanding the molecular signatures involved in the redox regulations that link central metabolism and stress pathways will help to define novel strategies for optimal fruit production and storage (Beauvoit et al., 2018).

AUTHOR CONTRIBUTIONS

All authors contributed to writing this review.

FUNDING

The authors are also grateful to the MetaboHUB (ANR-11-INBS-0010) and PHENOME (ANR-11-INBS-0012) projects for financial support. The doctoral school Sciences de la Vie et Santé at Université de Bordeaux is also acknowledged for granting PP with PhD funding for GD (bourse fléchée ministérielle 2018-2021).

ACKNOWLEDGMENTS

The authors thank Dr. Annick Moing for the invitation to contribute to this special issue on fruit metabolism. The authors are also grateful to the MetaboHUB (ANR-11-INBS-0010) and PHENOME (ANR-11-INBS-0012) projects for financial support. The doctoral school Sciences de la Vie et Santé at Université de Bordeaux is also acknowledged for granting PP with PhD funding for GD (bourse fléchée ministérielle 2018-2021).

REFERENCES

Alferez, F. M., Gerberich, K. M., Li, J.-L., Zhang, Y., Graham, J. H., and Mou, Z. (2018). Exogenous nicotinamide adenine dinucleotide induces resistance to citrus canker in citrus. *Front. Plant Sci.* 9, 1472. doi: 10.3389/fpls.2018.01472

Alhagdow, M., Mounet, F., Gilbert, L., Nunes-Nesi, A., Garcia, V., Just, D., et al. (2007). Silencing of the mitochondrial ascorbate synthesizing enzyme l-galactono-1,4-lactone dehydrogenase affects plant and fruit development in tomato. *Plant Physiol.* 145, 1408–1422. doi: 10.1104/pp.107.106500

Alhassan, N., Golding, J. B., Wills, R. B. H., Bowyer, M. C., and Pristijono, P. (2019). Long term exposure to low ethylene and storage temperatures delays calyx senescence and maintains 'Afourer' mandarins and navel oranges quality. *Foods* 8, 19. doi: 10.3390/foods8010019

Apel, K., and Hirt, H. (2004). Reactive oxygen species: metabolism, oxidative stress, and signal transduction. *Ann. Rev. Plant Biol.* 55, 373–399. doi: 10.1146/annurev.arplant.55.031903.141701

Araújo, W. L., Tohge, T., Osorio, S., Lohse, M., Balbo, I., Krahnert, I., et al. (2012). Antisense inhibition of the 2-oxoglutarate dehydrogenase complex in tomato demonstrates its importance for plant respiration and during leaf senescence and fruit maturation. *Plant Cell* 24, 2328–2351. doi: 10.1105/tpc.112.099002

Baldet, P., Bres, C., Okabe, Y., Mauxion, J.-P., Just, D., Bournonville, C., et al. (2013). Investigating the role of vitamin C in tomato through TILLING identification of ascorbate-deficient tomato mutants. *Plant Biotechnol.* 30, 309–314. doi: 10.5511/plantbiotechnology.13.0622b

Baldet, P., Ferrand, C., and Rothan, C. (2014). "Vitamins in Fleshy Fruit," in Fruit Ripening: Physiology, Signalling and Genomics, eds P. Nath, M. Bouzayen, A. K. Mattoo, and J. C. Pech (Wallingford: CABI), 127–150. doi: 10.1079/9781845939625.0127

Balmer, Y., Vensel, W. H., Tanaka, C. K., Hurkman, W. J., Gelhaye, E., Rouhier, N., et al. (2004). Thioredoxin links redox to the regulation of fundamental processes of plant mitochondria. *Proc. Nat. Acad. Sci.* 101, 2642–2647. doi: 10.1073/pnas.0308583101

Beauvoit, B., Belouah, I., Bertin, N., Cakpo, C. B., Colombié, S., Dai, Z., et al. (2018). Putting primary metabolism into perspective to obtain better fruits. *Ann. Bot.* 122, 1–21. doi: 10.1093/aob/mcy057

Beauvoit, B. P., Colombié, S., Monier, A., Andrieu, M.-H., Biais, B., Bénard, C., et al. (2014). Model-assisted analysis of sugar metabolism throughout tomato fruit development reveals enzyme and carrier properties in relation to vacuole expansion. *Plant Cell* 26, 3224–3242. doi: 10.1105/tpc.114.127761

Beekwilder, J., Hall, R. D., and Ric Vos, C. H. D. (2005). Identification and dietary relevance of antioxidants from raspberry. *BioFactors* 23, 197–205. doi: 10.1002/biof.5520230404

Belouah, I., Nazaret, C., Pétriacq, P., Prigent, S., Bénard, C., Mengin, V., et al. (2019). Modeling protein destiny in developing fruit. *Plant Physiol.* 180, 1709–1724 doi: 10.1104/pp.19.00086

Bindschedler, L. V., Dewdney, J., Blee, K. A., Stone, J. M., Asai, T., Plotnikov, J., et al. (2006). Peroxidase-dependent apoplastic oxidative burst in *Arabidopsis* required for pathogen resistance. *Plant J.* 47, 851–863. doi: 10.1111/j.1365-313X.2006.02837.x

Botella-Pavía, P., and Rodríguez-Concepción, M. (2006). Carotenoid biotechnology in plants for nutritionally improved foods. *Physiol. Plant.* 126, 369–381. doi: 10.1111/j.1399-3054.2006.00632.x

Bruemmer, J. H. (1969). Redox state of nicotinamide-adenine dinucleotides in citrus fruit. *J. Agric. Food Chem.* 17, 1312–1315. doi: 10.1021/jf60166a023

Bustamante, C. A., Monti, L. L., Gabilondo, J., Scossa, F., Valentini, G., Budde, C. O., et al. (2016). Differential metabolic rearrangements after cold storage are correlated with chilling injury resistance of peach fruits. *Front. Plant Sci.* 7, 1478. doi: 10.3389/fpls.2016.01478

Camejo, D., Martí, M. C., Román, P., Ortiz, A., and Jiménez, A. (2010). Antioxidant system and protein pattern in peach fruits at two maturation stages. *J. Agric. Food Chem.* 58, 11140–11147. doi: 10.1021/jf102807t

Centeno, D. C., Osorio, S., Nunes-Nesi, A., Bertolo, A. L. F., Carneiro, R. T., Araújo, W. L., et al. (2011). Malate plays a crucial role in starch metabolism, ripening, and soluble solid content of tomato fruit and affects postharvest softening. *Plant Cell* 23, 162–184. doi: 10.1105/tpc.109.072231

Cervilla, L. M., Blasco, B., Rios, J. J., Romero, L., and Ruiz, J. M. (2007). Oxidative Stress and Antioxidants in Tomato (Solanum lycopersicum) Plants Subjected to Boron Toxicity. *Annals of Botany* 100, 747–756. doi:10.1093/aob/mcm156.

Chaudhary, P., Sharma, A., Singh, B., and Nagpal, A. K. (2018). Bioactivities of phytochemicals present in tomato. Journal of Food Science and Technology, 55(8), 2833–2849. doi: 10.1007/s13197-018-3221-z

Chun, J., Lee, J., Ye, L., Exler, J., and Eitenmiller, R. R. (2006). Tocopherol and tocotrienol contents of raw and processed fruits and vegetables in the United States diet. *J. Food Compost. Anal.* 19, 196–204. doi: 10.1016/j.jfca.2005.08.001

Cocaliadis, M. F., Fernández-Muñoz, R., Pons, C., Orzaez, D., and Granell, A. (2014). Increasing tomato fruit quality by enhancing fruit chloroplast function. A double-edged sword? *J. Exp. Bot.* 65, 4589–4598. doi: 10.1093/jxb/eru165

Colombié, S., Beauvoit, B., Nazaret, C., Bénard, C., Vercambre, G., Le Gall, S., et al. (2017). Respiration climacteric in tomato fruits elucidated by constraint-based modelling. *New Phytol.* 213, 1726–1739. doi: 10.1111/nph.14301

Colombié, S., Nazaret, C., Bénard, C., Biais, B., Mengin, V., Solé, M., et al. (2015). Modelling central metabolic fluxes by constraint-based optimization reveals metabolic reprogramming of developing *Solanum lycopersicum* (tomato) fruit. *Plant J.* 81, 24–39. doi: 10.1111/tpj.12685

Coqueiro, D. S. O., de Souza, A. A., Takita, M. A., Rodrigues, C. M., Kishi, L. T., and Machado, M. A. (2015). Transcriptional profile of sweet orange in response to chitosan and salicylic acid. *BMC Genomics* 16, 288. doi: 10.1186/s12864-015-1440-5

Cory, H., Passarelli, S., Szeto, J., Tamez, M., and Mattei, J. (2018). The Role of Polyphenols in Human Health and Food Systems: A Mini-Review. Frontiers in Nutrition, 5(September), 1–9. doi: 10.3389/fnut.2018.00087

Cosio, C., and Dunand, C. (2009). Specific functions of individual class III peroxidase genes. *J. Exp. Bot.* 60, 391–408. doi: 10.1093/jxb/ern318

Dasgupta, A., and Klein, K. (2014). "*Antioxidant Vitamins and Minerals*," *in Antioxidants in Food, Vitamins and Supplements* (Elsevier), 277–294. doi: 10.1016/B978-0-12-405872-9.00015-X

Daudi, A., Cheng, Z., O'Brien, J. A., Mammarella, N., Khan, S., Ausubel, F. M., et al. (2012). The apoplastic oxidative burst peroxidase in *Arabidopsis* is a major component of pattern-triggered immunity. *Plant Cell* 24, 275–287. doi: 10.1105/tpc.111.093039

Davies, M. J. (2005). The oxidative environment and protein damage. *Biochim. Biophys. Acta* 1703, 93–109. doi: 10.1016/j.bbapap.2004.08.007

Deborde, C., Moing, A., Roch, L., Jacob, D., Rolin, D., and Giraudeau, P. (2017). Plant metabolism as studied by NMR spectroscopy. *Prog. Nucl. Magn. Reson. Spectrosc.* 10, 102–103. doi: 10.1016/j.pnmrs.2017.05.001

Ding, Z.-S., Tian, S.-P., Zheng, X.-L., Zhou, Z.-W., and Xu, Y. (2007). Responses of reactive oxygen metabolism and quality in mango fruit to exogenous oxalic acid or salicylic acid under chilling temperature stress. *Physiol. Plant.* 130, 112–121. doi: 10.1111/j.1399-3054.2007.00893.x

Eldahshan, O. A., Nasser, A., and Singab, B. (2013). Carotenoids. *J Pharmacogn Phytochem*, 8192(1), 2668735–5. doi 10.3945/an.113.004028

Eltelib, H. A., Badejo, A. A., Fujikawa, Y., and Esaka, M. (2011). Gene expression of monodehydroascorbate reductase and dehydroascorbate reductase during fruit ripening and in response to environmental stresses in acerola (*Malpighia glabra*). *J. Plant Physiol.* 168, 619–627. doi: 10.1016/j.jplph.2010.09.003

Emes, M. J. (2009). Oxidation of methionine residues: the missing link between stress and signalling responses in plants. *Biochem. J.* 422, e1–e2. doi: 10.1042/BJ20091063

Erkan, M., Wang, S. Y., and Wang, C. Y. (2008). Effect of UV treatment on antioxidant capacity, antioxidant enzyme activity and decay in strawberry fruit. *Postharvest Biology and Technology* 48, 163–171. doi: 10.1016/j.postharvbio.2007.09.028

Exposito-Rodriguez, M., Laissue, P. P., Yvon-Durocher, G., Smirnoff, N., and Mullineaux, P. M. (2017). Photosynthesis-dependent H_2O_2 transfer from chloroplasts to nuclei provides a high-light signalling mechanism. *Nat. Commun.* 8, 49. doi: 10.1038/s41467-017-00074-w

Fatemi, H., Mohammadi, S., and Aminifard, M. H. (2013). Effect of postharvest salicylic acid treatment on fungal decay and some postharvest quality factors of kiwi fruit. *Arch. Phytopathol. Plant Prot.* 46, 1338–1345. doi: 10.1080/03235408.2013.767013

Fischer, B. B., Hideg, É., and Krieger-Liszkay, A. (2013). Production, Detection, and Signaling of Singlet Oxygen in Photosynthetic Organisms. *Antioxid. Redox Signal* 18, 2145–2162. doi: 10.1089/ars.2012.5124

Fitzpatrick, T. B., Basset, G. J. C., Borel, P., Carrari, F., DellaPenna, D., Fraser, P. D., et al. (2012). Vitamin Deficiencies in Humans: Can Plant Science Help? *Plant Cell* 24, 395–414. doi: 10.1105/tpc.111.093120

Foyer, C. H. (2018). Reactive oxygen species, oxidative signaling and the regulation of photosynthesis. *Environ. Exp. Bot.* 154, 134–142. doi: 10.1016/j.envexpbot.2018.05.003

Foyer, C. H., and Noctor, G. (2011). Ascorbate and glutathione: the heart of the redox hub. *Plant Physiol.* 155, 2. doi: 10.1104/pp.110.167569

Fraga, C. G., Oteiza, P. I., and Galleano, M. (2018). Plant bioactives and redox signaling: (–)-Epicatechin as a paradigm. *Mol. Aspects Med.*, 61, 31–40. doi: 10.1016/j.mam.2018.01.007

Fu, L., Xu, B.-T., Xu, X.-R., Gan, R.-Y., Zhang, Y., Xia, E.-Q., et al. (2011). Antioxidant capacities and total phenolic contents of 62 fruits. *Food Chem.* 129, 345–350. doi: 10.1016/j.foodchem.2011.04.079

Gakière, B., Fernie, A. R., and Pétriacq, P. (2018a). More to NAD^+ than meets the eye: a regulator of metabolic pools and gene expression in *Arabidopsis*. *Free Radic. Biol. Med.* 122, 86–95 doi: 10.1016/j.freeradbiomed.2018.01.003

Gakière, B., Hao, J., de Bont, L., Pétriacq, P., Nunes-Nesi, A., and Fernie, A. R. (2018b). NAD^+ biosynthesis and signaling in plants. *Crit. Rev. Plant Sci.* 1–49. doi: 10.1080/07352689.2018.1505591

Gallie, D. R. (2013). Increasing vitamin C content in plant foods to improve their nutritional value—successes and challenges. *Nutrients* 5, 3424–3446. doi: 10.3390/nu5093424

Garcia, V., Stevens, R., Gil, L., Gilbert, L., Gest, N., Petit, J., et al. (2009). An integrative genomics approach for deciphering the complex interactions between ascorbate metabolism and fruit growth and composition in tomato. *C. R. Biol.* 332, 1007–1021. doi: 10.1016/j.crvi.2009.09.013

Gautier, H., Massot, C., Stevens, R., Sérino, S., and Génard, M. (2009). Regulation of tomato fruit ascorbate content is more highly dependent on fruit irradiance than leaf irradiance. *Ann. Bot.* 103, 495–504. doi: 10.1093/aob/mcn233

Geigenberger, P., and Fernie, A. R. (2014). Metabolic control of redox and redox control of metabolism in plants. *Antioxid. Redox Signaling* 21, 1389–1421. doi: 10.1089/ars.2014.6018

Geigenberger, ,. P., Thormählen, I., Daloso, D. M., and Fernie, A. R. (2017). The unprecedented versatility of the plant thioredoxin system. *Trends Plant Sci.* 22, 249–262. doi: 10.1016/j.tplants.2016.12.008

Gest, N., Garchery, C., Gautier, H., Jiménez, A., and Stevens, R. (2013a). Light-dependent regulation of ascorbate in tomato by a monodehydroascorbate reductase localized in peroxisomes and the cytosol. *Plant Biotechnol. J.* 11, 344–354. doi: 10.1111/pbi.12020

Gest, N., Gautier, H., and Stevens, R. (2013b). Ascorbate as seen through plant evolution: the rise of a successful molecule? *J. Exp. Bot.* 64, 33–53. doi: 10.1093/jxb/ers297

Giovinazzo, G., D'Amico, L., Paradiso, A., Bollini, R., Sparvoli, F., and DeGara, L. (2004). Antioxidant metabolite profiles in tomato fruit constitutively expressing the grapevine stilbene synthase gene: Antioxidant levels in tomato synthesizing resveratrol. *Plant. Biotechnol. J.* 3, 57–69. doi: 10.1111/j.1467-7652.2004.00099.x

Gomes-Rochette, N. F., Da Silveira Vasconcelos, M., Nabavi, S. M., Mota, E. F., Nunes-Pinheiro, D. C. S., Daglia, M., et al. (2016). Fruit as potent natural antioxidants and their biological effects. *Curr. Pharm. Biotechnol.* 17, 986–993. doi: 10.2174/1389201017666160425115401

Graßmann, J. (2005). "Terpenoids as Plant Antioxidants," in *Vitamins & Hormones* (Elsevier, London, UK). 72, 505–535. doi: 10.1016/S0083-6729(05)72015-X

Gugliandolo, A., Bramanti, P., and Mazzon, E. (2017). Role of vitamin E in the treatment of alzheimer's disease: evidence from animal models. *IJMS* 18, 2504. doi: 10.3390/ijms18122504

Hodges, M., Dellero, Y., Keech, O., Betti, M., Raghavendra, A. S., Sage, R., et al. (2016). Perspectives for a better understanding of the metabolic integration of photorespiration within a complex plant primary metabolism network. *J. Exp. Bot.* 67, 3015–3026. doi: 10.1093/jxb/erw145

Hu, M., Yang, D., Huber, D. J., Jiang, Y., Li, M., Gao, Z., et al. (2014). Reduction of postharvest anthracnose and enhancement of disease resistance in ripening mango fruit by nitric oxide treatment. *Postharvest Biol. Technol.* 97, 115–122. doi: 10.1016/j.postharvbio.2014.06.013

Huang, H., Liu, R., Niu, Q., Tang, K., Zhang, B., Zhang, H., et al. (2019). Global increase in DNA methylation during orange fruit development and ripening. *Proc. Natl. Acad. Sci. U.S.A.* 116, 1430–1436 doi: 10.1073/pnas.1815441116

Jaakola, L. (2013). New insights into the regulation of anthocyanin biosynthesis in fruits. *Trends Plant Sci.* 18, 477–483. doi: 10.1016/j.tplants.2013.06.003

Jiang, X., Lin, H., Lin, M., Chen, Y., Wang, H., Lin, Y., et al. (2018). A novel chitosan formulation treatment induces disease resistance of harvested litchi fruit to *Peronophythora litchii* in association with ROS metabolism. *Food Chem.* 266, 299–308. doi: 10.1016/j.foodchem.2018.06.010

Jimenez, A., Creissen, G., Kular, B., Firmin, J., Robinson, S., Verhoeyen, M., et al. (2002). Changes in oxidative processes and components of the antioxidant system during tomato fruit ripening. *Planta* 214, 751–758. doi: 10.1007/s004250100667

Jin, P., Zheng, C., Huang, Y., Wang, X., Luo, Z., and Zheng, Y. (2016). Hot air treatment activates defense responses and induces resistance against *Botrytis cinerea* in strawberry fruit. *J. Integr. Agric.* 15, 2658–2665. doi: 10.1016/S2095-3119(16)61387-4

Justi K. C., Visentainer J.V., Evelazio de Souza N, Matsushita M. (2000). Nutritional composition and vitamin C stability in stored camu-camu (Myrciaria dubia) pulp. *Arch Latinoam Nutr.* 50, 405–408.

Karaca, H. (2010). Use of ozone in the citrus industry. *Ozone: Sci. Eng.* 32, 122–129. doi: 10.1080/01919510903520605

Keutgen, A. J., and Pawelzik, E. (2007). Modifications of Strawberry Fruit Antioxidant Pools and Fruit Quality under NaCl Stress. *J. Agric. Food Chem.* 55, 4066–4072. doi: 10.1021/jf070010k

Khoo, H. E., Azlan, A., Tang, S. T., and Lim, S. M. (2017). Anthocyanidins and anthocyanins: colored pigments as food, pharmaceutical ingredients, and the potential health benefits. Food & Nutr. Res., 61(1), 1361779. doi: 10.1080/16546628.2017.1361779

Knecht, K., Sandfuchs, K., Kulling, S. E., and Bunzel, D. (2015). Tocopherol and tocotrienol analysis in raw and cooked vegetables: a validated method with emphasis on sample preparation. *Food Chem.* 169, 20–27. doi: 10.1016/j.foodchem.2014.07.099

Kumar, V., Irfan, M., Ghosh, S., Chakraborty, N., Chakraborty, S., and Datta, A. (2016). Fruit ripening mutants reveal cell metabolism and redox state during ripening. *Protoplasma* 253, 581–594. doi: 10.1007/s00709-015-0836-z

Lado, J., Zacarías, L., Gurrea, A., Page, A., Stead, A., and Rodrigo, M. J. (2015). Exploring the diversity in Citrus fruit colouration to decipher the relationship between plastid ultrastructure and carotenoid composition. *Planta* 242, 645–661. doi: 10.1007/s00425-015-2370-9

Lallu, N. (1997). Low temperature breakdown in kiwifruit. *Acta Hortic.* 444, 579–586. doi: 10.17660/ActaHortic.1997.444.89

Landi, L., De Miccolis Angelini, R. M., Pollastro, S., Feliziani, E., Faretra, F., and Romanazzi, G. (2017). Global transcriptome analysis and identification of differentially expressed genes in strawberry after preharvest application of benzothiadiazole and chitosan. *Front. Plant Sci.* 8, 235. doi: 10.3389/fpls.2017.00235

Lang, Z., Wang, Y., Tang, K., Tang, D., Datsenka, T., Cheng, J., et al. (2017). Critical roles of DNA demethylation in the activation of ripening-induced genes and inhibition of ripening-repressed genes in tomato fruit. *Proc. Natl. Acad. Sci. U.S.A.* 114, E4511–E4519. doi: 10.1073/pnas.1705233114

Leng, P., Yuan, B., and Guo, Y. (2013). The role of abscisic acid in fruit ripening and responses to abiotic stress. *J. Exp. Bot.* 65, 4577–4588. doi: 10.1093/jxb/eru204

Liu, Y., Yang, X., Zhu, S., and Wang, Y. (2016). Postharvest application of MeJA and NO reduced chilling injury in cucumber (*Cucumis sativus*) through inhibition of H_2O_2 accumulation. *Postharvest Biol. Technol.* 119, 77–83. doi: 10.1016/j.postharvbio.2016.04.003

López-Vidal, O., Camejo, D., Rivera-Cabrera, F., Konigsberg, M., Villa-Hernández, J. M., Mendoza-Espinoza, J. A., et al. (2016). Mitochondrial ascorbate–glutathione cycle and proteomic analysis of carbonylated proteins during tomato (*Solanum lycopersicum*) fruit ripening. *Food Chem.* 194, 1064–1072. doi: 10.1016/j.foodchem.2015.08.055

Lum, G. B., Shelp, B. J., DeEll, J. R., and Bozzo, G. G. (2016). Oxidative metabolism is associated with physiological disorders in fruits stored under multiple environmental stresses. *Plant Sci.* 245, 143–152. doi: 10.1016/j.plantsci.2016.02.005

Lüthje, S., and Martinez-Cortes, T. (2018). Membrane-bound class III peroxidases: unexpected enzymes with exciting functions. *Int. J. Mol. Sci.* 19, 2876. doi: 10.3390/ijms19102876

Ma, X., Wang, W., Bittner, F., Schmidt, N., Berkey, R., Zhang, L., et al. (2016). Dual and opposing roles of xanthine dehydrogenase in defense-associated reactive oxygen species metabolism in *Arabidopsis*. *Plant Cell* 28, 1108–1126. doi: 10.1105/tpc.15.00880

Macknight, R. C., Laing, W. A., Bulley, S. M., Broad, R. C., Johnson, A. A., and Hellens, R. P. (2017). Increasing ascorbate levels in crops to enhance human nutrition and plant abiotic stress tolerance. *Curr. Opin. Biotechnol.* 44, 153–160. doi: 10.1016/j.copbio.2017.01.011

Marmiroli, M., Mussi, F., Imperiale, D., Lencioni, G., and Marmiroli, N. (2017a). Abiotic stress response to As and As+Si, composite reprogramming of fruit metabolites in tomato cultivars. *Front. Plant Sci.* 8, 2201. doi: 10.3389/fpls.2017.02201

Marmiroli, M., Mussi, F., Imperiale, D., and Marmiroli, N. (2017b). Target proteins reprogrammed by As and As + Si treatments in *Solanum lycopersicum* L. fruit. *BMC Plant Biol.* 17, 210. doi: 10.1186/s12870-017-1168-2

Martí, M. C., Camejo, D., Olmos, E., Sandalio, L. M., Fernández-García, N., Jiménez, A., et al. (2009). Characterisation and changes in the antioxidant system of chloroplasts and chromoplasts isolated from green and mature pepper fruits. *Plant Biol. (Stuttg)* 11, 613–624. doi: 10.1111/j.1438-8677.2008.00149.x

Martí, R., Roselló, S., and Cebolla-Cornejo, J. (2016). Tomato as a source of carotenoids and polyphenols targeted to cancer prevention. *Cancers*, 8, 58. doi: 10.3390/cancers8060058

Martins, L., Trujillo-Hernandez, J. A., and Reichheld, J.-P. (2018). Thiol Based Redox Signaling in Plant Nucleus. *Front. Plant Sci.*, 9(May), 1–9. doi: 10.3389/fpls.2018.00705

Massot, C., Bancel, D., Lopez Lauri, F., Truffault, V., Baldet, P., Stevens, R., et al. (2013). High temperature inhibits ascorbate recycling and light stimulation of the ascorbate pool in tomato despite increased expression of biosynthesis genes. *PLoS ONE* 8, e84474. doi: 10.1371/journal.pone.0084474

Massot, C., Stevens, R., Génard, M., Longuenesse, J.-J., and Gautier, H. (2012). Light affects ascorbate content and ascorbate-related gene expression in tomato leaves more than in fruits. *Planta* 235, 153–163. doi: 10.1007/s00425-011-1493-x

Mehta, R. A., Cassol, T., Li, N., Ali, N., Handa, A. K., and Mattoo, A. K. (2002). Engineered polyamine accumulation in tomato enhances phytonutrient content, juice quality, and vine life. *Nat. Biotechnol.* 20, 613–618. doi: 10.1038/nbt0602-613

Melino, V. J., Soole, K. L., and Ford, C. M. (2009). Ascorbate metabolism and the developmental demand for tartaric and oxalic acids in ripening grape berries. *BMC Plant Biol.* 9, 145. doi: 10.1186/1471-2229-9-145

Millar, A. H., Whelan, J., Soole, K. L., and Day, D. A. (2011). Organization and regulation of mitochondrial respiration in plants. *Ann. Rev. Plant Biol.* 62, 79–104. doi: 10.1146/annurev-arplant-042110-103857

Miret, J. A., and Munné-Bosch, S. (2015). Redox signaling and stress tolerance in plants: a focus on vitamin E. *Ann. N. Y. Acad. Sci.* 1340, 29–38. doi: 10.1111/nyas.12639

Miret, J. A., and Munné-Bosch, S. (2016). Abscisic acid and pyrabactin improve vitamin C contents in raspberries. *Food Chem.* 203, 216–223. doi: 10.1016/j.foodchem.2016.02.046

Mittler, R. (2017). ROS are good. *Trends Plant Sci.* 22, 11–19. doi: 10.1016/j.tplants.2016.08.002

Mittler, R., Vanderauwera, S., Suzuki, N., Miller, G., Tognetti, V. B., Vandepoele, K., et al. (2011). ROS signaling: the new wave? *Trends Plant Sci.* 16, 300–309. doi: 10.1016/j.tplants.2011.03.007

Mounet-Gilbert, L., Dumont, M., Ferrand, C., Bournonville, C., Monier, A., Jorly, J., et al. (2016). Two tomato GDP-d-mannose epimerase isoforms involved in ascorbate biosynthesis play specific roles in cell wall biosynthesis and development. *J. Exp. Bot.* 67, 4767–4777. doi: 10.1093/jxb/erw260

Muñoz, P., and Munné-Bosch, S. (2018). Photo-oxidative stress during leaf, flower and fruit development. *Plant Physiol.* 176, 1004–1014. doi: 10.1104/pp.17.01127

Murillo, E., Meléndez-Martínez, A. J., and Portugal, F. (2010). Screening of vegetables and fruits from Panama for rich sources of lutein and zeaxanthin. *Food Chem.* 122, 167–172. doi: 10.1016/j.foodchem.2010.02.034

Nakamura, J., Morikawa-Ichinose, T., Fujimura, Y., Hayakawa, E., Takahashi, K., Ishii, T., et al. (2017). Spatially resolved metabolic distribution for unraveling the physiological change and responses in tomato fruit using matrix-assisted laser desorption/ionization–mass spectrometry imaging (MALDI–MSI). *Anal. Bioanal. Chem.* 409, 1697–1706. doi: 10.1007/s00216-016-0118-4

Ni, Z.-J., Hu, K.-D., Song, C.-B., Ma, R.-H., Li, Z.-R., Zheng, J.-L., et al. (2016). Hydrogen sulfide alleviates postharvest senescence of grape by modulating the antioxidant defenses. *Oxidative Med. Cell. Longevity* 2016, 1–14. doi: 10.1155/2016/4715651

Nimse, S. B., and Pal, D. (2015). Free radicals, natural antioxidants, and their reaction mechanisms. *RSC Adv.* 5, 27986–28006. doi: 10.1039/C4RA13315C

Noctor, G., and Mhamdi, A. (2014). Glutathione and NADPH in plant responses to H_2O_2. *Free Radic. Biol. Med.* 75 Suppl 1, S3–S4. doi: 10.1016/j.freeradbiomed.2014.10.830

Noctor, G., Mhamdi, A., and Foyer, C. H. (2014). The roles of reactive oxygen metabolism in drought: not so cut and dried. *Plant Physiol.* 164, 1636–1648. doi: 10.1104/pp.113.233478

Noctor, G., Reichheld, J.-P., and Foyer, C. H. (2018). ROS-related redox regulation and signaling in plants. *Semin. Cell Dev. Biol.* 80, 3–12. doi: 10.1016/j.semcdb.2017.07.013

O'Brien, J. A., Daudi, A., Butt, V. S., and Bolwell, G. P. (2012). Reactive oxygen species and their role in plant defence and cell wall metabolism. *Planta* 236, 765–779. doi: 10.1007/s00425-012-1696-9

Olas, B. (2018). Berry phenolic antioxidants - implications for human health? *Front. Pharmacol.*, 9(MAR), 1–14. doi: 10.3389/fphar.2018.00078

Osorio, S., Scossa, F., and Fernie, A. R. (2013a). Molecular regulation of fruit ripening. *Front. Plant Sci.* 4, 198. doi: 10.3389/fpls.2013.00198

Osorio, S., Vallarino, J. G., Szecowka, M., Ufaz, S., Tzin, V., Angelovici, R., et al. (2013b). Alteration of the interconversion of pyruvate and malate in the plastid or cytosol of ripening tomato fruit invokes diverse consequences on sugar but similar effects on cellular organic acid, metabolism, and transitory starch accumulation. *Plant Physiol.* 161, 628–643. doi: 10.1104/pp.112.211094

Padayachee, A., Day, L., Howell, K., and Gidley, M. J. (2017). Complexity and health functionality of plant cell wall fibers from fruits and vegetables. *Crit. Rev. Food Sci. Nutr.* 57, 59–81. doi: 10.1080/10408398.2013.850652

Palma, J. M., Sevilla, F., Jiménez, A., del Río, L. A., Corpas, F. J., Álvarez de Morales, P., et al. (2015). Physiology of pepper fruit and the metabolism of antioxidants: chloroplasts, mitochondria and peroxisomes. *Ann. Bot.* 116, 627–636. doi: 10.1093/aob/mcv121

Pan, Z., Liu, Q., Yun, Z., Guan, R., Zeng, W., Xu, Q., et al. (2009). Comparative proteomics of a lycopene-accumulating mutant reveals the important role of oxidative stress on carotenogenesis in sweet orange (*Citrus sinensis* [L.] osbeck). *Proteomics* 9, 5455–5470. doi: 10.1002/pmic.200900092

Pandey, V. P., Singh, S., Singh, R., and Dwivedi, U. N. (2012). Purification and characterization of peroxidase from papaya (*Carica papaya*) fruit. *Appl. Biochem. Biotechnol.* 167, 367–376. doi: 10.1007/s12010-012-9672-1

Pétriacq, P., de Bont, L., Hager, J., Didierlaurent, L., Mauve, C., Guérard, F., et al. (2012). Inducible NAD overproduction in *Arabidopsis* alters metabolic pools and gene expression correlated with increased salicylate content and resistance to Pst-AvrRpm1. *Plant J.* 70, 650–665. doi: 10.1111/j.1365-313X.2012.04920.x

Pétriacq, P., de Bont, L., Tcherkez, G., and Gakière, B. (2013). NAD: not just a pawn on the board of plant-pathogen interactions. *Plant Signal Behav.* 8, e22477. doi: 10.4161/psb.22477

Pétriacq, P., López, A., and Luna, E. (2018). Fruit decay to diseases: can induced resistance and priming help? *Plants* 7, 77. doi: 10.3390/plants7040077

Pétriacq, P., Ton, J., Patrit, O., Tcherkez, G., and Gakière, B. (2016). NAD acts as an integral regulator of multiple defense layers. *Plant Physiol.* 172, 1465–1479. doi: 10.1104/pp.16.00780

Pilati, S., Brazzale, D., Guella, G., Milli, A., Ruberti, C., Biasioli, F., et al. (2014). The onset of grapevine berry ripening is characterized by ROS accumulation and lipoxygenase-mediated membrane peroxidation in the skin. *BMC Plant Biol.* 14, 87. doi: 10.1186/1471-2229-14-87

Polidoros, A. N., Mylona, P. V., and Arnholdt-Schmitt, B. (2009). Aox gene structure, transcript variation and expression in plants. *Physiol. Plant.* 137, 342–353. doi: 10.1111/j.1399-3054.2009.01284.x

Purvis, A. C. (1997). Role of the alternative oxidase in limiting superoxide production by plant mitochondria. *Physiol. Plant.* 100, 165–170. doi: 10.1111/j.1399-3054.1997.tb03468.x

Qin, G., Meng, X., Wang, Q., and Tian, S. (2009a). Oxidative damage of mitochondrial proteins contributes to fruit senescence: a redox proteomics analysis. *J. Proteome Res.* 8, 2449–2462. doi: 10.1021/pr801046m

Qin, G., Wang, Q., Liu, J., Li, B., and Tian, S. (2009b). Proteomic analysis of changes in mitochondrial protein expression during fruit senescence. *Proteomics* 9, 4241–4253. doi: 10.1002/pmic.200900133

Queval, G., Jaillard, D., Zechmann, B., and Noctor, G. (2011). Increased intracellular H_2O_2 availability preferentially drives glutathione accumulation in vacuoles and chloroplasts: Oxidative stress and glutathione compartmentation. *Plant Cell and Environ.* 34, 21–32. doi: 10.1111/j.1365-3040.2010.02222.x

Quinlan, C. L., Treberg, J. R., Perevoshchikova, I. V., Orr, A. L., and Brand, M. D. (2012). Native rates of superoxide production from multiple sites in isolated mitochondria measured using endogenous reporters. *Free Radic. Biol. Med.* 53, 1807–1817. doi: 10.1016/j.freeradbiomed.2012.08.015

Raiola, A., Tenore, G., Barone, A., Frusciante, L., and Rigano, M. (2015). Vitamin E content and composition in tomato fruits: beneficial roles and bio-fortification. *IJMS* 16, 29250–29264. doi: 10.3390/ijms161226163

Rasmusson, A. G., Fernie, A. R., and van Dongen, J. T. (2009). Alternative oxidase: a defence against metabolic fluctuations? *Physiol. Plant.* 137, 371–382. doi: 10.1111/j.1399-3054.2009.01252.x

Rasmusson, A. G., Geisler, D. A., and Møller, I. M. (2008). The multiplicity of dehydrogenases in the electron transport chain of plant mitochondria. *Mitochondrion* 8, 47–60. doi: 10.1016/j.mito.2007.10.004

Rey, P., and Tarrago, L. (2018). Physiological roles of plant methionine sulfoxide reductases in redox homeostasis and signaling. *Antioxid. (Basel)* 7. doi: 10.3390/antiox7090114

Riedl, K. M., Choksi, K., Wyzgoski, F. J., Scheerens, J. C., Schwartz, S. J., and Reese, R. N. (2013). Variation in Lycopene and Lycopenoates, Antioxidant Capacity, and Fruit Quality of Buffaloberry (*Shepherdia argentea* [Pursh]Nutt.) *J. Food Sci.* 78, C1673–C1679. doi: 10.1111/1750-3841.12265

Roch, L., Dai, Z., Gomes, E., Bernillon, S., Wang, J., Gibon, Y., et al. (2019). Fruit salad in the lab: Comparing botanical species to help deciphering fruit primary metabolism. *Front. Plant Sci.* 10, 836. doi: 10.3389/fpls.2019.00836

Rodriguez-Casado, A. (2016). The health potential of fruits and vegetables phytochemicals: notable examples. *Crit. Rev. Food Sci. Nutr.* 56, 1097–1107. doi: 10.1080/10408398.2012.755149

Rogers, H., and Munné-Bosch, S. (2016). Production and scavenging of reactive oxygen species and redox signaling during leaf and flower senescence: similar but different. *Plant Physiol.* 171, 1560–1568. doi: 10.1104/pp.16.00163

Romanazzi, G., Sanzani, S. M., Bi, Y., Tian, S., Gutiérrez Martínez, P., and Alkan, N. (2016). Induced resistance to control postharvest decay of fruit and vegetables. *Postharvest Biol. Technol.* 122, 82–94. doi: 10.1016/j.postharvbio.2016.08.003

Saengnil, K., Chumyam, A., Faiyue, B., and Uthaibutra, J. (2014). Use of chlorine dioxide fumigation to alleviate enzymatic browning of harvested 'Daw' longan pericarp during storage under ambient conditions. *Postharvest Biol. Technol.* 91, 49–56. doi: 10.1016/j.postharvbio.2013.12.016

Sass-Kiss, A., Kiss, J., Milotay, P., Kerek, M. M., and Toth-Markus, M. (2005). Differences in anthocyanin and carotenoid content of fruits and vegetables. *Food Res. Int.* 38, 1023–1029. doi: 10.1016/j.foodres.2005.03.014

Schertl, P., and Braun, H.-P. (2014). Respiratory electron transfer pathways in plant mitochondria. *Front. Plant Sci.* 5, 163. doi: 10.3389/fpls.2014.00163

Skupien, K., and Oszmianski, J. (2004). Comparison of six cultivars of strawberries (Fragaria x ananassa Duch.) grown in northwest Poland. *Eur. Food Res. Technol.* 219, 66–70. doi: 10.1007/s00217-004-0918-1

Smeyne, M., and Smeyne, R. J. (2013). Glutathione metabolism and Parkinson's disease. *Free Radical Biology and Medicine* 62, 13–25. doi: 10.1016/j.freeradbiomed.2013.05.001

Smirnoff, N. (2018). Ascorbic acid metabolism and functions: a comparison of plants and mammals. *Free Radic. Biol. Med.* 122, 116–129. doi: 10.1016/j.freeradbiomed.2018.03.033

Smirnoff, N., and Arnaud, D. (2019). Hydrogen peroxide metabolism and functions in plants. *New Phytol.* 221, 1197–1214. doi: 10.1111/nph.15488.

Soubeyrand, E., Colombié, S., Beauvoit, B., Dai, Z., Cluzet, S., Hilbert, G., et al. (2018). Constraint-based modeling highlights cell energy, redox status and α-ketoglutarate availability as metabolic drivers for anthocyanin accumulation in grape cells under nitrogen limitation. *Front. Plant Sci.* 9, 421. doi: 10.3389/fpls.2018.00421

Stevens, R., Buret, M., Duffé, P., Garchery, C., Baldet, P., Rothan, C., et al. (2007). Candidate Genes and Quantitative Trait Loci Affecting Fruit Ascorbic Acid Content in Three Tomato Populations. *Plant Physiol.* 143, 1943–1953. doi: 10.1104/pp.106.091413

Stevens, R. G., Baldet, P., Bouchet, J.-P., Causse, M., Deborde, C., Deschodt, C., et al. (2018). A systems biology study in tomato fruit reveals correlations between the ascorbate pool and genes involved in ribosome biogenesis, translation, and the heat-shock response. *Front. Plant Sci.* 9, 137. doi: 10.3389/fpls.2018.00137

Sudheeran, P. K., Feygenberg, O., Maurer, D., and Alkan, N. (2018). Improved cold tolerance of mango fruit with enhanced anthocyanin and flavonoid contents. *Molecules* 23, 1832. doi: 10.3390/molecules23071832

Suzuki, N., Miller, G., Morales, J., Shulaev, V., Torres, M. A., and Mittler, R. (2011). Respiratory burst oxidases: the engines of ROS signaling. *Curr. Opin. Plant Biol.* 14, 691–699. doi: 10.1016/j.pbi.2011.07.014

Symons, G. M., Chua, Y.-J., Ross, J. J., Quittenden, L. J., Davies, N. W., and Reid, J. B. (2012). Hormonal changes during non-climacteric ripening in strawberry. *J. Exp. Bot.* 63, 4741–4750. doi: 10.1093/jxb/ers147

Thevenet, D., Pastor, V., Baccelli, I., Balmer, A., Vallat, A., Neier, R., et al. (2017). The priming molecule β-aminobutyric acid is naturally present in plants and is induced by stress. *New Phytol.* 213, 552–559. doi: 10.1111/nph.14298

Tian, S., Qin, G., and Li, B. (2013). Reactive oxygen species involved in regulating fruit senescence and fungal pathogenicity. *Plant Mol. Biol.* 82, 593–602. doi: 10.1007/s11103-013-0035-2

Torres, M. A., and Dangl, J. L. (2005). Functions of the respiratory burst oxidase in biotic interactions, abiotic stress and development. *Curr. Opin. Plant Biol.* 8, 397–403. doi: 10.1016/j.pbi.2005.05.014

Trobacher, C. P., Clark, S. M., Bozzo, G. G., Mullen, R. T., DeEll, J. R., and Shelp, B. J. (2013). Catabolism of GABA in apple fruit: subcellular localization and biochemical characterization of two γ-aminobutyrate transaminases. *Postharvest Biol. Technol.* 75, 106–113. doi: 10.1016/j.postharvbio.2012.08.005

Tzortzakis, N. G., and Economakis, C. D. (2007). Maintaining postharvest quality of the tomato fruit by employing methyl jasmonate and ethanol vapor treatment. *J. Food Qual.* 30, 567–580. doi: 10.1111/j.1745-4557.2007.00143.x

Valenzuela, J., Manzano, S., Palma, F., Carvajal, F., Garrido, D., and Jamilena, M. (2017). Oxidative stress associated with chilling injury in immature fruit: postharvest technological and biotechnological solutions. *Int. J. Mol. Sci.* 18, 1467. doi: 10.3390/ijms18071467

Wada, L., and Ou, B. (2002). Antioxidant Activity and Phenolic Content of Oregon Caneberries. *J. Agric. Food Chem.* 50, 3495–3500. doi: 10.1021/jf011405l

Wang, H., Guo, X., Hu, X., Li, T., Fu, X., and Liu, R. H. (2017). Comparison of phytochemical profiles, antioxidant and cellular antioxidant activities of different varieties of blueberry (Vaccinium spp.). *Food Chem.*, 217, 773–781. doi: 10.1016/j.foodchem.2016.09.002

Wargovich, M. J., Morris, J., Moseley, V., Weber, R., and Byrne, D. H. (2012). "Developing fruit cultivars with enhanced health properties," in *Fruit breeding. Handbook of plant breeding*. Eds. M. L. Badenes and D. H. Byrne (Boston, MA: Springer US), 37–68. doi: 10.1007/978-1-4419-0763-9_2

Wilkinson, S. W., Pastor, V., Paplauskas, S., Pétriacq, P., and Luna, E. (2018). Long-lasting β-aminobutyric acid–induced resistance protects tomato fruit against *Botrytis cinerea*. *Plant Pathol.* 67, 30–41. doi: 10.1111/ppa.12725

Wolfe, K. L., Kang, X., He, X., Dong, M., Zhang, Q., and Liu, R. H. (2008). Cellular Antioxidant Activity of Common Fruits. *J. Agric. Food Chem.*, 56(18), 8418–8426. doi: 10.1021/jf801381y

Wu, B., Guo, Q., Li, Q., Ha, Y., Li, X., and Chen, W. (2014). Impact of postharvest nitric oxide treatment on antioxidant enzymes and related genes in banana fruit in response to chilling tolerance. *Postharvest Biol. Technol.* 92, 157–163. doi: 10.1016/j.postharvbio.2014.01.017

Wu, F., Li, Q., Yan, H., Zhang, D., Jiang, G., Jiang, Y., et al. (2016). Characteristics of three thioredoxin genes and their role in chilling tolerance of harvested banana fruit. *Int. J. Mol. Sci.* 17, 1526. doi: 10.3390/ijms17091526

Yang, H., Wu, F., and Cheng, J. (2011a). Reduced chilling injury in cucumber by nitric oxide and the antioxidant response. *Food Chem.* 127, 1237–1242. doi: 10.1016/j.foodchem.2011.02.011

Yang, X.-Y., Xie, J.-X., Wang, F.-F., Zhong, J., Liu, Y.-Z., Li, G.-H., et al. (2011b). Comparison of ascorbate metabolism in fruits of two citrus species with obvious difference in ascorbate content in pulp. *J. Plant Physiol.* 168, 2196–2205. doi: 10.1016/j.jplph.2011.07.015

Yesbergenova, Z., Yang, G., Oron, E., Soffer, D., Fluhr, R., and Sagi, M. (2005). The plant Mo-hydroxylases aldehyde oxidase and xanthine dehydrogenase have distinct reactive oxygen species signatures and are induced by drought and abscisic acid. *Plant J.* 42, 862–876. doi: 10.1111/j.1365-313X.2005.02422.x

Young, A., and Lowe, G. (2018). Carotenoids—antioxidant properties. *Antioxidants* 7, 28. doi: 10.3390/antiox7020028

Zermiani, M., Zonin, E., Nonis, A., Begheldo, M., Ceccato, L., Vezzaro, A., et al. (2015). Ethylene negatively regulates transcript abundance of ROP-GAP rheostat-encoding genes and affects apoplastic reactive oxygen species homeostasis in epicarps of cold stored apple fruits. *J. Exp. Bot.* 66, 7255–7270. doi: 10.1093/jxb/erv422

Zhang, H., Ma, L., Wang, L., Jiang, S., Dong, Y., and Zheng, X. (2008). Biocontrol of gray mold decay in peach fruit by integration of antagonistic yeast with salicylic acid and their effects on postharvest quality parameters. *Biol. Control* 47, 60–65. doi: 10.1016/j.biocontrol.2008.06.012

Zhang, Y., Butelli, E., De Stefano, R., Schoonbeek, H.-J., Magusin, A., Pagliarani, C., et al. (2013). Anthocyanins double the shelf life of tomatoes by delaying overripening and reducing susceptibility to gray mold. *Curr. Biol.* 23, 1094–1100. doi: 10.1016/j.cub.2013.04.072

Zhang, Y., Li, Y., He, Y., Hu, W., Zhang, Y., Wang, X., et al. (2018). Identification of NADPH oxidase family members associated with cold stress in strawberry. *FEBS Open Bio.* 8, 593–605. doi: 10.1002/2211-5463.12393

Zuo, J., Wang, Q., Zhu, B., Luo, Y., and Gao, L. (2016). Deciphering the roles of circRNAs on chilling injury in tomato. *Biochem. Biophys. Res. Commun.* 479, 132–138. doi: 10.1016/j.bbrc.2016.07.032

Conflict of Interest Statement: The authors declare that the research was conducted in the absence of any commercial or financial relationships that could be construed as a potential conflict of interest.

ANNEX 4.

Guillaume Decros, Bertrand Beauvoit, Sophie Colombié, Cécile Cabasson, Stéphane Bernillon, Stéphanie Arrivault, Manuela Guenther, Isma Belouah, Sylvain Prigent, Pierre Baldet, Yves Gibon and Pierre Pétriacq (2019). Regulation of Pyridine Nucleotide Metabolism During Tomato Fruit Development Through Transcript and Protein Profiling.

frontiers in Plant Science

ORIGINAL RESEARCH
published: 11 October 2019
doi: 10.3389/fpls.2019.01201

Regulation of Pyridine Nucleotide Metabolism During Tomato Fruit Development Through Transcript and Protein Profiling

*Guillaume Decros[1], Bertrand Beauvoit[1], Sophie Colombié[1], Cécile Cabasson[1,2], Stéphane Bernillon[1,2], Stéphanie Arrivault[3], Manuela Guenther[3], Isma Belouah[1], Sylvain Prigent[1,2], Pierre Baldet[1], Yves Gibon[1,2] and Pierre Pétriacq[1,2]**

[1] UMR 1332 BFP, INRA, Univ. Bordeaux, Villenave d'Ornon, France, [2] MetaboHUB-Bordeaux, MetaboHUB, Phenome-Emphasis, Villenave d'Ornon, France, [3] Department 2, Metabolic Networks, Max Planck Institute of Molecular Plant Physiology, Potsdam-Golm, Germany

OPEN ACCESS

Edited by:
Michael James Considine, University of Western Australia, Australia

Reviewed by:
Jeffrey Charles Waller, Mount Allison University, Canada
Alberto A. Iglesias, National University of the Littoral, Argentina

***Correspondence:**
Pierre Pétriacq
pierre.petriacq@inra.fr

Specialty section:
This article was submitted to Plant Physiology, a section of the journal Frontiers in Plant Science

Received: 11 April 2019
Accepted: 02 September 2019
Published: 11 October 2019

Citation:
Decros G, Beauvoit B, Colombié S, Cabasson C, Bernillon S, Arrivault S, Guenther M, Belouah I, Prigent S, Baldet P, Gibon Y and Pétriacq P (2019) Regulation of Pyridine Nucleotide Metabolism During Tomato Fruit Development Through Transcript and Protein Profiling. Front. Plant Sci. 10:1201. doi: 10.3389/fpls.2019.01201

Central metabolism is the engine of plant biomass, supplying fruit growth with building blocks, energy, and biochemical cofactors. Among metabolic cornerstones, nicotinamide adenine dinucleotide (NAD) is particularly pivotal for electron transfer through reduction–oxidation (redox) reactions, thus participating in a myriad of biochemical processes. Besides redox functions, NAD is now assumed to act as an integral regulator of signaling cascades involved in growth and environmental responses. However, the regulation of NAD metabolism and signaling during fruit development remains poorly studied and understood. Here, we benefit from RNAseq and proteomic data obtained from nine growth stages of tomato fruit (var. Moneymaker) to dissect mRNA and protein profiles that link to NAD metabolism, including *de novo* biosynthesis, recycling, utilization, and putative transport. As expected for a cofactor synthesis pathway, protein profiles failed to detect enzymes involved in NAD synthesis or utilization, except for nicotinic acid phosphoribosyltransferase (NaPT) and nicotinamidase (NIC), which suggested that most NAD metabolic enzymes were poorly represented quantitatively. Further investigations on transcript data unveiled differential expression patterns during fruit development. Interestingly, among specific NAD metabolism-related genes, early *de novo* biosynthetic genes were transcriptionally induced in very young fruits, in association with NAD kinase, while later stages of fruit growth rather showed an accumulation of transcripts involved in later stages of *de novo* synthesis and in NAD recycling, which agreed with augmented NAD(P) levels. In addition, a more global overview of 119 mRNA and 78 protein significant markers for NAD(P)-dependent enzymes revealed differential patterns during tomato growth that evidenced clear regulations of primary metabolism, notably with respect to mitochondrial functions. Overall, we propose that NAD metabolism and signaling are very dynamic in the developing tomato fruit and that its differential regulation is certainly critical to fuel central metabolism linking to growth mechanisms.

Keywords: fruit, tomato, NAD, redox, development

INTRODUCTION

Plant metabolism is maintained by universal metabolic cornerstones including pyridine nucleotides such as nicotinamide adenine dinucleotide (NAD) (Noctor et al., 2006; Gakière et al., 2018b). NAD and its phosphorylated form NADP are ubiquitous electron carriers modulating energy homeostasis through the transport of electrons within reduction–oxidation (redox) processes (Geigenberger and Fernie, 2014; Gakière et al., 2018a). As a result of its capacity to transfer electrons, NAD(P) is present in the cell as oxidized or reduced forms, $NAD(P)^+$, and NAD(P)H, respectively, where NAD(P) refer to as the total pool of $NAD(P)^+$ and NAD(P)H. In plant cells, while NAD is mostly found as oxidized NAD^+, NADP mostly acts as a reductant (NADPH) (Noctor et al., 2006; Gakière et al., 2018b). For instance, the regeneration of reducing equivalents (NADPH) by the oxidative pentose phosphate pathway is necessary for the β-oxidation of fatty acids and for nitrogen assimilation in non-photosynthetic tissues (Neuhaus and Emes, 2000; Bowsher et al., 2007). Phosphorylation of NAD(H) to NADP(H) is catalyzed *via* highly conserved NAD^+ kinases (E.C. 2.7.1.23) and NADH kinases (E.C. 2.7.1.86) playing essential roles in metabolic and redox reactions including photosynthesis performance and reactive oxygen species (ROS) homeostasis, which are both crucial for plant growth and responses to stress (Turner et al., 2004; Waller et al., 2010; Li et al., 2014; Li et al., 2018a).

Plant cells produce NAD^+ from the amino acid aspartate *via* a *de novo* biosynthesis and a recycling pathway (**Figure 1**) (Katoh et al., 2006; Gakière et al., 2018b). Briefly, *de novo* synthesis starts with quinolinate formation in the chloroplast (Katoh et al., 2006) from aspartate and dihydroxyacetone phosphate by aspartate oxidase (AO; E.C. 1.4.3.16) plus quinolinate synthase (QS; E.C. 2.5.1.72) (**Figure 1**). Quinolinate phosphoribosyltransferase (QPT; E.C. 2.4.2.19) catalyzes the subsequent conversion of quinolinate to nicotinic acid (Na) mononucleotide (NaMN). The next biochemical reactions are cytosolic (Suda et al., 2003; Magni et al., 2004; Noctor et al., 2006; Hashida et al., 2007) and shared between NAD biosynthesis and recycling. This thus requires the transfer of NaMN to the cytosol, the transporter for which remains to be discovered. NaMN is adenylylated to nicotinic acid adenine dinucleotide (NaAD) by nicotinate mononucleotide adenylyl transferase (NaMNAT; E.C. 2.7.7.1); then, NAD synthetase (NADS; E.C. 6.3.1.5) finally amidates NaAD to NAD^+ (Gakière et al., 2018b). As for other nucleotides that are salvaged, NAD^+ can be recycled *via* the activity of nicotinamidases (NIC; E.C. 3.5.1.19) and nicotinic acid phosphorybosyltransferase (NaPT; E.C. 2.4.2.11) (**Figure 1**). Due to its toxicity, nicotinate is stored in plant cells as Na-conjugates such as nicotinate glucosides and trigonelline (*i.e.*, N-methylnicotinate) by glycosylation *via* Na glucosyltransferase (NaGT; E.C. 2.4.1.196) or methylation *via* Na-N-methyltransferase (NMT; E.C. 2.1.1.7) (Köster et al., 1989; Li et al., 2015; Li et al., 2017). While the topology of NAD^+ synthesis is well documented, the molecular and regulatory details of the corresponding biochemical pathways remain largely unknown, especially for fruit tissues. Deregulation of AO, QS, and QPT levels in *Arabidopsis thaliana* leaves has shown that such enzymes are critical in the control of pyridine nucleotide levels and its derivatives (Schippers et al., 2008; Macho et al., 2012; Pétriacq et al., 2012; Pétriacq et al., 2016). Na-glucosides have been shown to play a role in seed germination and contribute to resynthesis of NAD^+ in *Brassicaceae* (Li et al., 2017). Although the physiological role of trigonelline in plants remain unclear, trigonelline can also contribute, to a lesser extent, to the resynthesis of NAD^+ and undergoes long-distance transport in *Arabidopsis* (Upmeier et al., 1988; Wu et al., 2018).

Besides their redox functions, pyridine nucleotides can be directly consumed by signaling reactions that influence plant physiology through developmental processes and responses to environmental changes, most particularly stress mitigations (Hashida et al., 2009; Pétriacq et al., 2013; Gakière et al., 2018a). This includes calcium signaling (**Figure 1**), translational modification of target proteins by ADP-ribose transfer from NAD^+ *via* the poly-ADP-ribose polymerases (PARPs, E.C. 2.4.2.30) and mono-ADP-ribosyltransferase (E.C. 2.4.2.31), and epigenetic regulations *via* the sirtuin histone deacetylases (SIRs, E.C. 2.4.2.B14) (Hunt et al., 2004; Briggs and Bent, 2011; Kupis et al., 2016; Gakière et al., 2018b). Furthermore, Nudix hydrolases (NDXs, E.C. 2.4.2.13) can hydrolyze pyridine nucleotides and participate in signaling functions (Kraszewska, 2008). NAD(P)H can also undergo spontaneous and enzymatic hydrations that generate NAD(P)H hydrates, which can be subsequently repaired to NAD(P)H by NAD(P)H-hydrate dehydratases (E.C. 4.2.1.93/136) and epimerases (E.C. 5.1.99.6) (Niehaus et al., 2014). Several reviews have previously covered these aspects that link NAD^+ signaling to plant development and stress responses (Mahalingam et al., 2007; Hashida et al., 2009; Pétriacq et al., 2013; Gakière et al., 2018a; Gakière et al., 2018b). For instance, research on pyridine nucleotide signaling mostly focuses on photosynthetic tissues, sometimes roots and seeds (Hunt et al., 2007; Hunt and Gray, 2009; Hashida et al., 2012). In *Arabidopsis*, changes in $NAD(P)^+$ contents drastically alter growth phenotype, as exemplified particularly for genotypes that are affected for the first three enzymes of *de novo* biosynthesis (for a review see Gakière et al., 2018a). Following NAD(H) and NADP(H) levels in *Arabidopsis* developing leaves further indicate a continuous accumulation of the cofactors during foliar growth until the pools drop with flowering (Queval and Noctor, 2007). A positive correlation is observed between levels of NAD^+ and the resistance of *Arabidopsis* plants to several biotic changes, including fungal and bacterial infections (Zhang and Mou, 2009; Macho et al., 2012; Pétriacq et al., 2012; Pétriacq et al., 2016). In citrus plants, recent work highlights the importance of exogenous NAD^+ treatment in inducing resistance against citrus canker (Alferez et al., 2018). Furthermore, NAD^+ might leak from the cellular compartment and subsequently induce immune responses, which is further supported by the discovery of a lectin receptor kinase as a potential receptor for NAD^+ in *Arabidopsis*, also participating in basal resistance against bacterial pathogens (Zhang and Mou, 2009). Hence, the implication of pyridine nucleotides as signaling molecules is clearly established (Mou, 2017).

Only a handful of studies provide fruit-specific concentrations of NAD(H) and NAD(P)H. Although previous changes in pyridine nucleotides have been observed between green and red tomato fruits of MicroTom and Moneymaker cultivars (Centeno et al., 2011;

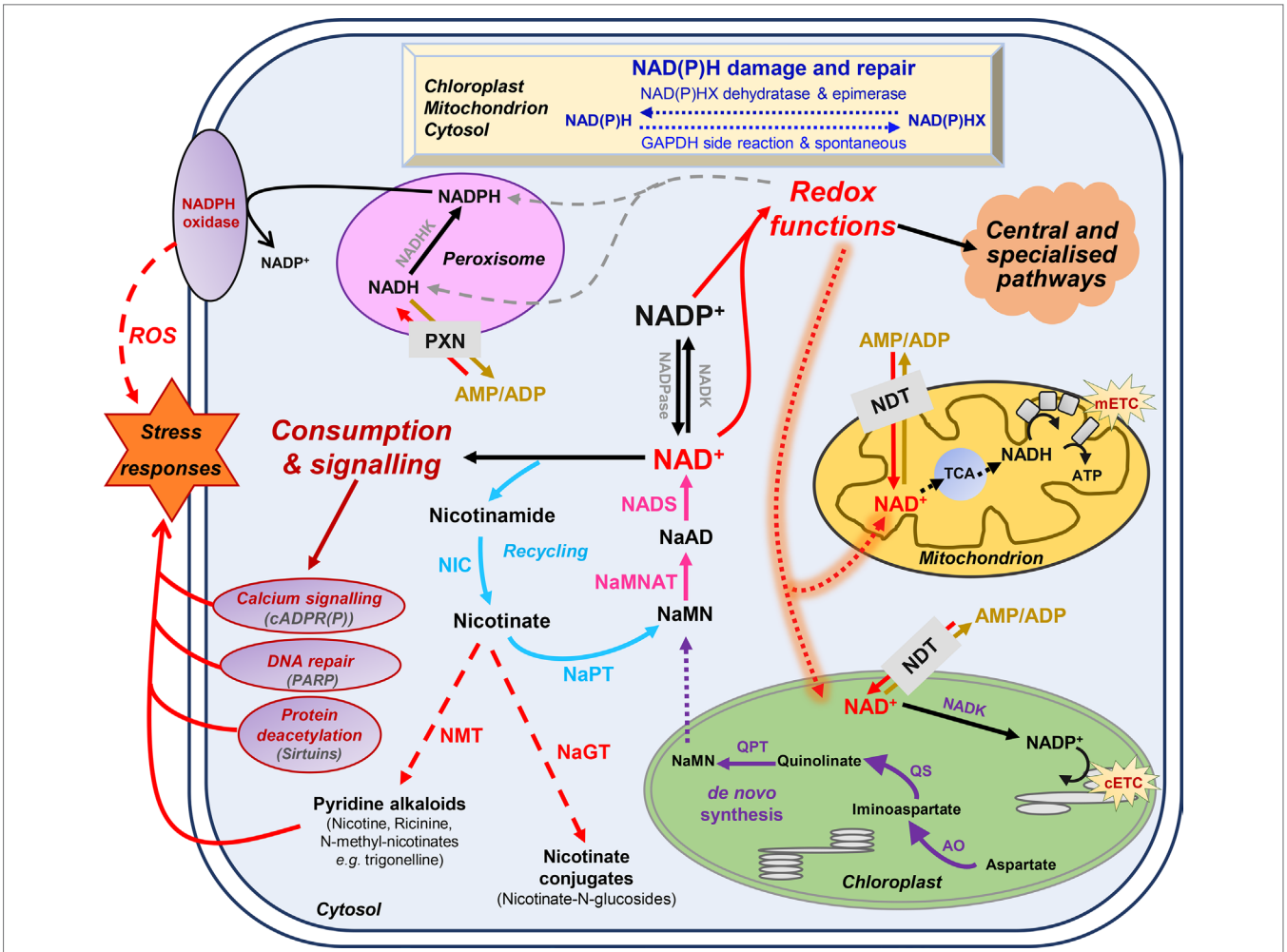

FIGURE 1 | Basics of nicotinamide adenine dinucleotide (NAD^+) metabolism in plant cells. Biosynthesis and utilization of pyridine nucleotides (Pétriacq et al., 2013). Dot arrows represent transport between the different cellular organelles. Purple and blue arrows indicate *de novo* synthesis pathway of NAD^+, and the recycling pathway, respectively. Pink arrows represent steps that are shared by these two synthesis pathways. Dashed red arrows indicate nicotinate metabolism. Indigo arrows show NAD(P)H damage and repair, which can be spontaneous or catalyzed by NAD(P)H-hydrate dehydratase and epimerase. AO, aspartate oxidase; ATP, adenosine triphosphate; cADPR(P), cyclic ADP-ribose (phosphate); cETC, chloroplastic electron transport chain; GAPDH, glyceraldehyde-3-phosphate dehydrogenase; mETC, mitochondrial electron transport chain; NaAD, nicotinic acid adenine dinucleotide; NADK, NAD kinase; NADP, NAD phosphate; NADPase, NADP phosphatase; NAD(P)HX, NAD(P)H hydrate; NaMN, nicotinic acid mononucleotide; NaMNAT, NaMN adenylyltransferase; NADS, NAD synthetase; NaGT, nicotinate N-glucosyltransferase; NaPT, nicotinate phosphoribosyltransferase; NDT, NAD^+ transporter; NIC, nicotinamidase; NMT, nicotinate N-methyltransferase; PARP, poly-ADP-ribose polymerase; PXN, peroxisomal NAD carrier; QPT, quinolinate phosphoribosyltransferase; QS, quinolinate synthase; ROS, reactive oxygen species; TCA, tricarboxylic acid cycle.

Osorio et al., 2013), to our knowledge, no developmental fruit series have been analyzed so far. Tomato fruit is not only an important crop that is widely used for human diet but also pivotal for fruit research (Li et al., 2018b). During tomato fruit development, a medium-scale stoichiometric model suggested that biomass synthesis required NADPH and higher ATP hydrolysis at the end of cell expansion (Colombié et al., 2015). This was further associated with a peak of CO_2 at the end of tomato ripening coinciding with climacteric respiration of tomato fruit and involved energy dissipation by the mitochondrial alternative oxidase. This was further confirmed by a more detailed stoichiometric model of the respiratory pathway, including alternative oxidase and uncoupling proteins (Colombié et al., 2017). In grape berry, reducing power equivalents (NADH and NADPH) were also associated with major carbon fluxes, thus supporting a strong link between central metabolism and pyridine nucleotides (Soubeyrand et al., 2018).

In the present work, as a first attempt to clarify the importance of pyridine nucleotides in the developing fruit, we used a developmental fruit series of nine growth stages of tomato fruit (var. Moneymaker) and measured pyridine nucleotide pools. We further examined quantitative data for transcript and protein levels previously obtained by RNAseq and proteomics (Belouah et al., 2019) and revealed changes in NAD(P) metabolism during fruit development. Our studies show that NAD(P) metabolism and signaling are very dynamic and crucial to the developing tomato fruit and link to central metabolism.

MATERIALS AND METHODS

Plant Material and Growth Conditions

Tomato fruit pericarps were obtained from *Solanum lycopersicum* L. var. Moneymaker as previously described (Biais et al., 2014). Briefly, tomato plants were grown under usual production greenhouse conditions in southern western France (44°23′56″N, 0°35′25″E) from June to October, using a nutrient solution (detailed in Biais et al., 2014) to adjust plant growth and water supply to the climate *via* a drip irrigation system that maintained 20–30% drainage (pH adjusted to 5.9, electrical conductivity to 2.2 mS.cm^{-1}). Flower anthesis was monitored on trusses 5, 6, and 7, and fruits were harvested at nine developmental stages (thereafter referred to as GS1 to 9), at about 8, 15, 21, 28, 34, 42 (mature green), 49 (turning), 50 (orange), and 53 (red ripe) days post anthesis (dpa). Seeds, jelly, and placenta were first removed for each fruit, and the resulting pericarp was cut into small pieces, which were immediately frozen in liquid nitrogen. Pericarp samples were ground to powder and stored at −80°C until further analysis.

Quantification of NAD(P) Contents in Tomato Fruit

Total cellular soluble pools of NAD^+, NADH, $NADP^+$, and NADPH were measured from fruit pericarps of nine developmental stages of tomato fruit according to a coupled enzyme assay described previously (Pétriacq et al., 2012) using HiT-Me Facility at MetaboHUB-Bordeaux (https://doi.org/10.15454/1.5572412770331912E12 Plateforme Metabolome Bordeaux, http://metabolome.cgfb.u-bordeaux.fr/en). Briefly, from the same fresh ground fruit material (20 mg), oxidized forms NAD^+ and $NADP^+$ were extracted in 200 µl HCl (0.2 N) and reduced forms NADH and NADPH in 200 µl NaOH (0.2 N) as detailed in (Queval and Noctor, 2007). Microplate measurements of oxidized NAD^+ and $NADP^+$ (Pétriacq et al., 2012) were confirmed from methanolic extracts using ion-pair liquid chromatography coupled to mass spectrometry (LCMS) technique described previously (Arrivault et al., 2009). Resulting metabolite levels were expressed in nmol.g^{-1} fresh weight (FW) for independent bioreplicates ($n = 3$) and checked for statistical significance by ANOVA for global variation and by binary comparison of Student's t test ($P < 0.05$). Volumes of cytosol and all organelles, except vacuole, were used to express metabolite pools as cellular concentrations by dividing pyridine nucleotide pools by the volume corresponding to each growth stage, as previously described (Beauvoit et al., 2014).

RNAseq and LC-MS/MS Proteomics of Developing Tomato Fruit

RNA and proteins were extracted and analyzed as described previously (Belouah et al., 2019) by RNAseq (GeT-PlaGe core facility, INRA Toulouse, France, http://get.genotoul.fr) and LCMS/MS-based proteomics (PAPPSO, INRA Moulon, France, http://pappso.inra.fr/index.php), respectively. Briefly, total RNA was isolated from frozen tissue powder of tomato pericarp using plant RNA Reagent (PureLink Kit, Invitrogen) followed by DNase treatment (DNA-free Kit, Invitrogen) and purification over RNeasy Mini spin columns (RNeasy Plant Mini Kit, QIAGEN), according to the manufacturer's instruction. RNA integrity was assessed using the RNA 600 Nano Kit with a Bioanalyzer 2100 system (Agilent Technologies). RNAseq was performed at the GeT-PlaGe core facility, INRA Toulouse (France). RNAseq libraries were prepared according to Illumina's protocols using the TruSeq Stranded mRNA Sample Prep Kit to analyze mRNA. Library quality was assessed using an Agilent Bioanalyzer, and libraries were quantified by quantitative PCR (qPCR) using the Kapa Library Quantification Kit. RNAseq experiments were performed on an Illumina HiSeq 2000 or HiSeq 2500 (2x100 bp).

Protein Extraction and Quantification

Total proteins from tomato pericarp were extracted as in (Faurobert et al., 2007). LC-MS/MS analyses were performed with a NanoLC-Ultra System (Nano-2D Ultra, Eksigent, Les Ulis, France) coupled with a Q Exactive Mass Spectrometer (Thermo Electron, Waltham, MA, USA) as in (Havé et al., 2018). For each sample, 800 ng (4 µl from a 0.200 ng.µl^{-1} solution) of protein digest were loaded onto a Biosphere C18 pre-column (0.1 × 20 mm, 100 Å, 5 µm; Nanoseparation) at 7.5 µl.min^{-1} and desalted with 0.1% (v/v) formic acid and 2% ACN. After 3 min, the pre-column was connected to a Biosphere C18 nanocolumn (0.075 × 300 mm, 100 Å, 3 µm; Nanoseparation). The raw MS output files and identification data were deposited online using the PROTICdb database (http://moulon.inra.fr/protic/tomato_fruit_development).

Protein identification was performed using the protein sequence database of *S. lycopersicum* Heinz assembly v 2.40 (ITAG2.4) downloaded from https://solgenomics.net/ (34,725 entries). A contaminant database, which contains the sequences of standard contaminants, was also interrogated. Criteria used for protein identification were (1) at least two different peptides identified with an E-value smaller than 0.01, and (2) a protein E-value (product of unique peptide E-values) smaller than 10^{-5}. Using reversed sequences as a decoy database, the false discovery rate for peptide and protein identification was respectively 0.05 and 0%.

Data Analysis of mRNA and Protein Profiles

Datasets consisted of 22,877 transcript and 2,375 protein profiles and were made publicly available *via* GEO repository (Barrett et al., 2013) with the accession number GSE12873 (https://www.ncbi.nlm.nih.gov/geo/query/acc.cgi?acc=GSE128739) for the transcripts. The proteomics data have been deposited to the ProteomeXchange Consortium *via* the PRIDE (Perez-Riverol et al., 2019) partner repository with the dataset identifier PXD012877.

Prior to uni- and multivariate statistical analyses, mRNA and protein data were pre-processed to normally distributed data by performing median normalization, cube-root transformation, and Pareto scaling of the data intensities as described previously (Belouah et al., 2019). Normalized datasets were then used to construct score plots of principal component analysis (PCA) for transcriptomic and proteomic overview using MetaboAnalyst v 4.0 (http://www.metaboanalyst.ca/), or dendrograms of clustering analysis by Pearson's correlation with complete clustering linkage using MeV v 4.9.0 (http://mev.tm4.org/). Significant markers of

both transcripts and proteins were determined by ANOVA after discarding false positives ($P < 0.01$ corrected for multiple testing by Bonferroni method). Details of ANOVA *P* values are given in Supplemental Tables S1-3. Transcript and protein features of NAD-dependent functions were selected by identifying domains (InterPro and GO) that were annotated to bind or process pyridine nucleotides using Assembly v 2.40 (ITAG v 2.4) from Sol Genomics (https://solgenomics.net/) and UniProt (https://www.uniprot.org/). Data mining of publicly available gene expression data was conducted using Tomato Expression Atlas (http://tea.solgenomics.net/) (Fernandez-Pozo et al., 2017). Functional annotation of mRNA and protein markers was performed based on gene ontology using Mercator4 v1.0 (https://plabipd.de/portal/mercator4) (Schwacke et al., 2019).

Enzymatic Activities of Dehydrogenases

Malate dehydrogenase and isocitrate dehydrogenase activities were measured according to an in-house protocol (Biais et al., 2014). Briefly, aliquots of about 20-mg FW were extracted by vigorous shaking with 500 µl extraction buffer composed of 20% (v/v) glycerol, 0.25% (w/v) bovine serum albumin, 1% (v/v) Triton-X100, 50 mM HEPES-KOH (pH 7.5), 10 mM $MgCl_2$, 1 mM EDTA, 1 mM EGTA, 1 mM ε-aminocaproic acid, 1 mM benzamidine, 10 mM leupeptin, 0.5 mM dithiothreitol, and 1 mM phenylmethylsulfonyl fluoride, which was added just before extraction. Enzyme activities were assayed using a robotized platform at HiT-Me Facility [(MetaboHUB-Bordeaux) http://metabolome.cgfb.u-bordeaux.fr/en] as previously described (Gibon et al., 2004; Studart-Guimarães et al., 2005; Gibon et al., 2006; Gibon et al., 2009; Steinhauser et al., 2010).

RESULTS

Tomato Fruit Development Is Associated With Changes in NAD(P) Pools

Fruit development can be divided into three partially overlapping phases, namely, cell division, cell expansion, and ripening (**Figure 2A**), which all have their own metabolic specificity (Beauvoit et al., 2018). As a first attempt to clarify the importance of pyridine nucleotides for fruit growth, we measured total cellular NAD^+, $NADP^+$, NADH, and NADPH pools from nine growth stages of tomato fruit (var. Moneymaker) (**Figure 2B**). Oxidized pools were also confirmed by LCMS (**Figure S1**). Global changes in the pools of these pyridine nucleotides were statistically significant (ANOVA followed by binary Student's *t* tests) and showed higher levels of both NAD(H) and NADP(H) in the very young fruit, with the highest pools observed at 8 days postanthesis (dpa) for growth stage 1 (GS1) and the lowest for mature green (GS6, 41 dpa) and for red ripe (GS9, 53 dpa) stages of tomato fruit, respectively. Reduced, oxidized, and total content of NAD(H) decreased until the end of cell division (GS4), then firstly increased during cell expansion (GS5–7) and secondly during ripening (GS8–9), while maintaining the NAD(H) pool mainly oxidized during fruit development. Since NAD(P) are mostly present in the chloroplasts, peroxisomes, mitochondria, and cytosol, but not in the vacuole (Donaldson, 1982; Gakière et al., 2018b), we could rule out the dilution effect due to the cell expansion (Beauvoit et al., 2014) and express NAD(P) contents as concentrations (**Figure 2C**). Differences in concentrations, except for NADH, were statistically significant during fruit growth (ANOVA followed by binary Student's *t* tests) and clearly indicated two distinct waves of accumulation for NAD(H) (*i.e.*, GS5–7 and GS7–9). Simultaneously, NADP(H) only increased during the beginning of development (from GS1 to GS4) as a result of a higher NADPH concentration (**Figure 2C**). Hence, this suggests a fine-tuned NAD(P) homeostasis during tomato fruit development.

Transcriptional Changes of NAD Biosynthesis and Metabolism Show Distinct Patterns During Tomato Fruit Growth

Next, in order to substantiate the changes in NAD(P), we examined transcript and protein profiles during tomato fruit development that were obtained from RNAseq and proteomics techniques (Belouah et al., 2019). Raw data (22,877 transcript and 2,375 protein features) were normalized as described previously (median-centered, cube root-transformed, and Pareto-scaled) (Belouah et al., 2019). We first focused on genes that were associated with NAD^+ biosynthesis and NAD(P)H damage and repair (**Figure 1**), which included 15 genes (**Figure 3A**). Clustering analysis of mRNA profiles (Pearson's correlation and complete clustering, **Figure 3A**) revealed two main statistically significant clusters (ANOVA with Bonferroni correction, $P < 0.01$ are listed in **Table S1**): one associated with the young fruit (stages 1–4) and another with the ripening fruit (stages 5–9). For the first cluster, early steps of *de novo* biosynthesis of NAD^+ and $NADP^+$ were transcriptionally up-regulated in the young fruit, including AO, QS and QPT, and NADK1 and NADK2 (**Figure 3A**). Interestingly, these enzymes are chloroplastic in *Arabidopsis* (Katoh et al., 2006) and assumed to be critical for NAD^+ and $NADP^+$ homeostasis, respectively (Pétriacq et al., 2012; Gakière et al., 2018a; Li et al., 2018a). For the second cluster, later stages of fruit growth coincided with the up-regulation of the expression of genes involved in final steps of NAD^+ biosynthesis (NaMNAT and NADS), NAD^+ recycling (NIC and NaPT), and NADP(H) production (NADK3 and NADK4) (**Figure 3A**). This suggests an accumulation of NAD^+ precursors during the beginning of development (GS1–4) followed by an active synthesis and recycling of $NAD(P)^+$ (GS5–9) concurrent with the increased NAD(H) content. Besides, NAD(P)XH epimerase and dehydratase genes are expressed all along fruit development suggesting a continuous NAD(P)H damage and repair (**Figure 3A**). Remarkably, protein profiles failed to include enzymes involved in NAD^+ synthesis, except for NaPT and NIC that followed mRNA profiles with higher levels during ripening (**Figure S2**). This might suggest that most NAD metabolism enzymes were poorly represented quantitatively (*i.e.*, below threshold of protein detection). To test this hypothesis, we checked the absolute expression levels of genes involved in NAD^+ synthesis as compared to other genes of central cellular functions (**Figure S3**). Raw data of mRNA profiles evidenced very low expression values for *AO* in tomato fruit, as compared

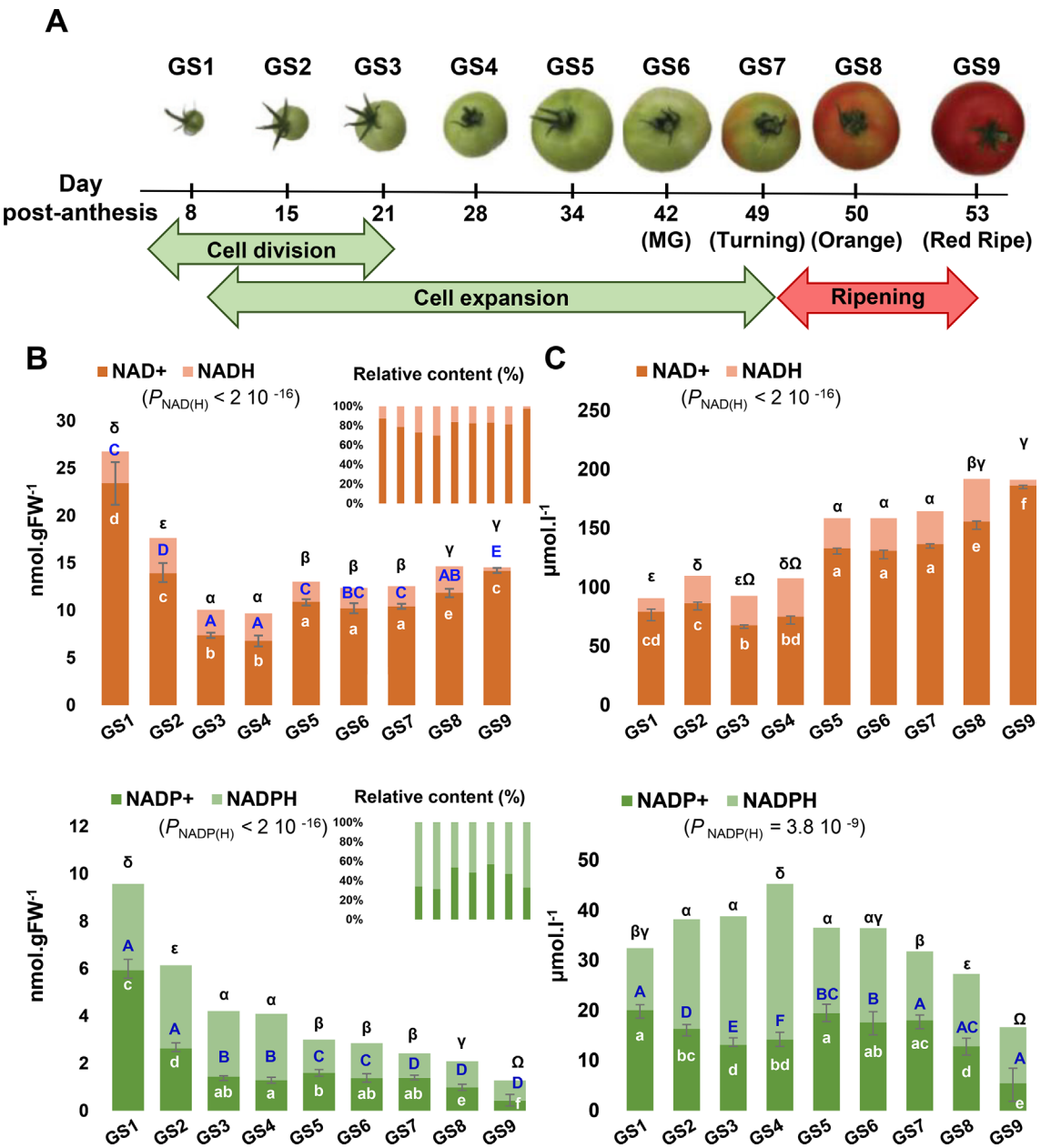

FIGURE 2 | Evolution of NAD(P) contents during tomato fruit development. NAD and NADP pools were measured for nine sequential growth stages (GS) of tomato fruit development **(A)**. Shown are bar plots of replicated metabolite quantifications (n = 3) **(B)** and of replicated metabolite quantifications (n = 3) normalized to the cytosol and organelles volumes **(C)**. Top and bottom error bars indicate SEM (standard error of the mean) for the reduced and oxidized forms, respectively. Statistical significance for total NAD(P) content is indicated by ANOVA P value. Binary comparisons between conditions are indicated by letters (oxidized form, in white), capital letters (reduced form, in blue), and symbols (total content, in black), according to Student's t test ($P < 0.05$). Left panel indicates the concentrations of NAD(P) in nmol.gFW^{-1} whereas the right panel indicates the NAD(P) concentrations in µmol.l^{-1}.

to *NIC and NaPT*, and more remarkably, as compared to actin- and enolase-related genes (**Figure S3A**). Complementarily, data mining of expression profiles from published datasets (http://tea.solgenomics.net/; Fernandez-Pozo et al., 2017) confirmed that the NAD$^+$ biosynthesis gene *AO* was expressed at low levels in fruit tissues as compared to other genes (**Figure S3B**), which can explain the absence of proteomic hits in our dataset.

Furthermore, we analyzed transcriptional changes of NAD$^+$ catabolism involved in signaling and metabolism of nicotinate including 13 genes of PARPs, SIR, NDXs, NaGTs, NMTs, and NaMe esterase that demethylates NaMe into Na (**Figure 3B**) (Gakière et al., 2018b). Clustering analysis (Pearson's correlation with complete clustering) unveiled three main significant clusters (ANOVA with Bonferroni correction, $P < 0.01$ are listed

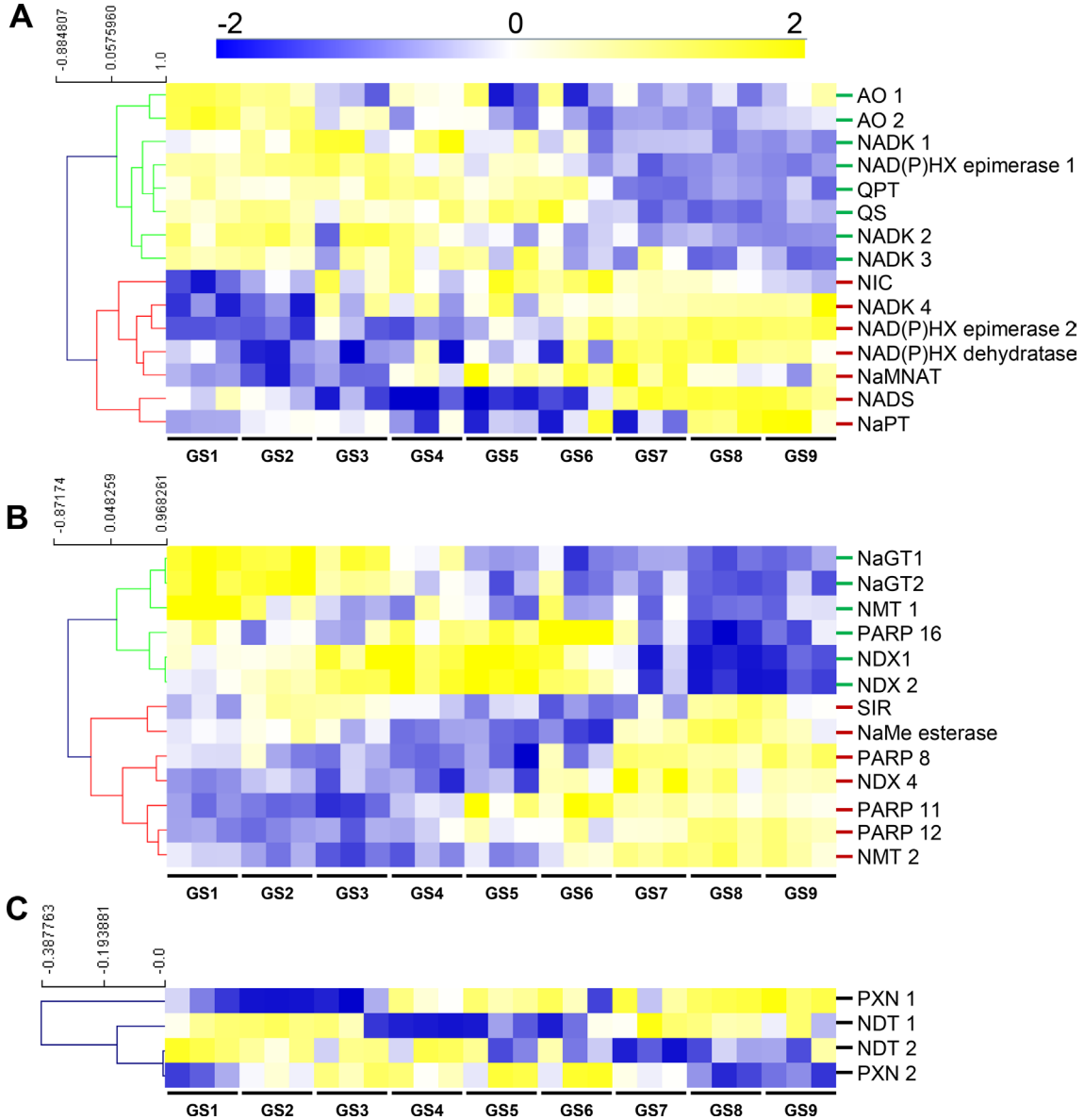

FIGURE 3 | NAD⁺ synthesis **(A)**, consumption **(B)**, and transport **(C)** show transcriptional changes during tomato fruit development. Transcript data were normalized (see *Materials and Methods*) then filtered for statistically significant features (ANOVA with Bonferroni correction, $P < 0.01$) and subjected to clustering analysis using MeV (http://mev.tm4.org/). Shown are Pearson's correlations after complete clustering of mRNA profiles. Names on the right refer to as enzymes of NAD⁺ synthesis **(A)**, consumption **(B)**, or putative transport **(C)**. NIC and NaPT were also found as significantly regulated during fruit growth for protein profiles (**Figure S2**). AO, aspartate oxidase; GS, growth stage; NADK, NAD kinase; NAD(P)HX, NAD(P)H hydrate; NaMNAT, NaMN adenylyltransferase; NAD(P)HX, NAD(P)H hydrate NADS, NAD synthetase; NaGT, nicotinate N-glucosyltransferase; NaPT, nicotinate phosphoribosyltransferase; NaMe, nicotinate methyl; NMT, nicotinate methyltransferase; NDT, nicotinamide adenine transporter; NDX, nudix; NIC, nicotinamidase; PARP, poly-ADP-ribose polymerase; PXN, peroxisomal NAD carrier; QPT, quinolinate phosphoribosyltransferase; QS, quinolinate synthase; SIR, sirtuin.

in **Table S1**). The young fruit correlated with an up-regulation of genes associated with NaGT and NMT functions, while older fruit (GS3–GS6) showed increased gene expression for PARP and NDX. The ripening fruit was associated with higher expression of genes associated with PARP, NMT, NaMe esterase, and NDX (**Figure 3B**).

Finally, we evaluated transcriptional changes of transporter genes that linked to putative pyridine nucleotide transport (**Figure 3C**). Transcript levels observed during early fruit development (GS1–4) correlated with the expression of NDT-like transporters suggesting an active transport of NAD(P) and its derivatives across the chloroplastic and mitochondrial membranes. Cell elongation (GS4–6) and ripening (GS7–9) phases were associated with higher expression of both PXN and NDT-like transporters, thus supporting the idea of an active NAD(P) transport during fruit development.

Altogether, RNAseq data demonstrate a profound reprogramming of NAD(P) metabolism during fruit growth, more specifically toward a stimulation of the synthesis of NAD^+ precursors (*AO*, *QS*, and *QPT*) in chloroplast of young fruits, which was concurrent with the expression of NDT-like transporters. This was followed at later stages of fruit development by an active synthesis (*NaMNAT* and *NADS*) and recycling (*NIC* and *NaPT*) (**Figure 3**), concomitantly with increased NAD(H) pools and concentrations (**Figure 2**).

Transcriptional Changes of Genes Associated to NAD(P)-Dependent Enzymes During Tomato Fruit Growth

To get a more global overview of the metabolic functions relating to pyridine nucleotides during tomato fruit growth, we analyzed the expression profiles of the genes that we could associate to NAD/P(H)-dependent functions. A selection of 442 NAD(P)-dependent features (see *Materials and Methods*) was subjected to PCA to display the global impact of growth stages on transcriptional changes for those features (**Figure 4A**). PCA explained 70% of the maximal variation in the mRNA profiles, where PC1 (59.6%) separated stages 1 to 6 from stages 7 to 9. This suggests a differential reprogramming at mRNA level of NAD(P)-dependent between cell division and expansion (GS1–6), and fruit ripening (GS7–9). Next, we filtered the same features for statistical significance (ANOVA with Bonferroni correction, $P < 0.01$ are listed in **Table S2**), which provided 119 mRNA markers that were retained for subsequent clustering analysis (Pearson's correlation, complete clustering) (**Figure 4B**). Tomato fruit development was associated with four clusters distributed along the different growth stages, for which functional classification was performed based on gene ontology using Mercator4 v1.0 (https://plabipd.de/portal/mercator4; (Schwacke et al., 2019). This led to the identification of 13 different functional categories (**Figure 4C**) in which mitochondrial activity (18% of the total significant features) is the largest category represented for all growth stages. Cluster 1 corresponded to the beginning of tomato fruit development (GS1 to 5) and contained 19 genes mainly involved in energy supply for central metabolism, *i.e.*, photosynthesis (21%) and mitochondrial activity (5%). Cluster 1 further harbors several genes linked to central metabolism such as lipid-, sugar-, lignin-, and cell wall–related metabolisms (11, 10, 16, and 5%, respectively). Cluster 2 covered cell division and cell expansion stages of fruit growth and contained 36 genes mostly related to central metabolism [*i.e.*, cell wall, sugar, lipid, amino acid metabolism (28, 8, 8, 5%, respectively)] that are essential to cell proliferation by providing building blocks (**Figure 4C**). In addition, cluster 2 presented a substantial proportion (25%) of unknown functions or of genes involved in specialized metabolism (17 and 8%, respectively). Cluster 3 was represented only by six genes which were expressed from GS4 to GS6 (*i.e.*, the end of fruit expansion) and that were annotated to pigment synthesis, lipid, amino acid, and cell wall metabolisms (17% each) (**Figure 4C**). Cluster 4 contained the larger number of significant mRNA markers (58) that coded for genes mostly involved in mitochondrial activity (34%), but also the maintenance of redox homeostasis, lipid, amino acid, secondary pathways (9% each), and protein degradation (2%). Overall, gene expression for NAD(P)-dependent functions during fruit growth emphasizes the importance of pyridine nucleotides as cornerstones of central metabolism, which provides building blocks and energy for development. Importantly, NAD(P)-related mitochondrial functions seem crucial for fruit growth, more specifically at the onset of ripening.

Protein Profiles for NAD(P)-Dependent Enzymes During Tomato Fruit Growth

In addition to mRNA profiles, we further examined protein profiles for NAD(P)-dependent enzymes through global analysis by PCA of 128 protein features from normalized data, and by clustering of 78 significant protein markers (ANOVA with Bonferroni correction, $P < 0.01$ are listed in **Table S3**). In contrast to transcript signatures (**Figure 4A**), PCA better segregated the protein patterns according to GS1, GS2, and GS3 then merged GS4 to GS6, separated GS7, and gathered GS8 and GS9 (**Figure 5A**). This suggests that proteomics of NAD(P)-dependent enzymes is particularly sensitive to fruit growth. Complete clustering analysis by Pearson's correlation resulted in three main clusters (**Figure 5B**) for which functional annotation of protein sequences was performed based on gene ontology using Mercator4 v1.0 leading to the identification of 12 different functional categories (**Figure 5C**) in which mitochondrial activity (19% of the total significant markers) was the largest category represented across all growth stages. To confirm the proteomic output, we measured enzyme activities of isocitrate dehydrogenase ($NADP^+$-dependent) and malate dehydrogenase (NAD^+-dependent) (**Figure S4**), which showed similar profile during fruit growth as compared to normalized protein concentration.

Firstly, cluster 1 is comprised of 27 NAD(P)-dependent proteins that accumulated mainly during the beginning of tomato fruit development (GS1–4) and during the ripening phases (GS7–9) for some of them (**Figure 5C**). This cluster could be divided into three segments; the first one contained enzymes involved in central metabolism (56%) such as cell wall-, sugar-, lipid-, and nitrogen-related metabolism and pentose phosphate pathway (15, 15, 11, 11, and 4%, respectively). The second portion is devoted to the energy production *via* the mitochondrial activity, constituting 15% of this cluster. The remaining part is represented by enzymes involved in specialized metabolism or unknown functions (15 and 15%, respectively) (**Figure 5C**). Secondly, cluster 2 included 28 proteins, which coincided with the fruit enlargement (GS1–6) within half of them that are stimulated during cell expansion (GS4–GS6). The most represented enzymes in this cluster are those involved in secondary pathways (29%) and mitochondrial functions (18%) (**Figure 5C**). Strikingly, central metabolism accounted for 42%, mainly because of cell wall and sugar metabolism (11% each) but also because of amino acid and lipid metabolism, glyoxylate cycle, and pentose phosphate pathway (7, 3, 3, and 7%, respectively) (**Figure 5C**). Finally, cluster 3 was constituted by 23 NAD(P)-dependent enzymes that were found during fruit ripening (from GS7 to GS9). Quite importantly, enzymes

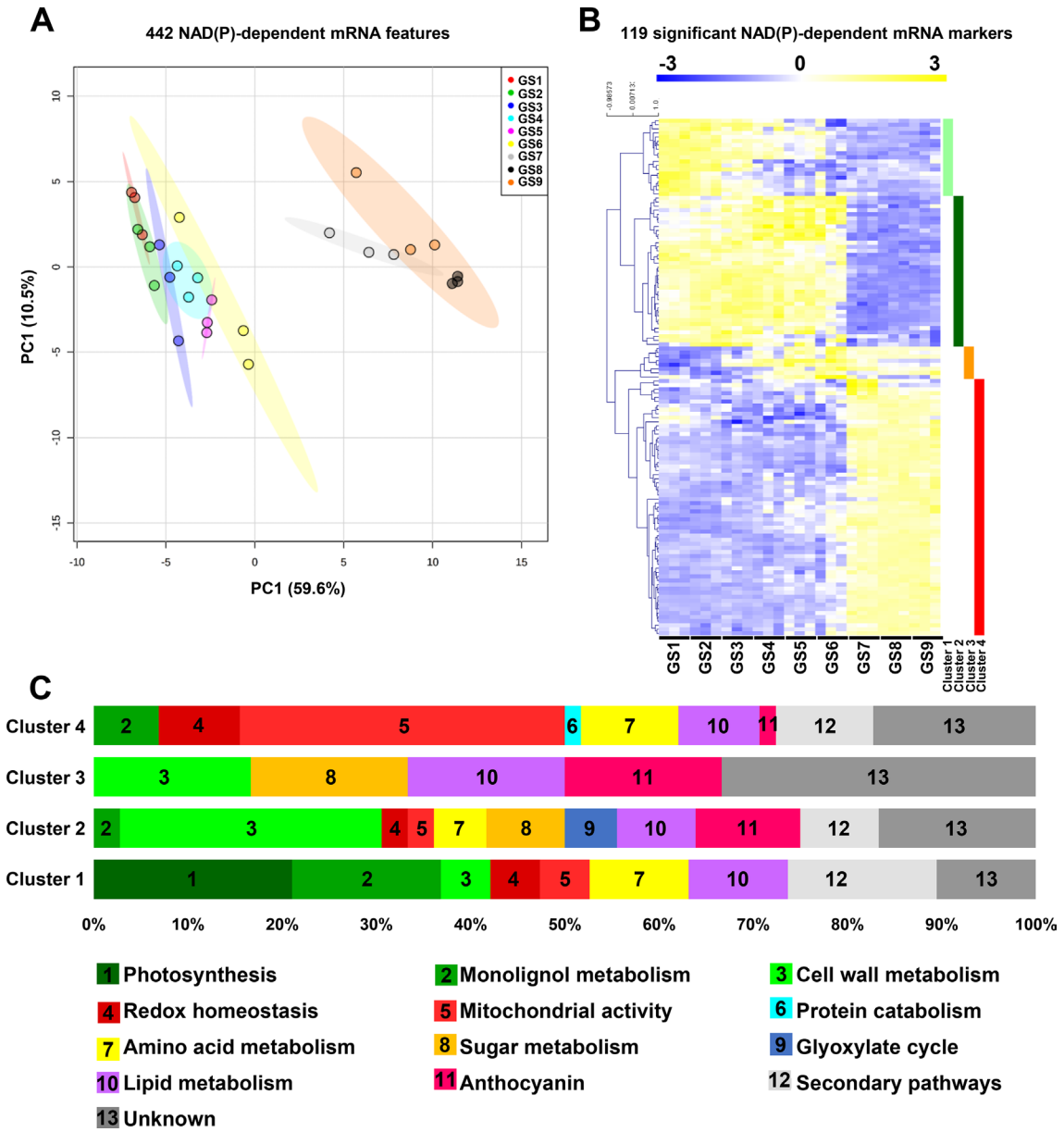

FIGURE 4 | Expression of genes for NAD(P)-dependent enzymes reveals distinct clusters during tomato fruit growth. Normalized transcript data of 442 transcript features of NAD(P)-dependent enzyme (see Materials and Methods) were visualized **(A)** for global impact of the growth stage of tomato fruit by PCA (with maximal variation given into brackets). Same features were then filtered (ANOVA with Bonferroni correction, $P < 0.01$) and subjected to clustering analysis **(B)** using MeV (http://mev.tm4.org/). Shown are Pearson's correlations after complete clustering of 119 significant mRNA profiles. Four clusters were identified and analyzed for functional classification based on their gene ontology annotations **(C)**. GS, growth stage.

involved in mitochondrial activity were mainly represented (26%) in this last cluster, followed by proteins participating in redox homeostasis (18%) and secondary pathways (13%). Central metabolism (21%) remained noticeable due to the presence of enzymes involved in lipid and amino acid metabolisms, pentose phosphate pathway, and protein degradation (9, 4, 4, and 4%, respectively) (**Figure 5C**). Hence, while protein and mRNA profiles of NAD(P)-dependent markers only showed partial overlap during tomato fruit growth, central metabolism and more particularly mitochondrial functions were critically linked to pyridine nucleotides.

DISCUSSION

Pyridine nucleotides have received considerable attention for their metabolic, redox, and signaling functions in plant tissues (Hashida et al., 2009; Pétriacq et al., 2013; Gakière et al., 2018a; Gakière et al., 2018b). However, very little is

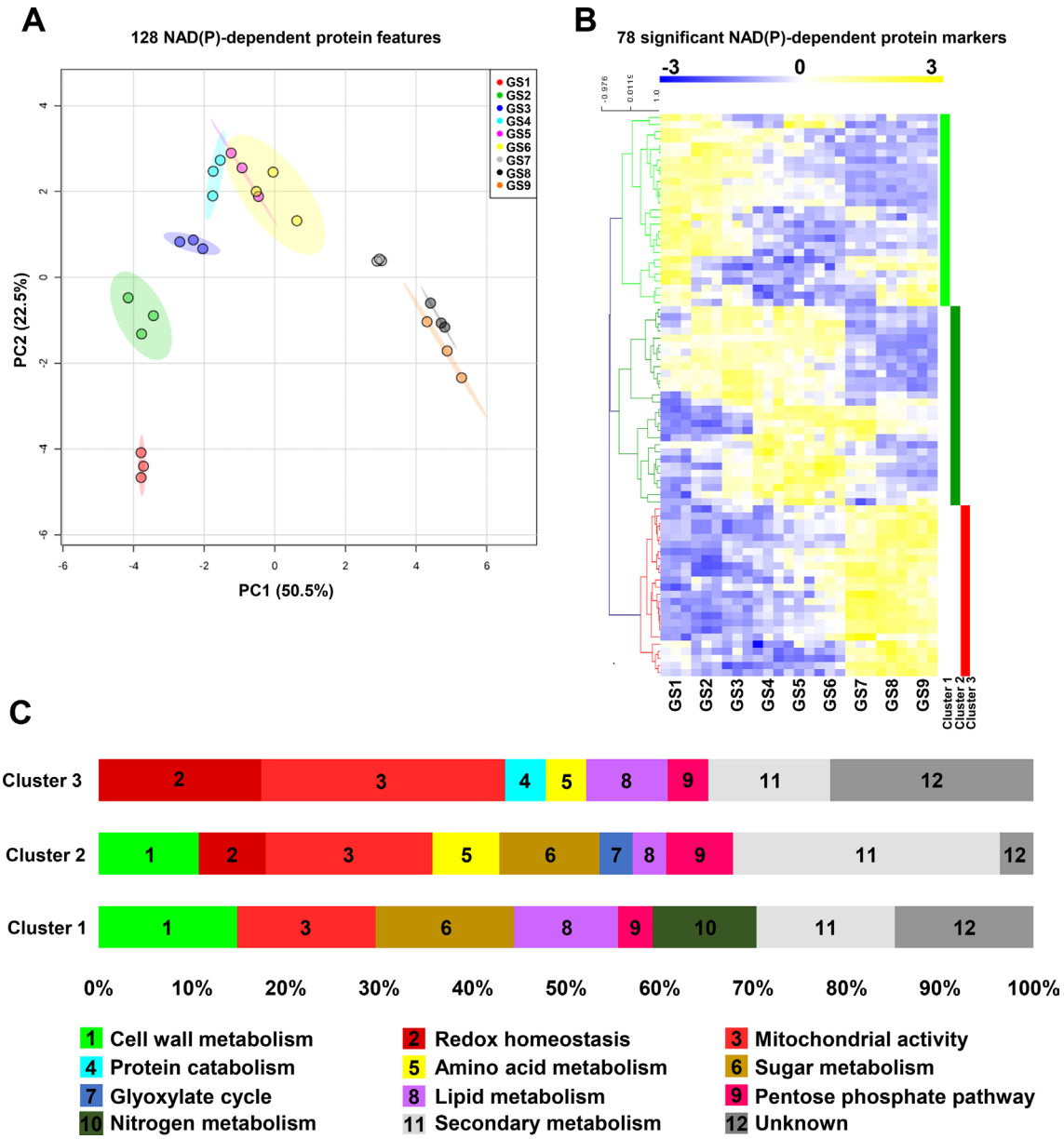

FIGURE 5 | Protein profiles for NAD(P)-dependent enzymes unveil distinct clusters during tomato fruit growth. Normalized protein data 127 NAD(P)-dependent enzyme (see Materials and Methods) were visualized **(A)** for global impact of the growth stage of tomato fruit by principal component analysis (PCA with maximal variation given into brackets). Same features were then filtered (ANOVA with Bonferroni correction, $P < 0.01$) and subjected to clustering analysis **(B)** using MeV (http://mev.tm4.org/). Shown are Pearson's correlations after complete clustering of 78 significant protein profiles. Four clusters were identified and analyzed for functional classification based on their gene ontology annotations **(C)**. GS, growth stage.

known about the importance of these metabolic cofactors for fruit growth. In this study, we examined the contribution of pyridine nucleotides to fruit growth by analyzing NAD(P) metabolism at transcriptome and proteome scales as well as NAD(P)$^+$ and NAD(P)H contents and concentrations during nine sequential stages of tomato fruit development.

Although previous changes in pyridine nucleotides have been observed between green and red tomato fruits of MicroTom and Moneymaker cultivars (Centeno et al., 2011; Osorio et al., 2013), our study presents for the first time the changes of NAD(P) contents and concentrations during nine sequential stages of tomato fruit development. As previously observed (Centeno et al., 2011), the highest contents (nmol.gFW^{-1}) were measured during early developmental phases (**Figure 2**), concomitantly with the expression of genes involved in early reactions of NAD$^+$ *de novo* synthesis (AO, QS, and QPT) (**Figure 3**), also assumed to control critically NAD(P) levels and its derivatives (Pétriacq et al., 2012; Pétriacq et al., 2016). Firstly, NAD(H) contents and concentrations

showed two distinct accumulations mainly caused by increased NAD^+ at the beginning of cell elongation and ripening (GS5 and GS8) (**Figure 2**). Concurrently, transcript analysis unveiled a stimulation of further steps of NAD^+ *de novo* synthesis and recycling pathway (**Figure 3A**). Secondly, NADP(H) contents dropped during cell division (GS1–4) whereas concentrations were augmented as a result of increased NADPH concentrations. Furthermore, cell expansion and ripening phases displayed a decrease in both NADP(H) contents and concentrations. Since NAD(P) are mostly present in organelles other than the vacuole (Donaldson, 1982; Gakière et al., 2018b), concentrations seem more relevant to understand the involvement of NADP(H) in fruit development (**Figure 2C**). However, pyridine nucleotide concentrations that are reported here and in previous studies represent pooled contents of subcellular metabolites rather than the *in vivo* original compartmentalized concentrations, which are known to differ between organelles (Gakière et al., 2018b). Such differences in subcellular concentrations might affect the enzyme activities that depend on pyridine nucleotides as cofactor. Meta-analysis of K_m values for plant dehydrogenases (Bar-Even et al., 2011) showed that total cellular concentrations of NAD(P) measured in our study were higher than the median K_m values of plant NAD(P)-dependent enzymes (**Figure S5**). This indicates that concentrations of pyridine nucleotides in the developing fruit are sufficiently high that they would not limit NAD(P)-dependent enzyme activities, as previously suggested (Bennett et al., 2009). In growing tissues, such as *Arabidopsis* pollen tubes (Hashida et al., 2012), or here in young tomato fruit that is characterized by a *turbo* metabolism due to high enzyme activities (Biais et al., 2014), plant development requires higher NAD^+ and reducing power (NADPH) (Gakière et al., 2018b). High concentrations of NADP(H) in young fruits (**Figure 2C**) might be associated with photosynthesis that remains active in green fruits, as detected in our transcript analysis (**Figure 4C**) and previously reported (Lytovchenko et al., 2011). Furthermore, mRNA and protein analyses indicated a primary accumulation of NAD^+ precursors (GS1–4) before the activation of *de novo* and recycling (GS4–9) pathways during tomato fruit growth (**Figure 3**), which correlated with both contents and concentrations of NAD(H). Interestingly, the stimulation of NaMNAT and NADS at transcript levels (**Figure 3A**) occurred just before the increase in NAD(H) concentrations (**Figure 2C**). On the other hand, catabolism of NAD(P) *via* signaling functions appeared continuous during fruit development but resulted from different catabolic pathways (**Figure 3B**) as well as transport of NAD(P) and their precursors (**Figure 3C**). This indicates that NAD(P) contents are sustained as key metabolic regulators for fruit growth by different synthesis and degradation pathways. Precursors are synthesized by early enzymes of *de novo* synthesis of NAD^+ (AO, QS, QPT); then, latter enzymes of synthesis and salvage routes (NaMNAT, NADS, NIC, NaPT, NaGT, and NAD(P)H-hydrate epimerase and hydratase) (**Figure 1**) allow for NAD(P) homeostasis. This agrees with previous works which have demonstrated the importance of AO, QS, and QPT in modulating NAD^+ levels that influence plant development (Katoh et al., 2006; Schippers et al., 2008; Pétriacq et al., 2012; Gakière et al., 2018a). Likewise, *Arabidopsis* NICs were also reported to influence NAD^+ contents (Hunt et al., 2007; Wang and Pichersky, 2007). Metabolism of nicotinate has also received recent attention in various plant species (Matsui et al., 2007; Li et al., 2015; Wu et al., 2018). In this context, we observed increased expression of NMT and NaMe esterase genes in the developing fruit (**Figure 3**), suggesting that Na metabolism is important to sustain NAD(P) homeostasis. Nicotinate conjugates are particularly difficult to measure *via* MS-based metabolomics due to unreliable ionizations of such compounds in the mass spectrometer, as it is the case for NAD^+ and nicotinamide (Guérard et al., 2011). Further research combining MS and NMR techniques is necessary to confirm the molecular and regulatory details of nicotinate metabolism in fruit.

In all biological systems, a plethora of cellular processes need NAD(P) as coenzymes, including both biosynthetic pathways and the catabolism of biomolecules which support energy production (Gakière et al., 2018a). Mitochondria are the powerhouse of the cell that ensure energy supply by regenerating NADH and providing ATP and are considered to contain the highest proportion of cellular NAD(H). Several studies have shown that modifying mitochondrial functions result in changes of NAD(P) contents that not only greatly influence plant growth (Dutilleul, 2003; Dutilleul et al., 2003; Dutilleul, 2005; Pellny et al., 2008; Meyer et al., 2009; Centeno et al., 2011; Osorio et al., 2013; Pétriacq et al., 2017) but also stress responses (Pétriacq et al., 2016; Gakière et al., 2018b), thus placing pyridine nucleotides as critical regulators of plant performance. In line with this, we demonstrated that NAD(P)-dependent enzymes appeared mainly related to central metabolic pathways, including one-fifth of mitochondrial functions (**Figures 4C** and **5C**). This agrees with a critical role of mitochondrial NAD(P) metabolism for tomato fruit growth, as elegantly demonstrated in mutant tomato fruit that are affected in TCA cycle (Araújo et al., 2012). Additionally, we showed that mRNAs and proteins that related to NAD(P)-dependent enzymes exhibited distinguishable profiles during fruit development. We further identified a global separation between ripening and previous developmental stages (*i.e.*, cell division and expansion) (**Figures 4A** and **5A**), based on the profiles of both NAD(P)-dependent mRNAs and proteins. This suggests a growth stage-dependent reprogramming of NAD(P) metabolism. Concurrently, we observed a growth stage-dependent stimulation of the different central metabolism branches (amino acid-, lipid-, sugar-, and cell wall–related metabolism) at both transcript and proteomic levels (**Figures 4C** and **5C**), thus emphasizing the link between NAD(P) and carbon and nitrogen metabolisms. This raises the question about NAD(P) signaling during fruit development (Hashida et al., 2018), as further exemplified by a notable proportion of NAD(P)-dependent enzymes that related to redox homeostasis at mRNA and protein levels, especially those involved in ascorbate–glutathione cycle, and other specialized pathways (e.g., anthocyanins biosynthesis). Here, we showed that cellular division phases displayed an increase in reducing power equivalent (NADPH) while cellular expansion and ripening phases harbored a higher oxidized state. Hence, pyridine nucleotides appear pivotal for fruit development in supplying energy and precursors for central metabolism while assuring redox homeostasis and secondary metabolites accumulation. For a better comprehension of NAD(P) involvement in cellular processes, future works should also include

the study of protein turnover, especially protein synthesis rate that has been shown to control protein levels in developing tomato fruit (Belouah et al., 2019).

Climacteric species (e.g., tomato, banana, kiwi.) are characterized by a metabolic shift from normal development state, known as climacteric crisis, that is associated with the conversion of starch into soluble sugars and CO_2 (Moing et al., 2001; Colombié et al., 2017), and which is concomitant with higher ATP levels and respiratory fluxes. Interestingly, from a transcript perspective, 50% of the significant NAD(P)-dependent genes that were identified as up-regulated during ripening belonged to enzymes involved in the key respiratory burst during ripening of climacteric fruits (**Figure 4**) in accordance with previous reports (Biais et al., 2014; Colombié et al., 2015; Colombié et al., 2017). Moreover, mitochondrial functions represented a notable proportion of both protein and transcript markers, and more specifically, a greater proportion (>75%) within the NAD(P)-dependent ripening-related markers, thus supporting the idea that climacteric respiration is *(i)* regulated by mitochondrial activity and *(ii)* essential for fruit ripening (**Figures 4B**, **C**). In tomato fruit, the energy peak results from an excessive carbon supply coming from starch and cell wall degradation, and a decrease in carbon demand as a result of arrested cell expansion (Colombié et al., 2017). In agreement, several sugar- and cell wall–related NAD(P)-dependent markers are identified to be up-regulated shortly before and during ripening (**Figures 4** and **5**). Besides, NAD(P)-dependent markers involved in redox homeostasis were also up-regulated mainly during ripening (**Figures 4** and **5**). Despite the energy peak and the control of redox balance, ripening is also associated with a wide range of metabolic processes resulting in organoleptic changes reflected by an increased sweetness, and nutritional value. This further agrees with a concurrent accumulation of soluble sugars and others amino acids coming from starch and protein degradation, respectively (Beauvoit et al., 2018). Here, functional clustering identified an increase of NAD(P)-dependent transcript and protein levels involved in protein catabolism only during ripening phases as well as amino acid-related metabolism markers (**Figures 4** and **5**). Finally, latter stages of NAD^+ synthesis and recycling were stimulated during ripening at both transcript and protein levels (**Figure 3**) that resulted in an augmented NAD(H) concentrations (**Figure 2**), probably to sustain the high metabolic activity during fruit-ripening process. Collectively, these results indicate that NAD(P) is a core component of tomato fruit ripening, which not only participates in the climacteric respiration *via* a stimulation of mitochondrial activity but also sustains energy supply for numerous biosynthetic pathways that relate pyridine nucleotide metabolism to fruit development and quality.

CONCLUSION

This study is a first step toward a better comprehension of the implication of NAD(P) in fruit development. Our results demonstrate a crucial role of NAD(P) during the whole process of fruit growth with distinct functions between the cellular division, expansion, and ripening stages. Further experiments are required to decipher which biochemical and molecular mechanisms are triggered by pyridine nucleotides and participate in the control of fruit development. Due to the high reactivity of such redox metabolites, metabolic modeling tools might provide a great alternative to predict fluxes of NAD(P) during fruit development and a better understanding of these mechanisms that will help to improve fruit performance, thus allowing better strategies for crop productions.

DATA AVAILABILITY STATEMENT

The datasets generated for this study can be found in https://www.ncbi.nlm.nih.gov/geo/query/acc.cgi?acc=GSE128739, GSE128739.

AUTHOR CONTRIBUTIONS

PP designed the work with inputs from GD, BB, SC, and YG. GD, IB, BB, SB, CC, SA, and MG performed the experiments. GD, BB, PP, SP and PB analysed the data with substantial data interpretation from all the authors. GD and PP wrote the manuscript with inputs from all the authors.

FUNDING

The authors are grateful for financial support from INRA BAP, University of Bordeaux and to the FRIMOUSS (ANR-15-CE20-0009-01), MetaboHUB (ANR-11-INBS-0010) and PHENOME (ANR-11-INBS-0012) projects. The doctoral school *Sciences de la Vie et Santé* at Université de Bordeaux is also acknowledged for granting PP with PhD funding for GD (bourse fléchée ministérielle 2018-2021).

SUPPLEMENTARY MATERIAL

The Supplementary Material for this article can be found online at: https://www.frontiersin.org/articles/10.3389/fpls.2019.01201/full#supplementary-material

REFERENCES

Alferez, F. M., Gerberich, K. M., Li, J.-L., Zhang, Y., Graham, J. H., and Mou, Z. (2018). Exogenous nicotinamide adenine dinucleotide induces resistance to citrus canker in citrus. *Front. Plant Sci.* 9, 1472. doi: 10.3389/fpls.2018.01472

Araújo, W. L., Nunes-Nesi, A., Nikoloski, Z., Sweetlove, L. J., and Fernie, A. R. (2012). Metabolic control and regulation of the tricarboxylic acid cycle in photosynthetic and heterotrophic plant tissues: TCA control and regulation in plant tissues. *Plant Cell Environ.* 35, 1–21. doi: 10.1111/j.1365-3040.2011.02332.x

Arrivault, S., Guenther, M., Ivakov, A., Feil, R., Vosloh, D., van Dongen, J. T., et al. (2009). Use of reverse-phase liquid chromatography, linked to tandem mass spectrometry, to profile the Calvin cycle and other metabolic intermediates in *Arabidopsis* rosettes at different carbon dioxide concentrations. *Plant J.* 59, 826–839. doi: 10.1111/j.1365-313X.2009.03902.x

Bar-Even, A., Noor, E., Savir, Y., Liebermeister, W., Davidi, D., Tawfik, D. S., et al. (2011). The moderately efficient enzyme: evolutionary and physicochemical trends shaping enzyme parameters. *Biochemistry* 50, 4402–4410. doi: 10.1021/bi2002289

Barrett, T., Wilhite, S. E., Ledoux, P., Evangelista, C., Kim, I. F., Tomashevsky, M., et al. (2013). NCBI GEO: archive for functional genomics data sets—update. *Nucleic Acids Res.* 41, 991–995. doi: 10.1093/nar/gks1193

Beauvoit, B., Belouah, I., Bertin, N., Cakpo, C. B., Colombié, S., Dai, Z., et al. (2018). Putting primary metabolism into perspective to obtain better fruits. *Ann. Bot.* 122, 1–21. doi: 10.1093/aob/mcy057

Beauvoit, B. P., Colombié, S., Monier, A., Andrieu, M.-H., Biais, B., Bénard, C., et al. (2014). Model-assisted analysis of sugar metabolism throughout tomato fruit development reveals enzyme and carrier properties in relation to vacuole expansion. *Plant Cell* 26, 3224–3242. doi: 10.1105/tpc.114.127761

Belouah, I., Nazaret, C., Pétriacq, P., Prigent, S., Bénard, C., Mengin, V., et al. (2019). Modeling protein destiny in developing fruit. *Plant Physiol.* 190, 1709–1724. doi: 10.1104/pp.19.00086

Bennett, B. D., Kimball, E. H., Gao, M., Osterhout, R., Van Dien, S. J., and Rabinowitz, J. D. (2009). Absolute metabolite concentrations and implied enzyme active site occupancy in *Escherichia coli*. *Nature Chem. Biol.* 5, 593–599. doi: 10.1038/nchembio.186

Biais, B., Bénard, C., Beauvoit, B., Colombié, S., Prodhomme, D., Ménard, G., et al. (2014). Remarkable reproducibility of enzyme activity profiles in tomato fruits grown under contrasting environments provides a roadmap for studies of fruit metabolism. *Plant Physiol.* 164, 1204–1221. doi: 10.1104/pp.113.231241

Bowsher, C. G., Lacey, A. E., Hanke, G. T., Clarkson, D. T., Saker, L. R., Stulen, I., et al. (2007). The effect of Glc6P uptake and its subsequent oxidation within pea root plastids on nitrite reduction and glutamate synthesis. *J. Exp. Bot.* 58, 1109–1118. doi: 10.1093/jxb/erl269

Briggs, A. G., and Bent, A. F. (2011). Poly(ADP-ribosyl)ation in plants. *Trends Plant Sci.* 16, 372–380. doi: 10.1016/j.tplants.2011.03.008

Centeno, D. C., Osorio, S., Nunes-Nesi, A., Bertolo, A. L. F., Carneiro, R. T., Araújo, W. L., et al. (2011). Malate plays a crucial role in starch metabolism, ripening, and soluble solid content of tomato fruit and affects postharvest softening. *Plant Cell* 23, 162–184. doi: 10.1105/tpc.109.072231

Colombié, S., Beauvoit, B., Nazaret, C., Bénard, C., Vercambre, G., Le Gall, S., et al. (2017). Respiration climacteric in tomato fruits elucidated by constraint-based modelling. *New Phytol.* 213, 1726–1739. doi: 10.1111/nph.14301

Colombié, S., Nazaret, C., Bénard, C., Biais, B., Mengin, V., Solé, M., et al. (2015). Modelling central metabolic fluxes by constraint-based optimization reveals metabolic reprogramming of developing *Solanum lycopersicum* (tomato) fruit. *Plant J.* 81, 24–39. doi: 10.1111/tpj.12685

Donaldson, R. P. (1982). Nicotinamide cofactors (NAD and NADP) in glyoxysomes, mitochondria, and plastids isolated from castor bean endosperm. *Arch. Biochem. Biophys.* 215, 274–279. doi: 10.1016/0003-9861(82)90305-8

Dutilleul, C. (2003). Leaf mitochondria modulate whole cell redox homeostasis, set antioxidant capacity, and determine stress resistance through altered signaling and diurnal regulation. *Plant Cell* 15, 1212–1226. doi: 10.1105/tpc.009464

Dutilleul, C. (2005). Mitochondria-driven changes in leaf NAD status exert a crucial influence on the control of nitrate assimilation and the integration of carbon and nitrogen metabolism. *Plant Physiol.* 139, 64–78. doi: 10.1104/pp.105.066399

Dutilleul, C., Driscoll, S., Cornic, G., Paepe, R. D., Foyer, C. H., and Noctor, G. (2003). Functional mitochondrial complex I is required by tobacco leaves for optimal photosynthetic performance in photorespiratory conditions and during transients. *Plant Physiol.* 131, 264–275. doi: 10.1104/pp.011155

Faurobert, M., Pelpoir, E., and Chaïb, J. (2007). Phenol extraction of proteins for proteomic studies of recalcitrant plant tissues. *Methods Mol. Biol.* 355, 9–14. doi: 10.1385/1-59745-227-0:9

Fernandez-Pozo, N., Zheng, Y., Snyder, S. I., Nicolas, P., Shinozaki, Y., Fei, Z., et al. (2017). The tomato expression atlas. *Bioinformatics* 33, 2397–2398. doi: 10.1093/bioinformatics/btx190

Gakière, B., Fernie, A. R., and Pétriacq, P. (2018a). More to NAD+ than meets the eye: a regulator of metabolic pools and gene expression in *Arabidopsis*. *Free Radic. Biol. Med.* 122, 86–95. doi: 10.1016/j.freeradbiomed.2018.01.003

Gakière, B., Hao, J., de Bont, L., Pétriacq, P., Nunes-Nesi, A., and Fernie, A. R. (2018b). NAD + biosynthesis and signaling in plants. *Crit. Rev. Plant Sci.* 37, 1–49. doi: 10.1080/07352689.2018.1505591

Geigenberger, P., and Fernie, A. R. (2014). Metabolic control of redox and redox control of metabolism in plants. *Antioxid. Redox Signal.* 21, 1389–1421. doi: 10.1089/ars.2014.6018

Gibon, Y., Blaesing, O. E., Hannemann, J., Carillo, P., Höhne, M., Hendriks, J. H. M., et al. (2004). A robot-based platform to measure multiple enzyme activities in *Arabidopsis* using a set of cycling assays: comparison of changes of enzyme activities and transcript levels during diurnal cycles and in prolonged darkness. *Plant Cell* 16, 3304–3325. doi: 10.1105/tpc.104.025973

Gibon, Y., Pyl, E.-T., Sulpice, R., Lunn, J. E., Höhne, M., Günther, M., et al. (2009). Adjustment of growth, starch turnover, protein content and central metabolism to a decrease of the carbon supply when *Arabidopsis* is grown in very short photoperiods. *Plant Cell Environ.* 32, 859–874. doi: 10.1111/j.1365-3040.2009.01965.x

Gibon, Y., Usadel, B., Blaesing, O. E., Kamlage, B., Hoehne, M., Trethewey, R., et al. (2006). Integration of metabolite with transcript and enzyme activity profiling during diurnal cycles in *Arabidopsis* rosettes. *Genome Biol.* 7, R76. doi: 10.1186/gb-2006-7-8-R76

Guérard, F., Pétriacq, P., Gakière, B., and Tcherkez, G. (2011). Liquid chromatography/time-of-flight mass spectrometry for the analysis of plant samples: a method for simultaneous screening of common cofactors or nucleotides and application to an engineered plant line. *Plant Physiol. Biochem.* 49, 1117–1125. doi: 10.1016/j.plaphy.2011.06.003

Hashida, S. N., Takahashi, H., and Uchimiya, H. (2009). The role of NAD biosynthesis in plant development and stress responses. *Ann. Bot.* 103, 819–824. doi: 10.1093/aob/mcp019

Hashida, S., Takahashi, H., Kawai-Yamada, M., and Uchimiya, H. (2007). *Arabidopsis thaliana* nicotinate/nicotinamide mononucleotide adenyltransferase (AtNMNAT) is required for pollen tube growth: AtNMNATis required for pollen tube growth. *Plant J.* 49, 694–703. doi: 10.1111/j.1365-313X.2006.02989.x

Hashida, S.-N., Miyagi, A., Nishiyama, M., Yoshida, K., Hisabori, T., and Kawai-Yamada, M. (2018). Ferredoxin/thioredoxin system plays an important role in the chloroplastic NADP status of *Arabidopsis*. *Plant J.* 95, 947–960. doi: 10.1111/tpj.14000

Hashida, S.-N., Takahashi, H., Takahara, K., Kawai-Yamada, M., Kitazaki, K., Shoji, K., et al. (2012). NAD+ Accumulation during Pollen maturation in *arabidopsis* regulating onset of germination. *Mol. Plant* 6, 216–225. doi: 10.1093/mp/sss071

Havé, M., Balliau, T., Cottyn-Boitte, B., Dérond, E., Cueff, G., Soulay, F., et al. (2018). Increases in activity of proteasome and papain-like cysteine protease in *Arabidopsis* autophagy mutants: back-up compensatory effect or cell-death promoting effect? *J. Exp. Bot.* 69, 1369–1385. doi: 10.1093/jxb/erx482

Hunt, L., and Gray, J. E. (2009). The relationship between pyridine nucleotides and seed dormancy. *New Phytol.* 181, 62–70. doi: 10.1111/j.1469-8137.2008.02641.x

Hunt, L., Holdsworth, M. J., and Gray, J. E. (2007). Nicotinamidase activity is important for germination. *Plant J.* 51, 341–351. doi: 10.1111/j.1365-313X.2007.03151.x

Hunt, L., Lerner, F., and Ziegler, M. (2004). NAD—new roles in signalling and gene regulation in plants. *New Phytol.* 163, 31–44. doi: 10.1111/j.1469-8137.2004.01087.x

Katoh, A., Uenohara, K., Akita, M., and Hashimoto, T. (2006). Early steps in the biosynthesis of NAD in *Arabidopsis* start with aspartate and occur in the plastid. *Plant Physiol.* 141, 851–857. doi: 10.1104/pp.106.081091

Köster, S., Upmeier, B., Komossa, D., and Barz, W. (1989). Nicotinic acid conjugation in plants and plant cell cultures of potato (*Solanum tuberosum*). *Z. Naturforsch. C.* 44, 623–628. doi: 10.1515/znc-1989-7-813

Kraszewska, E. (2008). The plant Nudix hydrolase family. *Acta Biochim. Pol.* 55, 663–671. doi: 19081844

Kupis, W., Pałyga, J., Tomal, E., and Niewiadomska, E. (2016). The role of sirtuins in cellular homeostasis. *J. Physiol. Biochem.* 72, 371–380. doi: 10.1007/s13105-016-0492-6

Li, B.-B., Wang, X., Tai, L., Ma, T.-T., Shalmani, A., Liu, W.-T., et al. (2018a). NAD kinases: metabolic targets controlling redox co-enzymes and reducing power partitioning in plant stress and development. *Front. Plant Sci.* 9, 379. doi: 10.3389/fpls.2018.00379

Li, W., Zhang, F., Chang, Y., Zhao, T., Schranz, M. E., and Wang, G. (2015). Nicotinate O-glucosylation is an evolutionarily metabolic trait important for seed germination under stress conditions in *Arabidopsis thaliana*. *Plant Cell* 27, 1907–1924. doi: 10.1105/tpc.15.00223

Li, W., Zhang, F., Wu, R., Jia, L., Li, G., Guo, Y., et al. (2017). A novel N-methyltransferase in *arabidopsis* appears to feed a conserved pathway for nicotinate detoxification among land plants and is associated with lignin biosynthesis. *Plant Physiol.* 174, 1492–1504. doi: 10.1104/pp.17.00259

Li, W.-Y., Wang, X., Li, R., Li, W.-Q., and Chen, K.-M. (2014). Genome-wide analysis of the NADK gene family in plants. *PLoS One* 9 (6), e101051. doi: 10.1371/journal.pone.0101051

Li, Y., Wang, H., Zhang, Y., and Martin, C. (2018b). Can the world's favorite fruit, tomato, provide an effective biosynthetic chassis for high-value metabolites? *Plant Cell Rep.* 37, 1443–1450. doi: 10.1007/s00299-018-2283-8

Lytovchenko, A., Eickmeier, I., Pons, C., Osorio, S., Szecowka, M., Lehmberg, K., et al. (2011). Tomato fruit photosynthesis is seemingly unimportant in primary metabolism and ripening but plays a considerable role in seed development. *Plant Physiol.* 157, 1650–1663. doi: 10.1104/pp.111.186874

Macho, A. P., Boutrot, F., Rathjen, J. P., and Zipfel, C. (2012). Aspartate oxidase plays an important role in *Arabidopsis* stomatal immunity. *Plant Physiol.* 159, 1845–1856. doi: 10.1104/pp.112.199810

Magni, G., Amici, A., Emanuelli, M., Orsomando, G., Raffaelli, N., and Ruggieri, S. (2004). Enzymology of NAD+ homeostasis in man. *Cell. Mol. Life Sci.* 61, 19–34. doi: 10.1007/s00018-003-3161-1

Mahalingam, R., Jambunathan, N., and Penaganti, A. (2007). Pyridine nucleotide homeostasis in plant development and stress. *Int. J. Plant Dev. Biol.* 1, 194–201.

Matsui, A., Yin, Y., Yamanaka, K., Iwasaki, M., and Ashihara, H. (2007). Metabolic fate of nicotinamide in higher plants. *Physiol. Plant* 131, 191–200. doi: 10.1111/j.1399-3054.2007.00959.x

Meyer, E. H., Tomaz, T., Carroll, A. J., Estavillo, G., Delannoy, E., Tanz, S. K., et al. (2009). Remodeled respiration in ndufs4 with low phosphorylation efficiency suppresses *Arabidopsis* germination and growth and alters control of metabolism at night. *Plant Physiol.* 151, 603–619. doi: 10.1104/pp.109.141770

Moing, A., Renaud, C., Gaudillère, M., Raymond, P., Roudeillac, P., and Denoyes-Rothan, B. (2001). Biochemical changes during fruit development of four strawberry cultivars. *J. Am. Soc. Hortic. Sci.* 126, 394–403. doi: 10.21273/JASHS.126.4.394

Mou, Z. (2017). Extracellular pyridine nucleotides as immune elicitors in *Arabidopsis*. *Plant Signal Behav.* 12. doi: 10.1080/15592324.2017.1388977

Neuhaus, H. E., and Emes, M. J. (2000). Nonphotosynthetic metabolism in plastids. *Annu. Rev. Plant Physiol. Plant Mol. Biol.* 51, 111–140. doi: 10.1146/annurev.arplant.51.1.111

Niehaus, T. D., Richardson, L. G. L., Gidda, S. K., ElBadawi-Sidhu, M., Meissen, J. K., Mullen, R. T., et al. (2014). Plants utilize a highly conserved system for repair of NADH and NADPH Hydrates. *Plant Physiol.* 165, 52–61. doi: 10.1104/pp.114.236539

Noctor, G., Queval, G., and Gakière, B. (2006). NAD(P) synthesis and pyridine nucleotide cycling in plants and their potential importance in stress conditions. *J. Exp. Bot.* 57, 1603–1620. doi: 10.1093/jxb/erj202

Osorio, S., Vallarino, J. G., Szecowka, M., Ufaz, S., Tzin, V., Angelovici, R., et al. (2013). Alteration of the interconversion of pyruvate and malate in the plastid or cytosol of ripening tomato fruit invokes diverse consequences on sugar but similar effects on cellular organic acid, metabolism, and transitory starch accumulation. *Plant Physiol.* 161, 628–643. doi: 10.1104/pp.112.211094

Pellny, T. K., Aken, O. V., Dutilleul, C., Wolff, T., Groten, K., Bor, M., et al. (2008). Mitochondrial respiratory pathways modulate nitrate sensing and nitrogen-dependent regulation of plant architecture in Nicotiana sylvestris. *Plant J.* 54, 976–992. doi: 10.1111/j.1365-313X.2008.03472.x

Perez-Riverol, Y., Csordas, A., Bai, J., Bernal-Llinares, M., Hewapathirana, S., Kundu, D. J., et al. (2019). The PRIDE database and related tools and resources in 2019: improving support for quantification data. *Nucleic Acids Res.* 47, D442–D450. doi: 10.1093/nar/gky1106

Pétriacq, P., de Bont, L., Genestout, L., Hao, J., Laureau, C., Florez-Sarasa, I., et al. (2017). Photoperiod affects the phenotype of mitochondrial complex I mutants. *Plant Physiol.* 173, 434–455. doi: 10.1104/pp.16.01484

Pétriacq, P., de Bont, L., Hager, J., Didierlaurent, L., Mauve, C., Guérard, F., et al. (2012). Inducible NAD overproduction in *Arabidopsis* alters metabolic pools and gene expression correlated with increased salicylate content and resistance to Pst-AvrRpm1. *Plant J.* 70, 650–665. doi: 10.1111/j.1365-313X.2012.04920.x

Pétriacq, P., de Bont, L., Tcherkez, G., and Gakière, B. (2013). NAD: not just a pawn on the board of plant-pathogen interactions. *Plant Signal Behav.* 8, 1–11. doi: 10.4161/psb.22477

Pétriacq, P., Ton, J., Patrit, O., Tcherkez, G., and Gakière, B. (2016). NAD acts as an integral regulator of multiple defense layers. *Plant Physiol.* 172, 1465–1479. doi: 10.1104/pp.16.00780

Queval, G., and Noctor, G. (2007). A plate reader method for the measurement of NAD, NADP, glutathione, and ascorbate in tissue extracts: application to redox profiling during *Arabidopsis* rosette development. *Anal. Biochem.* 363, 58–69.

Schippers, J. H. M., Nunes-Nesi, A., Apetrei, R., Hille, J., Fernie, A. R., and Dijkwel, P. P. (2008). The *Arabidopsis* onset of leaf death5 mutation of quinolinate synthase affects nicotinamide adenine dinucleotide biosynthesis and causes early ageing. *Plant Cell* 20, 2909–2925. doi: 10.1105/tpc.107.056341

Schwacke, R., Ponce-Soto, G. Y., Krause, K., Bolger, A. M., Arsova, B., Hallab, A., et al. (2019). MapMan4: a refined protein classification and annotation framework applicable to multi-omics data analysis. *Mol. Plant* 12, 897–892. doi: 10.1016/j.molp.2019.01.003

Soubeyrand, E., Colombié, S., Beauvoit, B., Dai, Z., Cluzet, S., Hilbert, G., et al. (2018). Constraint-based modeling highlights cell energy, redox status and α-ketoglutarate availability as metabolic drivers for anthocyanin accumulation in grape cells under nitrogen limitation. *Front. Plant Sci.* 9, 421. doi: 10.3389/fpls.2018.00421

Steinhauser, M.-C., Steinhauser, D., Koehl, K., Carrari, F., Gibon, Y., Fernie, A. R., et al. (2010). Enzyme activity profiles during fruit development in tomato cultivars and *Solanum* pennellii. *Plant Physiol.* 153, 80–98. doi: 10.1104/pp.110.154336

Studart-Guimarães, C., Gibon, Y., Frankel, N., Wood, C. C., Zanor, M. I., Fernie, A. R., et al. (2005). Identification and characterisation of the alpha and beta subunits of succinyl CoA ligase of tomato. *Plant Mol. Biol.* 59, 781–791. doi: 10.1007/s11103-005-1004-1

Suda, Y., Tachikawa, H., Yokota, A., Nakanishi, H., Yamashita, N., Miura, Y., et al. (2003). Saccharomyces cerevisiae QNS1 codes for NAD+ synthetase that is functionally conserved in mammals. *Yeast* 20, 995–1005. doi: 10.1002/yea.1008

Turner, W. L., Waller, J. C., Vanderbeld, B., and Snedden, W. A. (2004). Cloning and Characterization of two NAD kinases from *Arabidopsis*. Identification of a calmodulin binding isoform. *Plant Physiol.* 135, 1243–1255. doi: 10.1104/pp.104.040428

Upmeier, B., Thomzik, J. E., and Barz, W. (1988). Nicotinic acid-N-glucoside in heterotrophic parsley cell suspension cultures. *Phytochemistry* 27, 3489–3493. doi: 10.1016/0031-9422(88)80754-4

Waller, J. C., Dhanoa, P. K., Schumann, U., Mullen, R. T., and Snedden, W. A. (2010). Subcellular and tissue localization of NAD kinases from *Arabidopsis*: compartmentalization of *de novo* NADP biosynthesis. *Planta* 231, 305–317. doi: 10.1007/s00425-009-1047-7

Wang, G., and Pichersky, E. (2007). Nicotinamidase participates in the salvage pathway of NAD biosynthesis in *Arabidopsis*. *Plant J.* 49, 1020–1029. doi: 10.1111/j.1365-313X.2006.03013.x

Wu, R., Zhang, F., Liu, L., Li, W., Pichersky, E., and Wang, G. (2018). MeNA, controlled by reversible methylation of nicotinate, is an NAD precursor that undergoes long-distance transport in *Arabidopsis*. *Mol. Plant* 11, 1264–1277. doi: 10.1016/j.molp.2018.07.003

Zhang, X., and Mou, Z. (2009). Extracellular pyridine nucleotides induce PR gene expression and disease resistance in *Arabidopsis*. *Plant J.* 57, 302–312. doi: 10.1111/j.1365-313X.2008.03687.x

Conflict of Interest: The authors declare that the research was conducted in the absence of any commercial or financial relationships that could be construed as a potential conflict of interest.